

PROPRIETARY - FOR U.S. GOVERNMENT USE ONLY



**ARCO Alaska, Inc.**

RECEIVED

Anchorage, Alaska

MAR 22 1996

REGIONAL SUPERVISOR  
FIELD OPERATION  
MINERALS MANAGEMENT SERVICE

# **KUVLUM PREDECISION STUDIES**

**FINAL REPORT**

**June 1994**

(CONT'D)

**APPENDIX 6**

**DEVELOPMENT WELLS**

## APPENDIX 6: DEVELOPMENT WELLS

### Table of Contents

	<u>Page</u>
Summary	A6-1
Assumptions	A6-1

## **APPENDIX 6: DEVELOPMENT WELLS**

### **Summary**

The development wells were estimated to have a "most likely" cost of \$3.0MM/each. The estimated uncertainty of the development wells cost is shown in Figures A6-2 through A6-7. An optimistic cost is estimated to be 80% of the Most Likely cost. A pessimistic cost is estimated to be 150% of the Most Likely cost. As show in the following figures, a triangular distribution is assumed. The costs were developed based on the conditions encountered during the discovery well and experience from drilling Kuparuk River Unit development wells (similar to Kuvlum).

### **Assumptions**

The development wells were assumed to be 7000 ft. TVD and an average of 21 days per well. Detailed assumptions are included in this section in Figure A6-8.



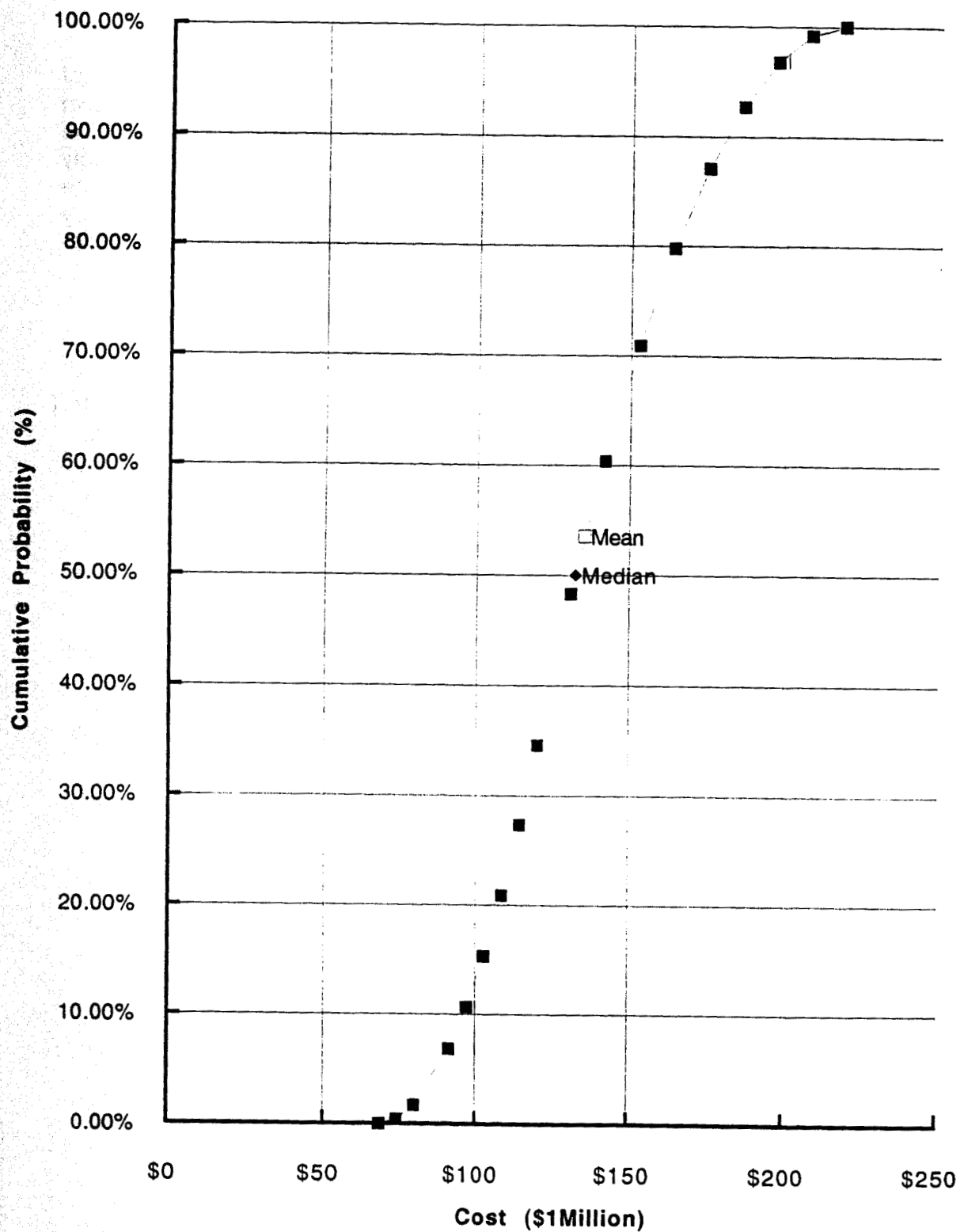


FIGURE A6-2  
Development Wells Cost (40 Wells) for Case 1

This Spread Sheet will compute the unique Triangular Probability Density Distribution and the unique Cumulative Probability Curve determined by the k%, Most Likely and k"% Cost Estimates

INPUT:			Costs in \$1,000,000		Development Well Cost (40 Wells) for Case 1.	
k' & k" Cost Estimate	0.1	\$96.00				
Most Likely Cost Estimate	b=	\$120.00				
k''' & k''' Cost Estimate	0.9	\$180.00				
			0% cost = \$68.04		100% Cost = \$218.50	
			See Table for Probability Density vs Cost, Mean & Median Costs			

To Calculate the Absolute Minimum Cost (0% Cost Estimate) which will be called "a" and the Absolute Maximum Cost (100% Cost Estimate) which will be called "c". Note the Most Likely Cost is called "b".

The k', Most Likely, and k''' Cost Estimates completely define the Triangular Probability Density Distribution and Cumulative Probability Curves. An iterative procedure has to be used to calculate "a" and "c"; that is, the 0% Cost Estimate and the 100% Cost Estimate, respectively.

First step is to determine which set of equations are applicable to find "a" and "c". This will depend on where the Most Likely Cost Estimate "b" lies relative to k' and k''' Cost Estimates.

Please note that k' Cost Estimate is always less than k''' Cost Estimate.

FOR THE ABOVE K'COST, MOST LIKELY COST AND K'''COST ESTIMATES USE

XXXXXXXX  
MIDDLE CASE  
XXXXXXXX

<p><b>CASE LEFT</b> If Most Likely Cost Estimate &lt; k' Cost Estimate c= 222.000000 D= 0.01156463 a= 49.05882353 Therefore k2 for Most Likely Cost Estimate is equal to 0.410204082 (k') (k'''-k') (1-k''')</p>	<p><b>CASE MIDDLE</b> If (k' Cost Estimate &lt; Most Likely Cost Estimate &lt; k''' Cost Estimate), iterate to Find Absolute Minimum 'a' and Maximum 'c' Cost Estimates. Try values of 'a' until c=c". Trial 'a'= 68.0397 c= 218.4985634 c'= 218.4985633 Delta=(c'-c")= 0.000710148 D= 0.013292847 0.0001 0.001 68.0398</p>	<p><b>CASE RIGHT</b> If (k' Cost Estimate &lt; k''' Cost Estimate &gt; Most Likely Cost Estimate), a= 54 c= 321.2727273 D= 0.007482993 (k') (k'''-k') (1-k''')</p>
--	---	--

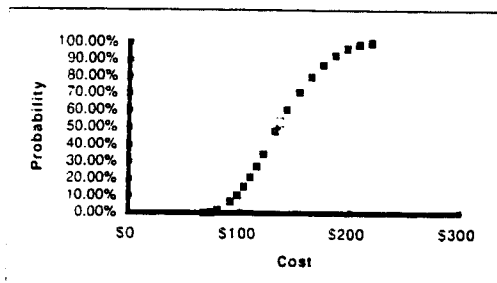
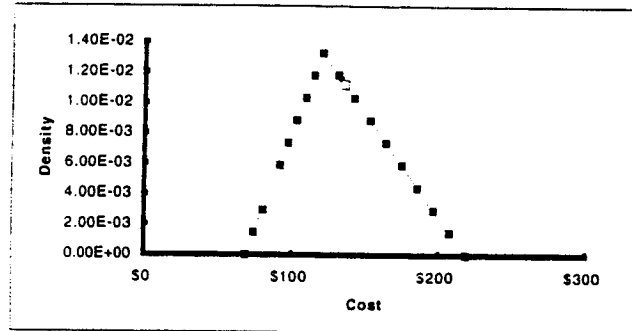
Is a < k' Cost Estimate? Yes, Valid  
Is k' < k'''? Yes, Valid

Please Note that you must enter the values calculated above into these slots before computing distributions.

Enter the Values of "a", "c", and D computed above	a= \$68.0397 c= \$218.4966 D= 0.01329285
--	--

Calculating Probability Density Distribution and Cumulative Probability Curves

	Cost in \$1,000,000 \$	Probability Density (1/\$)	Cumulative Probability %
	\$68	0.00E+00	0.00%
	\$74	1.48E-03	0.43%
	\$80	2.95E-03	1.71%
	\$91	5.91E-03	6.82%
	\$97	5.91E-03	6.82%
	\$97	7.38E-03	10.66%
	\$103	8.86E-03	15.35%
	\$108	1.03E-02	20.89%
	\$114	1.18E-02	27.29%
Most Likely	\$120	1.33E-02	34.54%
	\$131	1.18E-02	48.27%
	\$142	1.03E-02	60.40%
	\$153	8.86E-03	70.90%
	\$164	7.38E-03	79.79%
	\$175	5.91E-03	87.07%
	\$186	4.43E-03	92.73%
	\$197	2.95E-03	96.77%
	\$208	1.48E-03	99.19%
Absolute Maximum	\$218	0.00E+00	100.00%
MEAN COST	\$135.51	1.12E-02	53.53%
MEDIAN COST	\$132.42	0.01161712	50.00%



RSKWC12.xls Robert E. 12/14/93

FIGURE A6-3  
Development Wells Cost (40 Wells) for Case 1

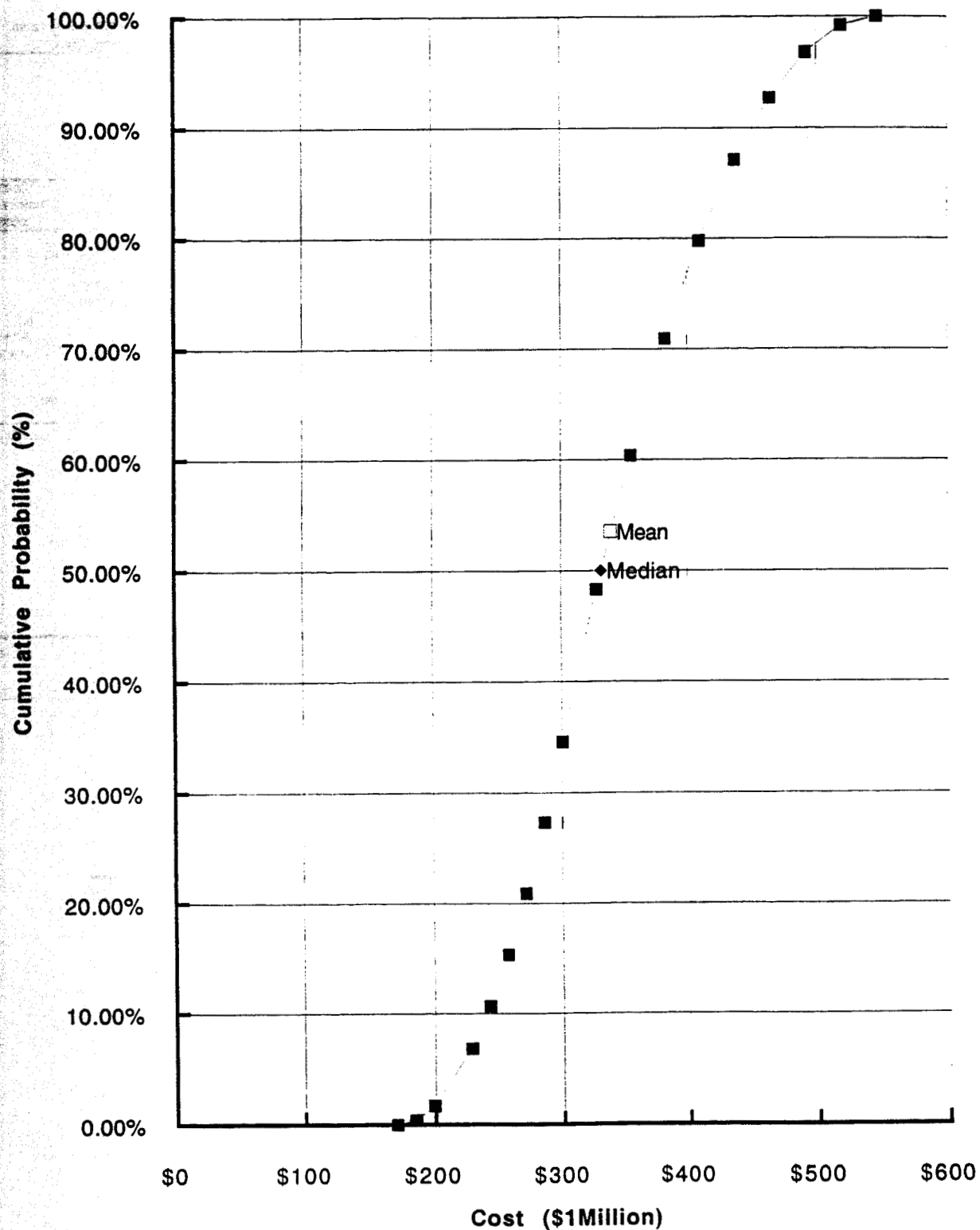


FIGURE A6-4  
Development Wells Cost (100 Wells) for Case 2 and Case 3

This Spread Sheet will compute the unique Triangular Probability Density Distribution and the unique Cumulative Probability Curve determined by the k%, Most Likely and k"% Cost Estimates

INPUT:			Costs in \$1,000,000		Development Wells Cost (100 Wells) for Case 2 and Case 3.	
k' & k" Cost Estimate	0.1	\$240.00				
Most Likely Cost Estimate	b=	\$300.00				
k''' & k''' Cost Estimate	0.9	\$450.00				
			0% cost = \$170.10		100% Cost = \$546.24	
See Table for Probability Density vs Cost, Mean & Median Costs						

To Calculate the Absolute Minimum Cost (0% Cost Estimate) which will be called "a" and the Absolute Maximum Cost (100% Cost Estimate) which will be called "c". Note the Most Likely Cost is called "b".

The k', Most Likely, and k''' Cost Estimates completely define the Triangular Probability Density Distribution and Cumulative Probability Curves. An iterative procedure has to be used to calculate "a" and "c"; that is, the 0% Cost Estimate and the 100% Cost Estimate, respectively.

First step is to determine which set of equations are applicable to find "a" and "c". This will depend on where the Most Likely Cost Estimate "b" lies relative to k' and k''' Cost Estimates.

Please note that k' Cost Estimate is always less than k''' Cost Estimate.

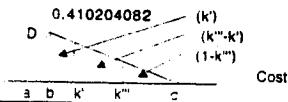
FOR THE ABOVE K'COST, MOST LIKELY COST AND K'''COST ESTIMATES USE

XXXXXXXX  
MIDDLE CASE  
XXXXXXXX

#### CASE LEFT

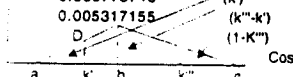
If Most Likely Cost Estimate < k' Cost Estimate  
 c= 555.00000  
 D= 0.00462585  
 a= 122.6470588

Therefore k2 for Most Likely Cost Estimate is equal to



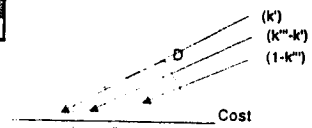
#### CASE MIDDLE

If (k' Cost Estimate < Most Likely Cost Estimate < k''' Cost Estimate), iterate to Find Absolute Minimum 'a' and Maximum 'c' Cost Estimates. Try values of 'a' until  
 c=c'. Trial 'a' = 170.0994  
 c' = 546.2403786  
 c'' = 546.2396048  
 Delta=(c'-c'')= 0.000773746  
 D= 0.005317155



#### CASE RIGHT

If (k' Cost Est. < k''' Cost Est. > Most Likely Cost Est.),  
 a= 135  
 c= 803.1818182  
 D= 0.002993197



Is a < k' Cost Estimate? Yes, Valid  
 Is k' < k'''? Yes, Valid

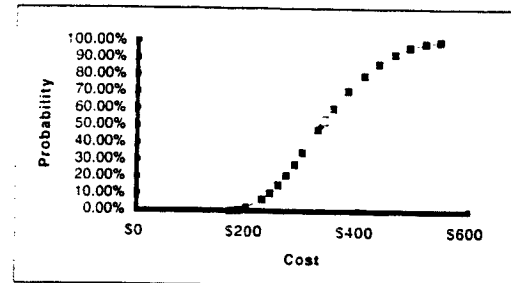
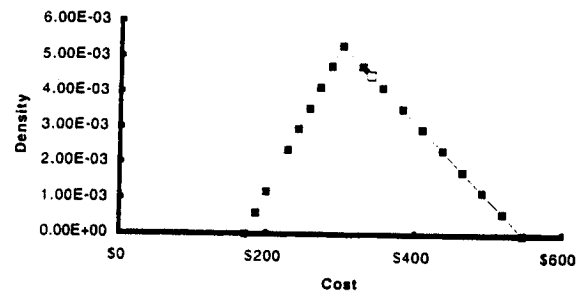
Please Note that you must enter the values calculated above into these slots before computing distributions.

Enter the Values of "a", "c", and D computed above

a= \$170.0994  
 c= \$546.2404  
 D= 0.00531716

Calculating Probability Density Distribution and Cumulative Probability Curves

	Cost in \$1,000,000 \$	Probability Density (1/\$)	Cumulative Probability %
	\$170	0.00E+00	0.00%
	\$185	5.91E-04	0.43%
	\$199	1.18E-03	1.71%
	\$228	2.36E-03	6.82%
	\$228	2.36E-03	6.82%
	\$242	2.95E-03	10.66%
	\$257	3.54E-03	15.35%
	\$271	4.14E-03	20.89%
	\$286	4.73E-03	27.29%
Most Likely	\$300	5.32E-03	34.54%
	\$327	4.73E-03	48.27%
	\$355	4.14E-03	60.40%
	\$382	3.54E-03	70.90%
	\$409	2.95E-03	79.79%
	\$437	2.36E-03	87.07%
	\$464	1.77E-03	92.73%
	\$492	1.18E-03	96.77%
	\$519	5.91E-04	99.19%
Absolute Maximum	\$546	0.00E+00	100.00%
MEAN COST	\$338.78	4.48E-03	53.53%
MEDIAN COST	\$331.04	0.004646865	50.00%



RSKWC12.xls Robert E. 12/14/93

FIGURE A6-5  
Development Wells Cost (100 Wells) for Case 2 and Case 3

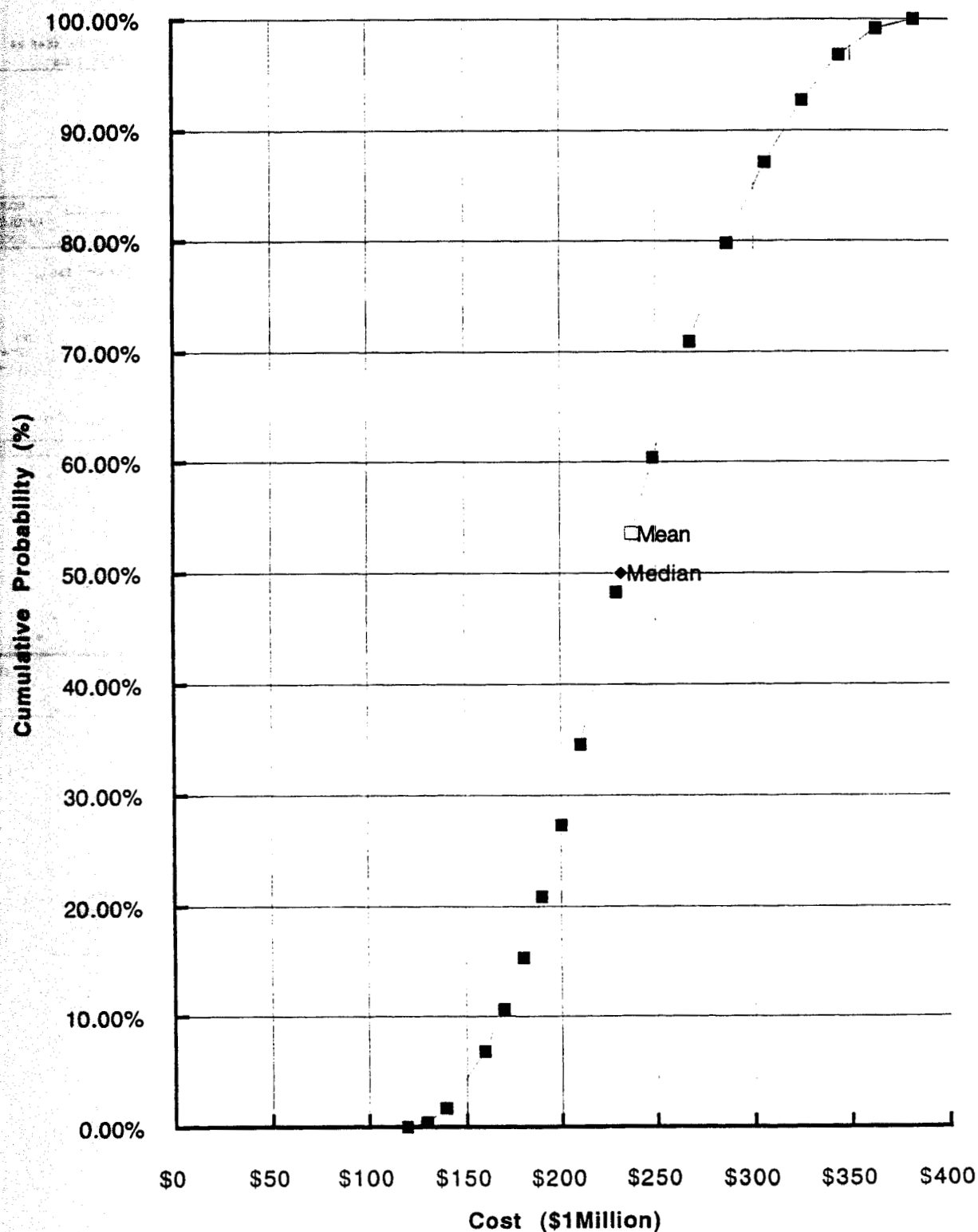


**FIGURE A6-6**  
**Development Wells Cost (70 Wells) for Intermediate Case between Case 2 and Case 3**

This Spread Sheet will compute the unique Triangular Probability Density Distribution and the unique Cumulative Probability Curve determined by the k%, Most Likely and k"% Cost Estimates

INPUT:			Development Wells Cost (70 Wells) for Intermediate Case between Case 1 and Case3.	
Costs in \$1,000,000			0% cost = \$119.07	100%Cost= \$382.37
k' & k"Cost Estimate	0.1	\$188.00	See Table for Probability Density vs Cost, Mean & Median Costs	
Most Likely Cost Estimate	b=	\$210.00		
k''' & k'''Cost Estimate	0.9	\$315.00		

To Calculate the Absolute Minimum Cost (0%Cost Estimate) which will be called "a" and the Absolute Maximum Cost (100% Cost Estimate) which will be called "c". Note the Most Likely Cost is called "b".

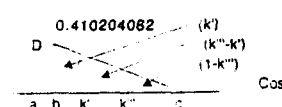
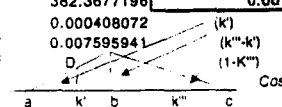
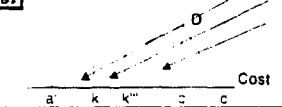
The k', Most Likely, and k'''Cost Estimates completely define the Triangular Probability Density Distribution and Cumulative Probability Curves. An iterative procedure has to be used to calculate "a" and "c"; that is, the 0%Cost Estimate and the 100% Cost Estimate, respectively.

First step is to determine which set of equations are applicable to find "a" and "c". This will depend on where the Most Likely Cost Estimate "b" lies relative to k' and k'''Cost Estimates.

Please note that k'Cost Estimate is always less than k'''Cost Estimate.

FOR THE ABOVE K'COST, MOST LIKELY COST AND K'''COST ESTIMATES USE

XXXXXXX  
MIDDLE CASE  
XXXXXXX

CASE LEFT		CASE MIDDLE		CASE RIGHT	
If Most Likely Cost Estimate < k'Cost Estimate		If (k'Cost Estimate < Most Likely Cost Estimate < k'''Cost Estimate), iterate to Find Absolute Minimum 'a' and Maximum 'c' Cost Estimates. Try values of 'a' until		If (k'Cost Est. < k'''Cost Est. > Most Likely Cost Est.),	
c=	388.50000	c=	382.3681277	a=	94.5
D=	0.00660836	c'=	382.3677196	c=	562.2272727
a=	85.85294118	c''=	119.0696	D=	0.004275996
Therefore k2 for Most Likely Cost Estimate is equal to		Delta=(c'-c'')=			
0.410204082		0.000408072			
					

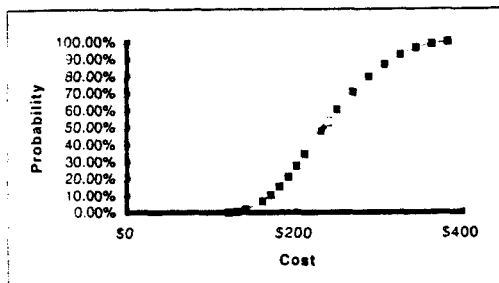
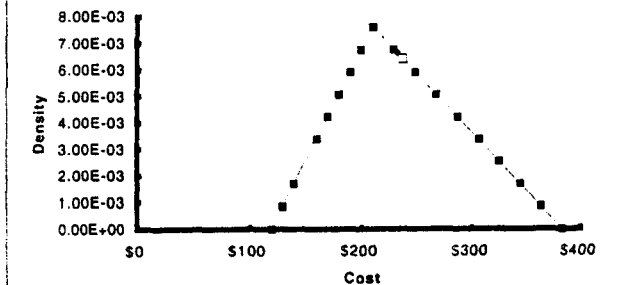
Is a < k'Cost Estimate? Yes, Valid  
Is k' < k'''? Yes, Valid

Please Note that you must enter the values calculated above into these slots before computing distributions.

Enter the Values of "a", "c", and D computed above	a=	\$119.0696
	c=	\$382.3681
	D=	0.00759594

Calculating Probability Density Distribution and Cumulative Probability Curves

	Cost in \$1,000,000	Probability Density (1/\$)	Cumulative Probability %
	\$119	0.00E+00	0.00%
	\$129	8.44E-04	0.43%
	\$139	1.69E-03	1.71%
	\$159	3.38E-03	6.82%
	\$159	3.38E-03	6.82%
	\$170	4.22E-03	10.66%
	\$180	5.06E-03	15.35%
	\$190	5.91E-03	20.89%
	\$200	6.75E-03	27.29%
	\$210	7.60E-03	34.54%
Most Likely	\$229	6.75E-03	48.27%
	\$248	5.91E-03	60.40%
	\$267	5.06E-03	70.90%
	\$287	4.22E-03	79.79%
	\$306	3.38E-03	87.07%
	\$325	2.53E-03	92.73%
	\$344	1.69E-03	96.77%
	\$363	8.44E-04	99.19%
Absolute Maximum	\$382	8.67E-04	100.00%
MEAN COST	\$237.15	6.40E-03	53.53%
MEDIAN COST	\$231.73	0.006638383	50.00%



RSKW12.xls Robert E. 12/14/93

FIGURE A6-7  
Development Wells Cost (70 Wells) for Intermediate Case between Case 2 and Case 3

# Kuvlum Development Well Cost

An average cost of \$3.0MM/development well was used. Below are the basic assumptions used in the cost estimate. The pages following contain the cost estimation calculation sheets.

## Basic Assumptions

- 16,000 acres per drillsite
- 100 wells per drillsite
- 13 3/8" surface casing
- 9 5/8" production casing
- 3 1/2" tubing
- 7000 ft TVD
- 1000'/day penetration rate for all depths
- Maximum departure of 16,000 ft
- \$75K rig operating day rate
- Ave time of 21 days per well

**Estimate Well Cost:****Input:**

No. Wells Per Drillsite =  (Max = 148)  
 Area Per Drillsite = 16,000 Acres

Rig Operating Day Rate = \$75/day  
 Rig Move Between Wells = 1 days/well  
 Rig Move Between DS's = 2 days/DS

WL Log Equip Cost =  \$M/Well  
 TC Log Equip Cost =  \$M/Well  
 Coring Equip Cost =  \$M/Well  
 Acid/Frac/Gravel Pack Cost =  \$M/Well

**Avg. Drilling Cost Per Well = \$3.0 MM**  
**Drilling Cost Per Drillsite = \$304.2 MM**

Note: Tubing-conveyed logging costs are being applied.

Apply tubing conveyed logging costs to wells with max hole angles exceeding:  Degrees  
 Core Every:  well Incr. Coring Time =  Days/Job

**Well Cost:**

Wells	Number Per Drillsite	Maximum Departure	Maximum Hole Angle	Measured Depth	Operating Days/Well	Hardware (\$MM/well)	Cost/Well (\$MM)	Total Cost (\$MM)
Type Well 1	4	1,867	16.1	7,260	15	0.63	2.2	8.8
Type Well 2	8	4,174	34.1	8,245	16	0.69	2.3	18.6
Type Well 3	4	5,600	43.0	9,137	17	0.75	2.5	9.8
Type Well 4	8	6,730	48.8	9,950	18	0.80	2.6	20.5
Type Well 5	8	7,697	53.0	10,701	19	0.84	2.8	22.1
Type Well 6	12	9,334	58.7	12,057	20	0.92	2.9	35.3
Type Well 7	8	10,053	60.7	12,678	21	0.96	3.0	24.2
Type Well 8	16	11,654	64.6	14,101	22	1.04	3.2	51.5
Type Well 9	20	13,059	67.2	15,384	24	1.12	3.4	67.8
Type Well 10	12	16,247	71.7	18,371	27	1.30	3.8	45.5
Average	@ 100 wells/DS	10,137	57.5	12,966	21	0.98	3.0	304.2

FIGURE A6-9



# DEVELOPMENT WELL COST ESTIMATOR

PROSPECT: Kuvlum Generic Well

**Estimate Well Characteristics:**

Well Type: Onshore Wells:  (Choose one, type 1)  
 Offshore Wells:  (Choose one, type 1)

Directional Wells:  (Choose one, type 1)  
 S - Shaped Wells:  (Choose one, type 1)

Well Spacing: 320 Acres/Well:  (Choose one, type 1)  
 160 Acres/Well:  (Choose one, type 1)  
 80 Acres/Well:  (Choose one, type 1)

Well Characteristics: TVD Depth =  7,000  foot Build Angle Rate =  3.0  Degrees/100'  
 Kickoff Depth =  250  foot Drop Angle Rate =  1.5  Degrees/100'  
 Vertical Tail =   foot

Casing Points: Casing Point 1 (TVD):  320  Cag Size  30" Time to Log & Case =  1  Days  
 Casing Point 2 (TVD):  1,000  Time to Log & Case =  1  Days  
 Casing Point 3 (TVD):  4,000  13-3/8" Time to Log & Case =  2  Days  
 Casing Point 4 (TVD):  7,000  9-5/8" Time to Log & Case =  3  Days

Time to Drill: Drilling Difficulty =  1.00 (Multiplier applied to drilling rate of penetration)

Depth	ROP
0 - 1000'	1000 ft/day
1000' - 4000'	1000 ft/day
4000' - 10,000'	1000 ft/day
10,000' - 12,000'	1000 ft/day
12,000' - 16,000'	1000 ft/day

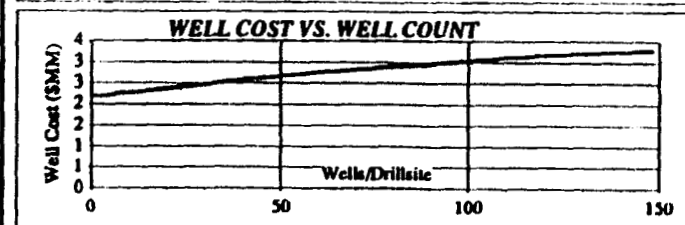
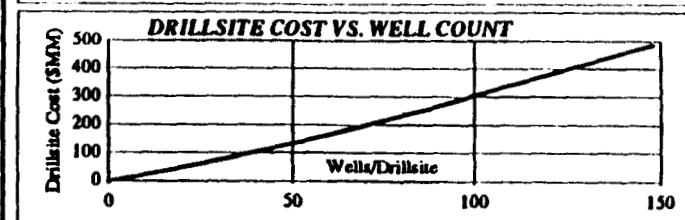
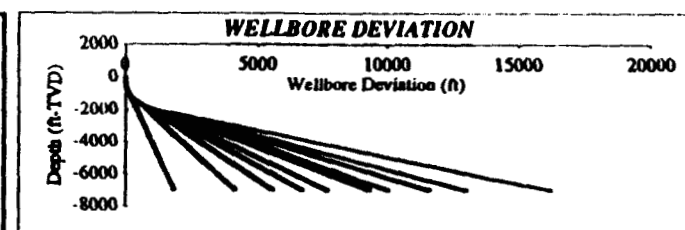


FIGURE A6-10

# CASING DETAILS

Wellhead Costs: Low Pressure (<12,000') = \$50 M  
 High Pressure (>12,000') = \$320 M  
 High Pressure Override: (type "x" to use high pressure wellhead regardless of well depth)

Casing Costs:

ONSHORE		
Casing Ft.	Size	Cost
0 - 500'	16"-20"	\$40/ft
500 - 4000'	13 3/8"	\$38/ft
4000' +	9 5/8"	\$38/ft
Tubing	3 1/2"	\$9/ft

OFFSHORE		
Casing Ft.	Size	Cost
0 - 500'	30"	\$100/ft
500 - 1500'	20"	\$69/ft
1500 - 5000'	13 3/8"	\$44/ft
5000' +	9 5/8"	\$32/ft
Tubing	3 1/2"	\$9/ft

Note: Above costs include cement and associated jewelry.  
 If casing point is within 2500 feet MD of TD, it is considered to be a hanging liner.

TYPE WELL 1:			
HARDWARE	MD	ONSHORE	OFFSHORE
Casing 1:	320	19,201	32,002
Casing 2:	1,016	38,808	70,432
Casing 3:	4,138	157,245	180,831
Casing 4:	7,260	203,281	233,773
Tubing:	7,010	56,000	64,492
Drilling Wellhead:		50,000	50,000
Total:		534,415	631,202

TYPE WELL 3:			
HARDWARE	MD	ONSHORE	OFFSHORE
Casing 1:	320	19,201	32,002
Casing 2:	1,021	38,789	70,432
Casing 3:	3,052	191,216	219,899
Casing 4:	9,137	253,836	294,200
Tubing:	8,887	71,093	81,757
Drilling Wellhead:		50,000	50,000
Total:		624,135	748,289

TYPE WELL 5:			
HARDWARE	MD	ONSHORE	OFFSHORE
Casing 1:	320	19,201	32,002
Casing 2:	1,021	38,789	70,432
Casing 3:	5,714	217,147	249,719
Casing 4:	10,701	299,621	344,564
Tubing:	10,451	83,606	96,147
Drilling Wellhead:		50,000	50,000
Total:		708,365	843,863

TYPE WELL 7:			
HARDWARE	MD	ONSHORE	OFFSHORE
Casing 1:	320	19,201	32,002
Casing 2:	1,021	38,789	70,432
Casing 3:	6,339	240,480	285,751
Casing 4:	12,678	354,983	408,233
Tubing:	12,428	99,434	114,338
Drilling Wellhead:		50,000	50,000
Total:		810,879	960,754

TYPE WELL 2:			
HARDWARE	MD	ONSHORE	OFFSHORE
Casing 1:	320	19,201	32,002
Casing 2:	1,021	38,789	70,432
Casing 3:	4,622	175,650	201,990
Casing 4:	8,245	230,872	265,503
Tubing:	7,993	63,964	73,558
Drilling Wellhead:		50,000	50,000
Total:		578,476	693,485

TYPE WELL 4:			
HARDWARE	MD	ONSHORE	OFFSHORE
Casing 1:	320	19,201	32,002
Casing 2:	1,021	38,789	70,432
Casing 3:	3,391	204,865	235,594
Casing 4:	9,950	278,588	320,376
Tubing:	9,700	77,597	89,236
Drilling Wellhead:		50,000	50,000
Total:		660,839	797,640

TYPE WELL 6:			
HARDWARE	MD	ONSHORE	OFFSHORE
Casing 1:	320	19,201	32,002
Casing 2:	1,021	38,789	70,432
Casing 3:	6,283	238,762	274,576
Casing 4:	12,057	337,597	388,237
Tubing:	11,807	94,456	108,625
Drilling Wellhead:		50,000	50,000
Total:		778,805	923,871

TYPE WELL 8:			
HARDWARE	MD	ONSHORE	OFFSHORE
Casing 1:	320	19,201	32,002
Casing 2:	1,021	38,789	70,432
Casing 3:	7,117	278,443	311,010
Casing 4:	14,101	394,825	454,848
Tubing:	13,851	110,807	127,428
Drilling Wellhead:		50,000	50,000
Total:		884,066	1,044,920

FIGURE A6-11

FIGURE A6-12

TJS 1/21/04 8:17 AM

TYPE WELL 2:			
HARDWARE	MD	ONSHORE	OFFSHORE
Casing 1:	320	19,201	22,002
Casing 2:	1,001	50,700	70,400
Casing 3:	7,031	209,370	335,475
Casing 4:	15,304	430,744	495,356
Tubing:	15,134	121,870	139,230
Drilling Wellhead:		50,000	50,000
Total:		949,782	1,120,494

TYPE WELL 16:			
HARDWARE	MD	ONSHORE	OFFSHORE
Casing 1:	320	19,201	22,002
Casing 2:	1,001	50,700	70,400
Casing 3:	8,012	234,042	305,000
Casing 4:	10,371	314,002	391,500
Tubing:	10,121	144,972	164,710
Drilling Wellhead:		50,000	50,000
Total:		1,103,205	1,295,782

FIGURE A6-12

**APPENDIX 7**

**TUNNELS FOR  
PIPELINE AND ACCESS**

## **APPENDIX 7: TUNNELS FOR PIPELINE AND ACCESS**

### **Table of Contents**

	<b><u>Page</u></b>
<b>Summary</b>	<b>A7-1</b>
<b>Woodward-Clyde Consultants Study Report (February 1994)</b>	
<b>"Kuvlum Evaluation Conceptual Study of Tunnels" - Executive Summary</b>	<b>A7-6</b>

## APPENDIX 7: TUNNELS FOR PIPELINE AND ACCESS

### Summary

The installation and protection of pipelines in the offshore Arctic along the Alaskan and Canadian coasts has been a concern to the industry for two decades because of the short summer season and potential ice gouging of the sea bed. The severity of the problem, both installation and protection, increases with the distance from the shoreline. Kuvlum, beyond the ice shear zone at 16-plus miles offshore, is clearly a location where these concerns are justified. There have been some summers where the ice conditions along the Alaska coast would have severely restricted or eliminated conventional lay barge, pipe pull and dredging/burial operations.

Recent advances in tunneling below bodies of water indicate that tunnels between the shore and the Kuvlum site and between Kuvlum platforms are technically feasible. Pipelines within tunnels offered safety, repair, maintenance and expansion advantages. Access between land and platform without regard to season was a positive. The flexibility of constructing a tunnel and then installing pipelines within that tunnel without regard to season or ice condition enhanced the attractiveness of applying this technology to a Kuvlum development.

Woodward-Clyde Consultants, Oakland, CA, was retained to apply recent tunnel technology to Kuvlum and to estimate the cost of a pipeline/access tunnel between shore and Kuvlum and between platforms. Several options were investigated. The tunnel option deemed most attractive was a 19-mile, single heading tunnel from Pt. Thomson to the Kuvlum site. The study concluded that tunnel construction for Kuvlum was technically feasible, but prohibitively expensive relative to more conventional pipeline construction and protection methods.

The expected installed cost of a tunnel from Pt. Thomson to Kuvlum was estimated by Woodward-Clyde to be between \$575 MM to \$725MM, as documented in their report. Distribution of tunnel costs for the Point Thomson and Flaxman options are computed and shown in Figures A7-2 through A7-5.

Better knowledge of the geotechnical/permafrost conditions between shore and Kuvlum and a reduction of tunnel requirements would reduce the estimated tunnel cost, but this reduction very probably would not reduce the cost to an economic level for Kuvlum.

The cover and executive summary from the Woodward-Clyde final report follow in this section. The full report is provided under separate cover.

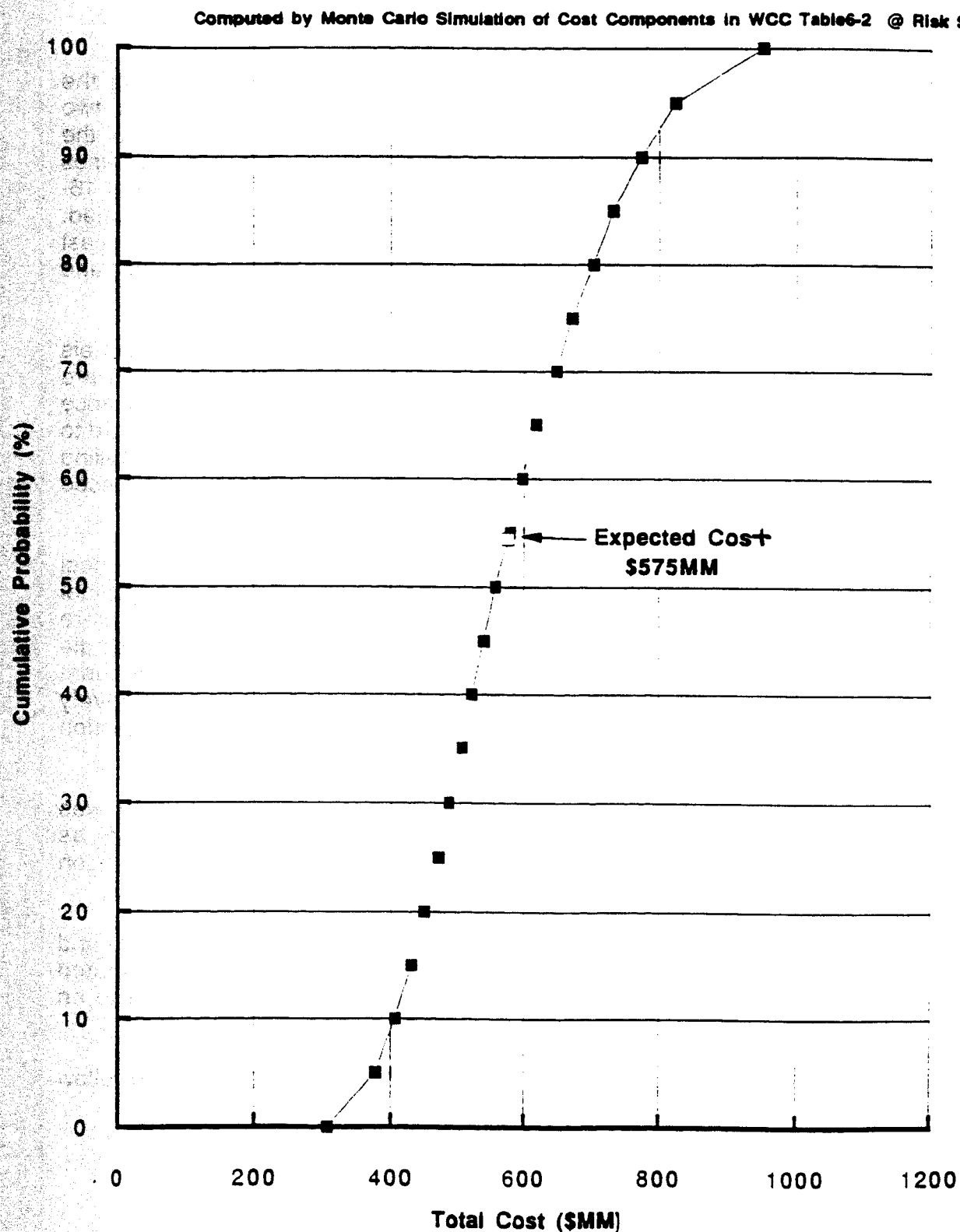


FIGURE A7-2  
Total Cost of Main Sales Pipeline Tunnel  
(Point Thomson Option)

**Reference:**

Woodward Clyde Consultants report "Kuvium Evaluation Conceptual Study of Tunnels" February 1994, Table 6-2.

**Procedure:**

"@Risk" Software is used here to compute Total Installed Cost of the Main Sales Pipeline Tunnel from Kuvium Main Platform to Flaxman Island (Flaxman Option). Infield Pipeline Tunnel Costs are excluded. The remaining 19 Component Costs in WCC Table 6-2 are shown in the table below.

Monte Carlo Simulation (Latin Hypercube) is used to compute the Total Installed Cost of the Tunnel from these 19 Cost Components. Figure A.8.2, presents the Cumulative Probability versus Total Installed Cost.

Component	WCC Table 6-2			Expected Cost of Components computed by @Risk Software  \$M
	Optimistic 10% Estimate	Most Likely Estimate	Pessimistic 90% Estimate	
<b>PRE-CONSTRUCTION</b>				
Environmental				
Permit Application Preparation	200.00	300.00	400.00	300
Environmental Studies	500.00	1,000.00	1,500.00	1,000
EIS Preparation	800.00	1,000.00	1,500.00	1,129
Permit Approval Process	400.00	600.00	800.00	600
Geotechnical Exploration				
*Office, Reports	1,123.88	1,125.00	1,500.00	1,306
*On-Shore Borings	696.80	697.50	1,000.00	843
*Off-Shore Borings	4,660.34	4,665.00	6,250.00	5,429
*Geophysical Surveys	314.69	315.00	600.00	453
Design				
Preliminary Design	1,200.00	1,500.00	2,000.00	1,586
Equipment Development	500.00	1,500.00	2,000.00	1,285
Final Design	3,000.00	4,000.00	5,000.00	4,000
Bid and Award	100.00	200.00	250.00	178
<b>CONSTRUCTION</b>				
Access Road	2,300.00	3,000.00	4,000.00	3,347
Site Facilities	24,000.00	26,000.00	28,000.00	26,000
Machine Delivery	20,000.00	22,000.00	23,000.00	21,570
SP Tunnel Construction	294,000.00	345,000.00	549,000.00	450,358
Main Platform Shaft Tunnel Connection	2,000.00	4,000.00	7,000.00	4,430
Site Restoration	300.00	700.00	1,000.00	657
Construction Management (10%)	23,310.00	40,070.00	71,200.00	50,628

Total Installed Expected Tunnel Cost = 575,099 \$M

"Where WCC Report shows the 10% and Most Likely Cost Components being equal, we will use the following procedure: 1. The 10% Cost will be equal to 0.999 Most Likely Cost and 2. The Cumulative Probability of this 10% Cost will not be 10% but rather it will be 1%. This procedure will yield nearly a right sided triangular probability density plot as intended by WCC.

**FIGURE A7-3**  
Distribution of Component Cost Estimates and Expected Cost  
for Main Sales Pipeline Tunnel (Point Thomson Option)



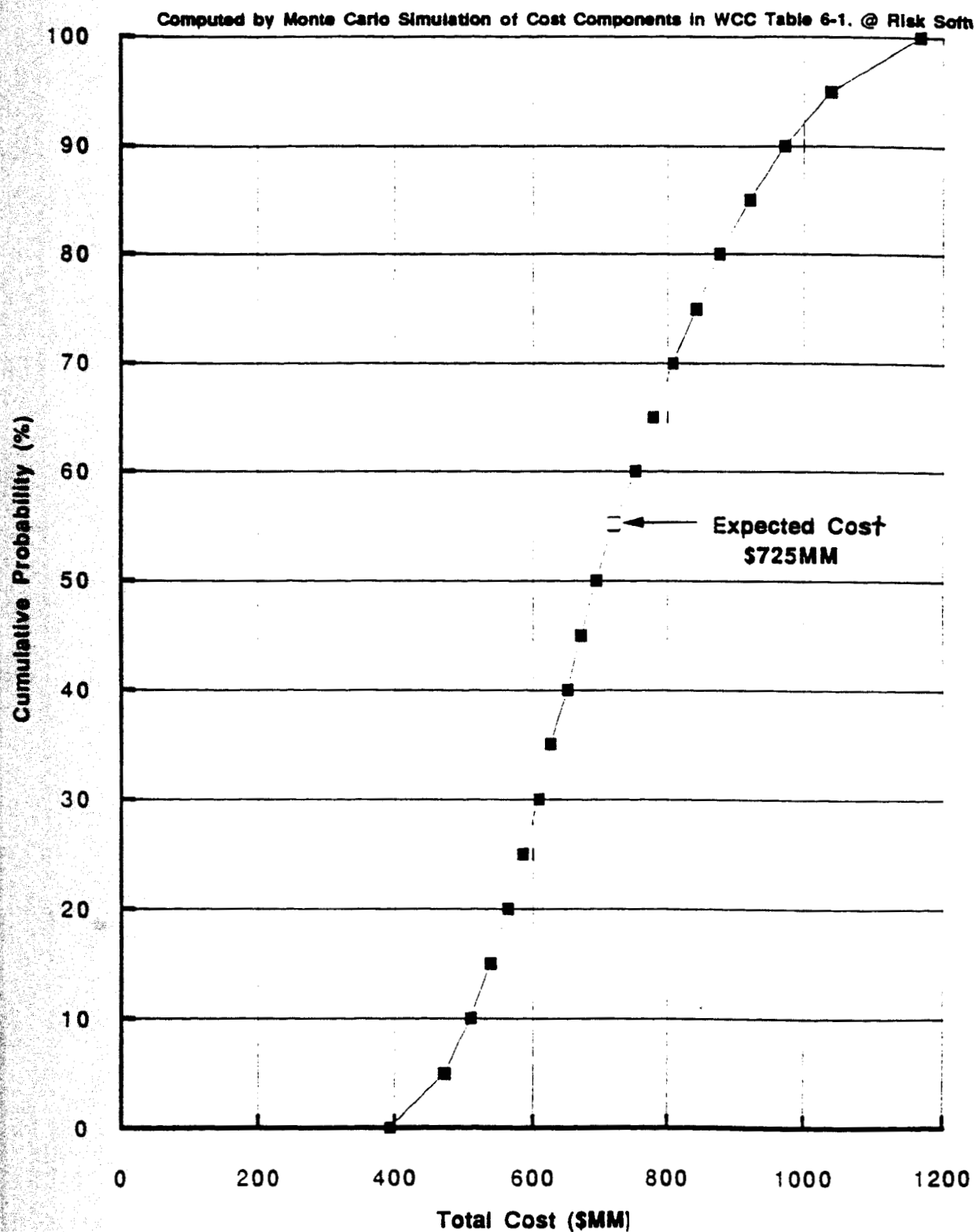


FIGURE A7-4  
Total Cost of Main Sales Pipeline Tunnel (Flaxman Option)

**Reference:**

Woodward Clyde Consultants report "Kuvium Evaluation Conceptual Study of Tunnels" February 1994. Table 6-1.

**Procedure:**

"@Risk" Software is used here to compute Total Installed Cost of the Main Sales Pipeline Tunnel from Kuvium Main Platform to Flaxman Island (Flaxman Option). Infield Pipeline Tunnel Costs are excluded. The remaining 19 Component Costs in WCC Table 6-1 are shown in the table below.

Monte Carlo Simulation (Latin Hypercube) is used to compute the Total Installed Cost of the Tunnel from these 19 Cost Components. Figure A.8.1. presents the Cumulative Probability versus Total Installed Cost.

Component	WCC Table 6-1			Expected Cost of Components computed by @Risk Software \$M
	*Optimistic 10% Estimate	Most Likely Estimate	Pessimistic 90% Estimate	
<b>PRE-CONSTRUCTION</b>				
Environmental				
Permit Application Preparation	200.0	400.0	600.0	400
Environmental Studies	1,000.0	2,000.0	2,500.0	1,785
EIS Preparation	1,000.0	1,500.0	2,000.0	1,500
Permit Approval Process	600.0	1,000.0	1,200.0	914
Geotechnical Exploration				
*Office, Reports	1,123.9	1,125.0	1,500.0	1,306
*On-Shore Borings	696.8	697.5	1,000.0	843
*Off-Shore Borings	4,660.3	4,665.0	6,250.0	5,429
*Geophysical Surveys	314.7	315.0	600.0	453
Design				
Preliminary Design	1,200.0	1,500.0	2,000.0	1,586
Equipment Development	500.0	1,500.0	2,000.0	1,285
Final Design	3,000.0	4,000.0	5,000.0	4,000
Bid and Award	100.0	200.0	250.0	178
<b>CONSTRUCTION</b>				
Ice Road	2,800.0	3,000.0	4,400.0	3,522
Site Facilities	24,000.0	26,000.0	28,000.0	26,000
Machine Delivery	42,000.0	44,000.0	46,000.0	44,000
SP Tunnel Construction	354,000.0	421,000.0	813,000.0	562,142
Main Platform Shaft Tunnel Connection	2,000.0	4,000.0	7,000.0	4,430
Site Restoration	500.0	1,000.0	2,000.0	1,215
Construction Management (10%)	42,530.0	49,900.0	90,040.0	64,121

Total Installed Expected Tunnel Cost = 725,109 \$M

\*Where WCC Report shows the 10% and Most Likely Cost Components being equal, we will use the following procedure: 1. The "10 % Cost will be equal to 0.999\*Most Likely Cost and 2. The Cumulative Probability of this 10% Cost will not be 10% but rather it will be 1%. This procedure will yield nearly a right sided triangular probability density plot as intended by WCC.

**FIGURE A7-5**  
**Distributions of Component cost Estimates and Expected Cost**  
**for Main Sales Pipeline Tunnel (Flaxman Option)**



**KUVLUM EVALUATION  
CONCEPTUAL STUDY  
OF TUNNELS**

Prepared for:  
ARCO Alaska, Inc.  
New Ventures Engineering  
P.O. Box 100360  
Anchorage, Alaska 99510

February 1994

**Woodward-Clyde**



Woodward-Clyde Consultants  
3501 Denali Street, Suite 101  
Anchorage, AK 99503

931033NA

## EXECUTIVE SUMMARY

---

A consortium of oil companies led by ARCO Alaska, Inc. (AAI) is considering alternative means for developing the Kuvlum Discovery, located in the Eastern Beaufort Sea about 16 miles offshore. AAI retained Woodward-Clyde Consultants (WCC) to evaluate the technical feasibility of an undersea tunnel link, and to develop conceptual-level cost estimates and schedules for the planning, investigation, design, and construction of the tunnels, shafts, and related items. WCC was to indicate uncertainty of these estimates of costs and schedules by presenting the 10%, Most Likely, and 90% Cost Estimates for each tunnel option. This report summarizes the results of WCC's evaluations.

Two tunnel options were studied. The Flaxman option would involve the construction of a 16-mile tunnel from Flaxman Island to a main production platform, a 5-mile tunnel from Flaxman Island to the mainland, and a 6-mile infield tunnel connecting the main platform to a second drilling platform. The Pt. Thomson option would involve a single tunnel constructed from the mainland to the main production platform, and the 6-mile infield tunnel. Pipelines constructed within these tunnels would transport oil from Kuvlum to either a land based or a near shore pipeline for transport to the Trans-Alaska Pipeline's Pump Station 1 at Prudhoe Bay. AAI desires that the tunnel to the main production platform be completed by September, 2001.

The Kuvlum project presents an unprecedented set of conditions for mining an undersea tunnel: the need to achieve high advance rates; the need to tunnel under high water pressure (4 to 6 bars); tunneling through abrasive and unstable sands and gravels; long tunnel headings with a single tunneling machine; the potential for high cutter wear; and difficult conditions under which to maintain the mining machine.

Nevertheless, it is considered that sufficient technology exists, through experience with past projects such as the Channel Tunnel, and ongoing projects such as the Storebaelt crossing in Denmark, to overcome the perceived problems to be encountered. A period for "equipment development" has been identified in the design schedule, to provide AAI and their designer the opportunity to address the specific issues with machine manufacturers.

The development schedules prepared illustrate the importance of a number of key, long-lead activities:

- the preparation and filing of permits and environmental compliance documents for construction;
- geotechnical exploration efforts;
- design of the tunnels, shafts, and support facilities;
- equipment development; and
- manufacture of the tunneling machine.

These activities are estimated to require on the order of 3.5 years to complete for the "Most Likely" scenarios. Construction of the tunnels that would connect the mainland to the main production platform are estimated to require between 3.2 and 3.6 years to complete. The Most Likely scenarios for the Flaxman and Pt. Thomson options would meet AAI's desired timetable if work were begun at the start of 1994.

The total costs for the "Most Likely" Flaxman and Pt. Thomson options, including environmental permitting, geotechnical investigations, design, temporary camp facilities, construction, and construction management, are estimated to be \$688.8 million and \$578.7 million, respectively. These costs exclude items to be addressed by AAI, such as the two platforms, the sales pipelines, the sales pipeline connections, and the pipeline to Prudhoe Bay.

In the planning of tunneling projects, as with other civil construction, contingencies are typically added to estimates of construction cost and time to reflect uncertainties in assumptions and conditions at the time the estimates are prepared. No contingencies are included in the above Most Likely estimates. A number of assumptions made in the development of the Most Likely estimates were modified in arriving at the 90% estimates.

The more conservative assumptions reflected in the 90% estimates resulted in significantly higher estimates of construction cost and time for the various options. The differences between the Most Likely and 90% estimates are considered representative of the contingencies that would otherwise be applied if the 90% estimates had not been prepared.

If the Kuvlum project is to be pursued any further, it is strongly recommended that estimates for environmental permitting, design, and construction costs and schedules be redeveloped based on the results of improved site specific information and data, detailed discussions with tunneling machine manufacturers, and a preliminary design effort. These efforts should be directed at reducing uncertainties related to the following:

- environmental constraints in the project area;
- nature of the subsurface conditions, related to soil types; potential for boulders; and bonded permafrost, warm permafrost, and thawed ground;
- tunneling machine requirements to cope with abrasive ground and adverse conditions under which machine maintenance would be performed;
- the frequency and duration of delays to tunnel progress owing to machine maintenance; and
- specific design requirements related to the precast concrete linings.

These efforts will improve the accuracy (reduce the uncertainty) of future estimates of cost and time.

**APPENDIX 8**

**OPERATION AND MAINTENANCE**

## APPENDIX 8: OPERATION AND MAINTENANCE

### Table of Contents

	<u>Page</u>
Summary	A8-1
A8.1 Kuvlum O&M Costs	A8-2
Variables	A8-2



## **APPENDIX 8: OPERATION AND MAINTENANCE**

### **Summary**

Operation and maintenance cost curves were developed using a Beaufort Sea offshore cost calculator. The curves generated have been plotted versus peak field oil rate. For the purposes of this economic evaluation, the O & M costs were assumed constant throughout the life of the field.

## **A8 OPERATION AND MAINTENANCE**

### **A8.1 Kuvlum O&M Costs**

The following cost curves were developed using a Beaufort Sea offshore O & M cost calculator. Various rate scenarios were used to develop the curves. The curves are used as building blocks for various development scenarios. For economic evaluation purposes, O & M costs are assumed to be constant over the life of the field.

For example: O & M for a two gravity based structure development, one processing/production and one production only, at equal rates of 200K BOPD would yield total O & M costs of \$200MM/yr. (140 + 60).

The following list contain some of the variables used in the cost calculator.

#### Variables

- Facility costs
- Production rate
- Number of producing well
- Number of injection wells
- Well depth
- Shore base costs
- Distance from existing infrastructure

### O & M Costs, Production Only

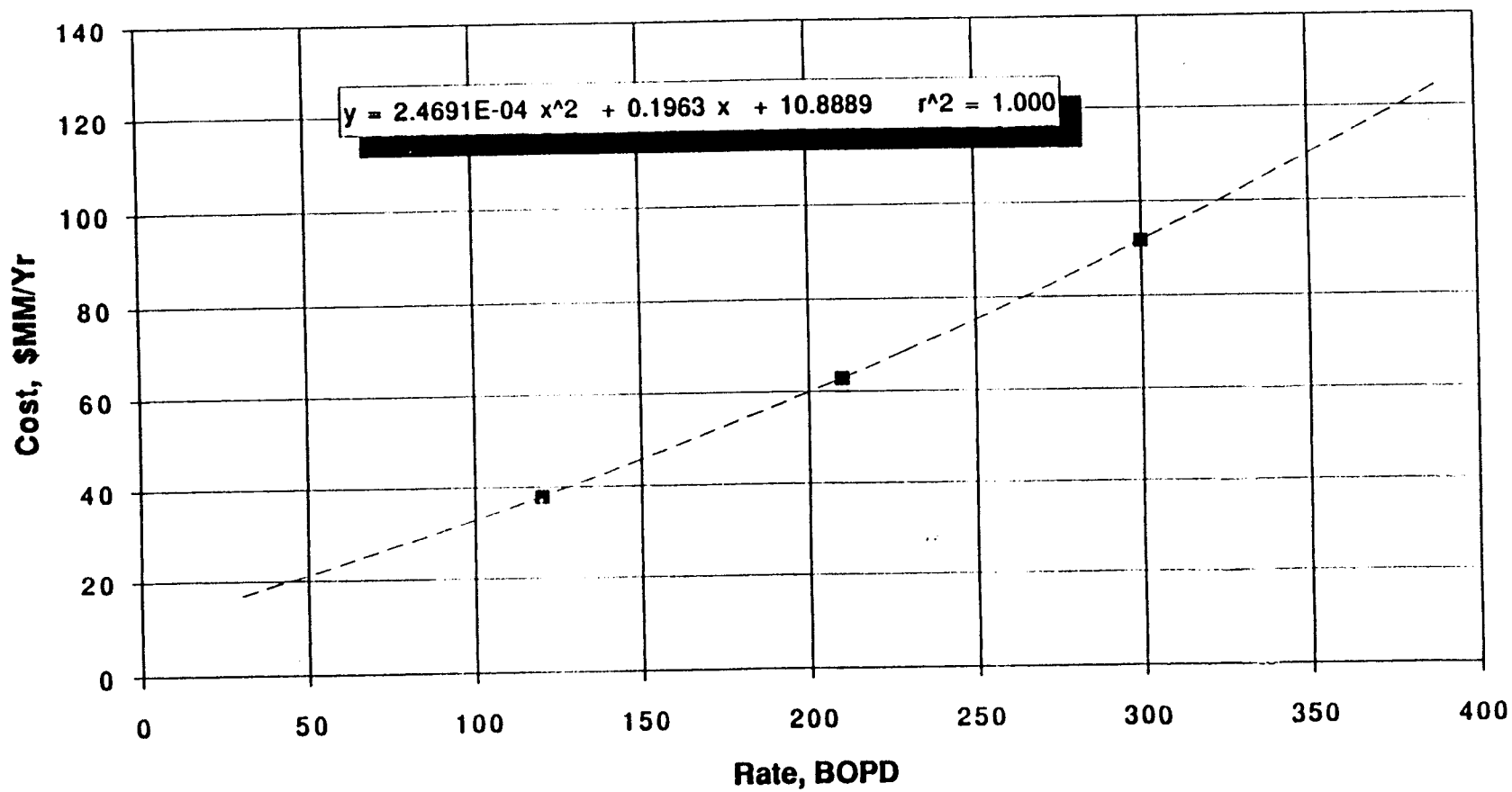


FIGURE A8-3

## O & M Costs, Processing and Production

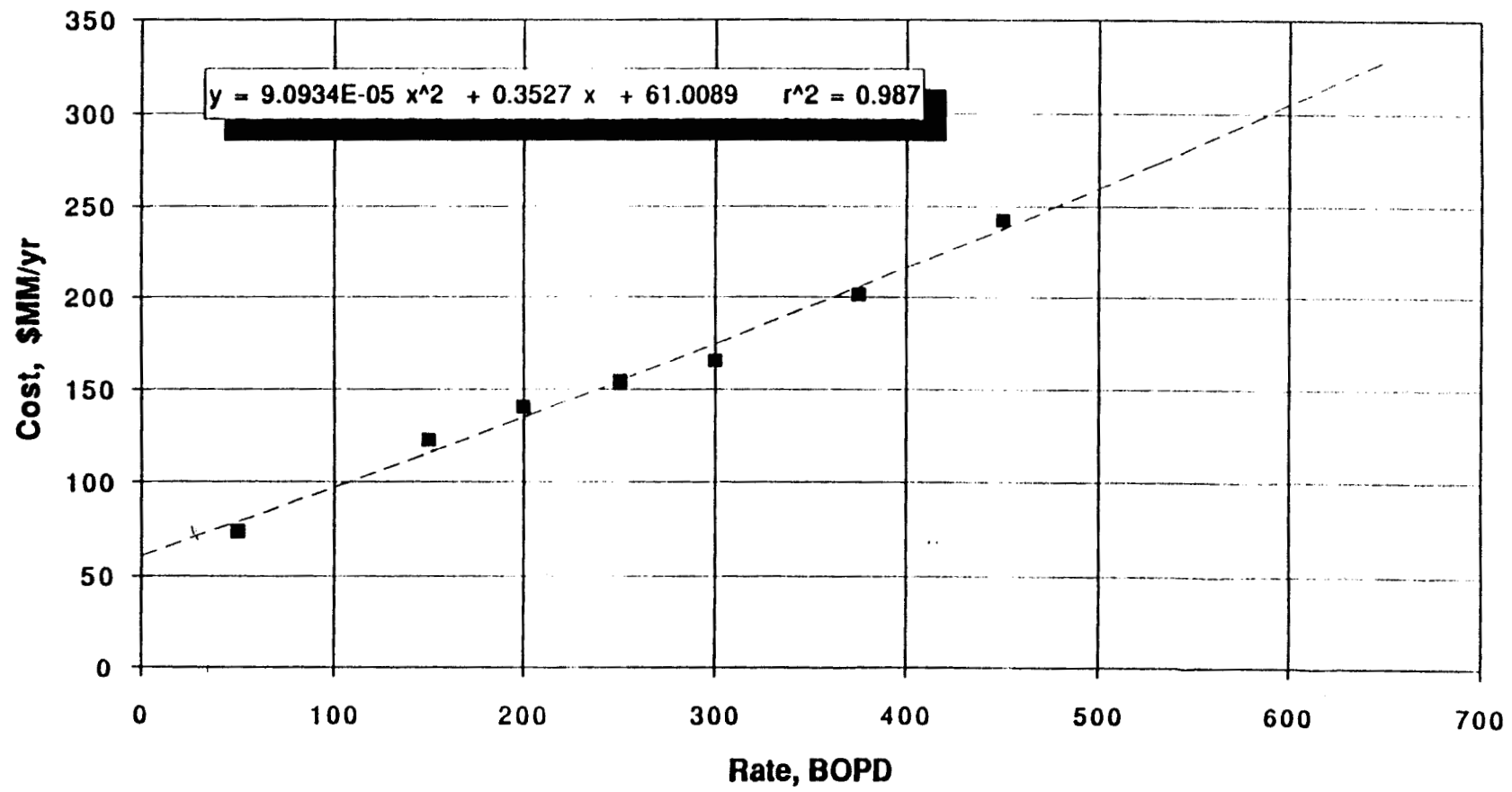


FIGURE A8-4

**APPENDIX 9**

**STATE OF ALASKA**  
**PRICE FORECAST**

**APPENDIX 9: STATE OF ALASKA PRICE FORECAST**

**Table of Contents**

	<b><u>Page</u></b>
<b>Summary</b>	<b>A9-1</b>
<b>Revenue Sources Book/Forecast &amp; Historical Data (State of Alaska)</b>	<b>A9-4</b>

## APPENDIX 9: STATE OF ALASKA PRICE FORECAST

### Summary

Included in the following section is the Alaska North Slope oil price forecast used in the economic evaluations. The forecast was generated from the following State of Alaska publication (included):

- *Revenue Sources Book, Forecast and Historical Data*, State of Alaska/Department of Revenue. Spring 1993.

The data in bold on the chart was obtained from the reference publication. Oil prices in years not provided by the publication were derived by interpolation. Prices beyond year 2005 were inflated at 3%, with no real growth.



**Date:** September 21, 1993 **File:** Kuvlum  
**Subject:** Kuvlum Generic Baseline Economics Program  
**From/Location:** J. M. Eldred, ATO 1286  
**Telephone:** 907/263-4347  
**To/Location:** S. F. Gritner, PRC-E1612

Per our 9/20 conversation, please proceed with the purchase and initial checkout of the OGRE program. I have attached the ANS price forecast to be used in the model (State of Alaska Revenue Sources Book). All other required input parameters will be supplied by me upon request. As a target date, I would like to have an initial run completed by early to mid-October (October 4-8). Please keep me posted on the progress and any information I need to provide.

Your time should be charged to TPA Y03866, Kuvlum 1993 Predecision Study.

*JME/amb*

Senior Engineer  
New Ventures Engineering

JME/amb  
Attachments

cc:	J. D. Allen, PRC-J1422	w/out attachment
	J. M. Bigger, PRC-J1409	w/out attachment
	W. C. Kazokas, PRC-J1437	w/out attachment
	J. B. Shelden, ATO 1296	w/out attachment
	R. E. Smith, PRC-J1411	w/out attachment



# State Forecast

State Price Forecasts: Revenue Sources Book, Forecast and Historical Data					Year to Year Changes			
Spring 1993					Enter Inflation Rate Assumption after 2005			
Scenarios for ANS Wellhead Price (\$/bbl)					3.00%			
Fiscal Year	Low	Mid	High		Fiscal Year	Low	Mid	High
1993	12.66	12.91	13.19		1993	1	1	1
1994	12.33	13.67	14.98		1994	0.9739	1.0589	1.1357
1995	12.89	14.50	15.76		1995	1.0454	1.0607	1.0521
1996	13.61	15.61	17.19		1996	1.0555	1.0765	1.0906
1997	14.36	16.80	18.75		1997	1.0555	1.0765	1.0906
1998	15.16	18.09	20.45		1998	1.0555	1.0765	1.0906
1999	16.00	19.47	22.30		1999	1.0555	1.0765	1.0906
2000	16.89	20.96	24.32		2000	1.0555	1.0765	1.0906
2001	17.15	21.69	25.82		2001	1.0152	1.0346	1.0615
2002	17.41	22.44	27.40		2002	1.0152	1.0346	1.0615
2003	17.67	23.21	29.09		2003	1.0152	1.0346	1.0615
2004	17.94	24.02	30.88		2004	1.0152	1.0346	1.0615
2005	18.21	24.85	32.78		2005	1.0152	1.0346	1.0615
2006	18.76	25.60	33.76		2006	1.0300	1.0300	1.0300
2007	19.32	26.36	34.78		2007	1.0300	1.0300	1.0300
2008	19.90	27.15	35.82		2008	1.0300	1.0300	1.0300
2009	20.50	27.97	36.89		2009	1.0300	1.0300	1.0300
2010	21.11	28.81	38.00		2010	1.0300	1.0300	1.0300
2011	21.74	29.67	39.14		2011	1.0300	1.0300	1.0300
2012	22.40	30.56	40.32		2012	1.0300	1.0300	1.0300
2013	23.07	31.48	41.52		2013	1.0300	1.0300	1.0300
2014	23.76	32.42	42.77		2014	1.0300	1.0300	1.0300
2015	24.47	33.40	44.05		2015	1.0300	1.0300	1.0300
2016	25.21	34.40	45.38		2016	1.0300	1.0300	1.0300
2017	25.96	35.43	46.74		2017	1.0300	1.0300	1.0300
2018	26.74	36.49	48.14		2018	1.0300	1.0300	1.0300
2019	27.54	37.59	49.58		2019	1.0300	1.0300	1.0300
2020	28.37	38.72	51.07		2020	1.0300	1.0300	1.0300

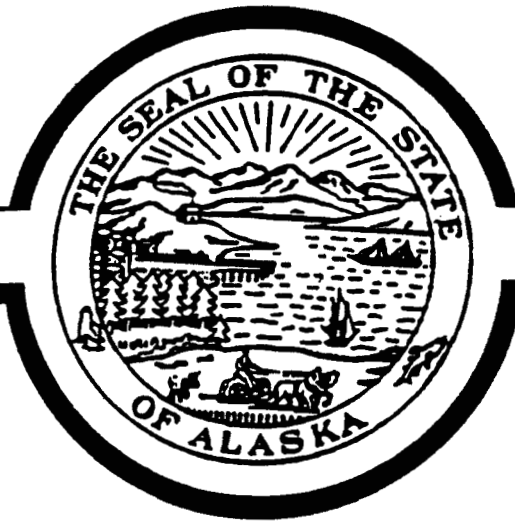
State only provides 1993-95, 2000, and 2005. (Bolded prices) The gaps between 1993-2005 are interpolated)  
 From 2005-2020, prices are simply inflated by 3%.

FIGURE A9-3

# REVENUE SOURCES BOOK

## FORECAST & HISTORICAL DATA

SPRING 1993



STATE OF ALASKA

*Walter J. Hickel, Governor*

DEPARTMENT OF REVENUE

*Darrel J. Rexwinkel, Commissioner*

# STATE OF ALASKA

## DEPARTMENT OF REVENUE

### OFFICE OF THE COMMISSIONER

WALTER J. HICKEL GOVERNOR

P. O. Box 110400  
Juneau, Alaska 99811-0400  
PHONE: (907) 465-2300  
FAX #: (907) 465-2389

March 5, 1993

The Honorable Walter J. Hickel  
Governor  
P.O. Box 110001  
Juneau, Alaska 99811-001

Dear Governor Hickel:

RE: Spring 1993 Revenue Sources Book

The Spring revenue forecast projects modestly different revenues than those we forecasted last Fall. Although oil prices fell significantly just after releasing the Fall estimates, prices have rebounded primarily due to the recent OPEC agreement. In addition, thanks to the diligent efforts of the Department's auditors and the Department of Law, the State received additional tax and royalty payments from prior years' oil production. As a result, FY 1993 Mid Scenario General Fund unrestricted revenues have been revised upward by \$114.7 million.

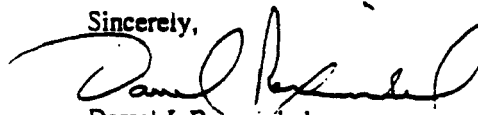
Mid Scenario FY 1994 General Fund unrestricted revenues have also been revised slightly upward by \$15.9 million. The Department continues to believe that increasing world oil consumption will keep pressure on supply resulting in oil prices at levels around \$18.00-\$19.00/bbl for Alaska North Slope quality oil. World oil consumption should rise as the global economy comes out of the current doldrums. Supply pressure should persist due to a continuing embargo of Iraqi production and a further slide in production from the Commonwealth of Independent States.

Alaska continues to rely on petroleum related revenues for approximately 85 percent of its revenue stream. This high degree of dependency on oil means that State revenues are particularly vulnerable to swings in the market price of oil and in the level of production. The scenario approach to forecasting oil prices is meant to illustrate how varying political and economic factors can easily result in significantly different oil prices. The range between the High and Low Scenarios encompasses a realistic range of possible revenue outcomes. However, as both the crash of 1986 and the spike in 1990 illustrate, either shortfalls or windfalls are possible. Over the long-run, our forecast demonstrates that oil price increases cannot be counted on to offset the decline in production from the mammoth Prudhoe Bay oil field.

Finally, I would like to stress that the forecast is based on conservative assumptions about future enhancements of petroleum reserves. Therefore, the forecast excludes new discoveries and development of oil or gas made possible by technological breakthroughs. Tax and royalty settlements are included in the forecast when collected. This means the recently announced \$630 million BP America settlement is not included.

I believe the revenues forecasted in this report represent our best estimate of future revenues.

Sincerely,



Darrel J. Rexwinkel  
Commissioner

# TABLE OF CONTENTS

---

<u>SECTION</u>	<u>PAGE</u>
REVENUE FORECAST SUMMARY	
<u>Outlook for Short-Term (FY 1993 - 1995)</u> .....	1
<u>Outlook for Long-Term (FY 1996 - 2010)</u> .....	2
REVENUE FORECAST: SHORT-TERM OUTLOOK (FY 1993 - 1995)	
<u>General Fund Unrestricted and Restricted Revenues</u> .....	3
<u>Petroleum Revenues</u>	
Importance of Petroleum Revenues .....	8
<u>Current Oil Market Situation</u>	
World Market .....	14
Alaska North Slope Market .....	15
<u>Forecast Assumptions</u>	
ANS Lower 48 Prices .....	16
Transportation Costs to Lower 48 Markets .....	18
Trans Alaska Pipeline System Tariffs .....	19
Wellhead Price for ANS .....	20
Oil Production Outlook .....	21

### **Other Non-Oil Revenue Sources Assumptions**

Oil Corporate Taxes .....	22
Non-Oil Corporate Taxes .....	22
Property Taxes .....	22
Alcoholic Beverage Taxes .....	22
Intergovernmental Receipts .....	22
Investment Earnings .....	23
Facilities and Related Charges .....	23

<b><u>Methodology</u></b> .....	23
---------------------------------	----

### **Scenarios over the Short-Term**

Low Scenario .....	24
Mid Scenario .....	26
High Scenario .....	28

### **REVENUE FORECAST:**

LONG-TERM OUTLOOK (FY 1996 - 2010) .....	33
--	----

<b>HISTORICAL REVENUES, PRICES AND PRODUCTION .....</b>	<b>49</b>
---	-----------

## FORECAST FIGURES

---

### FIGURE

### PAGE

1. General Fund Unrestricted Revenues, FY 1992 Actual and FY 1993 - 1995 Estimates .....	3
2. FY 92 General Fund Unrestricted Revenues .....	8
3. FY 92 General Fund Unrestricted Revenues (Detailed Petroleum Revenues as Percentages of the Total) .....	9
4. Percentage of General Fund Unrestricted Revenues Which Come from Petroleum (FY 1977 - 1995) .....	10
5. OPEC Production .....	14
6. ANS Spot Price, January 1988 - January 1993 .....	15
7. ANS at the U.S. Gulf (January 1990 - December 1995) .....	17
8. ANS at the U.S. West Coast (January 1990 - December 1995) .....	17
9. Total Transportation Costs to Lower 48, Pipeline and Tanker (January 1988 - January 1993) .....	18
10. ANS at the Wellhead (January 1990 - December 1995) .....	20
11. Simulated Oil Production, Total Alaska and Mid Case Prudhoe Bay (FY 1992 - 2010) .....	21
12. General Fund Unrestricted Revenue Projections	
Low Scenario, FY 1981 - 2010 .....	34
Mid Scenario, FY 1981 - 2010 .....	34
High Scenario, FY 1981 - 2010 .....	34

# FORECAST TABLES

<u>TABLE</u>	<u>PAGE</u>
1. General Fund Unrestricted Revenues and ANS Lower 48 Price (FY 1992 Actual and FY 1993 - 1995 Estimates) .....	1
2. General Fund Unrestricted Revenues and ANS Lower 48 Price (FY 1996 - 1998 and FY 2000) .....	2
3. General Fund Unrestricted Revenues (Details of FY 1992 and FY 1993 - 1995 Estimates) .....	4-6
4. General Fund Unrestricted Revenues: Petroleum Revenues as a Percentage of the Total .....	7
5. Alaska State Revenue Matrix Unrestricted General Fund, FY 1993 .....	12
6. Alaska State Revenue Matrix Unrestricted General Fund, FY 1994 .....	13
7. OPEC Production .....	14
8. Scenarios for ANS Oil Price, Gulf Coast and West Coast (FY 1993 - 1995, FY 2000, FY 2005) .....	16
9. Marine Transportation Costs, Valdez to Lower 48 (FY 1993 - 1995, FY 2000, FY 2005) .....	18
10. Scenarios for TAPS Tariffs (FY 1985 - 2005) .....	19
11. Scenarios for ANS Wellhead Price (FY 1993 - 1995, FY 2000, FY 2005) .....	20
12. Low Scenario Revenues, Oil Prices and Production (FY 1993 - 1995) .....	24
13. Low Scenario Global Oil Market Assumptions (FY 1992 - 1994) .....	25
14. Mid Scenario Revenues, Oil Prices and Production (FY 1993 - 1995) .....	26
15. Mid Scenario Global Oil Market Assumptions (FY 1992 - 1994) .....	27
16. High Scenario Revenues, Oil Prices and Production (FY 1993 - 1995) .....	28
17. High Scenario Global Oil Market Assumptions (FY 1992 - 1994) .....	29

Projected and Historical Crude Oil Spot Prices for Alaska  
North Slope Crude and Domestic Marker

18.	Low Scenario (FY1992 - 1995) .....	30
19.	Mid Scenario (FY1992 - 1995) .....	31
20.	High Scenario (FY1992 - 1995) .....	32
21.	Spring 1993 Forecast Assumptions .....	35

Detailed Revenue Projections

22.	Low Scenario (FY 1981 - 2010) .....	36-37
23.	Mid Scenario (FY 1981 - 2010) .....	38-39
24.	High Scenario (FY 1981 - 2010) .....	40-41

Petroleum Production Revenue Forecast

25.	Low Scenario (FY 1992 - 2010) .....	42
26.	Mid Scenario (FY 1992 - 2010) .....	43
27.	High Scenario (FY 1992 - 2010) .....	44

28.	Projected and Historical Crude Oil Prices. Alaska North Slope & Domestic Marker in 1992 Constant \$/barrel .....	45
-----	---	----

Simulated Oil Production

29.	Low Scenario (FY 1992 - 2010) .....	46
30.	Mid Scenario (FY 1992 - 2010) .....	47
31.	High Scenario (FY 1992 - 2010) .....	48

32.	Historical General Fund Unrestricted Revenues (FY 1978 - 1992) .....	50-51
-----	--	-------

33.	Historical Restricted Revenues and Total General Fund Revenues (FY 1978 - 1992) .....	52
-----	--	----

34.	Historical Petroleum Revenues (FY1959 - 1992) .....	53
-----	---	----

35.	Historical Prices and Production (FY 1978 - 1992) .....	54
-----	---	----



# REVENUE FORECAST SUMMARY

## Outlook for Short Term (FY 1993 - FY 1995)

Alaska's revenue outlook continues to rely heavily on petroleum revenues. The outlook for oil prices over the next two years depends primarily on how the Organization of Petroleum Exporting Countries (OPEC) responds to evolving market fundamentals. The strength of recovery of global economies, the timing of the lifting of United Nations (U.N.) sanctions on Iraqi crude exports, the increase in Saudi Arabia and Iran production capacity and the pace of decline in production from the Commonwealth of Independent States, are major factors that will also determine the relative strength or weakness of the crude oil market. Although new energy taxes have been proposed by President Clinton, no attempt is made to forecast the impact such taxes would have on the oil market.

The three oil price scenarios which underpin the revenue forecast are summarized as follows:

**Low Scenario:** A slow recovery from the global economic recession dampens oil consumption growth, U.N. sanctions are lifted and Iraqi crude returns to the global export market and Middle East production capacity increases which results in downward pressure on oil prices.

**Mid Scenario:** An upturn in the global economy results in moderate oil consumption growth, the U.N. embargo on Iraqi crude continues and a decline in non-OPEC production results in stronger oil prices by 1993 and beyond as OPEC's market share increases.

**High Scenario:** The global economy is vigorous by the end of 1993 with oil consumption putting pressure on available supply resulting in upward pressure on oil prices.

The following table illustrates the Alaska North Slope (ANS) Lower 48 oil price and General Fund unrestricted revenue outlook for the short term. Revenues considered to be program receipts in the state's budgeting process are not included. The scenarios presented in this forecast represent a probable range of outcomes. None of the scenarios will prove totally correct.

Table 1: General Fund Unrestricted Revenues and ANS Lower 48 Price						
	Low		Mid		High	
	(\$M)	(\$/bbl)	(\$M)	(\$/bbl)	(\$M)	(\$/bbl)
FY 1992 Actual	2,462.6	16.88	2,462.6	16.88	2,462.6	16.88
FY 1993	2,268.1	17.75	2,386.2	18.01	2,487.7	18.30
FY 1994	2,058.5	16.93	2,303.8	18.38	2,547.3	19.71
FY 1995	2,083.8	17.47	2,390.5	19.24	2,624.2	20.52

## Outlook for Long-Term (FY 1996 - FY 2010)

The long-term revenue outlook is dominated by the depletion of petroleum reserves of the Prudhoe Bay oil field. Higher oil prices in the future may offset some of the negative revenue impact of lower oil production levels. However, even in the high price scenario, inflation adjusted General Fund unrestricted revenues fall below \$2.0 billion by FY 2001. That compares to FY 1992 revenues of nearly \$2.5 billion.

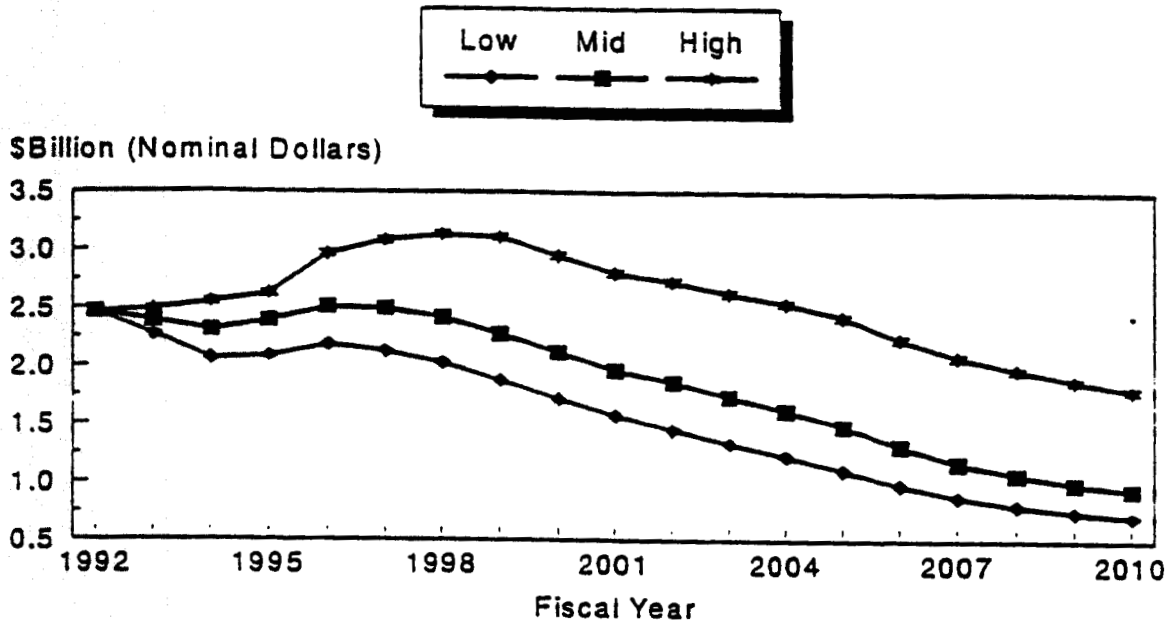
Long-term oil production scenarios show total Alaskan oil production falling to one-half of current levels by FY 2002 in all three scenarios. Oil prices are assumed to grow from current levels at roughly the rate of inflation in the Low Scenario, by 0.5 percent greater than the rate of inflation in the Mid Scenario and by 1.0 percent greater than the rate of inflation in the High Scenario.

This relatively gloomy long-term revenue forecast is based on an extrapolation of what is happening currently. This forecast does not include any revenues from new oil fields which may be discovered and developed, such as the Arctic National Wildlife Refuge (ANWR), nor does it factor in any allowance for technological developments which will increase production from Alaska's older fields. Further, no major revenues are forecast for development of the Arctic natural gas resource.

Table 2. General Fund Unrestricted Revenues and ANS Lower 48 Price						
	Low		Mid		High	
	(\$M)	(\$/bbl)	(\$M)	(\$/bbl)	(\$M)	(\$/bbl)
FY 1996	2182.0	18.74	2508.2	20.99	2966.4	22.68
FY 1997	2120.6	19.85	2491.8	22.68	3082.6	24.74
FY 1998	2023.9	20.42	2414.5	23.78	3181.5	26.20
FY 2000	1870.2	21.60	2416.8	26.14	2950.1	29.38

Figure 1

# General Fund Unrestricted Revenues FY 1992 Actual and FY 1993 - 1995 Estimates



## REVENUE FORECAST: SHORT-TERM OUTLOOK (FY 1993 - 1995)

### General Fund Unrestricted and Restricted Revenues

This section analyzes unrestricted revenues over the next two and a half years through the rest of FY 1993 to the end of FY 1995. Both unrestricted and restricted revenues flow into the General Fund, the account which finances most of the budget. The difference between these two types of revenues is in how the legislature can use them. Unrestricted revenues have no restrictions on their use. Restricted revenues carry some restriction on their use. For most restricted revenues, the restriction comes from the Federal government.

Because restricted revenues are specific in their use, discussions of revenues in this publication focus on unrestricted revenues. Program receipt revenues and restricted revenues designated in the state's budgeting process are not included in this forecast.

The following table shows all sources of unrestricted General Fund revenues for FY 1992 through FY 1995.

## GENERAL FUND UNRESTRICTED REVENUES

(Millions of Dollars)

TAXES	FY 1992	FY 1993 ESTIMATES			FY 1994 ESTIMATES			FY 1995 ESTIMATES		
	Actual	Low	Mid	High	Low	Mid	High	Low	Mid	High
<b>Income</b>										
Corporate - General	33.7	23.0	29.0	41.0	23.0	29.0	41.0	22.0	27.0	39.0
Corporate - Petroleum	165.5	150.0	220.0	260.0	106.0	132.0	178.0	106.0	132.0	178.0
Total (1)(2)	199.2	173.0	249.0	301.0	129.0	168.0	219.0	128.0	166.0	217.0
<b>Severance</b>										
Oil & Gas Production (1)	1022.2	974.3	992.6	1013.5	901.9	1000.7	1096.4	916.7	1032.5	1121.6
Oil & Gas Conservation	2.3	2.1	2.1	2.1	2.1	2.1	2.1	2.1	2.1	2.1
Oil & Hazardous Release (3)	28.7	26.7	26.7	26.7	26.7	26.7	26.7	26.2	26.2	26.2
Total	1053.2	1003.1	1021.4	1042.3	930.7	1029.5	1125.2	945.0	1060.8	1149.9
<b>Property</b>										
Oil & Gas (4)	62.0	62.8	62.8	62.8	52.6	52.6	52.6	56.6	56.6	56.6
<b>Sale/Use</b>										
Alcoholic Beverages	12.0	12.0	12.0	12.0	12.0	12.0	12.0	12.0	12.0	12.0
Fuel Taxes - Aviation (5)	10.7	10.5	10.5	10.5	10.5	10.5	10.5	10.9	10.9	10.9
Fuel Taxes - Highway	23.2	22.0	22.0	22.0	21.5	21.5	21.5	21.5	21.5	21.5
Fuel Taxes - Marine	9.4	9.5	9.5	9.5	9.7	9.7	9.7	9.7	9.7	9.7
Tobacco Products (6)	14.3	14.4	14.4	14.4	14.4	14.4	14.4	14.4	14.4	14.4
Total	62.6	68.4	68.4	68.4	68.1	68.1	68.1	68.5	68.5	68.5
<b>Miscellaneous - Other Taxes</b>										
Alaska Business License (7)	0.0	0.0	0.0	0.0	0.0	0.0	0.0	0.0	0.0	0.0
Fish (8)	30.1	21.0	27.0	36.0	21.0	27.0	36.0	21.0	27.0	36.0
Salmon Enhancement (9)	4.2	6.0	6.0	6.0	6.0	6.0	6.0	6.0	6.0	6.0
Seafood Marketing (10)	2.8	3.0	3.0	3.0	3.0	3.0	3.0	3.0	3.0	3.0
Insurance Companies	25.5	25.5	25.5	25.5	26.0	26.0	26.0	26.5	26.5	26.5
Electric & Telephone Coops (11)	2.1	2.0	2.0	2.0	2.0	2.0	2.0	2.0	2.0	2.0
Gaming (12)	1.5	1.5	1.5	1.5	1.5	1.5	1.5	1.5	1.5	1.5
Mining License Tax	0.5	0.5	0.5	0.5	0.5	0.5	0.5	0.5	0.5	0.5
Estate	1.0	1.0	1.0	1.0	1.0	1.0	1.0	1.0	1.0	1.0
Total	67.7	60.5	66.5	75.5	61.0	67.0	76.0	61.5	67.5	76.5
<b>TOTAL TAXES</b>	<b>1458.7</b>	<b>1367.8</b>	<b>1468.1</b>	<b>1550.0</b>	<b>1248.4</b>	<b>1392.2</b>	<b>1547.2</b>	<b>1252.6</b>	<b>1412.4</b>	<b>1568.5</b>

**I. FEES & PERMITS**

Business (7)(13)	5.3	5.0	5.0	5.0	5.0	5.0	5.0	5.0	5.0	5.0
Non-Business	27.1	27.0	27.0	27.0	27.0	27.0	27.0	27.0	27.0	27.0
Total	32.4	32.0	32.0	32.0	32.0	32.0	32.0	32.0	32.0	32.0

**INTERGOVERNMENTAL RECEIPTS**

Federal Shared Revenues (14)(15)	6.7	7.0	7.0	7.0	7.2	7.2	7.2	7.4	7.4	7.4
Section 8(g) Funds (14)(16)	4.7	4.7	4.7	4.7	4.7	4.7	4.7	4.7	4.7	4.7
Total	11.4	11.7	11.7	11.7	11.9	11.9	11.9	12.1	12.1	12.1

**STATE RESOURCE REVENUE****Sale/Use**

Bonus Sales (14)(17)(18)	2.6	37.8	37.8	37.8	0.0	0.0	0.0	0.0	0.0	0.0
Rents (14)(18)	3.9	5.0	5.0	5.0	5.5	5.5	5.5	6.0	6.0	6.0
Royalties (14)	702.4	730.0	745.8	762.7	696.7	783.5	861.1	713.9	816.3	890.0
Sale of State Property (7)	1.0	0.1	0.1	0.1	0.1	0.1	0.1	0.1	0.1	0.1
Gravel, Timber, etc. (7)	0.6	0.7	0.7	0.7	0.7	0.7	0.7	0.7	0.7	0.7
Total	710.5	773.6	789.4	806.3	703.0	789.8	867.4	720.7	823.10	896.8

Investment Earnings	101.8	61.0	63.0	65.7	32.0	53.7	63.9	34.5	72.0	82.2
---------------------	-------	------	------	------	------	------	------	------	------	------

**Facilities Related Charges**

Airports	3.4	2.0	2.0	2.0	2.5	2.5	2.5	3.0	3.0	3.0
Ferry System (19)	42.3	0.0	0.0	0.0	0.0	0.0	0.0	0.0	0.0	0.0
Other	2.3	2.0	2.0	2.0	2.5	2.5	2.5	2.5	2.5	2.5
Total	48.0	4.0	4.0	4.0	5.0	5.0	5.0	5.5	5.5	5.5

**Services Related Charges**

Court System	6.2	6.5	6.5	6.5	6.5	6.5	6.5	6.5	6.5	6.5
Other (20)	32.2	2.5	2.5	2.5	3.7	3.7	3.7	3.2	3.2	3.2
Total	38.4	9.0	9.0	9.0	10.2	10.2	10.2	10.4	10.4	10.4

TOTAL RESOURCE REVENUE	828.7	847.6	865.4	885.0	757.2	858.7	946.5	771.1	918.0	1002.6
------------------------	-------	-------	-------	-------	-------	-------	-------	-------	-------	--------

MISCELLANEOUS REVENUE (21)	61.4	2.0	2.0	2.0	2.0	2.0	2.0	2.0	2.0	2.0
----------------------------	------	-----	-----	-----	-----	-----	-----	-----	-----	-----

**TOTAL UNRESTRICTED  
REVENUE (22)**

2462.6	2268.1	2386.2	2487.7	2058.5	2303.8	2547.3	2083.8	2390.5	2624.2
--------	--------	--------	--------	--------	--------	--------	--------	--------	--------

MENTAL HEALTH TRUST (23)	152.1	136.1	143.2	149.3	123.5	138.2	152.8	125.0	143.4	157.5
--------------------------	-------	-------	-------	-------	-------	-------	-------	-------	-------	-------

- (1) FY 92 and FY 93 figures include corporate petroleum and oil and gas production tax settlements of \$156.3 million and \$114.9 million, respectively.
- (2) Figures include that portion (\$46.648 million in FY 92) annually shared through the municipal assistance program (AS 29.60.350).
- (3) Reflects enactment of the conservation surcharge on oil (Ch. 112, SLA 1989).
- (4) Figures only reflect the State's share of the total. The projected total property tax and the municipalities' share are as follows (millions \$): FY 93: \$310.6 and \$247.8; FY 94: \$314.7 and \$255.2; FY 95 \$315.7 and \$259.1, respectively.
- (5) Includes that portion annually shared to qualified municipalities (AS 43.40.010).
- (6) Figures reflect the increased millage rate for the General Fund portion from 5.5 to 12 mills per cigarette per AS 43.50.190.
- (7) Figures reflect the trend of shifting fees by various agencies from General Fund unrestricted revenues to restricted Program Receipts.
- (8) The figure of \$30.1 million is the remainder after tax credits have been applied. The amount of \$30.1 million must be further reduced by \$14.5 million in FY 92 for municipal revenue sharing (AS 43.75.130).
- (9) Provides annual funding based on collections for qualified regional aquaculture associations (AS 43.76.025).
- (10) Provides annual funding, based on collections, for the Alaska Seafood Marketing Institute (AS 16.51.160).
- (11) Figures include that portion (\$2.1 million for FY 92) annually refunded to local taxing authorities (AS 10.25.570).
- (12) Reflects enactment of the Gaming Reform Act (Ch. 99, SLA 1988), effective September 2, 1988.
- (13) Figures include that portion of amusement and gaming licenses (AS 43.35.050) and liquor licenses (AS 04.11.610) annually shared to qualified municipalities.
- (14) Net of Permanent Fund and Public School Fund contributions. For royalties this includes payment of prior year adjustments of \$24.8 million and \$6.3 million for FY 92 and FY 93, respectively.
- (15) National forest receipts transferred to organized and unorganized boroughs per Chapter 37, SLA 1991.
- (16) Reflects the OCS "8(g)" revenue sharing settlement monies. The General Fund share represents 49.5 percent of the aforementioned total, whereas the Permanent Fund receives 50.0 percent. The remaining 0.5 percent is distributed to the Public School Fund.
- (17) Figures for FY 92 and FY 93 reflect actual state lease sales: FY 92 (Sale 74, Cook Inlet, September, 1991, \$320,852—Sale 61, White Hills, January, 1992, \$2.4 million—Sale 68, Beaufort Sea, June, 1992, \$0); FY 93 (Sale 75, Kuparuk Uplands, December, 1992, \$9,750,111.21—Sale 76, Cook Inlet, January, 1993, \$65,269,166.65—Sale 67AW, Cook Inlet, January, 1993, \$2,433,863.85).
- (18) The Department of Natural Resources projects the following FY 93, FY 94, and FY 95 state lease sales: FY 93 (Sale 77, Nanushuk, May, 1993—Sale 70AW, Kuparuk Uplands, May, 1993); FY 94 (Sale 57, North Slope Foothills, September, 1993—Sale 75A, Colville, September, 1993—Sale 78, Cook Inlet, January, 1994); FY 95 (Sale 79, Yakataga, July, 1994—Sale 80, Shaviovik, November, 1994—Sale 81, Beaufort Sea, April, 1995). However, bonus bids are impossible to anticipate prior to sales; therefore, no estimates are provided.
- (19) Chapter 193, SLA 1990, establishes the Alaska Marine Highway System Fund, and provides that gross revenue of the State ferry system be deposited in the fund which may then be appropriated for operating and capital expenditures.
- (20) The figure for FY 92 contains reimbursement costs of \$25.3 million to the General Fund for legal services rendered per the EXXON VALDEZ oil spill settlement agreement.
- (21) The state received \$50.3 million in FY 92 from the EXXON VALDEZ oil spill case which was placed in a judgement settlement account within the General Fund.
- (22) The State, per AS 38.05.180, grants incentive credits against royalties, severance taxes, and rentals to the oil companies for drilling exploratory wells. The credits granted and applied for in FY 92 have not been subtracted from the aforementioned unrestricted revenues. Additional credits are anticipated in subsequent years.
- (23) Chapter 210, SLA 1990, allocates 6.0 percent of General Fund unrestricted revenues to the Mental Health Trust Income Account until such time as the original Mental Health Trust Lands are valued. The necessary expenses of Alaska's Mental Health Program must be met before funds in the Mental Health Trust Income Account may be expended for any other public purpose (AS 37.14.021). The amounts shown are included in the aforementioned Total Unrestricted Revenue figures. Currently, the Mental Health Lands Settlement per Chapter 66, SLA 1991 is pending before the courts.

The following table shows that petroleum revenues will dominate in the short-term under all three scenarios.

Table 4      General Fund Unrestricted Revenues:  
Petroleum Revenues as a Percentage of the Total

FY 1992 - 1995  
(Millions of Dollars)

	Total G. F. Unrestricted from Petroleum	Total G. F. Unrestricted Revenues	Percent
<u>FY 92 Actual</u>	2,007.4	2,462.6	82
<u>FY 93 Estimates</u>			
Low	1,998.4	2,268.1	88
Mid	2,102.5	2,386.2	88
High	2,180.3	2,487.7	88
<u>FY 94 Estimates</u>			
Low	1,807.7	2,058.5	88
Mid	2,026.3	2,303.8	88
High	2,238.6	2,547.3	88
<u>FY 95 Estimates</u>			
Low	1,836.2	2,083.8	88
Mid	2,087.4	2,390.5	87
High	2,289.2	2,624.2	87

## Petroleum Revenues

This section underlines the importance of petroleum revenues to Alaska's total revenues; discusses the current oil markets; sets out the petroleum forecast assumptions; describes the Low, Mid, and High Scenarios; and concludes with a note on methodology.

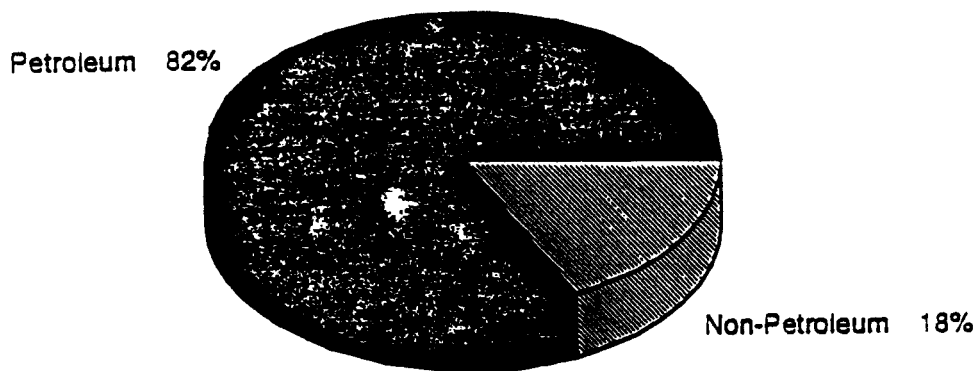
### **Importance of Petroleum Revenues**

Petroleum revenues accounted for 82 percent of all unrestricted General Fund revenues in FY 1992, and will continue to account for close to 80 percent of those revenues each year well into the 1990's.

The figure below shows the relationship of petroleum revenues to all revenues for FY 1992.

Figure 2

FY 92 General Fund Unrestricted Revenues



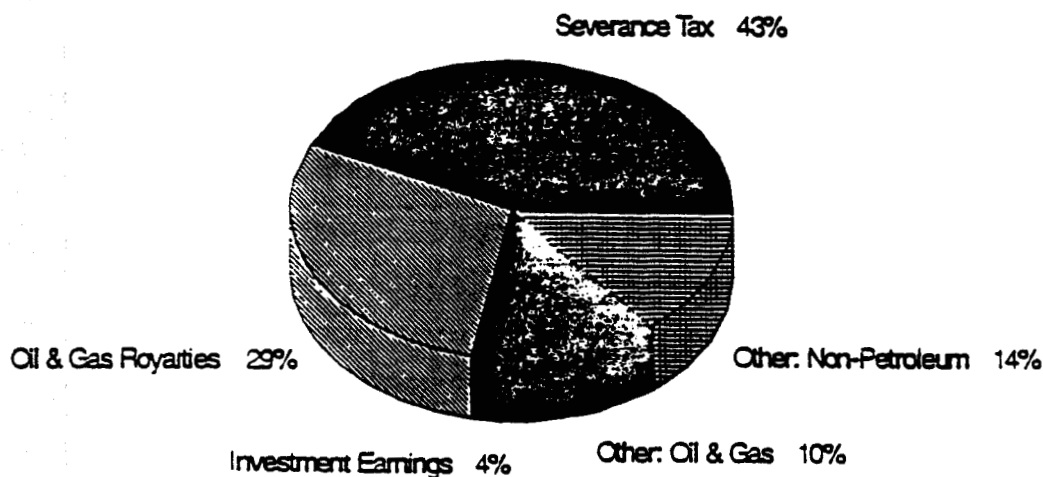


Petroleum revenues come from: (1) severance taxes (also called production taxes); (2) royalties on oil and gas the State owns; (3) corporate income taxes on corporations producing and transporting oil and gas; (4) oil and gas property taxes; and, (5) other oil and gas revenues (rents and bonuses).

Together, these petroleum revenues accounted for 82 percent of State revenues in FY 1992. The State also collects revenues in the form of interest earned on money invested in the State Treasury, which accounted for another four percent of the total General Fund unrestricted revenues. (Most of the earnings come from interest earned on petroleum revenues.) The following figure illustrates this.

Figure 3

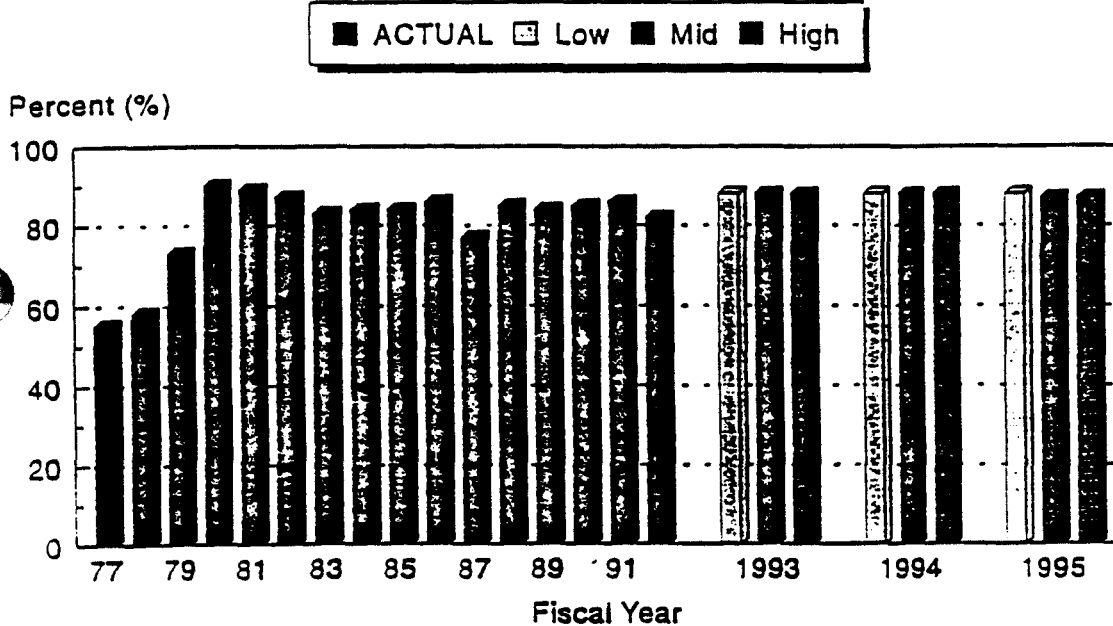
### FY 92 General Fund Unrestricted Revenues



The figure below shows that the State of Alaska has received most of its revenues from petroleum for a substantial period. Petroleum revenues comprised more than 77 percent of General Fund unrestricted revenues in FY 1992 for the thirteenth year in a row.

Figure 4

**Percentage of General Fund Unrestricted Revenues  
Which Come From Petroleum  
(FY 1977 - 1995)**



In this forecast we discuss only three of the many possible future price and production outcomes affecting Alaska oil revenues.

To assist in examining a greater number of possible future oil revenue outcomes, a revenue matrix has been developed for both FY 1993 and FY 1994. The Alaska State Revenue Matrices on the following two pages provide an estimate of State General Fund unrestricted revenues for various alternative ANS price and production levels.

Alaska State Revenue Matrix<sup>1</sup>  
Unrestricted General Fund  
(Millions of Dollars)

FY 1993

Alaska North Slope Production  
Millions of barrels/day

Avg ANS Lower 48 <sup>2</sup>	1.60	1.65	1.70	1.75	1.80	1.85	1.90	1.95	2.00
\$10.00	1,840	1,860	1,870	1,880	1,890	1,910	1,920	1,930	1,940
\$11.00	1,840	1,860	1,870	1,880	1,890	1,910	1,920	1,930	1,940
\$12.00	1,840	1,860	1,870	1,880	1,890	1,910	1,920	1,930	1,940
\$13.00	1,840	1,860	1,870	1,880	1,890	1,910	1,920	1,930	1,940
\$14.00	1,890	1,900	1,920	1,930	1,950	1,970	1,980	2,000	2,020
\$15.00	1,940	1,960	1,980	2,000	2,020	2,040	2,060	2,080	2,100
\$16.00	2,050	2,080	2,110	2,140	2,170	2,200	2,230	2,260	2,290
\$17.00	2,170	2,210	2,240	2,280	2,320	2,360	2,400	2,440	2,480
\$18.00	2,280	2,330	2,380	2,430	2,470	2,520	2,570	2,620	2,670
\$19.00	2,390	2,450	2,510	2,570	2,630	2,680	2,740	2,800	2,860
\$20.00	2,510	2,580	2,640	2,710	2,780	2,850	2,910	2,980	3,050
\$21.00	2,620	2,700	2,780	2,850	2,930	3,010	3,080	3,160	3,240
\$22.00	2,740	2,820	2,910	2,990	3,080	3,170	3,250	3,340	3,430
\$23.00	2,850	2,950	3,040	3,140	3,230	3,330	3,420	3,520	3,620
\$24.00	2,960	3,070	3,170	3,280	3,380	3,490	3,590	3,700	3,800
\$25.00	3,080	3,190	3,310	3,420	3,540	3,650	3,760	3,880	3,990
\$26.00	3,190	3,320	3,440	3,560	3,690	3,810	3,930	4,060	4,180
\$27.00	3,310	3,440	3,570	3,710	3,840	3,970	4,110	4,240	4,370
\$28.00	3,420	3,560	3,710	3,850	3,990	4,130	4,280	4,420	4,560
\$29.00	3,530	3,690	3,840	3,990	4,140	4,290	4,450	4,600	4,750
\$30.00	3,650	3,810	3,970	4,130	4,290	4,450	4,620	4,780	4,940

<sup>1</sup> Assumptions other than price and production are based on the Mid Scenario of the Department of Revenue Spring 1993 Forecast.

<sup>2</sup> The average ANS price for all lower 48 sales is approximately \$0.68/barrel less than the U.S. Gulf price in FY 1992.

Table 6

Alaska State Revenue Matrix<sup>1</sup>  
Unrestricted General Fund  
(Millions of Dollars)

FY 1994

Avg ANS <sup>2</sup> Lower 48	Alaska North Slope Production Millions of barrels/day								
	1.60	1.65	1.70	1.75	1.80	1.85	1.90	1.95	2.00
\$10.00	1,160	1,180	1,200	1,220	1,250	1,270	1,290	1,310	1,330
\$11.00	1,270	1,300	1,320	1,350	1,370	1,390	1,420	1,440	1,470
\$12.00	1,400	1,430	1,460	1,480	1,510	1,540	1,570	1,590	1,620
\$13.00	1,520	1,560	1,590	1,620	1,650	1,680	1,710	1,750	1,780
\$14.00	1,650	1,690	1,720	1,760	1,790	1,830	1,860	1,900	1,930
\$15.00	1,770	1,810	1,850	1,890	1,930	1,970	2,010	2,050	2,090
\$16.00	1,900	1,940	1,990	2,030	2,070	2,120	2,160	2,200	2,250
\$17.00	2,020	2,070	2,120	2,170	2,210	2,260	2,310	2,360	2,400
\$18.00	2,150	2,200	2,250	2,300	2,350	2,410	2,460	2,510	2,560
\$19.00	2,270	2,330	2,380	2,440	2,490	2,550	2,600	2,660	2,710
\$20.00	2,400	2,460	2,520	2,580	2,640	2,690	2,750	2,810	2,870
\$21.00	2,520	2,590	2,650	2,710	2,780	2,840	2,900	2,960	3,030
\$22.00	2,650	2,720	2,780	2,850	2,920	2,980	3,050	3,120	3,180
\$23.00	2,780	2,850	2,920	2,990	3,060	3,130	3,200	3,270	3,340
\$24.00	2,900	2,970	3,050	3,120	3,200	3,270	3,350	3,420	3,490
\$25.00	3,030	3,100	3,180	3,260	3,340	3,420	3,490	3,570	3,650
\$26.00	3,150	3,230	3,310	3,400	3,480	3,560	3,640	3,720	3,810
\$27.00	3,280	3,360	3,450	3,530	3,620	3,700	3,790	3,880	3,960
\$28.00	3,400	3,490	3,580	3,670	3,760	3,850	3,940	4,030	4,120
\$29.00	3,530	3,620	3,710	3,810	3,900	3,990	4,090	4,180	4,270
\$30.00	3,650	3,750	3,850	3,940	4,040	4,140	4,240	4,330	4,430

<sup>1</sup> Assumptions other than price and production are based on the Mid Scenario of the Department of Revenue Spring 1993 Forecast.

<sup>2</sup> The average ANS price for all lower 48 sales is approximately \$0.89/barrel less than the U. S. Gulf price in FY 1993.

## Current Oil Market Situation

### World Market

In February, OPEC agreed to a 23.582 million bbl/day ceiling for the second quarter of 1993. This agreement requires the cartel cut about 1.5 million bbl/day from its present production. This production strategy is an attempt to support prices which are currently about \$3.00/bbl under OPEC's \$21.00/bbl target.

Kuwaiti production has almost returned to its pre-War level. Though targeting an "all it can" initiative since the Gulf War, Kuwait has agreed to hold production at 1.6 million bbl/day through the second quarter. United Nations sanctions remain in place and Iraqi crude remains out of the worldwide market; this situation will continue until it can be shown that Iraqi weapons of mass destruction are destroyed. The earliest that Iraq could resume its oil exports is year-end 1993 or early 1994.

Worldwide economic recovery will fuel the demand for crude which is projected to increase by 500,000 bbls/day in 1993. The United States will be the driving force for this increase. No assessment of the impact of new energy taxes is made in this forecast. The call on OPEC for crude will increase by about 1 million bbl/day pushing prices upward in the short term.

Figure 5 OPEC Production  
Million Barrels/Day

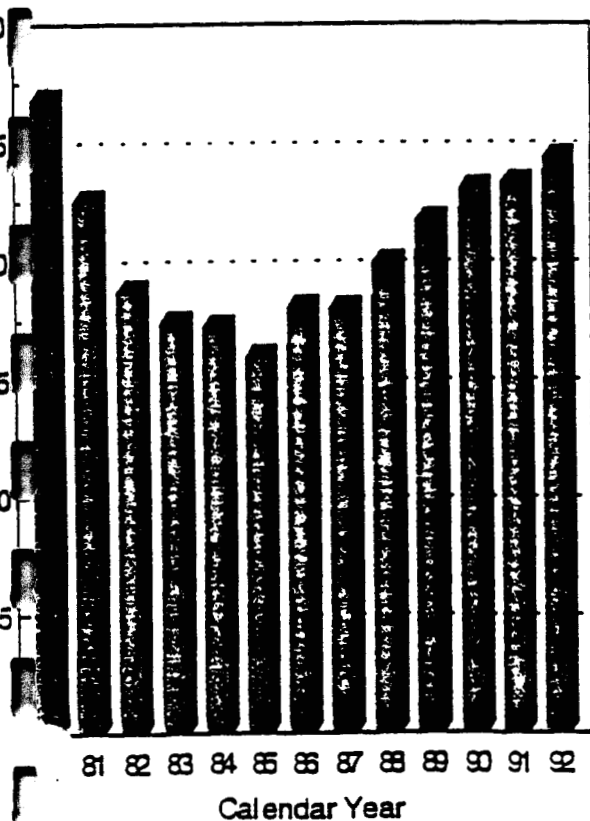


Table 7 OPEC Production<sup>1</sup>  
(Thousands of bbls/day)

Country	Production	
	Jan 93	O2 1993 Quota
Algeria	770	732
Ecuador**	....	....
Gabon	290	281
Indonesia	1,350	1,317
Iran	3,550	3,340
Iraq	450	400
Kuwait*	1,600	1,600
Libya	1,450	1,350
Nigeria	1,950	1,780
Qatar	460	364
Saudi Arabia*	8,500	8,000
UAE	2,270	2,161
Venezuela	2,360	2,267
<b>TOTAL</b>	<b>25,000</b>	<b>23,582</b>

Source: Platts Oilgram Price Report (2/5/93).

\* Share Neutral Zone output 1980-July 1990 and beginning in June 1991 due to Persian Gulf War.

\*\* Ecuador left OPEC January 1, 1992.

### Alaska North Slope Market

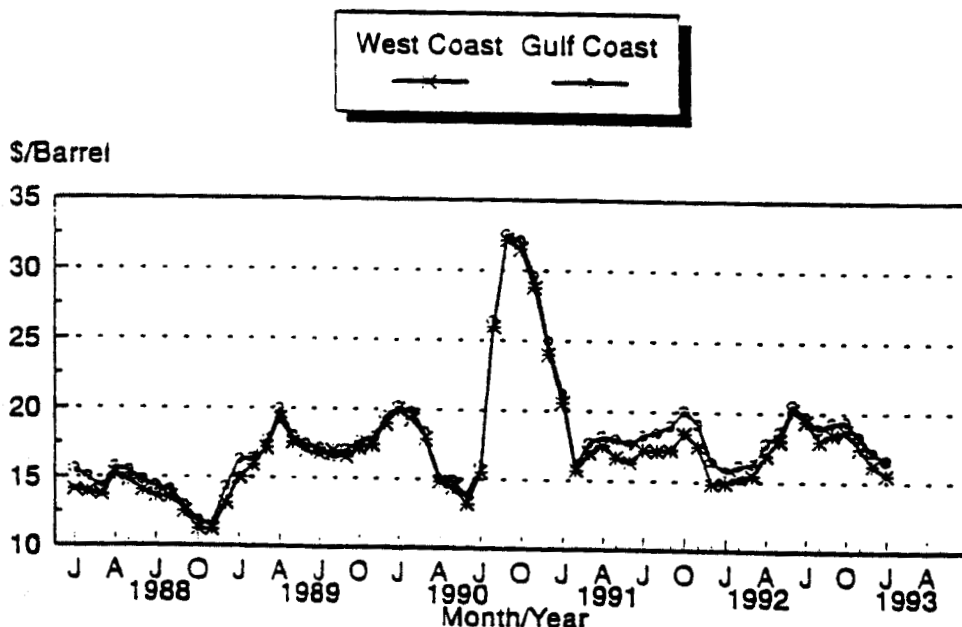
Alaska North Slope (ANS) prices have ranged between \$16.00 and \$19.00/bbl since last Fall. The stagnant global economy has dampened demand and kept downward pressure on oil prices. Additionally, continued over quota production by OPEC has kept an ample supply of crude in the market. FY 1993 ANS Lower 48 spot price is about \$18.11/bbl.

BP Exploration announced its official selling prices for March 1993 as \$16.78/bbl on the West Coast and \$17.90/bbl on the Gulf Coast. Recent spot prices have been running \$0.10/bbl lower than BP's official price.

Roughly 85 percent of ANS production is sold on the West Coast while 15 percent is marketed in the Eastern half of the United States and the Caribbean. As ANS production declines, it is expected that shipments to Eastern U.S. destinations are assumed to cease after 1996. Greater transportation costs to the more distant markets result in a Gulf Coast derived wellhead price which is lower than the West Coast price. Historical ANS spot prices are graphed below.

Figure 6

#### ANS Spot Price January 1988 - January 1993



## Forecast Assumptions

### **ANS Lower 48 Prices**

The oil price assumptions used in this forecast start with the spot price of ANS at the U.S. Gulf Coast. The price of West Coast ANS and the ANS royalty market basket are forecast based on their historical relationship to Gulf Coast ANS spot price. West Coast ANS sells at a discount to the Gulf Coast because total ANS production exceeds West Coast demand for sour crude oil. It is this crude surplus that necessitates the shipment of ANS to the Gulf. The short term price forecast for ANS is illustrated below.

Over the longer term, as demand on the West Coast grows and ANS production declines, the West Coast oil glut will disappear. In this forecast, West and Gulf Coast oil prices are assumed to converge when the West Coast surplus disappears. The long term forecast for ANS is also illustrated below.

Finally, starting with this forecast, collections of State severance taxes are now assumed to be based directly on spot price. This is a major change in forecasting methodology since in the past we incorporated into the forecast a difference between spot and taxpayer reported prices. This methodological change reflects the current system used to administer severance tax payments. Producers are now required to file a quarterly estimated tax-based payment.

The discussion of price forecast assumptions starts with the Gulf Coast ANS price and outlines the other variables which translate this price into the wellhead price for ANS crude oil. The wellhead price determines the value of production and thus, the state's severance tax and royalty income.

Table 8  
Scenarios for ANS Oil Price  
Gulf Coast and West Coast  
(\$/bbl)

<u>Fiscal Year</u>	<u>Low</u>		<u>Mid</u>		<u>High</u>	
	<u>West</u>	<u>Gulf</u>	<u>West</u>	<u>Gulf</u>	<u>West</u>	<u>Gulf</u>
1993	17.54	18.34	17.78	18.59	18.03	18.86
1994	16.81	17.75	18.25	19.27	19.57	20.67
1995	17.36	18.33	19.12	20.19	20.39	21.54
2000	21.60	21.60	26.14	26.14	29.38	29.38
2005	25.08	25.08	32.51	32.51	40.42	40.42



Over the long-run, demand on the West Coast will increase while ANS production is in decline; the oil glut on the West Coast will then disappear. In this forecast, West Coast and Gulf Coast oil prices are assumed to converge when the West Coast surplus disappears.

Figure 7

### ANS at the U. S. Gulf

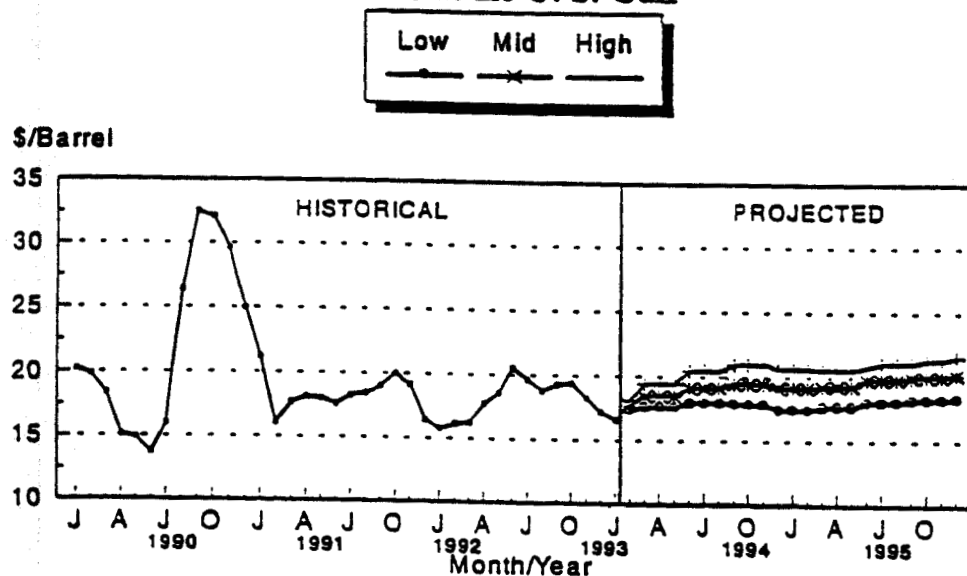
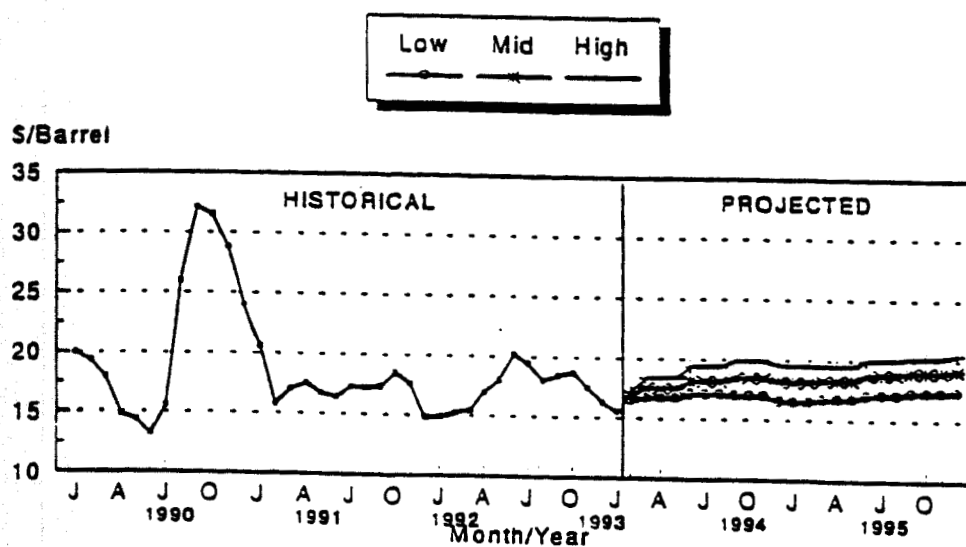


Figure 8

### ANS at the U. S. West Coast



## Transportation Costs to Lower 48 Markets

The weighted average Lower 48 shipping cost averaged \$1.66/bbl in FY 1992, \$0.30/bbl higher than in the prior year. This increase was mostly attributable to tight markets in the higher cost Gulf trade, where there is significant chartering, and results of the Oilspill Pollution Act of 1990 (OPA90).

As ANS production declines and West Coast petroleum demand increases, shipments to the Gulf will diminish. This will free up excess tonnage. Consequently, average shipping costs are expected to stay fairly constant over the next few years. In the long term the double hulling requirements of OPA90 will result in increased shipping costs.

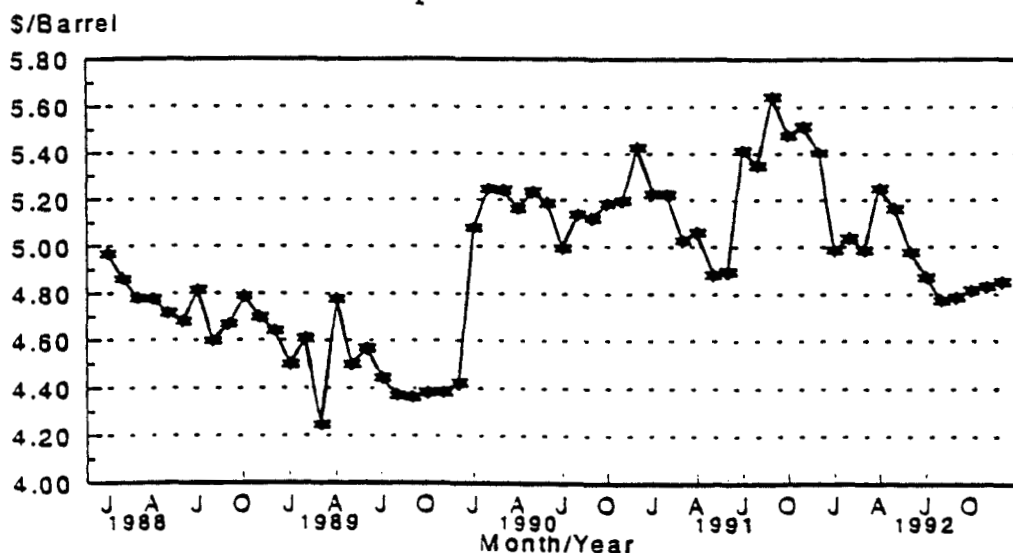
Table 9

### Marine Transportation Costs Valdez to Lower 48 (\$/bbl)

Fiscal Year	Low	Mid	High
1993	1.69	1.69	1.69
1994	1.68	1.69	1.69
1995	1.67	1.68	1.69
2000	1.53	1.58	1.62
2005	1.97	2.07	2.16

Figure 9

### Total Transportation Costs to Lower 48 Pipeline and Tanker



## Trans Alaska Pipeline System Tariffs

The Trans Alaska Pipeline System (TAPS) tariff is determined according to the TAPS Settlement Method, a ratemaking method agreed upon by the Pipeline owners and the State of Alaska. This agreement allowed an accelerated recovery of the construction costs and a fixed profit of an inflation adjusted \$0.35/bbl. This resulted in higher tariffs from 1977-85 in exchange for lower tariffs in the late 1980's and 1990's.

As can be seen in the table below, the tariff method has worked as intended with the exception of FY 1990 and FY 1991 when the tariff increased due to corrosion repairs, lower than expected TAPS throughput and oil spill mitigation expenditures due to the EXXON VALDEZ accident.

The 1993 average filed tariff was \$2.94/bbl. The filing is made on a calendar year basis while the table below is on a fiscal year basis.

Table 10

### Scenarios for TAPS Tariffs (\$/bbl)

<u>Fiscal Year</u>	<u>ACTUAL</u>	<u>Low</u>	<u>Mid</u>	<u>High</u>
1985	6.04			
1986	5.29			
1987	4.20			
1988	3.54			
1989	3.12			
1990	3.48			
1991	3.75			
1992	3.60			
1993		3.20	3.20	3.20
1994		2.98	2.99	3.00
1995		2.97	3.01	3.02
2000		3.00	3.18	3.08
2005		4.43	4.81	4.69

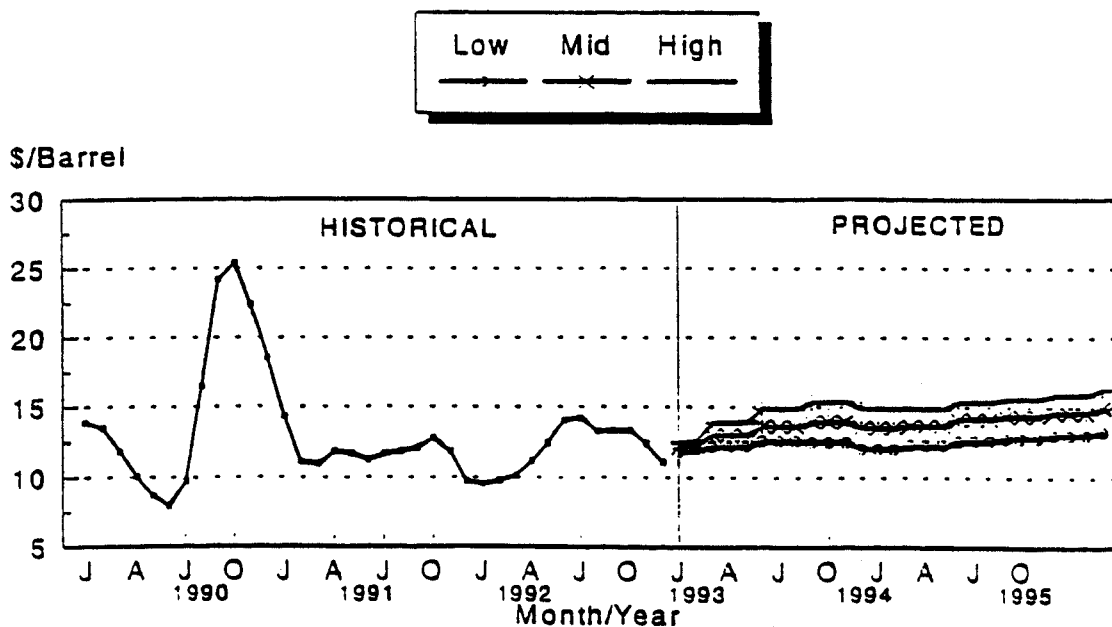
## Wellhead Price for ANS

The wellhead value of ANS, along with production, is the basis for both State severance tax and royalty. The wellhead value is calculated by subtracting the pipeline and marine transportation costs from the sales price (or transfer price at the refinery gate in the case of oil run through a producer's own refinery.)

Table 11  
Scenarios for ANS Wellhead Price  
(\$/bbl)

Fiscal Year	Low	Mid	High
1993	12.66	12.91	13.19
1994	12.33	13.67	14.98
1995	12.89	14.50	15.76
2000	16.89	20.96	24.32
2005	18.21	24.85	32.78

Figure 10  
ANS at the Wellhead



## Oil Production Outlook

Information for forecasting production comes from expertise at the Alaska Oil and Gas Conservation Commission, in-house engineering models, the operating companies, trade journals, technical reports and news releases. Annual production estimates are shown below.

Over the most recent quarter, North Slope daily oil production is at 96 percent of the rate seen during the same period a year ago. The seven percent decline in Prudhoe Bay liquid hydrocarbons continues to shape the production outlook for the entire state of Alaska. The GHX2 project will add 100,000 bbls/day to Prudhoe Bay in FY 1994.

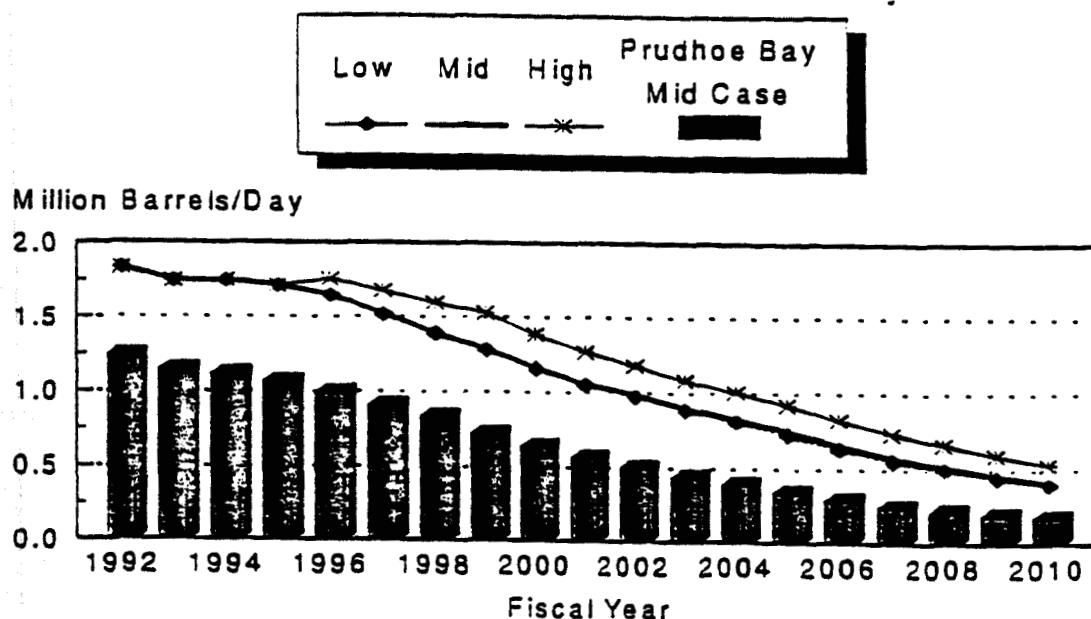
The Point McIntyre field is scheduled to commence production in the summer of 1993 and is expected to later peak at approximately 100,000 bbls/day. The Niakuk field is expected to start up a year later. Insofar as the Point McIntyre and Lisburne oil will be commingled at the latter's limited production facilities, the onset of Point McIntyre will cause a deferment of some Lisburne production.

Cook Inlet production continues to decline at a slow one percent annual rate. Recent developments at Granite Point, and discoveries at the West McArthur River field and the Sunfish prospect (North Forelands field), may stem that rate further. ARCO has announced commerciality of the latter, but has not disclosed the estimated reserves. Due to uncertainty these discoveries are not explicitly assumed in this forecast.

Despite the decline at the Prudhoe Bay field, continued success in reservoir management in all fields and exploration will hold statewide production decline in the near term to less than five percent per year.

Figure 11

### Simulated Oil Production Total Alaska and Mid Case Prudhoe Bay



## **Other Non-Oil Revenue Sources Assumptions**

### **Oil Corporate Taxes**

Oil corporate taxes for FY 1992 generated \$165.5 million compared to \$185.1 million collected in FY 1991. In FY 1993, the revenue outlook in this area is greater than FY 1992 due to corporate restructuring to promote more efficient operations and higher oil prices.

### **Non-Oil Corporate Taxes**

Non-petroleum corporate taxes generated \$33.7 million in FY 1992 compared to \$37.9 million in FY 1991. The drop in non-petroleum corporate tax revenue was due to the general slow down in business activity.

### **Property Taxes**

The current oil and gas property tax, which is levied at 20 mills on the full and true value of oil and gas property, is expected to continue to decline. The decrease for FY 1992 and FY 1993, as compared to previous forecasts, is greater due in part to investment delays and increased mill levies by the North Slope Borough, the Kenai Peninsula Borough and the City of Valdez. The municipalities in which taxable oil and gas property exists continue to receive the bulk of the property tax assessment.

### **Alcoholic Beverage Taxes**

The trends in alcohol consumption have been fairly steady over the last five years in all categories. The only notable exception has been a drop in wine consumption compared to the earlier period: FY 1984 through FY 1987. Current consumption trends for liquor, wine and beer, given population growth, demographics and income levels, are expected to continue generating revenues of between \$12 and \$13 million per year.

### **Intergovernmental Receipts**

Federal Shared Revenues, which consist of several categories, totaled \$12.8 million in FY 1991 but dropped to \$6.7 million in FY 1992 as anticipated. This is due primarily to the fact that the U.S. Forest Service (USFS) monies for timber sales were formerly allocated to only organized boroughs. The USFS has since notified the State that additional monies will be set aside for unorganized boroughs as well (Chapter 37, SLA 1991). The monies are intended to support roads and schools affected by national forest activities. The amount of Federal Shared Revenues which will go into the General Fund in FY 1993 should be about \$7 million.

Section 8(g) funds are the result of a negotiated settlement between the State and federal government several years ago with a specific payment schedule. The revenue figure increased from \$2 million in FY 1991 and will be \$4.7 million annually for the period FY 1992 through FY 1996 when the numbers will again be adjusted upward.

### **Investment Earnings**

The projections are based on projected out-going expenditures and incoming revenues with an assessment of yield on instruments and the length of maturity for the funds invested by the Treasury Division. FY 1992 investment earnings were \$101.8 million.

### **Facilities and Related Charges**

The main revenue item in this category is ferry system receipts which amounted to \$42.4 million in FY 1992. The legislature established the Alaska Marine Highway System Fund (Chapter 193, SLA 1990) which provides that the gross revenue of the state ferry system be deposited into the fund and then may be appropriated for operating and capital expenditures.

### **Methodology**

The Department of Revenue uses a wide variety of models and techniques to forecast petroleum severance taxes and royalties and the other non-petroleum sources. The main petroleum forecasting model is a marketing and production simulation model which projects severance tax and royalties on a company-by-company, field-by-field basis through the year 2050. This model, initially developed in 1978, can be run on either a scenario or iterative basis.

## Scenarios Over the Short-Term

### Low Scenario

**SUMMARY:** *The Low Scenario assumes a very slow worldwide economic recovery. As a result, oil consumption growth is assumed to grow slowly even with low oil prices. Steady increasing production from Saudi Arabia, Iran and Kuwait keeps downward pressure on oil prices in a stagnant market.*

Table 12 General Fund				
	Unrestricted Revenues	ANS Gulf Price (\$/bbl)	ANS Lower 48 Price (\$/bbl)	ANS Production (MMbbls/day)
EY 1993	2,268.1	18.34	17.75	1,703
EY 1994	2,058.5	17.75	16.93	1,704
EY 1995	2,083.8	18.33	17.47	1,674

#### Low Scenario assumptions:

1. Global economic growth averages 1.0 percent in 1993 with slow recovery in the United States, Japan and West Germany and the painful transition of the previously centrally planned economies into the global market continues to occur. The growth rate picks up to 1.5 percent in 1994 as the world economy begins to rebound.
2. Oil consumption grows slowly as the economic recession dampens the positive effect of low oil prices.
3. Non-OPEC production in both 1993 and 1994 holds steady as increases in such areas as the North Sea and newer frontier areas offset the continued decline from the Commonwealth of Independent States.
4. OPEC's market share under this scenario is 24.7 million bbl/day in 1993 and 25.1 million bbl/day in 1994.
5. Key OPEC producers Saudi Arabia, Iran and Kuwait continue to increase their capacity. Increased production from these three producers, as well as the possibility of the resumption of exports from Iraq, keep the market well supplied with continued downward pressure on oil prices.



Table 13

## Low Scenario

## Global Oil Market Assumptions

	<u>TOTAL GLOBAL OIL CONSUMPTION</u>	<u>OPEC CRUDE OIL PRODUCTION</u>	<u>OPEC NGL/COND. PRODUCTION</u>	<u>TOTAL NON-OPEC PRODUCTION</u>	<u>GLOBAL STOCK CHANGE</u>
<b>1992</b>					
Q1	67.7	24.1	2.0	41.0	-0.6
Q2	64.9	23.7	2.0	39.8	0.6
Q3	65.6	24.6	2.0	39.5	0.5
Q4	67.7	25.2	2.0	40.0	-0.5
YEAR	66.5	24.4	2.0	40.1	0.0
<b>1993</b>					
Q1	68.0	24.3	2.0	40.4	-1.3
Q2	65.0	24.4	2.0	39.7	1.1
Q3	65.6	24.6	2.0	39.7	0.8
Q4	68.1	25.6	2.0	40.5	0.0
YEAR	66.7	24.7	2.0	40.1	0.1
<b>1994</b>					
Q1	68.3	24.8	2.0	40.3	-1.3
Q2	65.4	24.8	2.0	39.6	1.1
Q3	65.9	25.1	2.0	39.6	0.8
Q4	68.4	26.0	2.0	40.4	0.0
YEAR	67.0	25.2	2.0	40.0	0.1

## Mid Scenario

**SUMMARY:** The Mid Scenario assumes that the global economy begins to pick up in 1993 and 1994 with the result that oil consumption grows in response to both relatively low oil prices and increased demand for oil. Oil prices begin to slowly drift upward as OPEC capacity expansion is required to meet growing demand, particularly with Iraq out of the market.

Year	General Fund Unrestricted Revenues	ANS Gulf Price (\$/bbl)	ANS Lower 48 Price (\$/bbl)	ANS Production (MM bbls/day)
1993	2386.2	18.59	18.01	1703
1994	2303.8	19.27	18.38	1704
1995	2390.5	20.19	19.24	1674

### Scenario assumptions:

- Global economic growth averages 2.5 percent in 1993 and 3.0 percent in 1994.
- Oil consumption grows by 0.5 million bbl/day in 1993 and 0.8 million bbl/day in 1994.
- Non-OPEC production continues to decline, as a result of a further decline from the Commonwealth of Independent States.
- OPEC market share under this scenario amounts to 25.5 million bbl/day in 1993 and 26.6 million bbl/day in 1994.
- This growing market share for OPEC will be accommodated by increased production from most member countries, in particular from Saudi Arabia, Iran and Kuwait. Iraq will remain embargoed. Pressure on capacity in OPEC will keep mild upward pressure on oil prices.

Table 15

## Mid Scenario

## Global Oil Market Assumptions

	<u>TOTAL GLOBAL OIL CONSUMPTION</u>	<u>OPEC CRUDE OIL PRODUCTION</u>	<u>OPEC NGL/COND. PRODUCTION</u>	<u>TOTAL NON-OPEC PRODUCTION</u>	<u>GLOBAL STOCK CHANGE</u>
<b>1992</b>					
Q1	67.7	24.1	2.0	41.0	-0.6
Q2	64.9	23.7	2.0	39.8	0.6
Q3	65.6	24.6	2.0	39.6	0.5
Q4	67.7	25.2	2.0	40.0	-0.5
YEAR	66.5	24.4	2.0	40.1	0.0
<b>1993</b>					
Q1	68.5	25.2	2.0	40.0	-1.3
Q2	65.5	25.2	2.0	39.3	1.1
Q3	66.0	25.5	2.0	39.3	0.8
Q4	68.6	26.5	2.0	40.1	0.0
YEAR	67.1	25.6	2.0	39.7	0.1
<b>1994</b>					
Q1	69.5	26.5	2.0	39.7	-1.3
Q2	66.5	26.5	2.0	39.0	1.1
Q3	67.0	26.8	2.0	39.1	0.8
Q4	69.6	27.8	2.0	39.8	0.0
YEAR	68.1	26.9	2.0	39.4	0.1

## High Scenario

**SUMMARY:** Global economic growth picks up rapidly in 1993 and 1994. This economic recovery spurs oil consumption increases which creates oil supply pressures leading to higher oil prices.

Table 16	General Fund	ANS Gulf	ANS Lower 48	ANS Production
	Unrestricted	Price (\$/bbl)	Price (\$/bbl)	(MM bbls/day)
Revenues				
FY 1993	2,487.7	18.86	18.30	1,703
FY 1994	2,547.3	20.67	19.61	1,704
FY 1995	2,624.2	20.54	20.52	1,674

### High Scenario assumptions:

1. World-wide economic growth averages 3.5 percent in both 1993 and 1994.
2. Oil consumption increases by 1.6 million bbl/day in 1993 and 1.2 million bbl/day in 1994 in response to vigorous economic growth.
3. Non-OPEC production continues to slide primarily due to further major declines in output from the Commonwealth of Independent States.
4. OPEC market share amounts to 27.1 million bbl/day in 1993 and 28.6 million bbl/day in 1994.
5. The 1993 and 1994 OPEC production levels assumed in this scenario are very close to current estimates of capacity. This causes significant upward pressure on oil prices.

Table 17

## High Scenario

## Global Oil Market Assumptions

	<u>TOTAL GLOBAL OIL CONSUMPTION</u>	<u>OPEC CRUDE OIL PRODUCTION</u>	<u>OPEC NGL/COND. PRODUCTION</u>	<u>TOTAL NON-OPEC PRODUCTION</u>	<u>GLOBAL STOCK CHANGE</u>
<b>1992</b>					
Q1	67.7	24.1	2.0	41.0	-0.6
Q2	64.9	23.7	2.0	39.8	0.6
Q3	65.6	24.6	2.0	39.5	0.5
Q4	67.7	25.2	2.0	40.0	-0.5
YEAR	66.5	24.4	2.0	40.1	0.0
<b>1993</b>					
Q1	69.3	26.8	2.0	39.3	-1.3
Q2	66.3	26.8	2.0	38.6	1.1
Q3	66.9	27.0	2.0	38.6	0.8
Q4	69.5	28.1	2.0	39.4	0.0
YEAR	68.0	27.2	2.0	39.0	0.1
<b>1994</b>					
Q1	70.6	28.2	2.0	39.1	-1.3
Q2	67.5	28.2	2.0	38.4	1.1
Q3	68.1	28.4	2.0	38.4	0.8
Q4	70.7	29.5	2.0	39.2	0.0
YEAR	69.2	28.6	2.0	38.8	0.1

Table 18

**Projected and Historical Crude Oil Spot Prices<sup>1</sup>**  
**For Alaska North Slope Crude and Domestic Marker**  
 (\$/barrel)

**Low Scenario**

	<u>Production</u> <u>Mon/YR</u>	<u>ANS at</u> <u>Wellhead</u>	<u>ANS at</u> <u>West Coast</u>	<u>ANS at</u> <u>Gulf Coast</u>	<u>WTI</u>
Historical	JUN 91	11.23	16.36	17.58	19.32
	JUL	11.72	17.26	18.30	21.41
	AUG	11.89	17.18	18.49	21.70
	SEP	12.14	17.31	19.05	21.87
	OCT	12.79	18.47	20.05	23.24
	NOV	11.86	17.57	19.16	22.51
	DEC	9.72	14.83	16.44	19.49
	JAN 92	9.51	14.92	15.74	18.80
	FEB	9.81	15.30	16.17	18.98
	MAR	10.17	15.50	16.29	18.91
	APR	11.21	16.96	17.77	20.23
	MAY	12.47	18.03	18.62	20.97
	JUN	14.04	20.20	20.56	22.37
	JUL	14.23	19.40	19.65	21.74
	AUG	13.26	17.97	18.82	21.33
	SEP	13.33	18.46	19.31	21.88
	OCT	13.33	18.71	19.43	21.67
	NOV	12.41	17.46	18.26	20.34
	DEC	11.09	16.23	17.19	19.38
	JAN 93	11.79	15.54	16.59	19.01
Projected	FEB	11.96	16.50	17.43	19.41
	MAR	12.18	16.68	17.62	19.62
	APR	12.18	16.68	17.62	19.62
	MAY	12.17	16.68	17.62	19.62
	QTR1 FY94	12.57	17.03	17.99	20.01
	QTR2 FY94	12.49	16.93	17.88	19.89
	QTR3 FY94	12.01	16.52	17.45	19.42
	QTR4 FY94	12.24	16.76	17.70	19.69
	QTR1 FY95	12.56	17.07	18.03	20.04
	QTR2 FY95	12.77	17.28	18.25	20.29
	QTR3 FY95	12.97	17.39	18.37	20.42
	QTR4 FY95	13.25	17.68	18.67	20.76

<sup>1</sup> Historical ANS spot prices are taken from Platt's Oilgram Price Report.

Table 19

**Projected and Historical Crude Oil Spot Prices  
For Alaska North Slope Crude and Domestic Marker<sup>1</sup>  
(\$/barrel)**

**Mid Scenario**

<b>Production Mon/YR</b>			<b>ANS at Wellhead</b>	<b>ANS at West Coast</b>	<b>ANS at Gulf Coast</b>	<b>WTI</b>
<b>Historical</b>	JUN	91	11.23	16.36	17.58	19.32
	JUL		11.72	17.26	18.30	21.41
	AUG		11.89	17.18	18.49	21.70
	SEP		12.14	17.31	19.05	21.87
	OCT		12.79	18.47	20.05	23.24
	NOV		11.86	17.57	19.16	22.51
	DEC		9.72	14.83	16.44	19.49
	JAN	92	9.51	14.92	15.74	18.80
	FEB		9.81	15.30	16.17	18.98
	MAR		10.17	15.50	16.29	18.91
	APR		11.21	16.96	17.77	20.23
	MAY		12.47	18.03	18.62	20.97
	JUN		14.04	20.20	20.56	22.37
	JUL		14.23	19.40	19.65	21.74
	AUG		13.26	17.97	18.82	21.33
	SEP		13.33	18.46	19.31	21.88
	OCT		13.33	18.71	19.43	21.67
	NOV		12.41	17.46	18.26	20.34
	DEC		11.09	16.23	17.19	19.38
	JAN	93	12.11	15.54	16.59	19.01
<b>Projected</b>	FEB		12.28	16.83	17.78	19.80
	MAR		12.96	17.51	18.50	20.60
	APR		12.96	17.51	18.50	20.60
	MAY		12.96	17.51	18.50	20.60
	QTR1	FY94	13.59	18.18	19.14	21.29
	QTR2	FY94	13.93	18.46	19.50	21.69
	QTR3	FY94	13.50	18.13	19.15	21.30
	QTR4	FY94	13.64	18.28	19.31	21.48
	QTR1	FY95	14.14	18.78	19.84	22.05
	QTR2	FY95	14.35	18.99	20.06	22.30
	QTR3	FY95	14.58	19.17	20.24	22.50
	QTR4	FY95	14.93	19.53	20.63	22.93

<sup>1</sup> Historical ANS spot prices are taken from Platt's Oilgram Price Report.

Table 20

**Projected and Historical Crude Oil Spot Prices  
For Alaska North Slope Crude and Domestic Marker<sup>1</sup>**  
(\$/barrel)

**High Scenario**

	Production Mon/YR	ANS at Wellhead	ANS at West Coast	ANS at Gulf Coast	WTI
Historical	JUN 91	11.23	16.36	17.58	19.32
	JUL	11.72	17.26	18.30	21.41
	AUG	11.89	17.18	18.49	21.70
	SEP	12.14	17.31	19.05	21.87
	OCT	12.79	18.47	20.05	23.24
	NOV	11.86	17.57	19.16	22.51
	DEC	9.72	14.83	16.44	19.49
	JAN 92	9.51	14.92	15.74	18.80
	FEB	9.81	15.30	16.17	18.98
	MAR	10.17	15.50	16.29	18.91
	APR	11.21	16.96	17.77	20.23
	MAY	12.47	18.03	18.62	20.97
	JUN	14.04	20.20	20.56	22.37
	JUL	14.23	19.40	19.65	21.74
	AUG	13.26	17.97	18.82	21.33
	SEP	13.33	18.46	19.31	21.88
	OCT	13.33	18.71	19.43	21.67
	NOV	12.41	17.46	18.26	20.34
	DEC	11.09	16.23	17.19	19.38
Projected	JAN 93	12.45	15.54	16.59	19.01
	FEB	12.62	17.17	18.14	20.20
	MAR	13.87	18.41	19.45	21.66
	APR	13.86	18.41	19.45	21.66
	MAY	13.86	18.41	19.45	21.66
	QTR1 FY94	14.86	19.38	20.47	22.77
	QTR2 FY94	15.35	19.87	20.99	23.35
	QTR3 FY94	14.86	19.52	20.61	22.93
	QTR4 FY94	14.85	19.51	20.60	22.92
	QTR1 FY95	15.32	19.98	21.11	23.46
	QTR2 FY95	15.56	20.23	21.37	23.75
	QTR3 FY95	15.87	20.46	21.61	24.02
	QTR4 FY95	16.29	20.89	22.07	24.53

<sup>1</sup>Historical ANS spot prices are taken from Platt's Oilgram Price Report.



## **REVENUE FORECAST: LONG-TERM OUTLOOK (FY 1996-2010)**

This section focuses on the long term from FY 1996 through FY 2010. It provides revenue projections for this period and also sets out the assumptions behind those projections for the Low, Mid, and High Scenarios.

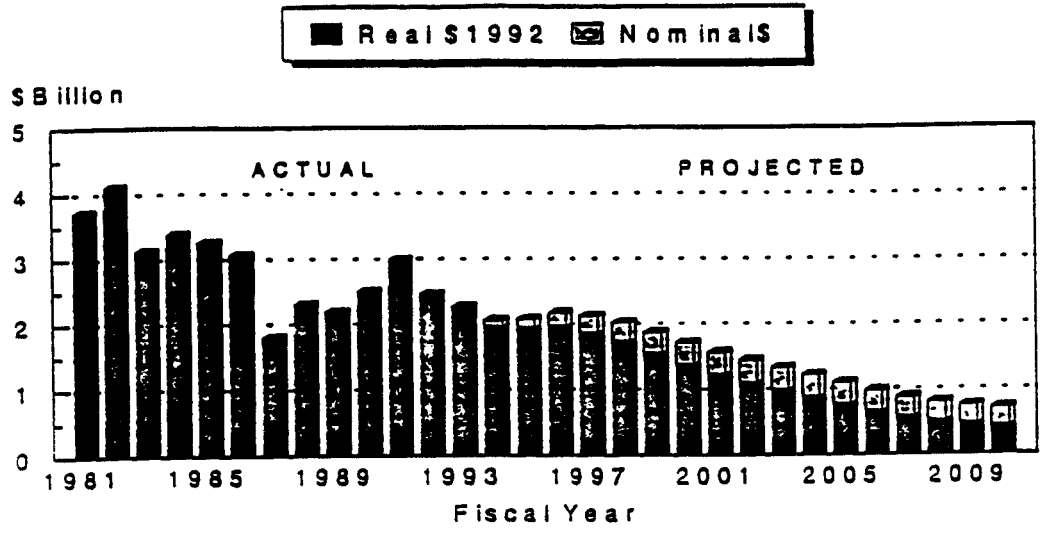
The assumptions for inflation rate, Alaska oil production, the TAPS tariff and average ANS Lower 48 price follow. The graphs on page 34 show the revenue projections for the three scenarios from FY 1981 through FY 2010 in both nominal and real dollar terms.

The following tables are then provided:

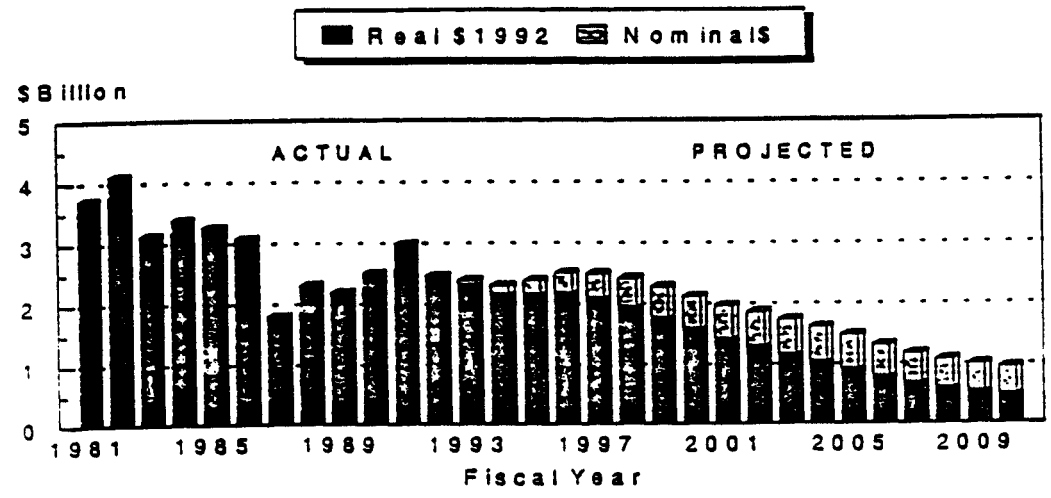
1. Detailed revenue projections for each category of revenues.
2. Petroleum production revenues by type and area of the state.
3. The expected and historical prices from FY 1992 - 2010 for ANS Wellhead and WTI.
4. Simulated production by field.

# General Fund Unrestricted Revenue Projections FY 1981 - 2010

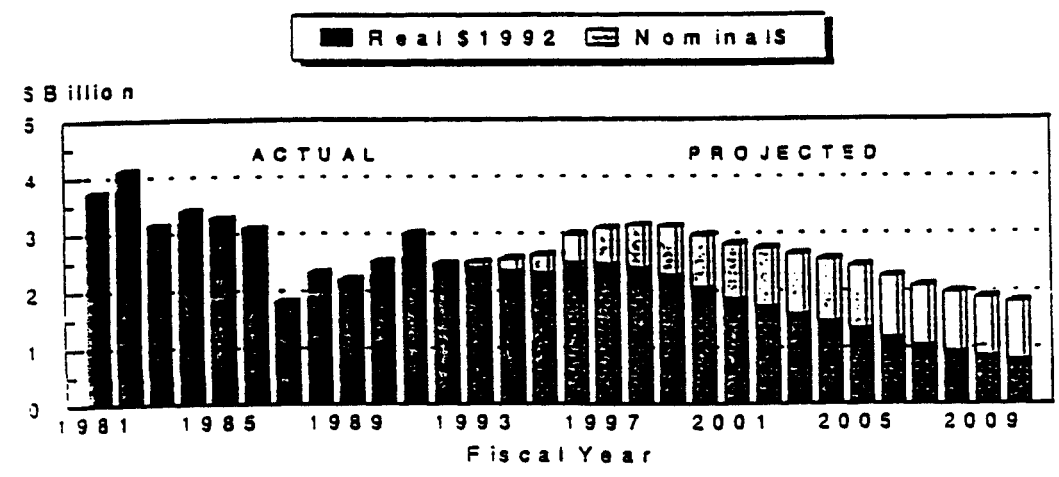
## Low Scenario



## Mid Scenario



## High Scenario



## Spring 1993 Forecast Assumptions

The following tables are part of the output from the Department of Revenue's simulation model, the Long-Run Fiscal Model (LRFM). All pertinent assumptions and footnotes are presented below:

- 1) Investment earnings are a function of expenditures and the resulting general investment fund balance.  
(Note: Permanent Fund earnings are excluded from the long-range revenue forecast.)  
Expenditures were assumed to increase at the scenario-specific inflation rate from the FY 92 base year.  
The real rate of return for investment earnings was assumed at 3.00% for all cases.
- 2) Non-petroleum/non-interest revenues beyond FY 93 were assumed to increase at the scenario-specific inflation rate.

Table 21

FY	INFLATION RATE (%)			ALASKA PRODUCTION (Millions of Barrels/day)			TAPS TARIFF (\$/bbl)			AVERAGE LOWER 48 (\$/bbl)		
	Low	Mid	High	Low	Mid	High	Low	Mid	High	Low	Mid	High
1992	3.09	3.09	3.09	1.833	1.833	1.833	3.602	3.602	3.602	16.88	16.88	16.88
1993	2.56	3.39	4.33	1.744	1.744	1.744	3.196	3.196	3.196	17.75	18.01	18.30
1994	2.62	3.67	4.56	1.746	1.746	1.746	2.975	2.988	3.000	16.93	18.38	19.71
1995	2.62	3.67	4.56	1.713	1.713	1.713	2.967	3.006	3.015	17.47	19.24	20.52
1996	2.85	3.81	4.84	1.644	1.647	1.757	2.766	2.852	2.883	18.74	20.99	22.68
1997	2.85	3.81	4.84	1.513	1.517	1.675	2.733	2.825	2.750	19.85	22.68	24.74
1998	2.85	3.81	4.84	1.387	1.392	1.595	2.577	2.688	2.658	20.42	23.78	26.20
1999	2.85	3.81	4.84	1.278	1.285	1.528	2.757	2.902	2.854	21.00	24.93	27.74
2000	2.85	3.81	4.84	1.152	1.158	1.382	2.998	3.184	3.078	21.60	26.14	29.38
2001	3.04	3.94	5.01	1.048	1.053	1.269	3.220	3.436	3.344	22.25	27.31	31.32
2002	3.04	3.94	5.01	0.971	0.985	1.179	3.461	3.706	3.624	22.93	28.53	33.38
2003	3.04	3.94	5.01	0.881	0.899	1.080	3.704	3.985	3.906	23.63	29.80	35.58
2004	3.04	3.94	5.01	0.804	0.824	1.005	4.021	4.343	4.251	24.34	31.13	37.92
2005	3.04	3.94	5.01	0.721	0.745	0.919	4.428	4.805	4.686	25.08	32.51	40.42
2006	3.04	3.94	5.01	0.631	0.653	0.819	4.942	5.388	5.220	25.84	33.96	43.08
2007	3.04	3.94	5.01	0.552	0.574	0.732	5.437	5.694	5.757	26.63	35.48	45.92
2008	3.04	3.94	5.01	0.495	0.514	0.660	5.967	6.608	6.372	27.44	37.06	48.95
2009	3.04	3.94	5.01	0.442	0.457	0.592	6.487	7.251	6.994	28.27	38.71	52.17
2010	3.04	3.94	5.01	0.397	0.410	0.533	7.085	7.981	7.716	29.13	40.44	55.57

Table 22

# Low Scenario Detailed Revenue Projections

(Millions of Dollars)

(1)	(2)	(3)	(4)	(5)	(6)	(7)	(8)	(9)	(10)	(11)	(12)
YR	SEVERANCE TAX	PROPERTY TAX	OIL&GAS INCTAX	GROSS ROYALTIES	MINERAL RENTS	BONUS SALES	SPECIAL PETRO SETTLEMENTS	TOTAL PETROLEUM REVENUES	NON-PETR NON-INTR REVENUES	GEN FUND INTEREST REVENUES	TOTAL REVS W/ PERM FND DEDICATION
81	1170.20	143.00	860.10	1501.60	7.90	14.10	0.00	3696.90	186.10	227.80	4110.80
82	1581.70	142.70	668.90	1553.20	26.40	10.30	0.00	3983.20	209.00	324.70	4516.90
83	1493.70	152.60	236.00	1447.40	54.20	73.10	0.00	3457.00	228.60	375.80	4061.40
84	1393.10	131.00	265.10	1409.00	21.90	16.70	0.00	3236.80	245.80	282.70	3765.30
85	1389.40	128.40	168.60	1390.30	23.70	23.60	0.00	3124.00	283.00	233.50	3640.50
86	1107.90	113.50	133.90	1098.20	44.50	70.10	460.70	3028.80	222.40	195.20	3446.40
87	648.50	102.50	120.40	591.60	29.10	1.00	85.20	1578.30	243.00	161.90	1983.20
88	818.70	96.20	158.00	953.50	24.20	11.30	329.00	2390.90	223.60	132.60	2747.10
89	698.80	89.70	166.00	818.70	18.00	23.00	259.70	2073.90	245.10	100.70	2419.70
90	1001.60	89.80	117.20	1004.43	21.00	0.00	156.80	2390.83	271.33	117.90	2780.06
91	1284.80	85.00	185.10	1292.83	21.30	38.30	398.59	3305.92	291.04	125.00	3721.96
92	1053.20	69.00	165.50	935.78	17.10	5.25	447.61	2693.44	353.40	101.80	3148.64
93	1003.10	62.80	150.00	991.20	19.30	76.30	9.40	2312.10	258.31	61.00	2631.41
94	930.75	59.60	106.00	948.13	21.85	0.00	9.40	2075.73	200.62	39.00	2315.35
95	944.98	56.60	106.00	971.68	20.76	0.00	9.40	2109.42	209.58	34.50	2353.50
96	994.01	52.70	104.00	1029.45	19.72	0.00	9.40	2209.28	215.87	41.33	2466.48
97	967.72	49.00	94.00	984.45	18.74	0.00	13.40	2127.31	222.34	43.17	2392.82
98	904.30	45.10	91.00	946.47	17.80	0.00	13.40	2018.07	229.01	41.80	2288.89
99	792.21	41.60	86.00	898.41	16.91	0.00	13.40	1848.53	235.88	39.94	2124.35
00	688.60	38.20	81.00	828.97	16.06	0.00	13.40	1666.23	242.96	36.93	1946.12
01	595.24	34.80	75.00	768.01	15.26	0.00	13.40	1501.71	250.25	33.77	1785.73
02	523.74	31.70	70.00	724.77	14.50	0.00	0.00	1364.71	257.76	30.93	1653.40
03	441.86	28.60	64.00	671.87	13.77	0.00	0.00	1220.10	265.49	28.83	1514.42
04	369.86	26.00	58.00	622.28	13.08	0.00	0.00	1089.22	273.45	26.35	1389.03
05	301.93	23.40	52.00	561.66	12.43	0.00	0.00	951.42	281.66	24.14	1257.22
06	225.88	21.30	46.00	495.79	11.81	0.00	0.00	800.78	290.11	21.85	1112.74
07	161.85	19.20	44.00	440.29	11.22	0.00	0.00	676.56	298.81	19.34	994.71
08	116.54	17.30	41.00	402.59	10.66	0.00	0.00	588.09	307.78	17.31	913.17
09	87.97	15.70	37.00	366.39	10.12	0.00	0.00	517.18	317.01	15.90	850.10
10	70.73	14.20	35.00	334.46	9.62	0.00	0.00	464.01	326.52	14.85	805.38

(13)	(14)	(15)	(16)	(17)	(18)	(19)	(20)	(21)
	TOTAL REVS W/PERM FND	PUB SCH	NPR-A	OTHER	PERM FUND	CONSTITUTIONAL BUDGET RESERVE		NET GEN FUND UNRESTRD REVENUES
FY	DEDICATION	FUND	FUND	FUNDS	DEDICATN	FUND	NOM \$	REAL 1222\$
81	4110.80	7.50	0.00	74.30	385.10	0.00	3718.20	
82	4516.90	8.00	0.00	0.00	400.50	0.00	4108.40	
83	4061.40	9.40	0.00	0.00	421.00	0.00	3631.00	
84	3765.30	9.00	0.00	0.00	366.20	0.00	3390.10	
85	3640.50	7.10	5.40	0.00	368.00	0.00	3260.00	
86	3446.40	6.50	41.00	0.00	323.40	0.00	3075.50	
87	1983.20	3.30	9.90	0.00	170.60	0.00	1799.40	
88	2747.10	6.60	1.00	15.80	417.90	0.00	2305.80	
89	2419.70	4.30	0.80	0.00	228.40	0.00	2186.20	
90	2780.06	5.13	0.60	0.00	267.10	0.00	2507.23	
91	3721.96	8.83	0.37	0.00	435.00	291.20	2986.56	
92	3148.64	15.04	0.13	0.00	337.80	333.07	2462.60	2462.60
93	2631.41	5.43	0.40	0.00	300.27	57.20	2268.11	2211.51
94	2315.35	4.85	0.40	0.00	251.61	0.00	2058.49	1955.92
95	2353.50	4.96	0.30	7.00	257.44	0.00	2083.80	1929.47
96	2466.48	5.25	0.10	7.00	272.16	0.00	2181.97	1964.39
97	2392.82	5.02	0.00	7.00	260.23	0.00	2120.57	1856.21
98	2288.89	4.82	0.00	10.00	250.13	0.00	2023.94	1722.53
99	2124.35	4.58	0.00	10.00	237.43	0.00	1872.34	1549.35
00	1946.12	4.23	0.00	10.00	219.20	0.00	1712.69	1377.97
01	1785.73	3.92	0.00	10.00	203.18	0.00	1568.63	1224.85
02	1653.40	3.70	0.00	10.00	191.77	0.00	1447.93	1097.27
03	1514.42	3.43	0.00	0.00	177.86	0.00	1333.13	980.49
04	1389.03	3.18	0.00	0.00	164.81	0.00	1221.04	871.57
05	1257.22	2.87	0.00	0.00	148.92	0.00	1105.43	765.78
06	1112.74	2.54	0.00	0.00	131.67	0.00	978.53	657.89
07	994.71	2.26	0.00	0.00	117.12	0.00	875.33	571.15
08	913.17	2.07	0.00	0.00	107.20	0.00	803.90	509.08
09	850.10	1.88	0.00	0.00	97.67	0.00	750.55	461.28
10	805.38	1.72	0.00	0.00	89.25	0.00	714.41	426.12

# Mid Scenario Detailed Revenue Projections

(Millions on Dollars)

(1)	(2)	(3)	(4)	(5)	(6)	(7)	(8)	(9)	(10)	(11)	(12)
EX	SEVERANCE TAX	PROPERTY TAX	OIL & GAS INC. TAX	GROSS ROYALTIES	MINERAL RENTS	BONUS SALES	SPECIAL PETRO SETTLEMENTS	TOTAL PETROLEUM REVENUES	NON-PETR NON-INTR REVENUES	GEN FUND INTEREST REVENUES	TOTAL REVS W/ PERM FND DEDICATION
81	1170.20	143.00	860.10	1501.60	7.90	14.10	0.00	3696.90	186.10	227.80	4110.80
82	1581.70	142.70	668.90	1553.20	26.40	10.30	0.00	3983.20	209.00	324.70	4516.90
83	1493.70	152.60	236.00	1447.40	54.20	73.10	0.00	3457.00	228.60	375.80	4061.40
84	1393.10	131.00	265.10	1409.00	21.90	16.70	0.00	3236.80	245.80	282.70	3765.30
85	1389.40	128.40	168.60	1390.30	23.70	23.60	0.00	3124.00	283.00	233.50	3640.50
86	1107.90	113.50	133.90	1098.20	44.50	70.10	460.70	3028.80	222.40	195.20	3446.40
87	648.50	102.50	120.40	591.60	29.10	1.00	85.20	1578.30	243.00	161.90	1983.20
88	818.70	96.20	158.00	953.50	24.20	11.30	329.00	2390.90	223.60	132.60	2747.10
89	698.80	89.70	166.00	818.70	18.00	23.00	259.70	2073.90	245.10	100.70	2419.70
90	1001.60	89.80	117.20	1004.43	21.00	0.00	156.80	2390.83	271.33	117.90	2780.06
91	1284.80	85.00	185.10	1292.83	21.30	38.30	398.59	3305.92	291.04	125.00	3721.96
92	1053.20	69.00	165.50	935.78	17.10	5.25	447.61	2693.44	353.40	101.80	3148.64
93	1021.40	62.80	220.00	1012.92	19.30	76.30	9.40	2422.12	271.37	63.00	2756.49
94	1029.57	59.60	139.00	1067.11	21.85	0.00	9.40	2326.53	213.20	53.70	2593.43
95	1060.74	56.60	139.00	1111.93	20.76	0.00	9.40	2398.43	221.24	79.00	2698.67
96	1133.58	52.70	131.00	1193.20	19.72	0.00	9.40	2539.60	227.88	69.97	2837.45
97	1129.93	49.00	128.00	1165.83	18.73	0.00	13.40	2504.89	234.71	73.79	2813.40
98	1078.30	45.10	120.00	1143.62	17.80	0.00	13.40	2418.22	241.75	73.04	2733.01
99	966.44	41.60	114.00	1112.22	16.91	0.00	13.40	2264.57	249.01	70.82	2584.39
00	858.16	38.20	111.00	1050.01	16.06	0.00	13.40	2086.83	256.48	66.66	2409.97
01	753.13	34.80	108.00	989.45	15.26	0.00	13.40	1914.04	264.17	62.02	2240.23
02	688.79	31.70	103.00	959.09	14.50	0.00	0.00	1797.08	272.10	57.52	2126.70
03	597.84	28.60	94.00	909.06	13.77	0.00	0.00	1643.27	280.26	54.88	1978.41
04	514.16	26.00	91.00	862.20	13.08	0.00	0.00	1506.44	288.67	50.89	1846.00
05	429.89	23.40	89.00	797.41	12.43	0.00	0.00	1352.13	297.33	47.39	1696.84
06	320.87	21.30	84.00	718.60	11.81	0.00	0.00	1156.94	306.25	43.50	1506.33
07	228.27	19.20	79.00	653.25	11.22	0.00	0.00	990.94	315.44	38.50	1344.87
08	164.40	17.30	74.00	606.07	10.66	0.00	0.00	872.43	324.90	34.29	1231.62
09	124.18	15.70	69.00	558.49	10.12	0.00	0.00	777.79	334.65	31.37	1143.51
10	101.24	14.20	65.00	518.09	9.62	0.00	0.00	708.15	344.68	29.18	1082.01

(13)	(14)	(15)	(16)	(17)	(18)	(19)	(20)	(21)
	TOTAL REVS W/ PERM FND	PUB SCH	NPR-A	OTHER	PERM FUND	CONSTITUTIONAL BUDGET RESERVE	NET GEN FUND UNRESTRD REVENUES	
FY	DEDICATION	FUND	FUND	FUNDS	DEDICATN	FUND	NOMI	REAL 1992\$
81	4110.80	7.50	0.00	74.30	385.10	0.00	3718.20	
82	4516.90	8.00	0.00	0.00	400.50	0.00	4108.40	
83	4061.40	9.40	0.00	0.00	421.00	0.00	3631.00	
84	3765.30	9.00	0.00	0.00	366.20	0.00	3390.10	
85	3640.50	7.10	5.40	0.00	368.00	0.00	3260.00	
86	3446.40	6.50	41.00	0.00	323.40	0.00	3075.50	
87	1983.20	3.30	9.90	0.00	170.60	0.00	1799.40	
88	2747.10	6.60	1.00	15.80	417.90	0.00	2305.80	
89	2419.70	4.30	0.80	0.00	228.40	0.00	2186.20	
90	2780.06	5.13	0.60	0.00	267.10	0.00	2507.23	
91	3721.96	8.83	0.37	0.00	435.00	291.20	2986.56	
92	3148.64	15.04	0.13	0.00	337.80	333.07	2462.60	2462.60
93	2756.49	5.54	0.40	0.00	307.15	57.20	2386.20	2308.02
94	2593.43	5.44	0.40	0.00	283.78	0.00	2303.81	2149.37
95	2698.67	5.66	0.30	7.00	295.18	0.00	2390.59	2151.25
96	2837.45	6.06	0.10	7.00	316.09	0.00	2508.20	2174.24
97	2813.40	5.92	0.00	7.00	308.70	0.00	2491.78	2080.67
98	2733.01	5.81	0.00	10.00	302.67	0.00	2414.53	1942.11
99	2584.39	5.65	0.00	10.00	294.25	0.00	2274.49	1762.28
00	2409.97	5.33	0.00	10.00	277.82	0.00	2116.82	1579.87
01	2240.23	5.02	0.00	10.00	261.83	0.00	1963.38	1409.83
02	2126.70	4.87	0.00	10.00	253.72	0.00	1858.11	1283.69
03	1978.41	4.61	0.00	0.00	240.49	0.00	1733.91	1152.10
04	1846.00	4.38	0.00	0.00	228.10	0.00	1613.52	1031.85
05	1696.84	4.05	0.00	0.00	211.04	0.00	1481.75	911.68
06	1506.33	3.65	0.00	0.00	190.34	0.00	1312.34	776.85
07	1344.87	3.32	0.00	0.00	173.16	0.00	1168.39	665.43
08	1231.62	3.08	0.00	0.00	160.72	0.00	1067.82	585.11
09	1143.51	2.84	0.00	0.00	148.18	0.00	992.49	523.23
10	1082.01	2.64	0.00	0.00	137.52	0.00	941.85	477.72

# High Scenario Detailed Revenue Projections (Millions on Dollars)

(1)	(2)	(3)	(4)	(5)	(6)	(7)	(8)	(9)	(10)	(11)	(12)
	SEVERANCE	PROPERTY	OIL & GAS	GROSS	MINERAL	BONUS	SPECIAL	TOTAL	NON-PETR	GEN FUND	TOTAL REVS
EY	TAX	TAX	INC TAX	ROYALTIES	RENTS	SALES	PETRO	PETROLEUM	NON-INTR	INTEREST	W/ PERM FND
							SETTLEMENTS	REVENUES	REVENUES	REVENUES	DEDICATION
81	1170.20	143.00	860.10	1501.60	7.90	14.10	0.00	3696.90	186.10	227.80	4110.80
82	1581.70	142.70	668.90	1553.20	26.40	10.30	0.00	3983.20	209.00	324.70	4516.90
83	1493.70	152.60	236.00	1447.40	54.20	73.10	0.00	3457.00	228.60	375.80	4061.40
84	1393.10	131.00	265.10	1409.00	21.90	16.70	0.00	3236.80	245.80	282.70	3765.30
85	1389.40	128.40	168.60	1390.30	23.70	23.60	0.00	3124.00	283.00	233.50	3640.50
86	1107.90	113.50	133.90	1098.20	44.50	70.10	460.70	3028.80	222.40	195.20	3446.40
87	648.50	102.50	120.40	591.60	29.10	1.00	85.20	1578.30	243.00	161.90	1983.20
88	818.70	96.20	158.00	953.50	24.20	11.30	329.00	2390.90	223.60	132.60	2747.10
89	698.80	89.70	166.00	818.70	18.00	23.00	259.70	2073.90	245.10	100.70	2419.70
90	1001.60	89.80	117.20	1004.43	21.00	0.00	156.80	2390.83	271.33	117.90	2780.06
91	1284.80	85.00	185.10	1292.83	21.30	38.30	398.59	3305.92	291.04	125.00	3721.96
92	1053.20	69.00	165.50	935.78	17.10	5.25	447.61	2693.44	353.40	101.80	3148.64
93	1042.30	62.80	260.00	1036.13	19.30	76.30	9.40	2506.23	292.12	65.70	2864.05
94	1125.24	59.60	178.00	1173.15	21.85	0.00	9.40	2567.24	233.84	63.90	2864.98
95	1149.89	56.60	178.00	1212.81	20.76	0.00	9.40	2627.46	241.65	89.90	2959.01
96	1345.89	52.70	173.00	1398.02	19.72	0.00	9.40	2998.73	248.90	102.26	3349.89
97	1418.38	49.00	169.00	1435.12	18.73	0.00	13.40	3103.63	256.37	115.55	3475.55
98	1441.28	45.10	167.00	1467.73	17.80	0.00	13.40	3152.31	264.06	119.51	3535.88
99	1397.57	41.60	161.00	1496.57	16.91	0.00	13.40	3127.05	271.98	121.44	3520.47
00	1285.78	38.20	154.00	1438.12	16.06	0.00	13.40	2945.56	280.14	120.46	3346.16
01	1182.97	34.80	148.00	1389.89	15.26	0.00	13.40	2784.32	288.54	114.11	3186.97
02	1135.38	31.70	141.00	1382.69	14.50	0.00	0.00	2705.27	297.20	108.48	3110.94
03	1048.54	28.60	138.00	1347.86	13.77	0.00	0.00	2576.77	306.11	106.27	2989.16
04	979.20	26.00	132.00	1328.91	13.08	0.00	0.00	2479.19	315.30	101.84	2896.33
05	902.70	23.40	129.00	1276.43	12.43	0.00	0.00	2343.96	324.76	98.49	2767.21
06	769.99	21.30	126.00	1199.74	11.81	0.00	0.00	2128.84	334.50	93.98	2557.32
07	664.23	19.20	121.00	1136.87	11.22	0.00	0.00	1952.52	344.54	86.54	2383.59
08	585.52	17.30	119.00	1089.67	10.66	0.00	0.00	1822.15	354.87	80.51	2257.53
09	530.77	15.70	111.00	1038.87	10.12	0.00	0.00	1706.46	365.52	76.18	2148.16
10	495.35	14.20	101.00	988.73	9.62	0.00	0.00	1608.90	376.48	72.49	2057.87



(13)	(14)	(15)	(16)	(17)	(18)	(19)	(20)	(21)
	TOTAL REVS W/PERM FND	PUB SCH	NPR-A	OTHER	PERM FUND	BUDGET RESERVE	CONSTITUTIONAL NET GEN FUND UNRESTRD REVENUES	
FY	DEDICATION	FUND	FUND	FUNDS	DEDICATION	FUND	NOM	REAL 1992
81	4110.80	7.50	0.00	74.30	385.10	0.00	3718.20	
82	4516.90	8.00	0.00	0.00	400.50	0.00	4108.40	
83	4061.40	9.40	0.00	0.00	421.00	0.00	3631.00	
84	3765.30	9.00	0.00	0.00	366.20	0.00	3399.10	
85	3640.50	7.10	5.40	0.00	368.00	0.00	3260.00	
86	3416.40	6.50	41.00	0.00	323.40	0.00	3075.50	
87	1983.20	3.30	9.90	0.00	170.60	0.00	1799.40	
88	2747.10	6.60	1.00	15.80	417.90	0.00	2305.80	
89	2419.70	4.30	0.80	0.00	228.40	0.00	2186.20	
90	2780.06	5.13	0.60	0.00	267.10	0.00	2507.23	
91	3721.96	8.83	0.37	0.00	435.00	291.20	2986.56	
92	3148.64	15.04	0.13	0.00	337.80	333.07	2462.60	2462.60
93	2864.05	5.66	0.40	0.00	313.09	57.20	2487.70	2384.38
94	2864.98	5.98	0.40	0.00	311.30	0.00	2547.30	2334.94
95	2959.01	6.17	0.30	7.00	321.34	0.00	2624.20	2300.43
96	3349.89	7.09	0.10	7.00	369.32	0.00	2966.58	2480.25
97	3475.55	7.27	0.00	7.00	378.73	0.00	3082.25	2458.30
98	3535.88	7.43	0.00	10.00	386.98	0.00	3131.47	2381.94
99	3520.47	7.57	0.00	10.00	394.26	0.00	3108.64	2255.32
00	3346.16	7.27	0.00	10.00	378.81	0.00	2950.08	2041.40
01	3186.97	7.03	0.00	10.00	366.04	0.00	2803.90	1847.63
02	3110.94	6.99	0.00	10.00	363.97	0.00	2729.98	1713.04
03	2989.16	6.81	0.00	0.00	354.70	0.00	2627.65	1570.12
04	2896.33	6.71	0.00	0.00	349.59	0.00	2540.03	1445.31
05	2767.21	6.44	0.00	0.00	335.75	0.00	2425.02	1314.00
06	2557.32	6.06	0.00	0.00	315.61	0.00	2235.65	1153.56
07	2383.59	5.74	0.00	0.00	299.08	0.00	2078.77	1021.41
08	2257.53	5.50	0.00	0.00	286.63	0.00	1965.40	919.60
09	2148.16	5.24	0.00	0.00	273.26	0.00	1869.66	833.05
10	2057.87	4.99	0.00	0.00	260.07	0.00	1782.81	760.67

Table 25

# Low Scenario Petroleum Production Revenue Forecast (Millions of \$)

Alaska North Slope								Cook Inlet							
Fiscal Year	Oil Royalty	Oil Severance	Cons. Tax	Hazardous Rel. Fund	Gas Royalty	Gas Severance	ANS Total	Oil Royalty	Oil Severance	Cons. Tax	Hazardous Rel. Fund	Gas Royalty	Gas Severance	Cook Inlet Total	State Total
1992	836.4	852.3	2.2	27.6	21.9	16.1	1756.3	22.3	0.0	0.1	0.7	26.8	16.0	65.9	1122.3
1993	909.1	918.0	2.1	25.9	30.7	18.5	1904.3	25.9	0.0	0.1	0.7	25.6	14.2	66.4	1270.7
1994	869.0	871.2	2.1	26.0	32.2	18.8	1819.2	24.8	0.0	0.1	0.7	22.1	11.9	58.7	1278.9
1995	889.7	885.0	2.0	25.5	34.2	19.5	1855.9	25.0	0.0	0.1	0.7	22.8	12.2	60.8	1316.7
1996	946.2	934.6	2.0	24.5	35.5	19.9	1962.7	25.0	0.0	0.1	0.7	22.8	12.2	60.8	1323.5
1997	899.9	910.5	1.8	22.5	33.7	19.2	1887.5	26.3	0.0	0.1	0.7	24.6	13.0	64.6	1352.2
1998	859.1	848.8	1.6	20.5	34.2	19.0	1783.2	27.1	0.0	0.1	0.7	26.1	13.7	67.6	1350.8
1999	811.5	739.6	1.5	18.8	33.6	17.7	1622.8	26.4	0.0	0.1	0.7	26.8	13.9	67.9	1290.6
2000	743.1	639.5	1.4	17.0	31.9	15.9	1448.7	26.4	0.0	0.1	0.6	27.6	14.2	68.9	1276.6
2001	683.4	549.1	1.2	15.3	30.7	14.4	1294.2	25.5	0.0	0.0	0.6	28.4	14.5	69.7	1243.9
2002	640.6	480.1	1.1	14.2	29.5	13.0	1178.5	25.5	0.0	0.0	0.6	29.2	14.7	70.0	1243.5
2003	588.6	401.0	1.0	12.8	27.8	11.5	1042.7	25.4	0.0	0.0	0.6	30.1	14.9	71.0	1193.7
2004	539.9	331.2	0.9	11.7	26.9	10.4	921.0	24.4	0.0	0.0	0.5	31.1	15.1	71.2	1122.1
2005	479.6	265.8	0.8	10.4	25.8	9.0	791.4	24.3	0.0	0.0	0.5	32.0	15.4	72.2	1063.6
2006	414.8	192.9	0.7	9.0	24.0	7.0	648.5	24.1	0.0	0.0	0.5	33.0	15.6	73.2	1021.7
2007	360.0	131.5	0.6	7.8	23.4	5.5	528.9	22.9	0.0	0.0	0.5	34.0	15.9	73.3	960.1
2008	322.6	88.2	0.6	7.0	22.4	4.1	444.8	22.6	0.0	0.0	0.4	35.0	16.2	74.3	919.1
2009	286.2	60.8	0.5	6.2	21.9	3.5	379.0	22.3	0.0	0.0	0.4	36.1	16.6	75.4	845.4
2010	255.2	44.3	0.4	5.5	21.2	3.2	329.8	20.9	0.0	0.0	0.4	37.1	16.9	75.4	805.2

8712

Table 26

# Mid Scenario Petroleum Production Revenue Forecast (Millions of \$)

Alaska North Slope								Cook Inlet							
Fiscal Year	Oil Royalty	Oil Severance	Cons. Tax	Hazardous Rel. Fund	Gas Royalty	Gas Severance	ANS Total	Oil Royalty	Oil Severance	Cons. Tax	Hazardous Rel. Fund	Gas Royalty	Gas Severance	Cook Inlet Total	State Total
1992	836.4	852.3	2.2	27.6	21.9	16.1	1756.4	22.3	0.0	0.1	0.7	26.8	16.0	65.9	1822.3
1993	930.1	936.1	2.1	25.9	33.0	20.2	1947.6	26.5	0.0	0.1	0.7	23.0	12.7	63.0	2010.7
1994	980.2	966.6	2.1	26.0	36.8	21.4	2032.9	26.6	0.0	0.1	0.7	23.6	12.7	63.7	2096.7
1995	1020.5	996.8	2.0	25.5	39.6	22.5	2106.8	27.1	0.0	0.1	0.7	24.7	13.2	65.9	2172.7
1996	1099.8	1069.8	2.0	24.6	41.5	23.3	2260.9	27.1	0.0	0.1	0.7	24.7	13.2	65.9	2266.8
1997	1069.4	1067.6	1.8	22.6	40.3	22.9	2224.5	29.0	0.0	0.1	0.7	27.1	14.3	71.2	2295.8
1998	1042.0	1016.8	1.7	20.6	41.7	23.1	2145.9	30.5	0.0	0.1	0.7	29.4	15.4	76.0	2221.9
1999	1009.1	907.2	1.5	18.9	42.1	22.1	2000.9	30.3	0.0	0.1	0.7	30.8	16.0	77.8	2078.7
2000	946.0	802.1	1.4	17.0	40.9	20.4	1827.7	30.9	0.0	0.1	0.6	32.3	16.6	80.4	1908.2
2001	885.2	699.7	1.2	15.4	40.0	18.8	1660.3	30.4	0.0	0.0	0.6	33.8	17.3	82.2	1786.6
2002	853.9	637.6	1.2	14.4	39.0	17.3	1563.3	30.8	0.0	0.0	0.6	35.4	17.8	84.6	1629.9
2003	803.6	549.3	1.0	13.1	37.4	15.5	1420.0	31.2	0.0	0.0	0.6	36.9	18.3	86.9	1506.9
2004	756.4	467.6	1.0	12.0	36.9	14.3	1288.1	30.4	0.0	0.0	0.5	38.6	18.8	88.5	1376.7
2005	690.5	385.7	0.9	10.8	36.1	12.6	1136.2	30.6	0.0	0.0	0.5	40.3	19.4	90.1	1226.3
2006	611.5	280.1	0.8	9.4	34.2	10.1	946.1	30.8	0.0	0.0	0.5	42.1	20.0	93.2	1039.5
2007	545.5	190.3	0.7	8.2	34.1	8.0	786.8	29.7	0.0	0.0	0.5	44.0	20.6	94.7	881.5
2008	497.2	128.6	0.6	7.3	33.2	6.2	673.1	29.7	0.0	0.0	0.4	45.9	21.3	97.6	770.5
2009	447.8	89.4	0.5	6.4	33.1	5.4	582.5	29.7	0.0	0.0	0.4	48.0	22.0	100.1	682.7
2010	407.1	66.9	0.5	5.7	32.7	4.9	517.8	28.2	0.0	0.0	0.4	50.1	22.8	101.5	619.3

966.6

Table 27

# High Scenario Petroleum Production Revenue Forecast (Millions of \$)

Alaska North Slope								Cook Inlet							
Fiscal Year	Oil Royalty	Oil Severance	Cons. Tax	Hazardous Rel. Fund	Gas Royalty	Gas Severance	ANS Total	Oil Royalty	Oil Severance	Cons. Tax	Hazardous Rel. Fund	Gas Royalty	Gas Severance	Cook Inlet Total	State Total
1992	836.4	852.3	2.2	27.6	21.9	16.1	1756.4	22.3	0.0	0.1	0.7	26.8	16.0	65.9	1822.3
1993	952.6	956.5	2.1	25.9	33.9	20.8	1991.8	26.5	0.0	0.1	0.7	23.0	12.7	60.0	2052.3
1994	1079.3	1059.1	2.1	26.0	40.9	23.8	2223.2	28.0	0.0	0.1	0.7	24.9	13.5	62.2	2285.4
1995	1114.8	1083.0	2.0	25.5	43.5	24.7	2293.6	28.5	0.0	0.1	0.7	26.0	13.9	69.1	2362.7
1996	1297.5	1276.2	2.1	26.3	46.1	26.7	2674.8	28.5	0.0	0.1	0.7	26.0	13.9	69.1	2749.9
1997	1329.9	1348.2	2.0	25.1	45.6	27.1	2777.8	30.8	0.0	0.1	0.7	28.8	15.2	75.7	2853.5
1998	1356.1	1369.9	1.9	23.9	47.3	28.3	2827.5	32.8	0.0	0.1	0.7	31.5	16.5	81.6	2909.0
1999	1382.0	1326.4	1.8	22.8	48.3	28.5	2809.0	32.9	0.0	0.1	0.7	33.4	17.3	84.3	2893.7
2000	1321.4	1217.3	1.7	20.6	47.6	27.3	2635.9	33.8	0.0	0.1	0.6	35.3	18.2	88.0	2723.9
2001	1271.0	1116.5	1.5	18.7	47.8	26.5	2461.0	33.7	0.0	0.0	0.6	37.4	19.2	90.9	2551.9
2002	1260.1	1070.1	1.4	17.5	47.9	25.7	2422.7	34.8	0.0	0.0	0.6	39.9	20.1	93.3	2416.0
2003	1222.4	985.2	1.3	16.0	47.1	24.5	2296.4	35.9	0.0	0.0	0.6	42.5	21.0	100.0	2396.4
2004	1200.2	916.5	1.2	14.9	47.7	24.0	2204.5	35.7	0.0	0.0	0.5	45.3	22.1	103.7	2308.2
2005	1143.4	841.1	1.1	13.5	48.0	23.2	2070.4	36.7	0.0	0.0	0.5	48.3	23.2	108.7	2179.1
2006	1063.6	710.7	1.0	12.0	47.0	21.3	1855.6	37.6	0.0	0.0	0.5	51.5	24.4	114.5	1969.7
2007	996.7	606.0	0.9	10.7	48.3	20.5	1683.0	37.0	0.0	0.0	0.5	54.9	25.7	118.1	1801.7
2008	944.9	528.1	0.8	9.6	48.5	19.4	1551.8	37.8	0.0	0.0	0.4	58.5	27.1	123.4	1675.2
2009	888.2	472.9	0.7	8.6	49.8	19.5	1439.0	38.6	0.0	0.0	0.4	62.4	28.7	130.0	1569.6
2010	834.2	436.7	0.6	7.7	50.7	19.7	1349.6	37.4	0.0	0.0	0.4	66.5	30.3	134.5	1484.1

Table 28

**Projected and Historical Crude Oil Prices  
Alaska North Slope Crude and Domestic Marker  
In 1992 Constant \$/barrel**

Fiscal Year	Low Scenario		Mid Scenario		High Scenario	
	WTI	ANS at Wellhead	WTI	ANS at Wellhead	WTI	ANS at Wellhead
1992	20.62	11.21	20.62	11.21	20.62	11.21
1993	19.99	12.35	20.10	12.49	20.20	12.65
1994	18.77	11.71	20.00	12.75	21.08	13.73
1995	18.87	11.93	20.20	13.05	20.99	13.81
1996	19.69	13.03	21.23	14.31	22.12	15.17
1997	20.27	13.72	22.09	15.28	23.02	16.20
1998	20.27	13.94	22.31	15.68	23.25	16.68
1999	20.27	13.76	22.54	15.63	23.48	16.72
2000	20.27	13.59	22.76	15.64	23.72	16.83
2001	20.27	13.45	22.88	15.61	24.07	17.04
2002	20.27	13.28	22.99	15.56	24.44	17.23
2003	20.27	13.11	23.11	15.51	24.80	17.44
2004	20.27	12.88	23.22	15.41	25.17	17.60
2005	20.27	12.61	23.34	15.29	25.55	17.76
2006	20.27	12.28	23.45	15.09	25.93	17.88
2007	20.27	12.10	23.57	15.04	26.32	18.12
2008	20.27	11.86	23.69	14.91	26.72	18.31
2009	20.27	11.68	23.81	14.83	27.12	18.55
2010	20.27	11.48	23.93	14.74	27.51	18.76

Table 29

Low Scenario Simulated Oil Production  
(Millions of barrels/day)

Fiscal Year	NGI's	Prudhoe	Kuparuk	Milne Point	Endicott	Libburne	West Sak	North Star	Niakuk	Point McIntyre	Sag Delta	Schrader Bluff	West Beach	Total ANS	Cook Inlet	State Total
1992	0.069	1.239	0.316	0.017	0.107	0.037	0.000	0.000	0.000	0.000	0.004	0.003	0.000	1.792	0.042	1.833
1993	0.073	1.141	0.321	0.016	0.114	0.031	0.000	0.000	0.000	0.000	0.003	0.003	0.001	1.703	0.041	1.744
1994	0.075	1.115	0.310	0.017	0.099	0.027	0.000	0.000	0.000	0.054	0.002	0.003	0.003	1.704	0.042	1.746
1995	0.076	1.063	0.310	0.015	0.089	0.019	0.000	0.000	0.010	0.083	0.001	0.002	0.006	1.674	0.039	1.713
1996	0.072	0.990	0.275	0.015	0.094	0.017	0.012	0.000	0.020	0.103	0.001	0.002	0.006	1.606	0.038	1.644
1997	0.065	0.906	0.248	0.011	0.087	0.016	0.012	0.000	0.021	0.103	0.001	0.002	0.005	1.476	0.037	1.513
1998	0.063	0.831	0.221	0.009	0.085	0.014	0.012	0.000	0.019	0.093	0.000	0.002	0.004	1.352	0.035	1.387
1999	0.061	0.717	0.191	0.008	0.083	0.013	0.019	0.049	0.016	0.084	0.000	0.001	0.003	1.244	0.034	1.278
2000	0.056	0.632	0.171	0.007	0.070	0.011	0.025	0.055	0.013	0.075	0.000	0.001	0.003	1.120	0.032	1.152
2001	0.053	0.560	0.155	0.006	0.061	0.009	0.037	0.055	0.011	0.068	0.000	0.001	0.002	1.017	0.031	1.048
2002	0.050	0.499	0.147	0.005	0.053	0.008	0.050	0.055	0.009	0.062	0.000	0.001	0.002	0.941	0.030	0.971
2003	0.046	0.438	0.135	0.004	0.046	0.007	0.063	0.049	0.008	0.053	0.000	0.001	0.002	0.853	0.028	0.881
2004	0.044	0.389	0.124	0.004	0.039	0.006	0.075	0.041	0.008	0.045	0.000	0.001	0.001	0.777	0.027	0.804
2005	0.042	0.339	0.116	0.003	0.034	0.005	0.075	0.033	0.007	0.039	0.000	0.001	0.001	0.695	0.026	0.721
2006	0.039	0.287	0.108	0.002	0.029	0.003	0.071	0.027	0.007	0.033	0.000	0.001	0.001	0.607	0.024	0.631
2007	0.037	0.242	0.099	0.000	0.025	0.000	0.064	0.025	0.006	0.028	0.000	0.001	0.001	0.529	0.023	0.552
2008	0.035	0.212	0.094	0.000	0.022	0.000	0.058	0.022	0.005	0.024	0.000	0.001	0.001	0.473	0.022	0.495
2009	0.034	0.190	0.086	0.000	0.015	0.000	0.052	0.019	0.004	0.020	0.000	0.001	0.001	0.422	0.020	0.442
2010	0.033	0.173	0.077	0.000	0.008	0.000	0.047	0.016	0.003	0.017	0.000	0.000	0.001	0.378	0.019	0.397

Table 30

### Mid Scenario Simulated Oil Production (Millions of barrels/day)

Fiscal Year	NGI's	Prudhoe	Kuparuk	Milne Point	Endicott	Lisburne	West Sak	North Star	Niakuk	Point McIntyre	Sag Delta	Schrader Bluff	West Beach	Total ANS	Cook Inlet	State Total
1992	0.069	1.239	0.316	0.017	0.107	0.037	0.000	0.000	0.000	0.000	0.004	0.003	0.000	1.792	0.042	1.833
1993	0.073	1.141	0.321	0.016	0.114	0.031	0.000	0.000	0.000	0.000	0.003	0.003	0.001	1.703	0.041	1.744
1994	0.075	1.115	0.310	0.017	0.099	0.027	0.000	0.000	0.000	0.054	0.002	0.003	0.003	1.704	0.042	1.746
1995	0.076	1.063	0.310	0.015	0.089	0.019	0.000	0.000	0.010	0.083	0.001	0.002	0.006	1.674	0.039	1.713
1996	0.072	0.990	0.275	0.015	0.097	0.017	0.012	0.000	0.020	0.103	0.001	0.002	0.006	1.609	0.038	1.647
1997	0.065	0.906	0.248	0.011	0.092	0.016	0.012	0.000	0.021	0.103	0.001	0.002	0.005	1.480	0.037	1.517
1998	0.063	0.831	0.221	0.009	0.090	0.014	0.012	0.000	0.019	0.093	0.000	0.002	0.004	1.357	0.035	1.392
1999	0.061	0.717	0.191	0.008	0.089	0.013	0.019	0.049	0.016	0.084	0.000	0.001	0.003	1.251	0.034	1.285
2000	0.056	0.632	0.171	0.007	0.076	0.011	0.025	0.055	0.013	0.075	0.000	0.001	0.003	1.126	0.032	1.158
2001	0.053	0.560	0.155	0.006	0.065	0.009	0.037	0.055	0.011	0.068	0.000	0.001	0.002	1.022	0.031	1.053
2002	0.050	0.499	0.147	0.005	0.057	0.008	0.050	0.055	0.009	0.072	0.000	0.001	0.002	0.955	0.030	0.985
2003	0.046	0.438	0.135	0.004	0.049	0.007	0.063	0.049	0.008	0.067	0.000	0.001	0.002	0.871	0.028	0.899
2004	0.044	0.389	0.124	0.004	0.042	0.006	0.075	0.041	0.008	0.063	0.000	0.001	0.001	0.797	0.027	0.824
2005	0.042	0.339	0.116	0.003	0.037	0.005	0.075	0.033	0.007	0.060	0.000	0.001	0.001	0.719	0.026	0.745
2006	0.039	0.287	0.108	0.003	0.031	0.004	0.071	0.027	0.007	0.052	0.000	0.001	0.001	0.629	0.024	0.653
2007	0.037	0.242	0.099	0.000	0.027	0.004	0.064	0.026	0.006	0.044	0.000	0.001	0.001	0.551	0.023	0.574
2008	0.035	0.212	0.094	0.000	0.023	0.002	0.058	0.023	0.005	0.038	0.000	0.001	0.001	0.492	0.022	0.514
2009	0.034	0.190	0.086	0.000	0.016	0.000	0.052	0.021	0.004	0.033	0.000	0.001	0.001	0.437	0.020	0.457
2010	0.033	0.173	0.077	0.000	0.009	0.000	0.047	0.018	0.003	0.028	0.000	0.000	0.001	0.391	0.019	0.410

Table 31

### High Scenario Simulated Oil Production (Millions of barrels/day)

Fiscal Year	NGI's	Prudhoe	Kuparuk	Milne Point	Endicott	Liburne	West Sak	North Star	Niakuk	Point McIntyre	Sag Delta	Schrader Bluff	West Beach	Total ANS	Cook Inlet	State Total
1992	0.069	1.239	0.316	0.017	0.107	0.037	0.000	0.000	0.000	0.000	0.004	0.003	0.000	1.792	0.042	1.833
1993	0.073	1.141	0.321	0.016	0.114	0.031	0.000	0.000	0.000	0.000	0.003	0.003	0.001	1.703	0.041	1.744
1994	0.075	1.115	0.310	0.017	0.099	0.027	0.000	0.000	0.000	0.054	0.002	0.003	0.003	1.704	0.042	1.746
1995	0.076	1.063	0.310	0.015	0.089	0.019	0.000	0.000	0.010	0.083	0.001	0.002	0.006	1.674	0.039	1.713
1996	0.072	1.093	0.280	0.015	0.098	0.017	0.012	0.000	0.020	0.103	0.001	0.002	0.006	1.719	0.038	1.757
1997	0.065	1.056	0.255	0.011	0.093	0.016	0.012	0.000	0.021	0.103	0.001	0.002	0.005	1.638	0.037	1.675
1998	0.063	1.023	0.230	0.009	0.092	0.014	0.012	0.000	0.019	0.093	0.000	0.002	0.004	1.560	0.035	1.595
1999	0.061	0.948	0.202	0.008	0.091	0.013	0.019	0.049	0.016	0.084	0.000	0.001	0.003	1.494	0.034	1.528
2000	0.056	0.844	0.182	0.007	0.077	0.011	0.025	0.055	0.013	0.075	0.000	0.001	0.003	1.350	0.032	1.382
2001	0.053	0.755	0.164	0.006	0.067	0.009	0.037	0.055	0.011	0.068	0.000	0.001	0.002	1.228	0.031	1.259
2002	0.050	0.679	0.155	0.005	0.058	0.008	0.050	0.055	0.009	0.077	0.000	0.001	0.002	1.149	0.030	1.179
2003	0.046	0.604	0.144	0.004	0.050	0.007	0.063	0.049	0.008	0.074	0.000	0.001	0.002	1.052	0.028	1.080
2004	0.044	0.541	0.132	0.004	0.043	0.006	0.086	0.041	0.008	0.072	0.000	0.001	0.001	0.978	0.027	1.005
2005	0.042	0.480	0.123	0.003	0.037	0.005	0.091	0.033	0.007	0.070	0.000	0.001	0.001	0.893	0.026	0.919
2006	0.039	0.416	0.114	0.003	0.032	0.004	0.091	0.027	0.007	0.060	0.000	0.001	0.001	0.795	0.024	0.819
2007	0.037	0.362	0.105	0.000	0.027	0.004	0.089	0.026	0.006	0.052	0.000	0.001	0.001	0.709	0.023	0.732
2008	0.035	0.322	0.099	0.000	0.023	0.003	0.080	0.023	0.005	0.045	0.000	0.001	0.001	0.638	0.022	0.660
2009	0.034	0.291	0.090	0.000	0.016	0.003	0.073	0.021	0.004	0.039	0.000	0.001	0.001	0.572	0.020	0.592
2010	0.033	0.266	0.082	0.000	0.010	0.002	0.066	0.018	0.003	0.033	0.000	0.000	0.001	0.514	0.019	0.533



## **HISTORICAL REVENUES, PRICES AND PRODUCTION**

This section reports on historical revenues, prices and production. The first two tables show General Fund revenues by type from FY 1978 - 91, and breaks them into unrestricted and restricted categories. Table 34 shows petroleum revenues by type from statehood to the present (FY 1959 - 91). And finally, historical prices and production (FY 1978-92) are shown in Table 35.

# Historical General and Unrestricted Revenues - Tax Portion -

(\$ millions)	FY 79	FY 80	FY 81	FY 82	FY 83	FY 84	FY 85	FY 86	FY 87	FY 88	FY 89	FY 90	FY 91	FY 92
Corporate - General	24.8	17.9	34.8	34.8	30.3	39.5	36.0	11.2	20.5	23.4	38.0	45.3	37.9	33.7
Corporate - Petroleum	232.6	547.5	860.1	668.9	236.0	265.1	168.6	133.9	120.4	158.0	166.0	117.2	185.1	165.5
Fiduciary	0.1	0.1	0.0	0.0	0.0	0.0	0.0	0.0	0.0	0.0	0.0	0.0	0.0	0.0
Individual	117.2	100.5	0.0	0.0	0.0	0.0	0.0	0.0	0.0	0.0	0.0	0.0	0.0	0.0
Total Income	374.7	666.0	894.9	703.7	266.3	304.6	204.6	145.1	140.9	181.4	204.0	162.5	223.0	199.2
Alaska Business License	28.2	4.2	5.4	5.5	6.9	19.9	38.8	2.1	1.5	1.4	1.0	0.1	0.0	0.0
Fish	11.9	14.6	20.7	22.8	20.5	19.0	18.7	21.1	26.5	22.5	26.7	25.1	31.1	30.1
Salmon Enhancement	0.0	0.0	0.0	2.4	2.6	2.2	2.6	4.3	4.4	5.8	9.5	6.5	6.2	4.2
Seafood Marketing	0.0	0.0	0.0	0.0	0.9	1.1	1.0	1.1	1.4	2.7	3.3	3.3	3.3	2.8
Insurance Companies	10.8	10.4	10.6	12.5	13.8	16.2	17.5	21.1	23.7	23.7	19.4	22.7	24.4	25.5
Other	1.2	2.1	1.2	1.4	1.6	2.0	2.1	2.2	2.3	2.4	3.2	4.6	4.1	4.1
Total Gross Receipts	52.8	31.3	37.9	44.6	46.3	60.4	80.7	51.9	59.8	58.5	62.1	62.3	69.1	66.7
Gravel, Timber, Etc.	1.7	1.6	2.7	0.0	0.0	0.0	0.0	0.0	0.0	0.0	0.0	0.0	0.0	0.0
Oil & Gas Production	173.6	506.2	1169.9	1581.1	1493.0	1392.4	1388.7	1107.4	647.3	816.4	696.4	972.3	1253.8	1022.2
Oil & Hazardous Release	0.0	0.0	0.0	0.0	0.0	0.0	0.0	0.0	0.0	0.0	0.0	26.9	28.0	28.7
Oil & Gas Conservation	0.2	0.3	0.3	0.6	0.7	0.7	0.7	0.5	1.2	2.3	2.4	2.4	2.3	2.3
Total Severance	175.5	508.1	1172.9	1581.7	1493.7	1393.1	1389.4	1107.9	648.5	818.7	698.8	1001.6	1284.1	1053.2
Oil & Gas Property	163.4	168.9	143.0	142.7	152.6	131.0	128.4	113.5	102.5	96.2	89.7	89.8	85.0	69.0
Vehicle Registration	0.2	0.1	0.2	0.0	0.0	0.0	0.0	0.0	0.0	0.0	0.0	0.0	0.0	0.0
Total Property	163.6	169.0	143.2	142.7	152.6	131.0	128.4	113.5	102.5	96.2	89.7	89.8	85.0	69.0
Alcoholic Beverages	7.4	7.4	8.3	9.0	10.4	13.0	13.9	13.3	12.6	12.1	11.8	12.0	12.2	12.0
Fuel Taxes - Aviation	3.4	4.0	4.1	6.3	8.7	8.1	8.0	8.1	8.5	9.0	10.1	9.4	10.7	10.7
Fuel Taxes - Highway	16.3	18.9	15.6	20.3	23.7	20.2	23.7	22.7	18.3	19.3	20.0	22.9	19.1	23.2
Fuel Taxes - Marine	2.6	3.2	3.5	3.7	4.3	3.9	4.3	5.3	5.4	5.3	7.2	9.2	10.0	9.4
Tobacco Products	1.7	1.6	1.7	1.2	2.0	2.0	2.0	4.2	6.6	6.1	6.4	11.0	14.0	14.3
Total Sale/Use	31.4	35.1	33.2	41.2	49.1	47.2	51.9	54.3	51.4	51.8	55.5	64.5	66.0	69.6
Estate	0.1	0.2	0.5	0.3	0.7	0.7	0.5	0.7	1.1	0.3	0.7	1.1	3.3	1.0
School	2.5	2.6	0.0	0.0	0.0	0.0	0.0	0.0	0.0	0.0	0.0	0.0	0.0	0.0
Total Other	2.6	2.8	0.5	0.3	0.7	0.7	0.5	0.7	1.1	0.3	0.7	1.1	3.3	1.0
Total Taxes	800.6	1412.3	2282.6	2514.2	2008.7	1937.0	1855.5	1473.4	1004.2	1206.9	1111.8	1381.8	1730.5	1458.7

## - Non-Tax Portion -

(\$ millions)	FY 72	FY 80	FY 81	FY 82	FY 83	FY 84	FY 85	FY 86	FY 87	FY 88	FY 89	FY 90	FY 91	FY 92
Business	7.5	8.1	9.1	10.8	10.8	10.8	11.9	11.3	10.0	8.6	8.1	6.7	5.8	5.3
Non-Business	<u>12.3</u>	<u>10.7</u>	<u>12.2</u>	<u>13.0</u>	<u>14.9</u>	<u>15.9</u>	<u>17.0</u>	<u>18.0</u>	<u>19.2</u>	<u>19.7</u>	<u>20.2</u>	<u>21.1</u>	<u>23.3</u>	<u>27.1</u>
Total Licenses & Permits	19.8	18.8	21.3	23.8	25.7	26.7	28.9	29.3	29.2	28.3	28.3	27.8	29.1	32.4
<b>Intergovernmental Receipts</b>														
Federal Shared Revenues	4.1	4.8	8.5	21.7	33.3	14.0	10.5	14.5	9.7	6.9	6.1	10.0	14.8	11.4
<b>State Resource Revenue</b>														
Bonus Sales	0.0	342.4	7.6	5.0	36.2	10.1	11.5	34.7	0.5	5.6	11.4	0.0	18.9	2.6
Investment Earnings	59.2	119.9	227.8	324.7	375.8	282.7	233.5	195.2	161.9	132.6	100.7	117.9	125.0	101.8
Rents	2.1	3.0	5.4	3.5	4.3	6.0	5.1	6.2	6.0	6.0	5.3	5.3	5.9	3.9
Royalties	249.2	688.2	1118.5	1157.3	1078.4	1047.5	1034.0	830.7	439.3	694.8	605.9	747.4	951.6	702.4
Sale of State Property	8.4	5.7	4.8	5.2	6.3	7.0	8.5	8.7	7.0	3.8	4.9	4.3	4.7	1.0
Gravel, Timber, etc.	<u>0.0</u>	<u>0.0</u>	<u>0.0</u>	<u>1.2</u>	<u>4.0</u>	<u>2.9</u>	<u>3.1</u>	<u>2.9</u>	<u>7.2</u>	<u>1.1</u>	<u>0.5</u>	<u>0.8</u>	<u>0.4</u>	<u>0.6</u>
Total Sale/Use	318.9	1159.2	1364.1	1496.9	1505.0	1356.2	1295.7	1078.4	621.9	843.9	728.7	875.7	1106.5	812.3
Airports	0.9	0.8	1.1	1.6	1.4	1.5	1.6	1.5	1.5	1.8	1.2	1.5	1.3	3.4
Ferry System	18.9	21.1	24.4	29.2	30.4	32.0	33.4	32.3	31.3	29.8	33.1	34.0	40.7	42.3
Other	<u>3.1</u>	<u>4.1</u>	<u>3.7</u>	<u>3.6</u>	<u>5.5</u>	<u>4.3</u>	<u>7.9</u>	<u>5.2</u>	<u>4.1</u>	<u>0.7</u>	<u>1.4</u>	<u>1.7</u>	<u>1.5</u>	<u>2.3</u>
Total Facilities Charges	22.9	26.0	29.2	34.4	37.3	37.8	42.9	39.0	36.9	32.3	35.7	37.2	43.5	48.0
Court System	2.8	2.8	2.9	3.5	4.2	4.1	4.5	5.1	5.3	5.5	6.0	5.8	6.4	6.2
Other	<u>2.3</u>	<u>2.0</u>	<u>4.1</u>	<u>6.1</u>	<u>5.9</u>	<u>4.8</u>	<u>5.2</u>	<u>4.1</u>	<u>4.8</u>	<u>2.0</u>	<u>1.9</u>	<u>3.2</u>	<u>7.3</u>	<u>32.2</u>
Total Services Charges	5.1	4.8	7.0	9.6	10.1	8.9	9.7	9.2	10.1	7.5	7.9	9.0	13.7	38.4
Total State Resource Revenue	346.9	1190.0	1400.3	1540.9	1552.4	1402.9	1348.3	1126.6	668.9	883.7	772.3	921.9	1163.7	898.7
Miscellaneous Revenue	7.2	6.7	5.5	7.8	10.9	9.5	16.8	13.0	16.9	16.1	10.0	10.9	14.9	61.4
Sub Total Non-Tax Revenue	378.0	1220.3	1435.6	1594.2	1622.3	1453.1	1404.5	1183.4	724.7	935.0	816.7	970.6	1222.5	1003.9
Less: Native Claims	45.6	131.4												
Plus: Income from prior years								418.7	70.5	163.9	257.7	154.8	33.6	
Total Non-Tax Revenue	332.4	1088.9	1435.6	1594.2	1622.3	1453.1	1404.5	1602.1	795.2	1098.9	1074.4	1125.4	1256.1	1003.9
Total Tax Revenue	800.6	1412.3	2282.6	2514.2	2008.7	1937.0	1855.5	1473.4	1004.2	1206.9	1111.8	1381.8	1730.5	1458.7
Total General Fund														
Unrestricted Revenue	1133.0	2501.2	3718.2	4108.4	3631.0	3390.1	3260.0	3075.5	1799.4	2305.8	2186.2	2507.2	2986.6	2462.6

# **Historical Restricted Revenues And Total General Fund Revenues**

Table 33

(\$ millions)	FY 78	FY 79	FY 80	FY 81	FY 82	FY 83	FY 84	FY 85	FY 86	FY 87	FY 88	FY 89	FY 90	FY 91	FY 92
<b>Federal Grants-In-Aid</b>															
Education	27.3	27.8	30.7	33.0	25.7	33.8	44.8	76.2	42.0	78.0	54.2	73.3	100.4	77.1	69.0
Social Services	57.7	57.8	60.0	68.7	60.4	80.7	91.2	100.7	125.2	156.4	154.2	167.4	194.7	211.8	254.3
Health	15.6	15.4	21.4	26.5	27.1	11.9	10.0	12.5	3.2	3.6	3.4	3.9	4.3	6.0	4.0
Natural Resources	7.9	10.1	6.5	8.3	12.4	15.0	14.2	18.1	17.9	27.8	28.4	30.0	35.8	54.6	41.5
Public Protection/Admin. of Justice	7.1	8.4	7.4	7.1	5.5	5.7	6.6	7.5	7.7	15.0	10.3	12.4	16.1	13.7	14.1
Development/Gen. Government	1.4	2.3	2.8	7.9	4.9	8.6	8.1	6.6	9.3	5.0	7.6	7.8	10.6	16.0	19.5
Transportation	<u>121.6</u>	<u>84.6</u>	<u>69.5</u>	<u>39.9</u>	<u>22.5</u>	<u>11.0</u>	<u>67.7</u>	<u>110.9</u>	<u>88.5</u>	<u>169.8</u>	<u>185.3</u>	<u>195.8</u>	<u>148.9</u>	<u>170.5</u>	<u>235.9</u>
<b>Total</b>	<b>238.6</b>	<b>206.4</b>	<b>198.3</b>	<b>191.4</b>	<b>158.5</b>	<b>166.7</b>	<b>242.6</b>	<b>332.5</b>	<b>293.8</b>	<b>455.6</b>	<b>443.4</b>	<b>490.6</b>	<b>510.8</b>	<b>549.7</b>	<b>638.3</b>
<b>Other Grants-In-Aid</b>															
Education	0.3	0.5	1.6	0.8	0.9	1.0	1.1	1.3	1.4	1.3	2.0	2.3	2.0	2.1	2.7
Health/Social Services	2.6	1.2	0.5	0.2	0.3	0.4	0.4	3.8	4.3	8.5	9.1	6.5	6.4	5.5	9.7
Natural Resources	1.4	1.2	0.6	2.4	1.4	1.0	0.9	0.9	1.4	2.3	6.0	6.2	5.7	7.5	15.2
Public Protection/Admin. of Justice	1.7	1.9	1.8	1.9	1.9	2.4	3.1	.9	2.0	5.7	5.1	5.3	10.3	9.5	12.6
Development/Gen. Government	1.3	1.6	4.1	2.6	3.3	5.3	15.6	6.5	3.6	3.8	5.2	14.0	21.1	1.2	1.2
Transportation	1.0	1.1	1.0	1.6	2.5	0.9	1.2	3.5	0.8	1.1	0.7	1.0	0.1	3.2	0.7
Oil Overcharge Fund	0.0	0.0	0.0	0.0	0.0	0.0	0.0	0.0	0.0	0.0	0.0	0.0	0.0	1.1	
Receipts for Services															<u>10.3</u>
<b>Total</b>	<b>8.3</b>	<b>7.5</b>	<b>9.6</b>	<b>9.5</b>	<b>10.3</b>	<b>11.0</b>	<b>22.3</b>	<b>16.9</b>	<b>13.5</b>	<b>22.7</b>	<b>28.1</b>	<b>35.3</b>	<b>45.6</b>	<b>30.1</b>	<b>52.4</b>
<b>Other Misc. Restricted Revenue</b>	<b>0.9</b>	<b>3.2</b>	<b>5.7</b>	<b>8.1</b>	<b>7.0</b>	<b>15.7</b>	<b>9.8</b>	<b>16.9</b>	<b>16.4</b>	<b>15.8</b>	<b>3.7</b>	<b>20.8</b>	<b>24.2</b>	<b>21.3</b>	<b>6.0</b>
<b>Total Restricted Revenue</b>	<b>247.8</b>	<b>217.1</b>	<b>213.6</b>	<b>209.0</b>	<b>175.8</b>	<b>193.4</b>	<b>274.7</b>	<b>366.3</b>	<b>323.7</b>	<b>494.1</b>	<b>475.2</b>	<b>546.7</b>	<b>580.6</b>	<b>601.1</b>	<b>696.7</b>
<b>Total Unrestricted Revenue</b>	<b>764.9</b>	<b>1133.0</b>	<b>2501.2</b>	<b>3718.2</b>	<b>4108.4</b>	<b>3631.0</b>	<b>3390.1</b>	<b>3260.0</b>	<b>3075.5</b>	<b>1799.4</b>	<b>2305.8</b>	<b>2186.2</b>	<b>2507.2</b>	<b>2986.6</b>	<b>2462.6</b>
<b>Total General Fund Revenue</b>	<b>1012.7</b>	<b>1350.1</b>	<b>2714.8</b>	<b>3927.2</b>	<b>4284.2</b>	<b>3824.4</b>	<b>3664.8</b>	<b>3626.3</b>	<b>3399.2</b>	<b>2293.5</b>	<b>2781.0</b>	<b>2732.9</b>	<b>3087.8</b>	<b>3587.7</b>	<b>3159.3</b>

Source: Department of Revenue, Revenue Sources FY 1978 - FY 1992. Updated March 1993.

# Historical Petroleum Revenues (Millions of Dollars)

Table 34

Y	Corporate Non-Petroleum	Corporate Petroleum	Oil/Gas Severance Tax	Property Tax	Reserve Tax	Fed. Min. Rents & Royalties (1)	Bonus Sales	Rents (1)	Royalties (1)	Oil/Gas <sup>(2)</sup> Special Settlements	Total Petroleum Revenues	Total G.P. Unrestricted Revenues	% of Total Unrestricted Revenues
59	1.4					3.1					3.1	25.4	12
60	1.7					5.8	4.0	0.1			9.9	48.0	21
61	1.4					2.4	1.6	0.2			4.2	40.5	10
62	1.8		0.2			4.5	20.3	1.0			26.0	68.9	38
63	2.2		0.3			8.6	17.9	1.0			27.8	71.6	39
64	1.8		0.3			8.7	4.7	1.2			14.9	67.0	22
65	1.9		0.3			8.3	5.9	1.9	0.1		16.5	83.0	20
66	4.1		0.3			7.7	10.8	2.5	0.3		21.6	86.5	25
67	3.5		0.5			7.7	8.6	2.8	1.9		21.5	86.6	25
68	3.8	0.1	10.2			7.5	21.8	2.9	9.5		43.0	112.7	38
69	4.2	0.1	5.6			7.8	0.8	3.3	16.9		34.5	112.4	31
70	4.9	0.4	7.9			8.2	900.0	3.1	19.3		938.9	1067.3	88
71	5.2	0.9	10.5			8.6	0.2	2.9	23.9		47.0	220.4	21
72	5.3	1.2	11.4			7.9	0.3	3.0	24.6		48.4	219.2	22
73	5.9	0.9	12.0			6.7	3.8	3.4	23.5		50.3	208.2	24
74	7.0	1.2	14.8			7.1	24.8	3.6	28.7		80.2	254.9	31
75	14.8	2.5	26.6	6.6		9.8	1.0	3.9	40.0		90.4	333.4	27
76	26.2	4.9	28.0	83.4	223.1	5.1		3.7	43.3		391.5	709.8	55
77	30.8	5.0	23.8	139.1	270.6	2.0*		2.8*	34.3*		477.6*	874.3	55
78	25.1	8.4	107.7	173.0		1.0*		1.8*	149.6*		441.5*	764.9	58
79	24.8	232.6	173.8	163.4		1.0*		1.6*	249.2*		821.6*	1133.0	73
80	17.9	547.5	506.5	168.9		1.2*	342.4*	1.8*	688.2*		2256.5*	2501.2	90
81	34.8	860.1	1170.2	143.0		1.2*	7.6*	3.7*	1118.5*		3304.3*	3718.2	89
82	34.8	668.9	1581.7	142.7		17.1*	5.0*	2.1*	1157.3*		3574.8*	4108.4	87
83	30.1	236.0	1493.7	152.6		27.2*	36.2*	2.5*	1078.4*		3026.6*	3631.0	83
84	39.5	265.1	1393.1	131.0		11.0*	10.1*	3.8*	1047.5*		2861.6*	3390.1	84
85	36.0	168.6	1389.4	128.4		8.2*	11.5*	3.4*	1034.0*		2743.5*	3260.0	84
86	11.2	133.9	1108.4	113.5		14.3*	34.7*	4.2*	830.7*	418.2*	2657.9*	3075.5	86
87	20.5	120.4	648.5	102.5		9.0*	0.5*	3.8*	439.3*	70.5*	1394.5*	1799.4	77
88	23.4	158.0	818.7	96.2		6.7*	5.6*	5.7*	694.8*	163.9*	1949.6*	2305.8	85
89	38.0	166.0	698.8	89.7		5.6*	11.4*	5.3*	605.9*	257.7*	1840.4*	2186.2	84
90	45.3	117.2	1001.6	89.8	0.0	6.3*	0.0*	4.2*	747.4*	154.8*	2121.4*	2507.2	85
91	37.9	185.1	1284.8	85.0	0.0	7.1*	18.9*	5.8*	951.6*	33.5*	2571.8*	2986.6	86
92	33.7	165.5	1053.2	69.0	0.0	5.8*	2.6*	4.2*	702.4*	4.7*	2007.4*	2462.6	82

\* Net of Permanent Fund contribution and constitutional Budget Reserve Fund deposits.

<sup>(1)</sup> These categories are primarily composed of oil/gas revenues; however, includes some additional revenues from other minerals (mostly coal).

<sup>(2)</sup> Not subject to budget reserve fund.

Table 35

## Historical Prices and Production

FY	Reported Alaska North Slope (\$/bbl)			Production (Millions of barrels/day)		
	<u>ANS West</u>	<u>ANS Gulf</u>	<u>ANS Lower 48</u>	<u>ANS</u>	<u>Cook</u>	<u>Total</u>
78	12.30	14.60	13.12	0.702	0.144	0.846
79	13.70	15.50	14.35	1.197	0.131	1.328
80	26.50	27.68	26.92	1.422	0.109	1.531
81	33.48	35.24	34.10	1.511	0.093	1.604
82	29.55	31.11	30.28	1.570	0.080	1.650
83	26.88	29.09	28.04	1.627	0.073	1.700
84	25.61	27.85	26.77	1.657	0.065	1.722
85	25.11	27.50	26.27	1.694	0.055	1.749
86	20.48	22.54	21.52	1.802	0.045	1.847
87	12.89	14.17	13.43	1.849	0.047	1.896
88	15.65	16.92	16.15	2.005	0.043	2.048
89	14.03	15.09	14.36	1.960	0.043	2.003
90	16.88	17.45	17.03	1.853	0.033	1.886
91	20.66	22.10	20.93	1.799	0.040	1.839
92	15.93	17.87	16.33	1.791	0.042	1.833

In accordance with 37.07.060(b)(4), Revenue Sources is compiled biannually by the Department of Revenue to assist the Governor in formulating a proposed comprehensive financial plan for presentation to the State Legislature. Within the publication are shown prior year actuals, revised current year estimates, and future year projections.

Anticipated State income is projected through the use of a number of data sources: 1) econometric models developed by the Department of Revenue to forecast unrestricted non-petroleum revenues; 2) a petroleum revenue model created by the Department's Oil and Gas Audit Division; and 3) estimates from individual State agencies.

The Department of Revenue thanks the various State agencies for their cooperation in computing anticipated revenues for publication in this document.

This publication was released by the Department of Revenue, produced at a cost of \$2.41 per copy to assist the Governor in formulating a proposed comprehensive financial plan for presentation to the State Legislature and printed in Anchorage, Alaska. This publication is required by AS 37.07.060.

**APPENDIX 10**

**MISCELLANEOUS  
STUDY MATERIAL**



## APPENDIX 10: MISCELLANEOUS STUDY MATERIAL

### Table of Contents

	<u>Page</u>
Summary	A10-1
A10.1 "Position Paper on Design Ice, Oceanographic, and Geotechnical Criteria For Production Concepts at the Kuvlum Prospect", Vaudrey & Associates, Inc. (January 1993)	
A10.2 "Kuvlum Summer Ice Statistics", Vaudrey & Associates, Inc. (December 1993)	
A10.3 "1993 Kuvlum Summer Ice Season", Vaudrey & Associates, Inc. (February 1994)	
A10.4 "Preliminary Burial Depth Profiles Along a Kuvlum Pipeline Route", Vaudrey & Associates, Inc. (August 1993)	
A10.5 "Kuvlum Design Ice Load Review", Vaudrey & Associates, Inc. (November 1993)	
A10.6 "Eastern Beaufort Sea Synthesis", Arctic Geoscience (July 1993)	
A10.7 "Bedrock Review, Eastern Beaufort Sea Synthesis", Arctic Geoscience (July 1993)	
A10.8 "Wellbore Geophysics Kuvlum Prospect," Arctic Geoscience (June 1993)	
A10.9 "Cost Schedule - Winter Geotechnical and Geophysical Site Investigation", Arctic Geoscience (July 1993)	
A10.10 "Cost Schedule - Summer Geotechnical and Geophysical Site Investigation", Arctic Geoscience (July 1993)	
A10.11 "Soil Profile for Conceptual Design of Kuvlum Structures", Arctic Geoscience (July 1993)	
A10.12 "Soil Profile for Conceptual Design of Pipelines and Tunnels", Arctic Geoscience (July 1993)	
A10.13 Oil and Gas Reserves and Economic Program (OGRE)	
A10.14 Kuvlum Predecision Studies Arctic Consultant Listing	

- A10.15 "Evaluation of SAR Satellite Imagery as a Data Source for Design and Operational Ice Criteria at ARCO's Kuvlum Field", Vaudrey & Associates, Inc. (March 1994)
- A10.16 "ARCO Alaska Floeberg Study - Executive Summary", Beaudril Ltd. (May 1993)
- A10.17 "Long Term Forecast of Breakup in the Vicinity of the Kuvlum Well - Final Report", Fairweather Forecasting (September 1993)
- A10.18 "Spectacled Eider and Tundra Swan Surveys: Kuvlum Corridor, Sagavanirktok River to Staines River - Draft Report", Alaska Biological Research, Inc. (January 1994)

## **APPENDIX 10: MISCELLANEOUS STUDY MATERIALS**

### **Summary**

Included in the following section are miscellaneous study materials generated and used during the course of these studies. The majority of these materials were generated as groundwork for further studies. In some instances, the work was groundwork for studies that were ultimately never performed.

POSITION PAPER  
ON  
DESIGN ICE, OCEANOGRAPHIC, AND GEOTECHNICAL CRITERIA  
FOR  
PRODUCTION CONCEPTS AT THE KUVLUM PROSPECT

by

K. D. Vaudrey

Prepared for:

ARCO ALASKA, INC.  
Anchorage, Alaska

ARCO EXPLORATION AND PRODUCTION TECHNOLOGY  
Plano, Texas

Prepared by:

VAUDREY & ASSOCIATES, INC.  
San Luis Obispo. California

January 1993

POSITION PAPER  
ON  
DESIGN ICE, OCEANOGRAPHIC, AND GEOTECHNICAL CRITERIA  
FOR  
PRODUCTION CONCEPTS AT THE KUVLUM PROSPECT

**EXECUTIVE SUMMARY**

Over the past 15-20 years the industry has been anticipating production from the Alaskan or Canadian Beaufort Sea by collecting environmental data (primarily ice-related) through a series of joint industry projects. Not all of these projects were equally valuable. Some did not address the necessary design parameters, while others failed to provide proper or sufficient information. The objective of this position paper is to pinpoint what type of design criteria is required, what data have already been acquired, what data need to be collected, and how the data will be analyzed to develop reasonable and defensible design criteria.

Initially, this paper briefly describes the most likely production concepts, including offshore platforms and subsea pipelines, for Arco's Kuvlum Field, located in 110 feet of water in the Camden Bay region of the Alaskan Beaufort Sea. In addition, operational ice and oceanographic conditions required for winter or summer construction seasons are discussed, including waves, currents, and length and severity of each ice season.

The environmental conditions and parameters that affect the design of each of the offshore production facilities are described, along with techniques to obtain the data. As examples, production structure design will probably be governed by an encounter with multiyear floe having an embedded ridge, if an encounter with a fresh-water ice island can be determined to be an extremely rare event. Subsea pipeline design and burial will be governed by the plowing depth of the seafloor and associated soil pressures developed by deep-keeled ice ridges.

The available ice, oceanographic, and geotechnical data are assessed and compared with the quantity and type of data required. Data analysis techniques and design methodologies are presented for determining environmental parameter statistics, computing global and local ice loads, and developing long-term ice forecasts.

Recommendations are made for additional data acquisition, either purchase of existing data bases or new data collection projects, and for additional data analysis and studies. It is recommended that multiyear floe diameter, thickness, and velocity data be acquired in 1993 and analyzed to compute design ice loads. In addition, a long-term prediction of an ice island impact with a production structure should be developed. The capability of long-range ice forecasting of the open-water season should be

investigated and improved. An analysis of the existing ice gouge data base should be performed to develop design ice gouge criteria, such as gouging depth and frequency and the number of new gouges that cross the proposed pipeline route each year. A total of \$560,000 of ice data acquisition and analysis studies are recommended, including \$300,000 for 1993 projects and \$260,000 for 1994 projects (including \$225,000 to purchase existing data bases).

Recommended oceanographic data acquisition and analysis include bathymetry measurements and wave, water level, and current predictions. Transects should be surveyed along the coast at probable pipeline landfall sites to determine shoreline stability. A total of \$185,000 of oceanographic data acquisition and analysis studies are recommended, including \$95,000 for 1993 projects and \$90,000 for 1994 projects.

Recommended geotechnical data acquisition and analysis include soil borings at the proposed production structure sites and compute the sliding resistance and bearing capacity of the platforms. In addition, soil boring and ice gouge data should be collected along the proposed pipeline routes to predict burial depths, compute applied soil pressures, and develop pipelaying criteria. The cost for the recommended 1993-94 geotechnical data acquisition and analysis studies has not been estimated.

Regarding the timing of these recommended data acquisition and analysis projects, if design criteria will be needed by 1994, most of these studies should be performed or at least started in 1993. Data bases can be updated with additional new information in 1994, but data should be collected and existing data bases analyzed this coming year. The design environmental criteria should not all be left to the last minute and put together in a shoddy manner for the regulatory agencies.

Selected references, research organizations, and arctic engineering consultants are given as potential sources to develop the environmental design criteria.

## TABLE OF CONTENTS

<u>Section</u>	<u>Page</u>
EXECUTIVE SUMMARY .....	i
1. BACKGROUND AND INTRODUCTION .....	1
2. ENVIRONMENTAL CONDITIONS .....	2
2.1 Offshore Platforms .....	2
2.1.1 Design Ice Feature .....	2
2.1.2 Extreme Ice Feature .....	4
2.1.3 Design Oceanographic Parameters .....	5
2.1.4 Geotechnical Data .....	5
2.2 Subsea Pipelines .....	6
2.2.1 Design Ice Parameters .....	6
2.2.2 Design Oceanographic Parameters .....	7
2.2.3 Design Geotechnical Parameters .....	7
2.3 Winter and Summer Construction and Installation .....	8
2.3.1 Operational Ice Conditions .....	8
2.3.2 Operational Oceanographic Conditions .....	8
3. DATA ANALYSIS AND DESIGN METHODOLOGIES .....	9
3.1 Ice Analysis .....	9
3.2 Oceanographic Analysis .....	11
4. RECOMMENDATIONS .....	12
4.1 Offshore Platforms .....	12
4.2 Subsea Pipelines .....	14
4.3 Winter and Summer Construction and Installation .....	15
5. REFERENCES AND SOURCES .....	16
5.1 Books, Papers, and Conference Proceedings .....	16
5.2 Research Organizations and Individuals .....	19

POSITION PAPER  
ON  
DESIGN ICE, OCEANOGRAPHIC, AND GEOTECHNICAL CRITERIA  
FOR  
PRODUCTION CONCEPTS AT THE KUVLUM PROSPECT

1. BACKGROUND AND INTRODUCTION

Over the past 15-20 years the industry has been anticipating production from the Alaskan or Canadian Beaufort Sea by collecting environmental data (primarily ice-related) through a series of joint industry projects. Not all of these projects were equally valuable. Some did not address the necessary design parameters, while others failed to provide proper or sufficient information. The objective of this position paper is to pinpoint what type of design criteria is required, what data have already been acquired, what data need to be collected, and how the data will be analyzed to develop reasonable and defensible design criteria.

Initially, this paper briefly describes the most likely production concepts, including offshore platforms and subsea pipelines, for Arco's Kuvlum Field, located in 110 feet of water in the Camden Bay region of the Alaskan Beaufort Sea. The environmental conditions and parameters that affect the design of each of the offshore production facilities are discussed, along with techniques to obtain the data. The available ice, oceanographic, and geotechnical data are assessed and compared with the quantity and type of data required. Data analysis techniques and design methodologies are presented for determining environmental parameter statistics, computing global and local ice loads, and developing ice forecasts.

Recommendations are made for additional data acquisition, either purchase of existing data bases or new data collection projects, and for additional data analysis and studies. Selected references, research organizations, and arctic engineering consultants are given as potential sources to develop the environmental design criteria.



## 2. ENVIRONMENTAL CONDITIONS

### 2.1 Offshore Platforms

The most likely production platforms to be located in 110 feet of water at the Kuvlum Field are either vertical-sided gravity caissons or broad-necked cones. Each could be constructed of either steel or concrete. In addition, other production structure concepts that should be considered are caisson-retained islands, sand-filled caissons, and a gravity-based structure resting on a gravel berm.

In addition to the above platform concepts in 110 feet of water, a temporary or permanent structure (or manmade gravel island) may be installed in shallow water within the landfast ice zone to facilitate construction and operation of a pipeline placed inside a tunnel. This tunnel may provide limited access to the main offshore platform or platforms.

#### 2.1.1 Design Ice Feature

Offshore platforms will be subjected to ice loading from different ice types and features during three or four separate seasons (e.g., freeze-up, winter, break-up, summer). Ice loading models will be used to develop the number of ice encounter scenarios expected for each season. Loads computed for each encounter require the statistical representation of a number of ice feature parameters.

Even though platforms will frequently encounter several first-year ice features (e.g., level and rafted sheet ice, ridges, rubble fields) throughout each winter ice season, these features will not produce the design global ice load for production platforms or islands. Formidable first-year ice features, such as floating ridges and rubble fields, simply cannot achieve the consolidated thickness of a multiyear floe or ridge. Computed ice loads from both deterministic and probabilistic ice load models developed by the industry over the past decade confirm that the governing design loads occur from encounters with and failures of multiyear floes and ridges. Therefore, the ice feature parameters presented here will be limited to those multiyear ice parameters required to develop design criteria for computing ice loads.

Multiyear Ice Concentration and Floe Size. Since multiyear ice will not be an annual occurrence at the Kuvlum Field, it is imperative that a sufficient sampling be collected when multiyear ice invades the Camden Bay region. Multiyear ice concentration and floe size are needed to determine encounter frequencies with platforms. In addition, floe size is required for momentum calculations during a summer multiyear floe impact with a structure.

The most reliable method of acquiring multiyear ice coverage and floe size data is synthetic aperture radar (SAR) imagery. Arco participated in joint industry projects to collect aircraft-borne SAR imagery in the Beaufort Sea during 1981-84. Two large SAR data bases acquired in 1989 and 1990 are available. Now that there are two SAR satellites (European since August 1991 and Japanese since February 1992) in orbit, this is the best source for obtaining additional years of data on these two important parameters.

Other methods, such as SLAR imagery taken from aircraft and LANDSAT and NOAA-AVHRR satellite imagery, are inconclusive and unreliable for identifying multiyear ice. They may be useful in a general sense but should not be used to develop design multiyear ice statistics.

Multiyear Floe and Ridge Thickness. A multiyear floe with embedded ridges is composed of relatively solid ice with little or no porosity. Next to the determination of the risk of encounter with a multiyear floe, the floe and embedded ridge thickness is the single most important parameter in computing the design ice load because of its significant deviation from the average value. Since we know the structure diameter, the ice thickness determines the contact area over which the design ice load acts. Compared to floe size or diameter data, relatively few multiyear floe thickness data point have been collected because they typically have required tedious field measurements using augers. More recently, data acquisition has improved by thermal drilling (much faster than augering) and 3-D underwater sonar mapping (combined with standard surveying on the surface). About 800 multiyear floe and ridge thicknesses are currently available to Arco through public information and joint industry projects. Another 1000 thickness data points have been found in other joint industry projects in which Arco did not participate.

Other techniques, such as electromagnetic sensors and impulse radar, may provide a large volume of data, but these two methods are largely interpretive and very unreliable for measuring the actual consolidated ice thickness. Combined submarine sonar and laser profilometry cannot discriminate between first-year and multiyear ice, and most submarine sonar data are collected in deeper water, not along the continental shelf.

Ice Velocity. Ice velocity is a required design parameter to predict the ice flux (amount of ice to move past a platform during a given season) in order to compute the encounter frequency of a multiyear collision. Velocity is also a necessary parameter in the computation of momentum during an open-water collision between a multiyear floe or ridge and a platform. In addition, the likely ice failure mode for a multiyear ice impact with a vertical-sided structure is crushing, which is highly dependent on the strain rate (a function of ice velocity).

Ice motion measurements are collected in landfast ice by using a wireline station anchored to the seafloor (appropriate for the shallow-water structure or island), but pack ice motion at the Kuvlum Field site is too dynamic for such measurements. Sequential satellite images can be used to determine the general trend or drift of the pack ice, but short-term (1-2 hours) ice motion of individual floes can be measured best, and most economically, using ARGOS ice buoys to transmit their position to satellites. There are over 2000 buoy-days (800 in the public domain and available to Arco) of ARGOS ice velocity data for the eastern Beaufort Sea; however, most of these data are limited to a few months or seasons.

Effective Ice Pressure. A variety of mechanical properties of multiyear ice, including compressive and flexural strength, elastic modulus, and Poisson's ratio, are required to compute the design horizontal ice loads. Once the mechanical properties are known, they are input to an empirical or theoretical description of the ice failure mode, generally considered to be a flexural failure for slope-sided structures and an indentation or crushing failure for vertical-sided structures. This is a very simplistic description of a complicated process, explaining why MIT and others are still trying to get a handle on ice behavior, after 20 years of laboratory and field measurements of mechanical properties and numerous attempts to describe the failure mechanisms. Arco has joined at least three previous projects (in addition to the MIT study) to develop a suitable ice failure criterion.

Model tests have been conducted to measure the ice forces on specific platform geometries generated by complicated ice features. Unfortunately, it is extremely difficult to scale all of the ice properties accurately at the same time, leading to some bizarre simulated ice formulations (e.g., urea ice, wax ice).

One major drawback to laboratory measurements and studies on ice as a continuum is that multiyear floes or other ice types do not behave as a homogeneous sheet of ice (imperfect contact of an irregular ice thickness with many embedded flaws and cracks). More recent studies have found that there is a pressure-area curve for ice that shows the effective failure ice pressure is reduced significantly with increasing contact area. This has been confirmed by full-thickness indentation tests and large-scale field experiments (especially at the Molikpaq structure and Hans Island).

#### 2.1.2 Extreme Ice Feature

Ice islands are tabular icebergs (fresh-water glacier ice, not sea ice) that calve from the ice shelves of Ellesmere Island and may become captured by the Beaufort Gyre. The typical thickness

range of an ice island is 30 to 60 meters. It is necessary to assess the risk of encounter between an ice island and a production structure. It is likely that the encounter frequency will indicate that ice islands are an extremely rare ice feature and need not be considered in the design; however, location, tracking, and forecasting the movement of ice islands may be prudent during the operation of the Kuvlum Field.

A study should be conducted to review historical ice island calving episodes, to estimate ice island population, size distribution, and typical ice island drift rates, and to predict the encounter frequency of an ice island with a structure. The purpose of this study would be to ensure that the expected return period (e.g. 1000's of years) for an ice island encounter greatly exceeds the return period (typically 100 years) used for design ice criteria. SAR satellite imagery can be used to estimate the current ice island population, locate potentially hazardous ice islands that exceed some "fragmented" size (e.g., 200 meters across), and track the hazardous islands.

#### 2.1.3 Design Oceanographic Parameters

Design Water Level, Waves, and Currents. Extreme water level and wave characteristics will be of critical importance to the design of the offshore production structures. This information will be required to determine wave forces on the production structures (or island) and to determine deck elevations and wave overtopping rates. The most reliable method of predicting design oceanographic conditions for the Beaufort Sea is an extremal analysis of historical storm hindcasts. Fortunately, Arco already has joined the development of an area-wide numerical hindcast analysis prepared for the Alaskan Beaufort Sea on a coarse grid. This information can be used to develop conditions for a fine grid at the Kuvlum Prospect, at a relatively low cost.

Extreme current conditions will also be important if the production structures are steep-sided, and therefore susceptible to toe scour. This information can be obtained from an extremal analysis of the data generated by the same numerical model used to analyze water levels.

Bathymetry. Detailed bathymetry will be needed at the site of the production structures. The relatively recent availability of GPS, which is a navigation system based upon a network of satellites maintained by the US Government, and which can provide position within 5 meters with a 95% confidence level, will greatly expedite the acquisition of such data.

#### 2.1.4 Geotechnical Data

Design basis geotechnical information includes soil types, distribution and engineering properties of the mudline and sub-

mudline sediments, locations and characteristics of relict permafrost, potential for encountering shallow gas, and the potential for sea bed instabilities. All of these data are necessary to compute sliding resistance for and to maintain the stability of gravity-based structures at the Kuvlum Field. If a caisson-retained structure or a submerged gravel berm is considered as a production concept, properties of the dredged fill material will be needed. The same holds true if a gravel island is chosen as the shallow-water production structure. Tunneling will require soils data along the entire pipeline route.

Some of these geotechnical data can be obtained from high resolution seismic profiles and geologic considerations. Site-specific data from soil borings are required to account for the complex combinations of geology, sediment deposition and reworking processes, and sediment types.

## 2.2 Subsea Pipelines

Pipeline concepts, including both intra-field and field-to-shore lines, will include armored and buried pipes in back-filled trenches. In addition, the pipelines may be placed inside of a tunnel until the field-to-shore pipeline reaches the landfast ice zone.

### 2.2.1 Design Ice Parameters

Ice Gouging. Ice gouges are produced by the plowing action of ice keels, both first-year and multiyear ridges. Design ice gouge criteria for pipelines are the gouge depth distribution, gouging frequency along the pipeline route as a function of water depth, seafloor slope, and ice movement. The most important ice gouging parameter is the age of existing gouges or the determination of how many new gouges cross the pipeline route each year.

It is difficult to estimate the frequency and depth of ice gouging indirectly by inference from ice keel measurements. Therefore, it is important to collect ice gouge data directly through side-scan sonar and precision fathometer records. There exists a study which analyzed over 10,000 gouges collected during a seven-year (1972-79) period by the US Geological Survey. In addition, Arco participated in a joint industry study that conducted a 3-year repetitive survey to determine the number of new gouges during successive years. Similar surveys have been conducted by the USGS. It is understood that a new gouge dating system has been developed, but needs field verification. Gouge infilling rate models have been developed in an attempt to determine the original gouge depth, but the models are difficult to calibrate without extensive information about seafloor soil types, bottom currents, reworking of sediments by new gouges, and year-to-year changes in summer storms.

Ice Ride-Up and Ice Pile-Up. The susceptibility of the coastline to ice ride-up and ice pile-up will be important in selecting the pipeline shore crossing and in locating pipeline support members. Such information was compiled during the early-to-mid 1980's in a series of freeze-up and break-up studies. Documentation of ice pile-up heights and ice encroachment distances onto the shore were acquired, along with a review of historical observations of similar events. A brief assessment of the ice ride-up and pile-up hazard should be performed for potential pipeline landfall locations.

#### 2.2.2 Design Oceanographic Parameters

Design Water Level, Waves, and Currents. Extreme water level and wave characteristics will be of critical importance to the design of the field-to-shore pipeline. This information will be required to determine potential storm-induced scouring in the nearshore zone and exposure of pipelines to grounded ice rubble formation and to determine potential storm-induced erosion at the pipeline shore crossing. As previously mentioned for offshore platforms, the most reliable method of predicting design oceanographic conditions for the Beaufort Sea is an extremal analysis of historical storm hindcasts, developed over a fine grid at the Kuvlum Prospect.

Bottom current conditions will also be important for estimating ice gouge depths and determining nearshore pipeline burial depths where ice gouging may be minimal. This information can be obtained from an extremal analysis of the data generated by the same numerical model used to analyze water levels.

Coastal Stability. The characteristics and stability of the coastline will be important in selecting and maintaining the pipeline shore crossing. Such information was compiled for the Point Thompson field, located to the southwest of Kuvlum Prospect, in 1983. If the pipeline will make landfall east of Flaxman Island (such as the vicinity of Brownlow Point), it is recommended that the stability of the coastline in the target area be assessed using a combination of historical survey data, historical aerial photographs, and present-day site visits and transect surveys.

#### 2.2.3 Design Geotechnical Parameters

All of the same design basis geotechnical information presented for offshore platforms are required for subsea pipelines to determine the susceptibility of the pipeline route to ice gouging, to compute the stresses in the reworked sediments above buried pipelines, and to assess the potential for sea bed instabilities while trenching for placement of buried pipelines.



Some of these geotechnical data can be obtained from high resolution seismic profiles and geologic considerations. Site-specific sediment layer and engineering property data from soil borings are required to account for the complex combinations of geology, sediment deposition and reworking processes, and sediment types.

## 2.3 Winter and Summer Construction and Installation

### 2.3.1 Operational Ice Conditions

Open-Water Season. Using historical satellite imagery and aerial observations, the expected break-up and freeze-up dates can be determined, based on a specified allowable ice coverage for a particular operation. Weekly ice charts are available for the past 21 years (1972-92) and aircraft observations/early satellite information is available from 1953 to 1975. From this same data base the expected number and duration of ice interruptions (greater than the threshold operational ice coverage) can be computed, as well as the length of the total construction season and the length of each uninterrupted portion of the season. Long-term forecasting may provide a tool for determining the probability of an early drilling or construction season by assessing the position of the multiyear ice edge and the midwinter pack ice motion.

Winter Ice Season. As mentioned above, the length of the winter construction season can be estimated by determining the expected freeze-up and break-up dates. Winter construction of pipelines and a shallow-water structure (e.g., gravel island) requires the knowledge of the thickness, roughness, and stability of the landfast ice. The stability and extent of the landfast ice zone can be determined by analyzing historical (LANDSAT) and current (SAR) satellite imagery acquired throughout the winter. In addition, the formation and extent of the grounded shear rubble that usually occurs along the 20-meter isobath can be studied as a stabilizing anchor for the landfast ice and as a potential source of vast, floating floebergs in the summer, which may represent a hazard to open-water operations.

### 2.3.2 Operational Oceanographic Conditions

Operational Waves and Currents. If a structure or pipeline is scheduled for installation during the open-water season, construction planning and towing route selection will benefit from a knowledge of the everyday wave and current climate. Statistics already have been developed for the Harrison Bay and Prudhoe Bay regions on the basis of a 4-year hindcast. This work can probably be extended to Camden Bay with far less effort than starting from scratch.

### 3. DATA ANALYSIS AND DESIGN METHODOLOGIES

Once the data for each design ice, oceanographic, or geotechnical parameter have been collected, a probability density function can be determined for each parameter provided there is a sufficient sample size to give representative or unbiased statistics. In addition, the data should be acquired over a number of years, not all gathered during the same year or season. Statistically, the number of years depends on the variability of the parameter. For instance, sheet ice thickness has a small standard deviation (about 10-20% of the mean) and does not require as many years of information to determine a representative distribution function. However, floe diameter, ridge thickness, and ice velocity have larger deviations and require more data points covering a longer time period to determine a complete distribution function, including the tail where the extreme or design values are found.

#### 3.1 Ice Analysis

Ice Load. Design loads for offshore platforms that are subject to ice hazards (e.g., multiyear floes/ridges) are computed by a series of logical steps. The first step is to define the probability of occurrence of certain ice loading events: that is, during the period of a year or season what is the likely range of multiyear impact events a platform will experience? The probability density function (pdf) of each of the multiyear ice parameters can be combined analytically (e.g., a Monte Carlo sampling technique) to provide an ensemble of ice loading events and the resulting peak load for each event. The maximum of all of the peak loads computed for a single year or season becomes the annual maximum load. The process is repeated for a very long trial period until a representative pdf for the annual or seasonal maximum ice load can be determined. The 100-year return period design multiyear ice load is the 99th percentile value of cumulative distribution function of the annual maximum load. This type of probabilistic ice load model is available and should be used to compute the design global ice loads for platforms at the Kuvlum Field.

For the purposes of design ice load calculation, the ice loading scenarios or events need to be divided into static and dynamic loads. The loading is considered static if the ice is relatively stationary and in contact with the platform, then experiences a sudden increase in load applied by natural driving forces, such as a storm wind. Two examples of static loads are winter landfast ice conditions and a multiyear floe lodged against the structure. Dynamic loading occurs when an ice feature strikes the platform with appreciable velocity, as an open-water encounter with a multiyear floe.

In addition to global ice loads acting on the whole structure, the pressure distribution of an ice feature in contact with any of the platform configurations is required for local structural design considerations (e.g., rib stiffener spacing, punching



shear capacity). Local ice forces over a limited area are generally much larger than the uniaxial compressive ice strength because of the confinement of the ice in contact with the structure. Local contact pressures have been measured experimentally by both instrumenting hulls of icebreakers and by field indentation tests.

Ice Forecasting. Short-term (2-3 days) ice forecasting is required for summer drilling and construction. This type of forecasting is currently employed by drilling rig operators, such as Beaudril (Kulluk) and Canmar (Explorer class drillships), who have a good working relationship between experienced ice observers and weather forecasters (e.g., Fairweather).

Long-term (2-3 months) ice forecasting is a desirable tool for early summer season drilling and construction, but it has shown very little "skill" (reliability). Discussions with Dr. Walsh at the University of Illinois and Gary Wohl of the Joint Ice Center indicate that there continues to be improvement in the ability to predict the severity of the upcoming summer by May. Wohl believes that the ability to forecast the break-up or first opening date is relatively good, based primarily on the proximity of the multiyear ice edge during late winter and on the pack ice motion during midwinter. However, the existing models seem to fall apart when it comes to predicting the length of the open-water season. Additional development of long-term forecasting of ice conditions for summer construction and towing appears worthwhile with the caveat that any forecasting model is just one tool to aid planning and operations, not the ultimate solution.

Long-term forecasting of an ice island impact with a platform should be investigated. The forecast should include identification of ice islands (with SAR satellite imagery) that are larger than some prescribed size. In addition, the forecast model should include the anticipated trajectory (along with an error band) and the probability and timing of potential impacts for offshore platforms at the Kuvlum Field. Long-term in this context may mean anywhere from six months to several years into the future. A short-term (two weeks to one month) supplement to this long-term model for ice islands could include the capability of forecasting the effects of any manmade perturbations to the trajectory of an ice island likely to collide with a structure.

Pipeline Burial. The ice gouge data can be analyzed to provide distributions of gouge depth as a function of water depth. The number of new gouges per kilometer of pipeline route per year can be determined from replicate sonar data (or from dating techniques or infilling rate models, if either prove reliable). In addition, directional statistics can be developed for gouge orientation. The design ice gouge depth can be determined from the gouge depth distribution, the expected new gouge frequency, the proposed lifetime of the pipeline, the length of the pipeline, and the angle between the pipeline route and the gouge orientation.

Design pipeline burial depths need to take into account, not only the design ice gouge depth, but the extent of soil deformation and resulting pressures induced from ice keels plowing the sediment above the buried pipeline.

### 3.2 Oceanographic Analysis

Wave Run-up and Overtopping. The elevation of wave run-up and the volume of wave overtopping for the design storm event can be used to optimize the deck or work surface elevation of the production structure. For preliminary design, these quantities can be predicted using the design wave and water level characteristics, and existing model test data and analytical methods. Scale model testing may be required for final design, especially if a structure of unconventional shape is adopted.

Armor Requirements. If a steep- or vertical-sided structure is to be utilized, the potential for wave-induced scour at the toe should be assessed to determine whether scour protection will be desirable. If, on the other hand, the production facility consists of a gravel island or a prefabricated core encased in gravel side slopes, an assessment will be required to determine the types of armor capable of withstanding the ice and wave loads at the site. The basis for this analysis will be the design wave characteristics described above, along with the design ice conditions.

Coastal Erosion. The design wave and water level conditions, in concert with coastal transect data, can be used to predict the erosion at the pipeline shore crossing which might result from the design storm. This information will be necessary to determine the required depth of burial for the pipeline in the nearshore area, as well as the setback between the shoreline and the point onshore at which burial is no longer required.

#### 4. RECOMMENDATIONS

##### 4.1 Offshore Platforms

##### 1993 Ice Data Acquisition and Analysis

1) Supplement the four years (1981-84) of SAR data with SAR satellite imagery from the Alaskan SAR Facility and analysis of the data to determine 1991-92 multiyear floe diameter distribution and multiyear ice fraction. As part of this project, use the acquired SAR satellite imagery to locate existing ice islands and estimate the current population.

2) Supplement the rather small data base of 800 multiyear floe and ridge thicknesses with 1993 field investigation in the Camden Bay region. During a one-week trip in March or April, an estimated 250 multiyear ice thicknesses can be acquired using Polar Alpine's thermal drill. This project is proposed in concert with the SAR imagery acquisition and analysis given in project (1).

3) Supplement the meager 2-year winter and 3-year summer ice velocity data base of less than 800 buoy-days in the Eastern Beaufort Sea with 1993 field investigation in the Camden Bay region. During two planned trips in March or April (2 buoys) and July (1 buoy), ARGOS buoys will be deployed in multiyear floes or vast floebergs. Each buoy will provide ice motion data 15-20 times per day over a 4-6 month period. The buoy deployment can be done as part of the multiyear thickness study presented in project (2).

4) Conduct midwinter ice reconnaissance, along with projects (2) and (3) above, to determine the extent of the shear rubble formation as a potential source of vast floebergs that could be a hazard to the 1993 summer drilling season.

Cost estimate for projects (1) through (4): \$175,000

5) Conduct a study to develop design ice loading criteria for selected production platform concepts. The criteria should include an analysis of the existing data bases to produce a series of probability distribution functions for multiyear ice parameters, such as floe diameter, multiyear ice concentration, floe and ridge thickness, velocity, and effective ice pressure.

Cost estimate: \$35,000

6) Conduct a study to provide a long-term prediction of an ice island impact with a platform, including a review of historical ice island calving episodes, an estimation of current ice island population, size distribution, and likely trajectories (with the help of SAR satellite imagery). The purpose of this study is to ensure that the expected return period (e.g. 1000's of years) for an ice island encounter greatly exceeds the return period (typically 100 years) used for design ice loading criteria.

Cost estimate: \$15,000

#### Purchase of Existing Ice Data

7) Supplement the four years (1981-84) of SAR data with two AOGA Projects 373 and 380, which provide an additional 25,000 multiyear floe diameters to the population distribution.

Cost estimate: ≈\$20,000 (ARCO cost).

8) Supplement the existing thickness data base with AOGA Projects 320 and 341, which provide an additional 950 multiyear floe and ridge thicknesses.

Cost estimate: ≈\$145,000 (ARCO cost).

9) Supplement the available ice velocity data base with AOGA Project 328, which provides an additional 1500 buoy-days (12 buoys deployed at different times during the winter) collected in the Camden Bay region during 1985-86.

Cost estimate: ≈\$60,000 (ARCO cost).

10) No additional ice strength or pressure measurements need to be acquired.

#### 1993 Oceanographic Data Acquisition and Analysis

11) Utilize existing storm hindcast data to predict wave, water level, and current conditions with return periods of 1, 10, 25, 50, and 100 years at the site of the proposed production structures and at several locations in the vicinity of the proposed pipeline route.

Cost estimate: \$25,000

12) Conduct a study to develop preliminary wave loads and minimum deck elevations for production structures and/or islands under consideration. The calculations will be based on the findings of Task 11 above.

Cost estimate: \$35,000

13) Acquire detailed bathymetry at the site of proposed production structures during the open-water season.

Cost estimate: \$30,000

### 1993 Geotechnical Data Acquisition and Analysis

14) Acquire soil borings at the Kuvlum Field and develop the design basis geotechnical properties for computing the sliding resistance and bearing capacity of the production platforms.

Cost estimate: Not estimated

### 4.2 Subsea Pipelines

#### 1993 Ice Data Acquisition and Analysis

1) Perform an analysis of existing ice gouge data base to develop preliminary design ice gouge criteria, including a set of statistics for ice gouge parameters, such as gouge depth, gouging frequency, gouge width, gouge orientation, and the number of new gouges that cross the pipeline route each year (if possible). In addition, the risk of damage to buried pipelines should be assessed, and it should be determined if additional gouge data need to be collected during the summer.

Cost estimate: \$20,000

2) Conduct a study to assess the ice ride-up and pile-up hazard for potential pipeline landfall locations.

Cost estimate: \$5,000

#### 1993 Oceanographic Data Acquisition and Analysis

3) Acquire detailed bathymetry along the proposed pipeline route during the open-water season.

Cost estimate: \$35,000

4) Perform a reconnaissance inspection of probable pipeline landfall sites during the open-water season, establish monumented survey transects, and obtain baseline data for use in determining shoreline stability.

Cost estimate: \$35,000

#### 1993 Geotechnical Data Acquisition and Analysis

5) Acquire soil borings and ice gouge data along the proposed pipeline route, interpret and reduce the data.

Cost estimate: Not estimated

#### 4.3 Winter and Summer Construction and Installation

##### 1993 Ice Data Acquisition and Analysis

1) Conduct a study using personal observations, photographs, and radar/satellite imagery to assess the risk of drilling or construction interruptions from vast floebergs (presumably refloated shear rubble). Study may include floeberg trajectories using ARGOS buoys.

Cost estimate: \$40,000 (initial effort being performed by Beaudril and funded by ARCO Alaska)

2) Investigate and improve long-term forecasting capability of summer season as a potential tool for construction planning or early summer drilling.

Cost estimate: \$35,000

##### 1993 or 1994 Ice Analysis

3) Conduct a study using historical data to develop adequate summer ice statistics for construction, platform towing and installation, and seafloor trenching and pipelaying. Study should determine expected length of summer construction season in the vicinity of the Kuvlum field, the number of expected ice interruptions, and the duration of each interruption.

Cost estimate: \$5,000

4) Conduct a study to assess the length of the winter construction season and the thickness, stability, and roughness of the landfast ice zone for possible winter construction of pipelines and a shallow-water structure. In addition, the formation and extent of the grounded shear rubble will be determined as an anchor for the landfast ice and as a potential source of vast floebergs in the summer.

Cost estimate: \$5,000

##### 1993 or 1994 Oceanographic Analysis

5) Conduct a study to develop operational wave and current conditions from existing hindcast data for used in planning summer construction and installation.

Cost estimate: \$25,000

## 5. REFERENCES AND SOURCES

### 5.1 Books, Papers, and Conference Proceedings

[for AOGA Projects see AOGA Book for summaries; if no costs are shown, ARCO was a participant; cost estimates shown are costs to ARCO, not total project cost]

#### General

American Petroleum Institute (API) RP2N (1988), Recommended Practice for Planning, Designing, and Constructing Fixed Offshore Structures in Ice Environments.

Canadian Standards Association (CSA) S471-M (1992), General Requirements, Design Criteria, the Environment, and Loads.

Sanderson, T. J. O. (1988), Ice Mechanics: Risks to Offshore Structures, Graham & Trotman, London.

Biannual proceedings of the POAC Conferences (1971-91) and IAHR Ice Symposiums (1970-92) and annual proceedings of the OMAE Conferences (1982-92).

#### Design, Feasibility, and Costs for Structure Concepts

AOGA Projects 106 and 121: In 1980 Brian Watt Assoc. did study on arctic cone test structure.

AOGA Project 233: In 1984 Brian Watt Assoc. did a study for exploration and production structures in the Lease Sale 87 area.

#### Multiyear Floe Diameter/Concentration

AOGA Projects 144, 177, 218, 257, and 266: Intera SAR imagery data acquisition with aircraft during winters of 1981-84.

AOGA Projects 120, 217, and 251: Bercha SLAR imagery data acquisition (of marginal value).

AOGA Project 373: Vaudrey analysis of Intera SAR imagery acquired in late winter 1989 [cost: ~\$15,000].

AOGA Project 380: Canatec analysis of Intera SAR imagery acquired in late winter 1990 [cost: ~\$5,000].

#### Multiyear Floe and Ridge Thickness

AOGA Project 139: Vaudrey field acquisition of 150 data points in 1981.

AOGA Projects 123, 195, 208, 262, and 277: Arctec field acquisition of 225 data points in 1981-85 from USCG Polar Star/Polar Sea cruises.

AOGA Projects 320 and 341: Arctec field acquisition of ≈950 data point in 1986-87 [cost: ≈\$145,000].

AOGA Project 280: Tekmarine and Polar Alpine field acquisition of ≈150 data points in 1984 [cost: \$120,000].

### Ice Velocity

APOA Project 222: Canmar compilation of ARGOS buoy data acquisition of ≈1300 buoy-days in the Beaufort Sea during 1979-85.

AOGA Project 328: Vaudrey field program and analysis of 12 ARGOS buoys deployed in the Camden Bay region during the winter of 1985-86 with over 2000 buoy-days of data covering the entire Beaufort Sea [cost: ≈\$60,000]

### Ice Loading and Effective Ice Pressure

Sanderson, T. J. O. (1988), Ice Mechanics: Risks to Offshore Structures, Graham & Trotman, London.

Vaudrey, K. (1991), Ice Conditions and Ice Loading Criteria for the SSDC/MAT Structure at the Cabot Prospect, prepared for ARCO Alaska, Inc. by Vaudrey & Associates, Inc.

AOGA Project 252: Arctec's local contact ice pressure study done in 1984.

AOGA Project 260: Coon & Assoc. in 1984 developed a failure criteria for sea ice and loads resulting from crushing.

AOGA Project 267: Brian Watt Assoc, in 1984 did a study on probabilistic ice load selection for caisson structures.

### Ice Islands

AOGA Project 33: Exxon's study in 1975 to develop a Monte Carlo model to estimate the risk of ice island collisions with structures [cost: \$10,000].

AOGA Project 363: Vaudrey & Assoc. ice island tracking study to determine a unique signature for identifying ice islands using remote sensing.



### Ice Forecasting

Barnett, D. (1980), A practical method of long-range ice forecasting for the north coast of Alaska, in Sea Ice Processes and Models, edited by R. Pritchard, Univ. of Washington Press.

Chapman, W. and J. Walsh (1991), Long-range prediction of regional sea ice anomalies in the arctic, Weather and Forecasting, Vol. 6, No. 2, p. 271-288.

### Ice Ride-Up and Ice Pile-Up

AOGA Projects 129, 160, 200, 246, 282, and 327: Vaudrey & Assoc. 1980-85 freezeup studies.

AOGA Projects 148, 191, 224, 274, and 319: Vaudrey & Assoc. 1981-85 breakup studies.

AOGA Projects 94, 102, and 118: OSI's 1979-80 freezeup and breakup ice movement studies.

### Summer Ice Season

AOGA Project 35: Amoco's summary of Bill Dehn's ice observations and interpretation for selected Beaufort Sea locations from 1953 and 1975.

AOGA Project 236: Arctec conducted a study on multiyear ice incursions into open-water areas of the Beaufort Sea.

AOGA Project 269: Brian Watt Assoc. performed a risk analysis of summer towing and installation operations.

AOGA Project 360, 370, 372, 381, and 386: Vaudrey & Assoc. studies in 1987-91 to analyze the summer ice conditions using satellite imagery and to determine drilling season ice statistics for four sites (including one at 70.5°N, 144°W) [cost: ~\$50,000].

Vaudrey, K. (1986), SSDC/MAT Mating Ice Conditions during August 1986, prepared for Tenneco by Vaudrey & Associates, Inc.

Navy/NOAA Joint Ice Center (1972-present), Weekly ice charts showing ice concentrations.

### Geotechnical and Ice Gouging

AOGA Project 335: McClelland Engineers study in 1984 to develop geotechnical design criteria for Lease Sale 87 [cost: \$9,500].

AOGA Project 326: R. J. Brown Assoc. conducted geotechnical centrifuge tests for arctic pipelines [cost: \$20,000]

AOGA Project 306: Harding Lawson Assoc. study to improve permafrost-related (seismic, electrical, and thermal properties) interpretation of geophysical data [cost: \$103,000].

Weeks, W. (1983), Statistical aspects of ice gouging on the Alaskan Shelf of the Beaufort Sea, CRREL Report 83-21.

AOGA Project 225: Harding-Lawson Assoc. ice gouging study to determine number of new annual gouges from repetitive tracks surveyed in 1983-85.

## 5.2 Research Organizations and Individuals

### Model Test Basins

US Army Cold Regions Research and Engineering Laboratory  
Hanover, New Hampshire  
Contact: Dr. Terry Tucker or Dr. Devinder Sodhi  
Phone: (603) 646-4100

Iowa Institute of Hydraulic Research  
Iowa City, Iowa  
Contact: Dr. Robert Ettema  
Phone: (319) 353-5696

Kvaerner Masa-Yards  
Helsinki, Finland  
Contact: Mr. Goran Wilkman  
Phone: +358 0 39 391

Hamburg Ship Model Basin  
Hamburg, Germany  
Contact: Dr. Joachim Schwarz  
Phone: (040) 69 20 30

### Theoretical Ice Mechanics and Constitutive Modeling

Dartmouth University  
Hanover, New Hampshire  
Contact: Dr. Erland Schulson  
Phone: (603) 646-2888

Massachusetts Institute of Technology  
Cambridge, Massachusetts  
Contact: Dr. Shyam Sunder  
Phone: (617) 253-7118

### Remote Sensing

Alaskan SAR Facility  
Fairbanks, Alaska  
Contact: Ms. Greta Reynolds  
Phone: (907) 474-7869

Applied Physics Laboratory  
University of Washington  
Seattle, Washington  
Contact: Mr. Drew Rothrock  
Phone: (206) 545-2262

National Snow and Ice Data Center  
Boulder, Colorado  
Contact: Dr. Roger Barry or Dr. Ronald Weaver  
Phone: (303) 492-5171

Jet Propulsion Laboratory  
Pasadena, California  
Contact: Dr. John Crawford (formerly with ARCO)  
Phone: (818) 354-6471

### Arctic Ocean Buoy Program

Polar Science Center  
University of Washington  
Seattle, Washington  
Contact: Dr. Roger Colony  
Phone: (206) ???-????

### Long-Term Ice Forecasting

Department of Atmospheric Sciences  
University of Illinois  
Urbana, Illinois  
Contact: Dr. John Walsh  
Phone: (217) 333-7521

Navy/NOAA Joint Ice Center  
Suitland, Maryland  
Contact: Mr. Gary Wohl  
Phone: (301) 763-5972

### Ice Island Properties and Tracking

Geophysical Institute  
University of Alaska  
Fairbanks, Alaska  
Contact: Dr. Martin Jeffries  
Phone: (907) 474-5257

### 5.3 Arctic Engineering Consultants

#### Ice-Related Field Investigations and Data Analysis

Vaudrey & Associates, Inc.  
1540 Marsh Street - Suite 105  
San Luis Obispo, California  
Contact: Dr. Kennon Vaudrey  
Phone: (805) 544-0940

frequently in joint venture with:

Polar Alpine, Inc.  
1442A Walnut Street - #236  
Berkeley, California  
Contact: Dr. William St. Lawrence  
Phone: (510) 524-1271

#### Ice Gouging Data Analysis

Vaudrey & Associates, Inc.  
1540 Marsh Street - Suite 105  
San Luis Obispo, California  
Contact: Dr. Kennon Vaudrey  
Phone: (805) 544-0940

#### Ice Load Modeling and Design Load Computation

Vaudrey & Associates, Inc.  
1540 Marsh Street - Suite 105  
San Luis Obispo, California  
Contact: Dr. Kennon Vaudrey  
Phone: (805) 544-0940

#### Ice Island Forecasting

Vaudrey & Associates, Inc.  
1540 Marsh Street - Suite 105  
San Luis Obispo, California  
Contact: Dr. Kennon Vaudrey  
Phone: (805) 544-0940

#### Short-Term Summer Ice Forecasting

Canadian Marine Drilling  
Calgary, Alberta  
Contact: Mr. Ben Danielewicz  
Phone: (403) 298-2813

Beaudril/Gulf Canada  
Calgary, Alberta  
Contact: Mr. Gary Pidcock  
Phone: (403) 233-3999

Oceanographic Data and Analysis and Coastal Processes

Coastal Frontiers Corporation  
9424 Eton Avenue, Suite H  
Chatsworth, California  
Contact: Mr. Craig Leidersdorf  
Phone: (818) 341-8133

Geotechnical Data and Analysis

any one of the following geotechnical firms:  
[all have Anchorage offices]

Dames & Moore, EBA Engineering, Harding Lawson Associates, and  
Woodward-Clyde Consultants.

In addition, there are McClelland Engineers and R. J. Brown.



## VAUDREY & ASSOCIATES, INC.

1540 Marsh Street - Suite 105  
San Luis Obispo, CA 93401  
Phone: (805) 544-0940  
Fax: (805) 544-0940

December 7, 1993

Mr. John Eldred  
New Ventures Engineering  
ARCO ALASKA, INC.  
P. O. Box 100360  
Anchorage, Alaska 99510-0360

Dear John:

### KUVLUM SUMMER ICE STATISTICS

We have developed a set of open-water ice statistics for summer construction at a site located approximately 10 to 12 miles northeast of Flaxman Island in the direction of the Kuvlum Prospect. Statistics are computed for an operational ice tolerance level of  $\leq 1$  tenth ice coverage. We used a 41-year data base, composed of the AOGA 35 data (1953-75) and existing weekly ice charts from the Navy-NOAA Joint Ice Center (1972-93). The data for individual years are presented in the attached Appendix. The following is a list of summer ice season definitions used in the column headings of the Appendix:

- **Break-Up Date:** First occurrence of an ice concentration of  $\leq 8$  tenths.
- **First OW Date:** First occurrence of an ice concentration of  $\leq 1$  tenth (defined as OW = open water) during the summer season.
- **Freeze-Up or Last OW Date:** Last occurrence of an ice concentration of  $\leq 1$  tenth (defined as OW = open water) prior to the onset of freeze-up.
- **Total OW Season:** Number of days between the first and last occurrence of open water.
- **Net OW Season:** Sum of all open water periods during the summer.
- **Maximum Continuous OW:** Duration of the longest open water period during the summer.
- **Ice Invasion:** Period of  $> 1$  tenth ice concentration between two open-water (OW) periods.

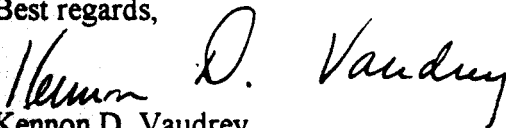
The following Table summarizes the summer season ice statistics developed from the data presented in the Appendix. Break-up, first open-water, and freeze-up dates and their respective standard deviations in days are determined. The probability that open water (OW) occurs is computed, along with the expected length in days of the Total OW Season, duration of the Net OW Season, and duration of the Maximum Continuous OW.

Often, the open water season is interrupted by one or more ice invasions. The conditional probability, given that open water occurs, is computed for the following number of invasions: (1) none, (2) one, (3) two, and (4) three or more invasions. Given the occurrence of an ice invasion, the expected duration of each invasion is determined. The expected duration of the Net Open Water (OW) Season for two and three consecutive summers is presented in the Table for construction scenarios that may require more than a single summer season to complete.

TABLE  
SUMMER SEASON ICE STATISTICS  
FOR A SITE 4-6 MILES SOUTHWEST  
OF THE KUVLUM PROSPECT

Parameter	Value
Operational Ice Tolerance	$\leq 1$ tenth ice concentration
<i>Dates</i>	
Break-Up Date	July 4 $\pm$ 11 days
First Open Water Date	August 6 $\pm$ 20 days
Freeze-Up Date or Last Open Water Date	October 8 $\pm$ 10 days
<i>Open Water (OW)</i>	
Probability that Open Water occurs	0.95
Expected Length of Total OW Season	58 $\pm$ 30 days
Expected Duration of Net OW Season	48 $\pm$ 29 days
Expected Duration of Maximum Continuous OW	41 $\pm$ 27 days
<i>Ice Invasions</i>	
Probability, given Open Water (OW)	
of None	0.436
of One	0.436
of Two	0.128
of Three or More	0.0
Expected Duration of Each Invasion	12 $\pm$ 8 days
<i>Multiple Summer Construction Seasons</i>	
Expected Duration of Net OW Season for	
Two Consecutive Summers	96 $\pm$ 41 days
Three Consecutive Summers	143 $\pm$ 50 days

Best regards,

  
Kennon D. Vaudrey

Attachment

cc: Mr. Junius Allen (ARCO-Plano) w/attachments

# APPENDIX

## SUMMER ICE DATA FOR KUVLUM CONSTRUCTION SITE COMPILED FOR 41-YEAR DATA BASE (1953-1993)

Year	Break-Up Date	First OW Date	Freeze-Up or Last OW Date	Total OW Season (days)	Net OW Season (days)	Maximum Continuous OW (days)	Number of Ice Invasions	Duration of Invasions (days)
1953	Jun 22	Sep 7	Unk.*	Unk.	6	6	0	N/A**
1954	Jul 28	Aug 8	Unk.	Unk.	36	30	1	6
1955	Jul 21	Never	Sep 20	0	0	0	N/A	N/A
1956	Jul 15	Aug 18	Oct 3	45	45	45	0	N/A
1957	Jun 23	Jul 16	Oct 4	80	74	68	1	6
1958	Jun 10	Jun 28	Oct 20	114	108	102	1	6
1959	Jul 4	Aug 14	Unk.	Unk.	54	54	0	N/A
1960	Jul 14	Aug 8	Oct 4	57	57	57	0	N/A
1961	Jun 28	Aug 7	Unk.	Unk.	44	44	0	N/A
1962	Jul 14	Aug 13	Unk.	Unk.	8	8	0	N/A
1963	Jun 21	Aug 20	Oct 19	60	60	60	0	N/A
1964	Jul 21	Sep 2	Oct 7	35	29	24	1	6
1965	Jul 4	Aug 2	Unk.	Unk.	18	12	1	36
1966	Jul 2	Jul 22	Unk.	Unk.	54	42	2	24
1967	Jul 4	Sep 20	Oct 3	13	13	13	0	N/A
1968	Jun 22	Jul 19	Oct 20	93	93	93	0	N/A
1969	Jun 9	Aug 26	Sep 24	16	16	16	0	N/A
1970	Jul 3	Sep 12	Sep 25	13	13	13	0	N/A
1971	Jul 10	Jul 27	Oct 1	66	42	24	2	24
1972	Jul 22	Aug 6	Oct 7	62	62	62	0	N/A
1973	Jul 10	Aug 21	Oct 8	48	48	48	0	N/A
1974	Jul 17	Sep 1	Oct 2	31	31	31	0	N/A
1975	Jul 28	Never	Sep 18	0	0	0	N/A	N/A
1976	Jul 8	Aug 22	Oct 11	50	38	24	1	12
1977	Jul 10	Aug 11	Oct 24	74	70	35	1	4
1978	Jul 5	Jul 16	Oct 8	84	62	42	1	22
1979	Jul 9	Jul 24	Oct 15	83	75	45	1	8
1980	Jul 2	Jul 20	Sep 3***	45	45	45	0	N/A
1981	Jun 28	Aug 18	Oct 4	47	47	47	0	N/A
1982	Jul 3	Aug 7	Oct 7	61	43	32	2	18
1983	Jun 21	Aug 9	Sep 30	51	30	18	1	21
1984	Jul 7	Jul 29	Oct 6	69	35	21	2	34
1985	Jun 30	Aug 4	Oct 8	65	57	42	1	8
1986	Jul 9	Aug 11	Oct 25	75	69	57	1	6
1987	Jun 29	Jul 18	Nov 1	106	106	106	0	N/A
1988	Jul 2	Jul 4	Aug 2***	29	17	10	1	12
1989	Jun 25	Jul 16	Oct 4	80	60	46	2	20
1990	Jun 22	Jul 3	Oct 15	104	97	83	1	7
1991	Jul 8	Aug 20	Oct 5	46	25	18	1	21
1992	Jul 3	Jul 14	Oct 12	90	83	63	1	7
1993	Jun 28	Jul 20	Oct 24	96	89	75	1	7

\* Unknown

\*\* Not Applicable

\*\*\* Last OW Date



Delivered to Chip  
2/18/94



## **FAX TRANSMISSION COVER SHEET**

**DATE:** February 18, 1994

**FROM:** Kennon Vaudrey  
Vaudrey & Associates, Inc.  
1540 Marsh Street, Suite 105  
San Luis Obispo, CA 93401  
**Phone:** (805) 544-0940  
**FAX:** (805) 544-0940

**TO:** John Eldred  
ARCO Alaska  
Anchorage, AK  
**Phone:** (907) 263-4347  
**FAX:** (907) 265-1462

**COMMENTS:**

Good Morning, John:

As per your phone request, attached is a copy of our letter report summarizing the 1993 summer ice season in the vicinity of the Kuvlum Prospect.

I will breakout the costs of this letter report separately on our next invoice. It took me 20 hours (cost:  $20 \times \$85/\text{hr} = \$1700$ ). Any questions, please call me.

Ken

**TOTAL PAGES:** 3 Pages (incl. Cover Sheet)

A10.3



## VAUDREY & ASSOCIATES, INC.

1540 Marsh Street - Suite 105

San Luis Obispo, CA 93401

Phone: (805) 544-0940

Fax: (805) 544-0940

February 18, 1994

Mr. John Eldred  
New Ventures Engineering  
ARCO ALASKA, INC.  
P. O. Box 100360  
Anchorage, Alaska 99510-0360

Dear John:

### 1993 KUVLUM SUMMER ICE SEASON

We have summarized the 1993 summer ice conditions in the Camden Bay region of the eastern Beaufort Sea and around the Kuvlum Prospect and ranked the season historically. The summary includes: (1) a description of the generic break-up and ice retreat mechanisms for the eastern Beaufort Sea, (2) an overview of the 1993 break-up and ice retreat in the Camden Bay region, and (3) a comparison of the 1993 summer at the Kuvlum Prospect based on ice edge location, length of open water season, air temperatures, and frequency of storms.

***Generic Break-Up and Ice Retreat Mechanisms.*** As air temperatures rise above freezing in May and early June, snow melts in the upland areas and the rivers begin flowing. Open leads and polynyas that form at this time offshore of the landfast ice do not refreeze. The primary mechanisms for ice deterioration and break-up in the Camden Bay region of the eastern Beaufort Sea are: (1) Mackenzie River discharge, (2) predominant east-southeasterly winds, and (3) high air temperatures.

Warm meltwater from the upland snow cover floods over the sea ice at the mouth of the Mackenzie River, accelerating ice break-up and melting in the Canadian Beaufort Sea. During mild ice summers in June and early July, prevalent east or southeasterly winds drive the Mackenzie River discharge westward along the Alaskan coast and move the ice further offshore in the eastern Beaufort Sea. High air temperatures, reported at coastal stations, combine with offshore winds to hasten the surface melting of the ice.

The landfast ice along the Alaskan Beaufort coast becomes delimited by the ice edge retreat in the Chukchi Sea to the west and in the Canadian Beaufort Sea to the east. Flood water from numerous rivers (primarily the Hula Hula, Canning, Sag, Kuparuk, and Colville) that flow into the Alaskan Beaufort Sea in early June initiates sea ice decay and reduces confinement along the coast which promotes break-up, typically in late June or early July.

After break-up occurs in the eastern Beaufort Sea, prevalent easterly winds, which circulate around the dome of high pressure usually present over the Arctic Ocean, tend to clear the broken ice away from the coast. During severe ice summers, the high pressure dissipates or moves eastward, which permits low-pressure cells to track across the Arctic Ocean from Siberia to Banks Island. Cyclonic circulation around these "lows" produce northerly and westerly winds which drive the pack ice south and keep it close to the coast.

In a normal northerly retreat, the ice edge in the eastern Beaufort Sea is typically located 20-40 miles offshore by mid-September. During the mildest summers, the ice may move as far north as 74°N. On the other hand, the Beaufort Sea does not open up at all during the severest summers. Freeze-up typically occurs in the vicinity of the Kuvlum site on October 5-7.

Secondary factors that may contribute to a mild ice year are: 1) frequent storm winds and 2) more solar radiation. A higher frequency of storm winds increases wave erosion of ice floes, breaking them in smaller pieces, and increasing the ice surface area exposed to warm-water currents. If summer cloud cover is less than normal, the higher solar radiation may accelerate ice deterioration and speed up the ice edge retreat.

**1993 Break-Up and Ice Retreat in Camden Bay.** Abnormally high air temperatures throughout the entire 1992-93 winter (December through April) retarded the ice growth and made the landfast ice thinner. A combination of (1) a thinner ice cover, (2) a continuation of unseasonably warm air temperatures in May and June, which produced an early Mackenzie River discharge, and (3) predominant east-southeasterly winds over the Canadian Beaufort Sea (due to a high pressure cell over the Archipelago) opened up a large polynya offshore of the Mackenzie Delta. This open water area, as much as 50 miles wide, extended as far west as Camden Bay by June 7.

A variable wind pattern and colder air temperatures during the last half of June stalled the very early ice edge retreat in the eastern Beaufort Sea, but strong easterly winds in early July opened up the entire route from Tuk to the Kuvlum site by July 13 (according to ice charts published by the Navy-NOAA Joint Ice Center). By mid-July, the 5 tenths ice edge had retreated northward to 71°N (about 40 miles north of the Kuvlum site), corresponding to a historical ice edge retreat that occurs once every 10 years (i.e., during 90% of the years, the ice edge is south of 71°N).

At this time, the landfast ice in the Camden Bay region had deteriorated to a concentration of only 3-5 tenths due to warm, fresh-water discharge from the Staines, Canning, and Hula Hula rivers and a return to warm air temperatures in July (6°F above normal). The warm air temperatures and early ice clearance of the nearshore zone in the Camden Bay region elevated the ocean surface temperatures, which were 2°-3°F above normal by midsummer.

The entire Canadian Beaufort Sea became virtually sea ice free out to 72°N by August 1, 1993. Predominant westerly winds in August retarded the rapid ice retreat, but did not produce any significant (> 5 tenths coverage) ice invasions of the Camden Bay region. Several belts and patches of ice (1-3 tenths coverage) moved into the area, but the relatively warm water quickly melted the ice as it neared the coast.

The potential floeberg hazard, which plagued the 1992 drilling season, was minimal in the summer of 1993 primarily because of a reduction in the areal extent of the shear zone during the 1992-93 winter. In addition, the very warm air temperatures and rapid, early retreat of the ice edge further reduced the threat from floebergs in 1993.

By September 1, the 5 tenths ice edge had retreated to almost 72°N north of Camden Bay, corresponding to an ice edge location that occurs once every 5 years. However, prevailing easterly winds, aided by two intense southeasterly storms on September 6-7 and September 12-14, drove the 5 tenths ice edge further offshore to 73.5°N by mid-September, corresponding to an ice edge location that occurs once every 10 to 20 years. The ice was so far away (almost 200 miles) that a strong westerly storm on September 16-19 and a northwesterly storm on September 26-27 did not produce any ice invasion of the Kuvlum drill site.

During October 1993, the edge of the perennial pack ice remained far offshore (between 73° and 74°N). Warm air temperatures continued throughout October (almost 10°F above normal) and into early November (averaging 17°F above normal for the first 10 days). A combination of high air and sea surface temperatures delayed freeze-up at the Kuvlum Prospect until October 23, about 2½ weeks later than normal. The young sheet ice in the Camden Bay region did not become 1-foot thick until mid-November or later.

Storms typically become more frequent during the early freeze-up season with the highest wind speeds usually occurring in November. In 1993 both September and October were very typical with four storms (two easterly and two westerly) occurring each month when the winds attained speeds of 25 knots or greater. Both months had the following percentage of time when the winds exceeded 20 knots: September, 15%; October, 22%. These values compare closely with their historical averages of 17% for September and 20% for October. November 1993 did not live up to its reputation as the windiest month, with only 6% of the time when winds exceeded 20 knots, compared to its average of 23%.

While an exceptionally mild summer ice season means little or no drilling downtime due to potential ice hazards, the long fetch length created by so much open water in the east-west direction can generate significant wave heights of 8-10 feet when a wind speed of 20-25 knots lasts 24 hours or more. Big waves can cause station keeping problems for the *Kulluk*, resulting in drilling downtime during storms, even when no ice is present.

**Summary and Historical Ranking.** Abnormally warm air temperatures throughout the winter and early summer of 1993 produced a thinner ice cover in the eastern Beaufort Sea and initiated an early Mackenzie River discharge. Easterly and southeasterly winds blew steadily in early June and again throughout July, producing a vast open-water lead in Camden Bay by early June and forcing the ice edge to retreat rapidly northward to 71°N by mid-July.


The entire Canadian Beaufort Sea became virtually sea ice free out to 72°N by August 1. Prevailing easterly winds during the first half of September drove the 5 tenths ice edge to 73.5°N north of Camden Bay. The ice edge remained 150-200 miles offshore for the remainder of the 1993 summer season.

Warm air temperatures continued throughout October and November. A combination of high air and sea surface temperatures delayed freeze-up at the Kuvlum Prospect until October 23, about 2½ weeks later than normal.

Open-water storms, which produced the only downtime experienced during the drilling season, were less severe in intensity and duration during August and occurred with typical frequency and strength in September and October 1993.

The summer of 1993 ranks as one of the 10% to 15% mildest ice seasons since 1953, based on the following parameters: (1) length of open water season, (2) extent of ice edge retreat, (3) air temperatures, and (4) frequency of storms. This ranking is equivalent to a return period of once every 7 to 10 years.

Best regards,

  
Kennon D. Vaudrey



## VAUDREY & ASSOCIATES, INC.

1540 Marsh Street - Suite 105  
San Luis Obispo, CA 93401  
Phone: (805) 544-0940  
Fax: (805) 544-0940

September 29, 1993

Mr. John Eldred  
New Ventures Engineering  
ARCO ALASKA, INC.  
P. O. Box 100360  
Anchorage, Alaska 99510-0360

Dear John:

### 1993 KUVLUM DRILLING SEASON EXTENSION

As requested by your telephone call on September 27, 1993, I have investigated the likelihood of extending the drilling season into mid-November 1993. The two key elements to my brief study are: (1) air temperatures and (2) sea surface temperatures.

Air Temperatures. The air temperatures from May through September 1993 have averaged 2° to 4° above normal. These higher than normal temperatures have contributed to a very mild summer ice season with the 5 tenths ice cover 150 miles north of the Kuvlum drill site.

Based on a paper by Jeff Rogers (1977) that included 56 years of Barrow air temperatures, October air temperatures have an 87% chance of being either normal (31%) or above normal (56%), given that the preceding summer months had above normal air temperatures. If October air temperatures are normal, it would take until October 15 (7-10 days later than normal) for freeze-up to occur, based on freezing-degree day accumulation alone.

Sea Surface Temperatures. The warm air temperatures and early ice clearance of the nearshore zone in the Camden Bay region have elevated the ocean surface temperatures. Reported sea surface temperatures are 34°F at the end of September, 2°-3°F higher than normal for the Camden Bay region. However, according to the Climatic Atlas, this temperature is roughly the same as the normal sea surface temperature offshore of Point Lay (on the Chukchi Sea coast) where the average freeze-up date is October 25.

The sea surface must cool to 29°F before freezing can take place. Even though the water temperature is quite warm now, if air temperatures drop below +10°F for a period of 2-3 days, the sea surface will cool rapidly and ice will start to form.

Ice Growth. Normal ice growth, based on freeze-up in early October, results in a 1-foot thick ice sheet by November 1 and a 2-foot thick ice sheet by late November. However, it is likely that freeze-up will be delayed until October 15-25. Assuming normal air temperatures prevail after freeze-up, it will take approximately three weeks to grow 1 foot of ice. It will take another four weeks for the ice sheet thickness to reach 2 feet.

Assume that the 1993 freeze-up will be delayed until October 20, the ice sheet will become 1 foot thick about November 10 and reach 2 feet thick around December 8.

Winds. Storms become even more frequent during the early freeze-up season with the highest wind speeds occurring in November, the windiest month of the year. Sustained winds of more than 20 knots occur almost 25% of the time in November with winds greater than 25 knots occurring 13% of the time.

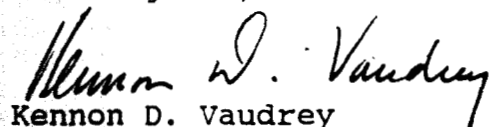
Summary and Recommended Action. Based on historical air and sea surface temperature records, it appears that freeze-up around the Kuvlum drill site will be delayed until October 20-23. Assuming normal conditions after freeze-up, the ice sheet should be 1 foot thick about November 10-12 and reach 2 feet thick around December 8-10.

Young first-year ice with a thickness of 1-2 feet should be within the station-keeping capability of the Kulluk, provided that the ice movement rate is not too great and that there are no old floes in the vicinity. Based on the expected freeze-up date and ice growth after freeze-up, the Kulluk should be able to continue drilling into mid-November.

If a third well is planned, I would recommend that several days of contingency be added to the drilling schedule for storm-related downtime due to high waves before freeze-up occurs and due to rapid ice movement after freeze-up.

Reference. J. Rogers (1977), A Meteorological Basis for Long-Range Forecasting of Summer and Early Autumn Sea Ice Conditions in the Beaufort Sea, POAC-77, St. John's, Newfoundland.

Best regards,

  
Kennon D. Vaudrey



## VAUDREY & ASSOCIATES, INC.

1540 Marsh Street - Suite 105  
San Luis Obispo, CA 93401  
Phone: (805) 544-0940  
Fax: (805) 544-0940

September 3, 1993

Mr. John Eldred  
New Ventures Engineering  
ARCO ALASKA, INC.  
P. O. Box 100360  
Anchorage, Alaska 99510-0360

Dear John:

### 1993 KUVLUM DRILLING SEASON EXTENSION

As requested by your telephone call on September 1, 1993, I have investigated the likelihood of extending the drilling season into late October 1993 and determined the probability of an ice invasion or interruption between now and freeze-up. The three key elements to my brief study are: (1) air temperatures, (2) traditional winds or storms during September and October, and (3) the current location of the ice edge relative to the Kuvlum site.

Air Temperatures. It was a very warm winter on the North Slope and the air temperatures from May through July 1993 have averaged 3° to 4° above normal. These higher than normal temperatures have contributed to a relatively mild summer ice season thus far. The warm air temperatures and early ice clearance of the nearshore zone in the Camden Bay region have elevated the ocean surface temperatures as well. Westerly winds in August, which are the major driving force for ice invasions and severe ice summers, have been mild and of short duration. Consequently, they have been unable to retard the ice edge retreat to the west and north, and the summer ice conditions have been relatively mild so far in 1993.

Winds. It is true that storms are more frequent and wind speeds increase during September and October (Figure 1 for the Stinson drill site), but the westerly and northwesterly direction of these winds decreases in favor of a more southerly component (as shown in Table 1 for the Stinson drill site). If a northwesterly storm does occur, the floes from the ice edge will diverge or spread apart and the warmer water will make them deteriorate or melt faster.

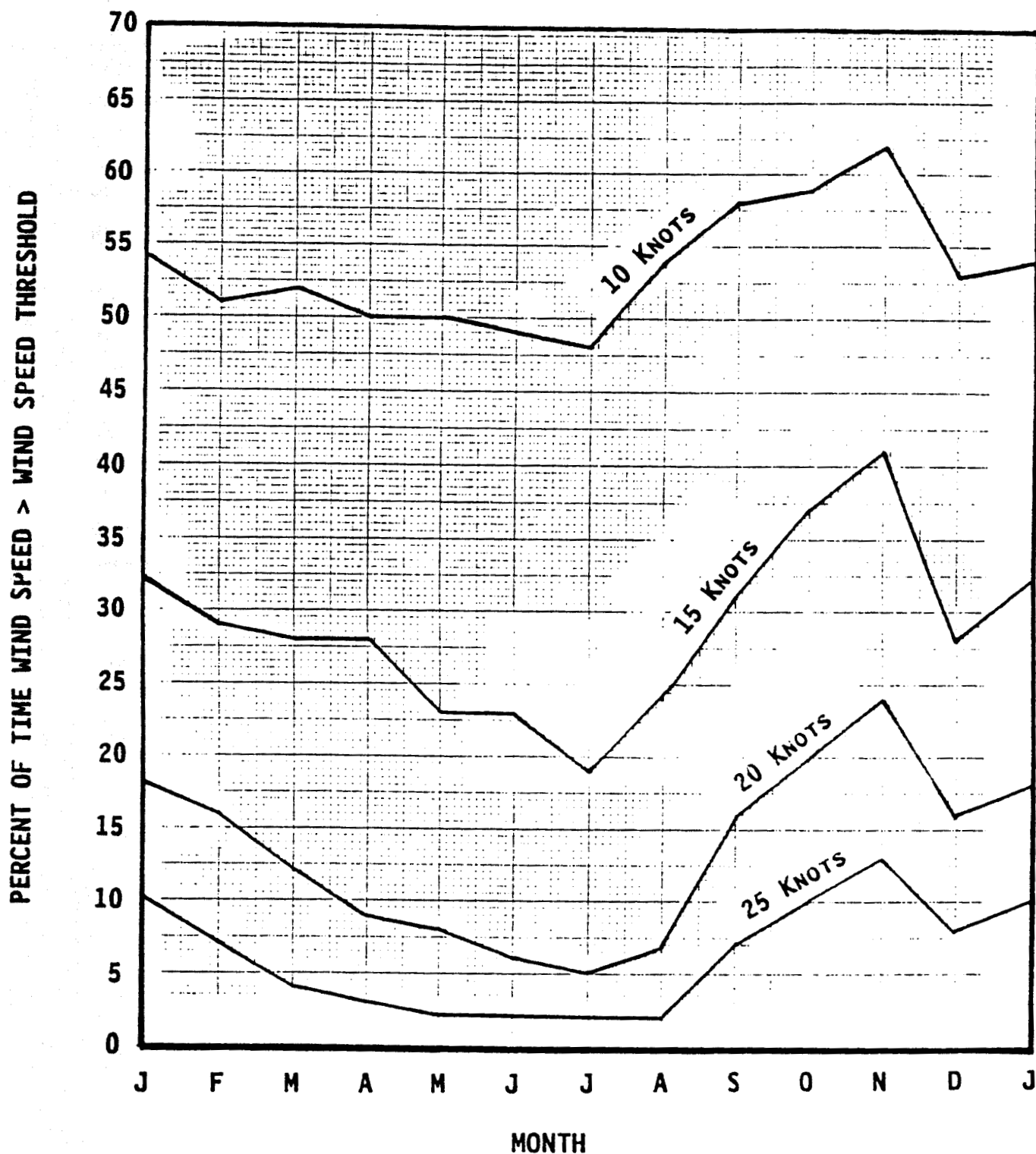


FIGURE 1 MONTHLY WIND SPEED EXCEEDENCE.





## VAUDREY & ASSOCIATES, INC.

1540 Marsh Street - Suite 105  
San Luis Obispo, CA 93401  
Phone: (805) 544-0940  
Fax: (805) 544-0940

August 6, 1993

Mr. John Eldred  
New Ventures Engineering  
ARCO ALASKA, INC.  
P. O. Box 100360  
Anchorage, Alaska 99510-0360

Dear John:

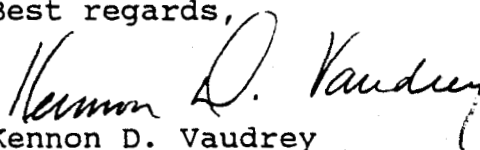
### PRELIMINARY BURIAL DEPTH PROFILES ALONG A KUVLUM PIPELINE ROUTE

Attached are five copies of our final report on the development of a set of preliminary burial depth profiles for a pipeline route from the 1992 Kuvlum drill site to Leffingwell Lagoon. At your request, I am sending you two bound copies and one unbound copy. In addition, I am forwarding two bound copies to Mr. Junius Allen in Plano.

I would be happy to assist you in determining what new ice gouge data, if any, need to be collected. Initially, I recommend that gouge depth information be extracted from the sonographs already collected in the Kuvlum vicinity as part of the shallow seismic surveys. Once analyzed these data should be combined with site-specific gouge data from AOGA 225 (Harding Lawson study) and then merged with the existing USGS gouge depth data base.

If you have any questions, please call me.

Best regards,

  
Kennon D. Vaudrey

Attachments

cc: Mr. Junius Allen (ARCO-Plano)

**PRELIMINARY  
BURIAL DEPTH PROFILES  
ALONG A  
KUVLUM PIPELINE ROUTE**



**VAUDREY & ASSOCIATES, INC.**

PRELIMINARY BURIAL DEPTH PROFILES  
ALONG A KUVLUM PIPELINE ROUTE

by

K. D. Vaudrey

Prepared for:

ARCO ALASKA, INC.  
Anchorage, Alaska

Prepared by:

VAUDREY & ASSOCIATES, INC.  
San Luis Obispo. California

July 1993

## TABLE OF CONTENTS

<u>Section</u>	<u>Page</u>
1. INTRODUCTION .....	1
2. ICE GOUGING PROCESSES .....	3
3. GOUGE DATA SOURCES AND SYNTHESIS .....	12
3.1 Gouge Density and Orientation .....	14
3.2 Ice Gouge Depth Distributions .....	14
4. GOUGE DEPTH STATISTICS .....	17
4.1 Computational Methods .....	17
4.2 Pipeline Burial Depth Profiles .....	21
5. RECOMMENDATIONS .....	34
6. REFERENCES .....	36

## LIST OF FIGURES

	<u>Description</u>	<u>Page</u>
Figure 1.	Pipeline Route Location Map.	2
Figure 2.	Characteristics of an Idealized Ice Gouge.	6
Figure 3.	Map Showing Location of the Sampling Lines [Weeks, 1983].	13
Figure 4.	Burial Depth Profile (RP = 100 Years, Lambda Values)	26
Figure 5.	Burial Depth Profile (RP = 200 Years, Lambda Values)	27
Figure 6.	Burial Depth Profile (RP = 500 Years, Lambda Values)	28
Figure 7.	Burial Depth Profile (RP = 1000 Years, Lambda Values)	29
Figure 8.	Burial Depth Profile (RP = 100 Years, Lambda-1 Values)	30
Figure 9.	Burial Depth Profile (RP = 200 Years, Lambda-1 Values)	31
Figure 10.	Burial Depth Profile (RP = 500 Years, Lambda-1 Values)	32
Figure 11.	Burial Depth Profile (RP = 1000 Years, Lambda-1 Values)	33

## LIST OF TABLES

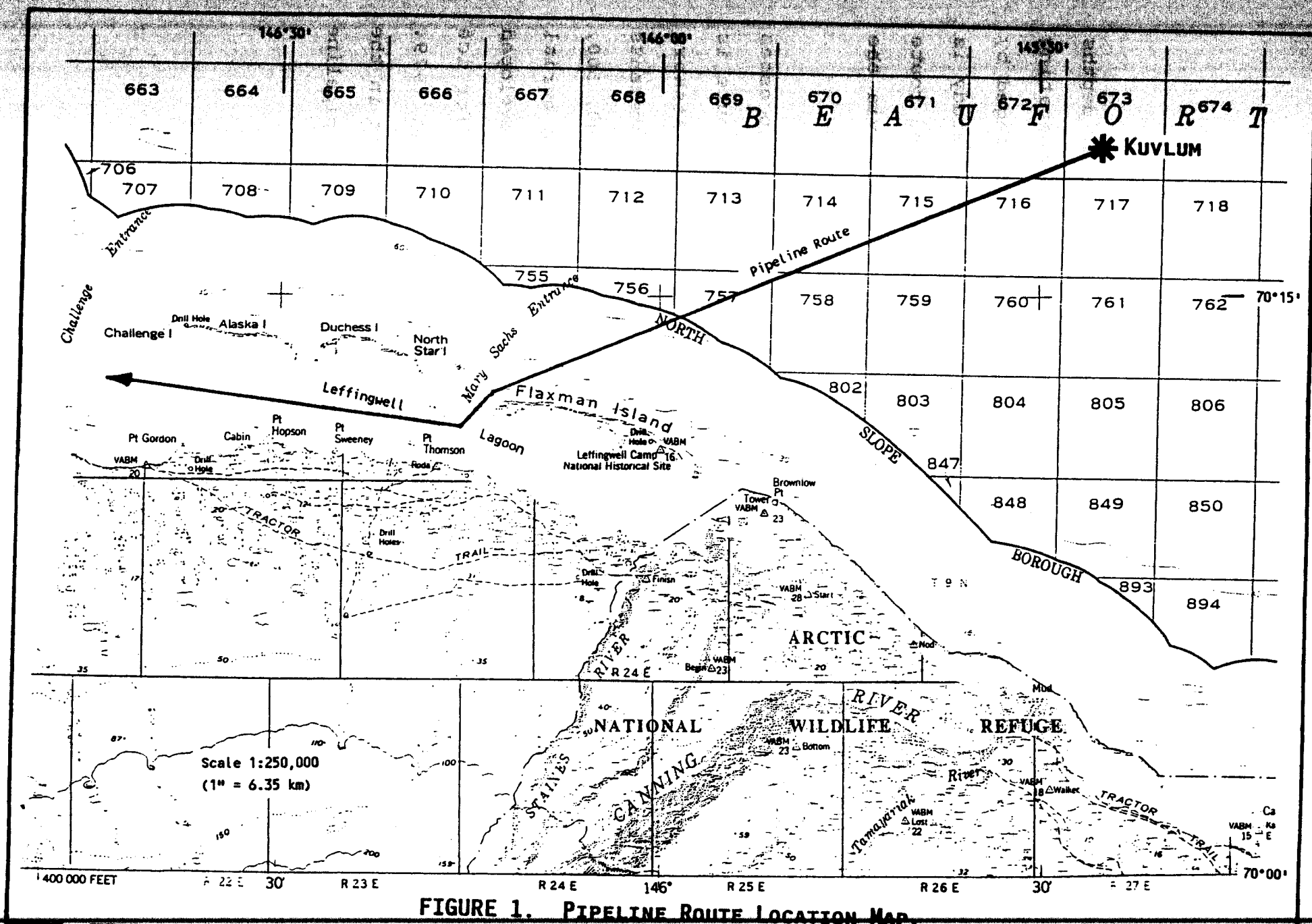
	<u>Description</u>	<u>Page</u>
Table 1.	Gouge Depth Histograms for a Series of Water Depth Intervals Along the the Alaskan Beaufort Sea Coast.	16
Table 2.	Extreme Gouge Depths for a Pipeline Route from Kuvlum to Leffingwell Lagoon.	24

PRELIMINARY BURIAL DEPTH PROFILES  
ALONG A KUVLUM PIPELINE ROUTE

1. INTRODUCTION

Gouge depths figure prominently in determining the burial depths required to provide sufficiently low risk, over the operating life of an offshore pipeline, that the pipe will be damaged by the keel of a moving ice feature. The purpose of this study is to develop a set of burial depth profiles for a pipeline route from the 1992 Kuvlum drill site to Leffingwell Lagoon via the Mary Sachs Entrance, just west of Flaxman Island (Figure 1).

Initially, this report briefly describes ice gouging processes and identifies ice gouging mechanisms. The pipeline route is divided into lagoon and offshore segments with the offshore segment further subdivided into 5-meter water depth increments (ranging from 5 to 35 meters). Return periods of 100, 200, 500, and 1000 years are selected for computing the pipeline burial depths. For this preliminary analysis, the methodology developed by Weeks (1983) is employed to compute the statistics for ice gouge depths measured by the USGS from 1972 through 1979. Recommendations are presented for removing uncertainties in the ice gouge data base, such that final design criteria for pipeline burial can be developed.



## 2. ICE GOUGING PROCESSES

The ice gouging process in the Alaskan Beaufort Sea is a complex interaction of the dynamic ice environment with the seafloor sediments. A process as dynamic and complicated as ice gouging produces a large regional variability in the ice gouge distribution, based primarily on ice movement, seafloor slope, geotechnical properties of the bottom sediments, and water depth.

Ice Regime. The ice environment of the Beaufort Sea varies greatly with the season and distance from shore. During the summer, much of the area along the selected pipeline route is ice-free, with the southern edge of the pack ice occurring between 10 and 100 kilometers offshore. New ice typically starts to form in early October. During the early stages of its formation, ice movement velocities range from an average of 7-8 km/day to more than 35 km/day during storms.

As winter progresses, numerous pressure ridges form in the moving ice, and in shallower areas many of these ridges become grounded. Zones of repeated and heavy grounding occur in water depths of roughly 15-20 meters offshore of the barrier islands, including Flaxman Island. Most winter ice movements are either easterly or westerly, roughly parallel to the shoreline. Additional ice movement around a grounded ridge fragment can enlarge the feature both in area and freeboard (sail height), producing a rubble pile.

Once the grounded ridge or shear rubble zone develops, the ice shoreward of these features remains relatively motionless until



break-up, beginning in late June or early July. Melting and positive storm surge during westerly storms permit formerly grounded ice features to float freely. However, some of the massive area of grounded ridges and rubble frequently remains on-bottom throughout most or even all of the summer. Associated with these grounded ice features at the 18-20 meter water depth is a break in the seafloor slope and changes in ice gouge character and sediment texture (Reimnitz and Barnes, 1974).

Ice Gouge Formation. The term "ice gouge" defines the characteristic seafloor furrow caused by the plowing action of ice keels. The disruption and reworking of seafloor sediments by ice keels are, in effect, dissipation mechanisms which subtract some of the energy input to the ice feature by atmospheric and oceanographic driving forces.

From a study of ice keel structure and available driving forces, Kovacs and Mellor (1974) concluded that virtually all ice keels have enough strength for gouging. They found that if energy is in the form of momentum of individual, free-drifting floes (driven by winds, currents, or waves), only short and shallow ice gouges would be created.

During the winter months deep-keeled ice ridges become part of an almost continuous ice canopy in the Alaskan Beaufort Sea. Storm winds acting over the surrounding ice cover can transmit enough energy to embedded ice ridges and rubble fields to produce long, deep ice gouges (Kovacs and Mellor, 1974).

Lewis (1977) contends that deeper gouges will occur in deeper water. It is generally agreed that the probability of encountering ice keels increases exponentially with decreasing keel depth. Only shallow keels can drift into or be formed in shallow water, and only deep keels can touch bottom in deeper water. The widely-scattered deep ice keels can collect more energy from wind stress than the more closely-spaced shallow keels. The expected result is fewer, but deeper, gouges in deep water. Of course, this conclusion is predicated on the premise that seafloor slope and soil resistance are equal in both shallow and deep water. Lewis' hypothesis was partially confirmed by Toimil (1978) who concluded that the density of ice gouges increases in a rough way with decreasing water depth, along with increasing slope gradients.

Gouge Characteristics. Immediately after ice gouges are formed, their measurable dimensions are usually narrower and shallower than the initial incision widths and depths due to slumping of berms formed along the gouge flanks (Figure 2). Seabed disruption by ice gouging extends beyond the original incision width of a specific gouge as a result of plastic deformation and compaction of the surrounding sediments (Reimnitz, et al., 1977). Most gouges are linear. The overall orientation along an ice gouge is the gouge trend. Frequently, ice gouges occur as sets of long, parallel furrows produced by the same ice movement event. Barnes, et al. (1984) speculates that these gouge multiplets are formed by first-year ice ridges with multiple keels.

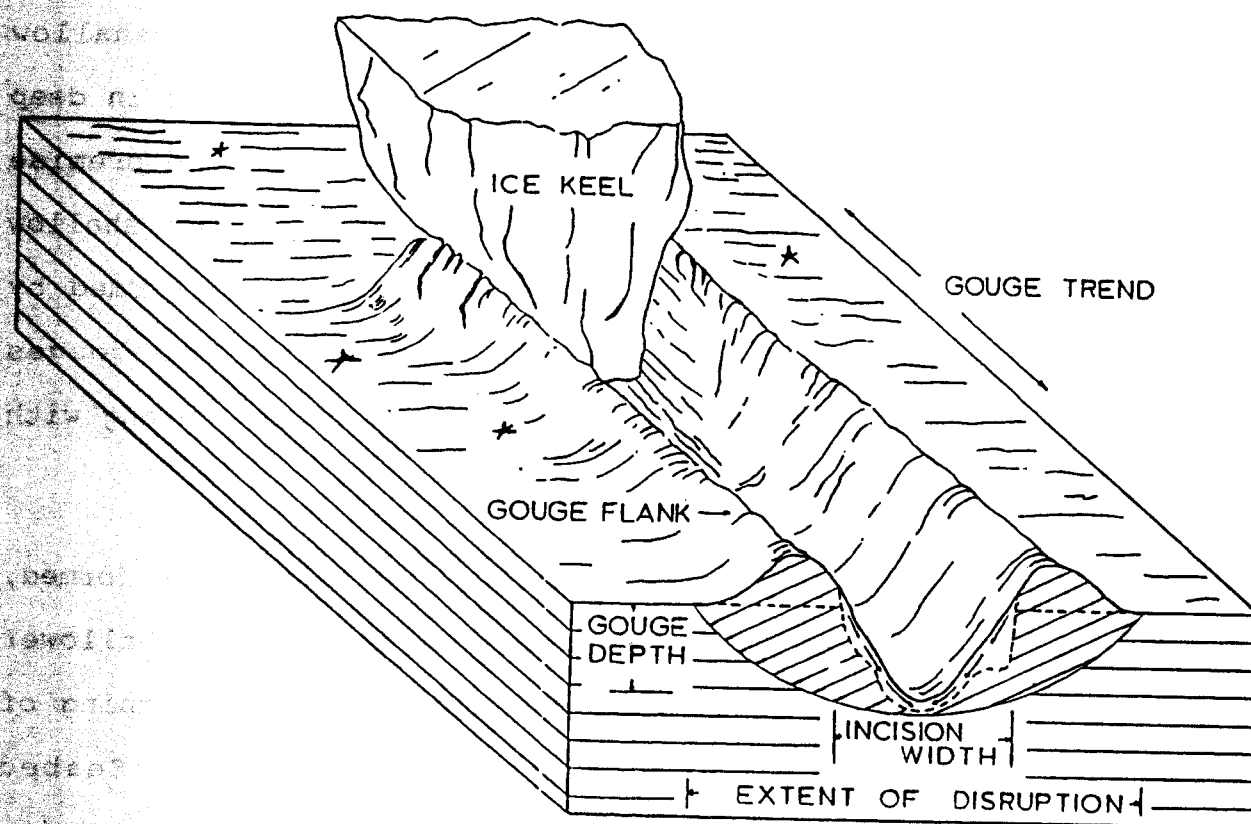


**FIGURE 2. CHARACTERISTICS OF AN IDEALIZED ICE GOUGE.**

Ice gouges in water less than 35 meters deep usually occur with a higher density and tend to have narrow widths, shallow incision depths, and no well-developed linear trends. Gouges in water deeper than 35 meters typically occur with a lower density and generally are wider, deeper, and more linear over long distances.

Obliteration. Wind-driven ice keels produce most of the gouges, but gouges are obliterated by ice gouge recurrence, sedimentation, and bedload transport by bottom currents. Shallow areas with sandy sediments exposed to vigorous waves and currents during the open water season will have all traces of ice gouging destroyed by the end of each summer season. Conversely, ice gouges in deeper water on the outer shelf, where bottom current activity is reduced, may be obliterated only by very slow settling of suspended material or by deposition of reworked sediment as new gouges cross existing ones.

Toimil (1978) observed that current-produced sand waves adjacent to, or within, individual ice gouges indicated rapid infilling and reworking of the gouges. In some cases gouges appear to be completely filled in and only narrow, linear ribbons of rippled bedforms mark former gouge flanks.

Age of Ice Gouges. "Recent" or "modern" in this context means within the last 200 years or so, whereas "relic" implies several thousand years. Modern ice gouging is known to occur in water depths between 5 and 35 meters, according to several early observers (Pelletier and Shearer, 1972; Reimnitz and Barnes, 1974; Lewis, 1977). As a recent example, an ice gouge crossed

the "glory hole" at Unocal's Hammerhead drill site in 30 meters of water in the Beaufort Sea during the winter of 1984-85. In addition, an ice gouge, approximately 3 meters deep, was observed in the vicinity of a grounded floeberg near the Kuvlum site during the 1992 summer drilling season. While ice gouging shoreward of the 5 meter isobath is probably frequent, the resulting microrelief is likely to be shallow and quickly obliterated by current and wave action.

The deepest water depth limit for recent ice gouging is open to considerable debate. Lewis (1977) and others thought that 50 meters is probably the limit for modern ice gouging since the deepest reported ice ridge keel, recorded in the Arctic Ocean by submarine sonar, is 47 meters. With extremely slow sedimentation rates, relic gouges in water depths greater than 50 meters should become progressively more shallow with increased depth, which is supported by a very limited data base acquired in the Canadian Beaufort Sea.

Reimnitz, et al. (1984) offer compelling arguments that deep-water ice gouges cannot be relic. If these gouges were formed when the sea level was lower and preserved for thousands of years, then they should be found across the entire shelf to a water depth of about 130 meters. However, ice gouging in the Alaskan Beaufort Sea is not found in water depths greater than 64 meters of water or greater than 58 meters in the Chukchi Sea (Toimil, 1978). In addition, Aagaard (1984) measured bottom currents in the deep-water Beaufort Sea strong enough to transport sediment and obliterate old gouges. This mode of ice

gouge obliteration is far different from an even sedimentation, postulated by Pelletier and Shearer (1972) and Lewis (1977), which would preserve the gouge relief for thousands of years.

This ongoing debate over the age of existing ice gouges has led to AOGA Project No. 388 (C-Core, 1993), entitled Pressure Ridge Ice Scour Experiment (PRISE), which is attempting to date extremely deep gouges by radioactive means. However, it has already been determined that the entire pipeline route out to the Kuvlum site is susceptible to modern or recent ice gouging; therefore, it remains to use existing ice gouge data and/or acquire additional ice gouge measurements to develop the ice gouge depth distribution and predict extreme ice gouge depths and their associated return periods.

Annual Gouging/Infilling Rates. Since the water depths along the Kuvlum pipeline route is shallow enough to be susceptible to modern ice gouging, dividing the ice gouge history into relic and recent time periods is not sufficiently precise to develop proper design criteria. It becomes necessary to estimate the annual gouging and infilling rates to determine how the gouge population for a region changes as new gouges form and old ones are obliterated.

During 1975-82 repetitive summer surveys out to water depths of 25 meters in 8 corridors of the Alaskan Beaufort Sea (Barnes and Rearic, 1983) gave a total of 2500 dated ice gouges, an average of 8.2 new gouges per kilometer. These new gouges disrupted an average of only 3% of the seafloor each year, but as much as 60%

over a single one-kilometer segment. In addition to large spatial differences, there was a high degree of temporal variability as well; for instance, the gouge intensity varied by a factor of 5 from year-to-year.

Site-specific tracklines (each 11 kilometers long) were repeated offshore Flaxman Island between 1979 and 1980 and again between 1981 and 1982. The water depth range was 7 to 26 meters. The number of new gouges averaged 6.3 per kilometer for 1979-80 and 3.9 per kilometer for 1981-82. These new gouges disrupted an average of only 1.6% of the seafloor each year.

In addition to this USGS study, AOGA Project No. 225 (Harding-Lawson Associates, 1986) also conducted a program to determine the repetitive effects of the seabed from 1983 through 1985. Unfortunately, out of the 10 sites repetitively surveyed, the only site offshore of Flaxman Island was limited to a water depth range of 3 to 9 meters. This trackline passed over an area of sandy bottom sediment where almost complete infilling or obliteration occurs during the following summer after gouge formation in the winter.

The average annual rate of new gouging, estimated from repetitive surveys, is sensitive to errors introduced by field operations, data interpretation, and year-to-year changes in ice conditions. Furthermore, repetitive surveys are expensive and provide only small data sets. If all of the gouge data is used, the statistical gouge characteristics can be modified by estimating the annual infilling rate based on regional sedimentation and

bedload transport (Weeks, Tucker, and Niedoroda, 1986; Environmental Science and Engineering, 1987; Niedoroda, 1990). Gouge infilling rates also are subject to considerable error due to lack of information about seafloor soil types, bottom currents, reworking of sediments by new gouges, and year-to-year changes in summer storms.

However, neither repetitive surveys nor infilling models can account for gouges that may never have been measured. For example, a shallow area of sandy sediments exposed to vigorous wave and current action during the open water season may have all traces of ice gouging eliminated by the end of each summer. Since all of the ice gouge data is collected near the end of the summer open-water season, most, if not all, of the ice gouges produced during the winter will no longer exist.



### 3. GOUGE DATA SOURCES AND SYNTHESIS

The most common method for obtaining ice gouge characteristics is to survey the area using side-scan sonar and a precision fathometer. All of the data contains information on gouge density (number of gouges measured per kilometer of trackline), gouge incision depth (with minimum values based on instrumentation resolution), gouge width, and gouge orientation or trend.

Until recently, there was no coordinated effort to obtain useful ice gouge characteristics. Gouge data were acquired primarily by the US Geological Survey (USGS) and by the oil industry. Ice gouge data have been collected in both the Canadian and Alaskan Beaufort Sea, starting in the early 1970's (Hnatiuk and Brown, 1977; Pelletier and Shearer, 1982).

Weeks, et al. (1983) analyzed seven years of gouge data acquired by the USGS in the Alaskan Beaufort Sea between 1972 and 1979 with a total trackline length of 1500 kilometers. Data were obtained both inside and seaward of the barrier islands to the 38-meter isobath. The location of the different sampling lines is shown in Figure 3, ranging from Smith Bay on the west to Camden Bay on the east.

Since only 4 or 5 tracklines are located near the Kuvlum pipeline route, there are insufficient site-specific gouge data to develop statistically representative distributions of ice gouge characteristics. Consequently, the entire Beaufort Sea data set presented by Weeks, et al. (1983) will be used in this study.

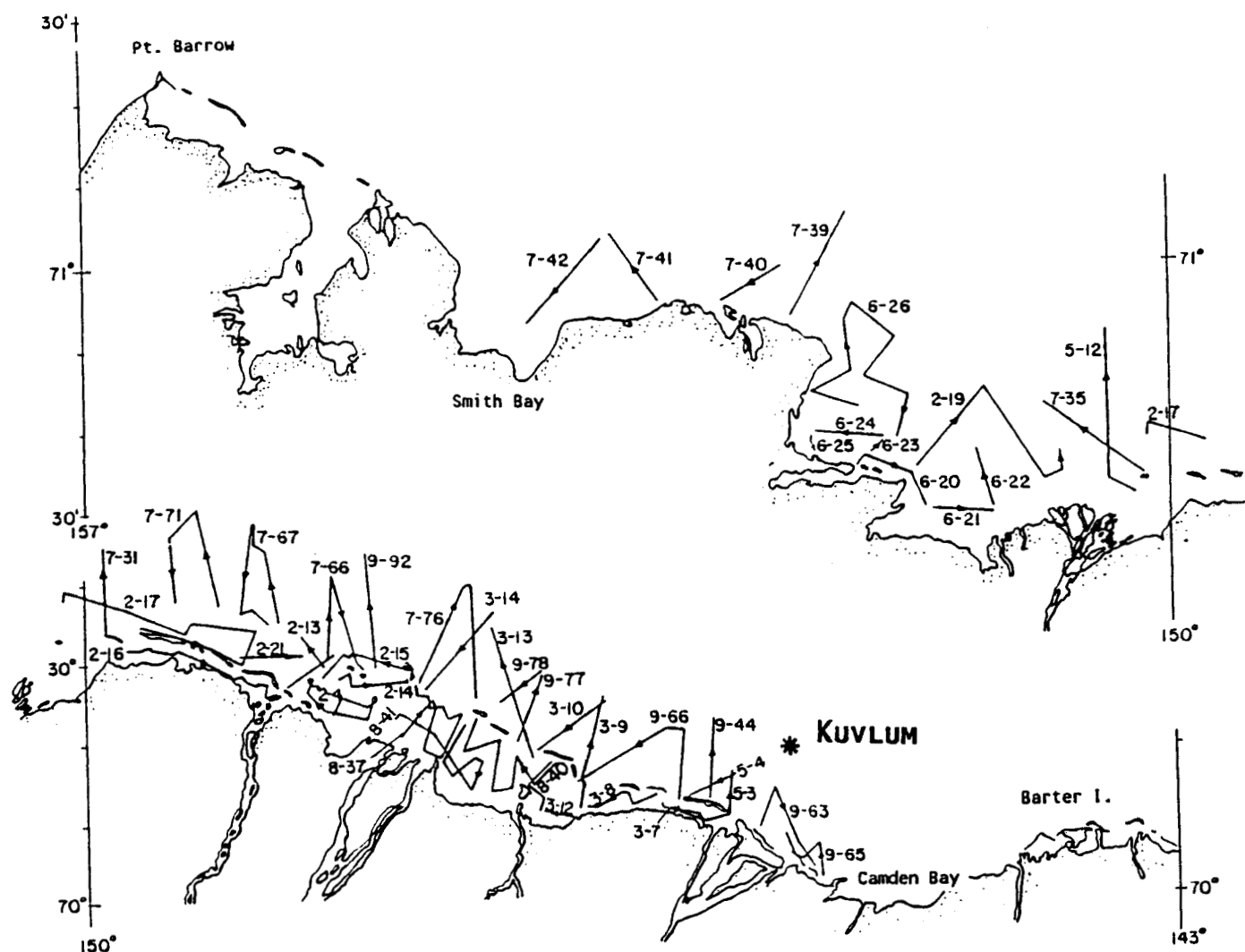


FIGURE 3. MAP SHOWING LOCATION OF THE SAMPLING LINES [WEEKS, 1983].

### 3.1 Gouge Density and Orientation

Ice gouge densities exceeding 50 per kilometer were common along the coast in 20 to 38 meters of water. Densities exceeding 100 gouges per kilometer were encountered in almost 25% of the 1-kilometer segments of the Beaufort Sea tracklines obtained in water depths greater than 20 meters. The average density was 81 gouges per kilometer for the 20-38 meter water depth range.

Gouge densities averaged 23 per kilometer in the 10-20 meter water depth range, and 9 per kilometer in water shallower than 10 meters offshore of the barrier islands. Inside the lagoons the average gouge density was less than 1 gouge per kilometer with a maximum density of 12 gouges per kilometer.

The dominant orientation of ice gouges has a well-developed east-west trend that parallel the coast and isobaths in the Alaskan Beaufort Sea. Specifically, north of Flaxman Island and in western Camden Bay the ice gouge orientation ranged between 090° and 100°.

While it is useful to have a general idea on the concentration and trend of existing ice gouges, the remainder of this report will focus on gouge incision depth, the most important gouge characteristic.

### 3.2 Ice Gouge Depth Distributions

In order to develop a preliminary set of burial depth profiles along the selected Kuvlum pipeline route (shown in Figure 1), it

is necessary to establish the gouge depth distribution as a function of water depth along the pipeline route. Side-scan sonar and fathometer records in the USGS gouge data (Weeks, et al., 1983) revealed some 20,340 individual ice gouges having a depth equal to or greater than 0.2 meter (the "cutoff" value based on the resolution of the fathometer used to collect the data).

Weeks found that the gouge depths are distributed as a negative exponential. Thus, the probability distribution function (PDF) of gouge depths will have the form

$$f(d) = \lambda \exp (-\lambda[d-c]) \quad (1)$$

where  $d$  is the gouge depth random variable,  $c$  is the cutoff gouge depth, and  $\lambda$  is the distribution parameter. A maximum likelihood estimate of  $\lambda$  is simply the reciprocal of the difference between the sample mean gouge depth ( $d_m$ ) and the cutoff depth ( $c$ ), written as:

$$\lambda = 1/(d_m - c) \quad (2)$$

A negative exponential distribution has been used to describe the depth of ice gouging elsewhere in the Canadian Beaufort and Alaskan Chukchi Seas (Lewis, 1977; Vaudrey, 1990).

Weeks separated the gouge depths into 5-meter water depth intervals for the lagoons and locations seaward of the barrier islands. In addition, the gouge depth data were placed in "bins" for each 0.2-meter depth interval. The depth intervals begin with 0.2 meter to account for the "cutoff" value based on the

resolution of the fathometer used to collect the data. The gouge depth data are presented in Table 1 as a series of histograms. The number of ice gouges, lambda ( $\lambda$ ) values, average gouge depth ( $d_m$ ), and cutoff values are included for each gouge depth histogram.

TABLE 1

GOUGE DEPTH HISTOGRAMS  
FOR A SERIES OF WATER DEPTH INTERVALS  
ALONG THE ALASKAN BEAUFORT SEA COAST

Midpoint of gouge depth (d) interval	Lagoons	Offshore of Barrier Islands (m)					
	0-5 m	5-10	10-15	15-20	20-25	25-30	30-35
0.3	61	609	1761	2110	4135	2427	764
0.5	3	78	532	616	1587	1486	520
0.7	1	13	196	184	428	604	241
0.9		6	61	85	250	482	176
1.1			24	34	93	252	86
1.3			7	11	41	94	47
1.5			5	5	28	72	33
1.7			1	1	8	23	10
1.9			0		3	12	11
2.1			0		3	5	1
2.3			1			4	1
2.5						1	1
2.7						1	1
2.9						0	1
3.1						0	0
3.3						0	0
3.5						1	0
3.7							0
3.9							1
N	65	706	2588	3046	6576	5464	1894
$\lambda$	8.66	7.43	5.03	5.09	4.48	2.98	2.71
$d_m$	0.32	0.33	0.40	0.40	0.42	0.54	0.57
c	0.20	0.20	0.20	0.20	0.20	0.20	0.20

#### 4. GOUGE DEPTH STATISTICS

##### 4.1 Computational Methods

After synthesizing the existing gouge depth data for the Alaskan Beaufort Sea, the next step is to find or develop a statistical model to process these data and assess the hazard to subsea structures posed by deep-keeled ice. It is a simple matter to use the exceedance probability function to determine the probability of occurrence for a given gouge depth if the average gouge depth ( $d_m$ ) and cutoff limit ( $c$ ) are known for a specific region or water depth. The exceedance probability is the complementary function of the cumulative distribution function (CDF), found by integration of equation (1) as

$$F_D(d) = 1 - \exp(-\lambda[d-c]) \quad (3)$$

Thus, the exceedance probability becomes

$$P[D \geq d] = 1 - F_D(d) = \exp(-\lambda[d-c]) \quad (4)$$

Unfortunately, application of the above solution is not particularly meaningful since it does not consider the occurrence rate of new gouges.

Ice Keels. Several researchers avoided the analysis of ice gouges directly and concentrated on ice keel data to estimate the annual gouging rate. Pilkington and Marcellus (1981) used laser profiles of ice ridges to estimate the distribution of underlying keel depths. By combining keels with ice movement rates, determined from drifting buoys, they developed ice keel, and by

inference ice gouge, time series. Wadhams (1983) followed a similar approach by utilizing ice keel profiles obtained directly from upward-scanning sonar attached to submarines.

Both of these methods require many assumptions to convert the measured keel data to a simulated gouge time history. For instance, sail height profiles of above-surface ice must assume some keel depth-to-sail height ratio before converting to equivalent ice gouges. On the other hand, keel profile statistics, computed for water depths sufficient to operate nuclear submarines, are assumed to be the same for deep-water pack ice as for ice that moves over the shallower Beaufort shelf. The number and depth of ice keels that are prevented from entering a region by grounded deep-keeled floes is not known. The use of profile keels to count gouges implies that every keel in the deep-water pack ice has sufficient strength to gouge the seafloor to the maximum floating depth of the keel, while remaining intact, across any type of bottom sediment in the region. Finally, strong winds that can change directions abruptly may produce numerous gouges from a single ice keel, by driving it back-and-forth across the same region.

Gouge Infilling. Another approach estimates the annual gouging rate by determining the obliteration rate. Lewis (1977) first investigated the computation of new ice gouges based on infilling. He assumed that the number and depth distribution of new gouges formed each year equaled the change in the total gouge depth distribution due to infilling. It would take about 5000 years to fill a 3-meter deep gouge, assuming a uniform

sedimentation rate of 0.6 millimeter per year (Lewis, 1977; Reimnitz et al., 1977) is the only active infilling process.

It is obvious that there are other infilling processes besides sedimentation. A gouged seafloor creates abrupt local relief that produces significant changes in sedimentation rates over short distances. Gouge embankments may be sites of rapid erosion or sloughing while the gouges, as depressions, act as a focus for much higher rates of sedimentation. Most importantly, large waves and wind-generated currents, associated with the presence of a large fetch in the open-water season over the Beaufort shelf, frequently obliterate gouges in shallow water and can rapidly infill gouges in deep water. Both Weeks, Tucker, and Niedoroda (1986) and Environmental Science and Engineering (1987) have tried to model gouge infilling from sedimentation and bedload transport.

This method of estimating the annual gouging rate has its own set of assumptions and limitations. It is difficult to accurately describe all of the variables (e.g., waves, currents, gouge profiles, bottom sediments, bathymetry, season duration) involved in the complex process of gouge infilling. However, the most limiting assumption is the requirement that there is a time-averaged equilibrium in the statistical characteristics of ice gouges in a region, resulting from a balance between the rates of gouge formation and obliteration over a period of several years. It is unlikely that such equilibrium exists on the Beaufort shelf where obliteration rates are much slower than gouge formation



from deep-draft ice keels. According to Niedoroda (1990), it is possible that equilibrium may occur in narrow range of water depths corresponding to the shear ice zone where the seafloor is almost saturated by gouges.

Rare Gouge Depths. In order to consider the annual gouging rate, Weeks et al. (1983) rewrote the exceedance probability for exponentially-distributed gouge depth data as

$$P[D \geq d] = \frac{n[D \geq d]}{N} = \exp(-\lambda[d-c]) \quad (5)$$

where  $n[D \geq d]$  is the expected number of gouges with depths greater than or equal to  $d$ , given that  $N$  gouges have occurred. In evaluating the ice gouge hazard,  $n[D \geq d]$  is equal to 1 because only a single deep gouge event is necessary to damage a subsea structure, such as a pipeline. The number of gouges ( $N$ ) which occur during a specified return period is given by

$$N = g_m T L \sin \theta \quad (6)$$

where  $g_m$  is the average annual gouging rate in number of new gouges per unit length of transect per year,  $T$  is the return period in years,  $L$  is the total length of transect of interest, and  $\theta$  is the angle between the transect and the dominant trend or average orientation of the gouges. Substituting equation (6) into (5) results in

$$\exp(-\lambda[d-c]) = \frac{1}{g_m T L \sin \theta} \quad (7)$$

and rewriting in terms of  $d$  gives

$$d = c + \frac{1}{\lambda} \ln (g_m T L \sin \theta) \quad (8)$$

In this case,  $d$  is the gouge depth associated with a specified return period,  $T$ .

Even though there are only limited repetitive ice gouge surveys to determine annual gouging rates for the Beaufort Sea, neither the ice keel method nor the gouge infilling approach is better than using equation (8) and available gouge data to develop gouge depth statistics.

The above method presented by Weeks et al. (1983) is not an extreme value analysis in the traditional sense since it utilizes the entire gouge depth distribution for a region or water depth range rather than the behavior of rare gouge events over a long period of time. However, the Weeks method is sufficient for this preliminary analysis, and an extreme value analysis using a numerical simulation model can be conducted prior to final design.

#### 4.2 Pipeline Burial Depth Profiles

Extreme Gouge Depths. The model developed in the previous section is used to compute the  $T$ -year gouge depths for a selected pipeline route (approximately 35 kilometers long) from the Kuvlum drill site to Leffingwell Lagoon via the Mary Sachs Entrance, west of Flaxman Island. The route is divided into two major segments, corresponding to the segment inside the lagoon (Zone L) and another segment offshore of the barrier islands (Zone O).

The offshore segment is further subdivided into six water depth ranges (Zones 01 to 06). Each water depth range corresponds to a 5-meter water depth increment with the total water depth ranging from 5 to 35 meters.

In order to use equation (8) to compute the T-year extreme ice gouge depth, it is necessary to define the annual gouge generation rate  $g_m$  along the pipeline route. The annual gouge generation rate ( $g_m$ ) was selected as a constant 5 gouges per kilometer per year for the entire offshore zone. This value for  $g_m$  is the average number of new gouges determined from two years of repetitive surveys conducted by the USGS in 1979-80 and in 1981-82 (Barnes and Rearic, 1983). It was assumed that  $g_m$  equals 1 new gouge per km-yr as an upper bound for the lagoon zone.

The angle  $\theta$  between the offshore segment of the pipeline route (070°) and the dominant gouge trend (100°) is assumed to be a constant of 30° for  $\theta$ . The pipeline direction for the lagoon segment is 095° and the gouge trend remains 100°, giving an angle of 5° for  $\theta$ .

Even though the length of each pipeline segment  $L_i$  is different for every water depth range, the total pipeline length  $L$  of 35 kilometers must be used in equation (8) in order to preserve the same level of risk for the entire line (Wheeler and Wang, 1985). The return periods (T) of 100, 200, 500, and 1000 years are equivalent to an annual risk (exceedance probability) of 1%, 0.5%, 0.2%, and 0.1%, respectively.

Thus, the T-year gouge depth  $d$  along the pipeline can be calculated by Equation (8), using a constant "cutoff" gouge depth ( $c$ ) of 0.2 meter and the set of  $\lambda$  values presented in Table 1 for various water depths. The route description and gouge characteristics for the Kuvlum pipeline route are presented in Table 2, along with the extreme gouge depths based on the Weeks methodology.

Another set of extreme gouge depths are presented for the same return periods, but using  $\lambda^{-1}$  values. Weeks, et al. (1983) speculated that the  $\lambda$  value for new gouges is about  $1 \text{ m}^{-1}$  less than for existing gouges. This assumption increases the T-year gouge depths by about 50% for the deeper water depth ranges (25 to 35 meters) and by about 25% for the shallower water depth ranges (10 to 25 meters).

Comparison with Canadian Beaufort Sea. Lewis and Blasco (1990) reported that two 7-meter deep gouges have been "observed" on the Canadian Beaufort shelf, one in 45 meters of water and the other in 50 meters. Out of a data base of 10,385 events the deepest recorded gouge is 6 meters, located in a 45-m water depth.

Approximately 880 new gouges were recorded during repetitive surveys conducted from 1974 through 1986. The deepest recorded new gouge depth is 4.5 meters in a 26-m water depth. The maximum annual gouge generation rate ranged from 5 to 8 gouges per km-yr for water depths of 20 to 35 meters. These values compare closely with the computed average annual gouge rate ( $g_m$ ) of 5 gouges per km-yr used in this study.

TABLE 2

EXTREME GOUGE DEPTHS  
FOR A PIPELINE ROUTE  
FROM KUVLUM TO LEFFINGWELL LAGOON

Parameters	Pipeline Route Zones						
	L	01	02	03	04	05	06
<u>Route Description</u>							
Length ( $L_i$ , km)	60*	5.4	3.2	3.3	8.3	9.7	5.1
Orientation	095°	070°	070°	070°	070°	070°	070°
Water Depth (m)	<5	5-10	10-15	15-20	20-25	25-30	30-35
<u>Gouge Parameters</u>							
Total Gouges	65	706	2588	3046	6576	5464	1894
Annual Gouge Rate ( $g_m$ , [km-yr] <sup>-1</sup> )	1	5	5	5	5	5	5
Lambda ( $\lambda$ , m <sup>-1</sup> )	8.66	7.43	5.03	5.09	4.48	2.98	2.71
Cutoff (c, m)	0.2	0.2	0.2	0.2	0.2	0.2	0.2
Gouge Trend	100°	100°	100°	100°	100°	100°	100°
<u>T-year Gouge Depths (m)</u>							
<u>Eq. (8) Results (using above <math>\lambda</math> values)</u>							
T = 100 years	0.92	1.42	2.00	1.98	2.23	3.25	3.55
T = 200 years	1.00	1.51	2.14	2.12	2.38	3.48	3.81
T = 500 years	1.11	1.64	2.32	2.30	2.59	3.79	4.14
T = 1000 years	1.19	1.73	2.46	2.44	2.74	4.02	4.40
<u>Eq. (8) Results (using <math>\lambda^{-1}</math> values)</u>							
T = 100 years	1.02	1.61	2.45	2.42	2.81	4.78	5.51
T = 200 years	1.11	1.72	2.62	2.59	3.01	5.13	5.91
T = 500 years	1.23	1.86	2.85	2.81	3.27	5.60	6.45
T = 1000 years	1.32	1.97	3.02	2.98	3.47	5.95	6.85

\* Lagoon pipeline length taken as 60 km assuming landfall is Endicott, but could be as little as 5 km if landfall is Pt. Thompson.

Lewis (1977) used a Gumbel extreme value analysis of Canadian Beaufort gouge data to determine the 100-year gouge depths of approximately 3.0-3.5 meters, 3.5-4.5 meters, and 4.5-5.0 meters for water depth range of 20-25 meters, 25-30 meters, and 30-35 meters, respectively. The corresponding gouge depths from Table 2 are 2.2-2.8 meters, 3.3-4.8 meters, and 3.6-5.5 meters, respectively. These Lewis values compare closely to the Weeks gouge depths for the two deeper water depth ranges, but are significantly greater for the 20-25 m water depth range.

Pipeline Burial Depths. It is important to note that using equation (8) results in extreme ice gouge depths, not pipeline burial depths. However, in this context, the terms "extreme gouge depth" and "pipeline burial depth" are identical, meaning that the distance from the existing seafloor to the top of the pipeline should be equal to or greater than the selected extreme gouge depth in order to provide the minimum adequate protection for the pipeline.

A set of preliminary design burial depth profiles are presented in Figures 4 through 7 for the selected Kuvlum pipeline route. Figures 4-7 show the pipeline burial depth profiles for the 100-year, 200-year, 500-year, and 1000-year return period ice gouge depths, respectively, using the  $\lambda$  values presented in Table 2. Another set of burial depth profiles are presented in Figures 8-11 for the same return periods, but using  $\lambda-1$  values. This assumption increases the required pipeline burial depth by about 25% to 50%, depending on the water depth.

**FIGURE 4**  
**BURIAL DEPTH PROFILE**  
**RP = 100 Years (Lambda)**

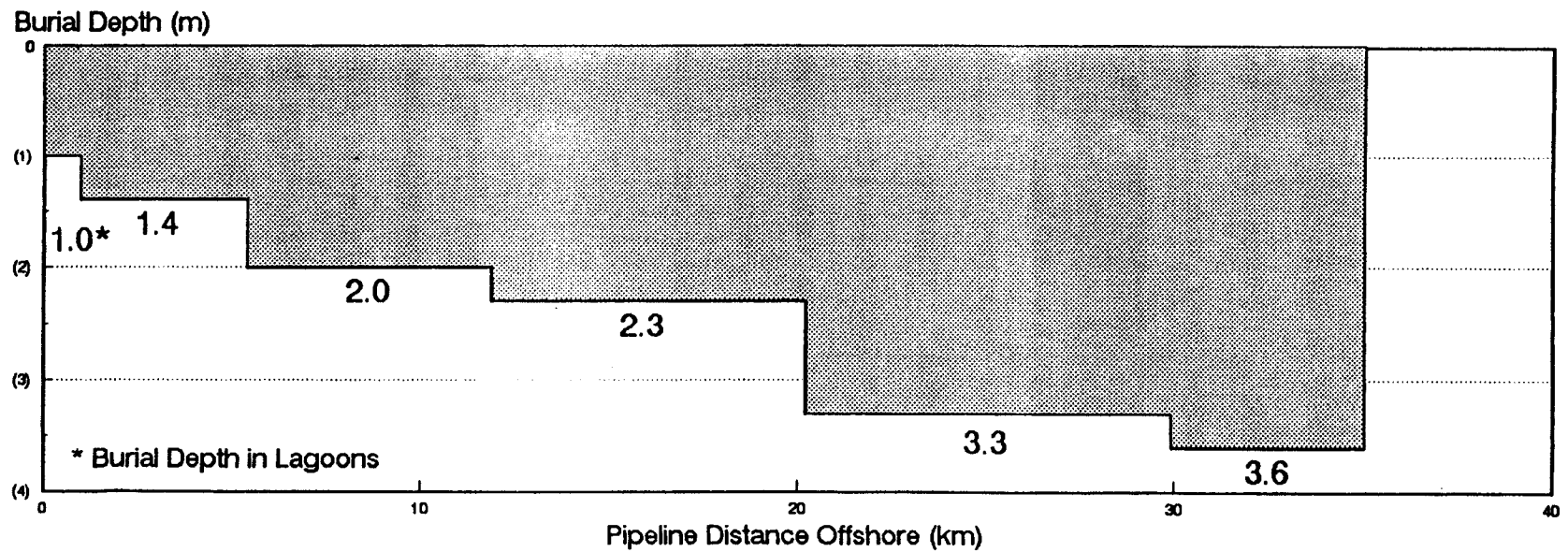
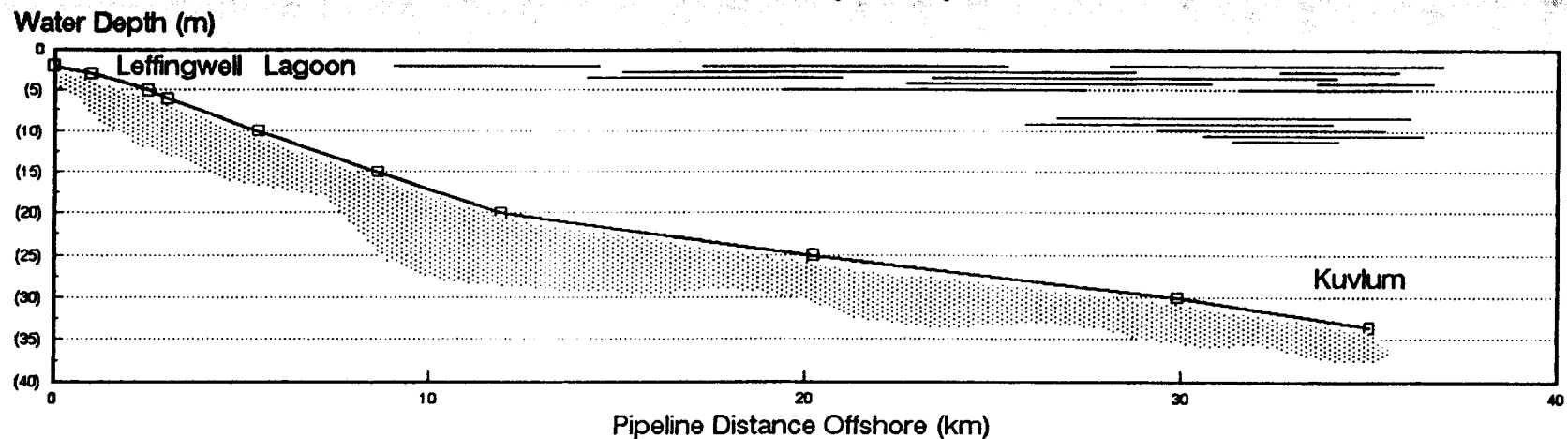


**FIGURE 5**  
**BURIAL DEPTH PROFILE**  
**RP = 200 Years (Lambda)**

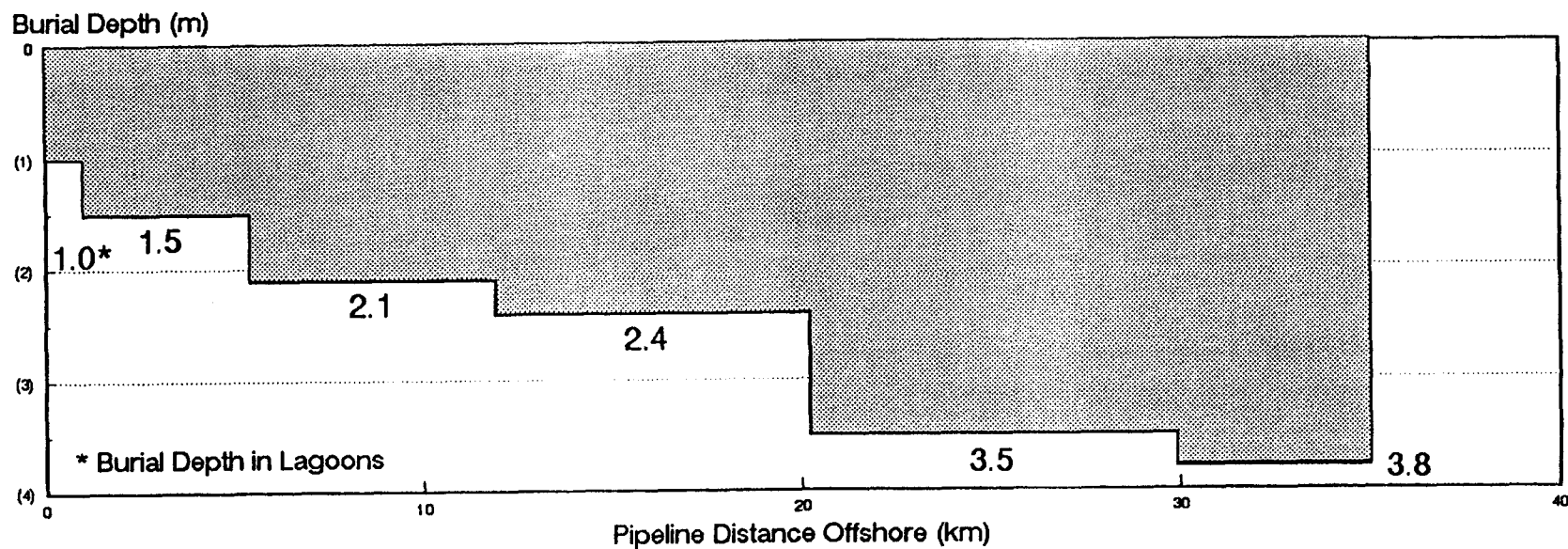
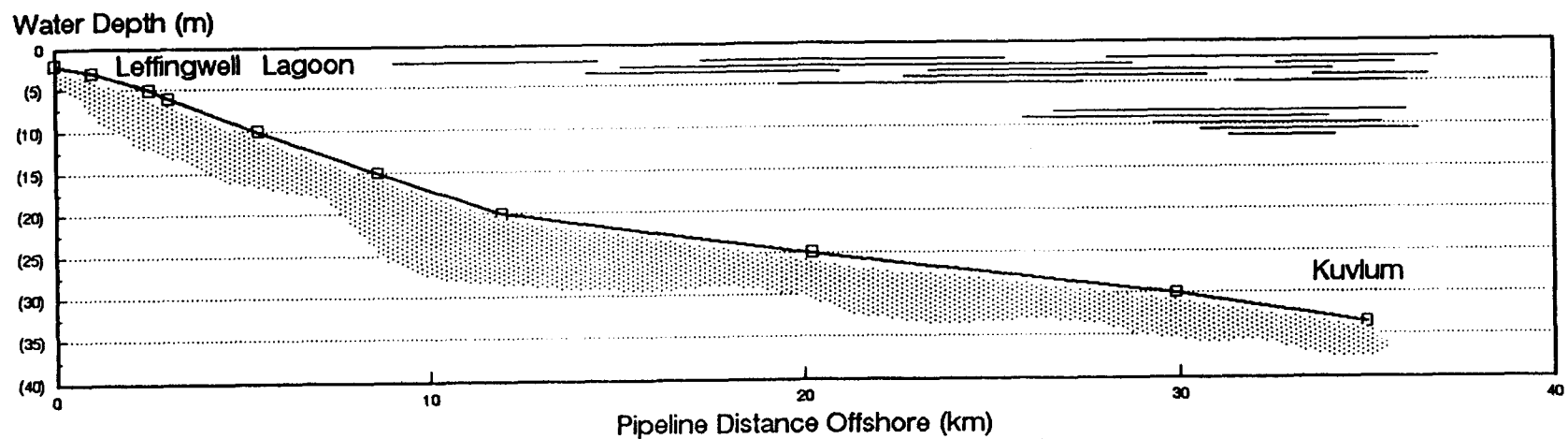




**FIGURE 6**  
**BURIAL DEPTH PROFILE**  
**RP = 500 Years (Lambda)**

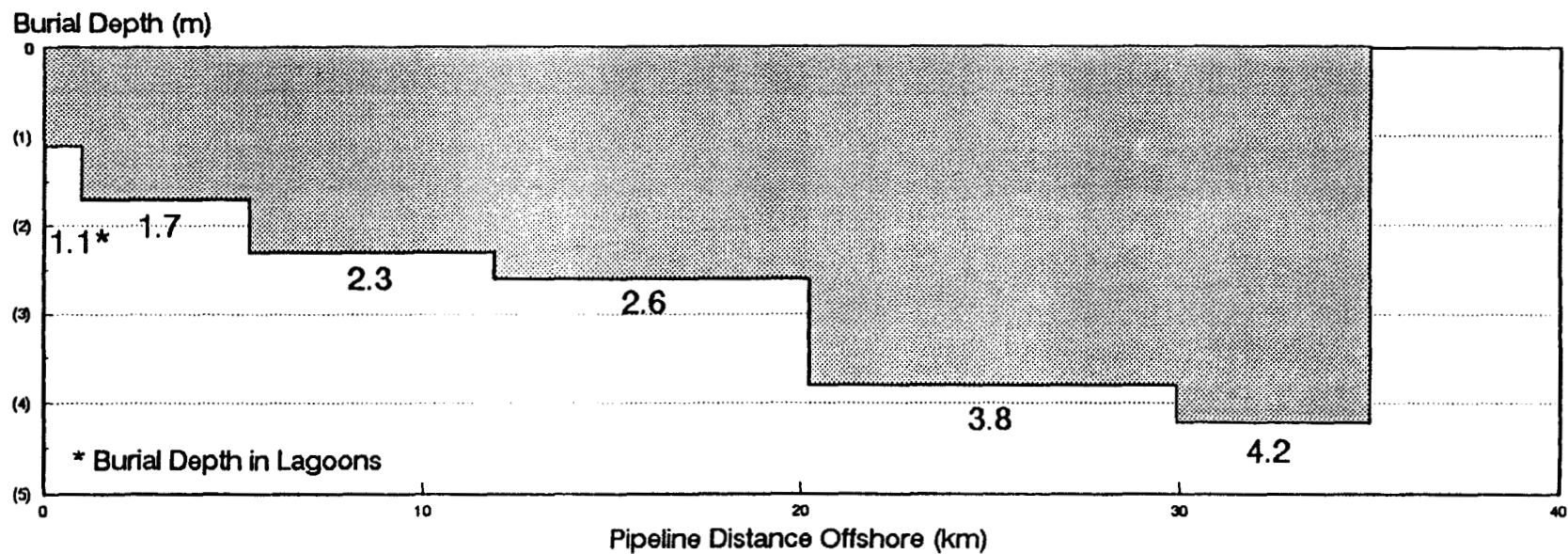
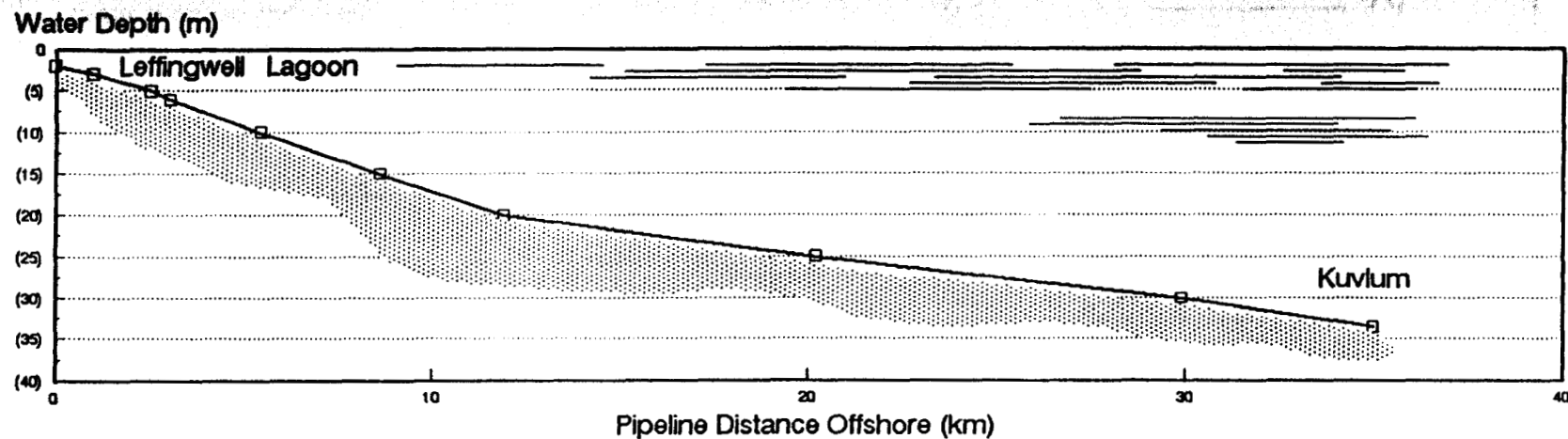


**FIGURE 7**  
**BURIAL DEPTH PROFILE**  
**RP = 1000 Years (Lambda)**

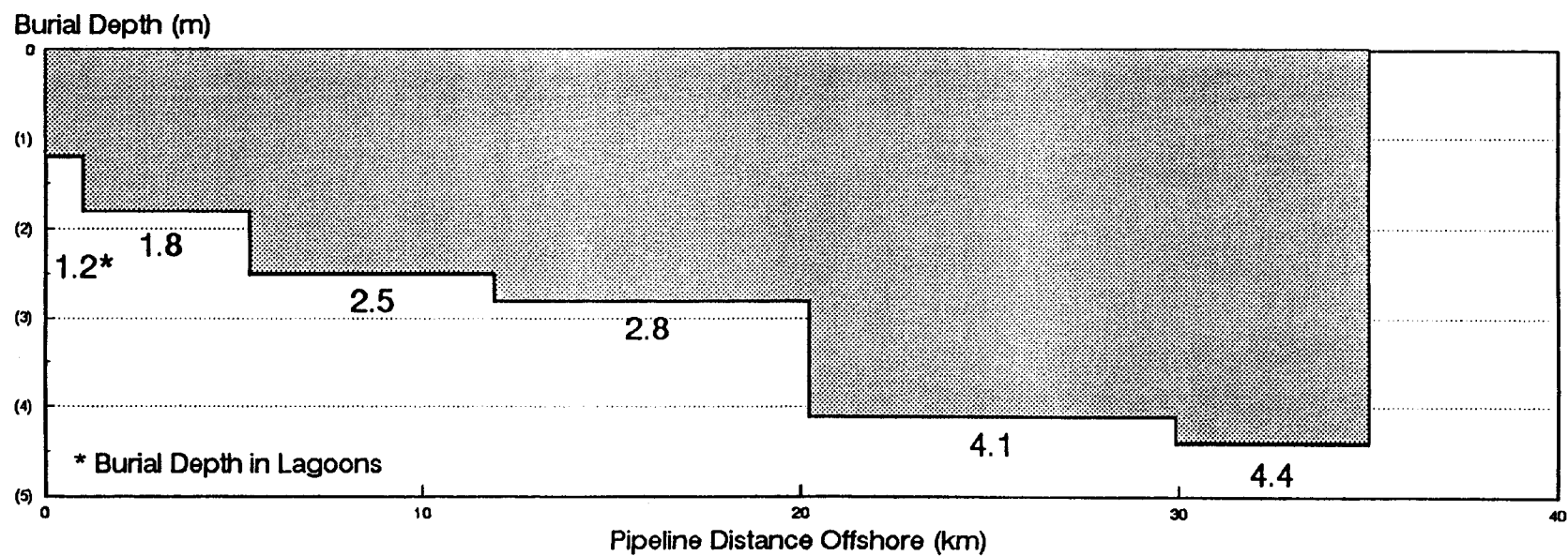
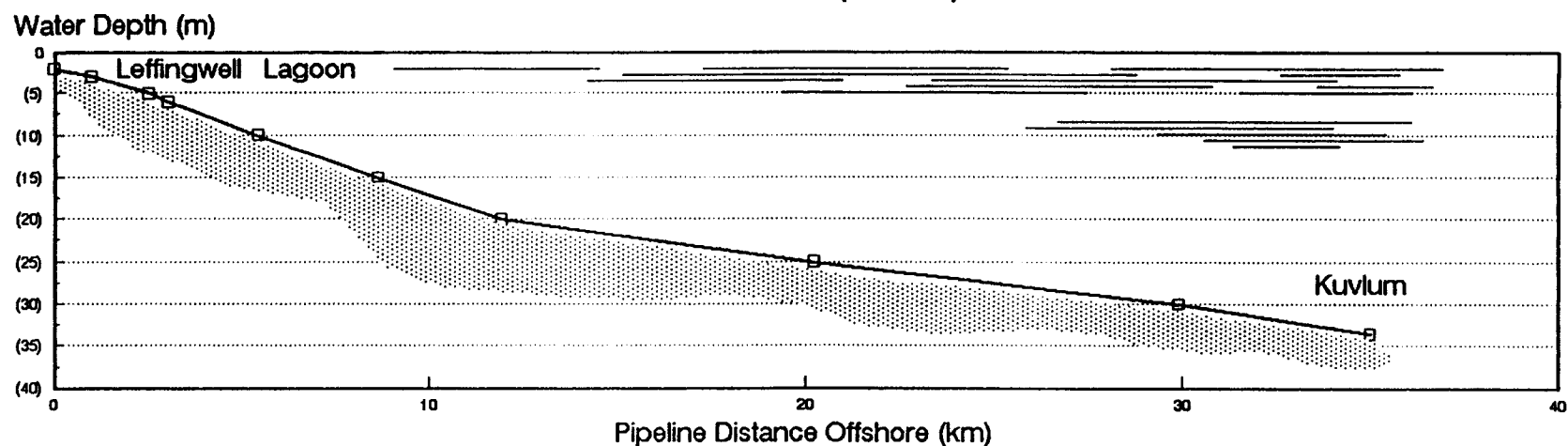


**FIGURE 8**  
**BURIAL DEPTH PROFILE**  
 RP = 100 Years ( $\Lambda = 1$ )

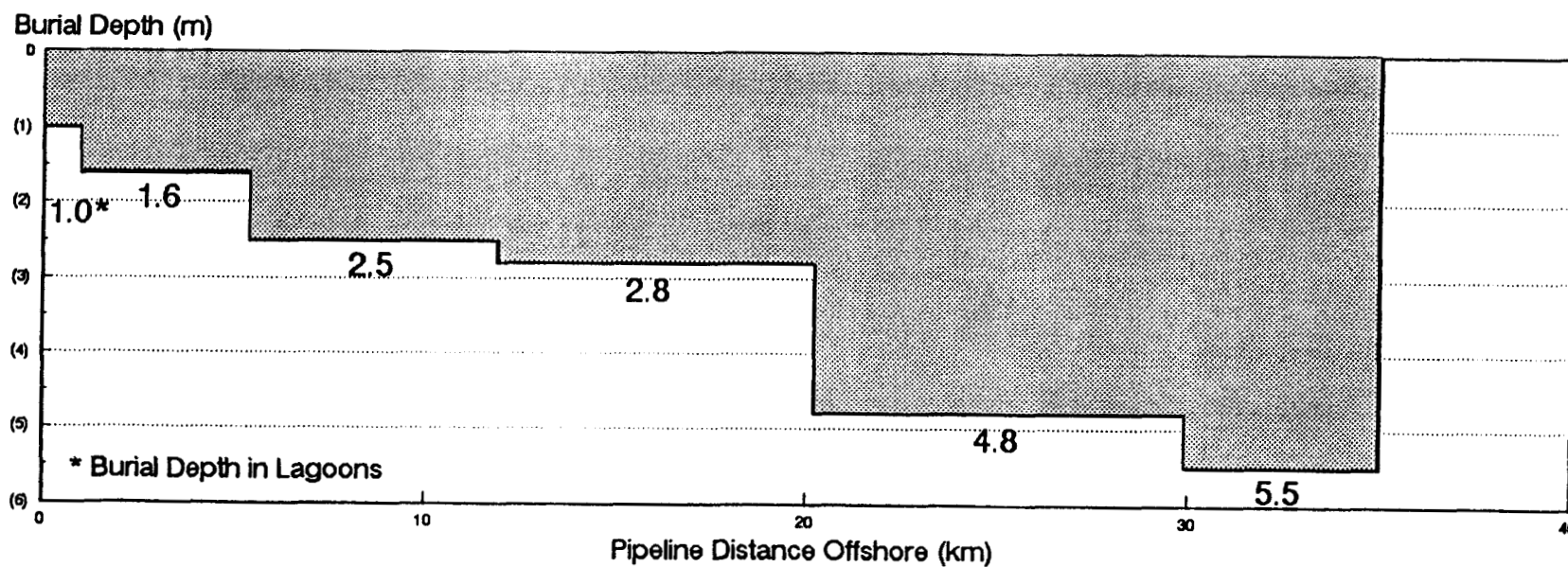
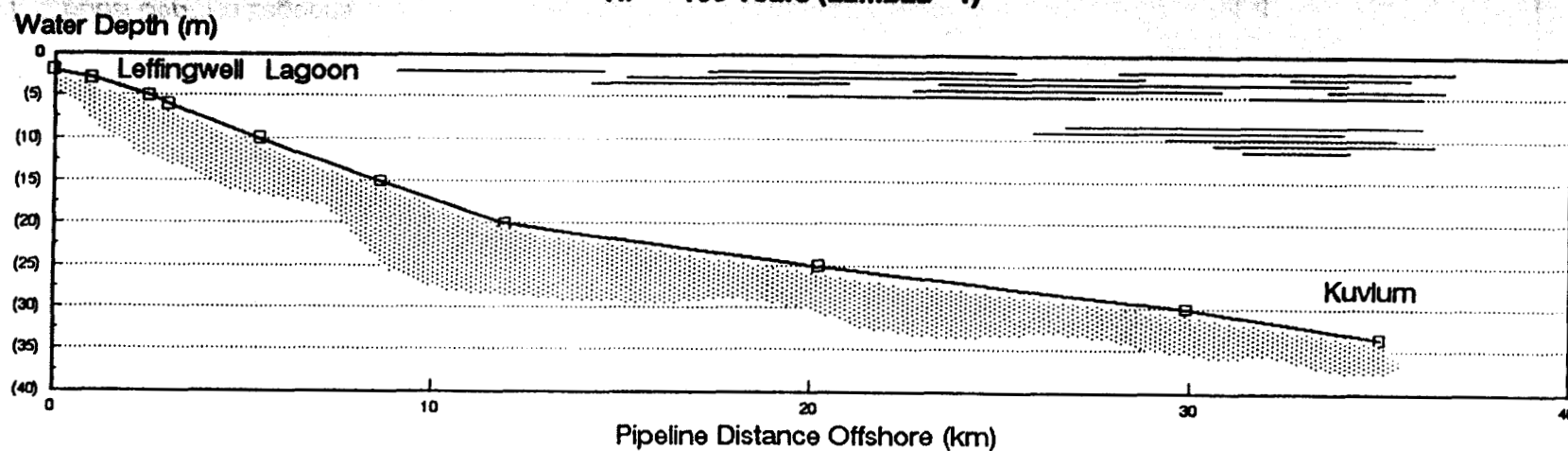


**FIGURE 9**  
**BURIAL DEPTH PROFILE**  
 RP = 200 Years ( $\Lambda - 1$ )

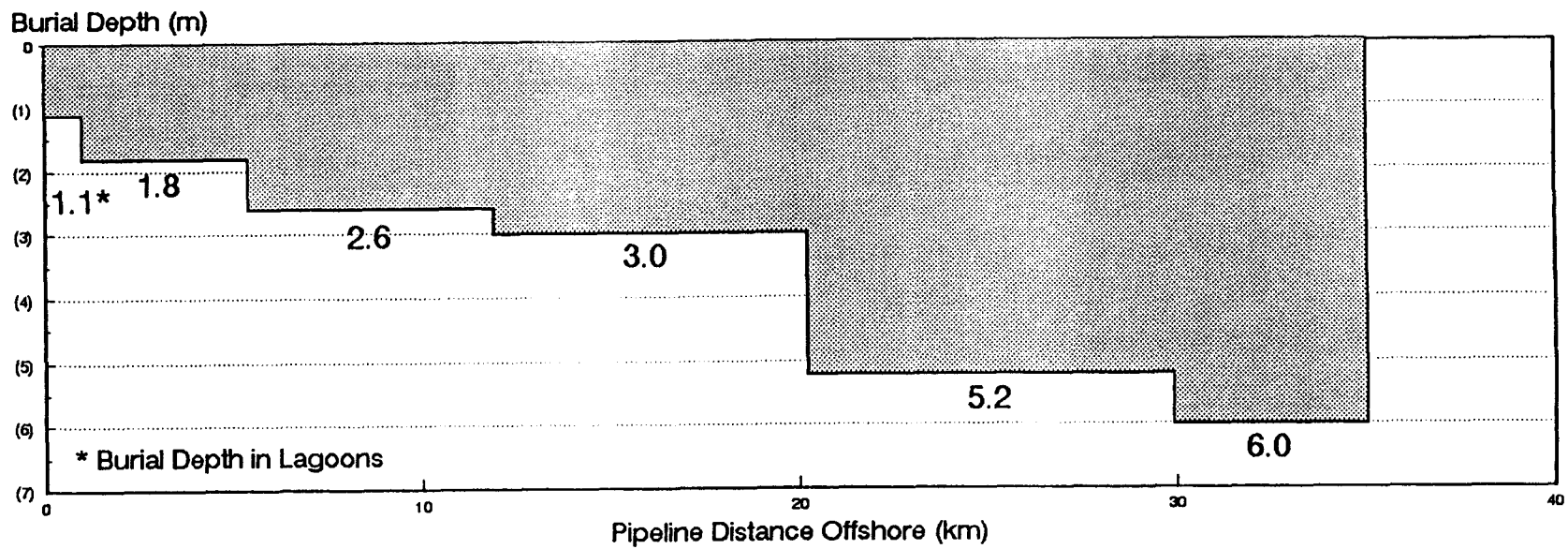
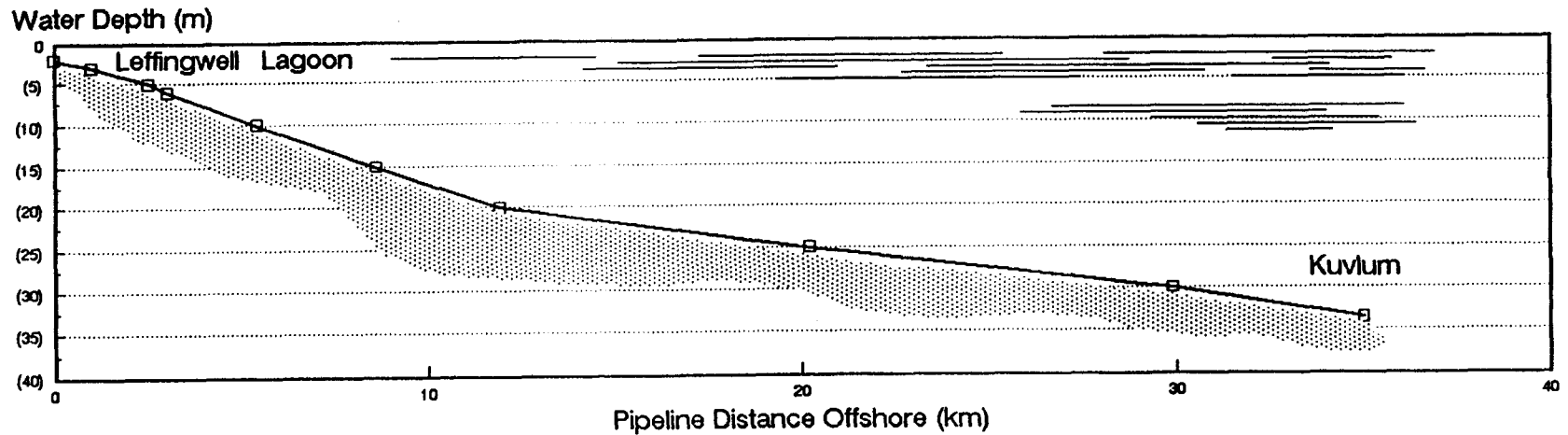


**FIGURE 10**  
**BURIAL DEPTH PROFILE**  
**RP = 500 Years (Lambda = 1)**

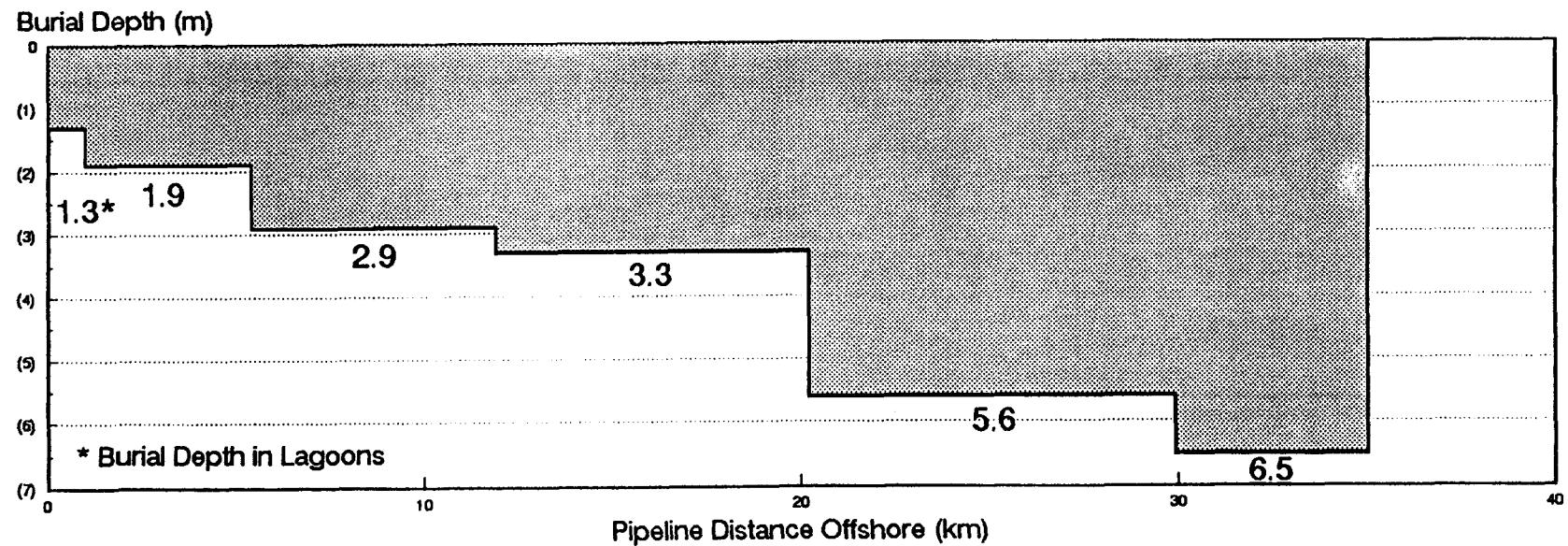
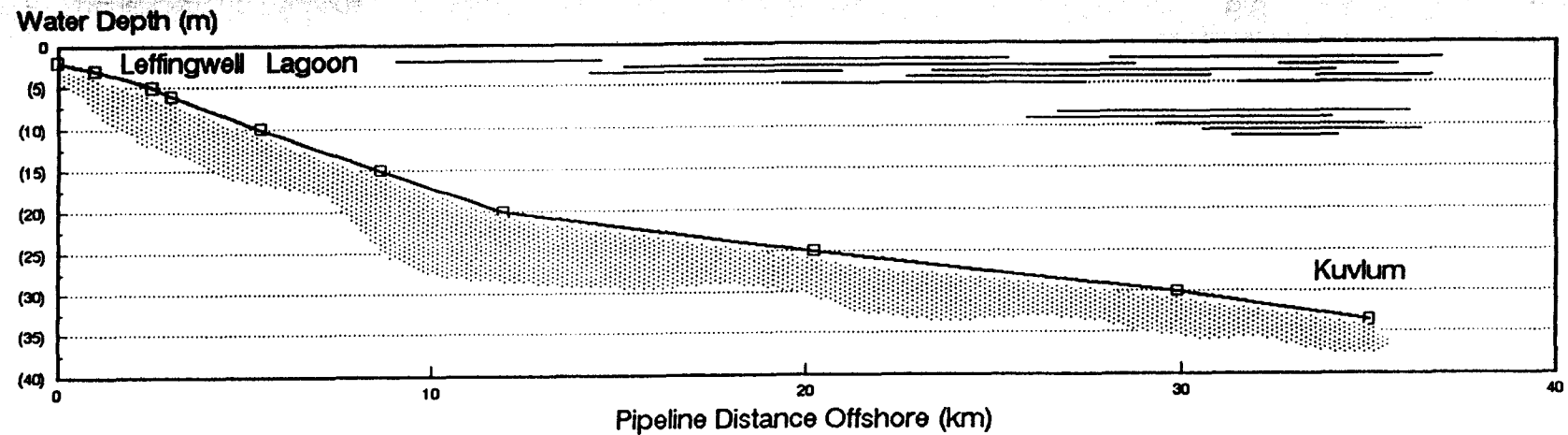
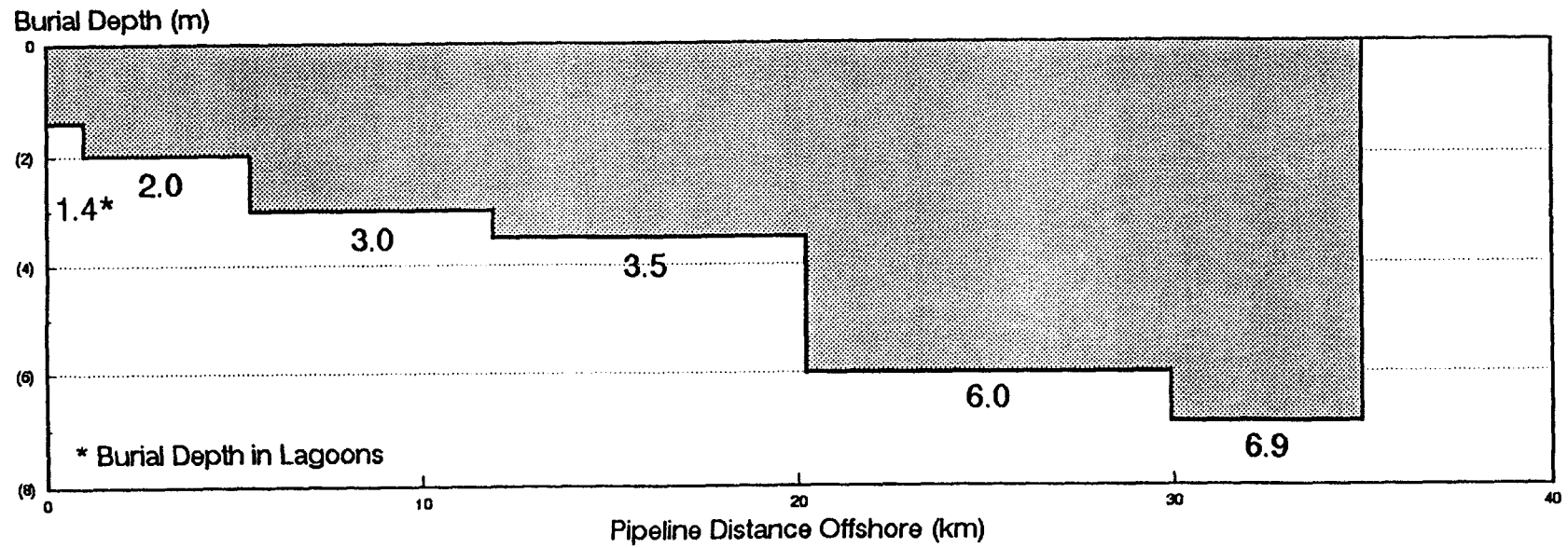
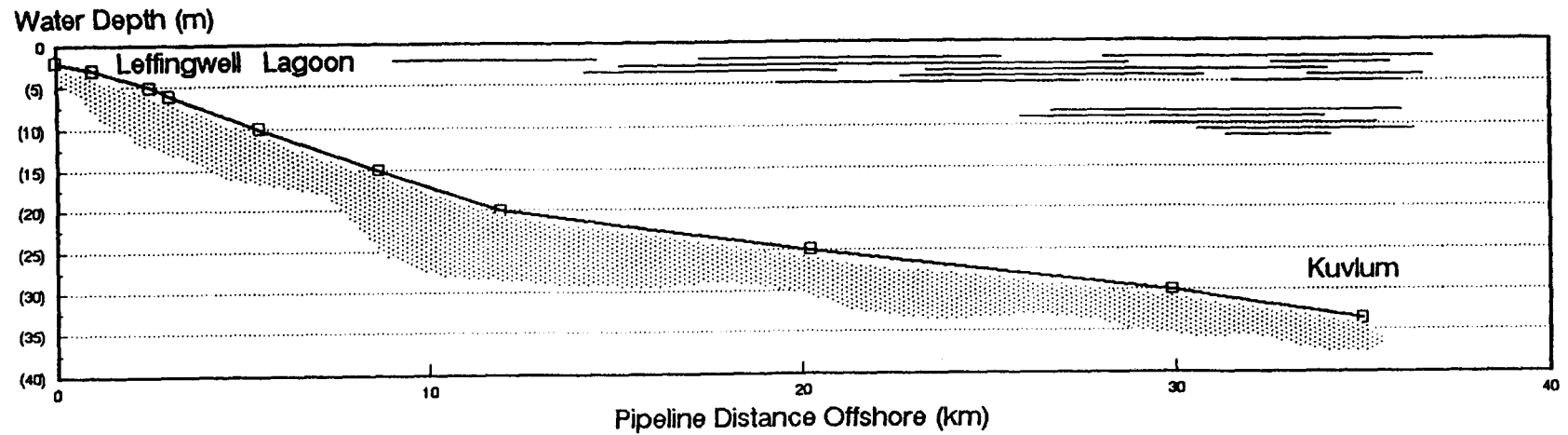


**FIGURE 11**  
**BURIAL DEPTH PROFILE**  
 RP = 1000 Years ( $\Lambda$  - 1)





## 5. RECOMMENDATIONS

This study is limited to one existing ice gouge data set collected by the USGS during the 1970's. In order to develop final design burial depth criteria for pipelines in the Kuvlum region, the following recommendations are presented to remove some of the uncertainty in the preliminary burial depth profiles developed in this report.

- 1) Additional repetitive, year-to-year surveys along the same tracklines are needed to establish a more reliable annual gouging rate ( $g$ ) and distribution parameter ( $\lambda$ ) for new gouges.
- 2) Site-specific ice gouge data should be acquired given that there is a wide variation over relatively short distances in the existing gouge data.
- 3) Existing and future ice gouge data should be compared with surface geotechnical maps to determine if there is a correlation between gouge depth and seafloor sediment thickness or soil type.
- 4) Design pipeline burial depths need to take into account, not only extreme ice gouge depths, but the extent of soil deformation and resulting pressures developed from ice keels plowing the sediment above buried pipelines.

- 5) Gouge data should be collected as early as possible in the summer season, especially in the nearshore zone, to measure the depth of recently formed gouges before early summer storms and bottom currents obliterate them.
- 6) Lithodynamics (movement of seafloor soils by waves and currents) may govern the depth of pipeline burial in shallow water, but very little or no littoral drift data have been collected.
- 7) Consistent resolution of fathometer instrumentation is necessary during any future gouge surveys so that the data bases can be merged and analyzed.
- 8) While the existing data base may not warrant any major improvements in computational methods, analysis techniques should account for the fact that other gouge characteristics, such as length, width, and orientation, are random variables. In addition, other distributions (e.g., gamma, lognormal) should be tested to see whether they fit the gouge depth data better than an exponential function.



## 6. REFERENCES

1. Aagaard, K. (1984), The Beaufort Undercurrent, in The Alaskan Beaufort Sea: Ecosystems and Environments edited by Barnes, Schell, and Reimnitz, Academic Press, NY, p. 47-71.
2. Barnes, P., E. Reimnitz and D. Rearic (1984), Ice Gouging Characteristics and Processes, in The Alaskan Beaufort Sea: Ecosystems and Environments edited by Barnes, Schell, and Reimnitz, Academic Press, NY, p. 159-183.
3. Barnes, P. and D. Rearic (1983), Characteristics of Ice Gouges Formed from 1975-82 on the Alaskan Beaufort Sea Inner Shelf, NOAA-OCSEAP Final Reports, Attachment G, p. 1-25.
4. C-Core (1993), Pressure Ridge Ice Scour Experiment, AOGA Project No. 388, St. John's, Newfoundland.
5. Environmental Science and Engineering Inc. (1987), Chukchi Sea Ice Gouge Infill Rate Estimation, prepared for Shell Development Company, Gainesville, Florida.
6. Harding-Lawson Associates (1986), Beaufort Sea Multiyear Ice Gouging Study, AOGA Project No. 225, Novato, California.
7. Hnatiuk, J. and K. Brown (1977), Sea Bottom Scouring in the Canadian Beaufort Sea, Offshore Technology Conference Paper No. OTC 2946, Houston, Texas.

8. Kovacs, A. and M. Mellor (1974), Sea Ice Morphology and Ice as a Geologic Agent in the Southern Beaufort Sea, in The Coast and Shelf of the Beaufort Sea, edited by Reed and Sater, Arctic Institute of North America, Arlington, Virginia, p. 113-161.
9. Lewis, C. (1977), Estimation of the Frequency and Magnitude of Drift-Ice Groundings from Ice Scour Tracks in the Canadian Beaufort Sea, POAC-77, St. John's, Newfoundland.
10. Lewis, C. and S. Blasco (1990), Character and Distribution of Sea Ice and Iceberg Scours, Workshop on Ice Scouring and the Design of Offshore Pipelines, Calgary, Alberta.
11. Niedoroda, A. (1990), Sea Ice Gouging (Scour), Chapter 34 in Handbook of Coastal and Ocean Engineering, edited by J. Herbick, Gulf Publishing, Houston.
12. Pelletier, B. and J. Shearer (1972), Sea Bottom Scouring in the Beaufort Sea of the Arctic Ocean, Marine Geology and Geophysics, Proceedings of the 24th International Geological Congress, Section 8, p. 251-261.
13. Pilkington, R. and R. Marcellus (1981), Methods of Determining Pipeline Trench Depths in the Canadian Beaufort Sea, POAC-81, Quebec City, Quebec, Canada.
14. Reimnitz, E. and P. Barnes (1974), Sea Ice as a Geologic Agent on the Beaufort Sea Shelf of Alaska, in The Coast and Shelf of the Beaufort Sea, edited by Reed and Sater, Arctic Institute of North America, Arlington, Virginia, p. 301-353.

15. Reimnitz, E., et al. (1977), Ice Gouge Recurrence and Rates of Sediment Reworking, Beaufort Sea, Alaska, Geology, Vol. 5, p. 405-408.
16. Reimnitz, E., P. Barnes, and L. Phillips (1984), Sixty-Meter Deep Pressure Ridge Keels in the Arctic Ocean Suggested from Geological Evidence, IAHR Ice Symposium, Hamburg, West Germany.
17. Toimil, L. (1978), Ice Gouged Microrelief on the Floor of the Eastern Chukchi Sea, Alaska: A Reconnaissance Survey, US Geological Survey Open File Report 78-693.
18. Vaudrey, K. (1990), Chukchi Sea Ice Gouging Study, prepared for Shell Development Company (proprietary), Vaudrey & Associates, Inc., San Luis Obispo, CA.
19. Wadhams, P. (1983), Predictions of Extreme Keel Depths from Sea Ice Profiles, Cold Regions Science and Technology, Vol. 6, p. 257-266.
20. Weeks, W. et al. (1983), Statistical Aspects of Ice Gouging on the Alaskan Shelf of the Beaufort Sea, CRREL Report 83-21, Hanover, NH.
21. Weeks, W., W. Tucker and A. Niedoroda (1986), Preliminary Simulation of the Formation and Infilling of Sea Ice Gouges, Ice Scour and Seabed Engineering Workshop, edited by Lewis et al., Calgary, Alberta, Canada.

22. Wheeler, J. and A. Wang (1985), Sea Ice Gouge Statistics,  
POAC-85, Narssarssuaq, Greenland.



## VAUDREY & ASSOCIATES, INC.

1540 Marsh Street - Suite 105

San Luis Obispo, CA 93401

Phone: (805) 544-0940

Fax: (805) 544-0940

November 2, 1993

Mr. John Eldred  
New Ventures Engineering  
ARCO ALASKA, INC.  
P. O. Box 100360  
Anchorage, Alaska 99510-0360

Dear John:

### KUVLUM DESIGN ICE LOAD REVIEW

After review of excerpts of the Sandwell report on the environmental overview and design ice loads for Kuvlum production structure concepts, I have prepared my comments in the following categories: (1) probabilistic ice load methodology, (2) multiyear ice parameters, (3) extreme ice feature encounter frequency, and (4) design ice load computation:

***Probabilistic Ice Load Methodology.*** Sandwell described their methodology as analogous to that specified in the CSA Code. Actually, there are two differences between the CSA Code and the Sandwell approach: (1) the CSA framework specifies the computation of the expected number of ice feature encounters with the structure before the ice load computation, not after as performed in the Sandwell model, and (2) the CSA Code calls for an extreme value analysis to assign probability distributions to the global ice loading of the structure.

(1) The reason for determining the expected number of impacts before computing the ice loads is that the probability distribution for the diameter and velocity of all multiyear floes and only those that impact the structure are not the same. In other words, larger and faster floes are more likely to encounter the structure. On the other hand, Sandwell first computes the global ice load for a single encounter, then assumes a specific number of seasonal ice feature encounters, and raises the cumulative distribution function for the global ice load to the power of the number of assumed ice feature encounters ( $N$ ). In the tail of the distribution, this operation is equivalent to multiplying the exceedance probability ( $1 - CDF$ ) by the number of ice encounters ( $N$ ) [see Fig. 3.6 of the Sandwell report]:

$$N(1 - CDF) \approx 1 - (CDF)^N$$

$$10(1 - 0.999) \approx 1 - (0.999)^{10}$$

$$0.01 \approx 0.0099551$$

if  $CDF$  approaches unity

The Sandwell approach is a perfectly acceptable alternative to computing the ice feature encounters first.

(2) Sandwell's description of the interaction conditions (Section 3.2.2) does not say whether the ice load exceedance probability distribution for repeated simulations of a single multiyear floe impact represents the peak or maximum load for each simulation. This should be clarified because it is necessary for an extreme value analysis that the annual exceedance probability distribution for a single impact represent the maximum value for each simulation. I believe that Sandwell's computations are correct, but the text should explicitly state that each ice load value is the maximum for each simulation.

**Multiyear Ice Parameters.** Sandwell states that most of the ice parameter distributions are contained in the Gulf Canada probabilistic ice load model. However, all of the figures in their draft report (e.g., Figure 2.4 Multiyear Floe Size and Thickness Distributions) were blank pages, which made evaluation of them exceedingly difficult. Consequently, I have used representative probability distribution functions developed for the Eastern Beaufort Sea region, and specifically Camden Bay, as input to our in-house probabilistic ice load model.

Based on 7 years of winter SAR imagery, the multiyear ice concentration can be modeled as a Beta distribution (average of 13% coverage for those seasons when multiyear ice was present) and the multiyear floe diameter distribution is determined to be a lognormal with an average of 450 meters. The multiyear floe thickness is also lognormally distributed with an average of 5.5 meters, based on a combination of almost 1500 measurements of nearshore and pack floes. Floe velocities (given that there was measurable ice movement) are exponentially distributed with an average of 0.2 meters per second, based on over 1000 buoy-days in the region. The ice failure pressure distribution is assumed to be a truncated normal distribution with an average of 1 MPa.

**Extreme Ice Feature Encounter Frequency.** Sandwell implied that the computed number of multiyear ice encounters is "unreasonably" high (based on "snapshots" of winter SAR imagery and "experience" in the area) even if reasonable values of concentration, floe size, and ice movement are used. I found this comment hard to comprehend since it says that the data must be wrong based on relatively few SAR images and almost non-existent "experience" of operating during the winter in the outer Camden Bay region. Consequently, I decided to compute the expected number of winter multiyear floe encounters with the available data to see how "unreasonable" they were.

As stated above, the Beta distribution for the multiyear ice concentration has an average of 13% coverage by area. However, this is a conditional probability distribution given that multiyear ice is present in the region. According to the several sources over the past 40 years, there were 15 years in which multiyear ice was present in the vicinity of the Kuvlum Prospect. This effectively reduces the average annual multiyear ice concentration to 5%. To determine the number of floe encounters ( $N$ ) per winter season we must convert the multiyear ice concentration ( $MY\%$ ) to the number of floes per unit area and compute the "swath" area ( $A_s$ ) swept out of the ice cover by the structure as the ice moves past.

Since concentration is a measure of the areal coverage of multiyear ice, the expected number of multiyear floe encounters per unit area ( $n$ ) can be determined by dividing the multiyear ice fraction ( $MY\%$ ) by the average floe area:

$$n = \frac{4MY\%}{100\pi E[D^2]}$$

where  $MP\%$  is the multiyear ice concentration in per cent and  $E[D^2]$  is the average of the square of the floe diameter, which is equal to the sum of the mean square and variance of the floe diameter. As stated previously, the average floe diameter is 450 meters.

A multiyear floe encounter with the structure will occur if the center of the floe lies within a swath of moving ice that has an average area equal to a rectangle with a width equal to the exposure width of the structure plus the average floe diameter. The length of the swath is equal to the seasonal ice flux (average daily ice movement, including days with no ice movement) multiplied by the typical season length. The swath area ( $A_s$ ) can be expressed as:

$$\text{Swath Area} = A_s = (S + E[D])ft$$

where  $S$  is the exposure width of the structure (110 meters),  $E[D]$  is the average floe diameter (450 meters),  $t$  is the typical length of the winter season (assumed to be 180 days), and  $f$  is the winter ice flux.

The average ice flux is determined to be 220 meters per day from several years of ARGOS buoy measurements limited to water depths of 20–40 meters in the Eastern Beaufort Sea. This water depth range lies within the transition or shear ice zone and includes the Kuvlum Prospect.

Thus, during a typical winter season, the total number of multiyear floe encounters ( $N$ ) with an 110-meter structure located in the Camden Bay region is computed to be:

$$N = nA_s = (2.18 \times 10^{-7} \text{ m}^2)(2.22 \times 10^7 \text{ m}^2) \approx 5 \text{ multiyear floe encounters per winter}$$

Using reasonable data input, I come up with a reasonable number of encounters for a typical winter season. I think that most of the discrepancy between Sandwell's estimate of multiyear floe encounters and mine occurs from their assumption that the average pack ice drift of 7–10 kilometers per day is representative of the transition zone, which remains relatively stationary between major storms during the winter.

Similarly, the number of multiyear floe encounters have been computed for a combined summer and freeze-up season when the multiyear floes attain the greatest velocities. Additionally, multiyear floes, surrounded by open water or thin, first-year ice, will be free to rotate upon impact, except for a limited number of potential "head-on" collisions. I estimate that approximately 20 multiyear floe encounters will occur during the combined summer and freeze-up seasons (from July 1 to November 30).

**Design Ice Load Computation.** Sandwell determined that the global design ice load for the 110-meter production structure was governed by a winter multiyear floe/ridge impact. I concur with this conclusion after executing one summer/freeze-up multiyear floe impact scenario using our in-house probabilistic ice load model. The load distribution was generated from 10,000 simulations of a multiyear floe impact. The 100-year return period global design ice load is computed to be 480 MN, and the 1000-year return period ice load is 750 MN, both calculated by a limited momentum approach for 20 impacts per summer/freeze-up season. The resulting summer global ice loads were significantly lower than those computed for the winter season. As stated by Sandwell, a lower ice failure pressure and little or no pack ice driving force are the primary factors contributing to the lower ice loads.

As a direct comparison of the governing winter design ice loads for a 110-meter structure as presented by Sandwell in Figure 3.5 of the draft report, I computed an ice load distribution based on 10,000 simulations and one impact per winter season. I used input probability density functions for the multiyear ice parameters as set forth in an earlier section of this letter. Initially, I assumed that there would be a sufficient pack ice driving force to produce full penetration of the structure into any multiyear floe coming in contact with the structure. A limited stress approach was used to compute the maximum ice load for each simulation. The results are plotted as Vaudrey1 on the attached figure, along with the Sandwell distribution from Figure 3.5 of their report.

A second ice load distribution was generated to determine the effect of changing from a limited stress to a limited momentum approach to account for thin, first-year ice in early winter and open-water lead formation during storms. If either of these two conditions exist, there may not be sufficient driving force to insure full penetration. The results of the limited momentum calculations are shown as Vaudrey2 on the attached figure. The difference between the limited stress (Vaudrey1) and the limited momentum (Vaudrey2) approaches are significant for most of the ice load distribution, but both plots converge in tail of the distribution, from which the design ice loads are selected. In fact, both of my ice load distributions and the Sandwell distribution converge at an exceedance probability of approximately 0.002 (equivalent to a 500-year return period for a single impact per winter season).

The fact that the Vaudrey1 and Vaudrey2 plots converge in the tail of the exceedance probability distribution simply indicates that full penetration is finally achieved by the limited momentum approach. Sufficient driving force to produce full penetration occurs as a result of sampling high velocities and large floe diameters from the tails of those multiyear ice parameter distributions.

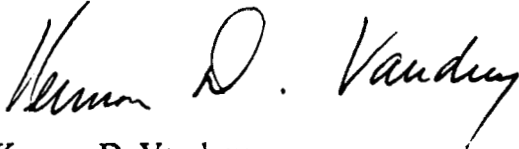
For 5 multiyear floe encounters per winter season, as computed previously, the 100-year return period design ice loads can be determined from the Vaudrey1 and Vaudrey2 ice load values for an exceedance probability of 0.002. This is equivalent to a 100-year return period or an exceedance probability of  $0.01 = 5(0.002)$ , as described earlier in the methodology section. Thus, the design ice load range becomes 1350–1450 MN or 300–325 thousand kips for a 100-year return period. These ice load values are roughly 15% less than the 1600–1700 MN range recommended in the Sandwell report, but the Sandwell loads are representative of 10 to 25 impacts per winter season, not 5. Using Figure 3.6 from the Sandwell report and a value of 5 winter impacts, the 100-year return period ice load is about 1450 MN, corresponding to the upper bound of my ice load range. As shown in the attached figure, all three ice load distributions have remarkable agreement in the tails of the distributions where exceedance probabilities are less than 0.002.



**Summary.** The Kuvlum design ice load review included:

- Evaluation of the probabilistic ice load methodology presented by Sandwell. It is recommended that the final report clarify that the ice load distribution represents the peak or maximum ice load for each simulation in order to insure a proper extreme value analysis.
- Development of a set of input distributions for multiyear ice concentration, floe diameter and thickness, ice velocity, and ice failure pressure. All of these probability distributions were based on data collected in the Eastern Beaufort Sea or, specifically, the Camden Bay region.
- Prediction of 5 multiyear floe encounters per winter season and approximately 20 multiyear floe impacts during the combined summer and freeze-up seasons. Both estimates are based on data measurements and personal experience in the vicinity of the Kuvlum Prospect.
- Computation of the global design ice loads for a 110-meter structure. The recommended design ice loads range between 1350 and 1450 MN (300–325 thousand kips) for a 100-year return period, based on 5 multiyear floe encounters per winter season. The ice loads compare very closely with the Sandwell loads in the tail of the distribution, which is the region of interest.

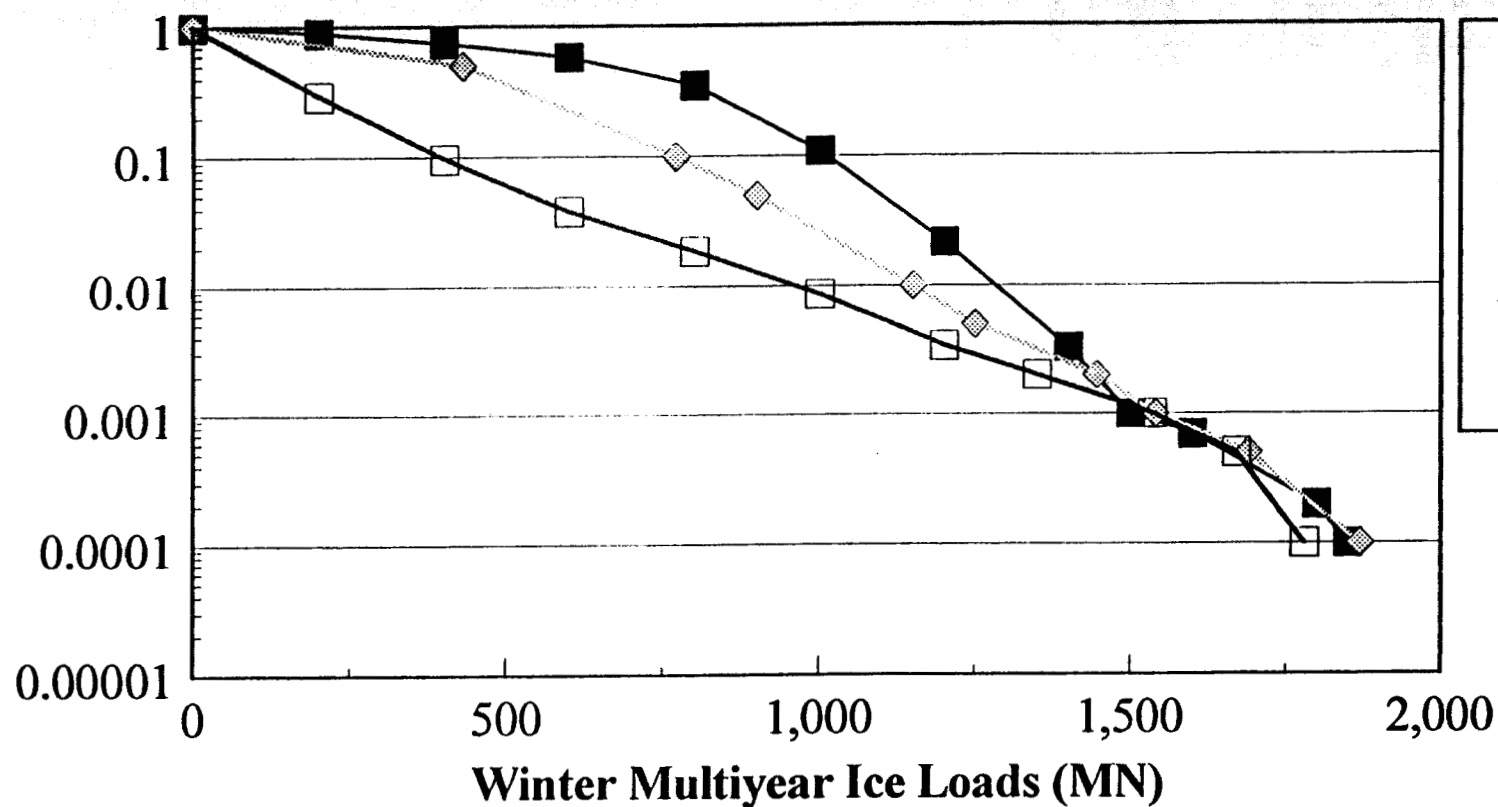
Best regards,



Kennon D. Vaudrey

Attachment

## Probability of Exceedance



Assumes one impact per season

Based on 10,000 simulations

## ***PROBABILISTIC MULTIYEAR LOADS FOR 110-METER STRUCTURE***

# **Arctic Geoscience Eastern Beaufort Sea Synthesis Summary**

Arctic Geoscience performed a synthesis of the Eastern Beaufort Sea area. Existing public geotechnical information was gathered into this document and regional area types have been classified. The cover and executive summary are provided in the following section. The full report was provided at the July 21, 1993 Kuvlum Predecision Studies Engineering meeting.

---

**EASTERN BEAUFORT SEA SYNTHESIS**  
**ARCO ALASKA INC.**

**JULY 1993**

**93-0033**

ARCTIC GEOSCIENCE  
10900 O'MALLEY CENTRE DRIVE, SUITE 205  
ANCHORAGE, ALASKA 99515  
(907) 522-4300

---

---

## EASTERN BEAUFORT SEA SYNTHESIS EXECUTIVE SUMMARY

This study was intended to synthesize existing geologic and geotechnical information of the near shore, middle shelf, and outer continental shelf regions of the Eastern Beaufort Sea, specifically from Mikkelsen Bay to Demarcation Bay. The synthesis was directed at identifying anticipated soil conditions in the study area as well as geologic, physiographic and oceanographic conditions that may have significance in engineering planning and designs for exploration and production activities. General knowledge of basic soil, geologic, and oceanographic conditions in a frontier environment is needed for various planning activities.

There are several areas of geotechnical investigation that are critical to Eastern Beaufort Sea development. This data is needed before strategic decisions on the types of development facilities and technologies can be made with confidence. Non-bonded Permafrost Soils - Evaluation of these materials would aid in predicting effects on pipelines, production well casings, and permanently founded structures. Ice-Bonded Soils in the Development Area - A boring program is required to identify the presence, location, depth, extent, and the temperature of ice-bonded soils, and is critical in areas of permanently founded production structures and buried pipelines. Detailed Distribution of Ice Gouging in the Development Area - Site seafloor surveys will investigate the distribution, frequency, and extent of ice gouging, and are critical in determining lithologic units and the base contact area for bottom founded structures.

The most effective approach to evaluating a frontier area is to develop a regional geologic synthesis with predictive models based on available geologic, geophysical, physiographic and oceanographic information. Using this regional model, the next step is to select key new soil boring locations and prioritize new high-resolution geophysical lines, bathymetric, current, and other oceanographic studies that will "infill" the data set.

Distribution of Permafrost in the North American Arctic seas is poorly understood in comparison to onshore permafrost. As developments extend offshore, the same level of understanding will be required. Investigations of extent, classification of type, and the performance of said type are required. Onshore classification systems, criteria and testing standards may need to be altered. The existing geophysical data set provides only a cursory evaluation of the variable depth to and extent of permafrost in the

---

**Eastern Beaufort Sea.** Most interpretations are based on local observations that are extrapolated to outlying regions.

The changes in regional features by geomorphic processes responsible for the active development or modification of the Arctic coast line need to be investigated, processes of erosion (thermal and hydraulic) understood, and included in engineering development planning and design efforts.

Regional soil conditions presented in the literature to date are limited and highly interpretive. Holocene sediments typically present lower soil strengths than the Pleistocene units and can be difficult to differentiate from Pleistocene soils of higher strengths due to ice gouging.

Only three deep soil borings are available in the study area, and are supplemented by analog seismic data with limited resolution. Existing literature recommends one borehole per 8000 square meters of surface area, or one soil test (insitu) per 2000 square meters. Common practice reported for structures in the Canadian Beaufort Sea are from one borehole per every 2000 square meters to one soil investigation per every 250 square meters for bottom founded Arctic caissons.

Considering these parameters for geotechnical studies associated with structure placement additional supporting information is needed. In evaluating the presentation of geotechnical data for stratigraphic units in this synthesis, it is prudent to realize that the geotechnical parameters depend more upon lithology than stratigraphy.

As ARCO Alaska Inc. continues with their Kuvlum Prospect development planning, the development of a geotechnical program for production development must be initiated with the oil company operator and a selected consultant as a team to define the scope of work and schedule. This interaction will assure the objectives of the owner are being met, and will reduce costs.

---

**EASTERN BEAUFORT SEA SYNTHESIS  
ARCO ALASKA, INC.**

**Table of Contents**

	<u>Page</u>
1.0 INTRODUCTION	1
1.1 Scope of Services	2
1.2 Basis for Study	2
1.3 Purpose	3
1.4 Acknowledgements	3
2.0 ELEMENTS OF THE ARCTIC	3
2.1 General	3
3.0 PHYSIOGRAPHY	4
4.0 GEOLOGY	5
4.1 Regional Framework	5
4.2 Geohazards	6
4.3 Quaternary Geology	7
4.3.1 Pleistocene and Holocene Sequences	8
4.4 Permafrost	8
4.5 Morphological Processes	12
5.0 SOIL CONDITIONS	12
5.1 Seafloor Morphology	12
5.2 Seafloor Soil Units	13
6.0 GEOTECHNICAL DATA SUMMARY	16
6.1 General - Available Data	16
6.2 Soil Strength	18
6.3 Index Testing Data	20
6.4 Permafrost effects on Seafloor Soils	21
7.0 INSITU TESTING SUMMARY	23
7.1 Cone Penetrometer Testing - <i>In-situ</i> Measurements	23
8.0 SEA ICE	24
8.1 Ice Zonation	24
8.2 Ice Movements	24
8.3 Ice Gouging	25
8.4 Mechanisms of Ice Gouging	25
8.5 Strudel Scour	26
9.0 GEOTECHNICAL SITE INVESTIGATIONS	26
9.1 General Overview	26
9.2 Recommendations for Geotechnical Program Planning	32

---

## TABLES

4.1.1	Summary of Permafrost Logging	12
5.2.1	Summary of Stratigraphic Units	14
6.1.1	Summary of Lithology	18
6.2.1	Data Summary Strength Testing	19
9.1.1	Typical Beaufort Sea Sampling Techniques	29

## FIGURES

Number	
1	Site Study Location Map
2	Regional Data Base Maps (Exploration Wells)
3	Regional Data Base Maps (Oceanographic Points)
4	Regional Data Base Maps (Soil Borings)
5	Regional Data Base Maps (Seismic Track Lines)
6	Regional Bathymetry Maps
7	Geologic Structure Map
8	Geologic Table
9	Shallow Gas and Gas Hydrates
10	Holocene Isopach
11	HLA/USGS Ground Temperature Profiles A
12	HLA/USGS Ground Temperature Profiles B
13	Depth to Permafrost Plot
14	Permafrost Section at Prudhoe Bay
15	Depth to Permafrost Observed at Stinson, Projected
16	Soil Unit (HLA)
17	Soil Unit (EBA)
18	Stratigraphic Units
19	Soil Zones 1A
20	Soil Zones 1B, 1C
21	Soil Zones 2A, 2B
22	Soil Zones 2C
23	Soil Zones 3A 3B
24	Soil Zones 4A 4B
25	Eastern Beaufort Sea Stratigraphic Cross Section
26	Eastern Beaufort Sea Stratigraphic Cross Section A-A'
	Lithology - Stratigraphy
27	Eastern Beaufort Sea Stratigraphic Cross Section A-A'
	Lithology - Permafrost
28	Eastern Beaufort Sea Stratigraphic Cross Section B-B'
	Lithology - Stratigraphy
29	Eastern Beaufort Sea Stratigraphic Cross Section B-B'
	Lithology - Permafrost
30	Eastern Beaufort Sea Stratigraphic Cross Section C-C'
	Lithology - Stratigraphy
31	Eastern Beaufort Sea Stratigraphic Cross Section C-C'
	Lithology - Permafrost
32	Unified Soil Classification Chart



## FIGURES

### Number

- 33 Frost Classification / Ground Ice Description
- 34 Key to Symbols for Cross Sections
- 35 Offshore Cross Section from HLA AOGA Study
- 36 HLA/USGS Borehole 5 Stratigraphic and Lithologic Log
- 37 HLA/USGS Borehole 12 Stratigraphic and Lithologic Log
- 38 HLA/USGS Borehole 15 Stratigraphic and Lithologic Log
- 39 HLA/USGS Borehole 18 Stratigraphic and Lithologic Log
- 40 Comparison of Estimated Shear Strength with  
Stratigraphic Units
- 41 Shear Strength verses Depth, Compilation
- 42 Comparison of Predicted Shear Strength with  
Stratigraphic Units to Available Shear Strength Data
- 43 Moisture Content Verses Depth, Compilation
- 44 Plastic Limit and Liquid Limit Verses Depth, Compilation
- 45 Dry Depth Verses Depth, Compilation
- 46 Salinity Verses Depth, Compilation
- 47 Freezing Point Depression Verses Depth, Compilation
- 48 Received Sample Temperature Verses Depth, Compilation
- 49 Cone Penetrometer Test Location
- 50 Qc Verses Depth, Compiled
- 51 Cu Verses Depth, Compiled
- 52 Friction Verses Depth, Compiled
- 53 F Ratio Verses Depth, Compiled
- 54 Relative Density Verses Depth, Compiled
- 55 Ice Zonation
- 56 Sea Floor Ice Gouging
- 57 Ice Gouging Statistics
- 58 Illustration of Ice Gouging
- 59 Illustration of River Drainage on Sea Ice
- 60 Typical Geotechnical Program Region
- 61 Typical Geotechnical Design Specification

## BIBLIOGRAPHY

## ATTACHMENTS

- A Tabular Coordinate Data
- B Tabular Geotechnical Data
- C Tabular Stratigraphic
- D Geophysical Well Log Review
- E Available Onshore Soil Borings
- F Oceanographic Data Review

# ARCTIC GEOSCIENCE

1330 E. HUFFMAN ROAD, SUITE 303 • ANCHORAGE, ALASKA 99515

July 21, 1993  
93-0033.02

ARCO Alaska Inc.  
ARCO PRODUCTION RESEARCH CENTER  
2300 West Plano Parkway  
Plano, Texas 75075-8499  
PRC-J-1422

Attention: Mr. Junius Allen

**Bedrock Review  
Eastern Beaufort Sea Synthesis  
ARCO Alaska, Inc.**

Gentlemen:

This letter transmits the results of our technical review of the data presented in Arctic GeoScience's Beaufort Sea Synthesis for the presence of "bedrock" in the "Kuvlum Prospect", and Camden Bay areas of the Eastern Beaufort Sea. This request was based on our discussion with Mr. Junius Allen on July 19, 1993. The interest in depth to "bedrock" was directed at providing information to support conceptual studies for tunneling in the offshore regions of the Beaufort Sea. We have reviewed the data in synthesis and have excerpted and expanded the information in the synthesis with the collected reference data base.

The users of the data presented in the synthesis must realize its limitations and the original purpose of the study. The synthesis is a compilation of work performed by other investigators. Arctic GeoScience compiled the data and summarized findings of these investigators to allow a reference for future planning. The next step in the synthesis is to review the data sets with new findings or cross correlation between various investigators to change or alter the regional mapping developed, and subsequently presented.

The initial response to the question of what is the depth to bedrock in the Eastern Beaufort Sea must initially be directed at what is "Bedrock" and by who's definition should the mappable unit if any be presented. We have reviewed this interpretive condition with respect to the data set available. This data set consists of seismic data from the geohazards site clearance at



"Kuvlum" and "Stinson", analog seismic data reported in open file USGS reports, downhole geophysical well logs, and the geotechnical properties presented by investigators working in the Eastern Beaufort Sea on various programs, both regional and site specific.

Initially, the terms "rock" and "soil" need to be understood in terms of the discipline making this distinction. As an example, what may be a mappable rock unit to the geologist may be soil to the civil engineer. Highly weathered sandstone or shale unit would appear on a geologist mapping or interpretations as structure horizon or mappable conformity, but due to weathering would have the physical properties of a soil. The definition of "soil" is significantly different between geologist, soil scientist, and civil engineers. It is prudent to remember that no universally accepted definition of "soil" and "rock" even within a given discipline exists (R. Johnson and J. DeGraff, 1988). The engineering definitions are governed by the need for quantifiable physical properties that may group materials together without regard for the more specialized classifications of the geologist or soil scientist.

Rock is defined as a naturally occurring consolidated or unconsolidated material composed of one or more minerals (Gary et al., 1972). Although this definition is useful to the geologist, it is apparent that the definition includes materials with physical properties that the engineer would consider to be engineering soils, unconsolidated materials. The commonly used engineering definition of rock is that of a hard, compact, naturally occurring aggregate of minerals (Krynine and Judd, 1957). The soil of the civil engineer is an aggregate of mineral grains that can be separated by gentle means such as agitation in water (Terzaghi and Peck, 1967).

Presented on page 8, section 4.3.1 "Pleistocene and Holocene Sequences" of the Beaufort Sea Synthesis, reference is made to the mapped thickness of the Holocene unit in the Eastern Beaufort Sea prepared by Dinter (1982) and illustrated as Figure 10. Dinter outlines an area of zero Holocene thickness north of Barter Island. Within this area, Craig, Sherwood and Johnson (1985) state that, consolidated bedrock may be exposed at or near the seafloor. The "geologic" interpretations made by these investigators of possible bedrock exposure at or near the seafloor being of Tertiary Age associated with the "Camden Bay Uplift" should be further referenced to the descriptions of the "Stratigraphy of the Beaufort Sea Shelf" presented on Figure 8. We have investigated these references by reviewing the seismic data from which the interpretations were based, and the high resolution seismic data collected for the "Kuvlum" and "Stinson" Prospects. To expand the depth to bedrock investigation we reviewed the geophysical well logs presented in Attachment D of the synthesis. The following discussion presents our engineering geologic review of the presence of a mappable bedrock contact.



### 1.0 Seismic Depth to Bedrock:

For seismic investigations the top of bedrock is defined by a sharp increase in the acoustical velocity of the subsurface due to the increase in the elastic moduli of the material with cementation. Frequently there is an associated increase in density. In a reference to acoustic velocities and bedrock, Caterpillar Tractor in edition 18 of their performance handbook states that shales, sandstones, siltstones, and claystones with acoustic velocities below 9,000 ft/sec are rippable with a D10N, from 9,000 to 10,800 ft/sec they are marginal and above 10,800 ft/sec they are non-rippable.

The compressional wave velocity of a medium is a function of the bulk modulus, the shear modulus, and the density of that medium. Compressional wave velocities for unconsolidated sediments range from 1,000 to 7,000 ft/sec, and for shales and sandstone from 5,000 to 18,000 ft/sec. For reflection seismology the compressional velocity may be extracted from a data processing parameter known as the stacking velocity. These values are normally posted on seismic sections to permit calculations of the depth associated with an event time on the record. Alternatively the raw shot records from the field contain shallow refraction data over the length of the active geophone spread. The compressional velocities can be calculated directly from this data to a depth not greater than the length of that active geophone spread.

The reflection coefficient on a seismic section is  $\frac{1}{2}$  the change in the logarithm of the density multiplied by the compressional velocity. Therefore a sharp change in velocity associated with the top of bedrock should result in a continuous substantial reflection on the seismic record.

In the Arctic environment permafrost complicates this investigation because the acoustic velocity in frozen soils ranges from that of ice (12,500 ft/s) to 18,000 ft/sec. This overlaps the range of competent rock. Permafrost is distinguished by noting the sharp decrease in velocity with depth at the bottom of the frozen soil. Seismic velocity tends to increase with depth in rocks of the same type, and decreases are associated with changes in lithology (from harder rocks to softer rocks) and not of the same magnitude as seen with permafrost. The top and bottom of permafrost zones are irregular enough that they do not yield seismic reflections. Permafrost zones are identified on reflection seismic sections by their impact on the travel times and stacking velocities of the events below those zones.

Unfortunately neither the seismic sections provided for the "Kuvlum" and "Stinson" sites nor



those acquired from the open literature include seismic stacking velocities. We have not been provided any raw shot data for refraction analysis and have failed to locate any supporting data for the study area in the public domain.

In the synthesis report, cross section A to A' (Figure 26&27) show no competent rock to a depth of 340 feet at Flaxman Island in USGS BH#18. This establishes an upper limit for the top of bedrock in this area. If we assume a compressional velocity of 6,000 ft/sec (typical for water saturated soils) this limits the reflector associated with the top of bedrock on the seismic section to below 110 milliseconds two way time. Similarly, soil boring performed at the "Stinson" Prospect to 100 feet penetration below mudline, did not report bedrock although over-consolidated soils were present, and sampling was only accomplished by the use of drive sampling techniques below 20 feet with somewhat limited success.

An examination of the high resolution seismic data acquired and presented for the geohazard surveys for the "Kuvlum" and "Stinson" wells do not show any major continuous regional reflectors of the type that would normally be associated with the transition from soil to competent rock. There are zones of shallow high amplitude reflections but their character is more consistent with gas saturated sands trapped between less permeable silts and clays than the transition to bedrock. This is also the earlier interpretation of this data set by the presenting investigators.

USGS line 81-32 in OCS Report MMS 85-011, attached Figure 1, shows shallow dipping beds (apparent dip of approximately 7°) which intersect or nearly intersect the sea floor and were interpreted in that report as bedrock of probable Tertiary age. This seismic line is approximately 3 miles north of the western tip of Barter Island, attached Figure 2. From Arctic GeoScience's Beaufort Sea Synthesis, Figure 17, we see this area as QPh/3B. Figure 23, of the same report describes QPh as very stiff and hard unconsolidated silts and clays of older Pleistocene age (pre-Illinoian) which are typically dipping with an angular unconformity marking the top of the Camden Bay uplift. The undrained shear strength is given as 4-8 ksf. This interpreted "bedrock" exposure correlates to the over-consolidated, hard marine soil unit. For engineering purposes, this unit may warrant further investigation for tunneling studies.

USGS seismic line 77-740, attached Figure 3, from the same reference shows an angular unconformity in it's southern ¾, with similarly dipping beds below it, at approximately 225 feet below the seafloor. This seismic line runs NE-SW just northeast of the "Kuvlum" well (attached Figure 2), and crosses the two "down to the north faults" shown on Figure 7 of the Beaufort

Sea Synthesis. This is likely to be the same unit but we have no direct evidence to this effect. We understand from conversations with ARCO Alaska drilling engineers that "glory hole" excavation for the exploratory drilling at "Kuvlum" has been, and is difficult.

The high resolution seismic data presented for the "Kuvlum" Prospect geohazards report was processed and displayed at a different scale than the USGS data. The attached Figure 4 through 7, display the interpretations prepared by the investigators, and our interpretation of the dipping beds presented by the USGS. It would be prudent to consider collecting the "Kuvlum" and "Stinson" high resolution seismic data and have the data reprocessed. The reprocessing would allow a second look for potential shallow bedding features, as well as allow alternative displays, such as a "squeezed" horizontal scale to facilitate interpretive efforts of this dipping unit. Additional site specific investigations directed at the upper 150 to 300 meters would be beneficial to map this unit from the "Kuvlum" Prospect to the coast. Further investigation of the upper 150 meters prior to mobilization of a specific geotechnical program could be accomplished by performing a high resolution geophysical investigation from a well support vessel, or drilling a soil boring intersecting the interpreted dipping beds, from the exploration drilling vessel onsite at "Kuvlum".

## 2.0 "Bedrock" Determination from Geophysical Well Logs

A geophysical well log analyst typically refer to bedrock as a consolidated formation. Bedrock can be determined from geophysical well logs (WL) by both reading cutoff values directly from the sonic log and by calculating mechanical parameters from log values. The determination based on mechanical properties requires establishing guidelines for defining bedrock based on calculated values. We have located well logs from the Chevron Karluk #1 and Exxon Pt. Thompson #2 wells as examples of data that is available in the area.

**SONIC LOG VALUE:** Bedrock can be determined from the borehole compensated sonic (sonic) tool based on log response in shales and in sand formations. Both techniques require establishing a log value to differentiate between bedrock and overlying soils.

Traditional sonic interpretation defines a formation as unconsolidated if the average compressional travel time ( $\Delta t_c$ ) of adjacent shales are greater than 100  $\mu\text{sec}/\text{ft}$  (Schlumberger 1972). Petrophysists derived this value empirically to force agreement with porosity values calculated from  $\Delta t_c$  and density, resistivity and neutron logs. We have well log data on the Chevron Karluk well #1 from approximately 2000 to 400 ft. None of the shale  $\Delta t_c$  values are



below 100  $\mu\text{sec}/\text{ft}$  indicating all formation material is unconsolidated. We also have well log data on the Exxon Pt Thompson #2 well from 2100 to 92 ft. This sonic log indicates  $\Delta t_c$  values greater than 100  $\mu\text{sec}/\text{ft}$  suggesting the entire interval is unconsolidated at this location.

Wet, unconsolidated sand produces an acoustic (sonic) velocity of 2000 to 6000 ft/sec while sandstone velocities vary from 6000 to 13,000 ft/sec (Table 1). This corresponds to sonic log values of 500 to 167  $\mu\text{sec}/\text{ft}$  for wet sand and 167 to 77  $\mu\text{sec}/\text{ft}$  for sandstone. The difference in acoustic velocity between wet sand and sandstone is due to the improved acoustic coupling between sand grains created by cementation. Using this criteria, bedrock is indicated by  $\Delta t_c$  less than 167  $\mu\text{sec}/\text{ft}$  in the clean sand formations. Consistent bedrock is located below 1300 ft in the Chevron Karluk #1 well. The Pt Thompson well #2 indicates the top of consolidated sand at approximately 1900 ft. Above these depths, both sonic logs show  $\Delta t_c$  in the clean sand intervals greater than 167  $\mu\text{sec}/\text{ft}$  (Above these depths  $\Delta t_c$  crosses below 167  $\mu\text{sec}/\text{ft}$  in intervals that are primarily shale.)

The Chevron Karluk #1 well is located in the vicinity of USGS borings 14 and 20. Neither of these borings encountered bedrock. USGS boring 14 was drilled to 120 ft and USGS boring 20 was drilled to 150 ft.

Figures 8 and 9 depict the sonic logs from the Chevron Karluk #1 and Exxon Pt. Thompson #2 wells. The 167  $\mu\text{sec}/\text{ft}$  cut off is marked on the sonic logs indicating bedrock and soils.

**MECHANICAL ROCK PROPERTIES CALCULATIONS:** Geophysical well log data can be used to calculate mechanical rock properties. These can be used to define rock competence which can be correlated to bedrock determination. The method of determining mechanical rock properties from WL data as described in two articles are presented below. These techniques rely primarily on sonic data but also utilize density, resistivity and gamma-ray data.

Tixier et al (1978) describe a method of calculating formation strength from density, sonic ( $\Delta t_c$ ), resistivity and gamma-ray logs. This technique is directed primarily at deep reservoir rock but can be adapted to shallow formations using consolidation corrections of sonic data. This method allows calculation of shear modulus (G) and poisson's ratio ( $\mu$ ). Shear modulus is related to shear strength ( $\tau$ ) by the relationship  $\tau = G\theta$ , where  $\theta$  = shear strain. The value of G will be that of the thawed formation material around the borehole. The authors derived this method using Gulf Coast information but have successfully applied it to well logs in Alaska, and Canada. Poisson's ratio has been derived empirically from work by Anderson using

formation shaliness (attached figure 10). Shaliness is derived from the gamma-ray or SP log. Shear modulus,  $G$ , is calculated using the formula  $G = A/t_c^2$  where  $A$  is a constant involving poisson's ratio.

Kowalski (1978) describes a method of calculating young's modulus ( $E$ ), bulk modulus ( $K$ ), shear modulus and poisson's ratio from well log data. This method requires bulk density ( $\rho$ ), shear travel time ( $\Delta t_s$ ) and  $\Delta t_c$ .  $\Delta t_s$  is not available on the well logs that are available to us at this time but estimates of  $\Delta t_s$  have been empirically derived for various rock types from  $\Delta t_c$  (see attached Figure 11). These calculations also require data from a density tool.

Calculations using the two methods described above can be used to confirm the validity of the two techniques. The next step in using this data will involve deriving appropriate cutoff limits to correlate mechanical properties to bedrock. We will also have to determine a method of distinguishing between over consolidated sediment and bedrock.

Well log data from the "Kuvlum" and "Stinson" Prospect exploration wells were not available to Arctic GeoScience during our synthesis. If the well log data for the upper 1,000 to 2,000 feet were available, similar evaluations could be performed, as well as investigation for the presence of bonded permafrost.

### 3.0 Geotechnical Data - Interpretations of "Bedrock"

In review of the geotechnical data compiled from limited soil borings performed in the Eastern Beaufort Sea, available values of soil strength ( $S_u$ ), and consolidation test results present physical properties to the geotechnical engineer of the QPh/3A unit of highly over-consolidated and very hard cohesive soils (silts and clays) with shear strengths greater than 4 ksf. USGS/HLA BH#18, north of Flaxman Island, penetrated to a depth of 300 plus feet below mudline. Bedrock was not reported in the geotechnical borehole logs. Similarly at "Stinson" soil borings to 100 feet did not report bedrock in the geotechnical logs, although over-consolidated soils were present and soil sampling was only accomplished by the use of drive sampling techniques. Soil boring 103, of the Dames and Moore - Fugro study, were drilled and sampled to a depth less than 150 feet penetration below mudline, and no reference was made in the geotechnical borehole logs to bedrock.

The soil borings performed and geotechnical data collected for Arctic bottom founded structure setdown and performance evaluations at "Stinson" and "Aurora" Prospects reported very hard





over-consolidated soils. Penetration of the structures "skirts" were limited and at "Aurora" Prospect as a gap of approximately 1.0 to 1.8 feet were measured (reported) between the base of the "MAT", and the seafloor. In review of the predicted soil zones prepared by EBA Engineering on Figure 17 of the Beaufort Sea Synthesis, and the results presented in this preliminary review, the hard Camden Bay soils could be interpreted to the extend further to the east than originally projected. Similarly the geotechnical properties of high shear strengths, over-consolidated soils at "Stinson" may also extend the 3A unit further to the west than is presently projected ( attached Figure 12). This stratigraphic zone of over-consolidated silts and clays may prove advantageous for site development planning and further investigation.

To further this study of the geotechnical properties of the regional soils, the shear strength profiles for each soil boring, and the results of cone penetrometer testing could be reviewed with the regional stratigraphic units. Figure 42 of the Beaufort Sea Synthesis presents a comparison of shear strength with the stratigraphic units. This could be further studied to correlate, and include the projected depth of Holocene soils at the soil boring location, the depth at which the cone penetrometer testing met refusal to the interpreted depth of Holocene soils, and the relationships of index testing, shear strength and consolidation indices within the projected soil units previously mapped by other investigators to the stratigraphic units. This study would be limited, due to the present distribution of geotechnical borings and cone penetrometer test locations in the "Kuvlum" study area, but would be more focused toward the interpretations of a geotechnical engineer as compared to past presentations by geologists, geophysicists, and geological engineers.

Arctic GeoScience appreciated this opportunity to assist ARCO Alaska Inc. with their development planning activities in the Eastern Beaufort Sea, Alaska. We continue to remain available. Should you have any questions or require any additional information please do not hesitate to contact the undersigned.

Sincerely,  
Arctic GeoScience



Michael G. Schlegel  
Consultant; Engineering Geology

---

REFERENCES:

Kowalski, John. (1978). Formation Strength Parameters from Well Logs. From SPWLA Reprint Volume, Acoustic Logging 1978. Houston, Texas.

Schlumberger. (1972). Log Interpretation Volume 1 - Principals Schlumberger Limited. New York, New York.

Redpath, Bruce B. (1973). Technical Report E-73-4 Seismic Refraction Exploration for Engineering Site Investigations, U.S. Army Engineer Waterways Experiment Station Explosive Excavation Research Laboratory. Livermore, California.

Tixier, M. P., Loveless, G. W., Anderson, R. A. (1978). Estimation of Formation Strength from the Mechanical-Properties Log. From SPWLA Reprint Volume, Acoustic Logging 1978. Houston, Texas.

---

TABLE 1

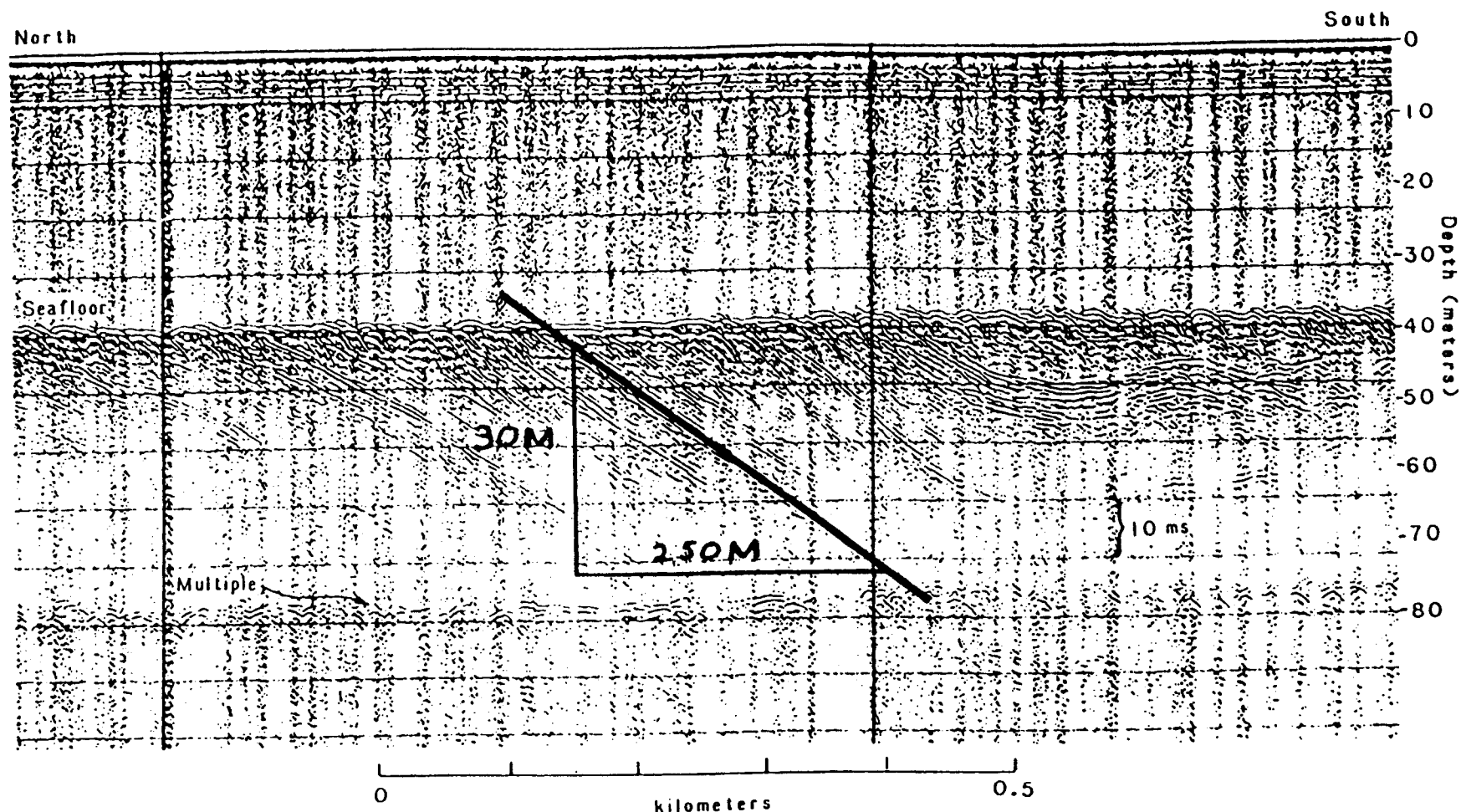
Table A2. Approximate range of velocities of longitudinal waves for representative materials found in the earth's crust.<sup>a</sup>

A. Classification According to Material			
Material	Velocity*		
	Ft./Sec.	M/Sec.	
Weathered surface material .....	1,000—2,000	305—610	
Gravel, rubble, or sand (dry) .....	1,500—3,000	468—915	
Sand (wet) .....	2,000—6,000	610—1,830	
Clay .....	3,000—9,000	915—2,750	
Water (depending on temperature and salt content) .....	4,700—5,500	1,430—1,680	
Sea water .....	4,800—5,000	1,440—1,530	
Sandstone .....	6,000—13,000	1,830—3,970	
Shale .....	9,000—14,000	2,750—4,270	
Chalk .....	6,000—13,000	1,830—3,970	
Limestone .....	7,000—20,000	2,140—6,100	
Salt .....	14,000—17,000	4,270—5,190	
Granite .....	15,000—19,000	4,580—5,800	
Metamorphic rocks .....	10,000—23,000	3,050—7,020	
Ice .....	12,050		
B. Classification According to Geologic Age			
Age	Type of Rock	Velocity	
		Ft./Sec.	M/Sec.
Quaternary	Sediments (various degrees of consolidation) .....	1,000—7,500	305—2,290
Tertiary	Consolidated Sediments ..	5,000—14,000	1,530—4,270
Mesozoic	Consolidated Sediments ..	6,000—19,500	1,830—5,950
Paleozoic	Consolidated Sediments ..	6,500—19,500	1,980—5,950
Archeozoic	Various .....	12,500—23,000	3,810—7,020
C. Classification According to Depth †			
	0—2000 ft. (0—600 M.)	2000—3000 ft. (600—900 M.)	3000—4000 ft. (900—1200 M.)
	Ft./Sec.	Ft./Sec.	Ft./Sec.
Devonian .....	13,300	13,400	13,500
Pennsylvanian .....	9,500	11,200	11,700
Permian .....	8,500	10,000	.....
Cretaceous .....	7,400	9,300	10,700
Eocene .....	7,100	9,000	10,100
Pleistocene-to-Oligocene	6,500	7,200	8,100

\* The higher values in a given range are usually obtained at depth.

† Data from B. B. Weatherly and L. Y. Faust, *Bull. Amer. Assoc. Petrol. Geologists*, 10 (1956) 1.

<sup>a</sup> Reprinted from pg. 660 of Jakosky<sup>2</sup>.



(USGS uniboom line from the Barter Island area showing shallow dipping bedrock of probable Tertiary age intersecting the seafloor. The rough seafloor surface may be caused by ice gouging or differential weathering of the bedrock units).

$$\text{DIP} = \text{ARCTAN}(30/250) = 7 \text{ DEGREES}$$

FROM OCS REPORT MMS 85-0111

For: **ARCTIC GEOSCIENCE**



Project Description:  
Title:

**EASTERN BEAUFORT SEA SYNTHESIS**

Client:

**ARCO Alaska, Inc.**

By:

JSH

Date:

8/2/93

Project No.

93-0033

Checked:

MGS

Date:

8/2/93

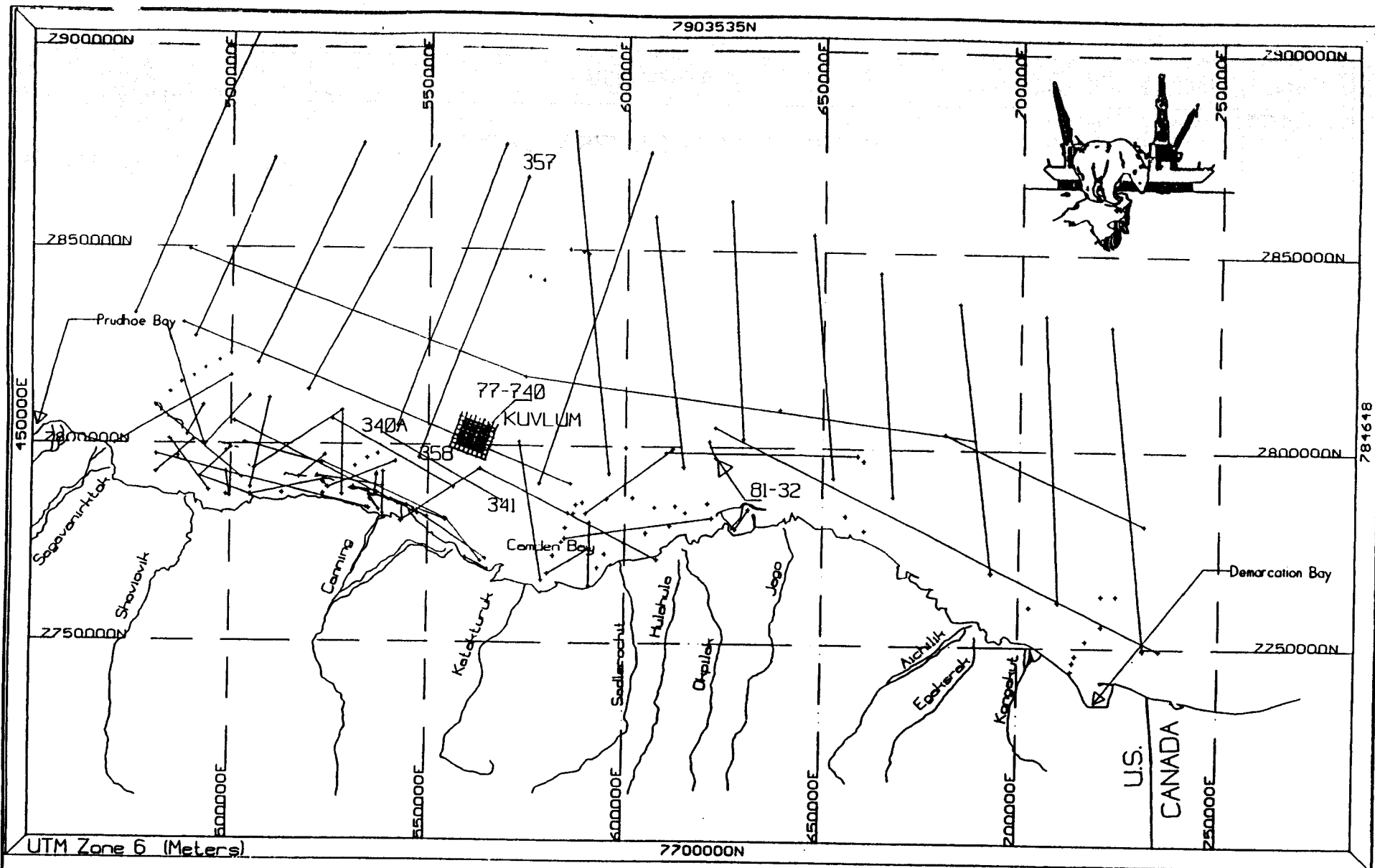
Sheet No.

Scale:

N/A

Figure 1

1 of 1



# EASTERN BEAUFORT SEA SEISMIC LINES

For: **ARCTIC GeoSCIENCE**



Project Description:  
Title:

**EASTERN BEAUFORT SEA SYNTHESIS**

Client:

**ARCO Alaska, Inc.**

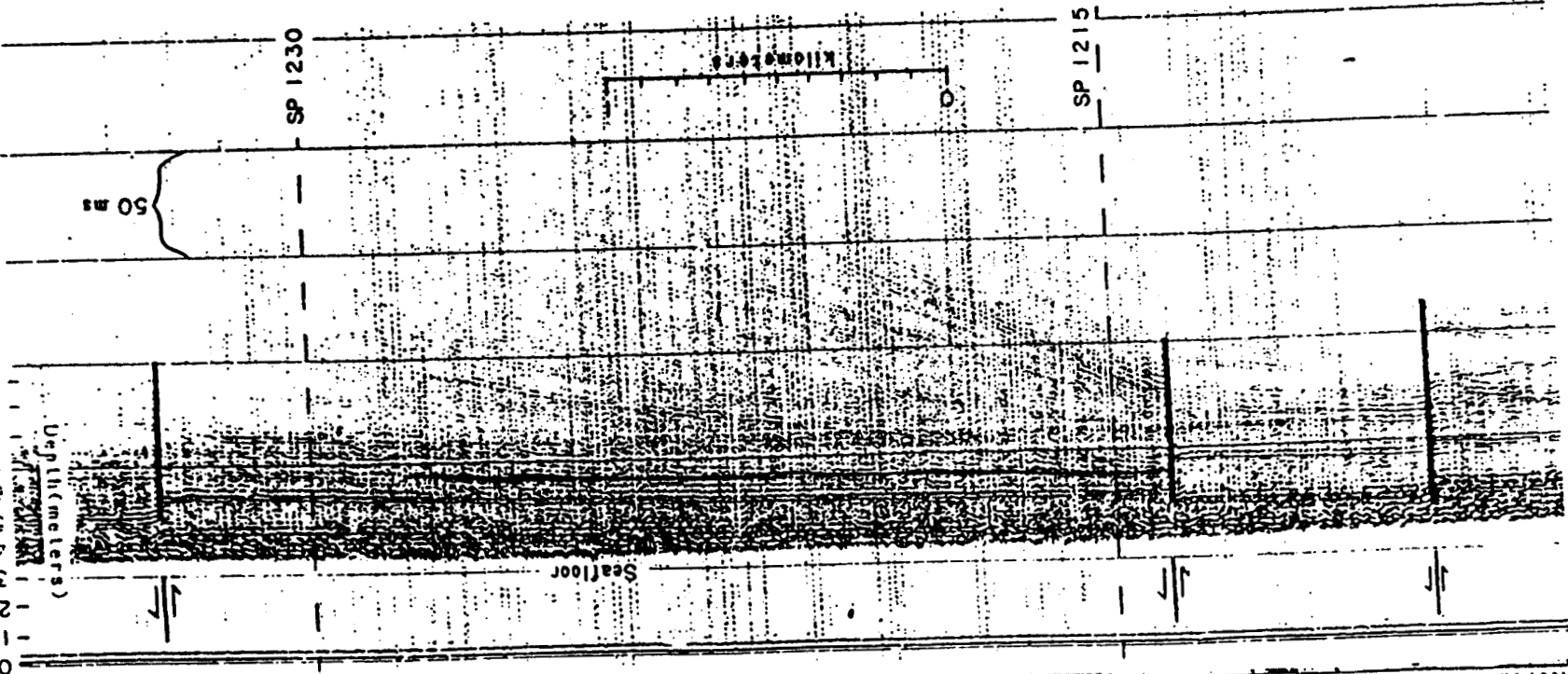
By: JSH	Date: 8/2/93	Project No. 93-0033
Checked: MGS	Date: 8/2/93	Sheet No.
Scale: N/A	Figure 2	1 of 1

North

South

Depth (meters)

0  
10  
20  
30  
40  
50  
60  
70  
80  
90  
100



(USGS uniboom line from the Barter Island area showing shallow bedrock of probable Tertiary age intersecting the seafloor. The rough seafloor surface may be caused by ice gouging or differential weathering of the bedrock units).

DIP = ARCTAN (30/250) = 7 DEGREES

FROM OCS REPORT MMS 85-0111

ARCTIC GEOSCIENCE



# EASTERN BEAUFORT SEA SYNTHESIS

ARCO Alaska, Inc.

Project Description:

By:

JSH

Date: 8/2/93

Checked:

MGS

Date: 8/2/93

Scale:

N/A

Figure 3

1 of 1

83-0033

Project No.

Sheet No.

SW

PROPOSED WELLSITE C-2

NE

1100

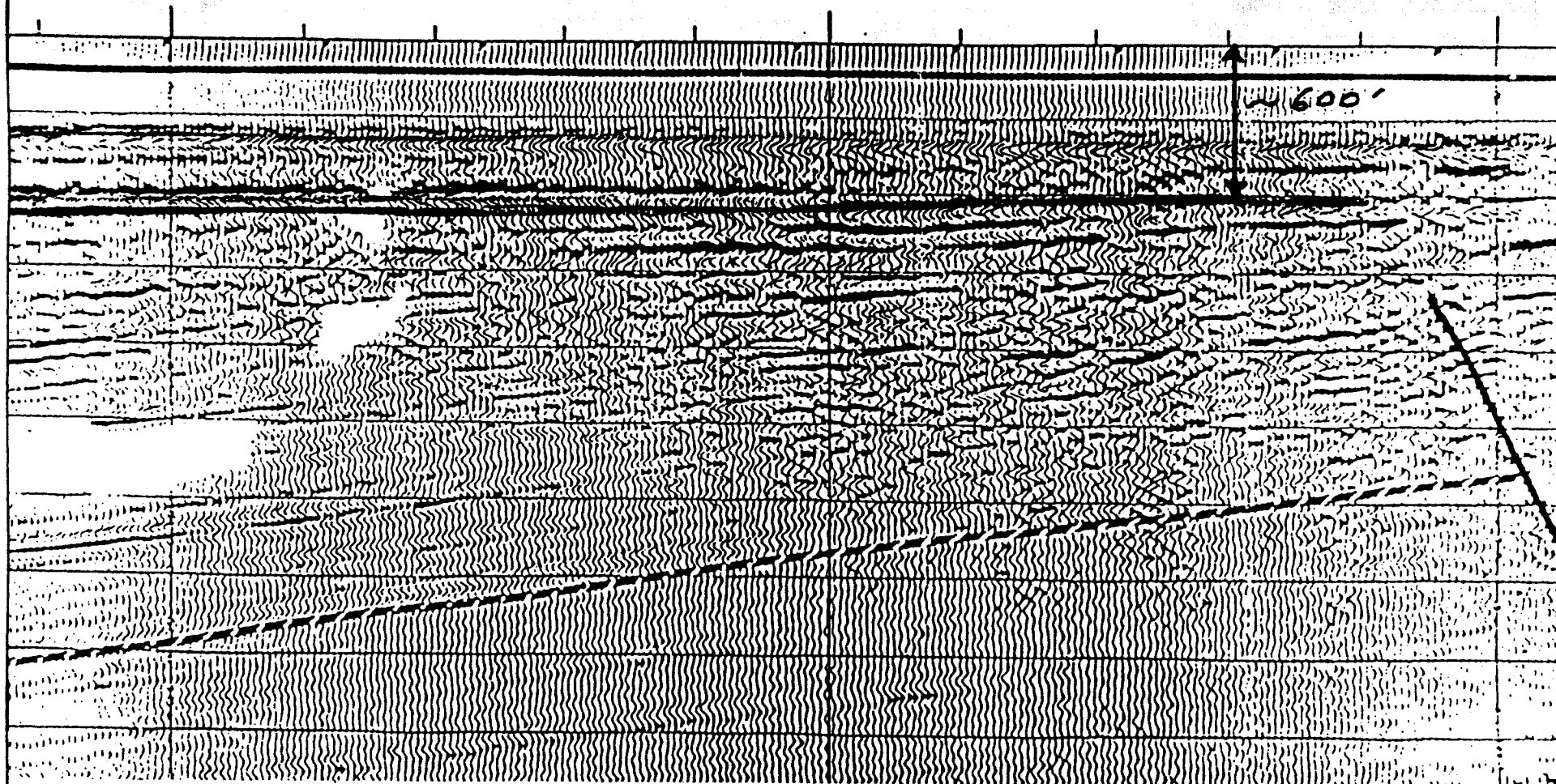
104'

1150


TIE LINE 123

1200

111'



## KUVLUM GEOHAZARDS DATA

For: <b>ARCTIC GEO SCIENCE</b> 	Project Description:		By:	Date:	Project No.
	Title:		JSH	8/2/93	93-0033
	Client:		Checked:	Date:	Sheet No.
EASTERN BEAUFORT SEA SYNTHESIS		MGS	8/2/93		
ARCO Alaska, Inc.		Scale:	N/A	Figure 4	1 of 1

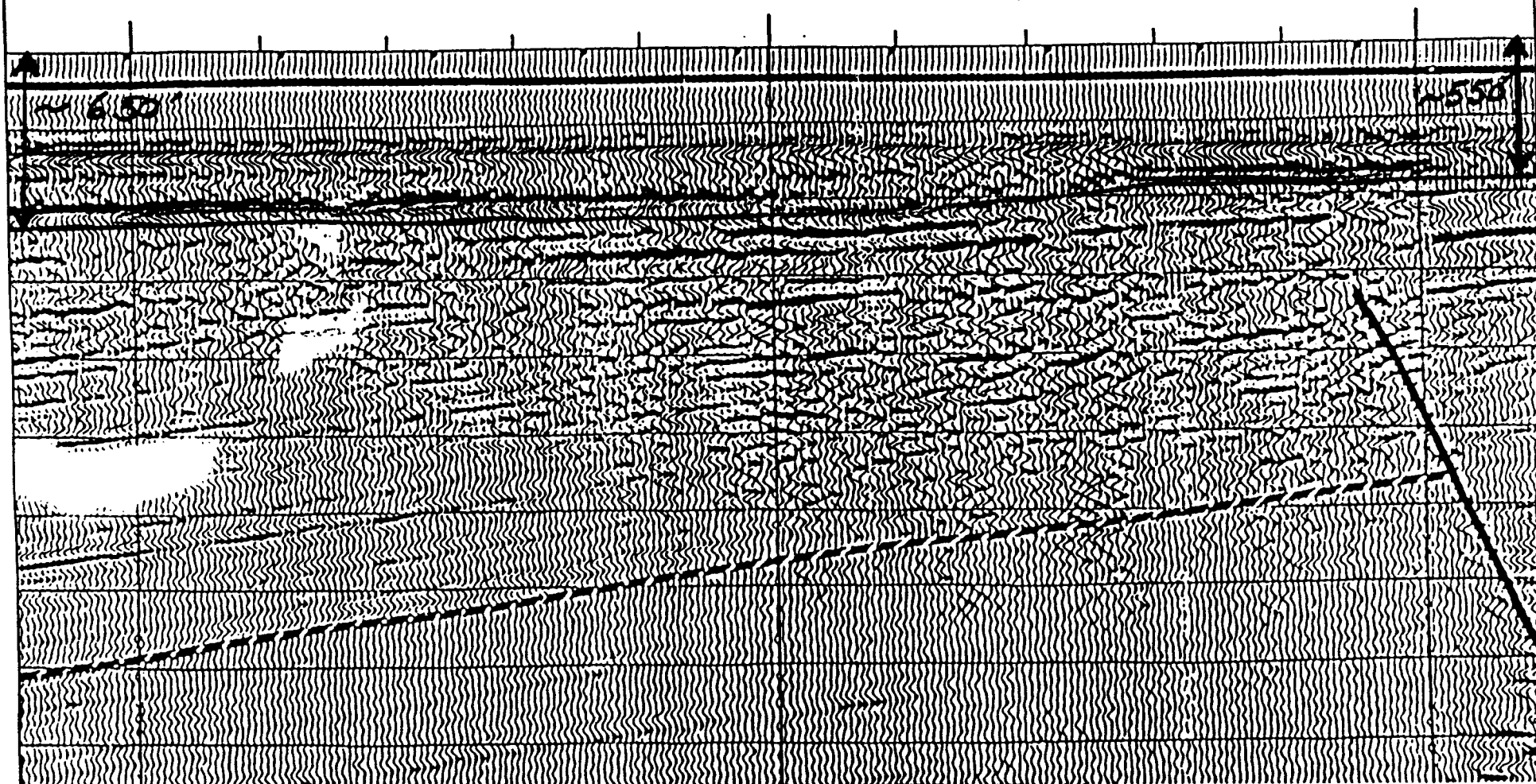
SW

PROPOSED WELLSITE C-2  
TIE LINE 123

NE

1100  
104'

1150

1200  
111'

## KUVLUM GEOHAZARDS DATA

For:

ARCTIC GeoSCIENCE

Project Description:  
Title:

EASTERN BEAUFORT SEA SYNTHESIS

Client:

ARCO Alaska, Inc.

By:

JSH

Date:

8/2/93

Project No.

93-0033

Checked:

MGS

Date:

8/2/93

Sheet No.

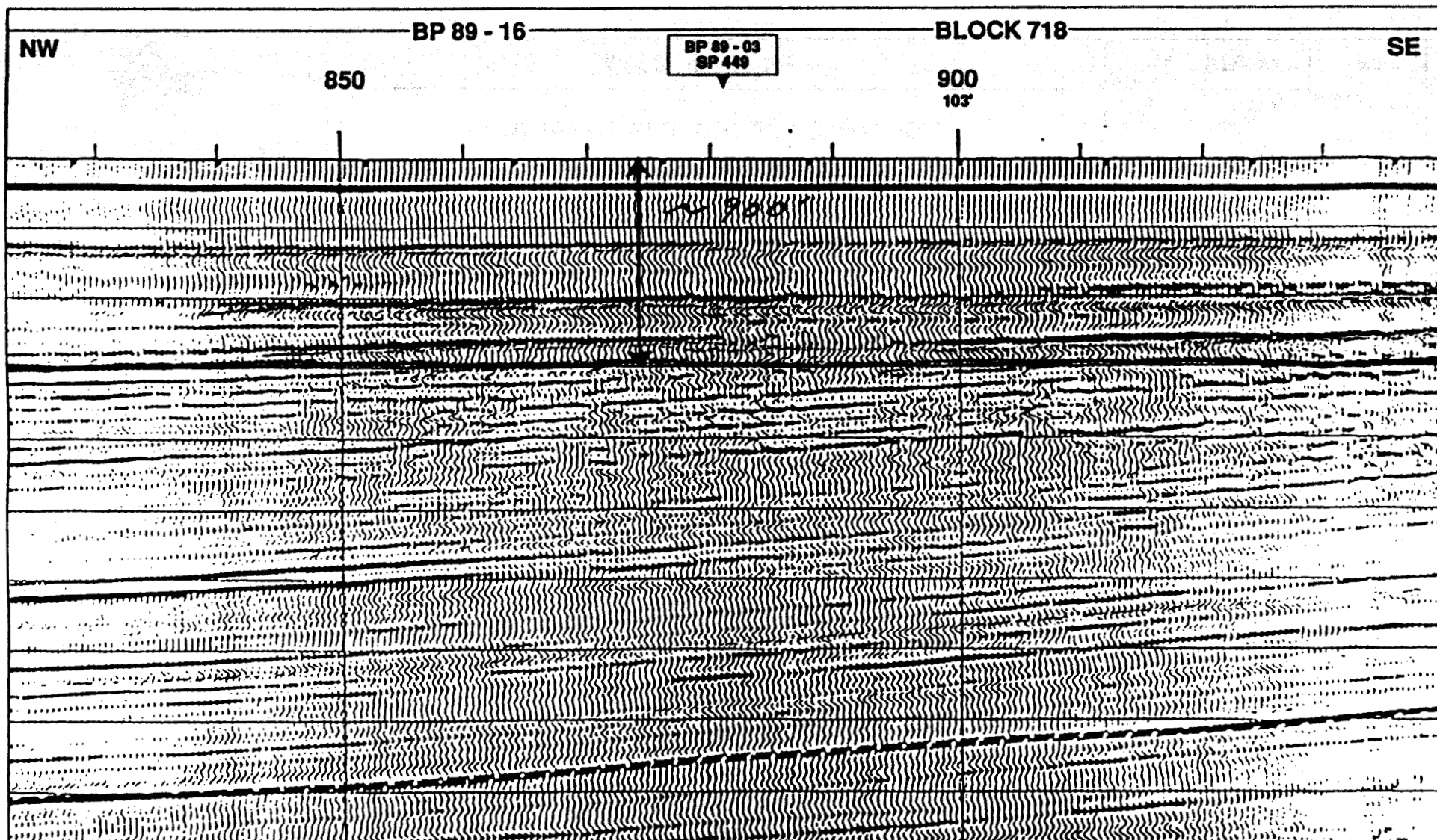
Scale:

N/A


Figure 5

1 of 1





### KUVLUM GEOHAZARDS DATA

For: <b>ARCTIC GEO SCIENCE</b> 	Project Description: <b>EASTERN BEAUFORT SEA SYNTHESIS</b>	By: <b>JSH</b>	Date: <b>8/2/93</b>	Project No. <b>93-0033</b>	
	Client: <b>ARCO Alaska, Inc.</b>	Checked: <b>MGS</b>	Date: <b>8/2/93</b>	Sheet No. <b>1 of 1</b>	
	Scale: <b>N/A</b>		Figure 6		

SW

PROPOSED WELLSITE C-2  
TIE LINE 123

NE

1100  
104'

1150

1200  
111'

## KUVLUM GEOHAZARDS DATA

For: **ARCTIC GEO SCIENCE**Project Description:  
Title:

EASTERN BEAUFORT SEA SYNTHESIS

Client:

ARCO Alaska, Inc.

By:

JSH

Date:

8/2/93

Project No.

93-0033

Checked:

MGS

Date:

8/2/93

Sheet No.

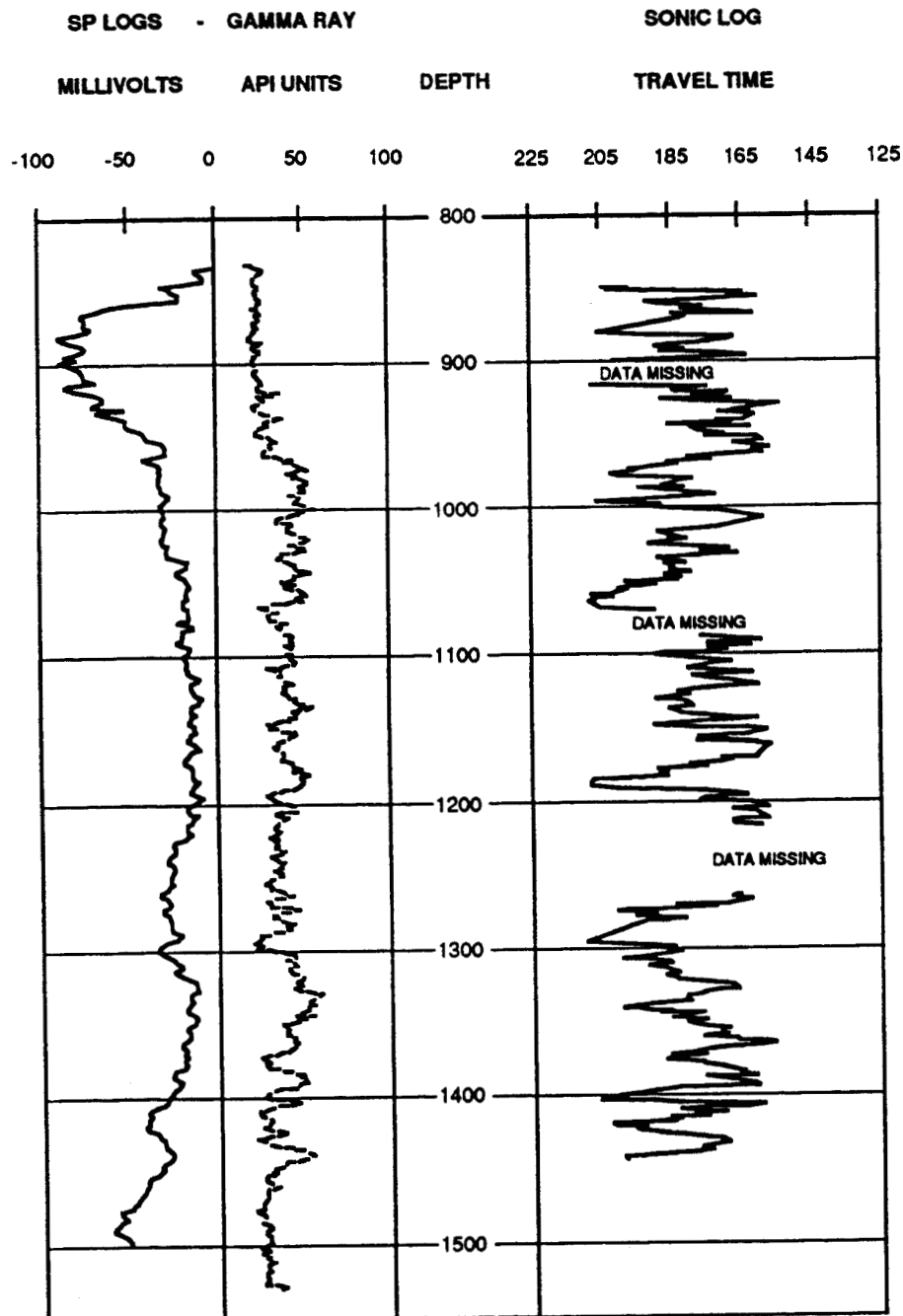
Scale:

N/A

Figure 7

1 of 1

# POINT THOMPSON NO. 2



For **ARCTIC GEOSCIENCE**



Project Description:  
Title:

**EASTERN BEAUFORT SEA SYNTHESIS**

Client:

**ARCO, ALASKA Inc.**

By: **DH**

Date: **7/22/93**

Checked:  
**MGS**

Date: **7/22/93**

Scale:  
**As/Noted**

**Figure 8**

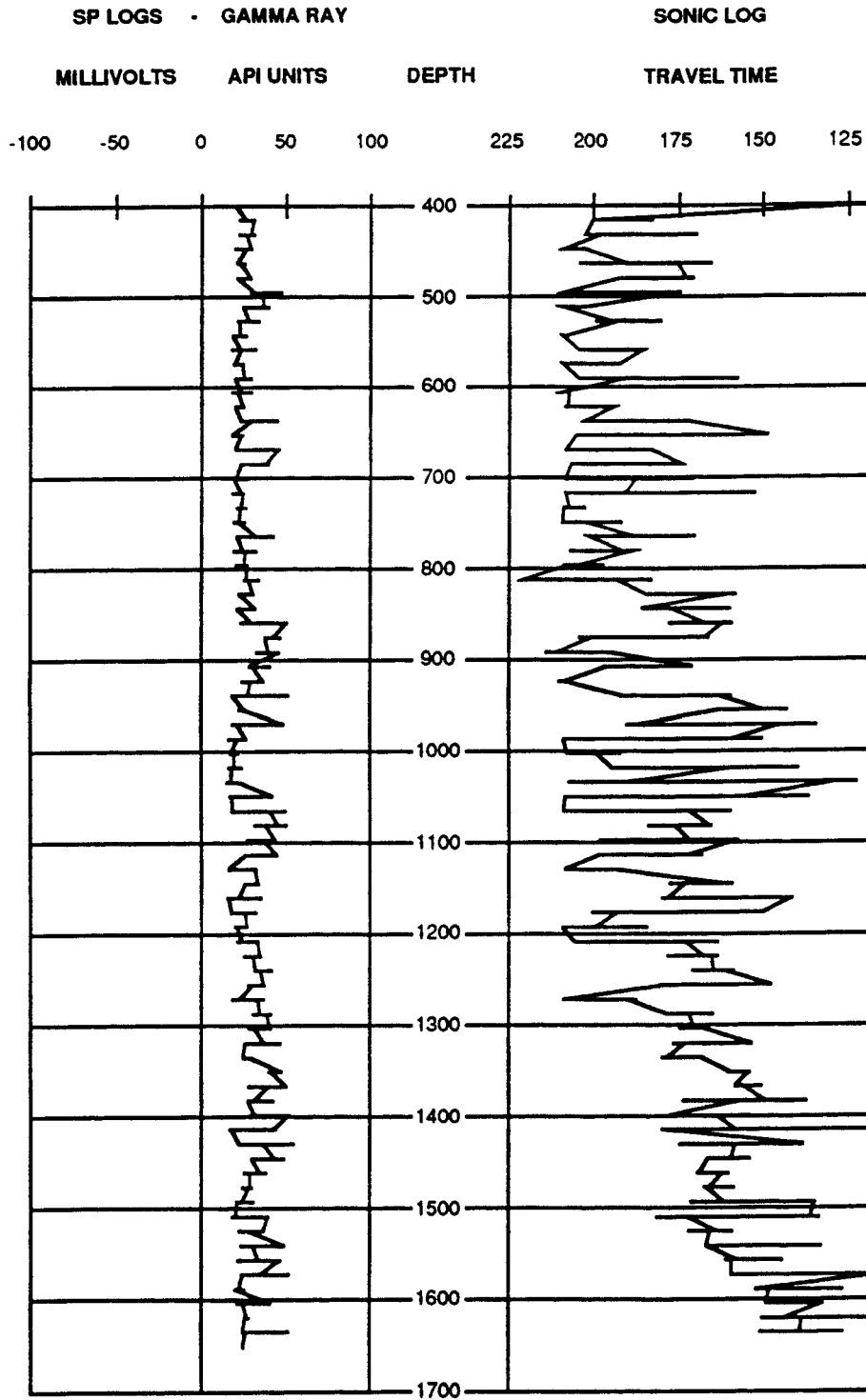
Project No.

**93-0033**

Sheet No.

**1 of 1**

# KARLUK NO. 1



For: **ARCTIC GEOSCIENCE**



Project Description:  
Title:

**EASTERN BEAUFORT SEA SYNTHESIS**

Client:

**ARCO, ALASKA Inc.**

By: **DH**

Checked:  
**MGS**

Scale:  
**As/Noted**

Date: **7/22/93**

Date: **7/22/93**

**Figure 9**

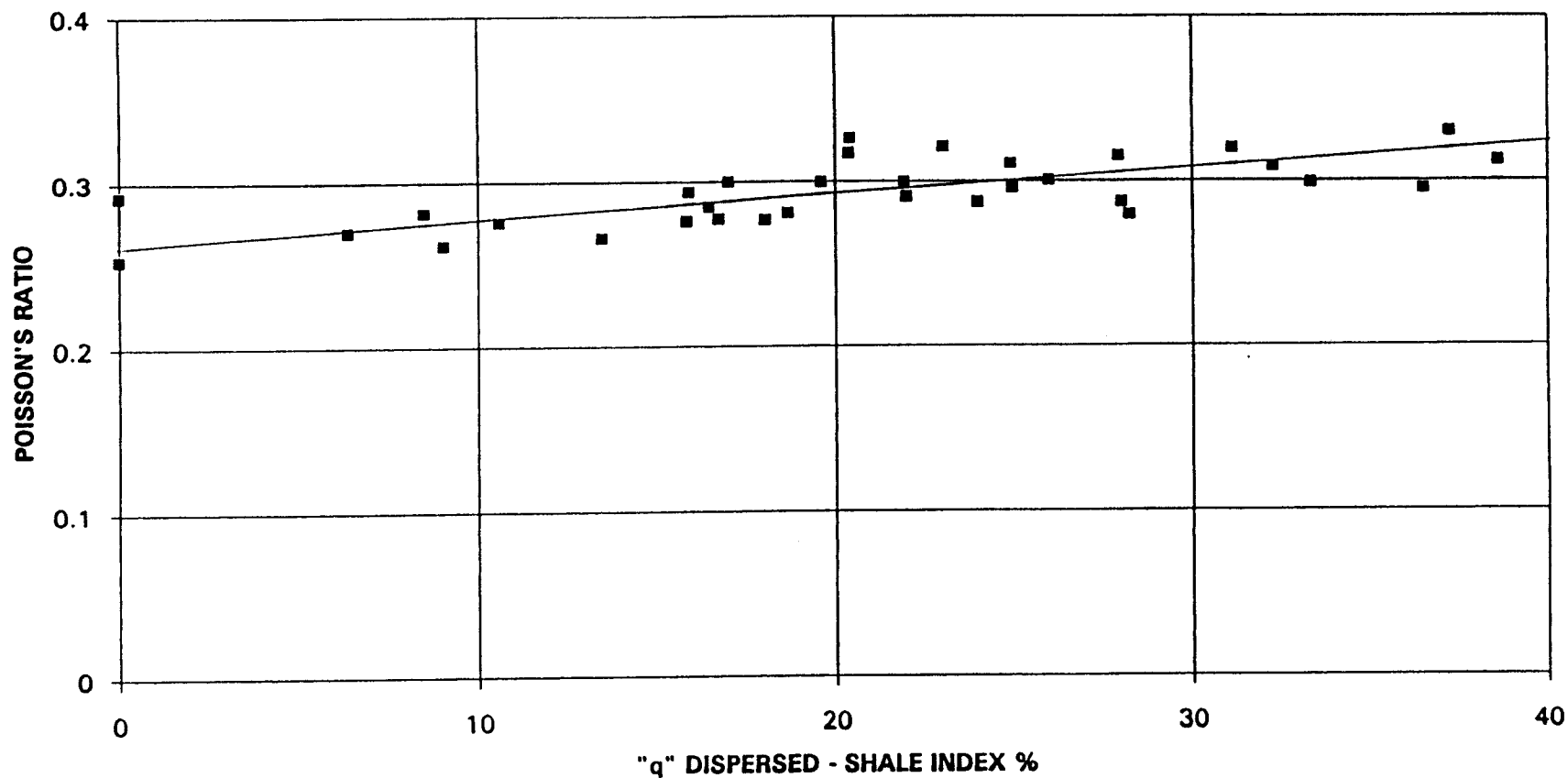
Project No.

**93-0033**

Sheet No.

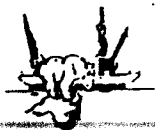
**1 of 1**

# EMPERICAL RELATIONSHIP BETWEEN POISSON'S RATIO AND SHALINESS



FROM ANDERSON (1973)

For: **ARCTIC GEO SCIENCE**



Project Description:  
Title:

**EASTERN BEAUFORT SEA SYNTHESIS**

Client:

**ARCO Alaska, Inc.**

By:

JSH

Date:

7/22/93

Project No.

93-0033

Checked:

MGS

Date:

7/22/93

Sheet No.

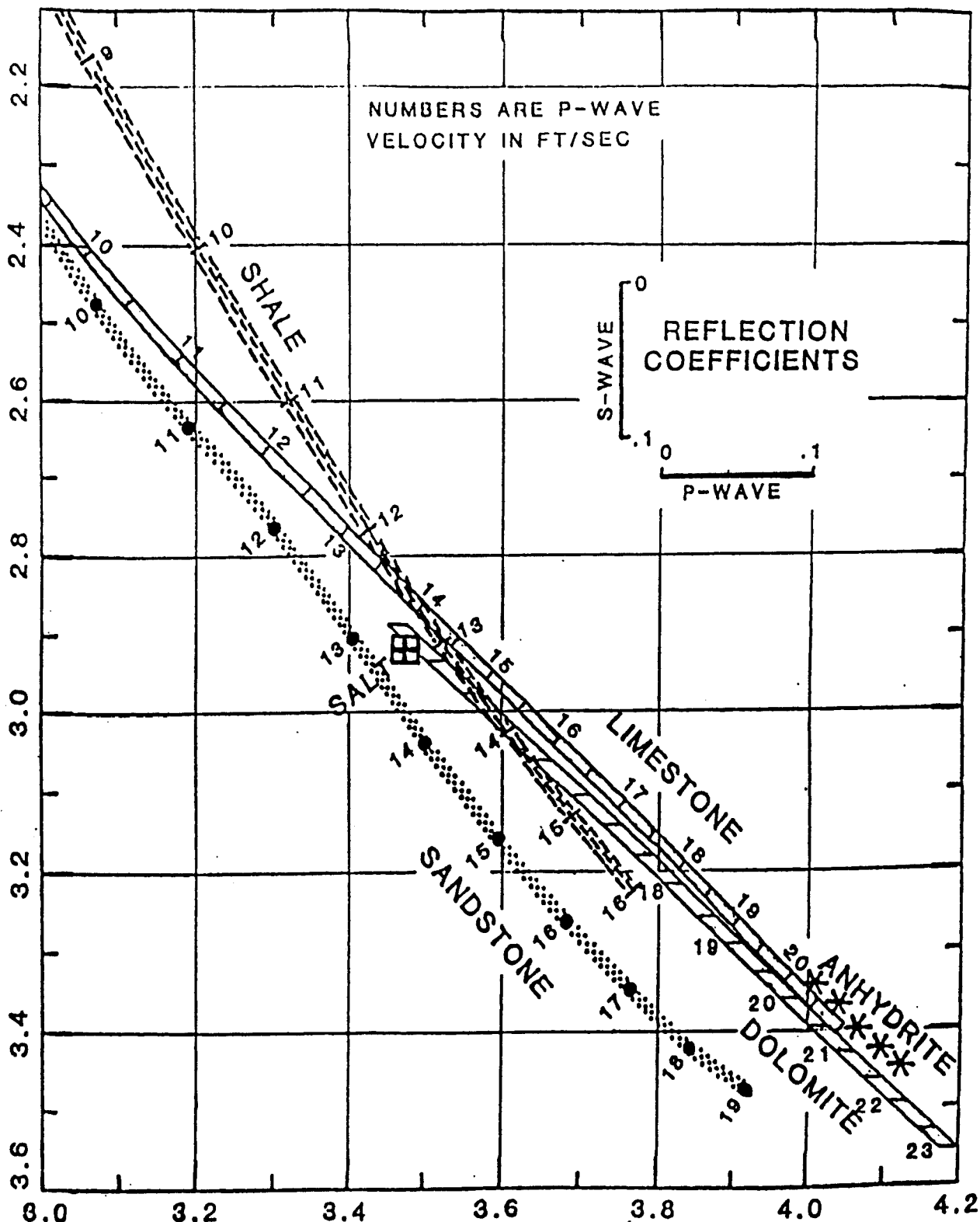
Scale:

N/A

Figure 10


1 of 1

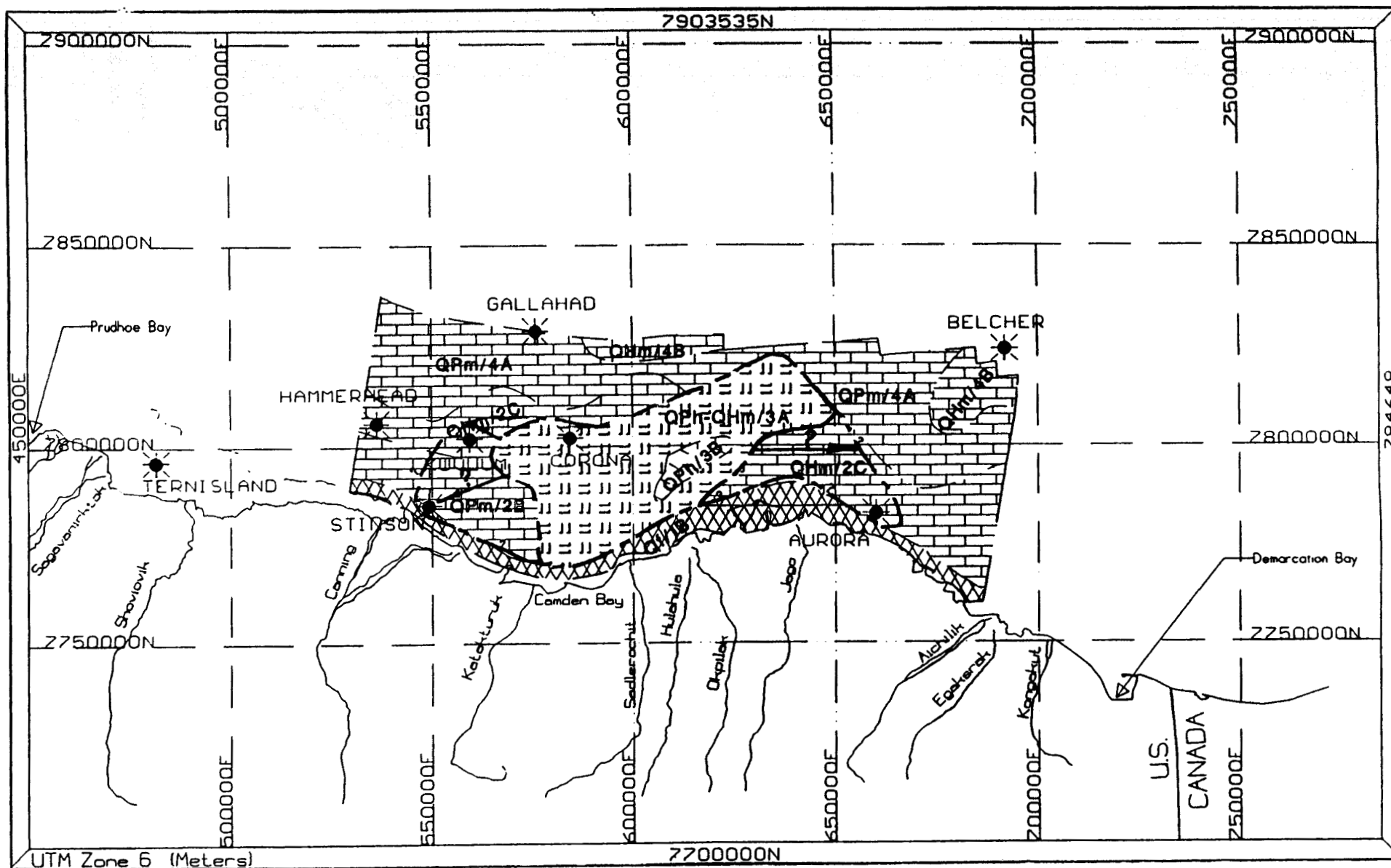
Ln  $\rho$  Vs



Ln  $\rho$  Vp



For: <b>ARCTIC GeoSCIENCE</b> 	Project Description: Title: <b>EASTERN BEAUFORT SEA SYNTHESIS</b>	By: <b>DH</b> Date: <b>7/22/93</b>	Project No.: <b>93-0033</b>
	Client: <b>ARCO ALASKA, INC.</b>	Checked: <b>MGS</b> Date: <b>7/22/93</b>	Sheet No.:
		Scale: <b>N/A</b> Figure <b>11</b>	



UTM Zone 6 (Meters)

# BEAUFORT SOIL UNITS

From: EBA - ARCO Stinson Study

For: **ARCTIC GeoSCIENCE**



Project Description:  
Title:

## EASTERN BEAUFORT SEA SYNTHESIS

Client:

ARCO Alaska, Inc.

By:

JSH

Date:

8/3/93

Project No.

93-0033

Checked:

MGS

Date:

8/3/93

Sheet No.

Scale:

N/A

Figure 12

1 of 1

# ARCTIC GEOSCIENCE

1330 E. HUFFMAN ROAD, SUITE 303 • ANCHORAGE, ALASKA 99515

June 18, 1993  
93-0033

ARCO Alaska Inc.  
Post Office Box 100360  
Anchorage, Alaska 99510-0360

Attention: Mr. John M. Eldred  
Sr. Facilities Engineer

**Wellbore Geophysics  
Kuvlum Prospect  
Beaufort Sea, Alaska**

Gentlemen:

This letter is in response to our past conversations regarding the presence of ice bonded permafrost in the offshore regions of the Beaufort Sea. We have collected geophysical well logs from one onshore exploration well ( Pt. Thompson #2) and another from an exploration well drilled from a Barrier Island (Karluk #1). The geophysical data collected can be utilized to evaluate the presence and condition of the permafrost in the wellbore. This technique is described in professional papers included with this submittal. The evaluation of the available well logs would assist in extending the data base being assembled for ARCO's future development planning at "Kuvlum Prospect". The following text briefly summarizes our approach, and ability to review the wellbore geophysical logs.

Our preliminary investigation of petrophysical properties of permafrost indicate that we are able to identify several properties including the percentage of pore space occupied by free liquid verses the total porosity ( $\phi_{eff}/\phi_{total}$ ),  $R_w$ , NaCl concentration and temperature of the undisturbed permafrost.

We located two sets of geophysical well logs in the area of study from the public record (AOGCC) that included measurements of the shallow permafrost zone. These were Exxon's Point Thompson #2 well and Chevron's Karluk #1 well located in the Eastern Beaufort Sea. The data available was from approximately 400 ft to 3000 ft. The well log suites included Dual Induction Resistivity, SP, Gamma-Ray, and Borehole Compensated Sonic tools.





Our evaluation followed procedures described in (Desai and Moore, 1968). We have also located two additional articles describing techniques for identifying Hydrates (Collett, 1983) and (Pearson et al, 1983), accompany this transmittal. We have incorporated their techniques where applicable.

We have identified other available well logs that cross ice-bonded permafrost zones to further identify petrophysical changes, in the public record should this study be continued.

#### DESCRIPTION OF PROCEDURES FOLLOWED:

The following discussion is a description of the procedures followed in evaluating the geophysical well logs in permafrost. Figures 1 through 3 depict sections of the well logs used to evaluate the analysis techniques used in this investigation.

Initially, we reviewed the logs continuance of the data, and for data quality. The Point Thompson Sonic log was missing data due to poor print quality of the available record. The lack of caliper data hindered the evaluation of the sonic log quality., because we were not able to identify cycle skips due to washouts verses tool response to shallow formations. The deep resistivity (ILD) exhibits very high resistivity in the sands due to the presence of ice in the pore space as expected. The shallow resistivity (LL8) reads much lower, as this is responding to the thawed zone in the sand strata. The SP log exhibits larger negative deflection near the top of the logged interval as  $R_w$  decreases. We have selected three zones to test the evaluation method.

Our next step involved calculating the temperature distribution for the well and zones of interest. The borehole temperature environment is depicted on Figure 4. The extent of thawing is dependent on the length of time the formation is exposed to the drilling mud and the mud temperature. We were able to identify the extent of thawing of material around the borehole and the temperature of the undisturbed permafrost at depth. We can refine this work to include temperature corrections for latent heat, should ARCO be interested in continuing this study.

Resistivity of the water in the pore space ( $R_w$ ) was calculated from the SP log using standard methods.  $R_w$  was calculated by following guidelines presented in

Schlumberger Log Interpretation Principles Volume 1 (1972). Computation of  $R_w$  values allowed us to calculate the NaCl concentration in the zone of study.

After computing values for  $R_w$ , we determined the  $\phi_{eff}/\phi_{total}$  ratio for each zone using  $R_w$  at formation temperature.

Table 1 is a summary of the data set calculated for the Exxon, Point Thompson #2 well.

**Table 1**  
**Point Thompson #2 Well**  
**Summary of Petrophysical Properties**

DEPTH (feet)	TEMP OF UNDISTURBE D PERMAFROST	$R_w$	NaCl	$\phi_{eff}/\phi_{total}$
900	14.8°F	0.31 @ 62°F	26,000 PPM	0.18
1500	24.6°F	0.54 @ 62°F	13,000 PPM	0.20
2010	33.0°F	1.70 @ 62°F	3,000 PPM	1.00

Note that  $R_w$  decreases and NaCl concentration increases as interpretations continue up the wellbore. This is consistent with the concentration of naturally occurring salts present in the pore spaces of the formation as the interstitial water freezes with decreasing temperatures. The  $\phi_{eff}/\phi_{total}$  ratio also decreases as expected in shallower depths of the wellbore. Permafrost occurs to approximately 1900 ft in the Point Thompson #2 well. The  $\phi_{eff}/\phi_{total}$  ratio calculates at 1.00 below this depth, confirming there is no frozen water occupying the pore space which helps confirm the validity of the process. Figure 5, graphically displays the change in  $R_w$  and  $\phi_{eff}/\phi_{total}$  in the Point Thompson #2 well with depth.

Table 2 is a computation of temperature at a depth of 900 feet in the Point Thompson #2 wellbore. The formation temperature is calculated from the methods outlined in Desai and Moore's publication entitled "Well Log Interpretation in Permafrost"

**Table 2**  
**Point Thompson #2 Well**  
**Radial Temperature Distribution for Depth 900 Feet**

RADIUS FROM BOREHOLE CENTER (FT)	TEMPERATURE	TEMPERATURE CORRECTED FOR LATENT HEAT
1.46	35.00°F	TO BE CALCULATED
2.0	25.20°F	TO BE CALCULATED
2.5	17.85°F	TO BE CALCULATED
3.0	7.07°F	TO BE CALCULATED
4.0	-1.75°F	TO BE CALCULATED
5.0	-8.12°F	TO BE CALCULATED
8.0	-11.55°F	TO BE CALCULATED
10.0	-14.00°F	TO BE CALCULATED

We can continue our evaluation of the permafrost conditions by calculating the temperature corrected for latent heat which will allow identification of the thawed, transition and undisturbed permafrost zones. This can be performed if requested

**ADDITIONAL INFORMATION:**

The following information will help to improve the accuracy of this technique and allows for further evaluation of petrophysical data.

Well log data collected from shallower wells, preferably data that crosses the ice-bonded contact. This information is available in selected wells. Well logging has been performed to 92 feet in the Point Thompson #2 well. This data was not available to us at this time. This shallow evaluation is supported by Sellmann and Chamberlain (1979) identification of the ice-bonded permafrost boundary to be between 0 and 140 meters offshore in the Beaufort Sea based on drilling and seismic reflection data.

Information on accurate values of Sonic Travel Time ( $\Delta t$ ) of the matrix and chemistry of interstitial fluid in the shallow permafrost. This data can be obtained from crossplots and core sample measurements.

Caliper information of the well bore to evaluate the quality of the sonic data.

Density and/or Neutron data to assist in cross plots for matrix parameters and porosity information.

Drilling records identifying the length of time the zone of interest has been exposed to the drilling mud. This will allow us to better understand the radial temperature distribution around the borehole.

Micro Resistivity log (MSFL or MLL) to insure measurement of thawed zone resistivity.

Core data of the permafrost.

Any of the above information will improve the quality of information obtained in these investigations. We can continue to investigate the procedures identified here by researching additional techniques and acquiring additional well information.

#### FURTHER STUDY:

We can continue the process of locating well logs that have obtained measurements across the ice-bonded permafrost boundary to further identify the petrophysical changes. Our presented interpretive theory is based on the assumption that salt water will invade the pore space above the ice-bounded zone in the offshore regions of the Beaufort Sea. This increase or change in formation salinity will change the SP and resistivity response as the value of  $R_w$  will also change at this location. Additionally, we can further our study by attempting to identify and refine values for  $Dt$  of the matrix and fluid at these shallow depths.

Arctic GeoScience and Watson Co. appreciated this opportunity to provide technical services in support of ARCO Alaska's planning activities at your "Kuvlum Prospect" in the Beaufort Sea, Alaska. We hope our services to date have been of value to ARCO Alaska Inc. Should you have any questions or require any additional information please do not hesitate to contact the undersigned.

Sincerely,  
Arctic GeoScience



Michael G. Schlegel  
Consultant; Engineering Geology

## REFERENCES:

Collett, T. S., (1983), Detection and Evaluation of Natural Gas Hydrates from Well Logs, Prudhoe Bay, Alaska, Department of Geology/Geophysics, University of Alaska, Fairbanks

Desai, K. P., and Moore, E. J. (1968). Well Log Interpretation in Permafrost. The Log Analyst, January - February.

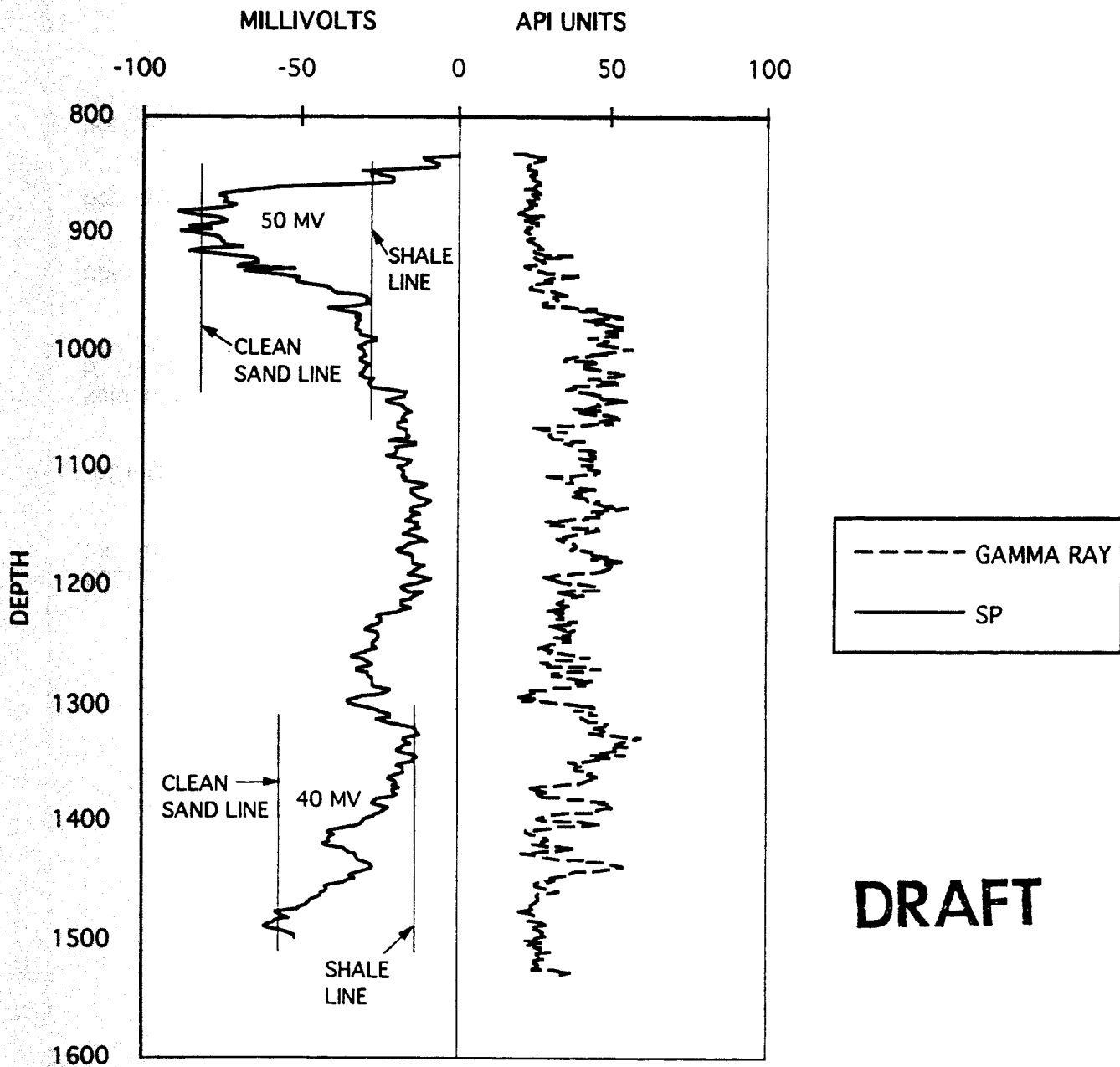
Exxon Well Point Thompson Number 2. Anchorage Oil and Gas Conservation Commission. Anchorage, Alaska.

Pearson, C., Murphy, J., Halleck, P., Hermes, R., and Mathews, M. (1983). Sonic and Resistivity Measurements on Berea Sandstone Containing Tetrahydrofuran Hydrates: A Possible Analog to Natural Gas Hydrate Deposits, Earth Sciences Division. Los Alamos National Laboratory. Los Alamos, New Mexico.

Schlumberger Log Interpretation Volume 1 - Principles. (1972). Schlumberger Limited. New York, N. Y.

Sellmann, P. V., and Chamberlain, E. J. (1979). Permafrost Beneath the Beaufort Sea: Near Prudhoe Bay, Alaska. U. S. Army - Cold Region Research and Engineering Laboratory. Hanover, New Hampshire.

# SP AND GAMMA RAY LOGS

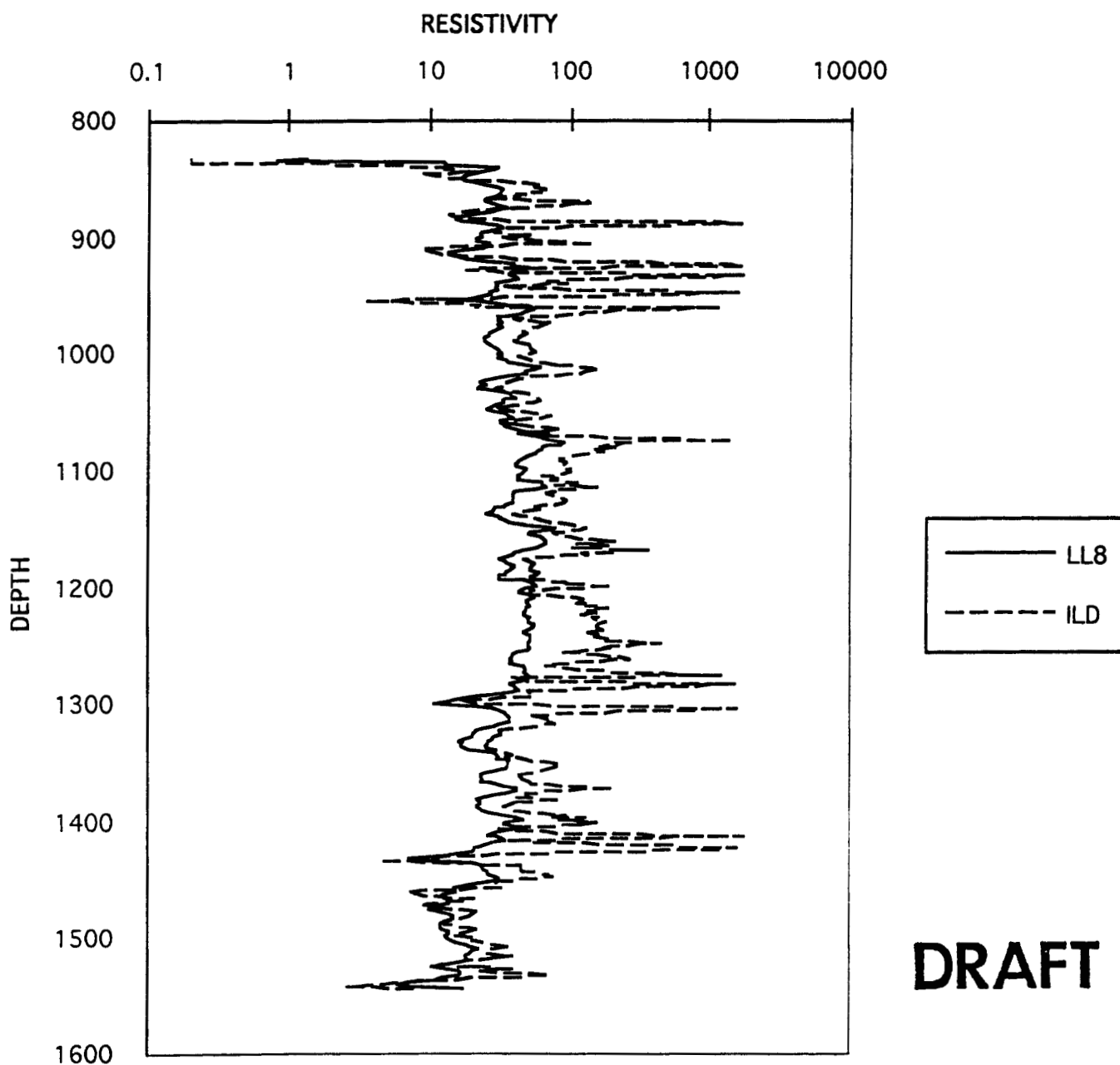


**DRAFT**

NOTE DECREASE IN SP DEFLECTION IN SAND FROM SHALE BASE AT 1500 FT COMPARED TO 900 FT DUE TO INCREASING  $R_w$  WITH DEPTH

For:	Project Description:	By:	Date:	Project No.
	Title:	DH	6/17/93	
	Client:	Checked:	Date:	Sheet No.
ARCTIC GeoSCIENCE	PERMAFROST LOG EVALUATION NORTH SLOPE, ALASKA	MGS	6/17/93	1 of 1
	ARCO Alaska, Inc.	Scale:	Figure 1	
		NA		

# RESISTIVITY LOGS



**DRAFT**

NOTE HIGH ILD (DEEP) RESISTIVITY INDICATIVE OF ICE IN THE FORMATION PORE SPACE. LL8 (SHALLOW) RESISTIVITY READS LOWER FROM THE THAWED ZONE.

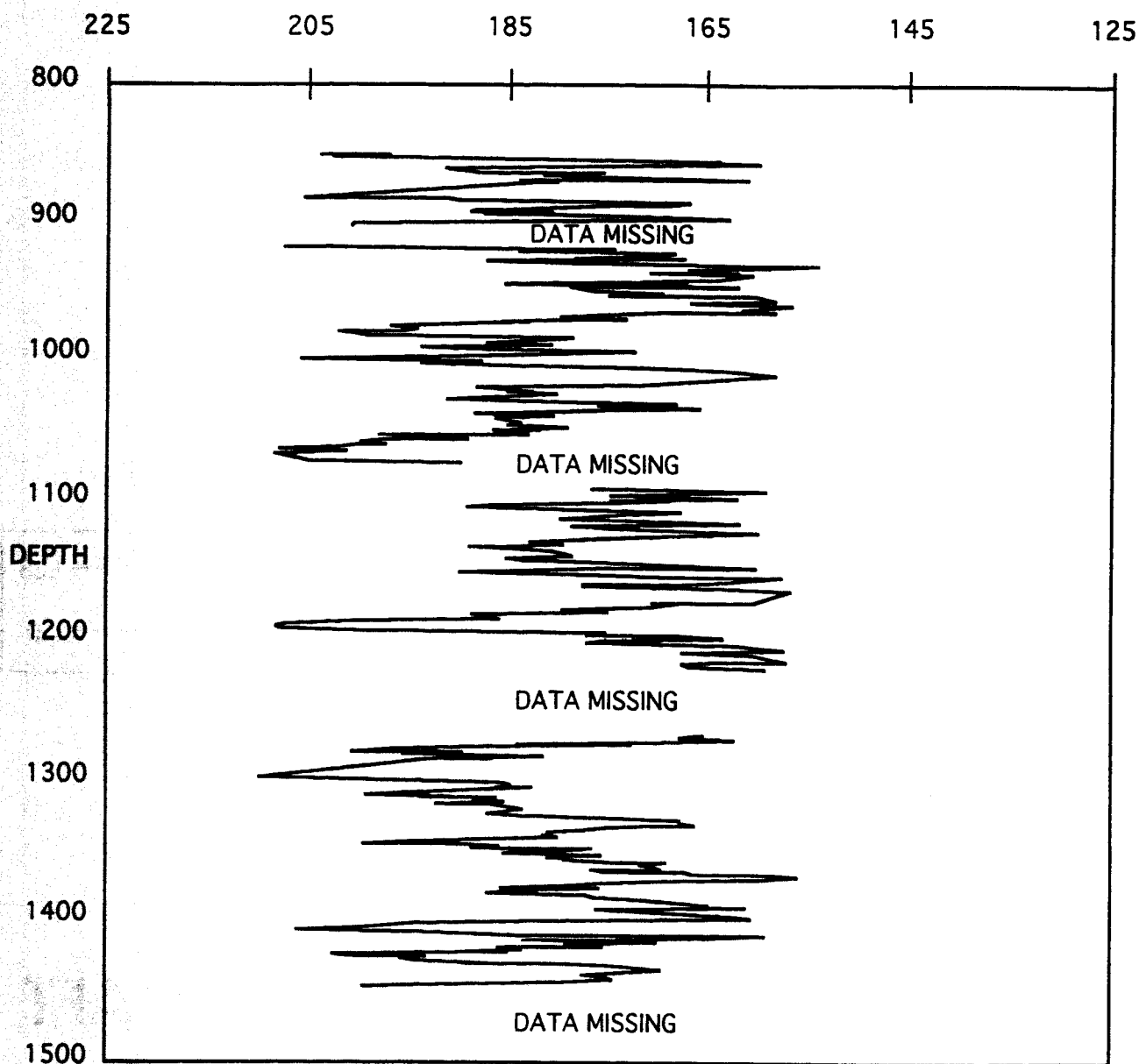
**ARCTIC GeoSCIENCE**

Client:	Project Description: Title:	By: DH	Date: 6/17/93	Project No.
	PERMAFROST LOG EVALUATION		Checked: MGS	
	NORTH SLOPE, ALASKA		Date: 6/17/93	Sheet No.
	ARCO Alaska, Inc	Scale: NA	Figure 2	1 of 1



# SONIC LOG

## TRAVEL TIME



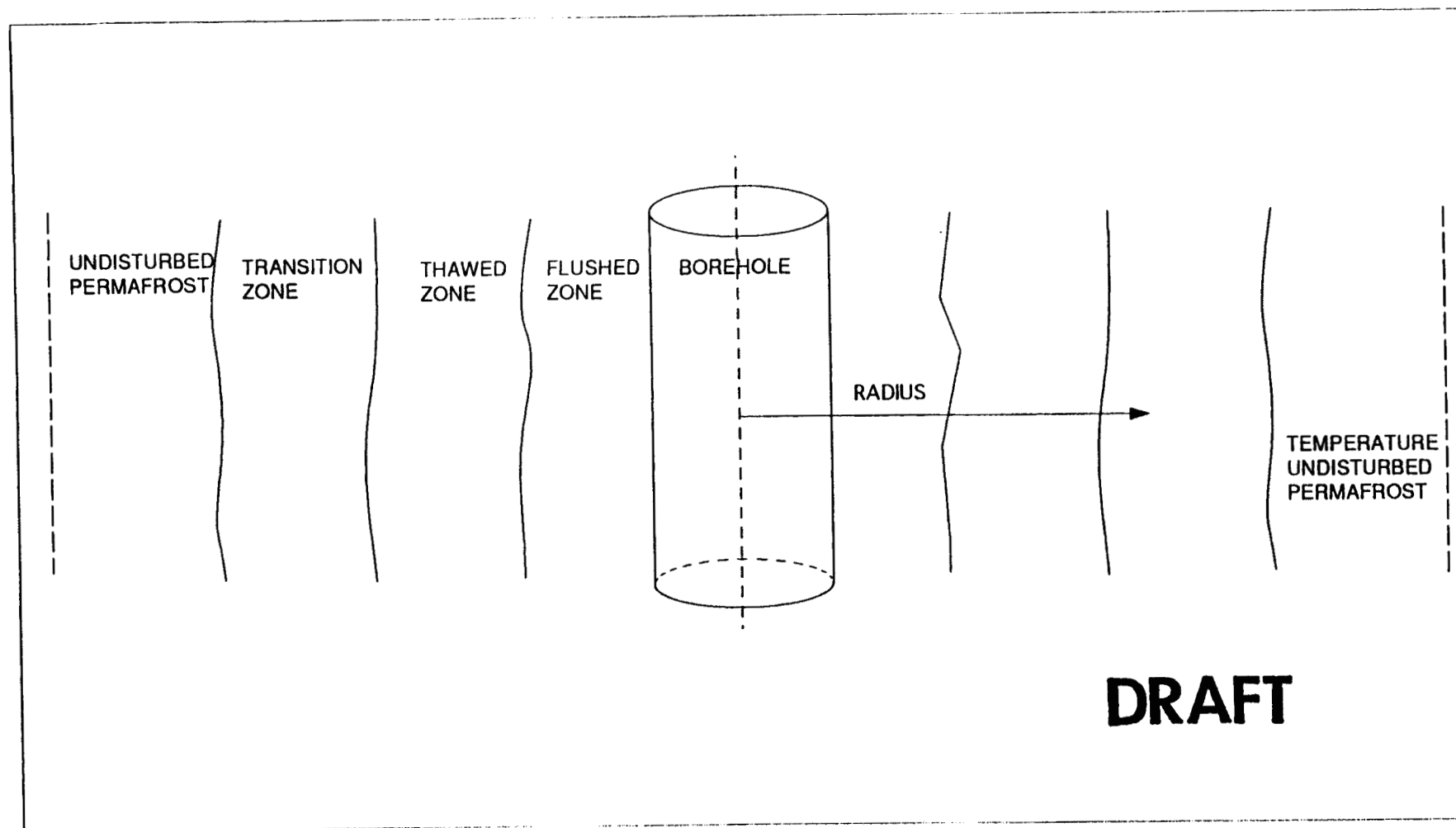
NOTE HIGH IRREGULAR TRAVEL TIMES

**DRAFT**

For:	Project Description:	By:	Date:	Project No.
	Title:	DH	6/17/93	
	<b>PERMAFROST LOG EVALUATION</b>	Checked:	Date:	Sheet No.
	NORTH SLOPE, ALASKA	MGS	6/17/93	
	Client:	Scale:	Figure 3	1 of 1
	ARCO Alaska, Inc.	NA		

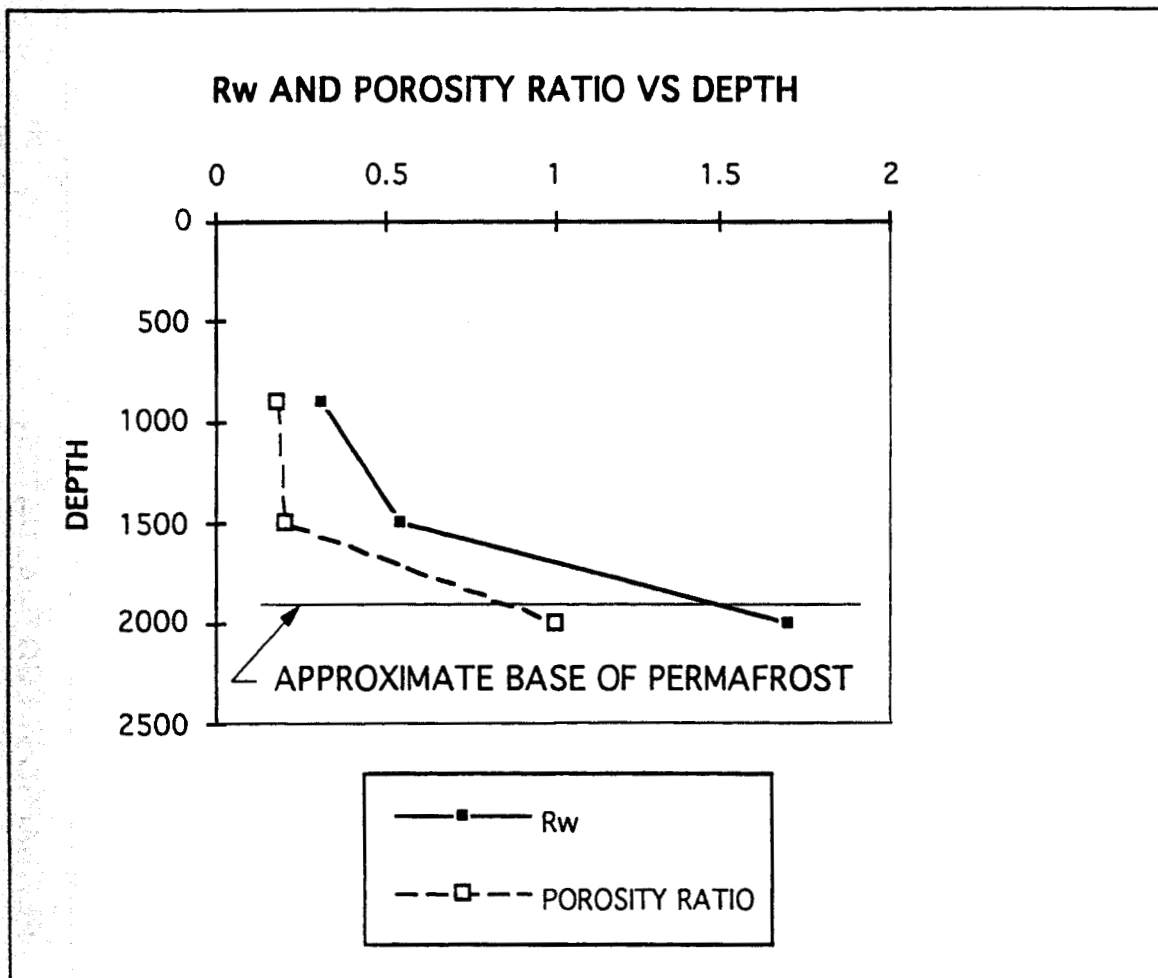
**ARCTIC GeoScience**

# BOREHOLE TEMPERATURE ENVIRONMENT



**DRAFT**

For:  <b>ARCTIC GEO SCIENCE</b>	Project Description: Title: <b>PERMAFROST LOG EVALUATION</b> <b>NORTH SLOPE, ALASKA</b>	By: <b>DH</b>	Date: <b>6/17/93</b>	Project No.  Sheet No.
	Client: <b>ARCO Alaska, Inc.</b>	Checked: <b>MGS</b>	Date: <b>6/17/93</b>	
		Scale: <b>N/A</b>	Figure 4	1 of 1



DRAFT

**ARCTIC GeoSCIENCE**

Project Description:  
**PERMAFROST LOG EVALUATION**  
 NORTH SLOPE, ALASKA

Client: **ARCO Alaska, Inc.**

By: DH

Checked: MGS

Scale: NA

Date: 6/17/93

Date: 6/17/93

Figure 5

Project No.

Sheet No.

1 of 1

DETECTION AND EVALUATION OF NATURAL GAS HYDRATES FROM WELL LOGS,  
PRUDHOE BAY, ALASKA

Timothy S. Collett

Department of Geology/Geophysics, University of Alaska, Fairbanks, Alaska 99701 USA

The purpose of this study is to develop techniques for the detection and evaluation of in-situ gas hydrates from well log data and to determine possible geologic controls on the occurrence of hydrates in the North Slope region of Alaska. Several new methods of evaluation for subsurface gas hydrate were developed and incorporated with existing techniques. For each of 125 wells examined as part of this study the geothermal gradient was determined and the theoretical stability zone for methane hydrate was calculated. Among these, there was 102 apparent hydrate occurrences in 32 wells. A subsurface structural-stratigraphic framework was established to a depth of 1,000 meters. This sediment package is characterized by three deltaic depositional sequences. The high frequency of hydrate occurrences in the structurally up-dip region of the Kuparuk Oil Field suggests that upward migration of free gas preceded hydrate development in the zone of hydrate stability.

INTRODUCTION

Significant quantities of gas hydrates have been detected in many permafrost regions of the world; in western Siberia, in the Mackenzie Delta of Canada, and on the North Slope of Alaska (Kvenvolden et al. 1980). In 1970 Makogon reported that the Messoyakha field in western Siberia had reserves in the billions of cubic meters of methane gas frozen as gas hydrates (Figure 1). Although gas hydrates have been identified in many regions, their significance and geographical extent have seldom been studied. Work done in the Messoyakha field showed that injections of methanol into the hydrate zones could increase gas reserves by 54% above what would be expected in an equal volume of reservoir rocks filled with free gas (Makogon 1981).

In-situ hydrates can occur in permafrost and can also occur below the base of the permafrost at temperatures above the freezing point of water (Figure 2). Various schemes for hydrate development have been postulated. One theory suggests that a gas hydrate could be part of a preexisting gas reservoir, which was frozen in place. It has been suggested that a hydrate body could form by a flux of free gas into a zone of methane hydrate stability and be frozen in place. Another theory states the possibility that free gas could be trapped at the base of the permafrost and be frozen into hydrate. Hydrates can also be found in association with decaying biomatter, such as coal, which would serve as a source for the methane needed for hydrate development (Pratt 1979).

The overall study of in-situ gas hydrates has been limited, with only several preliminary studies completed (Pratt 1971, Bily and Dick 1974, Kvenvolden et al. 1980). The work of Bily and Dick (1974) provided the most conclusive study to date on the occurrence and detection of in-situ natural gas hydrates. Bily and Dick incorporated well logs including dual induction, sonic, and mud logs as potential hydrate detection devices.

Published research to date into the gas hydrates of the Prudhoe Bay region is limited to the work of Osterkamp and Payne (1981), and also Pratt (1979).

CONSIDERATIONS FOR HYDRATE OCCURRENCE

The depth and thickness of the zone of potential hydrate stability can be calculated if the mean annual temperature, geothermal gradient, lithostatic pressure gradient, and gas density are known. The past mean surface temperature at Prudhoe Bay was  $-10.9^{\circ}\text{C}$  and the lithostatic pressure gradient is  $9.84 \text{ kPa/m}$  (Lachenbruch et al. 1982). The mean value of  $-10.9^{\circ}\text{C}$  can be viewed as the average surface temperature with which the deep permafrost is presently in equilibrium.

The high number of methane gas shows on the mud logs and several sets of detailed gas analysis from drill stem tests suggest that the dominant gas type in the upper units in Prudhoe Bay is methane.

The geothermal gradients needed to predict the thickness of the hydrate are not generally available. Lachenbruch et al. (1982) observed three geothermal gradients from different bore holes along the Alaskan arctic coast. The lowest geothermal gradient was calculated at Cape Thompson, which was  $2.0^{\circ}\text{C}/100 \text{ m}$ , at Pt. Barrow the gradient was  $2.3^{\circ}\text{C}/100 \text{ m}$  and the geothermal gradient at Cape Simpson was  $3.3^{\circ}\text{C}/100 \text{ m}$  (Lachenbruch et al. 1982). The variance in the geothermal gradient is due to differences in thermal conductivity.

The variance in the geothermal gradient indicates that no one regional gradient should be used to calculate the thickness of the zone of potential hydrate occurrence. The geothermal gradient was calculated separately for each well, the base of the permafrost was assumed to be at  $-1^{\circ}\text{C}$  (Lachenbruch et al. 1982), and a temperature gradient was calculated to the base of the permafrost.

Formerly, the base of the permafrost was assumed to be in equilibrium at  $0^{\circ}\text{C}$ , but due to freezing point depression the interface is now believed to be at equilibrium at  $-1^{\circ}\text{C}$  with an error of  $\pm 0.5^{\circ}\text{C}$  (Lachenbruch et al. 1982). Freezing point depression is related to several factors that may affect the thermal stability of the phase boundary. These factors include the presence of salt ions in solution, the existence of freeze-back pressure, and variations in the types of solids and fluid saturation levels.

Obviously it is impossible to make a reliable temperature estimate at the base of the permafrost in a well bore. However, the error in a regional geothermal gradient would be more significant than using a calculated gradient for each well bore, in which the base of the permafrost is assumed to be at  $-1^{\circ}\text{C}$ . The values for the depth to the base of the permafrost were taken directly from the work of Osterkamp on permafrost thickness evaluation from well log data on the North Slope.

Figure 3 illustrates how the depth to the base of the permafrost and a methane hydrate stability curve were used to determine the depth and thickness of the zone of potential methane hydrate stability. In this example the depth to the base of the permafrost is 532 m with a mean annual ground temperature of  $-10.9^{\circ}\text{C}$ . Assuming that the temperature at the base of the permafrost is  $-1^{\circ}\text{C}$ , the geothermal gradient within the permafrost for this bore hole would be  $1.9^{\circ}\text{C}/100\text{ m}$ . In Figure 3 a  $1.0^{\circ}\text{C}/100\text{ m}$  geothermal gradient within the permafrost has been plotted along with a calculated  $3.2^{\circ}\text{C}/100\text{ m}$  gradient below the base of the permafrost. The geothermal gradient changes abruptly at the base of the permafrost due to a change in thermal conductivity. Therefore, the geothermal gradient was modified below the base of the permafrost in the calculation of the thickness of the zone of potential hydrate stability. The ratio used to manipulate the gradient below the base of the permafrost was given by Lachenbruch et al. (1982). This ratio indicated that the gradient increase by a factor of 1.73 from within the permafrost to the unfrozen strata below the base of the permafrost. A methane hydrate stability curve has also been plotted using a hydrostatic pressure gradient of  $9.84\text{ kPa/m}$  (Lachenbruch et al. 1982). The lower boundary of the zone of methane hydrate stability is marked by the lower intersection of the geothermal gradient with the methane stability curve. The upper boundary of the zone of methane hydrate stability is defined by the upper intersection of the methane stability curve and the geothermal gradient. In Figure 3 the upper boundary of the zone is marked by H1 at 177 m. While the lower hydrate boundary is marked by H2 at 957 m, delineating a zone of potential hydrate occurrence 780 m thick.

The methane hydrate stability curve indicates that the geothermal gradient must be less than  $3.7^{\circ}\text{C}/100\text{ m}$  for methane gas hydrate to form at Prudhoe Bay. For the geothermal gradient to intersect the methane hydrate stability curve the gradient must be equal to or less than  $3.6^{\circ}\text{C}/100\text{ m}$ , which would correspond with a minimum permafrost depth of 290 m. In other words methane hydrate should not exist at Prudhoe Bay if the

depth to the base of the permafrost is less than 290 m. The dashed line in Figure 2 represents the 290 m depth contour on the base of the permafrost. If the above line of reasoning is correct, methane hydrate occurrences should be limited to areas north of this contour. The thickness of the zone of potential hydrate occurrence ranged from nothing at the 290 m permafrost contour to more than 1,000 m near Mikkelsen Bay, where the methane hydrate was found to be potentially stable to a depth of 1,119 m.

#### LOG EVALUATION

The recognition of gas hydrate in well log data is not straightforward, and often the zones of potential hydrate occurrence are not logged, or the quality of the logs may be poor. Another problem in the evaluation of hydrates from well log data is the lack of prior quantitative work.

The work by Bily and Dick (1974) on the evaluation of natural occurring gas hydrates in the Mackenzie Delta is one of only a few papers dealing with the detection of in-situ natural gas hydrates using wire line logs. Bily and Dick discovered that when a hydrate zone was penetrated during drilling, there was a marked increase in the amount of gas in the drilling mud. The hydrate units recorded a relatively high resistivity on the dual induction log and a slight spontaneous potential deflection in comparison to a free gas. Sonic logs also indicated an increase in acoustic velocity.

The first confirmation of the existence of in-situ natural gas hydrate was not until 1972, when ARCO/EXXON were successful in recovering the first natural gas hydrate in a frozen state. The sample was recovered from a depth of 666 m in the Northwest Eileen State #2 well in Prudhoe Bay. The Northwest Eileen well was drilled with cool drilling muds in an attempt to reduce thawing of the permafrost and hydrate. The methane hydrate saturated sample was recovered in a pressurized core barrel, and a simple test was devised to check for the presence of hydrate. The pressure within the core barrel was allowed to equilibrate with the surface pressure, and the core barrel was resealed and warmed above in-situ temperatures. The pressure within the barrel began to rise, indicating the presence of thawing hydrate. This process was repeated several times with similar results. The hydrate sample had a gas composition of 99.17% methane (P. Barker, personal communication, ARCO Alaska Inc., Anchorage, Alaska).

The confirmed hydrate occurrence in the Northwest Eileen well presents itself as an ideal starting point for the development of log evaluation techniques in a hydrate zone. Log responses for the hydrate zone in the Eileen well are graphically represented in Figure 4.

The following list summarizes various log responses, incorporating the methods developed in this study with the evaluation techniques developed by Bily and Dick (1971) in the Mackenzie Delta. The ability of each log to distinguish hydrates from free gas and ice bearing permafrost is also indicated.

1. Mud Log On a mud log there is a pronounced gas kick associated with a hydrate, due to thawing during drilling. The mud log serves as the best tool available for the differentiation of a hydrate saturated unit from gas-free ice-bearing permafrost.
2. Dual Induction Log There is a relatively high resistivity deflection on the dual induction log in a gas hydrate zone, in comparison to that in a free gas zone. The long normal is separated from the short normal due to thawing next to the bore hole. If a unit were hydrate saturated within ice-bearing permafrost, the resistivity response on the dual induction log for the hydrate unit would not be significantly different than the log responses for the surrounding ice-bearing permafrost. Hence, it is impossible without the usage of the mud log to distinguish between hydrate and permafrost. Below the base of the permafrost the high resistivity deflection associated with the hydrate is distinct from the surrounding non ice-bearing zones, but may be similar to that of a free gas.
3. Spontaneous Potential (SP) There is a relatively lower (less negative) spontaneous potential deflection in a hydrate zone when compared to that associated with free gas. The frozen hydrate limits the penetration of mud filtrate thus reducing the negative spontaneous potential.
4. Caliper Log The caliper log in a hydrate interval usually indicates an oversized well bore due to spalling associated with the decomposition of a hydrate. Because the caliper log also indicates an enlarged bore hole in ice-bearing permafrost, it is only useful in detecting hydrates below the base of the ice-bearing permafrost.
5. Sonic Log Acoustic velocities in hydrate are relatively high ranging from 3.1 km/s to 4.4 km/s. Because the sonic velocity of ice-bearing permafrost is very similar to that of gas hydrate, the sonic log cannot be used to detect hydrates within the upper ice-bearing permafrost zone, but it is helpful below the base of the ice-bearing permafrost.
6. Neutron Porosity In a hydrate zone there is an increase in the neutron porosity; this contrasts with the apparent reduction in neutron porosity in a free gas zone. If a unit is hydrate saturated and occurs within the ice-bearing permafrost zone the neutron porosity log would theoretically indicate an increased or reduced neutron porosity, depending on the amount of free gas associated with the hydrate in comparison to that of the surrounding ice-bearing permafrost. Below the base of the permafrost a hydrate unit exhibits a relatively higher neutron porosity compared to water saturated or free gas saturated zones. However, thawing near the well bore complicates the neutron log interpretation.
7. Drilling Rate In a hydrate zone the relative drilling rate decreases, due to the

cemented nature of the hydrate. There is a very similar drilling rate response within ice-bearing permafrost, and therefore drilling rate change is not useful as a hydrate detector within the permafrost.

8. Cross Plots In a cross plot of the resistivity and transit time for a series of stratigraphic units saturated with either hydrate or free gas and below the base of the ice-bearing permafrost, there is a grouping of units with similar constituents. Hydrate saturated units fall in a region of relatively higher resistivity and faster transit times while free gas saturated units fall in an area of lower resistivity and slow transit times. Differences are relative and not absolute; the cross plots show a simple clustering of similar properties. A resistivity/transit time cross plot of units that are above the base of the permafrost is not useful as a hydrate indicator, due to the similarity in resistivity and transit time velocities in hydrates and in permafrost.

In the Prudhoe Bay wells the dual induction and mud log are the most valuable tools available for the detection of gas hydrates; caliper and sonic logs are helpful but less definitive. The neutron porosity log showed great promise, but the lack of neutron surveys did not allow adequate assessment of it as a hydrate detection device. Many problems still exist in the evaluation of in-situ hydrates from well log data, and the addition of new evaluation techniques such as the use of cross plots and the addition of the neutron logs has only slightly improved the subjective nature of hydrate detection.

#### HYDRATE OCCURRENCE IN PRUDHOE BAY

In this study, a structural-stratigraphic framework of 32 key markers within the Tertiary and Upper Cretaceous strata was picked from the gamma ray logs and was established to a depth of 1,000 m. Thirty-three distinct units were defined and described from direct interpretation of the gamma ray logs. The gamma ray surveys were correlated with three complete sets of drill core chips and four petrographic strip logs.

The upper 1,000 m of strata in Prudhoe Bay is characterized by a gentle dip to the northeast, ranging from 20 to 28 m/km and is dominated by three distinct coarsening-upwards deltaic sequences. Howitt (1971) suggested that deposition of the upper units in Prudhoe Bay was more or less continuous in an aqueous environment.

One hundred twenty-five wells were examined for potential hydrate occurrence, with 102 definite occurrences in 32 different wells. Hydrates occurred in relative porous discrete units. Many of the wells had multiple zones of hydrate occurrence, with each hydrate unit ranging from 2 to 28 m thick.

Hydrate occurrences appeared to be regionally isolated to the Kuparuk oil field to the west of Prudhoe Bay, indicated in Figure 1. In the Kuparuk region there are four laterally continuous hydrate saturated sands and two less extensive

units. The lateral extent of each hydrate saturated unit has been graphically represented in a three-dimensional block diagram in Figure 5. An east-west cross section through the Kuparuk oil field has been plotted in Figure 6, along with associated hydrate accumulations and inferred environments of deposition.

The presence of a structural control on the occurrence of hydrate is apparent upon close examination of all hydrate zones. With several minor exceptions, all hydrate occurrences are below marker 12, which marks the base of a nonporous prodelta shale. Hydrates were found exclusively between markers 12 and 19.

The sediment package between marker 12 and 19 is described as a deposit of shaly sand with thick interbeds of clean sand and shale, which were deposited in a delta front foreshore environment. There are several notable impermeable shale breaks which act as caps for relatively porous sand units which are hydrate saturated. Due to the interbedded nature of the sediments the hydrate occurs in multiple discrete units, within one well there may be as many as eight different hydrate saturated units.

A subjective A, B or C value has been assigned to each hydrate occurrence in an attempt to quantify the degree of hydrate saturation. The magnitude of the resistivity kick and the gas show associated with each hydrate occurrence was used to calculate the relative saturation of each hydrate. The letter A was assigned to a unit if it appeared to be highly saturated with methane hydrate, B and C indicate a relative decrease in hydrate saturation.

In the cross section in Figure 6 the hydrate appears to be concentrated in the southwest up-dip direction, with a decrease in hydrate saturation down-dip to the northeast. The anomalous occurrence of hydrate in the Kuparuk region, along with the greater saturation of hydrate up-dip, suggests that the free gas necessary for hydrate development may have migrated into place. The source for the free gas may be from either local biological decay in the upper units, or the gas could have migrated from a deeper mature gas zone.

As noted in the cross section of Figure 6, there are a number of hydrate occurrences within the permafrost. The occurrence of hydrate within the permafrost represents a time restraint on the formation of hydrate. Since permafrost is impermeable to gas migration, the hydrate must have developed in the upper intervals before the formation of the permafrost to the present depth.

A possible scenario for the formation of hydrate in the North Slope would begin with free gas migration either from local diagenesis or from depth through a relatively permeable sand unit along the base of an impermeable prodelta shale. The overlying shale unit would act as a cap to vertical gas migration.

The migrating free gas could be trapped in the up-dip direction by a series of different trapping mechanisms. The two most probable trapping mechanisms would be a self-forming hydrate trap and an impermeable ice-bearing trap. The existence of a porosity/permeability trap or a fault trap is unlikely.

The rate of free gas migration and the existence of possible porosity/permeability traps in the hydrate saturated sands are not easily delineated due to the lack of data. The only data available on the porosity/permeability characteristics of the upper units are from stratigraphic logs prepared by the American Stratigraphic Company. The porosity within the hydrate saturated sands varies little, from 38 to 46% (American Stratigraphic Company). The existence of a porosity/permeability trap for the up-dip free gas migration is not likely due to the lack of variation in the lateral porosity in the same units. The unconsolidated nature of the upper units would not lend itself to the formation of a porosity/permeability trap.

The evidence that there is little faulting past the Lower Cretaceous reduces the likelihood of fault traps.

The free gas could have formed a trap when the gas entered the hydrate stability field. As the migrating gas moved into the zone of hydrate stability, the gas would be frozen in place. The frozen hydrate would be impermeable to free gas migration and would continue to thicken as free gas is trapped and frozen in place.

The impermeable permafrost could also form an up-dip trap to free gas migration. As the free gas migrated up-dip along the bedding plane, the gas would be trapped at the base of the permafrost and be frozen in place.

The actual occurrence of hydrate does not favor either the self-forming trapping model or the permafrost trapping model. However, the laterally continuous nature of the hydrate occurrences suggests possible reorganization of the hydrate by multiple periods of freezing and thawing.

## CONCLUSIONS

The major findings of this study are:

1. Several well logs have been found to be indicative of the presence of hydrate. Although no single log is definite by itself, used in combination they permit at least a subjective evaluation of hydrate occurrences. For example, the development of new evaluation techniques such as the use of cross plots and the addition of the neutron porosity log as a hydrate detector has reduced the subjective nature of the hydrate evaluation. Hydrate occurrences were identified by a variety of different well logs. The internal consistency of their determination, and their application in a large number of wells, indicate the validity of the method.
2. The recognition of the primarily structural-stratigraphic control on the up-dip gas migrational model for the hydrate accumulations was a significant contribution. The correlation of the actual hydrate occurrences identified in well log data with the structural-stratigraphic framework has allowed the development of a conceptual model for hydrate formation in the North Slope region.

3. The method for determining the zone of hydrate stability was refined to take into account both the difference in thermal conductivity between ice bearing and water bearing strata and the shallow depth limit of the stability zone. The method used for estimating the local geothermal gradients allows estimation of temperature profiles during warmer periods in the Earth's history which, in turn, has provided insight concerning the original formation and accumulation of the actual gas hydrate occurrences.

#### REFERENCES

- Bily, C., and Dick, J. W. L., 1974, Naturally occurring gas hydrates in Mackenzie Delta, N.W.T.: Bulletin of Canadian Petroleum Geology, v. 22, no. 3, p. 340-352.
- Howitt, F., 1971, Permafrost geology in Prudhoe Bay, Alaska: World Petroleum, September, p. 28-34.
- Kvenvolden, D. A., and McMenamin, M. A., 1980, Hydrates of natural gas: A review of their geologic occurrence: U.S. Geological Survey Circular 825, 11 p.
- Lachenbruch, A. H., Sass, J. H., Marshall, B. V., and Moses, T. H., 1982, Permafrost, heat flow, and the geothermal regime at Prudhoe Bay, Alaska: Journal of Geophysical Research, v. 87, no. B11, p. 9301-9316.
- Makogon, Y. F., 1981, Hydrates of natural gas: Tulsa, Okla., Penn Well Publishing Company, 237 p.
- Pratt, R. M., 1979, Gas hydrate evaluation and recommendations Natural Petroleum Reserve, Alaska: U.S. Geological Survey Special Report TC-7916, 27 p.
- Osterkamp, T. E., and Payne, M. W., 1981, Estimates of permafrost thickness from well logs in northern Alaska: Cold Regions Science and Technology, v. 5, p. 13-27.

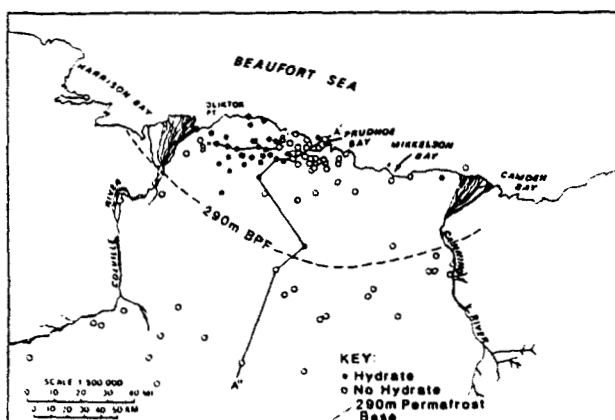


FIGURE 1 Base map of study area Hydrate occurrences have been denoted.

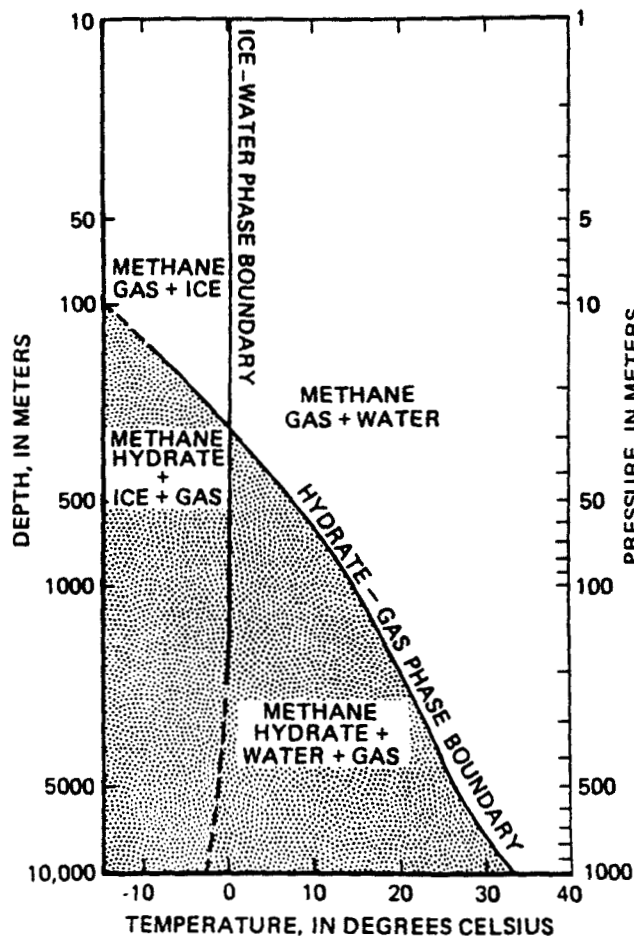


FIGURE 2 Phase boundary diagram showing free methane gas and methane hydrate pattern for a freshwater pure methane system (Kvenvolden et al. 1980).



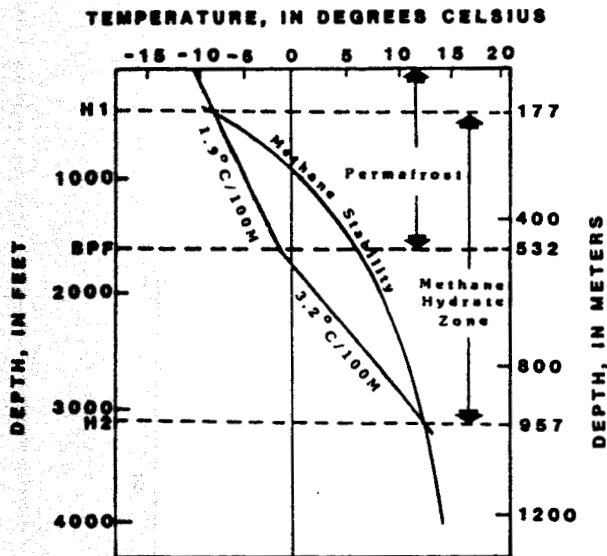


FIGURE 3 Thickness calculation of the methane hydrate stability zone in North-west Eileen State No. 2 well.

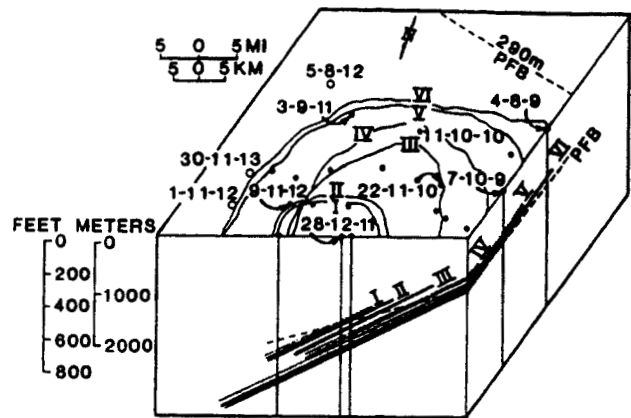


FIGURE 5 Block diagram representation of the hydrate occurrence in the Kuparuk Oil Field.

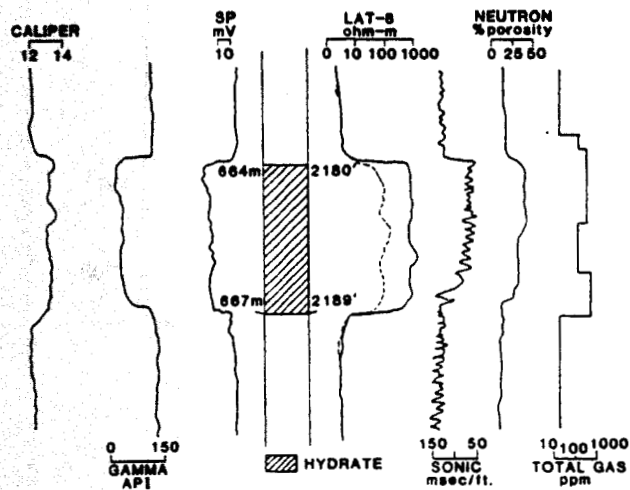


FIGURE 4 Hydrate characteristics in well log data from Northwest Eileen State No. 2 well.

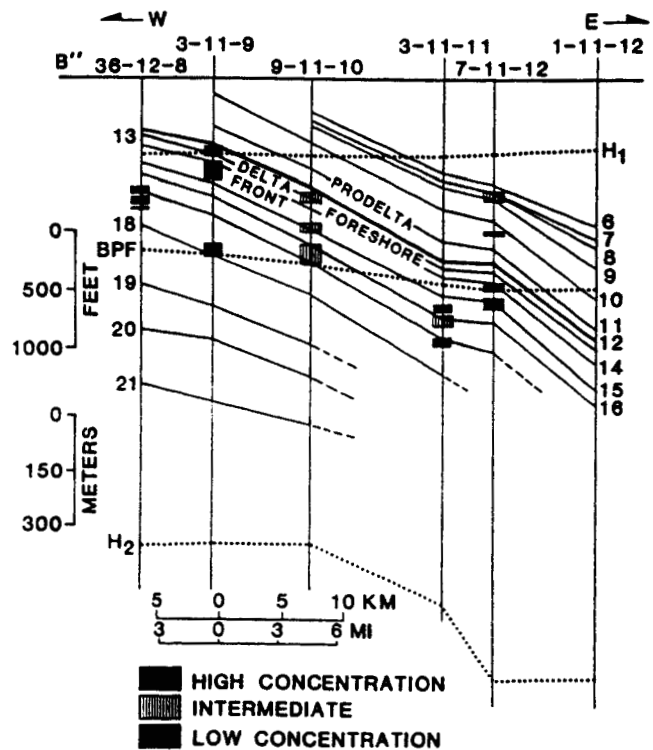


FIGURE 6 East-west cross section through the Kuparuk Oil Field Hydrate occurrences are plotted with degree of saturation indicated.

# WELL LOG INTERPRETATION IN PERMAFROST

By  
K. P. DESAI and E. J. MOORE  
Sinclair Oil & Gas Company  
Tulsa Research Center

**EDITOR'S NOTE:** *As the authors of this paper point out, permafrost covers a significant portion of North America (22%) to depths as great as 1,300 feet. Although the permafrost has yet to be proven economically important in terms of petroleum reserves, some hydrocarbon accumulations have been found. Thus a knowledge of the characteristics of this material could become of great importance to us.*

*Doctors Desai and Moore have done an outstanding job in investigating and in here describing these characteristics. Of particular note are the dramatic changes in resistivity and acoustic properties of permafrost at the freezing point of water. These changes could in turn significantly affect our normal interpretive approaches in Formation Evaluation. Techniques for handling these problems are described by the authors. This paper was presented at the SPWLA Eighth Annual Symposium.*

## ABSTRACT

Permafrost or permanently frozen ground covers a large portion of the arctic sedimentary basins of Canada and Alaska. The thickness of the permafrost layer varies up to a maximum of 1300'. Some accumulations of hydrocarbons in the permafrost have been reported.

First, a method is described for establishing the temperature distribution around a well bore in these unique surroundings. Then, the basic borehole environments which might occur under a variety of drilling and completion programs are discussed. The laboratory determined data is presented to show the effects of below freezing temperatures upon fluid and rock properties. At their freezing points, brine saturated rocks exhibit marked changes in both their electrical and acoustical properties. Finally an interpretation from actual field logs, based on the previously described investigation, is given.

These studies show that a knowledge of temperature distribution and variations in physical properties with temperature are essential to a correct quantitative interpretation of well logs from permafrost. The proper field procedures prior to logging also are important.

## INTRODUCTION

Continuous permafrost or permanently frozen ground occupies over 22% of the land area of the Northern Hemisphere, including a large portion of the arctic sedimentary basins of Canada and Alaska.<sup>1</sup> Though this permafrost may reach a thickness of 1300' in northern Alaska, with some accumulations of hydrocarbons being reported,<sup>2,3</sup> the commercial potential of this unusual layer still remains in considerable doubt. Nevertheless, an investigation of some of the physical properties of permafrost with a view towards utilizing this information in the interpretation of logs run in this unique environment promised to be a particularly interesting problem. While the results presented here may have more academic than practical value, at this time, they do illustrate the need for an accurate understanding of the physical properties of an environment before a reliable interpretation of its logs can be attempted.

## DISTRIBUTION OF TEMPERATURE

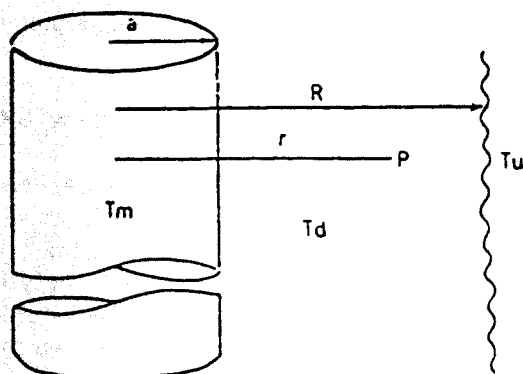
This investigation showed that in the permafrost environment many of the physical properties of rocks are acutely sensitive to relatively small changes in temperature. It is therefore essential, in accurately interpreting well logs in this environment, to have a precise knowledge of the temperature distribution around the borehole.

To accomplish this we must first understand the vertical distribution of temperature in the undisturbed permafrost. It differs in several ways from a normal distribution. First, of course, the temperatures are much lower, ranging anywhere from 40°F to 60°F cooler. Second, the average geothermal gradient is higher, around 1.7°F/100' in northern Alaska, with a range of  $\pm 0.3^\circ\text{F}/100'$ . The minimum temperature in the permafrost occurs just below the zone of seasonal variation, at a depth of 75'  $\pm 25'$ , depending to a large extent on geographical location and surface features. This minimum temperature is approximately the same as the mean annual ground temperature which experience has shown to be approximately 5.5°F higher than the mean annual air temperature. The difference can be attributed in part to heating of the ground surface by solar radiation and to the insulating effect of snow cover.<sup>4</sup> Average minimum permafrost temperatures are in the range from 15°F to 20°F.

Therefore, to construct an approximate picture of the temperature distribution in undisturbed permafrost only a knowledge of the mean annual air temperature in the vicinity under consideration is needed in addition to the general information presented in the preceding paragraph. For example, at Umiat, Alaska on the Arctic Slope the annual mean air temperature is 10.8°F.<sup>5</sup> Then the minimum permafrost temperature would be 16.3°F at a depth of 75'. Below that point the permafrost temperature would increase at the rate of approximately 1.7°F for each 100' of depth until the base of the permafrost is reached at around 1000'. If the proper logs have been run at a given location, the exact vertical temperature distribution may be determined even more accurately as illustrated in the section on the interpretation of actual field logs.

A knowledge of the vertical distribution of temperature in the undisturbed permafrost is essential to any calculation of the radial distribution of temperature from a borehole in the thermally disturbed environment. If no heat is used in melting the ice, the differential equation representing the flow of heat out from a borehole at any point P, see Figure 1, can be written in terms of cylindrical coordinates as follows:

$$\frac{\partial^2 T}{\partial r^2} + \frac{\partial T}{r \partial r} = \frac{1}{K} \frac{\partial T}{\partial t} \quad \text{for } r > a \quad (1)$$



#### LEGEND

- $a$  = RADIUS OF A BOREHOLE
- $r$  = LATERAL DISTANCE FROM THE CENTER OF THE BOREHOLE TO ANY POINT P
- $R$  = MAXIMUM RADIUS OF DISTURBED ZONE
- $T_d$  = DISTURBED TEMPERATURE AT ANY POINT
- $T_m$  = MUD TEMPERATURE
- $T_u$  = UNDISTURBED FORMATION TEMPERATURE
- $t$  = TIME FROM WHEN DRILLING STARTED AT A GIVEN DEPTH UNTIL LOGGING STARTED
- $K$  = THERMAL DIFFUSIVITY

FIGURE 1

TEMPERATURE DISTRIBUTION AROUND A BOREHOLE FILLED WITH MUD

The boundary conditions are:

$$T(r, 0) = T_u; \quad T(a, t) = T_m;$$

$$T \text{ is finite as } r \rightarrow \infty$$

The various symbols in the above equation are defined in Figure 1.

Assuming the undisturbed formation temperature to be zero, an exact solution for Eq. (1) has been developed by Carslaw and Jaeger.<sup>6</sup> A graphical presentation of an approximate solution to Eq. (1) is shown in Figure 2. A number of the curves of Figure 2 were verified by programming the exact solution of Eq. (1) on a high speed computer. To facilitate its field use, this graphical solution has been modified as illustrated in Figure 3.

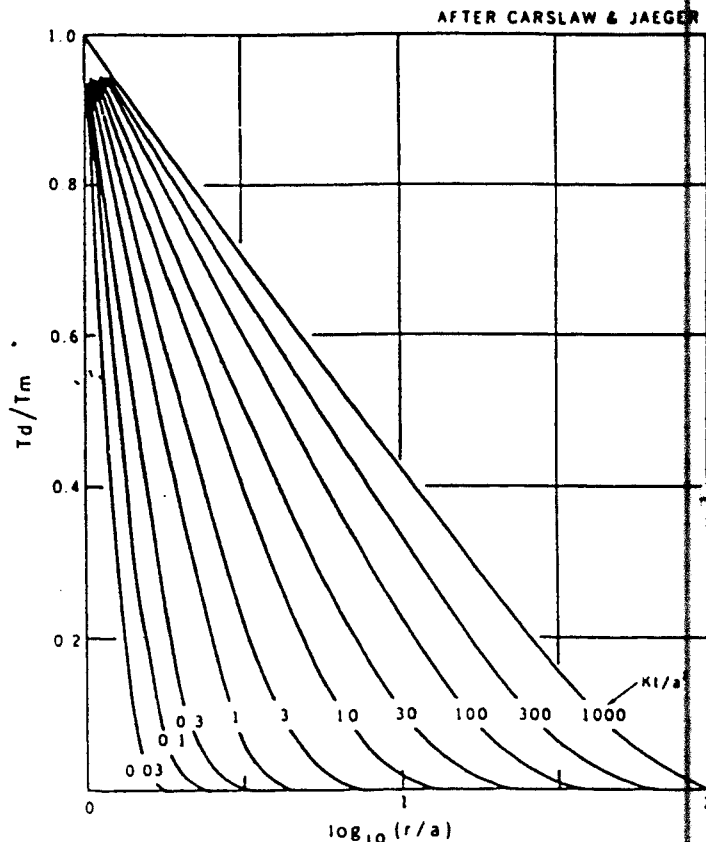


FIGURE 2

GRAPHICAL PRESENTATION OF THE APPROXIMATE SOLUTION OF EQUATION (1)

Figure 3 is a plot of  $r/a$  versus  $(T_d - T_u) / (T_m - T_u)$  for a series of  $Kt/a^2$  values. From the literature,<sup>7</sup> a good average value for  $K$  in permafrost is .04 ft.<sup>2</sup>/hr. For the optimum utilization of Figure 3, the time interval between the conclusion of drilling and the beginning of logging should not be more than a few hours. After choosing the appropriate value for  $Kt/a^2$ , the ratio  $(T_d - T_u) / (T_m - T_u)$  is determined for any number of  $r/a$  values. Knowing the undisturbed permafrost temperature,  $T_u$ , and the mud temperature,  $T_m$ , the radial distribution of temperature in the disturbed permafrost borehole environment can be determined at any given depth (see Figure 4).

However, as previously mentioned, Eq. (1) does not account for the heat required to accomplish the phase change from ice to water at the freezing temperature. About 80 calories are required to convert one gram of ice at zero degree Centigrade to water. This required latent heat of fusion complicates the determination of the radial distribution of temperature.

In solving this problem the total amount of heat  $H_t$  supplied by the drilling mud to a thermally disturbed zone 1' thick was calculated using the equation

$$H_t = \pi \rho C_p \int_a^R T(r) d(r^2) \quad (2)$$

where  $R$  is the maximum radial distance of the disturbed zone,  $\rho$  is the density and  $C_p$  is the specific heat of the formation. The integral can be evaluated by plotting  $Td$  vs  $r^2$  from Eq. (1) and then manually determining the area under the curve using a planimeter. In the case of the permafrost zone analyzed later in the article, this heat was 14,600 BTU's. Knowing formation porosity, the latent heat required to change ice into water in a cubic foot of rock was determined. In our example, it was 2070 BTU's. Next, the  $Td$  vs  $r^2$  curve was redrawn so that the amount of heat under the new curve plus the necessary total latent heat of fusion was equal to the BTU's determined initially using Eq. (2). For our zone of interest,

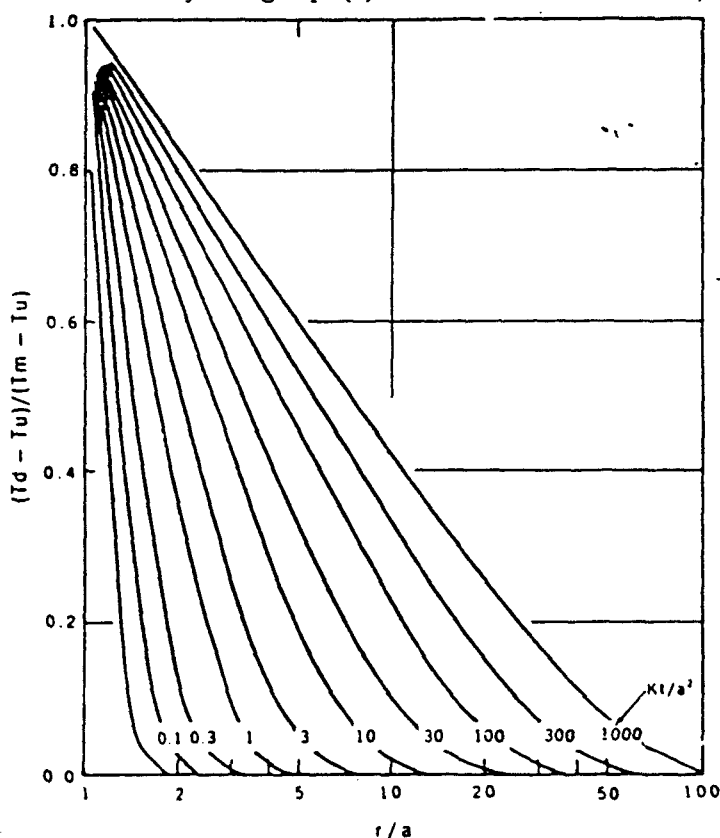


FIGURE 3

MODIFIED GRAPHICAL SOLUTION

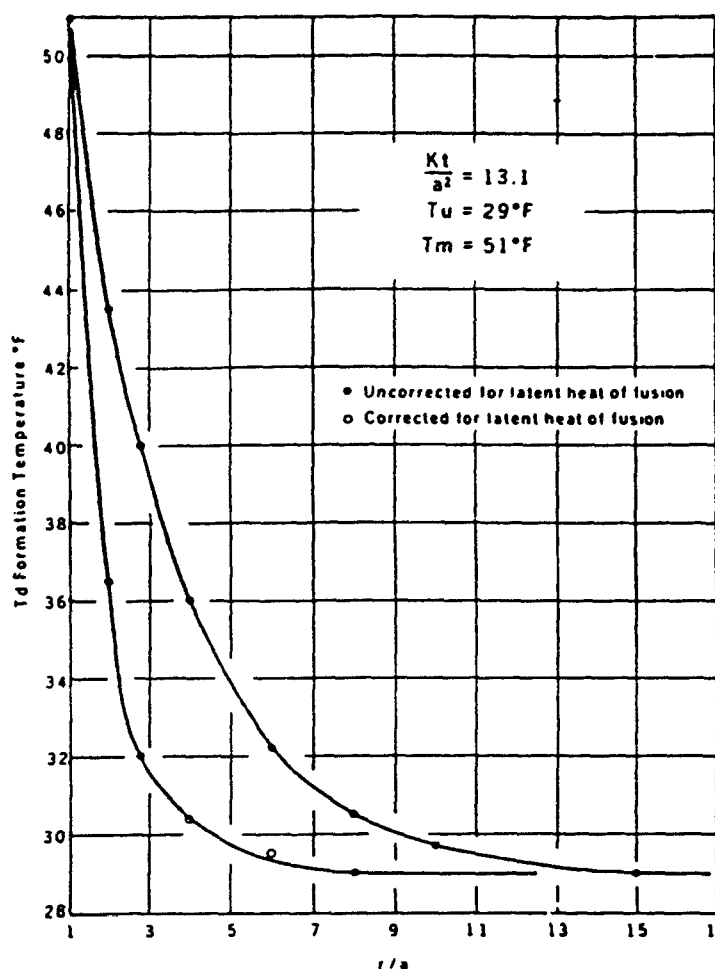


FIGURE 4

DISTURBED FORMATION TEMPERATURE  
 $T_d$  VERSUS THE RATIO  $r/a$

3760 BTU's was determined under the new  $T_d$  vs  $r^2$  curve and the rest of the heat went into changing ice to water up to a radial distance of 1.4' from the axis of the borehole. The data from the preceding  $T_d$  vs  $r^2$  curves are presented more conveniently in Figure 4 as  $T_d$  vs  $r$ .

Because of the modified lateral temperature distribution, more heat was supplied by the mud than was initially determined from Eq. (2). Therefore, while the first  $T_d$  vs  $r$  curve shows the maximum disturbed zone and the modified  $T_d$  vs  $r$  curve yields the minimum disturbed zone, the true curve falls between these two and quite close to the latter.

Notice that this general method for the graphical determination of disturbed formation temperatures applies regardless of the formation temperature. Figure 5 has been prepared to show the effects of thermal invasion in the case where formation temperatures are higher than mud temperatures.

## BOREHOLE ENVIRONMENTS

When the drill penetrates the undisturbed permafrost it superimposes, to some extent, a radial distribution of

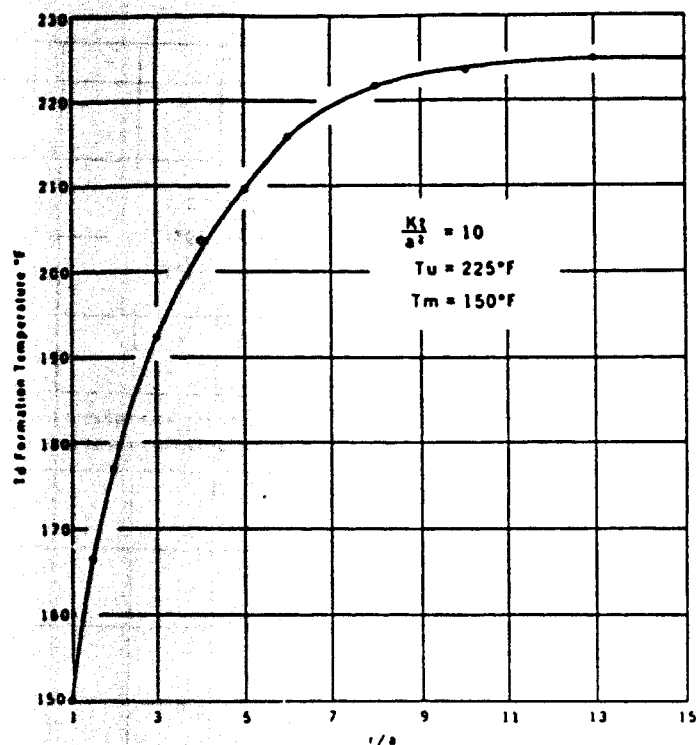


FIGURE 5  
DISTURBED FORMATION TEMPERATURE  
 $T_d$  VERSUS THE RATIO  $r/a$

temperature upon the existing layered distribution. The resultant thermal distribution depends, to a great extent, upon the temperature and the type of drilling fluid as well as upon the time this fluid is exposed to the formation

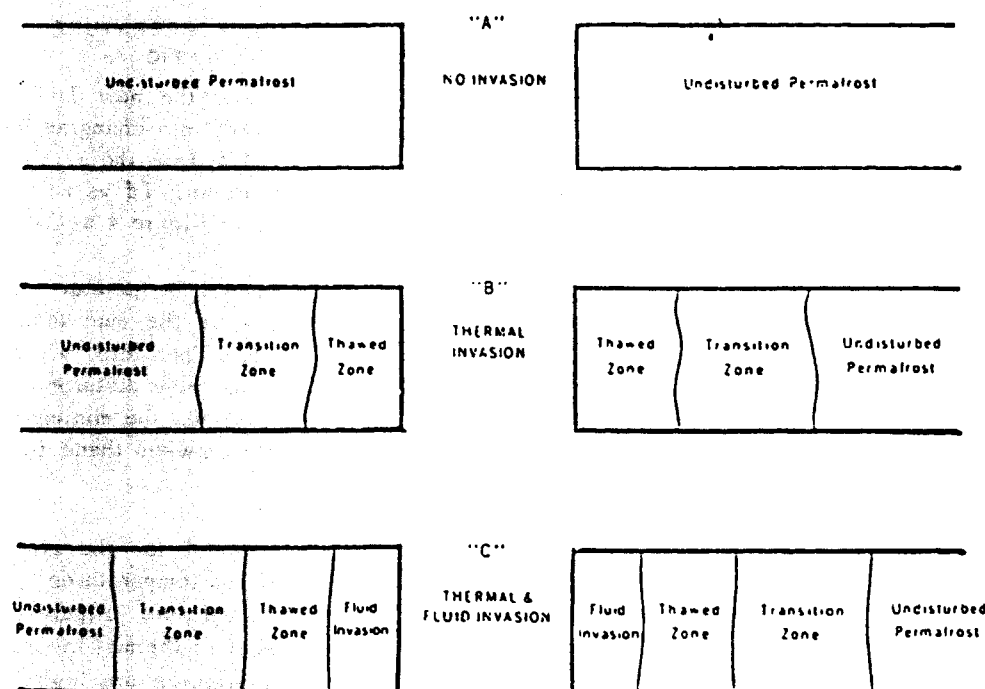


FIGURE 6  
IDEALIZED BOREHOLE (ENVIRONMENTS)

wall. The three basic idealized environments which might occur as a result of various drilling and completion practices are illustrated in Figure 6. Since the permafrost remains essentially undisturbed in environment "A", the distribution of temperature depends solely on its geothermal gradient. In environment "B" the permafrost suffers thermal invasion; the method for calculating the resultant lateral distribution of temperature has just been described in the previous section. In environment "C" the permafrost experiences both thermal and fluid invasion. Here the method previously described for calculating the radial distribution of temperature may still be used. In this case an addition to the calculated radius of the thawed zone can be made to account for the invasion of mud filtrate. A study of the proper suite of logs in addition to other information on a particular well would be needed before the optimum addition could be assigned.

Obviously there are about as many possible temperature distributions in the disturbed permafrost as there are sets of borehole conditions. In the previous section, methods for determining this distribution from a known set of conditions were illustrated. The importance of knowing this thermal distribution is more fully appreciated as the effects of sub-freezing temperatures upon fluid and rock properties are observed.

#### EFFECT OF TEMPERATURE UPON FLUID POROSITIES

Any change in temperature will affect the properties of a brine. Above its freezing point these properties change gradually as a function of temperature but below this point, the changes may be abrupt and of considerable magnitude. At its freezing temperature, a salt solution begins to separate into two distinct physical phases, one solid, the other liquid. As the temperature is lowered, the volume of the solid phase increases while that of the liquid phase decreases. To complicate the situation still further, the liquid phase also is continually increasing in salinity. This process continues until the brine has been cooled to its eutectic temperature where it remains till the liquid phase is completely transformed into the solid phase, both ice and salt. The phase diagram for NaCl and  $H_2O$  is shown in Figure 7.

For the purposes of log interpretation the relationship between brine volume, concentration and below freezing temperature of pure NaCl solutions is more conveniently illustrated by reprocessing the data of Figure 7 and presenting it as shown in Figure 8. Here effective porosity,  $\phi_{eff}$ , represents the volume of the

remaining brine in the pore spaces per unit volume of rock as its temperature is lowered below the freezing point. The decrease in brine volume, expressed as a relative porosity, for a water saturated rock, is plotted against concentration and temperature. The curved lines represent brines of varying initial salt concentrations. If the distribution of temperature in the permafrost has been calculated by the method previously described, and the concentration of the unfrozen brine is also known, then the volume of both the solid and liquid phases in the pore spaces can be calculated as well as the concentration of the remaining brine. Because of the severe contrasts in the electrical and acoustical properties of the solid and liquid phases of the brine, an exact knowledge of their relative volumes as a function of temperature is essential to an accurate interpretation of well logs.

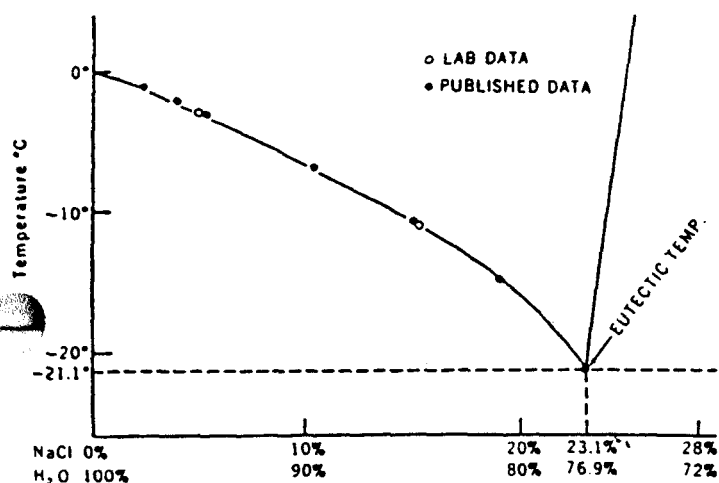


FIGURE 7  
PHASE DIAGRAM FOR NaCl & H<sub>2</sub>O

It is equally essential to know the variation in the physical properties of these two phases as a function of below freezing temperatures. The relationship between brine resistivity, temperature and concentration, Figure 9, was determined in the laboratory. The equipment for obtaining these data consisted of a four-electrode conductivity cell placed in a fluid-filled container located in a deep freeze unit whose temperature could be lowered to -28°C, well below the minimum temperatures encountered in the permafrost. Due to the phenomena of supercooling it was possible to measure the resistivities of these fluids to as much as 10°C below their normal freezing temperatures. In addition, the velocity, or its reciprocal the interval travel time, of acoustic energy through these brines was determined as a function of temperature and concentration (Figure 10). The equipment for making acoustic measurements is shown in block diagram form as Figure 11. Thermocouples were

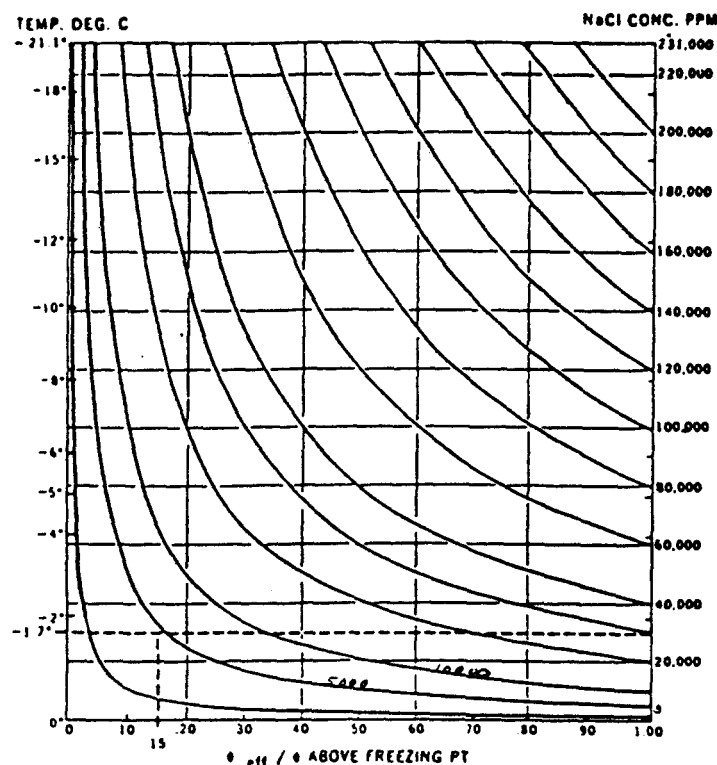


FIGURE 8  
RELATIVE POROSITY VS CONCENTRATION  
AND TEMPERATURE

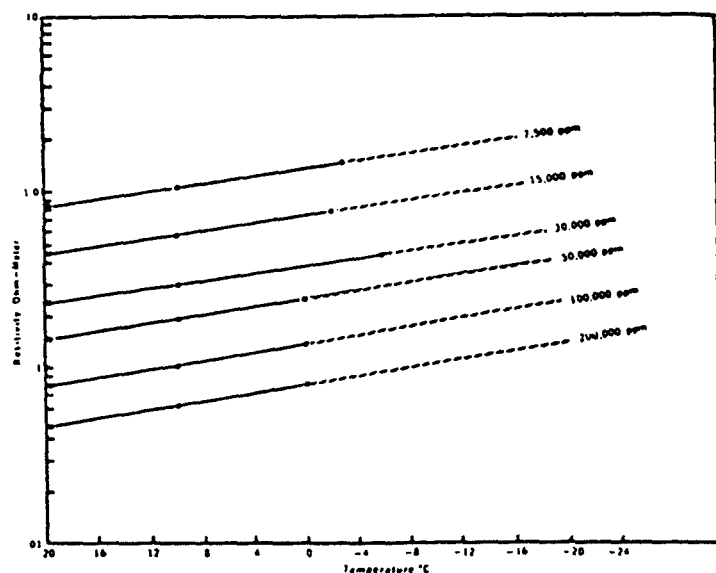


FIGURE 9  
 $R_w$  VS TEMPERATURE FOR NaCl BRINES

utilized to obtain reliable temperature data. Based on our own laboratory measurements the resistivity of ice could be considered as infinite, while its acoustic velocity was found to be about 12,500 ft./sec. Finally in Figure 12 the acoustic travel time is shown as a function of temperature for a refined mineral oil. Like ice, resis-

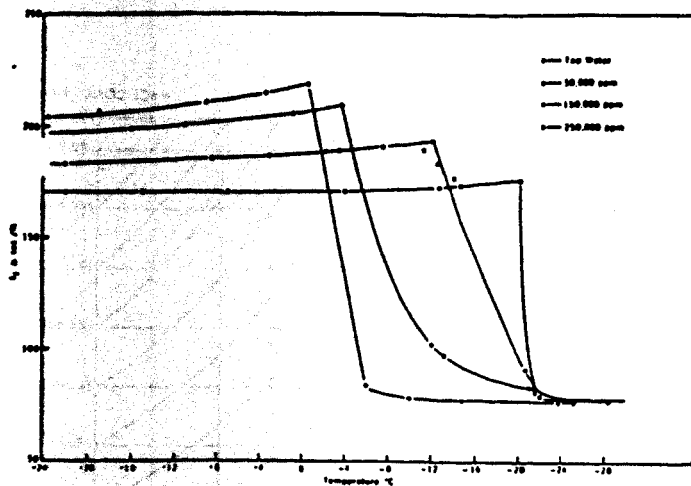


FIGURE 10

$\rho_f$  VS TEMPERATURE FOR NaCl BRINES

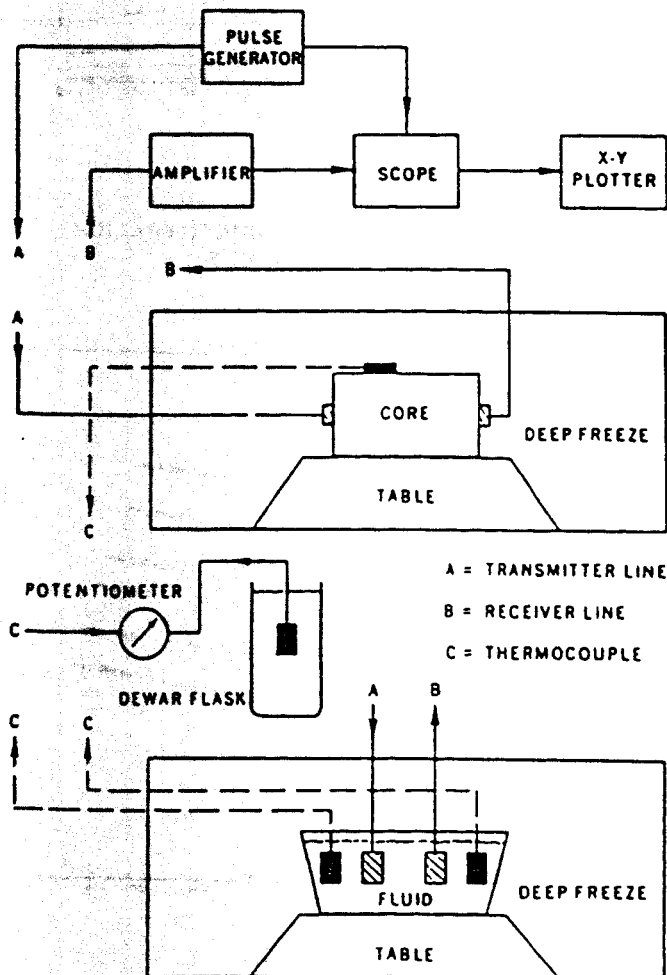


FIGURE 11

EQUIPMENT FOR OBTAINING TRAVEL TIME  
VS TEMPERATURE DATA

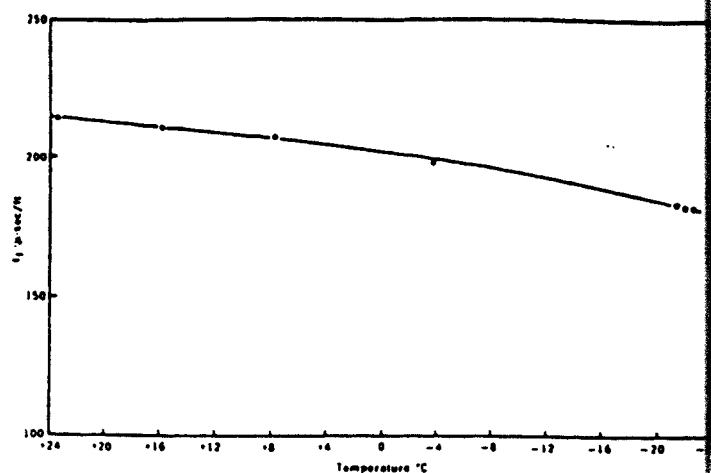


FIGURE 12

$\rho_f$  VS TEMPERATURE FOR OIL

tivity of oil can be considered infinite. Thus, we have determined the relationships between temperature and some pertinent physical properties of materials normally occupying the pore spaces of rocks.

### EFFECT OF TEMPERATURE UPON ROCK PROPERTIES

If we determine these general relationships as a function of temperature for rocks saturated to varying degrees with these same materials, we can establish meaningful logging parameters for permafrost. Figure 13 illustrates the effect of brine concentration and temperature upon the resistivity,  $R_o$ , of a 100% water saturated rock. From this figure and Figure 9 we have sufficient data to calculate the effect of temperature upon the formation factor-porosity relationship. This effect is illustrated in Figure 14. The experimental points on each

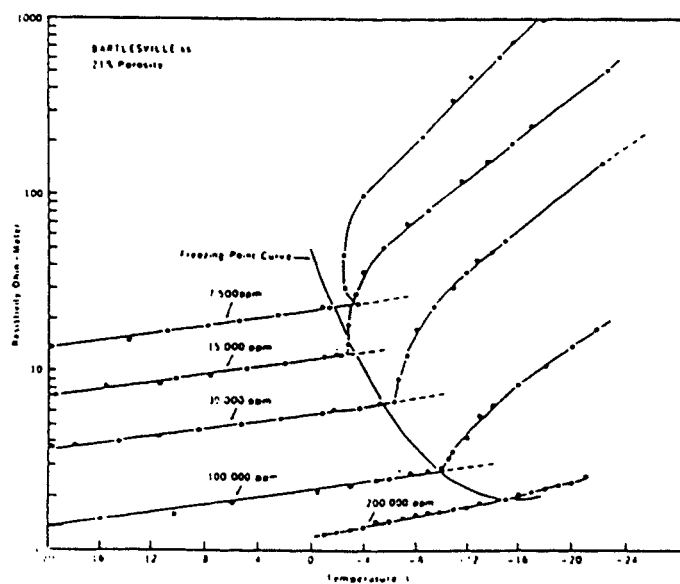


FIGURE 13

$R_o$  VS TEMPERATURE FOR NaCl BRINES

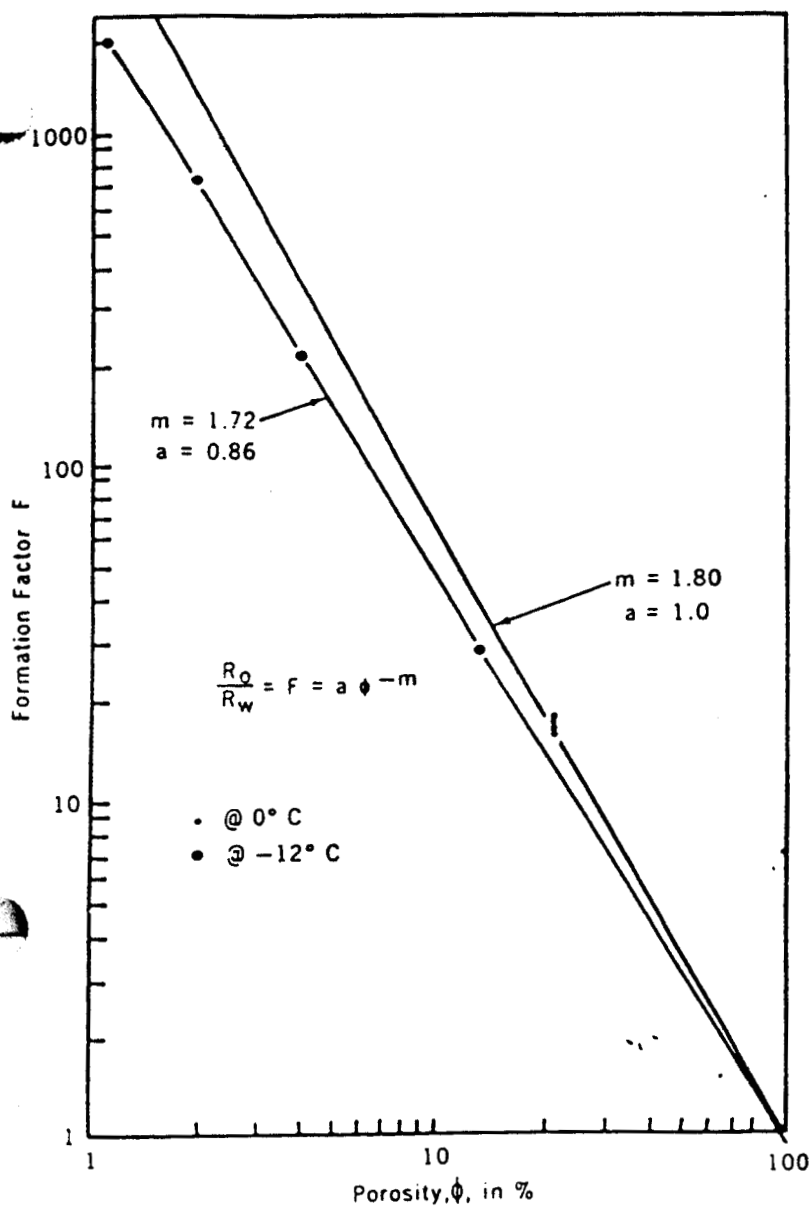


FIGURE 14

$$F = a \phi^{-m} \text{ VS TEMPERATURE}$$

slope line correspond to a different concentration of the brine saturant. All measurements were made on a single Bartlesville sand core with a true porosity of 21%. The three porosities on the  $-12^{\circ}\text{C}$  curve are effective porosities due to the phase changes illustrated in Figure 8. In Figure 15 is shown the effect of water saturation and temperature upon the resistivity,  $R_t$ , of a partially water saturated rock is shown in Figure 15. From this figure, the effect of temperature upon the resistivity index-water saturation relationship can be calculated. This is depicted in Figure 16. Note that this relationship seems to be essentially unaffected by the permafrost temperatures. This could be due to ice growing out from the pore surfaces at a fairly uniform rate resulting in a tendency of the system to retain the original pore configuration.

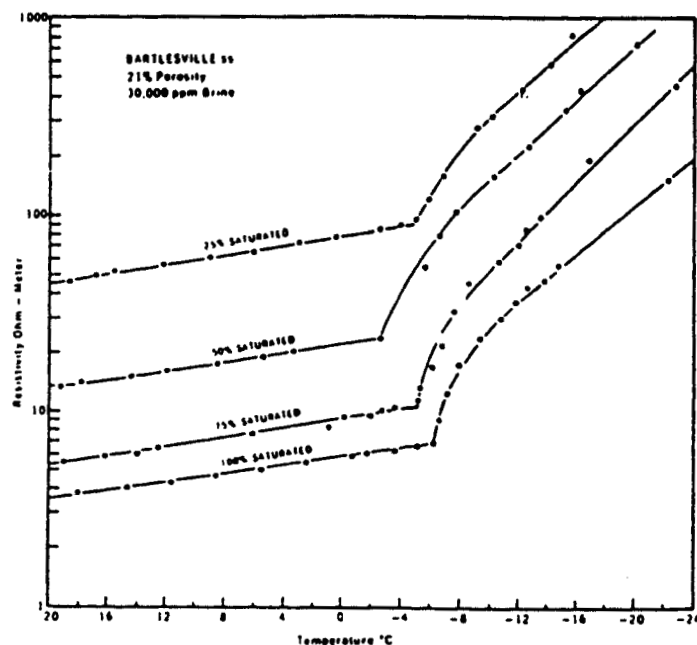


FIGURE 15

$$R_t \text{ VS TEMPERATURE FOR VARIOUS } S_{w^*s}$$

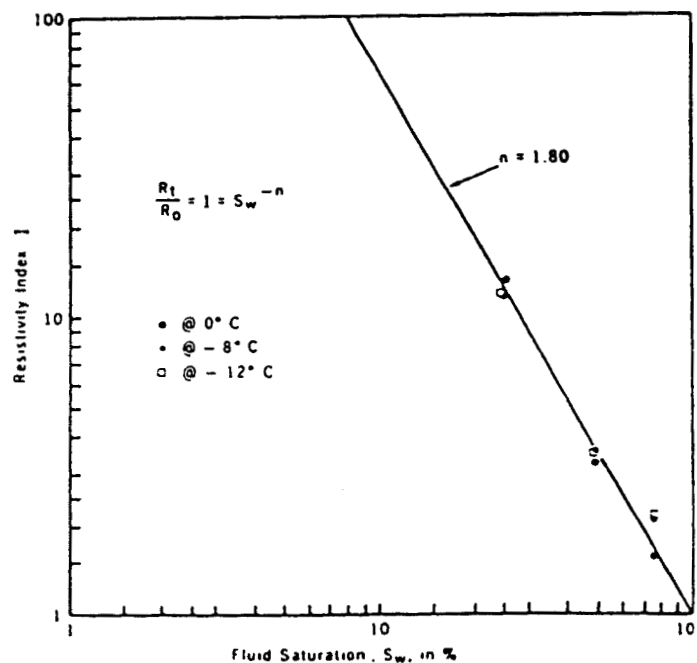


FIGURE 16

$$I = S_w^{-n} \text{ VS TEMPERATURE}$$

Figure 17 illustrates the effect of temperature upon the interval travel time of a compressional wave through a porous sandstone core saturated with brine. The changes taking place in the acoustic properties of the rock at its freezing temperature appear to be just as severe as the changes in its electrical properties. From these data and Figure 10 the matrix travel time of a saturated rock



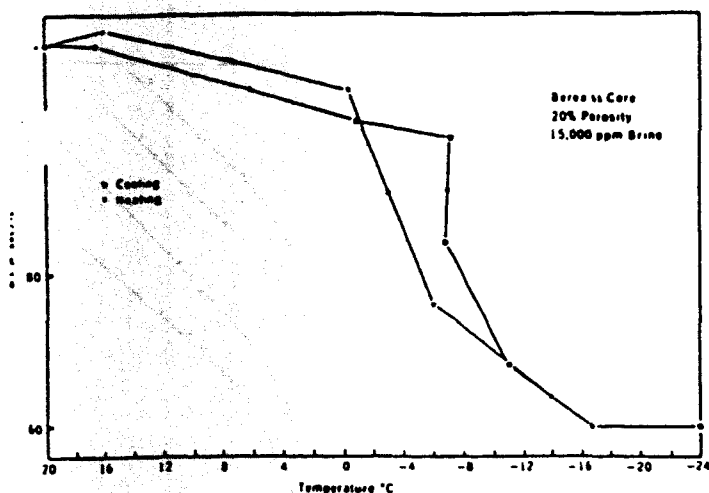


FIGURE 17

#### Δt VS TEMPERATURE FOR WATER SATURATED ROCK

can be determined as a function of temperature by using the time average equation. This is an important logging parameter in the interpretation of acoustic logs. Computations reveal that the matrix travel time decreased from 88  $\mu$ -sec/ft at 20°C to 55  $\mu$ -sec/ft at -24°C. Most of this decrease can be attributed to the pressure of the expanding ice in the pore spaces upon the rock matrix.

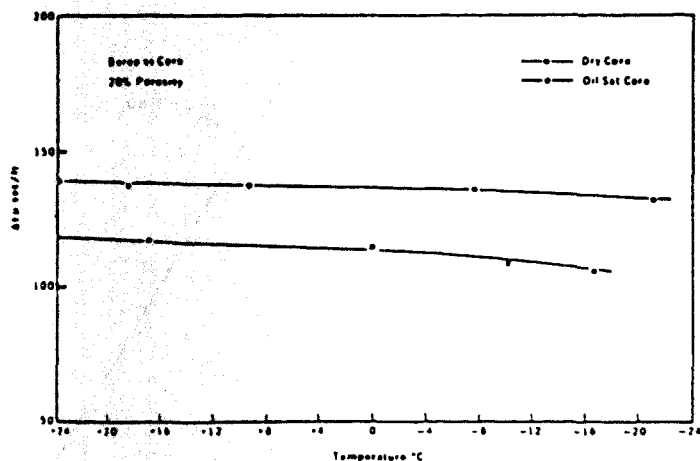


FIGURE 18

#### Δt VS TEMPERATURE FOR ROCK SAMPLES

Figure 18 shows the changes in acoustic travel times through an oil saturated core as a function of temperature. Calculated matrix travel times for a Berea sandstone core in this case decreased from 93  $\mu$ -sec/ft at 17°C to 85  $\mu$ -sec/ft at -16.5°C. Since the density of oil increases with decreasing temperature, no expansion-pressure upon the rock matrix would be expected. The smaller reduction in matrix travel time bears this out. Still the change is enough to be significant. It can, in part at least, be explained by the normal increase in acoustic velocity through rocks as their temperature is

lowered.<sup>8</sup> This is verified to some degree by the measured change in travel time through a dry rock (Figure 18) which also decreased significantly with lower temperatures. These times, of course, are not matrix travel times as we define them because in this case, the least time and the least distance paths do not coincide as is assumed when using the time average equation. The effect of temperature on the full acoustic wave form of a water saturated core is displayed in Figure 19. Probably more than any other illustration, this figure dramatizes the effect of temperature upon the acoustic properties of permafrost and also suggests the possibilities of wave form analysis as a diagnostic interpretation method.

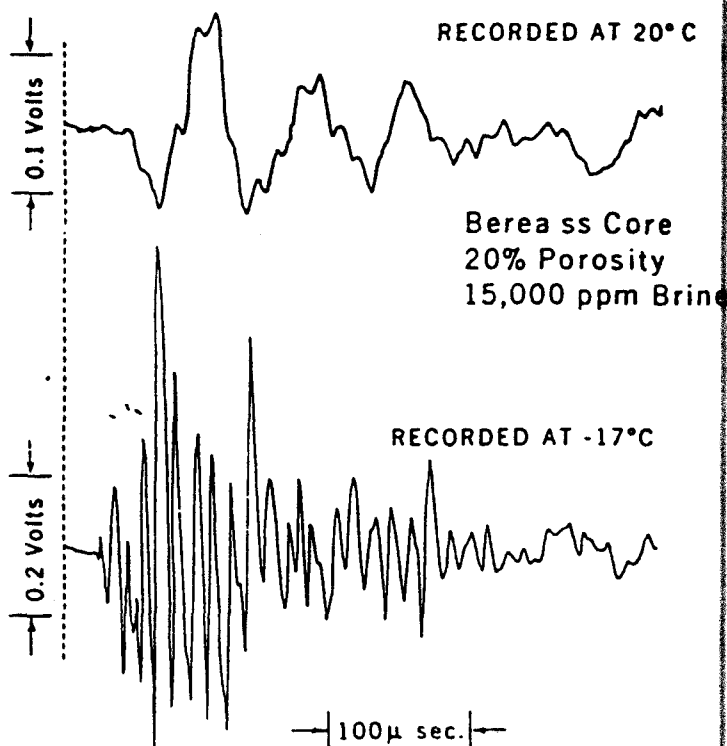


FIGURE 19

#### EFFECT OF TEMPERATURE ON WAVE FORM OF 100% BRINE SATURATED CORE

#### INTERPRETATION OF ACTUAL FIELD LOGS

In this section, the previously described information is applied to the interpretation of the permafrost horizon of a well on the North Slope in Alaska. Figure 20 displays some of the logs run in the permafrost, the remainder are shown in Figure 21. The suite of logs in Figure 20 was assembled because they seemed to identify the permafrost layer the most positively. A knowledge of the presence and the extent of the permafrost can be of value to the geophysicist as well as to the log analyst, since a high velocity permafrost layer can also complicate seismic record interpretation.

In this well the SP, resistivity and acoustic logs all

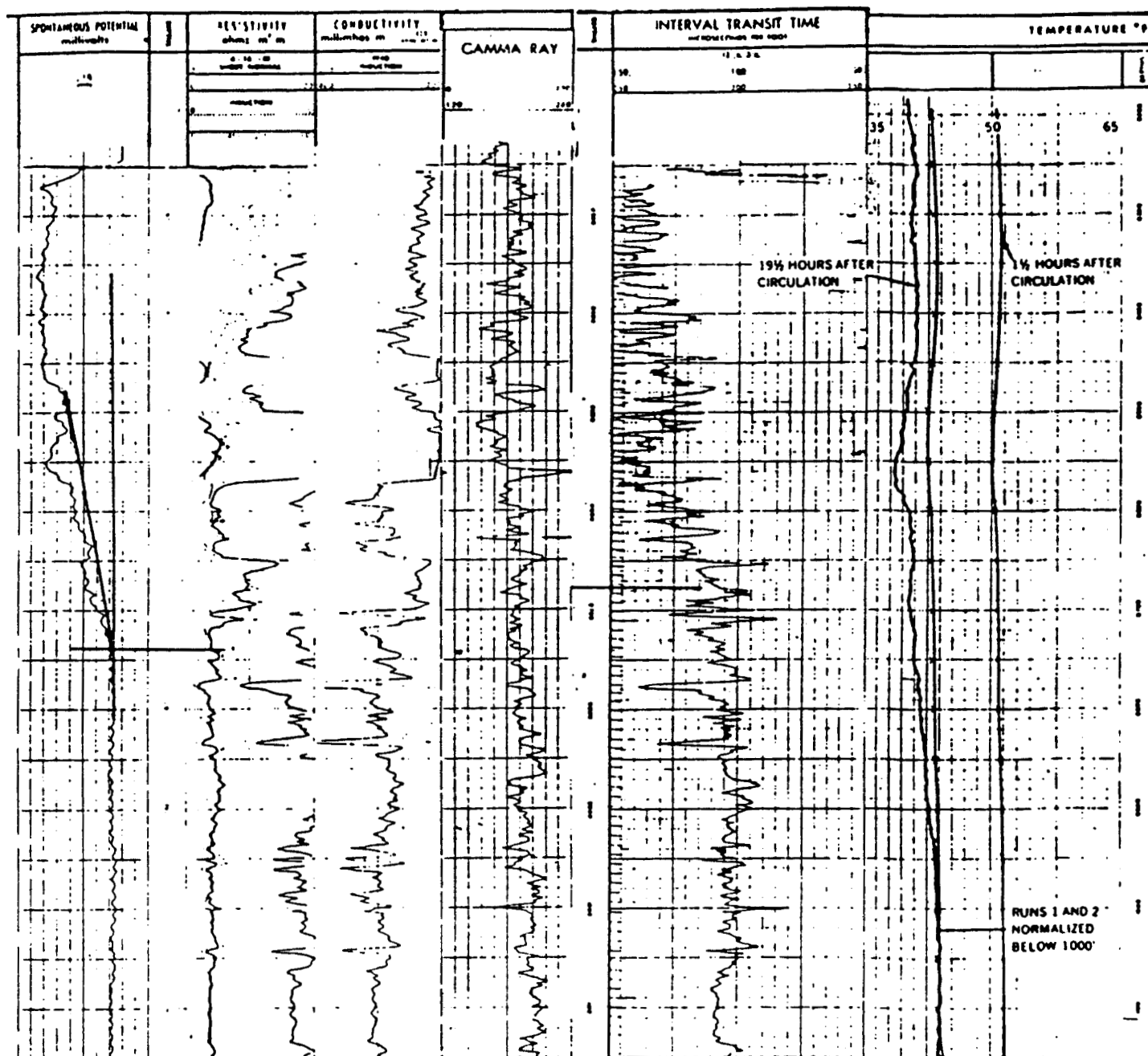


FIGURE 20

#### IDENTIFICATION OF PERMAFROST LAYER FROM LOGS

indicate the presence of a permafrost layer with an approximate thickness of  $700' \pm 50'$ . The SP drift reflects the increased concentration of the remaining fluid in the pore spaces of the permafrost layer. The greater diffusion of negative ions into the borehole, because of their higher mobilities, causes the shift in the SP baseline starting near the base of the permafrost. The sharp contrast in resistivities of formations above and below the freezing point was shown previously in Figures 13 and 15. In the case of the acoustic log, the low velocity is the response to a thawed zone rather than to the undisturbed permafrost itself.

On the other hand, the temperature logs only detect the presence of the permafrost. They do not define its vertical extent with any great accuracy. This is because the temperature logs, having no depth of investigation, only respond to the true geothermal gradient, thus softening any actual contrast between the permafrost and the unfrozen sediments immediately below. In addition, between the two temperature surveys presented in Figure 20, all of the other logs were run in the hole, which superimposes an additional smearing effect on the true temperature distribution.

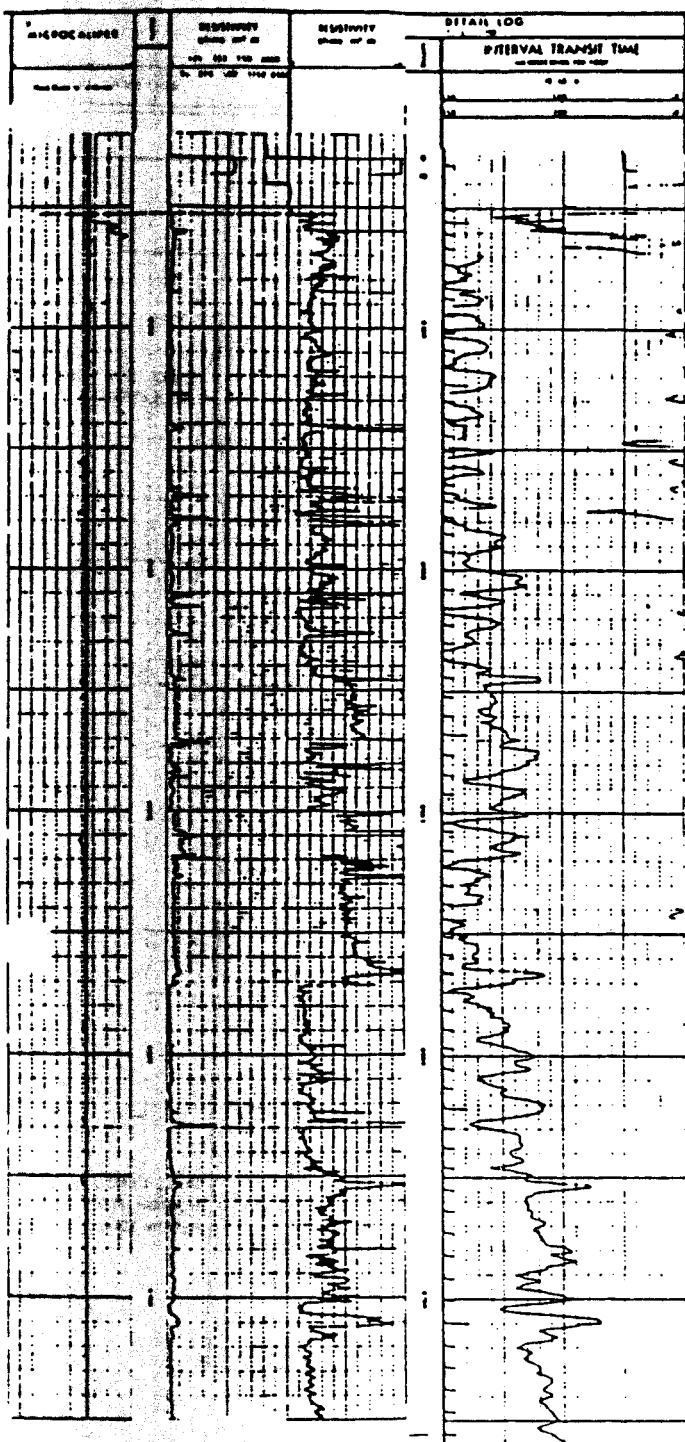


FIGURE 21

#### DETERMINATION OF $R_{MLL}$ AND $\Delta t$ FROM LOGS

Drilling and completion practices in this well understandably were not tailored to optimum log interpretation in permafrost. For instance, both the caliper log and the bit size information on the log heading show a 12 1/4" diameter hole. The borehole corrections for many tools in this size hole may be as much as 10%. Correc-

tions of this magnitude often introduce significant uncertainties into the recorded log data. One way to improve this situation, if quantitative log interpretation is desired, would be to drill through the permafrost first with an 8" bit, log the section, and then ream the hole to the 12 1/4" diameter required by completion considerations.

The following steps are taken to interpret the logs of Figures 20 and 21 in the interval 520' - 570'.

#### 1. The Undisturbed Permafrost Temperature is Determined.

Assuming the permafrost layer is a horizontal slab, the expression for the flow of heat through it may be written as

$$\frac{Q}{t} = k \frac{(T_1 - T_2)}{d} \quad (3)$$

where  $\frac{Q}{t} = 2.9 \times 10^{-6} \frac{\text{cal}}{\text{cm}^2 \cdot \text{sec}}$ , the average rate of heat flow per unit area through the permafrost. <sup>9</sup>

$k = .008 \frac{\text{cal}}{\text{sec} \cdot \text{cm} \cdot \text{deg}}$ , the average thermal conductivity of the permafrost. <sup>9</sup>

Here,  $T_1 = 0^\circ\text{C}$  at the base of the permafrost and

$T_2 = \text{minimum temperature at approximately } 50' = -7.2^\circ\text{C}.$

From the logs of Figure 20, the base of the permafrost was estimated to be at 700'. Therefore,

$d = 650' = 198 \times 10^2 \text{ cm}$ , the thickness of the permafrost from minimum temperature to base, and

$$T_1 - T_2 = \frac{d}{k} \times \frac{Q}{t} = \frac{198 \times 10^2}{8 \times 10^{-3}} \times 2.9 \times 10^{-6}$$

Since  $\frac{T_1 - T_2}{d} = \frac{-7.2^\circ\text{C}}{650'} = -1.11^\circ\text{C}/100' = 2^\circ\text{F}/100'$ ,

the undisturbed permafrost temperature at 550',

$$T_u = (700 - 550) \times -1.11^\circ\text{C}/100' = -1.67^\circ\text{C} = 29^\circ\text{F}.$$

#### 2. The Radial Distribution of Temperature is Calculated.

$T_m = \text{mud temperature} = 51^\circ\text{F} = 10.5^\circ\text{C},$

$t = \text{time mud exposed to formation} = 85 \text{ hours},$

$T_u = \text{undisturbed formation temperature} = 29^\circ\text{F},$

$a = \text{radius of borehole} = 6\text{-}1/8", \text{ and}$

$K = \text{thermal diffusivity} = .04 \text{ ft}^2/\text{hr}$

$$\text{Thus, } Kt/a^2 = \frac{.04 \times 85}{.26} = 13.1.$$

From Figures 3 and 4,  $r$  vs  $T_d$  is determined as shown in Table 1:

$r$ in ft.	$r/a$	$\frac{T_d - T_u}{T_m - T_u}$	$T_d$ in °F	$T_d$ Corrected for Latent Heat	
0.5	1	1.000	51	51	thawed
1	2	0.660	43.5	36.5	zone
1.4	2.8	0.500	40.0	32.0	-----
2	4	0.320	36.0	30.4	transition
3	6	0.144	32.2	29.5	zone
4	8	0.070	30.5	29.0	-----
5	10	0.030	29.7	29.0	undisturbed
7.5	15	0.000	29.0	29.0	permafrost

3. The value of  $R_w$  in the Thawed Zone is obtained from the SP Curve using

$$SP = 25 \text{ mv and}$$

$$R_{mf} = 2.6 \Omega\text{-m at } 50^\circ\text{F}$$

This yields

$$R_w = 1.75 \Omega\text{-m at } 50^\circ\text{F or an}$$

NaCl Concentration of 4500 ppm.

4. The Ratio of Effective Porosity in Undisturbed Permafrost to Actual Porosity in Thawed Zone is found as follows:

Given the Concentration of formation water above freezing point = 4500 ppm and the undisturbed permafrost temperature of  $-1.7^\circ\text{C}$ , the concentration of the brine remaining in the effective pore space is, from Figure 8, 30,000 ppm and  $\phi_{eff}/\phi = 0.15$

5. To Determine the porosity in the Thawed Zone, a plot of  $R_{MLL}$  vs  $\Delta t$  extracted from the logs shown in Figure 21 is prepared. From this plot, shown in Figure 22, apparent matrix and fluid travel times of  $90 \mu\text{-sec/ft}$  and  $265 \mu\text{-sec/ft}$  respectively are obtained. Using an average  $140 \mu\text{-sec/ft}$  travel time through the zone of interest and the time average equation, the porosity,  $\phi$ , is 27.4%.

Assuming  $R_{MLL} = R_{xo}$ , the formation factor  $F =$

$$\frac{R_{xo}}{R_{mf}} = \frac{27}{2.6} = 10.4 \quad \text{for } m = 1.8, \phi = 27\%.$$

6.  $R_o$ , in the Undisturbed Permafrost, is computed from

$$\phi = 27\%,$$

$$\text{Temperature} = -1.7^\circ\text{C}.$$

$$\text{NaCl Concentration (salt in remaining brine)}$$

$$= 30,000 \text{ ppm}$$

$$\text{and } \phi_{eff}/\phi = .15$$

The effective porosity,  $\phi_{eff} = .15 \times 27 = 4.05\%$ ; for

$m = 1.8, F = 315$ . From Figure 9 with 30,000 ppm at  $-1.7^\circ\text{C}$ ,  $R_w = .39 \Omega\text{-m}$  in the undisturbed permafrost. Then  $R_o = F R_w = 315 \times .39 = 123 \Omega\text{-m}$ .

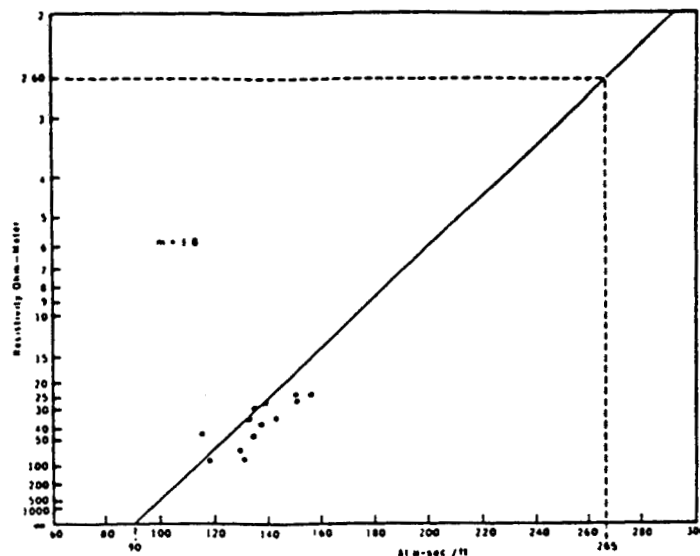


FIGURE 22  
 $R_{MLL}$  VS  $\Delta t$  PLOT

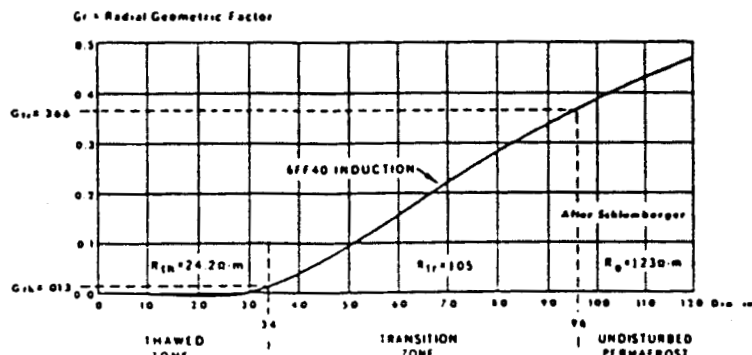


FIGURE 23  
CONDUCTIVITY CONTRIBUTIONS IN  
DISTURBED PERMAFROST

7. Water Saturation in the Undisturbed Permafrost is calculated as illustrated in Figure 23; this is accomplished by first calculating the response of the induction log,  $R_{ILO}$ , in the zone of interest, assuming that this zone is 100% water saturated. Then,  $R_{ILO}$  is compared to the recorded value  $R_{IL}$  to determine the resistivity index  $I$ .

According to the geometric factor concept,

$$\frac{1}{R_{ILO}} = \frac{G_{th}}{R_{th}} + \frac{G_{tr} - G_{th}}{R_{tr}} + \frac{1 - G_{tr}}{R_o} \quad (6)$$

where  $G_{th}$  = geometric factor for the thawed zone,

$G_{tr}$  = geometric factor at the outer limit of disturbed or transition zone,

$R_{tr}$  = the resistivity of the transition zone, and

$R_o$  = the resistivity of the undisturbed permafrost.

The extent of the thawed and transition zones calculated from the temperature data of Figures 3 and 4 and shown in Table I are 34" and 96" in diameter respectively. The radial response characteristics of the 6FF40 induction log are such that  $G_{th}$  is about .013 and  $G_{tr}$  is about 0.366 (see Figure 23).

Taking the average  $R_w$  of the thawed zone to be 2.2 and determining an  $F$  of 11 for  $m = 1.8$  and  $\phi = 27\%$ ,  $R_{th} = F R_w = 11 \times 2.2 = 24.2 \Omega\text{-m}$ .

Using an average temperature in the transition zone of  $29.8^\circ\text{F}$  or  $-1.2^\circ\text{C}$ , the ratio  $\phi_{eff}/\phi = 0.20$  from Figure 8. The concentration of the remaining brine = 22,000 ppm. From Figure 9,  $R_w = .54$  @  $-1.2^\circ\text{C}$ . The effective porosity =  $.20 \times 27 = 5.4\%$ ; for  $m = 1.8$ ,  $F = 195$ . Then,  $R_{tr} = F R_w = 195 \times .54 = 105 \Omega\text{-m}$ .

$R_o$ , the resistivity of the undisturbed permafrost in the zone of interest, if 100% water saturated, was computed in the preceding section to be  $123 \Omega\text{-m}$ .

Substituting the preceding values in Eq. (4) give

$$\frac{1}{R_{ILo}} = \frac{0.013}{24.2} + \frac{0.366 - 0.013}{105} + \frac{1 - 0.366}{123}$$

$$= 0.00054 + 0.00336 + 0.00515 = 0.00905.$$

Then  $R_{ILo} = 110 \Omega\text{-m}$ .

The average  $R_{IL} = 120 \Omega\text{-m}$  for the zone of interest, so

$$\text{Resistivity Index} = \frac{R_{IL}}{R_{ILo}} = \frac{120}{110} = 1.09; \text{ for } n = 1.8,$$

$$S_w = 95\%.$$

An analysis of the cuttings from this section revealed no stains, fluorescence or shows of hydrocarbons. It is very important to remember that in permafrost high porosity and high resistivity do not necessarily mean oil in place.

If this formation had been 75% saturated with oil its resistivity would have been approximately  $1560 \Omega\text{-m}$ . To distinguish accurately between high and very high resistivities a focussed resistivity log might be more appropriate. Also it is quite possible that a density log might provide more satisfactory porosity data than the acoustic log provides.

## CONCLUSIONS

1. A knowledge of the temperature distribution in permafrost and the substantial variation in a given physical property of permanently frozen ground with temperature are both imperative if an accurate interpretation of well logs in permafrost is desired.

2. Of equal importance is the utilization of the optimum drilling, mud, logging and completion programs.

## REFERENCES

1. Black, R. F. "Permafrost - A Review," Bulletin GSA, Vol. 65, pp. 839-856 (1954).
2. U.S.G.S. Prof. Paper 305, A-J, Part 5, "Subsurface Geology and Engineering Data, Exploration of Naval Petroleum Reserve No. 4," Test Wells Nos. 1-26, Alaska (1959).
3. Baptist, O. C., "Oil Production from Frozen Reservoir Rocks, Umiat, Alaska," Trans. AIME, Vol. 216, pp. 437-440, TN 2045 (1959).
4. Brown, J. E., and Johnston, G. H., "Permafrost and Related Engineering Problems," Endeavour, Vol. 23, No. 89, pp. 66-72 (May 1964).
5. Gates, G. L., and Caraway, W. H., "Effect of Completion Fluids on Well Productivity in Permafrost Umiat Field, Alaska," JPT, pp. 33-40 (October 1960).
6. Carslaw, H. S., and Jaeger, J. C., "Conduction of Heat in Solids," Oxford University Press (1959).
7. Wolfe, L. H., and Thieme, J. O., "Physical and Thermal Properties of Frozen Soil and Ice," SPE Journal, Vol. 4, No. 1, pp. 67-72 (March 1964).
8. Hughes, D. S., and Cross, J. H., "Elastic Wave Velocities in Rocks at High Pressures and Temperatures," Geophysics, Vol. 16, No. 4, pp. 577-593 (October 1951).
9. Misener, A. D., "Heat Flow and Depth of Permafrost at Resolute Bay, Cornwallis Island, N.W.T., Canada," Trans. Amer. Geoph. Union, Vol. 36, No. 6, pp. 1055-1060 (December 1955).

## ACKNOWLEDGEMENTS

The authors wish to express their thanks to the management of the Sinclair Oil & Gas Company for permission to publish this paper. They also wish to thank W. P. Cecil for his part in performing the laboratory experiments described and discussed in this paper.

SONIC AND RESISTIVITY MEASUREMENTS ON BEREJA SANDSTONE  
CONTAINING TETRAHYDROFURAN HYDRATES:  
A POSSIBLE ANALOG TO NATURAL GAS HYDRATE DEPOSITS

C. Pearson, J. Murphy, P. Halleck, R. Hermes, and M. Mathews

Earth and Space Sciences Division, Los Alamos National Laboratory  
Los Alamos, New Mexico 87545 USA

Deposits of natural gas hydrates exist in arctic sedimentary basins and in marine sediments on continental slopes and rises. However, the physical properties of such sediments, which may represent a large potential energy resource, are largely unknown. In this paper, we report laboratory sonic and resistivity measurements on Bereja sandstone cores saturated with a stoichiometric mixture of tetrahydrofuran (THF) and water. We used THF as the guest species rather than methane or propane gas because THF can be mixed with water to form a solution containing proportions of the proper stoichiometric THF and water. Because neither methane nor propane is soluble in water, mixing the guest species with water sufficiently to form solid hydrate is a difficult experimental problem, particularly in a core. Because THF solutions form hydrates readily at atmospheric pressures it is an excellent experimental analog to natural gas hydrates. Hydrate formation increased the sonic P-wave velocities from a room temperature value of 2.5 km/s to 4.5 km/s at  $-5^{\circ}\text{C}$  when the pores were nearly filled with hydrates. Lowering the temperature below  $-5^{\circ}\text{C}$  did not appreciably change the velocity however. In contrast, the electrical resistivity increases nearly two orders of magnitude upon hydrate formation and continues to increase more slowly as the temperature is further decreased. In all cases the resistivities are nearly frequency independent to 30 kHz and the loss tangents are high, always greater than 5. The dielectric loss shows a linear decrease with frequency, suggesting that ionic conduction through a brine phase dominates at all frequencies, even when the pores are nearly filled with hydrates. We find that the resistivities are strongly a function of the dissolved salt content of the pore water. Pore water salinity also influences the sonic velocity, but this effect is much smaller and only important near the hydrate formation temperature.

INTRODUCTION

Hydrates are a crystalline form of water containing voids or cavities that can trap other (guest) molecules which play an important role in stabilizing the hydrate structure. Two types of hydrates (types 1 and 2) are known to form. The first type contains only relatively small cavities ( $>8.6 \text{ \AA}$  in diameter) that can trap guest species smaller than ethane, whereas the second type contains a mixture of small and large ( $9.5 \text{ \AA}$  in diameter) cavities that can trap molecules as large as isobutane. Most of the common constituents of natural gas form hydrates, usually type 1, but type 2 hydrates can also form if significant amounts of  $\text{C}_3\text{H}_8$ ,  $\text{C}_4\text{H}_{10}$ , or  $\text{CO}_2$  are present.

Until recently, natural gas hydrates were widely known only as a nuisance that condensed in gas transmission lines. Then Soviet investigators reported natural gas hydrate deposits in the Siberian Arctic. These early reports were confirmed with the discovery of large natural gas hydrate deposits in arctic North America and in marine sediments. Research interest in hydrates increased as hydrates became not only a potential engineering problem in the Arctic, but also a potential energy resource. Although a considerable body of experimental data exists on the

electrical properties of pure crystalline hydrate (see Davidson 1973, for a summary) these measurements are usually conducted at frequencies far higher than those used in exploration geophysics and surprisingly little is known about the physical properties of sediments containing hydrates in their pores except for the pioneering work by Stoll and Bryan (1979).

In this paper, we present laboratory sonic and resistivity measurements on Bereja Sandstone cores containing tetrahydrofuran (THF) hydrate. Tetrahydrofuran was used as a guest species instead of methane or some other constituent of natural gas because THF hydrate is stable at moderate temperatures ( $+4^{\circ}\text{C}$ ) and atmospheric pressures, which greatly simplifies experimental procedures. A second major advantage of THF hydrate is that the guest is mixable with water. This eliminates the problem of ensuring complete mixing between the guest species and water, which is a formidable problem inside the pore spaces of sedimentary rock. Because the crystal structure of hydrates is largely independent of the guest species, the physical properties of THF-hydrate-containing samples are probably similar to the physical properties of a natural gas hydrate deposit formed in similar rocks. This is particularly likely if the natural hydrates form from gas-containing molecules large enough to form type 2 hydrates.

This paper focuses on sonic and electrical measurements because preliminary calculations (Pearson 1982) show that sonic velocities and resistivities are more strongly affected by the presence of hydrates than are other physical properties such as densities or thermal conductivities. In addition, seismic and electrical methods are the most commonly applied exploration geophysical techniques. Clearly a detailed understanding of the electrical and acoustic properties of hydrates is necessary to design and interpret geophysical surveys over natural gas hydrate deposits.

During this study we restricted our electrical measurements to the frequency range from 10 Hz to 30 kHz because most exploration geophysical surveys are conducted at these relatively low frequencies. In addition Olhoeft (1977) demonstrates that the electrical properties of permafrost at higher frequencies are very variable. If hydrated sediments are similar in this respect, then even if surveys could be conducted at higher frequencies, the results would be very difficult to interpret.

#### EXPERIMENTAL METHOD

The samples were cylindrical cores approximately 5 cm long and 2.54 cm in diameter cut perpendicular to the bedding plane from a block of Berea sandstone. The ends were ground parallel to ensure good contact between the ends of the samples and the electrodes or transducers. Samples were saturated with a stoichiometric mixture of THF and water (18 parts water to 1 part THF; Gough and Davidson 1971) under vacuum. As part of the study, various amounts of NaCl were added to the fluid. The concentration of salt is reported by the molarity of the water NaCl solution before THF was added to the mixture. Because temperature is an important variable in our study, all measurements were conducted in a NESLAB RTE-8 constant temperature bath. We left the sample in the bath for 24 hours, well after a temperature change, to ensure the sample had equilibrated with the bath. Because the crystalline water that formed in the pores disassociated near 4°C which is near the disassociation temperature of THF hydrates (Gough and Davidson 1971) and significantly above the melting point of ice, THF hydrate apparently formed in the pore spaces of the rock, not water ice.

The electrical measurements were conducted using a two-electrode system similar to that described by Collett and Katsube (1973). We used a Princeton Applied Research model 5204 lock-in analyzer, which can measure the in-phase and quadrature components of the voltage drop across the precision resistor, and were able to calculate the real and imaginary components of the resistivity, the phase angle, and the complex relative permittivity. The complex electrical properties (i.e., the complex permittivity ( $K^*$ ) and the loss tangent ( $D$ ) were calculated using the following equations presented by Collett and Katsube (1973).

$$D = \frac{P''}{\sqrt{[P^*]^2 - (P')^2}}, \text{ and} \quad (1)$$

$$K^* = \frac{1}{\omega [P^*] \epsilon_0} \quad (2)$$

where  $[P^*]$  and  $P'$  are the magnitude complex resistivity and the real part of the complex resistivity respectively,  $\omega$  is the frequency, and  $\epsilon_0$  is the permittivity of free space. The real ( $K'$ ) part of the relative permittivity can be calculated from  $K^*$  using

$$K' = \frac{K^*}{1+D^2} \quad (3)$$

Two-electrode systems of this type are subject to several systematic errors, among which are inductive and capacity coupling between the leads, current leakage around the sample, transfer impedances between the sample and the electrodes and contact polarization (Olhoeft 1975). We minimized coupling between the leads by using shielded wires. Calibration using known resistors showed that coupling and resistance in the leads had a negligible effect on our measurements. Current leakage was minimized by jacketing the samples tightly in shrink tubing before conducting measurements. We minimized transfer impedance between the electrode and the sample by spring loading the electrodes and using a conducting brine as an interstitial fluid. Polarization processes at the electrodes can also cause errors in two-electrode measurements, particularly if the sample is highly resistive or the measurement frequency is high. These effects may cause the small-frequency dependence above 1 kHz in the high resistivity curves in Figures 1 and 2. However we always used 200-Hz measurements when comparing resistivities because, at these frequencies, the

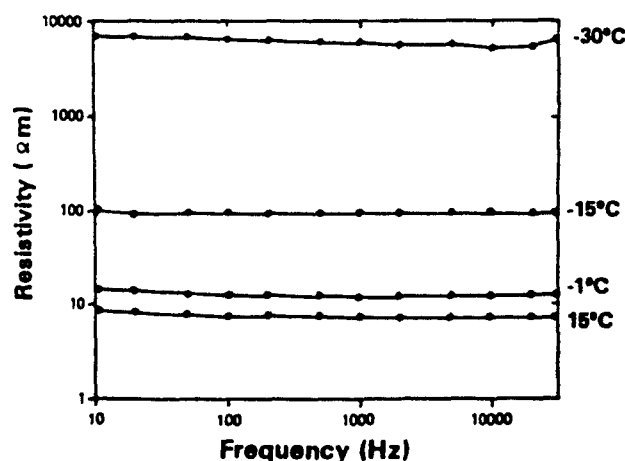


FIGURE 1 Resistivity as a function of temperature and frequency for a Berea core saturated with 0.5 N NaCl THF solution.

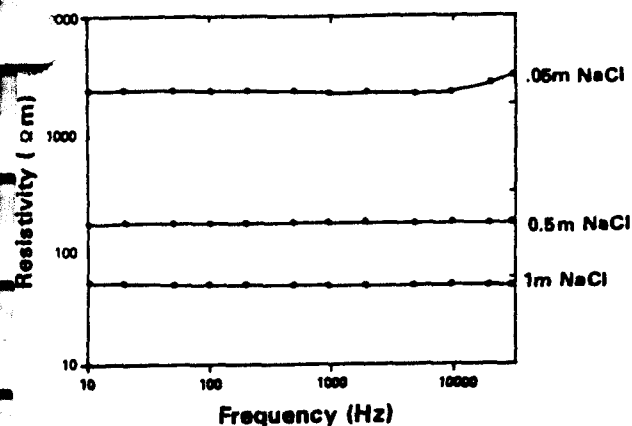


FIGURE 2 Resistivity as a function of frequency and salinity at  $-24^{\circ}\text{C}$ .

resistivities were frequency independent. Rust (1952) compared resistivity measurements on porous sedimentary rocks using both two- and four-electrode (which avoid most of the experimental problems described above) techniques. He concluded that, as long as the sample is saturated with a conductive fluid, either method gives an accurate measure of the complex resistivity.

Sonic measurements were conducted using the pulse transmission described by Mattaboni and Schreiber (1967). We used Valpey Fisher LTZ-5 1-MHz piezoelectric transducers that were attached to the sample by a spring-loading device. All measurements (both sonic and electric) were conducted at atmospheric pressure, except for a small axial load,  $>0.1$  MPa, which was applied to ensure that the electrode or transducer remained in contact with the sample. Olhoeft (1977) found the electrical properties of permafrost to be strongly pressure dependent from 10 Hz to 10 kHz. Thus, care must be taken when using our results to interpret geophysical surveys over natural hydrate deposits because the *in situ* pressure will always be much greater than atmospheric pressure.

#### ELECTRICAL RESULTS

As shown in Figures 1 and 2, the resistivities of Berea cores containing THF hydrates are functions of both temperature and salinity at which the measurements were made. However, to 30 kHz, the resistivities are nearly independent of frequency. Figures 1 and 2 plot the complex resistivity, but because the imaginary component of the resistivity was always very small, usually less than 10% of the real component, the real and complex resistivities are nearly equal. As a result, loss tangents are very high, often in excess of 100. Both the real relative permittivity and the imaginary part which is proportional to the dielectric loss are linear functions of frequency. The log linear relationship between the dielectric loss and frequency (Figure 3) is particularly important because the dielectric loss is a parameter that describes the motion of electric charge. If the material displays

conduction that arises not from the effect of polarization on the displacement current but from actual charge transport, Hasted (1974) shows that

$$\epsilon = \epsilon_{\text{dielectric}} + \frac{\sigma}{4\pi\omega\epsilon_0} \quad (4)$$

Here  $\epsilon_{\text{dielectric}}$  is the component of the dielectric loss associated with loss from polarization currents. With a dielectric loss mechanism such as that from water molecules and in the absence of conductors, will normally show a strong peak when plotted vs. frequency. However, if conduction dominates the polarization effects,  $\epsilon$  will be inversely proportional to frequency. Thus, the slope of the line from Figure 3, which is (0.994) calculated using least square regression techniques, implies that conduction is much more important than polarization effects in determining the electrical properties of hydrate-containing Berea sandstone cores.

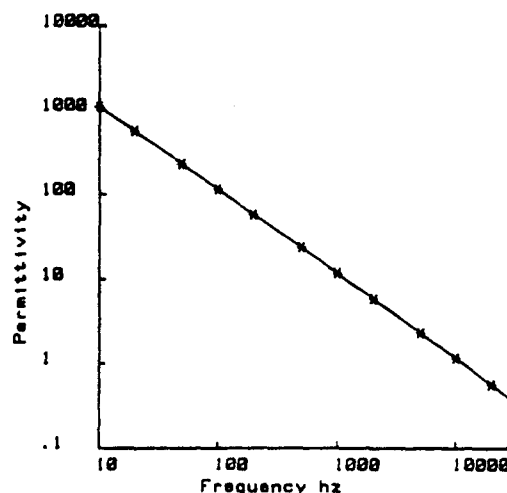


FIGURE 3 Imaginary part of the relative permittivity  $\times 10^{-4}$  vs. frequency for a Berea core saturated with a 0.5 N NaCl THF solution at  $-24^{\circ}\text{C}$ .

The effect of temperature and salinity on the resistivities of the Berea cores also suggests that the electric currents flow because of ionic conduction in an unfrozen brine phase, which is present in the rock even after hydrates start to form. The exponential increase in resistivity with temperature occurs because lowered temperatures cause the proportion of hydrates in the pores to increase, further constricting the brine phase. The decrease in resistivity as the salinity increases (shown in Figure 2) is caused by an increase in the ionic concentration of the brine phase. The additional ions present probably also inhibit the formation of hydrates increasing the amount of brine present in the pores.

The electrical properties of hydrate-containing sediments can be quantitatively understood using Archie's law ( $\rho = \rho_w \phi^{-m} S_w^{-n}$ ), an empirical



relationship between water content and the resistivity of water-saturated sediments. Here  $\rho$  is the resistivity of the sediments,  $\rho_w$  is the pore water resistivity,  $S_w$  is the fraction of the porosity occupied by liquid water, and  $a$ ,  $m$ , and  $n$  are empirically derived parameters. This equation also applies to rocks where the pore spaces are partially filled with ice or hydrates. However, as the amount of liquid water decreases,  $S_w$  and  $\rho_w$  are both reduced,  $S_w$  because some of the available pore space is now filled with a solid nonconductor, and  $\rho_w$  because the dissolved salts are concentrated in the remaining unfrozen brine. If the brine is not very near saturation, the effect on hydrate or ice formation of  $\rho_w$  is relatively easy to quantify because an increase in salt concentration causes a linear decrease in  $\rho_w$ . Because hydrates of ice exclude all of the dissolved salts as they form, the salt concentration of the brine inclusions is inversely proportional to the volume fraction of liquid water, if we assume that the sediments were initially water saturated. In addition, the resistivity of aqueous solutions increases exponentially with decreasing temperatures. Including both the temperature and concentration effects, the resistivity of a partially frozen brine at temperature  $T$  is thus proportional to  $(C)^T S_w$ , where  $C$  is a constant. Substituting this relationship into Archie's equation and dividing by the resistivity at  $0^\circ\text{C}$ , we find that the ratio of frozen ( $\rho_f$ ) and thawed ( $\rho_t$ ) resistivities is

$$\rho_f/\rho_t = C^{-T} S_w^{1-n} \quad (5)$$

Archie's law accounts for the rapid decrease in resistivity as a function of temperature (see Figure 4). Because  $N$  is usually equal to 2, the

resistivity is inversely proportional to  $S_w$ . As the temperature decreases, the concentration of the brine at equilibrium with hydrates increases, causing  $S_w$  to decrease and the resistivity to increase. Increasing the molarity of the salt solution causes the resistivity to decrease because the increased salinity of the pore water inhibits the formation of hydrates, which increases the amount of unfrozen water ( $S_w$ ) present.

In order to compare the electrical properties of partially frozen sediments with the measurements on hydrate containing sediments described above, we performed a series of electrical measurements on a Berea sandstone sample saturated with an 0.5 N NaCl solution. Because this sample did not contain any THF, ice rather than hydrates formed when the temperature of the sample was reduced below freezing. As was the case with hydrates, the complex resistivities were frequency independent and a linear relationship existed between  $\log(E)$  and  $\log$  frequency. The relationship between hydrate and ice containing samples is shown in Figure 4. Note that the curves are similar in that both curves show an exponential decrease in resistivity with temperature. The quantitative difference between the curves is probably caused by differing amounts of crystalline hydrates and ice in the pore spaces. Such differences are not unexpected because ice and THF hydrates have different stability curves and dissociation temperatures. The resistivity of ice reaches a nearly constant value at  $-4^\circ\text{C}$ , the freezing point of a 0.5 N NaCl solution, whereas the THF-containing sample does not reach plateau until  $+2^\circ\text{C}$ , presumably the dissociation temperature of THF hydrates in a 0.5 N NaCl solution.

#### SEISMIC RESULTS

Sonic P-wave velocities, measured on hydrate-containing Berea sandstone cores as a function of temperature, are shown in Figure 5. This figure

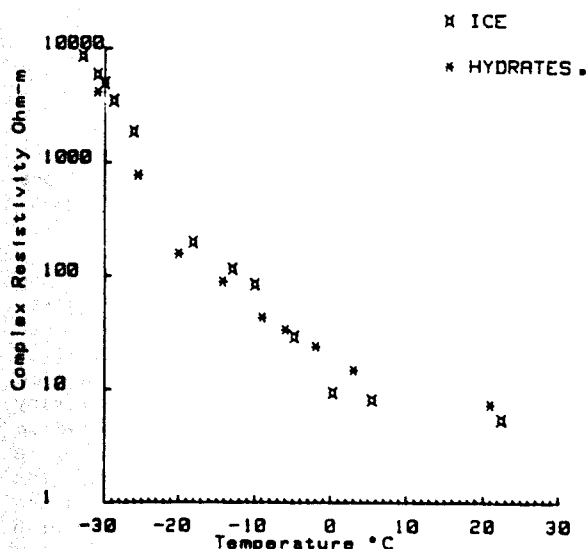


FIGURE 4 Resistivity as a function of temperature for two Berea sandstone samples, one saturated with 0.5 N NaCl THF solution and one saturated with a 0.5 N NaCl solution without THF.

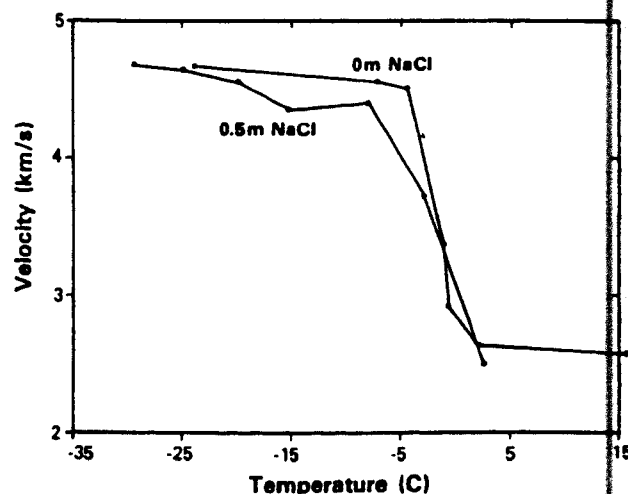


FIGURE 5 Sonic velocities vs. temperature for two Berea cores showing the effect of salinity.

shows results from cores saturated with two different NaCl solutions. Note that in both cases the sonic velocities increase from 2.5 to 4.5 km/s when hydrates begin to form in the pore spaces. Once hydrates form, the velocities reach a plateau where further cooling produces very little change.

As shown in Figure 5 the salinity of the saturating liquid has very little effect on the sonic velocities once hydrates have formed in the cores. However cores saturated with saline water and THF approach the high-velocity plateau more gradually than do samples saturated with pure water and THF. Thus the behavior of sonic velocities as a function of temperature contrasts with the electrical resistivity measurements in that electrical resistivities decrease rapidly as a function of temperature even after the pore spaces of the sample are probably nearly full of hydrates, while sonic velocities rapidly increase when hydrates start to form in the pore spaces. Then the velocities reach a plateau where further cooling produces very little change in sonic velocities. The difference in the temperature dependence of sonic velocities and resistivities illustrates a fundamental difference in the mechanism by which electrical and acoustic signals are transmitted in rock. Electrical signals are transmitted through the brine phase so electrical properties remain sensitive to the amount of brine present, even when the fraction of the pore volume containing brine becomes very small. In contrast, acoustic pulses are transmitted primarily through the solid matrix, so once the pore volume is largely filled with hydrates, a further decrease in the small brine fraction produces only a negligible change in velocity. However the slower asymptotic approach in the brine-rich sample suggests that amount of fluid in the unfrozen brine phase does have some effect on velocity when the brine phase consists of a relatively large amount of fluid.

The compressional velocity of hydrates forming in a sediment can probably be understood using a three-phase time-averaged equation, first proposed by Timur (1968) for partially frozen sediments and since tested by several other authors. The compressional velocity ( $V_p$ ) is related to the velocity of ice ( $V_s$ ), the velocity of the brine inclusions ( $V_b$ ), and the velocity of the solid matrix ( $V_m$ ) by

$$1/V_p = \frac{\phi(S_w)}{V_b} + \frac{\phi(1-S_w)}{V_s} + \frac{(1-\phi)}{V_m} \quad (6)$$

Because of the similarities between the seismic velocities of ice and hydrates, this equation can probably be used to calculate the velocity of a mixture of hydrates and brine in sedimentary rock. Note that Equation 6 depends linearly on  $S_w$ , in contrast to Equation 5 which, if  $n = 2$ , is inversely proportional. The difference in electrical and sonic properties as a function of temperature can be explained by the difference in the dependence of Equations 5 and 6 on  $S_w$ . The electrical properties are inversely proportional to  $S_w$  so the electrical resistivity remains sensitive to changes in  $S_w$  even when very little unfrozen water remains in the rock. In contrast,

in Equation 6  $S_w$  enters directly as a term added to other quantities. Thus as  $S_w$  becomes small it has a negligible effect on the seismic velocity.

We performed no sonic measurements on Berea samples that did not contain a THF hydrate mixture so we could not compare the effect of THF hydrates and ice on the sonic velocities. However because our measurements are very similar to results published by Pandt and King (1979) for partially frozen sediments, we expect ice and hydrates to have nearly the same effect on the sonic velocities.

## CONCLUSIONS

Several significant conclusions can be drawn from this study: (1) the resistivities and sonic velocities of Berea sandstone cores are strongly affected by the presence of either ice or hydrates. Resistivities increased by an order of magnitude and continued to increase rapidly as further decreases in temperature reduced the amount of unfrozen brine present in the rock. The sonic velocities, in contrast, rapidly increased when hydrates began to form in the cores but soon approached a limiting value. Further cooling produced only a very small increase in sonic velocities. (2) Ice and hydrates produce very similar changes in the sonic and electrical properties of Berea sandstone. Any differences can probably be ascribed to differing amounts of unfrozen brine present in the pores. This suggests that it may be difficult to distinguish permafrost and hydrate-containing layers using ordinary geophysical techniques. (3) The salinity of the pore water in which the hydrates form has a strong effect on the resistivities but a very small effect on the sonic velocities. We suggest that the effect of temperature and salinity on resistivities and sonic velocities can be explained if the samples obey Archie's law for resistivities and the three-phase rule for velocities. (4) Resistivities of hydrate containing cores are nearly frequency independent in the range from 10 Hz to 30 kHz. However, both the dielectric constant and the dielectric loss decrease rapidly as a function of frequency. The log linear relationship between frequency and dielectric loss suggests that the electrical properties of the hydrate containing samples are controlled by ionic conduction in a frozen brine phase.

Our experimental results show that the presence of hydrates has a strong effect on the acoustic and electric properties of sediments compared to unfrozen or unhydrated sediments. An increase of several orders of magnitude in electrical resistivities can easily be detected using a variety of electrical exploration techniques. Also an 80% increase in sonic velocity is sufficient to produce a very strong reflection in seismic reflection data and can easily be detected in seismic refraction surveys. This very strong velocity contrast may account for strong reflections that are often observed at the bottom of possible hydrate bearing horizons in marine seismic surveys (Shipley et al. 1979).

## ACKNOWLEDGMENTS

We thank the ESS-3 Rock Mechanics Group, especially Tom Dey, without whose help this research could not have been undertaken. We would also like to thank Tom Shankland who reviewed this paper and made many helpful suggestions. This research was supported by the U.S. Department of Energy.

## REFERENCES

- Collett, L. S. and T. J. Katsube, Electrical parameters of rocks in developing geophysical techniques, *Geophysics*, 38, 76-91, 1973.
- Davidson, D. W., Clathrate hydrates in water, a comprehensive treatise, F. Frank, ed., Plenum Press, New York, 2, 115-234, 1973.
- Gough, S. R. and D. W. Davidson, Composition of tetrahydrofuran hydrate and the effect of pressure on the decomposition, *Canadian Journal of Chemistry*, 49, 2691-2699, 1971.
- Hasted, J. B., *Aqueous Dielectrics*, Chapman and Hall, London, 302 pp., 1974.
- Mattaboni, P. and E. Schreiber, Method of pulse transmission measurements for determining sound velocities, *J. Geophys. Res.*, 72, 5160-5163, 1967.
- Olhoeft, G. R., Electrical properties of permafrost, Ph.D thesis, Dept. of Physics, Univ. of Toronto, Toronto, Canada, 1975.
- Olhoeft, G. R., Electrical properties of natural clay permafrost, *Canadian Journal of the Earth Sciences*, 14, 16-24, 1977.
- Pandt, B. I. and M. S. King, A study of the effect of pore water salinity on some physical properties of sedimentary rocks at permafrost temperatures, *Canadian Journal of the Earth Sciences*, 16, 1566-1580, 1979.
- Pearson, C. F., Physical properties of natural gas hydrate deposits, Los Alamos National Laboratory report LA-9422-MS, 1982.
- Rust, C. F., Electrical resistivity measurements on reservoir rock samples by the two-electrode and four-electrode methods, *Petroleum Transactions, American Institute of Mining Engineers*, 195, 217-224, 1952.
- Shipley, T. H., M. H. Houston, R. T. Buffler, F. J. Shaub, K. J. McMillen, J. W. Ladd and J. L. Worzel, Seismic evidence for widespread possible gas hydrate horizons on continental slopes and rises, *American Association of Petroleum Geologists Bulletin*, 63, 2204-2213, 1979.
- Stoll, R. D. and G. M. Bryan, Physical properties of sediments containing gas hydrates, *J. Geophys. Res.*, 84, 1629-1634, 1979.
- Timur, A., Velocity of compressional waves in porous media at permafrost temperatures, *Geophysics*, 33, 584-595, 1968.

C 3527



## PERMAFROST BENEATH THE BEAUFORT SEA: NEAR PRUDHOE BAY, ALASKA

by P.V. Sellmann and E.J. Chamberlain,  
U.S. Army-Cold Regions Research and  
Engineering Laboratory

This paper was presented at the 11th Annual OTC in Houston, Tex., April 30-May 3, 1979. The material is subject to correction by the author. Permission to copy is restricted to an abstract of not more than 300 words.

### ABSTRACT

The occurrence and properties of subsea permafrost near Prudhoe Bay, Alaska, were investigated by drilling and probing. Nine holes were drilled and 27 sites were probed with a cone penetrometer. The deepest drill hole was 65.1 m below the seabed, while a depth of 14.1 m was reached with the cone penetrometer. Engineering and chemical properties were determined from core samples and point penetration resistance data were obtained with the penetrometer. Thermal profiles were acquired at both the drill and probe sites.

Temperatures below 0°C were observed in all the drill and penetrometer holes logged, although frozen sediments were encountered only occasionally. Seasonally frozen sediments were observed near the seabed at each site. The degree of ice bonding, or strength, could be related to seabed temperature and was greatest in shallow water (<2 m). The penetrometer resistance and thermal data indicated that deeper ice-bonded sediments occur, for example approximately 12.7 m below the seabed in 2 m of water off the Sagavanirktok delta.

Of eight holes drilled offshore, it appeared that four encountered bonded permafrost. In general, the position of the ice-bonded permafrost interface was extremely irregular. The depth below the seabed to this interface at various distances from shore along the line studied was 28.8 m at 1 km, 65.1 m at 3.5 km, 44.1 m at 6.8 km, and 29.5 m at 17.2 km.

Shallow, overconsolidated marine sediments were found in the upper fine-grained section at all of the drill sites investigated; the degree of overconsolidation varied considerably among the sites. This fine-grained section was up to 10 m thick and covered sands and coarse gravels.

### INTRODUCTION

Scientific and engineering investigations conducted by several nations bordering the Arctic Basin

References and illustrations at end of paper.

have documented the existence of subsea permafrost. Many questions concerning distribution, and particularly the properties, of these perennially frozen sediments still remain.

The earliest quantitative studies commenced around 1953 in the USSR. The Soviet investigations have continued, with emphasis on field observation and theoretical studies.<sup>1</sup>

Few studies were conducted in North America prior to the extensive activity stimulated by petroleum exploration in the arctic regions. Early direct observations and theoretical models of subsea permafrost by Lachenbruch and others<sup>2,3</sup> were based on studies made near Barrow, Alaska. Lewellen<sup>4,5</sup> followed these investigations with drilling and probe studies in the same region.

In the Canadian Beaufort Sea, probably the first evidence of permafrost and ice-bonded sediment was obtained during an Arctic Petroleum Operators Association drilling program.<sup>6</sup> Shearer et al.<sup>7</sup> observed the occurrence of pingo-like features on the outer shelf. Hunter et al.<sup>8,9,10</sup> followed these studies with an extensive investigation of the distribution of ice-bonded permafrost. These studies, which were largely based on examination of seismic records, showed extensive subsea permafrost.

Recently, in the U.S. Beaufort Sea near Prudhoe Bay, Alaska, investigations were conducted to provide data on permafrost distribution and properties based on drilling, probing and seismic studies.<sup>11-19</sup> These investigations have shown that there are substantial areas of permafrost beneath the Beaufort Sea. They have also provided some information on its engineering, chemical and physical properties. This paper summarizes the results of the studies conducted by the U.S. Army Cold Regions Research and Engineering Laboratory in the Prudhoe Bay area during the spring of 1976 and 1977.

We obtained information on engineering properties, pore water chemistry, and temperature through drilling, sampling and probing. The locations of our 9 drill holes and 27 penetrometer sites are shown in Fig. 1. These sites were selected to represent a

range of thermal and geological settings. Parameters such as water depth, distance from shore, and proximity to offshore islands, bars and shoal areas account for some of the differences between the sites.

The drill holes were placed mainly on line 2 (Fig. 1), which extended true north from shore to several kilometers seaward of Reindeer Island. This line was selected to correspond with a study line initially established by Osterkamp and Harrison.<sup>11</sup> We selected three other study lines for drilling and probing. One (line 1) extended offshore from Prudhoe Bay across a shoal area between Gull and Niakuk Islands into the open waters of the Beaufort Sea. Another (line 3) was roughly perpendicular to the others and extended along the 2-m isobath from Stump Island to the Sagavanirktok River. The remaining line (line 4) crossed Stump Island.

## METHODS

### Drilling and Sampling

Complete details covering equipment and procedures are provided in two operational reports.<sup>20,21</sup> The drilling equipment used was fairly conventional, the unique aspect being that it was completely housed on sleds.

The upper part of every section drilled was fine-grained, and emphasis was placed on obtaining continuous samples in this material. Sampling below these fine-grained sediments in the sands and gravels was done at greater intervals, grain size and casing placement procedures often controlling the spacing.

Most of the samples obtained during the study were taken by drive sampling. Wash samples were also collected, usually at 0.6-m intervals. All cores were subsampled to provide material for determining engineering properties and pore water chemistry, and for geological and paleontological analysis.

### Engineering Property Determinations

Index properties including grain size, liquid and plastic limits, density, water content, and organic content were all determined using established procedures.

Undrained, unconsolidated triaxial compression tests were conducted on specimens prepared from undisturbed core. The test specimens were nominally 50 mm in diameter and 115 mm long. Confining pressures and temperatures were selected to approximate in situ conditions. The strain rate for the strength tests was  $7.5 \times 10^{-4} \text{ s}^{-1}$ .

The consolidation tests were also conducted using standard procedures. Samples were nominally 45 mm in diameter and 25 mm high. The maximum stress applied was 4600 kPa.

The temperature was maintained within  $0 \pm 1^\circ\text{C}$  for all strength and consolidation tests. None of the test specimens contained ice at these temperatures. Details of these tests are provided by Sellmann and Chamberlain.<sup>22</sup>

We encountered difficulties in using the standard procedures for determining the maximum past pressure (preconsolidation pressure)  $p_c$  because many of the void ratio ( $e$ ) versus log effective stress ( $p'$ ) curves did not have sharp, well defined breaks. As a result, the  $p_c$  values reported are our best

estimates. Actual values could vary considerably.

### Pore Water Chemical Analysis

The pore water chemistry studies discussed were conducted at CRREL by I.K. Iskandar and F.W. Page. They analyzed water extracted from the sediments for pH and alkalinity, and for sodium, potassium, calcium, magnesium, chloride and sulfate concentrations.<sup>23</sup> Iskandar et al.<sup>17</sup> have published additional information, including data from the University of Alaska studies.

### Penetrometer Equipment

A penetrometer device was prefabricated at CRREL and evaluated during the first field season as a means of obtaining engineering property data from the seabed. Encouraging results from this first-year program provided the basis for the design and construction of a formal field test unit.

A cone penetrometer was selected because it appeared to offer the best combination of versatility, simplicity and data productivity. It was used to acquire both engineering data and thermal profiles. The primary testing mode was static, although a dynamic capability was included.

The penetrometer, including equipment for automatic data acquisition, was completely housed in a heated building mounted on skis. A large crawler tractor transported the unit and provided the reaction force for testing. The probe design was similar to the Dutch "mantle cone" described by Heijnen,<sup>24</sup> with provisions for separate measurements of point resistance and side friction. The cone and friction shoe were 63.5 mm in diameter. Maximum probe penetration velocity was approximately 20 mm/s. A detailed discussion of the entire apparatus and its operation is given by Blouin et al.<sup>18</sup>

### Sediment Temperature Measurements

After the penetrometer was driven to refusal, we made temperature observations with a thermistor in the fluid-filled bore of the penetrometer rod. Initial observations indicated that temperature equilibrium was reached in 6 to 8 hours after the penetrometer was driven. To ensure equilibrium the probe was allowed to remain in place overnight before temperature readings were made.

The temperature measurements were made from the bottom up, normally at 1.5-m intervals. In the upper part of the profiles, where temperature gradients were the steepest, we made observations at closer intervals.

Five to twenty minutes was usually required for a single measurement, depending on the amount of temperature change between positions. The thermistor resistance was displayed continuously on a digital ohm-meter so that temperature changes could be observed. The equilibrium temperature for each measurement was established as the resistance where less than a 1-ohm change occurred in one minute. For the thermistors employed, a 1-ohm change is approximately equal to  $0.0035^\circ\text{C}$ . In a few cases temperature fluctuations as large as  $0.05^\circ\text{C}$  occurred near the top of the sediments as a result of convection.

USGS personnel obtained temperature profiles from access tubes placed in the deeper drill holes. These holes were repeatedly logged until the ice

became unsafe. The techniques employed were similar to those used at the penetrometer sites. The procedures and the results have been reported.<sup>19,25</sup>

## RESULTS

### Material Properties

Profiles of the index properties and hole lithology are shown in Figs. 2-8. All holes have fine-grained surface sections of marine sediments (fine sand, silt and clay) 2.1 to 12.0 m thick. These sediments commonly contain a few rounded pebbles - material possibly ice-rafted from nearby beaches. Sands and gravels with occasional layers of silt and clay underlie the fine-grained marine sediments at all of the sites.

The properties of the fine-grained sediments are quite variable, both with depth and from site to site.

At site PB-1, which is located near the middle of Prudhoe Bay along line 1 (see Fig. 1), soft organic silts dominate the 4.5-m-thick fine-grained section. In the upper three-quarters of this section, water content (Fig. 2) exceeds or nearly exceeds the liquid limits (41 to 43%). Near the boundary between the fine-grained sediments and the underlying sands and gravels, the water content falls markedly to below 20% in non-plastic silty sediments.

At site PB-5, which is also along line 1 but seaward of the shoal separating Prudhoe Bay from the Beaufort Sea, the water content (Fig. 5) ranges from 24 to 37%, also exceeding the liquid limits. Thicker (7.1 m) non-plastic inorganic sands and silts dominate this site.

At site PB-6, the drill site nearest the shore along line 2, the water content is below 20% in principally non-plastic interbedded sands and silts 3 m thick (Fig. 6). Further seaward along this line at site PB-7 in thicker (4.5 m) but similar sediments, water content ranges from 26 to 38%, with one value as low as 9% just above the sands and gravels (Fig. 7).

Continuing further seaward along line 2 to site PB-3, which was located approximately midway between the shore and Reindeer Island, the fine-grained sediments are dominated by silts of low plasticity. These sediments are approximately 5 m thick. Water content (Fig. 4) ranges from 20 to 42%, increasing with depth. In the shallow part of these silts the water content is near the plastic limit, but it increases steadily to the liquid limit with increasing depth.

Just shoreward of Reindeer Island at site PB-8 the fine-grained section is 12 m thick and is dominated by the clay sizes. Water content (Fig. 8) ranges from 20% in the upper half of this section to 40% in the lower half. In the upper half the water content falls near the plastic limit. In the lower half it ranges between the liquid and plastic limits.

The most uniform fine-grained section was observed at site PB-2, which is located seaward of Reindeer Island. The sediments are approximately 7.5 m thick, with water content ranging between 20 and 22% (Fig. 3). In all cases the water content was at or below the plastic limit.

The implication of the relationship between the moisture content and Atterberg limit data is that

much of the fine-grained marine sediments are overconsolidated, and those at PB-2 and certainly some of those at site PB-8 are highly overconsolidated.

### Consolidation Properties

The consolidation test results support our initial observation that at most of the sites the fine-grained sediments are overconsolidated. However, there appears to be considerable variation in the degree of overconsolidation.

The estimated values for the preconsolidation pressure ( $p_c$ ) range from a low of 540 kPa at site PB-8 to .900 kPa at PB-2, with overconsolidation ratios ( $p_c/p_o'$ , the ratio of preconsolidation pressure to effective overburden pressure) varying from 2.2:1 at PB-7 to 1091:1 at PB-5. The specimens are, thus, lightly to highly overconsolidated.

It is interesting to compare the results at sites PB-2 and PB-8. Fig. 3 shows  $p_c$  to be uniformly high (>1800 kPa) at PB-2 over the depth profiled, while at PB-8  $p_c$  varies between 540 and 1550 kPa (Fig. 8). The sediment types at these two sites are similar; therefore, it appears that they have been subject to quite different processes.

### Strength Tests

The strength determinations discussed in this section are for the fine-grained sections from which good "undisturbed" cores could be obtained.

The shear strength profile for site PB-1 is shown in Fig. 2. These sediments are soft and weak to a depth of 2.5 m below the seabed, with a maximum shear strength of 45 kPa. At 4.1 m the shear strength increases to .35 kPa near the transition between the shallow silt and clay and the deeper sands and gravels.

Just seaward of the shoal that separates Prudhoe Bay from the Beaufort Sea at site PB-5, the maximum shear strength ranged between 35 and 63 kPa to a depth of 7.1 m below the seabed (Fig. 5). Non-plastic inorganic sands and silts dominated this site.

The five sites along line 2 (Fig. 1) provide considerable information on the variability of the sediments in this region. For the two sites nearest shore (PB-6 and PB-7) only one sample from a silty sand layer 1.4 m below the seabed was tested. The shear strength  $S_u$  of this material was 76 kPa, which is probably representative of the unfrozen sandy sediments found in this region.

Further seaward, at PB-3, the shear strength ranges from 25 to 120 kPa (Fig. 4), the weaker samples coming from the high moisture content sediments in the lower portion of the fine-grained section. Just shoreward of Reindeer Island at PB-8,  $S_u$  ranges from 25 to 100 kPa, with considerable variation occurring over the entire 12-m-thick section (Fig. 8).

At the most seaward site, PB-2, considerably higher  $S_u$  values were observed (Fig. 3). Shear strength values ranged from 85 kPa at shallow depths to more than 260 kPa 8 m below the seabed.

### Penetrometer Observations

Penetration Resistance Data. In general, penetration resistance values were low in the upper few meters and approached refusal (40 MPa) at depths between 10 and 14 m below the seabed. The spread between maximum and minimum penetration values was

narrow in the upper 4 m, compared with the wider range of values observed in the material below. However, in shallow water, where seasonally frozen sediments were encountered, very high penetration resistance was observed. We found that variations in the resistance data could be readily correlated with geologic features and the occurrence of frozen material. Extremely high penetration resistance in coarse-grained sediments caused termination of probing at all sites.

Blouin et al.<sup>18</sup> give a detailed discussion of all penetrometer records. A summary of these data obtained along line 1 is shown in Fig. 9.

**Temperature Profiles.** Temperature profiles were obtained at 18 of the 27 probe sites. Subsea sediment temperatures were below 0°C at all sites.

Profiles obtained along line 1 are shown in Fig. 10. Along this line, the lowest temperatures were observed at sites PH-4, PH-5 and PH-9. These sites are in a region where the sea ice freezes to the shoal sediments that separate Prudhoe Bay from the Beaufort Sea. Seaward of this shoal, at PH-1, PH-2 and PH-3, the temperature profiles are warmer and have much shallower gradients.

Shoreward of the shoal, at PH-6 and PH-8, the temperatures fall in between these two extremes, the temperatures in the upper 4 m of sediment being more like those observed in the shoal area and the deeper temperatures more like those seaward of the shoal.

Profiles along the other two study lines<sup>18</sup> provide similar data.

#### Chemistry Data

The salinity data obtained by Page and Iskandar<sup>23</sup> provided another means of establishing information on permafrost properties. This information permitted calculation of the freezing point of the pore water, and when coupled with thermal data helped establish where frozen sediments could be expected, as summarized in Fig. 11.

#### DISCUSSION

##### Engineering Properties

The high shear strengths of the fine-grained sediments that constitute the upper part of the sections indicate that these sediments are overconsolidated, which, of course, supports the earlier observations made from the Atterberg limit, water content, and consolidation test results. But as previously mentioned, the magnitudes of the overconsolidation pressures are uncertain in many cases because of difficulties in interpreting the consolidation test results.

Following the suggestions of Berre<sup>26</sup> we used a modified version of Skempton's<sup>27</sup> relationship between the ratio  $S_u/p_c$  and the plasticity index  $I_p$  to estimate  $p_c$  from the strength data.

There is generally good agreement with one exception between these  $p_c$  values and those obtained from the consolidation tests at PB-2 (Fig. 3). However at the other site (PB-8) where there are sufficient data to make this comparison (Fig. 8) the estimated values are considerably less.

Berre<sup>26</sup> believes that  $S_u$  for overconsolidated clays is influenced less by disturbance during sampling

than the  $p_c$  values obtained from the consolidation test, and therefore that his method is preferable for obtaining  $p_c$ . For the purpose of our discussion, we have assumed that he is correct.

We have established, then, that most of the fine-grained sediments studied are overconsolidated. The degree of overconsolidation and the magnitude of the preconsolidation pressures, however, are quite variable. Preconsolidation pressures estimated from the strength data range from a low of 90 kPa at site PB-3 to a high of 1850 kPa at PB-2. Overconsolidation ratios vary from 2.2 at PB-8 to 1090 at PB-5.

The preconsolidation pressures are nearly constant with depth at PB-2 and PB-5, the average values being much greater at PB-2 (1635 kPa versus 475 kPa), and the preconsolidation pressure increases with depth at PB-1 (300 to 1800 kPa) and decreases with depth at PB-3 (1000 to 90 kPa) and PB-8 (1000 to 100 kPa).

The range and variability of  $p_c$  and  $p_c/p'$  from site to site and at different depths are difficult to explain. In an earlier paper<sup>16</sup> we dismissed the traditional overconsolidation mechanisms such as: 1) accumulation and subsequent erosion of overburden, 2) desiccation, and 3) glaciation. We also rejected the possibility that the forces of drifting ice caused the overconsolidation, and came to the conclusion that freezing and thawing was most likely the mechanism. We supported this theory with laboratory freeze-thaw consolidation test results.

At that time we had  $p_c$  data for site PB-2 only and assumed that the other two sites (PB-1 and PB-3) were normally consolidated. We also had concluded that the sediments at PB-2 were no more than 10,000 years old, and thus had always been submerged and had frozen and thawed during the passage of the transient barrier island, Reindeer Island. More recent dating of these sediments<sup>28</sup> suggests that their age is much greater than 10,000 years and that they may have been exposed to freezing temperatures during a period of low sea level that followed their deposition.<sup>29</sup>

It is possible, then, that during this exposure desiccation caused or contributed to the overconsolidation. However, because similar ice-saturated frozen clays have been observed on shore<sup>30</sup> this is doubtful. We believe, now, that the overconsolidation is the result of complex geological, chemical and thermal processes. As we are uncertain in most cases precisely what happened, we will defer speculating on the processes other than to say that: 1) Brown and Rashid<sup>31</sup> suggest that changes in chemistry can cause a low degree of overconsolidation, and 2) it appears that a few meters of sediments have been eroded locally,<sup>32</sup> which could also have caused a low degree of overconsolidation. It is also probable that Reindeer Island passed over site PB-2 and that it induced freezing as it is doing today.<sup>13,33</sup> And the large differences between the overconsolidation pressures and ratios at sites PB-2 and PB-8 are probably due to the more recent freezing and thawing of sediments at PB-2.

The highly overconsolidated clays play an important role in the degradation of ice-bonded permafrost in this region of the Beaufort Sea. According to Hopkins,<sup>32</sup> wherever the highly overconsolidated silt or clay is preserved on the sea bottom, ice-bonded permafrost lies close to the sea floor, the dense sediments inhibiting the infiltration of more saline waters into the deeper sands and gravels.



These dense clays may create access problems for obtaining gravel for drilling pads, etc. Conventional hydraulic dredges would probably not work well in these sediments. Most likely, mechanical cutters would be required to break through to the gravels.

#### Penetration Resistance

Because of the ease and speed with which the point resistance profiles were obtained, we were able to identify sediment types, distribution and bearing capacity over a large area.

Unique penetration characteristics were identified with sediment types and frozen sediment by comparing penetration resistance curves with drill hole logs and temperature profiles. Subtle variations in grain size as well as depositional patterns and frozen zones were apparent.

The resulting correlations allowed us to establish stratigraphic cross sections along each of the study lines. These sections show the distribution of sediments and zones where they may be frozen.

For instance, the stratigraphic section along line 1 (Fig. 12) shows a distinct difference between the sediments seaward and shoreward of the shoal separating Prudhoe Bay from the Beaufort Sea. A weak fine-grained section occurs from the surface down to stronger coarser-grained sediments at PH-6, PH-7 and PH-8. A similar section occurs under the shoal at PH-5 and PH-9, but is capped with sandy sediment. Seaward of the shoal the surface sand and silt unit increases in thickness and caps a weaker fine clayey silt section.

Furthermore, from the penetration resistance and temperature profiles, we determined that the shallow sediments in the shoal region (PH-4, PH-5 and PH-9) were seasonally frozen. Similarly, the sediments near the bottom of PH-5 were found to be frozen (possibly perennially frozen).

A discussion of the stratigraphic sections along the other study lines can be found in Blouin et al.<sup>18</sup>

#### Sediment Temperatures

The temperature profiles obtained with the penetrometer differ considerably from site to site. In areas where the sea ice was near or in contact with the seabed (water depth less than 2 m) the temperature at the seabed ranged from  $-2.2$  to  $-11.4^{\circ}\text{C}$ , with the temperatures apparently being controlled by the length of time the sea ice was in contact with the bed.

In water depths greater than 2 m, where sea water circulation was possible beneath the ice, the variation was much less,  $-1.7$  to  $-2.3^{\circ}\text{C}$ . In the center of Prudhoe Bay (PH-6), which is apparently a closed basin because of the sea ice freezing to the shoal separating it from the Beaufort Sea, the seabed temperature was  $-3.4^{\circ}\text{C}$  in 2.93 m of water. Extremely cold saline brines approaching 60 ppt were also observed in this region, indicating that little or no circulation occurs to flush the salts excluded during the freezing of the sea ice.

The highest temperature measured at the bottom of a probe hole was  $-0.8^{\circ}\text{C}$ , which was at PH-2 approximately 6 m below the seabed. This site was located in an open marine environment along line 1 with a water depth of 3.2 m.

The lowest temperature measured at depth in a probe hole was  $-3.4^{\circ}\text{C}$  12.7 m below the seabed at PH-27, which is on line 3 off the Sagavanirktok River delta in 1.89 m of water.

The temperature profiles in the deeper drill holes also differed considerably, depending on depth and site location. The temperatures at the bottom of the drill holes ranged from  $-1.7$  to  $-2.5^{\circ}\text{C}$ . The lowest bottom hole temperature was obtained almost a kilometer from shore at site PB-6, 28 m below the seabed.

The sediment temperatures at all the probe and drill sites increase with depth to depths ranging from 4 to 10 m, and then, with the exception of PH-5 and PH-9, decrease with depth, indicating that perennially frozen sediments occur at all sites. The temperature profiles at PH-5 and PH-9 do not show this trend, simply because the probe did not reach beyond the depth of seasonal cooling.

The relative accuracy of the thermal data is best demonstrated by comparing the probe results with those taken in the drill holes. In Fig. 13 the probe temperature profiles are superimposed on the drill hole profiles.

We can see that there is a general cooling of the drill holes during the time between the first observation made immediately after drilling was completed and the last measurements made before breakup of the sea ice. This cooling is attributed to two factors: 1) the establishment of thermal equilibrium in the sediments that were disturbed by drilling, and 2) seasonal cooling of the sediments.

Fig. 13 shows that there is good agreement between the probe and drill hole data. The small differences can be attributed to thermal disturbances induced during the drilling activity, to seasonal cooling, and to local temperature variations. (The probe observations were not made at precisely the same locations as the drill hole observations.)

The results are encouraging, especially if one considers the greater productivity of the penetrometer device and the time required for the drill holes to come to equilibrium. The advantage of the drill hole method, of course, is that greater depths can be reached and strongly ice-bonded sediments can be penetrated.

#### Chemistry

Another means of establishing the position of seasonally and perennially frozen sediments was through comparison of pore water freezing point profiles calculated by Page and Iskandar<sup>23</sup> from the salinity data with the thermal profiles obtained from the drill holes. We show these profiles for all the drill holes in Fig. 11.

One can see that the temperature near the seabed is below the freezing point of the interstitial water in all cases, which indicates that the bed sediments are seasonally frozen. Although we did not observe ice during drilling, it is quite possible that ice and water are in equilibrium in these sediments, with little bonding of sediments occurring. The decrease in freezing temperatures below this zone, which is the result of increases in salinity, probably reflects brine exclusion from above during freezing.



The freezing point and temperature data also suggest that perennially frozen sediments occur near the bottoms of all the drill holes except PB-1 and PB-5. With the exception of PB-8 this observation agrees extremely well with observations made during the drilling program. At PB-8 it appears that we stopped short of perennially frozen sediments.

#### Depth to Perennially Frozen Sediments

Although perennially frozen sediments appear to occur at all of the sites investigated, the depths are extremely variable and currently unpredictable.

Fig. 14 shows a composite of data for the location of the top of ice-bonded permafrost along line 2. Our data and that of our colleagues at the U.S. Geological Survey and the University of Alaska are included in this figure. Superimposed on these data is our estimate of the depth to perennially ice-bonded sediments. One can see that there is good agreement between the drill and probing estimates and those obtained by seismic means.

We attribute the difference between the seismic data and the probe and drill hole data principally to differences in alignment of the study lines (see Fig. 1).

Several distinct regions occur along this profile:

- 1) The near-shore shallow water (<1 m) region where perennially frozen sediments lie close to the seabed,
- 2) The region seaward to PB-3 where the depth to ice-bonded permafrost falls to 50 or 60 m,
- 3) The 140-m-deep depression between PB-3 and PB-8,
- 4) The very shallow perennially frozen sediments in the region of Reindeer Island,
- 5) The shallow rising ice-bonded permafrost table beyond Reindeer Island.

Hopkins<sup>32</sup> believes that the dense overconsolidated clays play an important role in controlling the position of the top of ice-bonded permafrost by keeping the salt water from gaining access to the porous gravel substrate beneath. "Consequently, thawing of ice in the shallow bonded permafrost could progress only by heat and salt diffusion."

Hopkins also believes that the deeply thawed region between PB-3 and PB-8 was a river bed in Pleistocene times, during which the dense overconsolidated clays were eroded and the deeper gravels were thawed to tens of meters. As the sea level rose, this valley was flooded early, and in the absence of the impervious dense clays the salty sea water gained ready access to the gravels, thawing them to even greater depths.

We also believe that the overconsolidated clays restrict the depth of thawing. In addition, we think that other factors such as 1) the initial degree of ice saturation of the sediments, 2) variations in mean annual seabed temperature, and 3) thermal perturbations introduced by transient features also play an important role. For instance, we can see in Fig. 15 that the mean annual seabed temperature along line 2 decreases with increasing distance from shore. (These values were determined by extrapolating the straight line segments of the drill hole temperature to the seabed, and assuming the intercept to be the mean annual seabed temperature.) Thus, the depth to

perennially frozen sediments is decreasing far offshore.

#### CONCLUSIONS

In the Prudhoe Bay region of the Beaufort Sea fine-grained sediments cover coarser dense sands and gravels interspersed occasionally with finer grained sediments. The thickness of the fine-grained section ranges from 3 to 10 m at the sites investigated. The properties of these materials vary greatly from soft, weak sediments in the center of Prudhoe Bay to stiff, highly overconsolidated sediments north of Reindeer Island.

All of the fine-grained sediments appear to be overconsolidated, but the degree of overconsolidation varies widely. The densest, most uniform and most highly overconsolidated clays occur seaward of Reindeer Island. We believe that freezing and thawing has probably caused the overconsolidation of these fine-grained sediments.

The sands and gravels appear to be a good source of borrow material and good materials for some types of foundations. Access to them, however, may be restricted in shallow water locations where the fine-grained sediments freeze seasonally and in the regions of dense overconsolidated clays.

In general, the salinity in the interstitial water in the sediments was similar to that of sea water and was fairly uniform with depth. The largest variations were encountered close to shore, where highly saline sea water has infiltrated into the surface layer of sediments. These brines formed as a result of salt exclusion during the formation of sea ice. Other large variations in salinity observed were associated with the partial seasonal freezing of the interstitial water in sediments located near the seabed. The pore water chemistry data coupled with the thermal data were useful in confirming the position of zones where ice can be anticipated in the sediments.

Although we did not observe segregated ice during our study, the occurrence of ice-rich sediments cannot be discounted. Ice-rich sediments are extremely likely to occur in shallow coastal sites, particularly to the west of Prudhoe Bay in areas where rapid coastal retreat is occurring. Ice has been seen in the Humble C-1 Reindeer Island hole<sup>33</sup> and in the Canadian Beaufort Sea.<sup>34</sup>

Permafrost properties and distribution are extremely variable in the marine environment as they are on land, with greater potential for variability because of saline waters and complex thermal histories imposed by varying coastal processes. Of particular concern and interest is the rising ice-bonded permafrost table seaward of Reindeer Island because of the high potential for segregated ground ice at shallow depths far out on the continental shelf.

#### ACKNOWLEDGMENTS

We wish to acknowledge S.E. Blouin, I.K. Iskandar, F.W. Page, H. Ueda, D.E. Garfield and A. Delaney of CRREL as well as our co-workers D.M. Hopkins, D. Carter, V. Marshall, and R. Hartz of the U.S. Geological Survey, for their contributions to this project. The efforts of R.I. Lewellen are also greatly appreciated. This work was supported by the Bureau of Land Management and managed by the National Oceanic and Atmospheric Administration as part of their Outer

Continental Shelf Environmental Assessment Program. The study was a cooperative effort undertaken with the U.S. Geological Survey, Menlo Park, California. The Office of Naval Research, Naval Arctic Research Laboratory provided some of the equipment used during the field activities.

#### REFERENCES

1. Are, F.E.: "The Subsea Cryolithic Zone of the Arctic Ocean," In: Regional and Thermophysical Investigations of Frozen Soils (Rocks) in Siberia, Academy of Sciences of the USSR, Siberian Branch, Published by: The Yakutsk Book Publishing House (1976).
2. Lachenbruch, A.H.: "Thermal Effects of the Ocean on Permafrost," Geol. Soc. Am. Bull. (1957), No. 68, 1515-1529.
3. Lachenbruch, A.H., Brewer, M.C., Greene, G.W., and Marshall, B.V.: "Temperatures in Permafrost," In: Temperature-Its Measurement and Control in Science and Industry, Vol. 3, Part 1, Reinhold, N.Y. (1978), 791-803.
4. Lewellen, R.I.: "The Occurrence and Characteristics of Nearshore Permafrost, Northern Alaska," In: Permafrost, North American Contributions to the Second International Conference, NAS/NRC (1973), 131-136.
5. Lewellen, R.I.: "Subsea Permafrost Research Techniques," Symposium on Research Techniques in Coastal Environments, Louisiana State University (1976).
6. Golden, Brawner, and Associates: "Bottom Sampling Program, Southern Beaufort Sea," Arctic Petroleum Operators Association Report No. 3. (1970).
7. Shearer, J.M., MacNab, R.F., Pelletier, B.R., and Smith, T.B. "Submarine Pingos in the Beaufort Sea," Science (1971) 179, 816-818.
8. Hunter, J.A., Judge, A.S., MacAulay, H.A., Good, R.L., Gagne, R.M., and Burns, R.A.: "The Occurrence of Permafrost and Frozen Sub-sea-bottom Materials in the Southern Beaufort Sea," Geological Survey of Canada and Earth Physics Branch, Dept. of Energy, Mines and Resources (Canada), Beaufort Sea Technical Report #22 (1976), 174 p.
9. Hunter, J.A., Neave, K.G., MacAulay, H.A., and Hobson, G.D.: "Interpretation of Sub-seabottom Permafrost in the Beaufort Sea by Seismic Methods. Part I: Seismic Refraction Methods," In: Proceedings of the Third International Conference on Permafrost (1978), Vol. 1, 514-520.
10. Hunter, J.A., Neave, K.G., MacAulay, H.A., and Hobson, G.D.: "Interpretation of Sub-seabottom Permafrost in the Beaufort Sea by Seismic Methods. Part II: Estimating the Thickness of the High-Velocity Layer," In: Proceedings of the Third International Conference on Permafrost (1978), Vol. 1, 521-526.
11. Osterkamp, T.E. and Harrison, W.D.: "Subsea Permafrost at Prudhoe Bay, Alaska: Drilling Report and Data Analysis," University of Alaska, Geophysical Institute Report UAG-R-245 (1976).
12. Osterkamp, T.E. and Harrison, W.D.: "Subsea Permafrost Probing, Thermal Regime and Data Analysis," Quarterly Report, April-June 1978 to National Oceanic and Atmospheric Administration, Outer Continental Shelf Environmental Assessment Project (1978).
13. Osterkamp, T.E. and Harrison, W.D.: "Subsea Permafrost Probing, Thermal Regime and Data Analysis," Quarterly Report, October-December 1978, to National Oceanic and Atmospheric Administration, Outer Continental Shelf Environmental Assessment Project (1978).
14. Harrison, W.D. and Osterkamp, T.E.: "A Coupled Heat and Salt Transport Model for Subsea Permafrost," University of Alaska Geophysical Institute, UAG-R-247 (1976), 21 p.
15. Rogers, J.C. and Morack, J.L.: "Geophysical Investigation of Offshore Permafrost at Prudhoe Bay, Alaska," In: Proceedings of the Third International Conference on Permafrost (1978), Vol. 1, 560-566.
16. Chamberlain, E.J., Sellmann, P.V., Blouin, S.E., Hopkins, D.M., and Lewellen, R.I.: "Engineering Properties of Subsea Permafrost in the Prudhoe Bay Region of the Beaufort Sea," In: Proceedings of the Third International Conference on Permafrost (1978), Vol. 1, 629-635.
17. Iskandar, I.K., Osterkamp, T.E., and Harrison, W.D.: "Chemistry of Interstitial Water from the Subsea Permafrost, Prudhoe Bay, Alaska," In: Proceedings of the Third International Conference on Permafrost (1978), Vol. 1, 93-98.
18. Blouin, S.E., Chamberlain, E.J., Sellmann, P.V., and Garfield, D.E.: "Determining Sub-sea Permafrost Characteristics with a Cone Penetrometer - Prudhoe Bay, Alaska," Cold Regions Science and Technology (1971) 1, No. 1.
19. Lachenbruch, A.H. and Marshall, B.V.: "Subsea Temperatures and a Single Tentative Model for Offshore Permafrost at Prudhoe Bay, Alaska," U.S. Geological Survey Open-File Rept. 77-395 (1977).
20. Sellmann, P.V., Lewellen, R.I., Ueda, H.T., Chamberlain, E.J., and Blouin, S.E.: "Operational Report: 1976 USACRREL-USGS Subsea Permafrost Program, Beaufort Sea, Alaska," U.S. Army Cold Regions Research and Engineering Laboratory Special Report 76-12 (1976).
21. Sellmann, P.V., Chamberlain, E.J., Ueda, H.T., Blouin, S.E., Garfield, D.E., and Lewellen, R.I.: "Operational Report - 1977 CRREL-USGS Subsea Permafrost Program, Beaufort Sea, Alaska," U.S. Army Cold Regions Research and Engineering Laboratory Special Report 77-41 (1977).
22. Sellmann, P.V. and Chamberlain, E.J.: "The Properties and Distribution of Subsea Permafrost Near Prudhoe Bay, Alaska," Final Report, USACRREL-USGS Subsea Permafrost Program, Beaufort Sea, Alaska (in preparation).
23. Page, F.W., and Iskandar, I.K., "Geochemistry of Subsea Permafrost at Prudhoe Bay, Alaska," U.S. Army Cold Regions Research and Engineering Laboratory Special Report 78-14 (1978).
24. Heijnen, W.J.: "Penetration Testing in Netherlands," Proceedings of European Symposium on Penetration Testing, Vol. 1, National Swedish Building Research, Stockholm, Sweden (1974).
25. Marshall, B.V.: Personal Communication (1978).
26. Berre, T.: Marine Geotechnique (1978).
27. Skempton, A.W.: "Discussion on the Planning and Design of the New Hong Kong Airport," Proc. Inst. Civ. Eng. (1957) 7, 305-310.
28. Hopkins, D.M.: "Offshore Permafrost Studies and Shoreline History of Chukchi and Beaufort Seas as an Aid to Predicting Offshore Permafrost Conditions," Quarterly Report, October-December 1978, to National Oceanic and Atmospheric Administration, Outer Continental Shelf Environmental Assessment Project (1978).
29. Barnes, P.W. and Hopkins, D.M., eds.: "Geological Sciences," In: Environmental Assessment of the Alaskan Continental Shelf, Interim Synthesis; Beaufort/Chukchi, U.S. National Oceanic

and Atmospheric Administration and U.S. Bureau of Land Management, Boulder, Colorado (1978), 101-133.

30. Hopkins, D.M.: Personal Communication (1978).
31. Brown, J.D. and Rashid, M.A.: "Geotechnical Properties of Nearshore Sediments of Canso Strait, Nova Scotia," *Can. Geotech. J.* (1974) **12**, 44-57.
32. Hopkins, D.M.: "Offshore Permafrost Studies, Beaufort Sea, Alaska," Quarterly Report, April-September 1978, to National Oceanic and

Atmospheric Administration, Outer Continental Shelf Environmental Assessment Project (1978).  
 33. Humble C-1: "Reindeer Island, Drill Log of Reindeer Island Hole," Drilled by Younger Brothers Drilling Co., Humble Oil Production Department Files, Los Angeles, California (unpublished).  
 34. MacKay, J.R.: "Offshore Permafrost and Ground Ice, Southern Beaufort Sea, *Can. J. Earth Sci.* (1972) **10**, No. 6, 979.

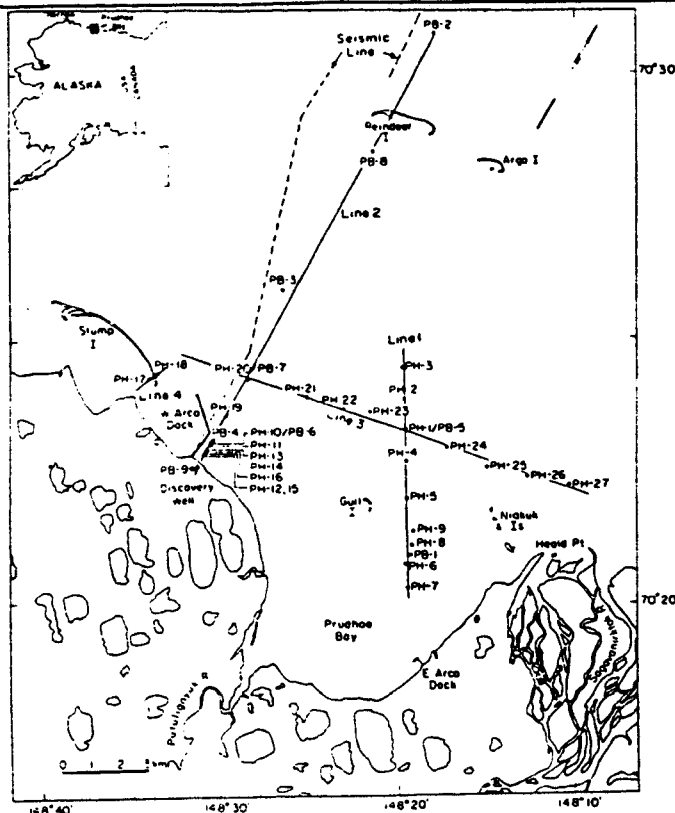


Fig. 1 - Site locations and major study lines (PB indicates drill hole, PH probe hole, except for PB-4 which is a 1976 probe hole location). The dashed line indicates the location of Rogers' seismic data shown in Figure 14.

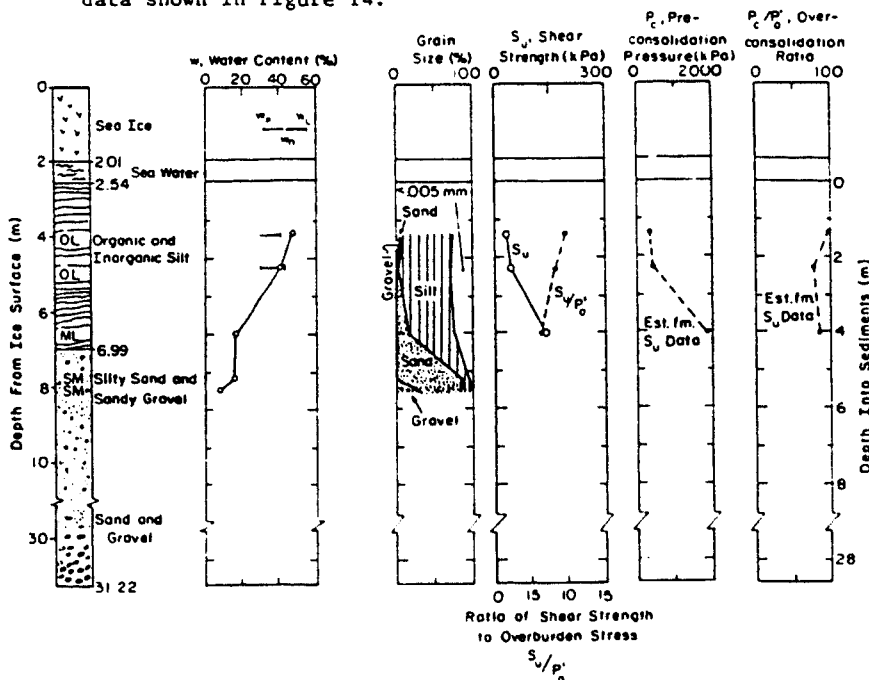


Fig. 2 - Drill hole log and engineering properties for site PB-1.

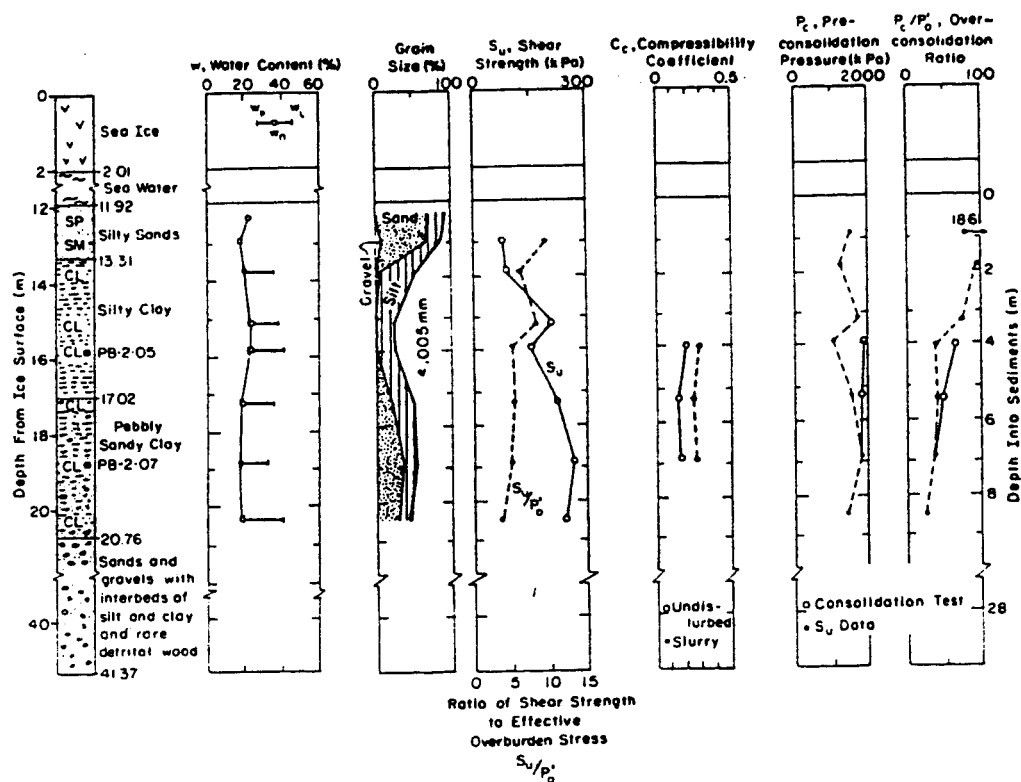


Fig. 3 - Drill hole log and engineering properties for site PB-2.

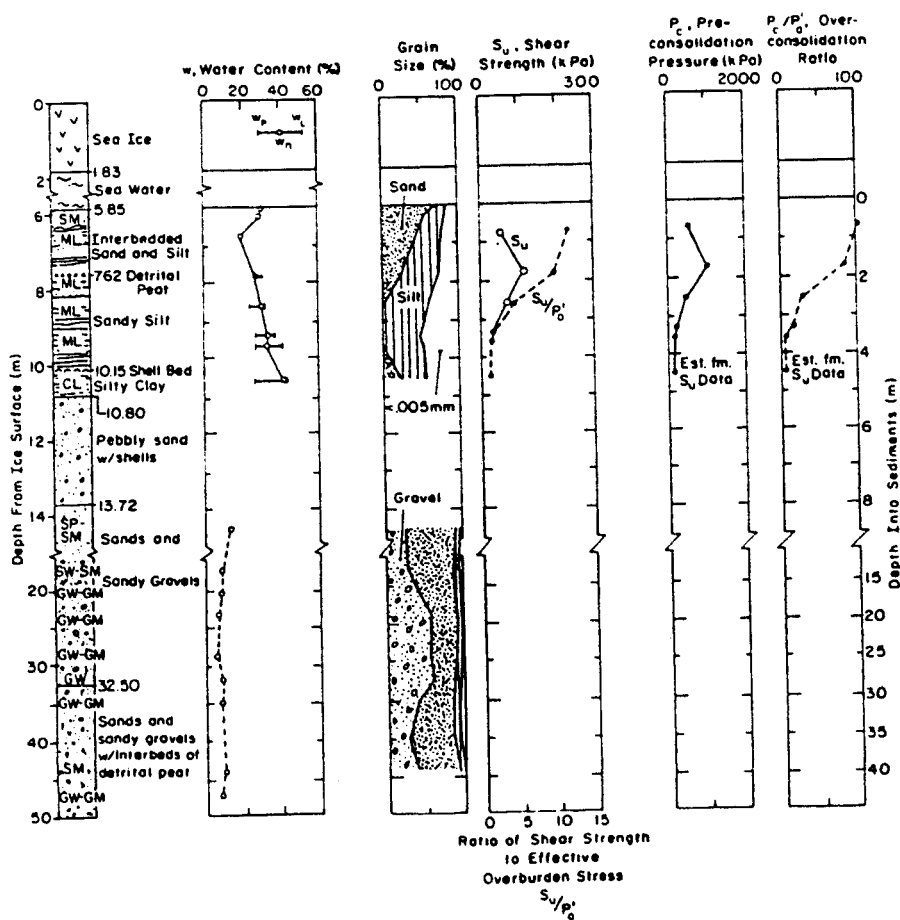


Fig. 4 - Drill hole log and engineering properties for site PB-3.

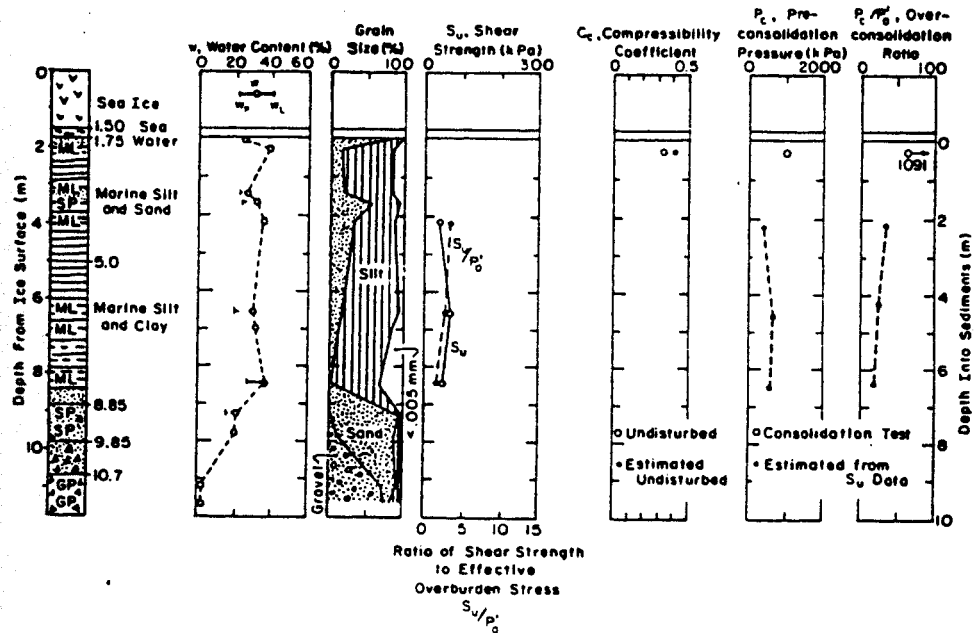


Fig. 5 - Drill hole log and engineering properties for site PB-5.

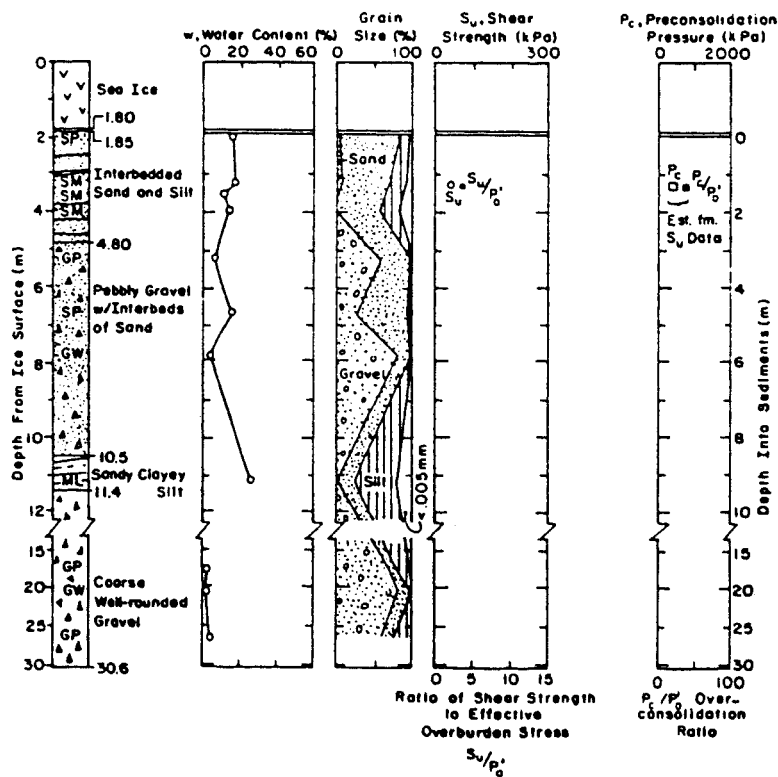


Fig. 6 - Drill hole log and engineering properties for site PB-6.

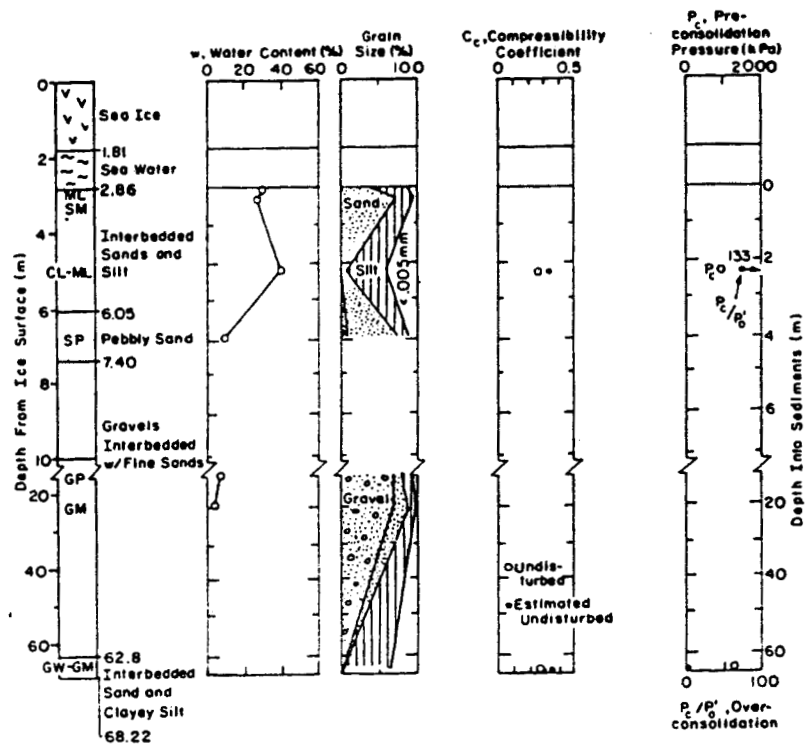


Fig. 7 - Drill hole log and engineering properties for site PB-7.

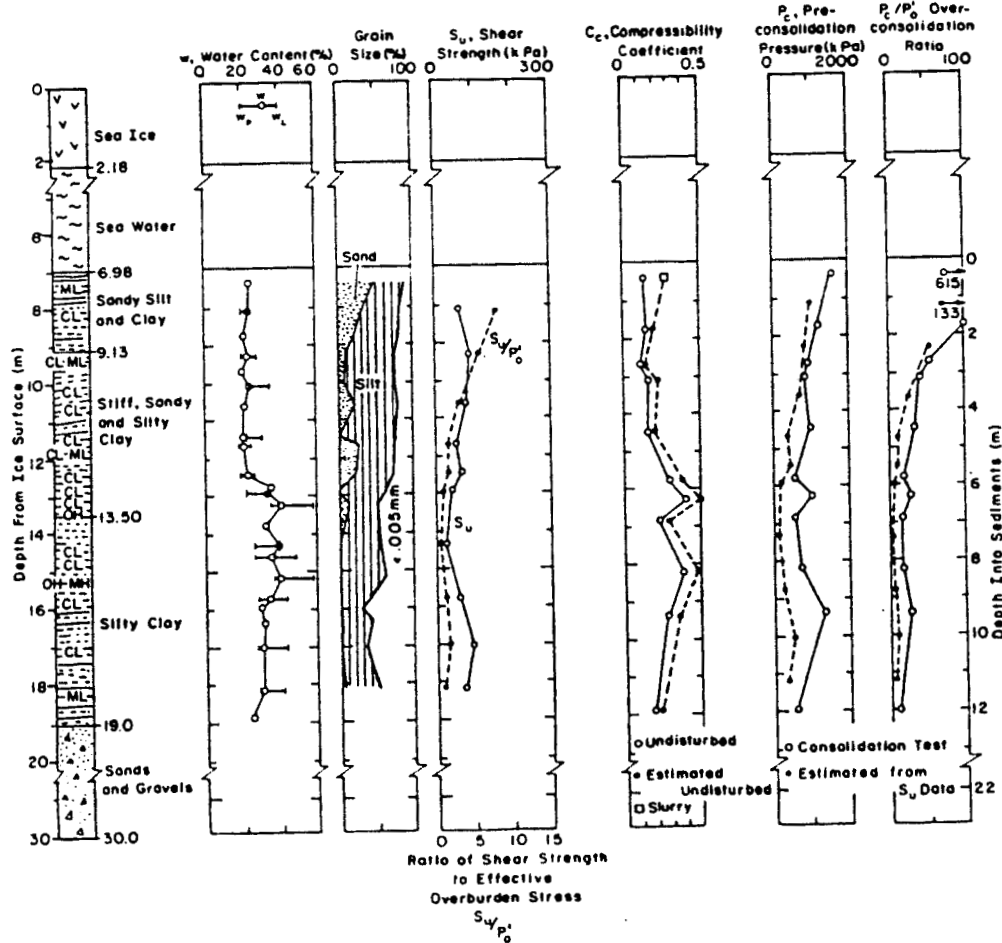


Fig. 8 - Drill hole log and engineering properties for site PB-8.

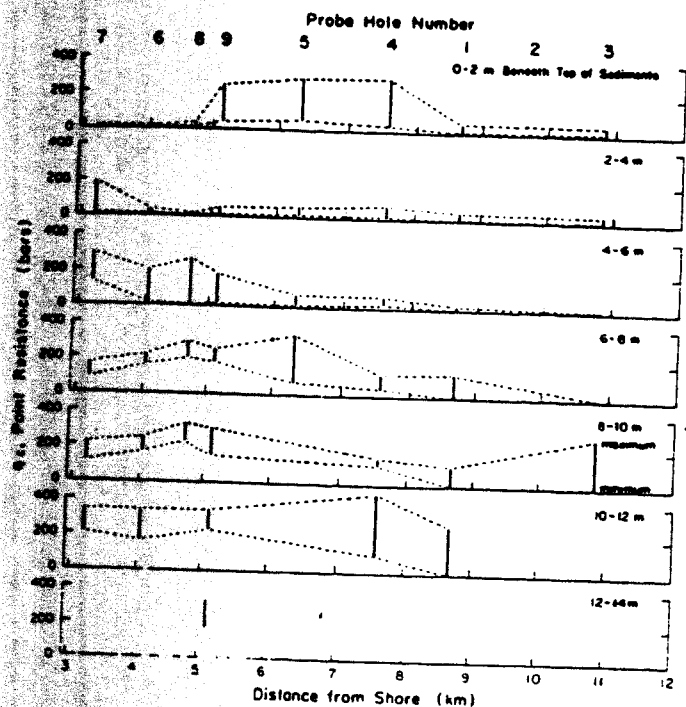


Fig. 9 - Summary of penetration resistances along line 1.  
(1 bar = 100 kPa.)

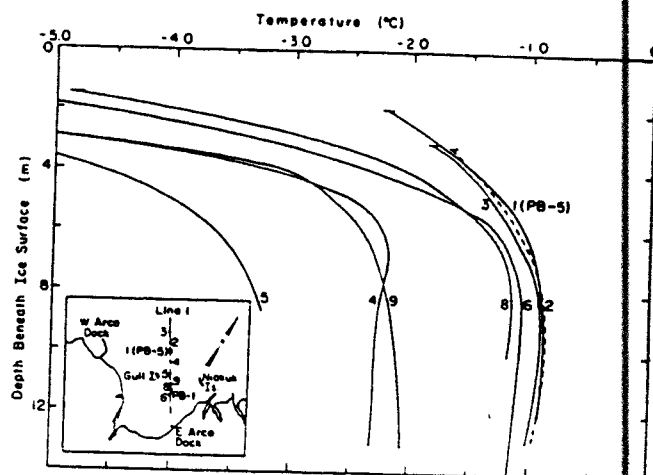


Fig. 10 - Temperature profiles along line 1.

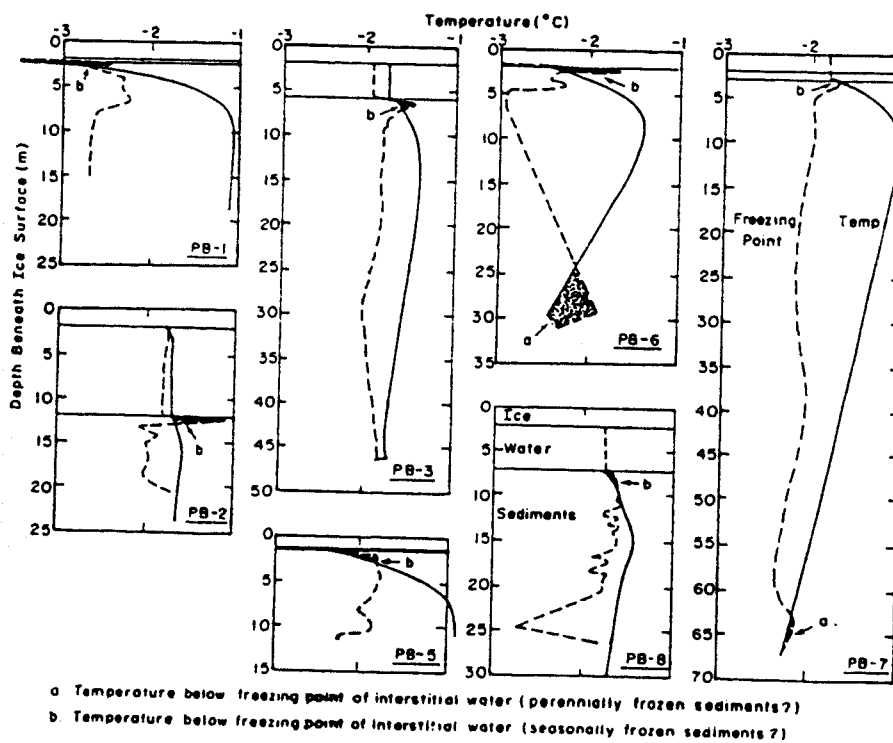


Fig. 11 - Comparison of the calculated freezing point and temperature profiles.

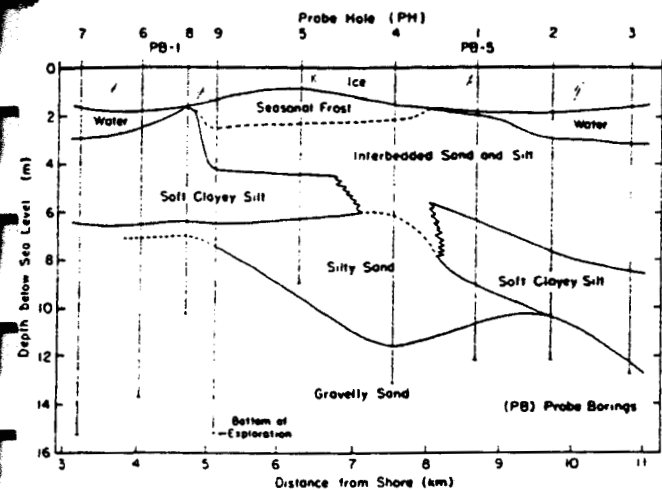


Fig. 12 - Stratigraphic section along line 1.

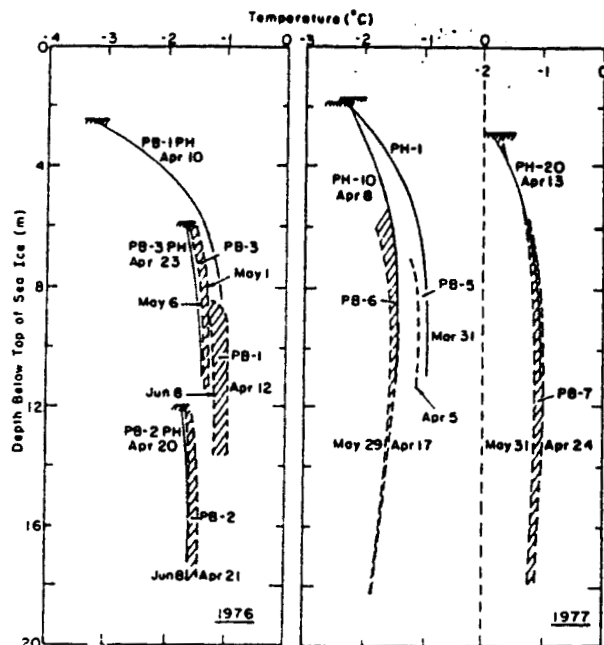


Fig. 13 - Comparison of drill hole and probe temperature profiles.

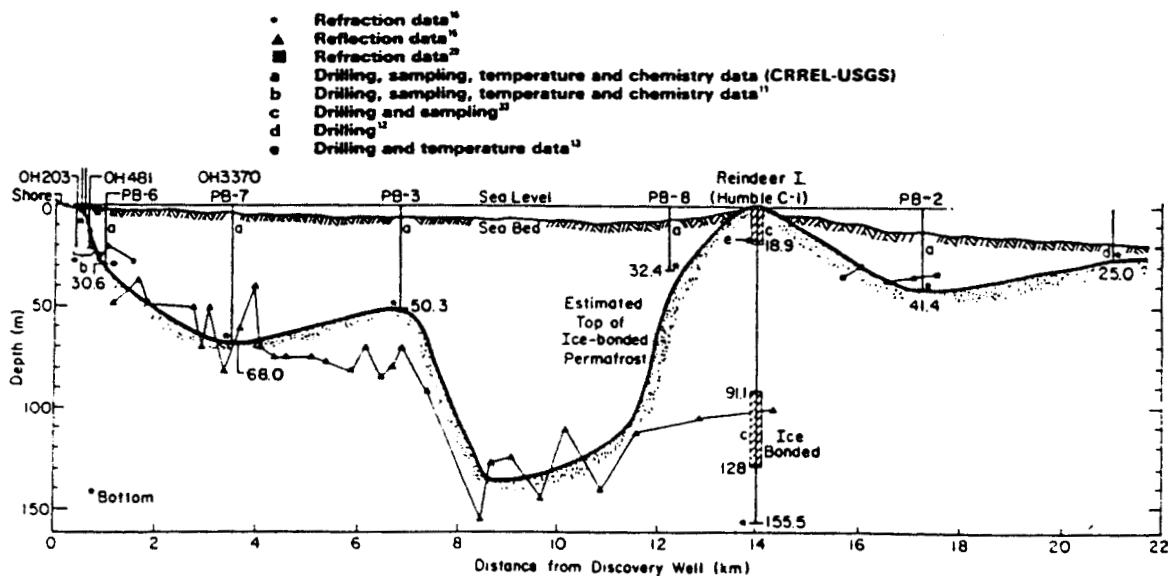


Fig. 14 - Summary of available data on depth to ice-bonded permafrost along line 2. Dark shaded line is our estimate of the position of the top of ice-bonded permafrost.

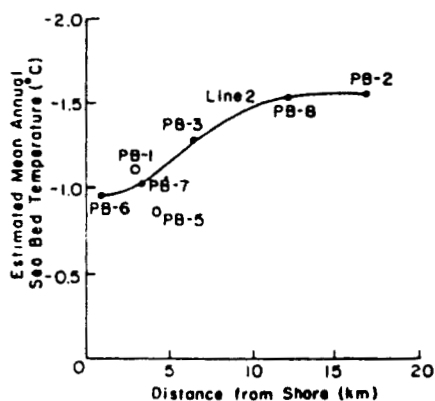


Fig. 15 - Mean annual seabed temperatures estimated from drill hole temperature profiles.



**COST SCHEDULE**  
**WINTER GEOTECHNICAL AND GEOPHYSICAL SITE INVESTIGATION**  
**93-0033**

DISBURSEMENT FEE = D 10.0%

PROGRAM BASED ON UTILIZING POLYGON SUPPORT ( LIMITED OFFSHORE ACCESS)

Item Description	Estimated Quantity	Unit	Unit Price	D	Estimated Total Amount
<b>1.0 MOBILIZATION/DEMOBILIZATION</b>					
<b>1.1 PLANNING AND CUSTOMS</b>					
1. PREPARATION WORK PLAN w/ ARCO	24	hour	\$85		\$2,040.00
2. COMMUNICATIONS	1	lump sum	\$500	Y	\$550.00
3. OPERATIONS PLANNING	80	hours	\$85		\$6,800.00
4. CONSUMABLES, ADMIN EXPENSES	1	lump sum	\$750		\$750.00
<b>TOTAL COST FOR PLANNING AND MOBILIZATION</b>					<b>\$10,140.00</b>
<b>1.2 MOBILIZATION GEOPHYSICAL EQUIPMENT PERSONNEL TO ANCH</b>					
<b>1.0 SEAFLOOR HAZARDS Bathy-Sonar</b>					
1.1 Foreward Look Sonar, FATHO,	1	lump sum	\$55,000	Y	\$60,500.00
2.2 PERSONNEL	60	hour	\$105		\$6,300.00
2.3 CONSUMABLES	1	lump sum	\$3,500	Y	\$3,850.00
<b>TOTAL COST FOR MOBILIZATION GEOPHYSICAL EQUIPMENT</b>					<b>\$70,650.00</b>
<b>1.3 MOBILIZATION ARCTIC GEOSCIENCE</b>					
<b>1.0 PROGRAM PLANNING</b>					
1.1 ARCTIC GEOSCIENCE	80	hour	\$85		\$6,800.00
1.2 CONSUMABLES	1	lump sum	\$1,500		\$1,500.00
1.3 VESSEL COMM. (RADIO PHONE)	1.0	lump sum	\$3,500		\$3,500.00
1.4 TECH SUPPORT	60.0	hour	\$65		\$3,900.00
<b>TOTAL COST FOR ARCTIC GEOSCIENCE MOB</b>					<b>\$15,700.00</b>
<b>1.4 MOBILIZATION EQUIP/ PERS. ANC TO PRUDHOE BAY</b>					
<b>1.0 TRANSPORTATION TO DEADHORSE</b>					
1.1 AK AIRLINES (ANC-DH-ANC)	16	RT FLTS	\$785	Y	\$13,816.00
2.0 TRANSPORT EQUIP - TRUCK	2	LOADS	\$3,500	Y	\$7,700.00
3.0 MISC. SUPPORT - CATCO OFFLOAD	40	\$/HR	\$145	Y	\$6,380.00
3.1 PICK-UP TRUCK	7	\$/day	\$150	Y	\$1,155.00
3.2 ACCOMS IN TUK, MISC SUPPORT	6	days	\$175	Y	\$1,155.00
<b>TOTAL COST FOR EQUIP/PERS.MOBILIZATION</b>					<b>\$30,206.00</b>

**COST SCHEDULE**  
**WINTER GEOTECHNICAL AND GEOPHYSICAL SITE INVESTIGATION**  
**93-0033**

**2.0 MOBILIZATION GEOTECHNICAL PROGRAM - FROM ANCH.**

1. GEOTECH DRILL	1	lump sum	\$35,000	Y	\$38,500.00
2. CPT - ARCTIC GEOSCIENCE consumables	1	lump sum	\$4,500		\$4,500.00
3. ONSITE LAB	1	lump sum	\$3,500		\$3,500.00
4. COMPUTER	1	prj prgrm	\$1,750		\$1,750.00
5. GEO/ ENG.	80	hours	\$85		\$6,800.00
6. CONSUMABLES	1	lump sum	\$3,500		\$3,500.00

**TOTAL COST FOR MOBILIZATION GEOTECHNICAL**

**\$58,550.00**

**3.0 REMOTE CAMP MOBILIZATION W/ FUEL**

1.0 CATCO REMOTE CAMP	1	24/MAN	\$86,450	Y	\$95,095.00
-----------------------	---	--------	----------	---	-------------

**TOTAL COST FOR REMOTE CAMP**

**\$95,095.00**

**4.0 MOBILIZATION NAVIGATION NET**

1. WESTERN GEOPHYSICAL	CR 1	lump sum	\$17,500	Y	\$19,250.00
2. LCMF	1	lump sum	\$24,850	Y	\$27,335.00

**TOTAL COST FOR NAVIGATION**

**\$27,335.00**

**5.0 DAILY OPERATING GEOPHYSICAL AND GEOTECH PRGRM**

1.0 ROLLIGON -TRACTOR TRAILER	6	\$/HR	\$345	Y	\$2,277.00
1.1 RD-85	6	\$/HR	\$185	Y	\$1,221.00
2.0 LCMF	1	\$/day	\$3,540	Y	\$3,894.00
3.0,4.0 SEAFLOOR HAZ EQUIP/PERS	1	\$/day	\$12,500	Y	\$13,750.00
5. ARCTIC GEOSCIENCE (3 men and lab)	1	\$/day	\$2,950		\$2,950.00
6. CONSUMABLES	1	\$/day	\$125		\$125.00
7. COMMUNICATIONS	1	\$/day	\$150		\$150.00
8. CATCO CAMP	24	\$/MANday	\$150	Y	\$3,960.00
9. GEOTECH DRILLER	24	\$/hr	\$265	Y	\$6,996.00
10 CPT EQUIP ( ARCTIC GEO EQUIP)	1	\$/day	\$2,100		\$2,100.00

**TOTAL DAILY COST FOR GEOPHYSICAL AND GEOTECHNICAL PROGRAM**

**\$37,423.00**

**6.0 DAILY OPERATING GEOTECH PRGRM**

1. ROLLIGON -TRACTOR TRAILER	6	\$/HR	\$345	Y	\$2,277.00
2. RD-85	6	\$/HR	\$185	Y	\$1,221.00
3. LCMF	1	\$/day	\$3,540	Y	\$3,894.00
4. ARCTIC GEOSCIENCE (3 men and lab)	1	\$/day	\$2,950		\$2,950.00
5. CONSUMABLES	1	\$/day	\$125		\$125.00
6. COMMUNICATIONS	1	\$/day	\$150		\$150.00
7. CATCO CAMP	24	\$/MANday	\$150	Y	\$3,960.00
8. GEOTECH DRILLER	24	\$/hr	\$265	Y	\$6,996.00
9. CPT EQUIP ( ARCTIC GEO EQUIP)	1	\$/day	\$2,100		\$2,100.00

**TOTAL DAILY COST FOR GEOTECHNICAL PROGRAM**

**\$23,673.00**

**COST SCHEDULE**  
**SUMMER GEOTECHNICAL AND GEOPHYSICAL SITE INVESTIGATION**  
**93-0033**

**FOR GENERAL PLANNING**

**DAILY RATES SHOULD ALSO INCLUDE ICE AND WEATHER MONITORING  
COSTS FOR SERVICES BY WEATHER SERVICE AND DR. LEWELLEN  
THESE COST TYPICALLY ADD TO THE PROGRAM \$950 TO \$1,150 PER DAY**

**ESTIMATED DATA PROCESSING, LABORATORY TESTING, REPORTING COST  
APPROXIMATELY 15 PERCENT OF THE TOTAL PROGRAM BUDGET**

**COST SCHEDULE**  
**WINTER GEOTECHNICAL AND GEOPHYSICAL SITE INVESTIGATION**  
**93-0033**

DISBURSEMENT FEE = D 10.0%

**PROGRAM BASED ON UTILIZING HELICOPTER SUPPORT**

Item Description	Estimated Quantity	Unit	Unit Price	D	Estimated Total Amount
<b>1.0 MOBILIZATION/DEMOBILIZATION</b>					
<b>1.1 PLANNING AND CUSTOMS</b>					
1. PREPARATION WORK PLAN w/ ARCO	24	hour	\$85		\$2,040.00
2. COMMUNICATIONS	1	lump sum	\$500	Y	\$550.00
3. OPERATIONS PLANNING	80	hours	\$85		\$6,800.00
4. CONSUMABLES, ADMIN EXPENSES	1	lump sum	\$750		\$750.00
<b>TOTAL COST FOR PLANNING AND MOBILIZATION</b>					<b>\$10,140.00</b>
<b>1.2 MOBILIZATION GEOPHYSICAL EQUIPMENT PERSONNEL TO ANCH</b>					
<b>1.0 SEAFLOOR HAZARDS Bathy-Sonar</b>					
1.1 Foreward Look Sonar, FATHO,	1	lump sum	\$55,000	Y	\$60,500.00
2.2 PERSONNEL	60	hour	\$105		\$6,300.00
2.3 CONSUMABLES	1	lump sum	\$3,500	Y	\$3,850.00
<b>TOTAL COST FOR MOBILIZATION GEOPHYSICAL EQUIPMENT</b>					<b>\$70,650.00</b>
<b>1.3 MOBILIZATION ARCTIC GEOSCIENCE</b>					
<b>1.0 PROGRAM PLANNING</b>					
1.1 ARCTIC GEOSCIENCE	80	hour	\$85		\$6,800.00
1.2 CONSUMABLES	1	lump sum	\$1,500		\$1,500.00
1.3 VESSEL COMM. (RADIO PHONE)	1.0	lump sum	\$3,500		\$3,500.00
1.4 TECH SUPPORT	60.0	hour	\$65		\$3,900.00
<b>TOTAL COST FOR ARCTIC GEOSCIENCE MOB</b>					<b>\$15,700.00</b>
<b>1.4 MOBILIZATION EQUIP/ PERS. ANC TO PRUDHOE BAY</b>					
<b>1.0 TRANSPORTATION TO DEADHORSE</b>					
1.1 AK AIRLINES (ANC-DH-ANC)	16	RT FLTS	\$785	Y	\$13,816.00
2.0 TRANSPORT EQUIP - TRUCK	2	LOADS	\$3,500	Y	\$7,700.00
3.0 MISC. SUPPORT - CATCO OFFLOAD	40	\$/HR	\$145	Y	\$6,380.00
3.1 PICK-UP TRUCK	7	\$/day	\$150	Y	\$1,155.00
3.2 ACCOMS IN TUK, MISC SUPPORT	6	days	\$175	Y	\$1,155.00
<b>TOTAL COST FOR EQUIP/PERS.MOBILIZATION</b>					<b>\$30,206.00</b>

**COST SCHEDULE**  
**WINTER GEOTECHNICAL AND GEOPHYSICAL SITE INVESTIGATION**  
**93-0033**

**2.0 MOBILIZATION GEOTECHNICAL PROGRAM - FROM ANCH.**

1. GEOTECH DRILL	1	lump sum	\$35,000	Y	\$38,500.00
2. CPT - ARCTIC GEOSCIENCE consumables	1	lump sum	\$4,500		\$4,500.00
3. ONSITE LAB	1	lump sum	\$3,500		\$3,500.00
4. COMPUTER	1	prj prgrm	\$1,750		\$1,750.00
5. GEO/ ENG.	80	hours	\$85		\$6,800.00
6. CONSUMABLES	1	lump sum	\$3,500		\$3,500.00

**TOTAL COST FOR MOBILIZATION GEOTECHNICAL** \$58,550.00

**3.0 REMOTE CAMP MOBILIZATION W/ FUEL**

1.0 CATCO REMTE CAMP	1	24/MAN	\$86,450	Y	\$95,095.00
----------------------	---	--------	----------	---	-------------

**TOTAL COST FOR REMOTE CAMP** \$95,095.00

**4.0 MOBILIZATION NAVIGATION NET**

1. WESTERN GEOPHYSICAL	CR	1	lump sum	\$17,500	Y	\$19,250.00
2. LCMF		1	lump sum	\$24,850	Y	\$27,335.00

**TOTAL COST FOR NAVIGATION** \$27,335.00

**5.0 DAILY OPERATING GEOPHYSICAL AND GEOTECH PRGRM**

1. ERA 212 HELICOPTER	1	\$/day	\$5,425	Y	\$5,967.50
1.2 FLIGHT HOURS wet ( 3HR MIN)	6	\$/HR	\$1,050	Y	\$6,930.00
3. LCMF	1	\$/day	\$3,540	Y	\$3,894.00
4. SEAFLOOR HAZ EQUIP/PERS	1	\$/day	\$12,500	Y	\$13,750.00
5. ARCTIC GEOSCIENCE (3 men and lab)	1	\$/day	\$2,950		\$2,950.00
6. CONSUMABLES	1	\$/day	\$125		\$125.00
7. COMMUNICATIONS	1	\$/day	\$150		\$150.00
8. CATCO CAMP	24	\$/MANday	\$150	Y	\$3,960.00
9. GEOTECH DRILLER	24	\$/hr	\$265	Y	\$6,996.00
10 CPT EQUIP ( ARCTIC GEO EQUIP)	1	\$/day	\$2,100		\$2,100.00

**TOTAL DAILY COST FOR GEOPHYSICAL AND GEOTECHNICAL PROGRAM** \$46,822.50

**6.0 DAILY OPERATING GEOTECH PRGRM**

1. ERA 212 HELICOPTER	1	\$/day	\$5,425	Y	\$5,967.50
1.2 FLIGHT HOURS wet ( 3HR MIN)	3	\$/HR	\$1,050	Y	\$3,465.00
3. LCMF	1	\$/day	\$3,540	Y	\$3,894.00
4. ARCTIC GEOSCIENCE (3 men and lab)	1	\$/day	\$2,950		\$2,950.00
5. CONSUMABLES	1	\$/day	\$125		\$125.00
6. COMMUNICATIONS	1	\$/day	\$150		\$150.00
7. CATCO CAMP	24	\$/MANday	\$150	Y	\$3,960.00
8. GEOTECH DRILLER	24	\$/hr	\$265	Y	\$6,996.00
9. CPT EQUIP ( ARCTIC GEO EQUIP)	1	\$/day	\$2,100		\$2,100.00

**TOTAL DAILY COST FOR GEOTECHNICAL PROGRAM** \$29,607.50

**COST SCHEDULE**  
**SUMMER GEOTECHNICAL AND GEOPHYSICAL SITE INVESTIGATION**  
**93-0033**

---

**FOR GENERAL PLANNING**

**DAILY RATES SHOULD ALSO INCLUDE ICE AND WEATHER MONITORING  
COSTS FOR SERVICES BY WEATHER SERVICE AND DR. LEWELLEN  
THESE COST TYPICALLY ADD TO THE PROGRAM \$950 TO \$1,150 PER DAY**

**ESTIMATED DATA PROCESSING, LABORATORY TESTING, REPORTING COST  
APPROXIMATELY 15 PERCENT OF THE TOTAL PROGRAM BUDGET**

**COST SCHEDULE**  
**SUMMER GEOTECHNICAL AND GEOPHYSICAL SITE INVESTIGATION**  
**93-0033**

DISBURSEMENT FEE = D 10.0%

PROGRAM BASED ON UTILIZING A CANADIAN FLAGGED VESSEL

Item Description	Estimated Quantity	Unit	Unit Price	D	Estimated Total Amount
<b>1.0 MOBILIZATION/DEMobilIZATION</b>					
<b>1.1 PLANNING AND CUSTOMS</b>					
1. PREPARATION WORK PLAN w/ ARCO	24	hour	\$85		\$2,040.00
2. PERMAN STOHLER	1	lump sum	\$7,500	Y	\$8,250.00
3. COMMUNICATIONS	1	lump sum	\$500	Y	\$550.00
4. OPERATIONS PLANNING	80	hours	\$85		\$6,800.00
5. CONSUMABLES, ADMIN EXPENSES	1	lump sum	\$750		\$750.00
<b>TOTAL COST FOR PLANNING AND MOBILIZATION</b>					<b>\$18,390.00</b>
<b>1.2 MOBILIZATION GEOPHYSICAL EQUIPMENT PERSONNEL TO ANCH</b>					
<b>1.0 MULTI-CHANNEL - SUBBOTTOM</b>					
1.1 EQUIPMENT: MULTI-CHANNEL	1	lump sum	\$80,000	Y	\$88,000.00
1.2 TRANSFER TO TUK CAN	10.0	days	\$3,500	Y	\$38,500.00
1.3 CONSUMABLES	1.0	lump sum	\$5,000	Y	\$5,500.00
<b>2.0 SEAFLOOR HAZARDS</b>					
2.1 SIDE SCAN, FATHO, 3.5, WSMS	1	lump sum	\$25,000	Y	\$27,500.00
2.2 PERSONNEL	100	hour	\$105		\$10,500.00
2.3 CONSUMABLES	1	lump sum	\$3,500		\$3,500.00
3.0 COMMUNICATIONS, EQUIP MANIFEST	1	lump sum	\$2,500		\$2,500.00
<b>TOTAL COST FOR MOBILIZATION GEOPHYSICAL EQUIPMENT</b>					<b>\$176,000.00</b>
<b>1.3 MOBILIZATION ARCTIC GEOSCIENCE</b>					
<b>1.0 PROGRAM PLANNING</b>					
1.1 ARCTIC GEOSCIENCE	80	hour	\$85		\$6,800.00
1.2 CONSUMABLES	1	lump sum	\$1,500		\$1,500.00
1.3 VESSEL COMM. (RADIO PHONE)	1.0	lump sum	\$3,500		\$3,500.00
1.4 TECH SUPPORT	60.0	hour	\$65		\$3,900.00
<b>TOTAL COST FOR ARCTIC GEOSCIENCE MOB</b>					<b>\$15,700.00</b>

ARCTIC GEOSCIENCE

**COST SCHEDULE**  
**SUMMER GEOTECHNICAL AND GEOPHYSICAL SITE INVESTIGATION**  
**93-0033**

**1.4 MOBILIZATION EQUIP/ PERS. ANC TO TUK CANADA**

**2.0 TRANSPORTATION TO TUK AND RETURN**

2.1 SECURITY AVIATION (ANC-TUK-ANC)	2	RT FLTS	\$6,543	Y	\$14,394.60
2.2 PERS TRAVEL 8 MEN 4 -6HR DAYS	200	hour	\$85		\$17,000.00
2.3 TRANSPORT EQUIP - TRUCK & BARGE	4	LOADS	\$3,500	Y	\$15,400.00
BARGE (NTCL)	2	mob/demob	\$4,800	Y	\$10,560.00
3.0 MISC. SUPPORT-TRANSF IN INUVIK	40	\$/HR	\$145	Y	\$6,380.00
3.1 PICK-UP TRUCK	7	\$/day	\$150	Y	\$1,155.00
3.2 CRANES, ETC. IN TUK	36	hour	\$175	Y	\$6,930.00
3.3 ACCOMS IN TUK, MISC SUPPORT	6	days	\$175	Y	\$1,155.00

**TOTAL COST FOR EQUIP/PERS.MOBILIZATION**

**\$72,974.60**

**2.0 MOBILIZATION GEOTECHNICAL PROGRAM - FROM CANADA**

1. FOUNDEX - GEOTECH DRILL	1	lump sum	\$65,000	Y	\$71,500.00
2. CPT - FOUNDEX consumables	1	lump sum	\$3,500	Y	\$3,850.00
3. ONBOARD LAB	1	lump sum	\$7,500		\$7,500.00
4. COMPUTER	1	prj prgrm	\$3,750		\$3,750.00
5. GEO/ ENG.	80	hours	\$85		\$6,800.00
6. CONSUMABLES	1	lump sum	\$3,500		\$3,500.00

**TOTAL COST FOR MOBILIZATION GEOTECHNICAL**

**\$96,900.00**

**3.0 MARINE VESSEL CHARTER MINIMUM**

1. CANMAR SUPPLIER V	30	DAYS	\$16,200	Y	\$534,600.00
2. M/V FRANK BRODERICK ( OPTION)	30	DAYS	\$43,000	Y	\$1,419,000.00
3. BARGE/ MOD U.S BEAUF VESSEL	30	DAYS	\$18,000	Y	\$594,000.00

**TOTAL COST FOR MARINE VESSEL**

**\$534,600.00**

**4.0 MOBILIZATION NAVIGATION NET**

1. WESTERN GEOPHYSICAL	CR	1	lump sum	\$17,500	Y	\$19,250.00
2. LCMF		1	lump sum	\$24,850	Y	\$27,335.00

**TOTAL COST FOR NAVIGATION**

**\$27,335.00**



**COST SCHEDULE**  
**SUMMER GEOTECHNICAL AND GEOPHYSICAL SITE INVESTIGATION**  
**93-0033**

**5.0 DAILY STANBY GEOPHYSICAL PRGRM ( AT THE DOCK, VESSEL MOBILIZATION )**

1. SUPPLIER V	1	\$/day	\$8,100	Y	\$8,910.00
2. MULTI-CHANNEL EQUIP/PERS	1	\$/day	\$5,820	Y	\$6,402.00
3. LCMF	1	\$/day	\$2,540	Y	\$2,794.00
4. SEAFLOOR HAZ EQUIP/PERS	1	\$/day	\$3,800	Y	\$4,180.00
5. ARCTIC GEOSCIENCE	2	\$/day	\$920		\$1,840.00
6. CONSUMABLES	1	\$/day	\$125		\$125.00
7.0 COMMUNICATIONS	1	\$/day	\$150		\$150.00
8. CANMAR FOOD	8	\$/day	\$50	Y	\$440.00

**TOTAL COST FOR STANDBY**

**\$24,841.00**

**6.0 DAILY STANBY GEOPHYSICAL AND GEOTECH PRGRM ( AT THE DOCK, VESSEL MOBILIZATION )**

1. SUPPLIER V	1	\$/day	\$8,100	Y	\$8,910.00
2. MULTI-CHANNEL EQUIP AND PERS	1	\$/day	\$5,820	Y	\$6,402.00
3. LCMF	1	\$/day	\$2,540	Y	\$2,794.00
4. SEAFLOOR HAZ EQUIP/PERS	1	\$/day	\$3,800		\$3,800.00
5. ARCTIC GEOSCIENCE	1	\$/day	\$2,150		\$2,150.00
6. CONSUMABLES	1	\$/day	\$125		\$125.00
7.0 COMMUNICATIONS	1	\$/day	\$150		\$150.00
8. CANMAR FOOD	15	\$/day	\$50	Y	\$825.00
9.0 FOUNDEX	1	\$/day	\$2,750	Y	\$3,025.00

**TOTAL COST FOR STANDBY GEOPHYSICAL AND GEOTECHNICAL PROGRAM**

**5 x \$28,181.00 = 140,905**

**7.0 DAILY STANBY GEOTECH PRGRM ( AT THE DOCK, VESSEL MOBILIZATION )**

1. SUPPLIER V	1	\$/day	\$8,100	Y	\$8,910.00
3. LCMF	1	\$/day	\$2,540	Y	\$2,794.00
5. ARCTIC GEOSCIENCE	1	\$/day	\$2,150		\$2,150.00
6. CONSUMABLES	1	\$/day	\$125		\$125.00
7.0 COMMUNICATIONS	1	\$/day	\$150		\$150.00
8. CANMAR FOOD	8	\$/day	\$50	Y	\$440.00
9.0 FOUNDEX - GEOTECH DRILL	1	\$/day	\$2,750	Y	\$3,025.00

**TOTAL COST FOR STANDBY GEOTECHNICAL PROGRAM**

**\$17,594.00**

**8.0 DAILY OPERATING GEOPHYSICAL PRGRM**

1. SUPPLIER V (FIRST 30 DAYS)	1	\$/day	\$0	Y	\$0.00
2. MULTI-CHANNEL EQUIP AND PERS	1	\$/day	\$6,820	Y	\$7,502.00
3. LCMF	1	\$/day	\$3,540	Y	\$3,894.00
4. SEAFLOOR HAZ EQUIP/PERS	1	\$/day	\$4,250		\$4,250.00
5. ARCTIC GEOSCIENCE	2	\$/day	\$920		\$1,840.00
6. CONSUMABLES	1	\$/day	\$125		\$125.00
7.0 COMMUNICATIONS	1	\$/day	\$150		\$150.00
8. CANMAR FOOD	8	\$/day	\$50	Y	\$440.00

**TOTAL DAILY COST FOR GEOPHYSICAL**

**\$18,201.00**

**COST SCHEDULE**  
**SUMMER GEOTECHNICAL AND GEOPHYSICAL SITE INVESTIGATION**  
**93-0033**

**9.0 DAILY OPERATING GEOPHYSICAL AND GEOTECH PRGRM**

1. SUPPLIER V (FIRST 30 DAYS)	1	\$/day	\$0	Y	\$0.00
2. MULTI-CHANNEL EQUIP AND PERS	1	\$/day	\$5,820	Y	\$6,402.00
3. LCMF	1	\$/day	\$3,540	Y	\$3,894.00
4. SEAFLOOR HAZ EQUIP/PERS	1	\$/day	\$4,250		\$4,250.00
5. ARCTIC GEOSCIENCE (2 men and lab)	1	\$/day	\$2,950		\$2,950.00
6. CONSUMABLES	1	\$/day	\$125		\$125.00
7. COMMUNICATIONS	1	\$/day	\$150		\$150.00
8. CANMAR FOOD	15	\$/day	\$50	Y	\$825.00
9. FOUNDEX - GEOTECH DRILLER	14	\$/hr	\$265	Y	\$4,081.00
10. CPT EQUIP (OPT. ARCTIC GEO EQUIP)	1	\$/day	\$2,100	Y	\$2,310.00

**TOTAL DAILY COST FOR GEOPHYSICAL AND GEOTECHNICAL PROGRAM**

**\$24,987.00**

**10.0 DAILY OPERATING GEOTECH PRGRM**

1. SUPPLIER V (FIRST 30 DAYS)	1	\$/day	\$0	Y	\$0.00
3. LCMF	1	\$/day	\$3,540	Y	\$3,894.00
5. ARCTIC GEOSCIENCE (3 men and lab)	1	\$/day	\$2,950		\$2,950.00
6. CONSUMABLES	1	\$/day	\$125		\$125.00
7. COMMUNICATIONS	1	\$/day	\$150		\$150.00
8. CANMAR FOOD	8	\$/day	\$50	Y	\$440.00
9. FOUNDEX - GEOTECH DRILLER	24	\$/hr	\$285	Y	\$7,524.00
10. CPT EQUIP (OPT. ARCTIC GEO EQUIP)	1	\$/day	\$2,100	Y	\$2,310.00

**TOTAL DAILY COST FOR GEOPHYSICAL AND GEOTECHNICAL PROGRAM**

**\$17,393.00**

**DAILY RATES DO NOT INCLUDE FUEL OR LUBE FOR VESSEL OR EQUIPMENT**

**COST SCHEDULE**  
**SUMMER GEOTECHNICAL AND GEOPHYSICAL SITE INVESTIGATION**  
**93-0033**

**FOR GENERAL PLANNING**

**ESTIMATED DATA PROCESSING, LABORATORY TESTING, REPORTING COST**  
**APPROXIMATELY 15 PERCENT OF THE TOTAL PROGRAM BUDGET**

Field Program

14 days

Date: July 23, 1993

Subject: Soil Profile for Conceptual Design of Kuvlum Structures

From: Junius Allen PRC J1422

Phone: 214 754 3079

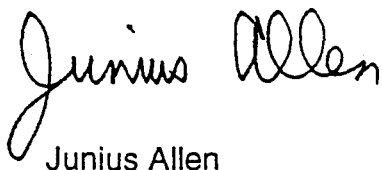
To: Bob Smith PRC J1411

Two soil profiles are attached which I propose for use of conceptual design of structures for the Kuvlum prospect.

The profile labelled "Middle and Outer Shelf Stratigraphy" is the most likely profile for soils in the Kuvlum area. Other borings in the general area, the hard bottom encountered in drilling the glory hole for the current well, and Mike Schlegel's reports of the hard bottom encountered in setting down the structure at the previous Kuvlum well and at another prospect make us somewhat confident that this is a typical profile for the area. Figure 17 of Schlegel's report shows a Kuvlum well solidly in the region labelled QHm/2c which this profile characterizes.

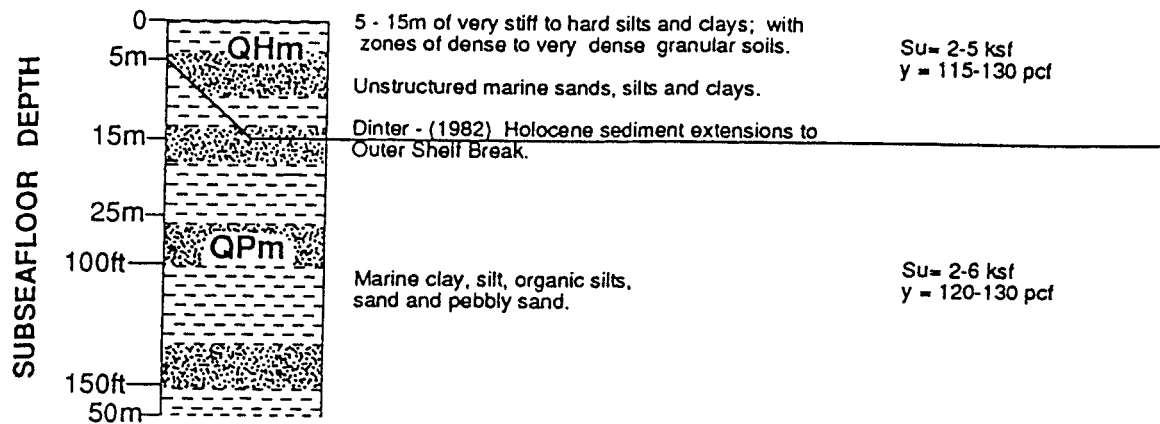
Because of the wide east-west extent of the Kuvlum reservoir, we have to consider the possibility that a structure near the fringes of the reservoir may have a profile more like that which is labelled Camden Bay Uplift Stratigraphy, which is also attached. Figure 17 shows this area off to the east of Kuvlum.

For executing the structures study, I recommend using 2 ksf over a controlling depth for the primary structure and checking sensitivity or having a secondary case with a 15 foot thick layer of 0.5 ksf material over 2 ksf material.

  
Junius Allen

# Middle and Outer Shelf Stratigraphy

## Zone 2C



### Notes

- 1) Locations of soil units are shown on Figures 9 and 10.
- 2) Su = Undrained shear strength.  
 $\phi$  = Angle of internal friction  
 $\gamma$  = Wet unit weight
- 3) Geotechnical properties are estimated and are for non-bonded soils; limitations on their applicability are discussed in text.
- 4) Because of modern ice gouging, surficial soils 0.5 - 3 m thick (depending on water depth) may be weaker than shown on the soil profiles.

## PREDICTED SOIL PROFILES

Modified from data provided in:  
 EBA - Stinson Geotechnical Synthesis,  
 and HLA AOGA Studies

ARCTIC GeoSCIENCE



Project Description:  
 Title:

EASTERN BEAUFORT SEA SYNTHESIS

Client:

ARCO Alaska, Inc.

By:

JSH

Date:

7/1/93

Project No.

93-0033

Checked:

MGS

Date:

7/1/93

Sheet No.

1 of 1

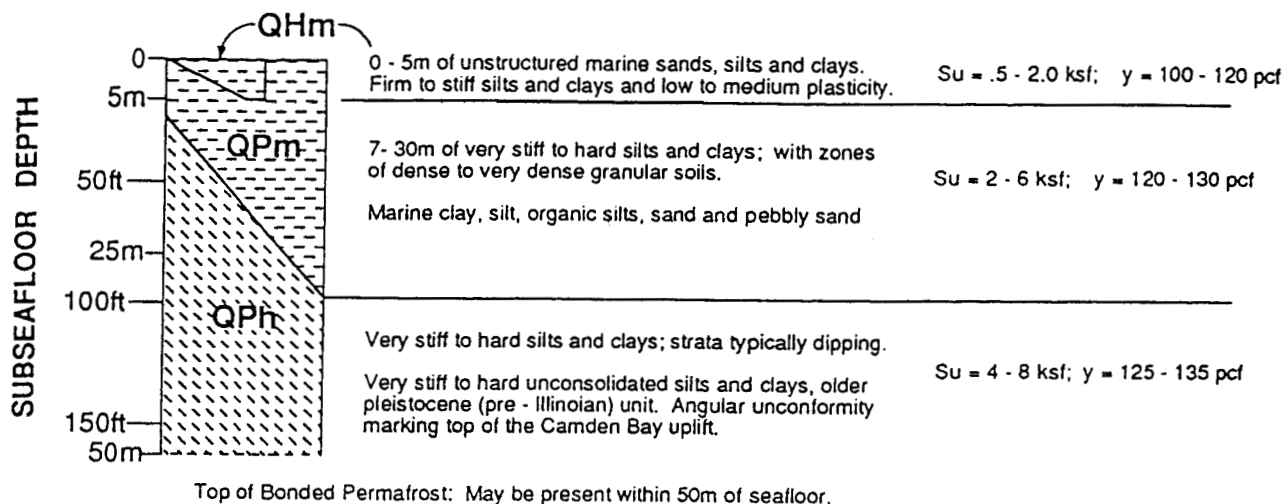
Scale:

N/A

Figure 22

# CAMDEN BAY UPLIFT Stratigraphy

## Zone 3A



### Notes

- Locations of soil units are shown on Figures 9 and 10.
- $S_u$  = Undrained shear strength.  
 $\phi$  = Angle of internal friction  
 $\gamma$  = Wet unit weight
- Geotechnical properties are estimated and are for non-bonded soils; limitations on their applicability are discussed in text.
- Because of modern ice gouging, surficial soils 0.5 - 3 m thick (depending on water depth) may be weaker than shown on the soil profiles

## PREDICTED SOIL PROFILES

Modified from data provided in:  
EBA - Stinson Geotechnical Synthesis,  
and HLA AOGA Studies

ARCTIC GEO SCIENCE



Project Description:  
Title:

EASTERN BEAUFORT SEA SYNTHESIS

Client:

ARCO Alaska, Inc.

By:

JSH

Date:

6/2/93

Checked:

MGS

Date:

6/2/93

Project No.

93-0033

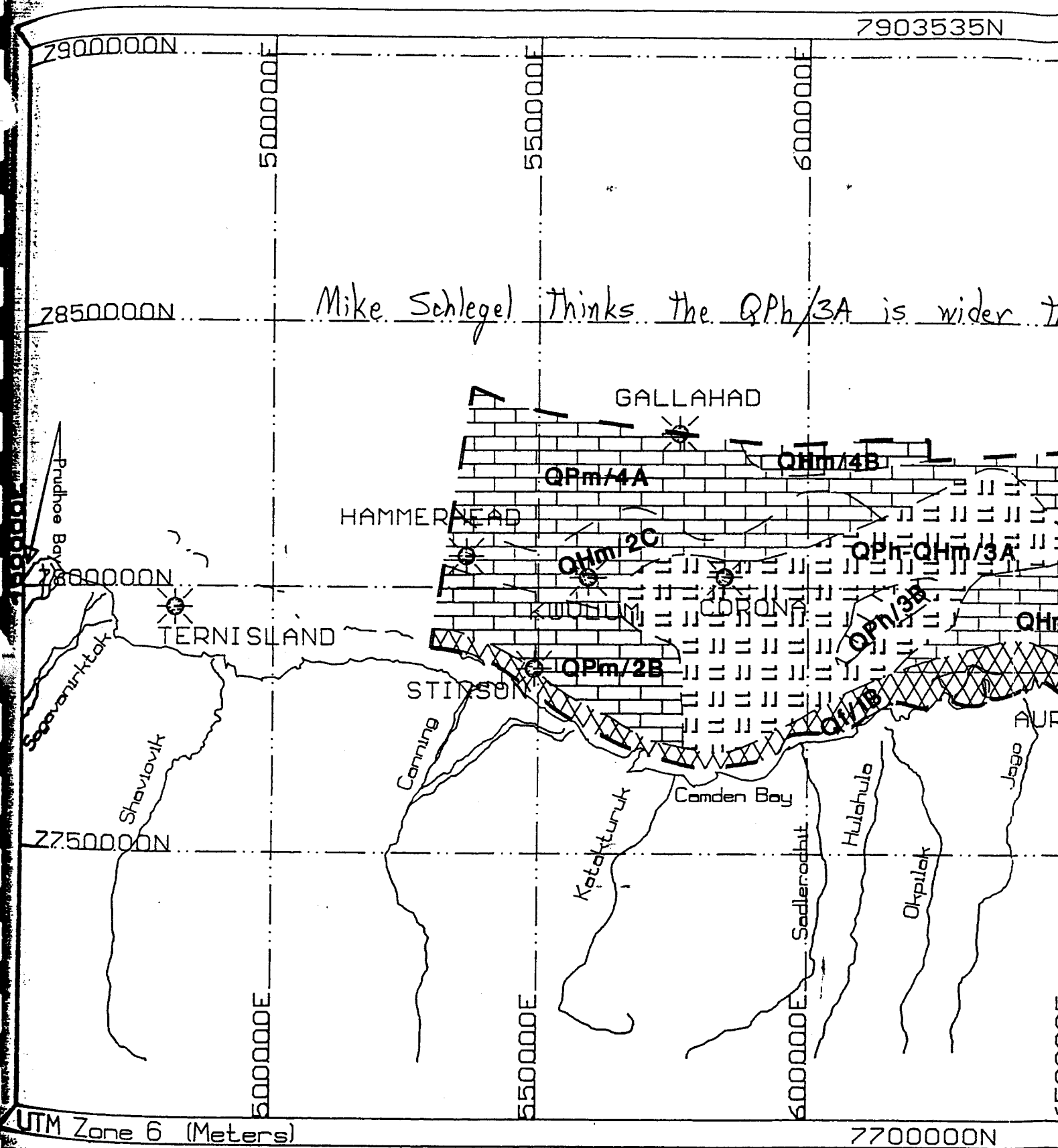
Sheet No.

1 of 1

Scale:

N/A

Figure 23



BEAUFORT SOIL U

ARCO ALASKA INC.

SYNTHESIS

EASTERN BEAUFORT SEA, ALA

ARCTIC GEO SCIENCE

is shown here.

BELCHER



2C

RA

Aichilik

Egokserok

Kongokut

Demarcation Bay

U.S.A.

CANADA

2250000N

2800000N

2850000N

2900000N

2000000E

2500000E

784648

From EBA - ARCO Stinson Study

VITS

(A

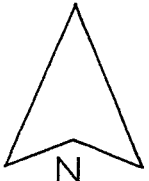


FIGURE 17

Put a thin lag deposit over Zone 1B to get the RF/1B profile.

Date: August 17, 1993

Subject: Soil Profile for Conceptual Design of Pipelines and Tunnels

From: Junius Allen PRC J1422

Phone: 214 754 3079

To: Bob Smith PRC J1411

Soil profiles are attached which I recommend for use of conceptual design of pipelines and tunnels for the Kuvlum prospect. These profiles are taken from the Eastern Beaufort Sea Synthesis compiled by Arctic GeoScience. The profiles are listed below in the order they would be encountered by a pipeline route from onshore to the Kuvlum platform site. Two routes are given below.

#### Route 1 - Crossing Flaxman Island

1. Soil Unit QH/1c. The area of this unit is south of Flaxman Island and is shown crosshatched in green on Figure 16. The profile is shown in the lower half of Figure 20. Though the surficial part of the profile is labelled QHm, this profile is still applicable to the unit. Tunnelling would possibly go to a depth deeper than the bottom of the profile. Therefore the profile can be assumed to be dense to very dense sands and gravels below the maximum depth shown.
2. Soil Unit Qf/QPu/2A. This unit is north of Flaxman Island and is a relatively thin strip shown in white on Figure 16. The profile is shown in the upper half of Figure 21. Again, tunnelling would possibly go to a depth deeper than the bottom of the profile. Therefore assume dense to very dense sands and gravels exist below the maximum depth shown.
3. Soil Unit QPm/2B. This unit is shown with blue lines on Figure 16. The profile is shown in the lower half of Figure 21. Again, assume dense to very dense sands and gravels exist below the maximum depth shown.
4. Soil Unit QHm/2c. This unit is shown with green lines on Figure 17. The profile is shown in Figure 22. Assume that the soil below the profile can be diverse ranging from stiff marine clay and silt to very dense sands and gravels.

#### Route 2 - East of Flaxman Island

1. QHd/1A or Qf/1B. The listing of two units, which are very similar, stems from having two different interpretations of data in the area. The QHd/1A unit is shown with green triangles in Figure 16 and the profile is shown in the upper half of Figure 19. The Qf/1B unit is shown as a purple crosshatched area on Figure 17 and the

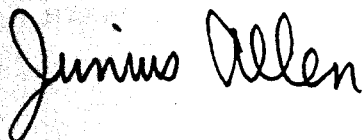


profile would consist of the upper half of Figure 20 with a thin lag deposit of gravel, cobbles, and boulders imposed at the top. Assume that the subprofile labelled Sag Delta characterizes the strip rather than the subprofile labelled Colville Delta.

2. Qf/QPu 2A or QPm/2B. See descriptions above.

3. QHm/2C. See description above.

Assume that rock, by the civil engineer's definitions, would not be encountered until a depth of well below 1000 feet. Rock would not be encountered in some areas until below 2000 feet.



Junius Allen

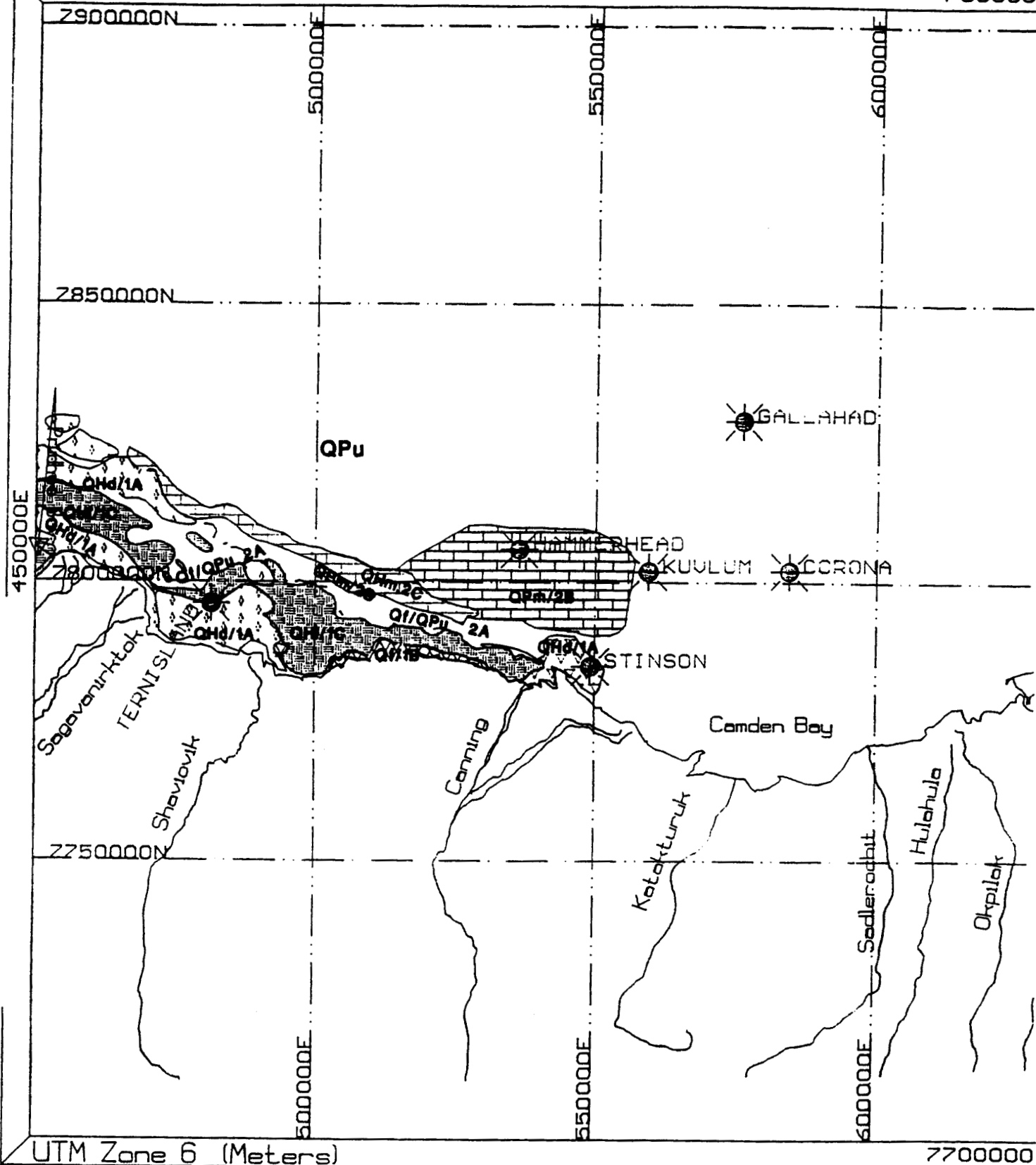


Fig. 16

BEAUFORT SOI

ARCTIC GEOS. JENSE

ARCO ALASKA  
SYNTHESIS  
EASTERN BEAUFORT SE

7903535N

2900000N

500000E

550000E

600000E

2850000N

GALLAHAD

QPM/4A

QHM/4B

HAMMERHEAD

QHM/2C

QPM-QHM/3A

QPM/3B

QPM/2B

QHM/1B

ERNISLAND

STIMPSON

Canning

Kotakturuk

Camden Bay

Sadlerodbit

Hulahulo

Okpikak

500000N

500000E

550000E

600000E

7700000N

Scale 6 (Meters)

Fig. 17

BEAUFORT SOIL

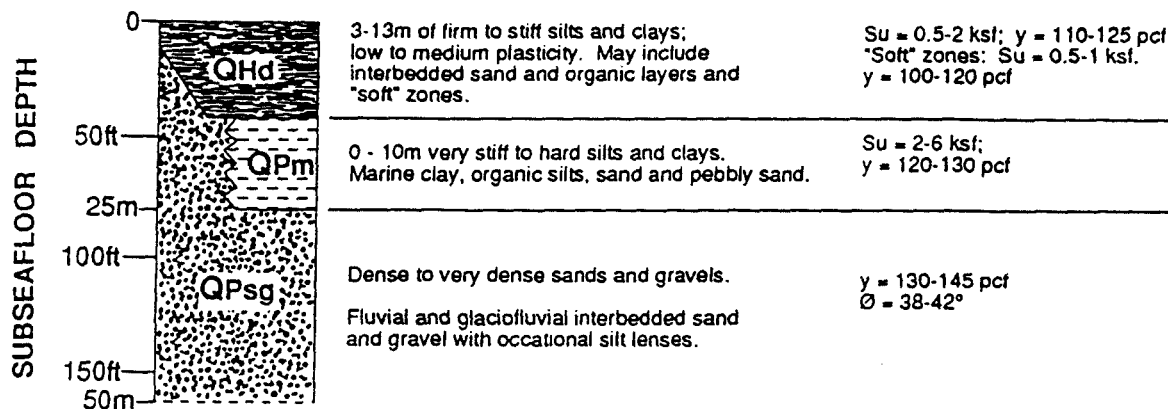
ARCO ALASKA INC.

SYNTHESIS

EASTERN BEAUFORT SEA. A

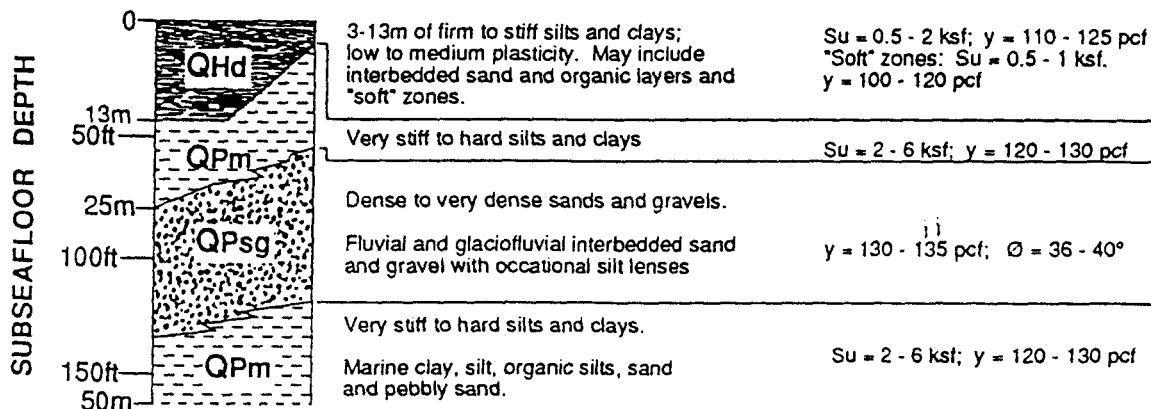
# Nearshore Stratigraphy

## Zone 1A Eastern Half (Prudhoe Bay Area)



Top of Bonded Permafrost: Present at highly variable depths ranging from about 5m to greater than 60m.

## Zone 1A Western Half (Prudhoe Bay Area)



Top of Bonded Permafrost: Present at highly variable depths ranging from about 5m to greater than 60m.

### Notes

- Locations of soil units are shown on Figures 9 and 10
- Su = Undrained shear strength  
 $\phi$  = Angle of internal friction  
 $\gamma$  = Wet unit weight
- Geotechnical properties are estimated and are for non-bonded soils; limitations on their applicability are discussed in text
- Because of modern ice gouging, surficial soils 0.5 - 3 m thick (depending on water depth) may be weaker than shown on the soil profiles.

## PREDICTED SOIL PROFILES

Modified from data provided in:  
EBA - Stinson Geotechnical Synthesis,  
and HLA AOGA Studies

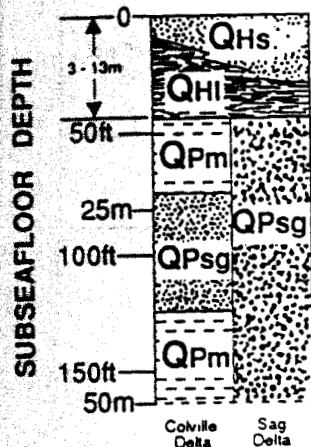
ARCTIC GEO SCIENCE



Project Description: Title:	By: JSH	Date: 6/2/93	Project No. 93-0033
	Checked: MGS	Date: 6/2/93	
Client: ARCO Alaska, Inc.	Scale: N/A	Figure 19	Sheet No. 1 of 2

# Nearshore Stratigraphy

## Zone 1B



Loose to medium dense silty fine sands. Coastal, Shoals  $\gamma = 120 - 135$  pcf,  $\phi = 30 - 38^\circ$

Firm to stiff silts and clays; may include organic and "soft" zones.

$S_u = 0.5 - 2$  ksf;  $\gamma = 11 - 125$  pcf  
 "Soft" zones:  $S_u = 0.5 - 1$  ksf  
 $\gamma = 100 - 120$  pcf

Colville R. Delta: Very stiff to hard silts and clays and dense to very dense sands.

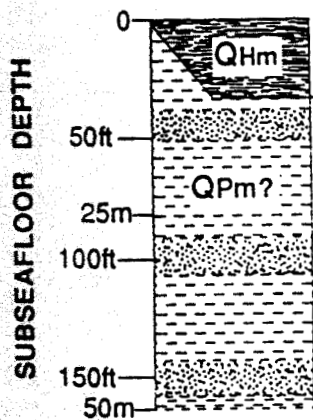
Silts and clays:  $S_u = 2 - 6$  ksf  
 $\gamma = 120 - 130$  pcf  
 Sands:  $\gamma = 130 - 135$  pcf;  $\phi = 36 - 40^\circ$

Sag R. Delta: Dense to very dense sands and gravels.

$\gamma = 130 - 145$  pcf  
 $\phi = 38 - 42^\circ$

Top of Bonded Permafrost: Present at highly variable depths ranging from about 5m to greater than 60m.

## Zone 1C



0-10m of firm to stiff silts and clays and loosed to medium dense sands; may include "soft" zones.

Silts and clays;  $S_u = 0.5 - 2$  ksf  
 $\gamma = 110 - 125$  pcf.  
 "Soft" zones:  $S_u = 0.5 - 1$  ksf;  
 $\gamma = 100 - 120$  pcf.  
 Sands:  $\gamma = 120 - 135$  pcf;  $\phi = 30 - 38^\circ$

Very stiff to hard silts and clays and dense to very dense sands.

Silts and clays;  $S_u = 0.5 - 2$  ksf,  
 $\gamma = 120 - 130$  pcf.  
 Sands:  $\gamma = 130 - 135$  pcf;  $\phi = 36 - 40^\circ$

Top of Bonded Permafrost: Present at highly variable depths

### Notes

- Locations of soil units are shown on Figures 9 and 10
- $S_u$  = Undrained shear strength  
 $\phi$  = Angle of internal friction  
 $\gamma$  = Wet unit weight
- Geotechnical properties are estimated and are for non-bonded soils; limitations on their applicability are discussed in text.
- Because of modern ice gouging, surficial soils 0.5 - 3 m thick (depending on water depth) may be weaker than shown on the soil profiles

## PREDICTED SOIL PROFILES

Modified from data provided in:  
 EBA - Stinson Geotechnical Synthesis,  
 and HLA AOGA Studies

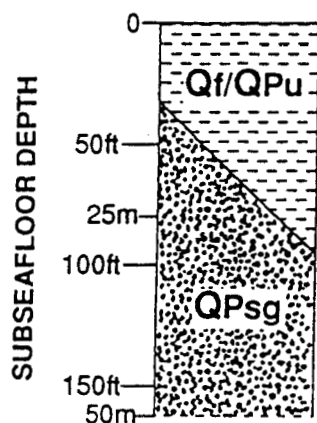
ARCTIC GEOSCIENCE



Project Description: Title:	By: JSH	Date: 6/2/93	Project No. 93-0033
	Checked: MGS	Date: 6/2/93	Sheet No.
Client: ARCO Alaska, Inc.	Scale: N/A	Figure 20	2 of 2

# Middle Shelf Stratigraphy

## Zone 2A



10 - 30m of very stiff to hard silts and clays.

$S_u = 2 - 6 \text{ ksf}$   
 $\gamma = 120 - 130 \text{ pcf}$

A thin lag deposit of gravel, cobbles and boulders/

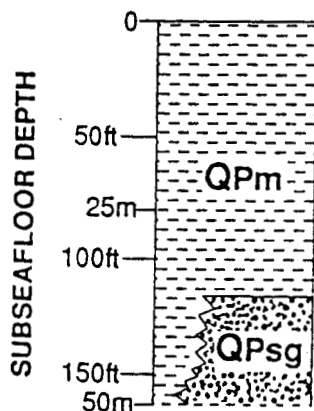
Undifferentiated geologic unit for which insufficient data was available to satisfactorily identify the unit.

Dense to very dense sands and gravels.

$\gamma = 130 - 145 \text{ pcf}$   
 $\phi = 38 - 42^\circ$

Top of Bonded Permafrost: May be present less than 20m below seafloor over much of area.

## Zone 2B



> 30m of very stiff to hard silts and clays.

$S_u = 2 - 6 \text{ ksf}$   
 $\gamma = 120 - 130 \text{ pcf}$

Marine clay, silt, organic silts, sand and pebbly sand

Dense to very dense sands or sands and gravels.

$\gamma = 130 - 145 \text{ pcf}$   
 $\phi = 36 - 42^\circ$

Top of Bonded Permafrost: May be present at variable depths typically ranging from about 10m to 50m.

### Notes

- 1) Locations of soil units are shown on Figures 9 and 10.
- 2)  $S_u$  = Undrained shear strength.  
 $\phi$  = Angle of internal friction  
 $\gamma$  = Wet unit weight
- 3) Geotechnical properties are estimated and are for non-bonded soils; limitations on their applicability are discussed in text.
- 4) Because of modern ice gouging, surficial soils 0.5 - 3 m thick (depending on water depth) may be weaker than shown on the soil profiles.

## PREDICTED SOIL PROFILES

Modified from data provided in:  
EBA - Stinson Geotechnical Synthesis,  
and HLA AOGA Studies

ARCTIC GEOSCIENCE



Project Description:  
Title:

EASTERN BEAUFORT SEA SYNTHESIS

Client:

ARCO Alaska, Inc.

By:

JSH

Date:

6/2/93

Checked:

MGS

Date:

6/2/93

Scale:

N/A

Figure 21

Project No.

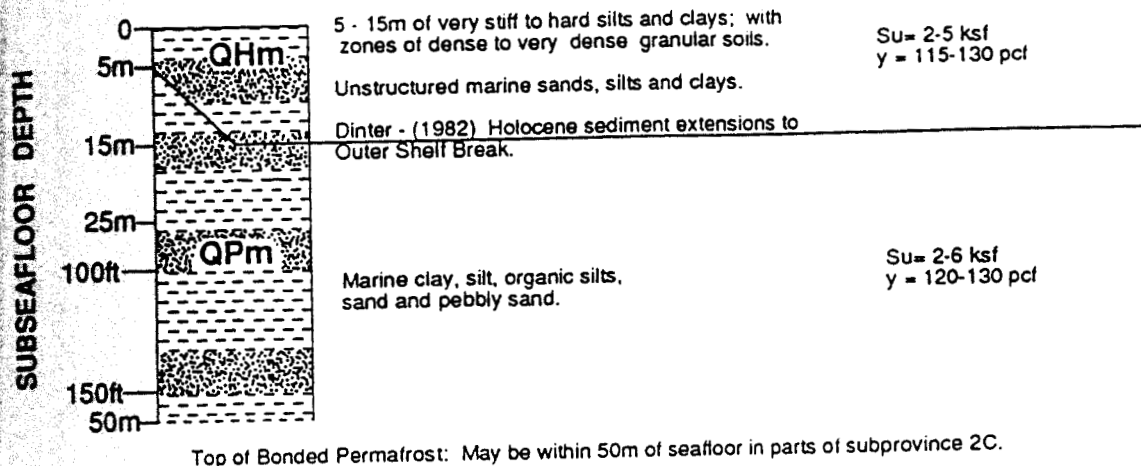
93-0033

Sheet No.

1 of 1

# Middle and Outer Shelf Stratigraphy

## Zone 2C




### Notes

- 1) Locations of soil units are shown on Figures 9 and 10.
- 2)  $S_u$  = Undrained shear strength.  
 $\phi$  = Angle of internal friction  
 $\gamma$  = Wet unit weight
- 3) Geotechnical properties are estimated and are for non-bonded soils; limitations on their applicability are discussed in text.
- 4) Because of modern ice gouging, surficial soils 0.5 - 3 m thick (depending on water depth) may be weaker than shown on the soil profiles.

## PREDICTED SOIL PROFILES

Modified from data provided in:  
EBA - Stinson Geotechnical Synthesis,  
and HLA AOGA Studies

<b>ARCTIC GEOSCIENCE</b> 	Project Description:		By:	Date:	Project No.
	EASTERN BEAUFORT SEA SYNTHESIS		JSH	7/1/93	93-0033
	Client:		Checked:	Date:	Sheet No.
	ARCO Alaska, Inc.		MGS	7/1/93	1 of 1
			Scale:	Figure 22	
			N/A		

**APPENDIX**

~~SECRET~~  
---  
A10.13

*Included in this Appendix are the printouts from the Oil and Gas Reserves and Economic Program (OGRE). Complete printouts are provided for Cases 1, 2, and 3. The input cost data for each case is taken from the most likely (ML) cost for each of the components.*



OGRE(R) \ . BATAK  
 FILE NAME: KUVLUM ( 17)  
 CASE NAME: MIN ECON SIZE  
 CMD NAME: STDJ5319( 300)

DATA PORT

DATE: 02/25/94  
 TIME: 09:53:23

101 DETERMINE MINIMUM ECONOMIC SIZE  
 102 PROD 100 WELLS RESERVES = 200 MMBLS  
 103 SINGLE (LARGE) DRILLING & PRODUCTION PLATFORM

117 CASE \$COM

\* 107 KUVLUM DEVELOPMENT PROJECT  
 \* 120 01 94 12 1 1 94 10 1  
 \* 131 DRILL ACRS 7 DELAY 0 0 0  
 \* 132 PRODFAC ACRS 7 DELAY 0 0 0  
 \* 133 PIPELINE ACRS 7 DELAY 0 0 0  
 \* 134 DRILSITE ACRS 7 DELAY 0 0 0  
 168!  
 169! TOTAL TAX IS 39 PERCENT  
 \* 170 39  
 \* 600 SET IDCAMORT = MAJOR

	W.I. FRACTION	OP. COST (\$/W/MO)	OP. COST (\$/MO.)	ADV. TAX (PCT)	MAJOR PH. NAME	PROD DATE (MO/DY/YR)	
210	1.000000000	.00	.00	.000	OIL	1/ 1/ 0	
	PHASE NAME	CUM PROD (MUNITS)	REV. INT FRACTION	PRICE (\$/UNIT)	DEV. TAX (PCT)	NO. OF WELLS	RATIO TO MAJOR PH
221	OIL	.000	.87500000	.000	.000	1.0	

300 CASE \$RESERVES200MM

300 SERIES LINES:

	MAN	OIL
* 305	FACT	1000.000
* 310		
* 311	12.	10000.000
* 312	12.	14000.000
* 313	12.	14000.000
* 314	12.	14000.000
* 315	12.	14000.000
* 316	12.	14000.000
* 317	12.	13600.000
* 318	12.	12600.000
* 319	12.	11600.000
* 320	12.	10600.000
* 321	12.	9200.000
* 322	12.	8200.000
* 323	12.	7600.000
* 324	12.	6800.000
* 325	12.	6200.000
* 326	12.	5400.000
* 327	12.	4800.000
* 328	12.	4400.000
* 329	12.	3800.000
* 330	12.	3400.000
* 331	12.	3000.000
* 332	12.	2600.000
* 333	12.	2200.000
* 334	12.	2000.000
* 335	12.	2000.000

\* 600 DATA : 12.33 12.89 13.61 14.36  
 \* 605 15.16 16.00 16.89 17.15 17.41 17.67 17.94  
 \* 610 18.21 18.76 19.32 19.90 20.50 21.11  
 \* 615 21.74 22.40 23.07 23.76 24.47 25.21  
 \* 620 25.96 26.74 27.54 28.37 29.22 30.10  
 \* 621 31.00 31.93  
 611! OPERATING COST  
 615 DATA OPCOST 1000 : 0 0 0 0 0 0  
 616 6272 LIFE  
 617!  
 618!  
 619!  
 620 DATA OPCOST : ESC 3 %  
 630 DATA ESCINV : 0 3 TO FRAME 40  
 800! INVESTMENTS FOR THE COASTAL PIPELINE  
 801!

	INV NAME	INV. POINT	(G OR N)	TANG-M\$	INTANG-M\$	LSEHLD-M\$	RISK FRAC	OVHD FLAG
802	PIPELINE	-54.000 MOS	G	6500.000	.000	.000	1.000	
803	PIPELINE	-42.000 MOS	G	6500.000	.000	.000	1.000	
804	PIPELINE	-30.000 MOS	G	58500.000	.000	.000	1.000	
805	PIPELINE	-18.000 MOS	G	52000.000	.000	.000	1.000	
806	PIPELINE	-6.000 MOS	G	6500.000	.000	.000	1.000	
807!	INVESTMENTS FOR THE MAIN PIPELINE							
808	PIPELINE	-54.000 MOS	G	7400.000	.000	.000	1.000	
811	PIPELINE	-42.000 MOS	G	7400.000	.000	.000	1.000	
812	PIPELINE	-30.000 MOS	G	66600.000	.000	.000	1.000	
813	PIPELINE	-18.000 MOS	G	59200.000	.000	.000	1.000	
814	PIPELINE	-6.000 MOS	G	7400.000	.000	.000	1.000	
815!								
816!	INVESTMENTS FOR MAIN PRODUCTION PLATFORM							
817!	STRUCTURE							
818	PRODFAC	-42.000 MOS	G	105000.000	.000	.000	1.000	
819	PRODFAC	-30.000 MOS	G	157500.000	.000	.000	1.000	
820	PRODFAC	-18.000 MOS	G	157500.000	.000	.000	1.000	
821	PRODFAC	-6.000 MOS	G	105000.000	.000	.000	1.000	
822!	PRODUCTION FACILITIES							
823	PRODFAC	-30.000 MOS	G	14850.000	.000	.000	1.000	
824	PRODFAC	-18.000 MOS	G	103950.000	.000	.000	1.000	
825	PRODFAC	-6.000 MOS	G	178200.000	.000	.000	1.000	
827!	INVESTMENTS FOR PERMITTING							
828	PRODFAC	-66.000 MOS	G	5000.000	.000	.000	1.000	
829	PRODFAC	-54.000 MOS	G	5000.000	.000	.000	1.000	
830	PRODFAC	-42.000 MOS	G	5000.000	.000	.000	1.000	
831	PRODFAC	-30.000 MOS	G	5000.000	.000	.000	1.000	
832!	DELINEATION WELLS THEN PRODUCTION WELLS							
833!								
834	DRILL	-6.000 MOS	G	10800.000	61200.000	.000	1.000	
835	DRILL	-72.000 MOS	G	10530.000	59670.000	.000	1.000	
836	DRILL	6.000 MOS	G	10800.000	61200.000	.000	1.000	
837	DRILL	18.000 MOS	G	10800.000	61200.000	.000	1.000	
838	DRILL	30.000 MOS	G	12600.000	71400.000	.000	1.000	
839!								
840	ESC	USING ESCINV						
850	NOLOSS OFF							

DETERMINE M1 M ECONOMIC SIZE  
 PROD 100 WELL RESERVES = 200 MMBLS  
 SINGLE (LARGE) DRILLING & PRODUCTION PLA

DATE: 02/25/94  
 TIME: 09:53:23  
 FILE: KUVLUM  
 GETI: 17

# RESERVES AND ECONOMICS

## KUVLUM DEVELOPMENT PROJECT

AS OF JANUARY 1, 1994

-END- MO-YR	---GROSS PRODUCTION---		---NET PRODUCTION---		---PRICES---		NO. OF WELLS	-----OPERATIONS, M\$-----			
	OIL, MMBL	GAS, MMCF	OIL, MMBL	GAS, MMCF	OIL \$/B	GAS \$/M		OIL REVENUE	GAS REVENUE	OTHER REVENUE	TOTAL REVENUE
12-94	.000	.000	.000	.000	12.33	.00	.0	.000	.000	.000	.000
12-95	.000	.000	.000	.000	12.89	.00	.0	.000	.000	.000	.000
12-96	.000	.000	.000	.000	13.61	.00	.0	.000	.000	.000	.000
12-97	.000	.000	.000	.000	14.36	.00	.0	.000	.000	.000	.000
12-98	.000	.000	.000	.000	15.16	.00	.0	.000	.000	.000	.000
12-99	.000	.000	.000	.000	16.00	.00	.0	.000	.000	.000	.000
12- 0	10000.000	.000	8750.000	.000	16.89	.00	1.0	147787.500	.000	.000	147787.500
12- 1	14000.000	.000	12250.000	.000	17.15	.00	1.0	210087.500	.000	.000	210087.500
12- 2	14000.000	.000	12250.000	.000	17.41	.00	1.0	213272.500	.000	.000	213272.500
12- 3	14000.000	.000	12250.000	.000	17.67	.00	1.0	216457.500	.000	.000	216457.500
12- 4	14000.000	.000	12250.000	.000	17.94	.00	1.0	219765.000	.000	.000	219765.000
12- 5	14000.000	.000	12250.000	.000	18.21	.00	1.0	223072.500	.000	.000	223072.500
12- 6	13600.000	.000	11900.000	.000	18.76	.00	1.0	223244.000	.000	.000	223244.000
12- 7	12600.000	.000	11025.000	.000	19.32	.00	1.0	213003.000	.000	.000	213003.000
12- 8	11600.000	.000	10150.000	.000	19.90	.00	1.0	201985.000	.000	.000	201985.000
12- 9	10600.000	.000	9275.000	.000	20.50	.00	1.0	190137.500	.000	.000	190137.500
12-10	9200.000	.000	8050.000	.000	21.11	.00	1.0	169935.500	.000	.000	169935.500
12-11	8200.000	.000	7175.000	.000	21.74	.00	1.0	155984.500	.000	.000	155984.500
12-12	7600.000	.000	6650.000	.000	22.40	.00	1.0	148960.000	.000	.000	148960.000
12-13	6800.000	.000	5950.000	.000	23.07	.00	1.0	137266.500	.000	.000	137266.500
12-14	6200.000	.000	5425.000	.000	23.76	.00	1.0	128898.000	.000	.000	128898.000
12-15	5400.000	.000	4725.000	.000	24.47	.00	1.0	115620.750	.000	.000	115620.750
12-16	4800.000	.000	4200.000	.000	25.21	.00	1.0	105882.000	.000	.000	105882.000
12-17	4400.000	.000	3850.000	.000	25.96	.00	1.0	99946.000	.000	.000	99946.000
12-18	3800.000	.000	3325.000	.000	26.74	.00	1.0	88910.500	.000	.000	88910.500
12-19	3400.000	.000	2975.000	.000	27.54	.00	1.0	81931.500	.000	.000	81931.500
12-20	3000.000	.000	2625.000	.000	28.37	.00	1.0	74471.250	.000	.000	74471.250
12-21	2600.000	.000	2275.000	.000	29.22	.00	1.0	66475.500	.000	.000	66475.500
12-22	2200.000	.000	1925.000	.000	30.10	.00	1.0	57942.500	.000	.000	57942.500
12-23	2000.000	.000	1750.000	.000	31.00	.00	1.0	54250.000	.000	.000	54250.000
12-24	2000.000	.000	1750.000	.000	31.93	.00	1.0	55877.500	.000	.000	55877.500
12-25	.000	.000	.000	.000	.00	.00	1.0	.000	.000	.000	.000
S TOT	200000.000	.000	175000.000	.000	20.58	.00	1.0	3601164.000	.000	.000	3601164.000
REM.	.000	.000	.000	.000	.00	.00	.0	.000	.000	.000	.000
TOTAL	200000.000	.000	175000.000	.000	20.58	.00	.0	3601164.000	.000	.000	3601164.000

-END- MO-YR	-----OPERATIONS, M\$-----				-----CAPITAL COSTS, M\$-----				10.00 PCT CUM. DISC	
	SEVERANCE TAXES	AD VAL TAXES	NET OPER EXPENSES	OPERATIONS CASH FLOW	TANGIBLE COSTS	INTANG. COSTS	LSEHOLD COSTS	SALVAGE VALUE	CASH FLOW BTAX, M\$	CUM. DISC BTAX, M\$
12-94	.000	.000	.000	.000	15530.000	59670.000	.000	.000	-75200.000	-74967.313
12-95	.000	.000	.000	.000	19467.000	.000	.000	.000	-19467.000	-91841.000
12-96	.000	.000	.000	.000	131445.510	.000	.000	.000	-131445.510	-195418.171
12-97	.000	.000	.000	.000	330495.281	.000	.000	.000	-330495.281	-432168.649
12-98	.000	.000	.000	.000	419420.858	.000	.000	.000	-419420.858	-705307.162
12-99	.000	.000	.000	.000	356940.487	70947.573	.000	.000	-427888.061	-958627.699
12- 0	.000	.000	89869.152	57918.348	12895.765	73076.001	.000	.000	-28053.417	-979744.383
12- 1	.000	.000	92565.227	117522.273	13282.638	70288.281	.000	.000	28971.355	-959517.597
12- 2	.00	.000	95342.183	117930.317	15961.303	904.4	.000	.000	11521.630	-954372.950
12- 3	30	.000	98202.449	118255.051	.000	0	.000	.000	118255.051	-906537.093
12- 4	100	.000	101110.600	118255.051	.000	0	.000	.000	118255.051	-800000.000

12- 5	.000	104182.978	118889.522	.000	.000	.000	118889.522	-823171.163
12- 6	.000	107308.467	115935.533	.000	.000	.000	115935.533	-787936.318
12- 7	.000	110527.721	102475.279	.000	.000	.000	102475.279	-759623.557
12- 8	.000	113843.553	88141.447	.000	.000	.000	88141.447	-737484.934
12- 9	.000	117258.860	72878.640	.000	.000	.000	72878.640	-720843.988
12-10	.000	120776.625	49158.875	.000	.000	.000	49158.875	-710639.599
12-11	.000	124399.924	31584.576	.000	.000	.000	31584.576	-704679.308
12-12	.000	128131.922	20828.078	.000	.000	.000	20828.078	-701106.177
12-13	.000	131975.880	5290.620	.000	.000	.000	5290.620	-700281.064
12-14	.000	135935.156	-7037.156	.000	.000	.000	-7037.156	-701278.790
12-15	.000	140013.211	-24392.461	.000	.000	.000	-24392.461	-704422.752
12-16	.000	144213.607	-38331.607	.000	.000	.000	-38331.607	-708914.196
12-17	.000	148540.015	-48594.015	.000	.000	.000	-48594.015	-714090.491
12-18	.000	152996.216	-64085.716	.000	.000	.000	-64085.716	-720296.392
12-19	.000	157586.102	-75654.602	.000	.000	.000	-75654.602	-726956.576
12-20	.000	162313.685	-87842.435	.000	.000	.000	-87842.435	-733986.693
12-21	.000	167183.096	-100707.596	.000	.000	.000	-100707.596	-741313.719
12-22	.000	172198.589	-114256.089	.000	.000	.000	-114256.089	-748870.767
12-23	.000	177364.546	-123114.546	.000	.000	.000	-123114.546	-756273.456
12-24	.000	182685.483	-126807.983	.000	.000	.000	-126807.983	-763205.065
12-25	.000	.000	.000	.000	.000	.000	.000	-763205.065
S TOT	.000	.000 3276563.169	324600.831 1315438.842	369409.238	.000	.000	-1360247.250	-763205.065
REM.	.000	.000 .000	.000 .000	.000 .000	.000	.000	.000	-763205.065
TOTAL	.000	.000 3276563.169	324600.831 1315438.842	369409.238	.000	.000	-1360247.250	-763205.065

DATE: 02/25/94  
TIME: 09:53:23  
FILE: KUVLUM  
GET: 17

## KUVLUM DEVELOPMENT PROJECT

AS OF JANUARY 1, 1994

BTAX RATE OF RETURN (PCT)		.00	ATAX RATE OF RETURN (PCT)		.00	-----PRESENT WORTH PROFILE-----		
BTAX PAYOUT YEARS		31.00	ATAX PAYOUT YEARS		31.00	DISC	PW OF NET	PW OF NET
BTAX PAYOUT YEARS (DISC)		31.00	ATAX PAYOUT YEARS (DISC)		31.00	RATE	BTAX, M\$	ATAX, M\$
BTAX NET INCOME/INVEST		.19	ATAX NET INCOME/INVEST		.51	----	-----	-----
BTAX NET INCOME/INVEST (DISC)		.30	ATAX NET INCOME/INVEST (DISC)		.46	2.0	-1360247.249	-829750.821
PRODUCTION START DATE		1/ 1/ 0	PROJECT LIFE (YEARS)		31.00	5.0	-1105451.631	-719077.866
MONTHS IN FIRST LINE		12.00	DISCOUNT RATE (PCT)		10.00	8.0	-909099.669	-644953.750
GROSS WELLS		1.00	PRIOR DEPL. BASIS (M\$)		.000	10.0	-808527.100	-611285.521
			PRIOR DEPR. BASIS (M\$)		.000	12.0	-763205.065	-595177.219
						15.0	-725841.115	-579911.690
						18.0	-677187.922	-556042.639
						20.0	-633084.263	-530395.438
						25.0	-606216.738	-512576.537
MAX. OIL PR. (/B)		31.93	MAX. GAS PRICE (\$/M)		.00			

CUMULATIVE OIL (BBL) .000  
REMAINING OIL (BBL) 200000.000  
ULTIMATE OIL (MBBL) 200000.000

CUMULATIVE GAS (MMCF)  
REMAINING GAS (MMCF)  
ULTIMATE GAS (MMCF)

.000  
.000  
.000

INITIAL W.I. FRACTION 1.00000000  
INITIAL NET OIL FRACTION .87500000  
INITIAL NET GAS FRACTION .00000000

FINAL W.I. FRACTION  
FINAL NET OIL FRACTION  
FINAL NET GAS FRACTION

1.00000000  
.87500000  
.00000000

30.0	-483330.956	-423712.573
35.0	-432950.059	-383517.898
40.0	-389287.389	-347488.851
45.0	-351682.566	-315682.194
50.0	-319374.625	-287831.845
60.0	-267728.497	-242379.747
70.0	-229277.792	-207843.269
80.0	-200272.227	-181422.374
90.0	-178066.926	-160997.566
100.0	-160815.474	-145022.966

OGRE(R) 1 BATA  
 FILE NAME. KUVLUM ( 17)  
 CASE NAME: MIN ECON SIZE  
 CMD NAME: STDY0930( 300)

DATA PORT

DATE: 02/24/94  
 TIME: 16:09:34

101 DETERMINE MINIMUM ECONOMIC SIZE  
 102 PROD 100 WELLS RESERVES = 400 MMDBLS  
 103 SINGLE (LARGE) DRILLING & PRODUCTION PLATFORM

117 CASE \$CON  
 \* 107 KUVLUM DEVELOPMENT PROJECT  
 \* 120 01 94 12 1 1 94 10 1  
 \* 131 DRILL ACRS 7 DELAY 0 0 0  
 \* 132 PRODFAC ACRS 7 DELAY 0 0 0  
 \* 133 PIPELINE ACRS 7 DELAY 0 0 0  
 \* 134 DRILLSITE ACRS 7 DELAY 0 0 0  
 168!  
 169! TOTAL TAX IS 39 PERCENT  
 \* 170 39  
 \* 600 SET IDCAMORT = MAJOR

	W.I. FRACTION	OP. COST (\$/W/MO)	OP. COST (\$/MO.)	ADV. TAX (PCT)	MAJOR PH. NAME	PROD DATE (MO/DY/YR)	
210	1.00000000	.00	.00	.000	OIL	1/ 1/ 0	

	PHASE NAME	CUM PROD (MUNITS)	REV. INT FRACTION	PRICE (\$/UNIT)	SEV. TAX (PCT)	NO. OF WELLS	RATIO TO MAJOR PH
221	OIL	.000	.87500000	.000	.000	1.0	

300 CASE \$RESERVES200MM

300 SERIES LINES:

	MAN	OIL
* 305	FACT	
* 310		2000.000
* 311	12.	10000.000
* 312	12.	14000.000
* 313	12.	14000.000
* 314	12.	14000.000
* 315	12.	14000.000
* 316	12.	14000.000
* 317	12.	13600.000
* 318	12.	12600.000
* 319	12.	11600.000
* 320	12.	10600.000
* 321	12.	9200.000
* 322	12.	8200.000
* 323	12.	7600.000
* 324	12.	6800.000
* 325	12.	6200.000
* 326	12.	5400.000
* 327	12.	4800.000
* 328	12.	4400.000
* 329	12.	3800.000
* 330	12.	3400.000
* 331	12.	3000.000
* 332	12.	2600.000
* 333	12.	2200.000
* 334	12.	2000.000
* 335	12.	2000.000

610 CA LOW

```

* 600 DATA C      : 12.33 12.89 13.61 14.36
* 605 15.16 16.00 16.89 17.15 17.41 17.67 17.94
* 610 18.21 18.76 19.32 19.90 20.50 21.11
* 615 21.74 22.40 23.07 23.76 24.47 25.21
* 620 25.96 26.74 27.54 28.37 29.22 30.10
* 621 31.00 31.93
611! OPERATING COST
615 DATA OPCOST 1000 : 0 0 0 0 0 0
616 7484 LIFE
617!
618!
619!
620 DATA OPCOST : ESC 3 %
630 DATA ESCINV : 0 3 TO FRAME 40
800! INVESTMENTS FOR THE COASTAL PIPELINE
801!

```

[illegible]



DETERMINE MII 4 ECONOMIC SIZE  
 PROD 100 WELLS RESERVES = 400 MMBBLS  
 SINGLE (LARGE) DRILLING & PRODUCTION PLA

DATE: 02/24/94  
 TIME: 16:09:34  
 FILE: KUVLUM  
 GETS: 17

# RESERVED AND ECONOMICS

## KUVLUM DEVELOPMENT PROJECT

AS OF JANUARY 1, 1994

-END- MO-YR	---GROSS PRODUCTION---		---NET PRODUCTION---		---PRICES---		NO. OF WELLS	---OPERATIONS, M\$---			
	OIL, MMBL	GAS, MMCF	OIL, MMBL	GAS, MMCF	OIL \$/B	GAS \$/M		OIL REVENUE	GAS REVENUE	OTHER REVENUE	TOTAL REVENUE
12-94	.000	.000	.000	.000	12.33	.00	.0	.000	.000	.000	.000
12-95	.000	.000	.000	.000	12.89	.00	.0	.000	.000	.000	.000
12-96	.000	.000	.000	.000	13.61	.00	.0	.000	.000	.000	.000
12-97	.000	.000	.000	.000	14.36	.00	.0	.000	.000	.000	.000
12-98	.000	.000	.000	.000	15.16	.00	.0	.000	.000	.000	.000
12-99	.000	.000	.000	.000	16.00	.00	.0	.000	.000	.000	.000
12- 0	20000.000	.000	17500.000	.000	16.89	.00	1.0	295575.000	.000	.000	295575.000
12- 1	28000.000	.000	24500.000	.000	17.15	.00	1.0	420175.000	.000	.000	420175.000
12- 2	28000.000	.000	24500.000	.000	17.41	.00	1.0	426545.000	.000	.000	426545.000
12- 3	28000.000	.000	24500.000	.000	17.67	.00	1.0	432915.000	.000	.000	432915.000
12- 4	28000.000	.000	24500.000	.000	17.94	.00	1.0	439530.000	.000	.000	439530.000
12- 5	28000.000	.000	24500.000	.000	18.21	.00	1.0	446145.000	.000	.000	446145.000
12- 6	27200.000	.000	23800.000	.000	18.76	.00	1.0	446488.000	.000	.000	446488.000
12- 7	25200.000	.000	22050.000	.000	19.32	.00	1.0	426006.000	.000	.000	426006.000
12- 8	23200.000	.000	20300.000	.000	19.90	.00	1.0	403970.000	.000	.000	403970.000
12- 9	21200.000	.000	18550.000	.000	20.50	.00	1.0	380275.000	.000	.000	380275.000
12-10	18400.000	.000	16100.000	.000	21.11	.00	1.0	339871.000	.000	.000	339871.000
12-11	16400.000	.000	14350.000	.000	21.74	.00	1.0	311969.000	.000	.000	311969.000
12-12	15200.000	.000	13300.000	.000	22.40	.00	1.0	297920.000	.000	.000	297920.000
12-13	13600.000	.000	11900.000	.000	23.07	.00	1.0	274533.000	.000	.000	274533.000
12-14	12400.000	.000	10850.000	.000	23.76	.00	1.0	257796.000	.000	.000	257796.000
12-15	10800.000	.000	9450.000	.000	24.47	.00	1.0	231241.500	.000	.000	231241.500
12-16	9600.000	.000	8400.000	.000	25.21	.00	1.0	211764.000	.000	.000	211764.000
12-17	8800.000	.000	7700.000	.000	25.96	.00	1.0	199892.000	.000	.000	199892.000
12-18	7600.000	.000	6650.000	.000	26.74	.00	1.0	177821.000	.000	.000	177821.000
12-19	6800.000	.000	5950.000	.000	27.54	.00	1.0	163863.000	.000	.000	163863.000
12-20	6000.000	.000	5250.000	.000	28.37	.00	1.0	148942.500	.000	.000	148942.500
12-21	5200.000	.000	4550.000	.000	29.22	.00	1.0	132951.000	.000	.000	132951.000
12-22	4400.000	.000	3850.000	.000	30.10	.00	1.0	115885.000	.000	.000	115885.000
12-23	4000.000	.000	3500.000	.000	31.00	.00	1.0	108500.000	.000	.000	108500.000
12-24	4000.000	.000	3500.000	.000	31.93	.00	1.0	111755.000	.000	.000	111755.000
12-25	.000	.000	.000	.000	.00	.00	1.0	.000	.000	.000	.000
S TOT	400000.000	.000	350000.000	.000	20.58	.00	1.0	7202328.000	.000	.000	7202328.000
REM.	.000	.000	.000	.000	.00	.00	.0	.000	.000	.000	.000
TOTAL	400000.000	.000	350000.000	.000	20.58	.00	.0	7202328.000	.000	.000	7202328.000

-END- MO-YR	---OPERATIONS, M\$---				---CAPITAL COSTS, M\$---				10.00 PCT	
	SEVERANCE TAXES	AD VAL TAXES	NET OPER EXPENSES	OPERATIONS CASH FLOW	TANGIBLE COSTS	INTANG. COSTS	LEASEHOLD COSTS	SALVAGE VALUE	CASH FLOW BTAX, M\$	CUM. DISC BTAX, M\$
12-94	.000	.000	.000	.000	15530.000	59670.000	.000	.000	-75200.000	-74967.313
12-95	.000	.000	.000	.000	19415.500	.000	.000	.000	-19415.500	-91796.361
12-96	.000	.000	.000	.000	131392.465	.000	.000	.000	-131392.465	-195331.733
12-97	.000	.000	.000	.000	333445.644	.000	.000	.000	-333445.644	-434195.705
12-98	.000	.000	.000	.000	443788.124	.000	.000	.000	-443788.124	-723202.859
12-99	.000	.000	.000	.000	400703.084	70947.573	.000	.000	-471650.657	-1002431.958
12- 0	.000	.000	107235.449	188339.551	12895.765	73076.001	.000	.000	102367.786	-947298.756
12- 1	.000	.000	110452.512	309722.488	13282.638	75268.281	.000	.000	221171.570	-839027.214
12- 2	.000	.000	113766.087	312778.913	15961.303	.94	.000	.000	206370.226	-747181.623
12- 3	.000	.000	117179.070	315735.930	.000	.00	.000	.000	315735.930	-619461.930
12- 4	.000	.000	.000	.000	.000	.00	.000	.000	.000	.000

12-5	.000	.000	124318.275	321829.725	.000	.000	.000	321829.725	-394622.582	
12-6	.000	.000	128044.734	318443.266	.000	.000	.000	318443.266	-297842.079	
12-7	.000	.000	131886.076	294119.924	.000	.000	.000	294119.924	-216580.068	
12-8	.000	.000	135842.658	268127.342	.000	.000	.000	268127.342	-149234.110	
12-9	.000	.000	139917.938	240357.062	.000	.000	.000	240357.062	-94351.515	
12-10	.000	.000	144115.476	195755.524	.000	.000	.000	195755.524	-53716.625	
12-11	.000	.000	148438.940	163530.060	.000	.000	.000	163530.060	-22857.048	
12-12	.000	.000	152892.108	145027.892	.000	.000	.000	145027.892	2023.001	
12-13	.000	.000	157478.872	117054.128	.000	.000	.000	117054.128	20278.501	
12-14	.000	.000	162203.238	95592.762	.000	.000	.000	95592.762	33831.623	
12-15	.000	.000	167069.335	64172.165	.000	.000	.000	64172.165	42102.819	
12-16	.000	.000	172081.415	39682.585	.000	.000	.000	39682.585	46752.562	
12-17	.000	.000	177243.857	22648.143	.000	.000	.000	22648.143	49165.071	
12-18	.000	.000	182561.173	-4740.173	.000	.000	.000	-4740.173	48706.044	
12-19	.000	.000	188038.008	-24175.008	.000	.000	.000	-24175.008	46577.819	
12-20	.000	.000	193679.149	-44736.649	.000	.000	.000	-44736.649	42997.501	
12-21	.000	.000	199489.523	-66538.523	.000	.000	.000	-66538.523	38156.461	
12-22	.000	.000	205474.209	-89589.209	.000	.000	.000	-89589.209	32230.913	
12-23	.000	.000	211638.435	-103138.435	.000	.000	.000	-103138.435	26029.357	
12-24	.000	.000	217987.588	-106232.588	.000	.000	.000	-106232.588	20222.445	
12-25	.000	.000	.000	.000	.000	.000	.000	.000	20222.445	
S TOT	.000	.000	3909725.567	3292602.433	1386414.522	369409.238	.000	.000	1536778.673	20222.445
REM.	.000	.000	.000	.000	.000	.000	.000	.000	.000	20222.445
TOTAL	.000	.000	3909725.567	3292602.433	1386414.522	369409.238	.000	.000	1536778.673	20222.445

DATE: 02/24/94  
TIME: 16:09:34  
FILE: KUVLUM  
GET: 17

## KUVLUM DEVELOPMENT PROJECT

AS OF JANUARY 1, 1994

				-----PRESENT WORTH PROFILE-----		
				DISC	PW OF NET	PW OF NET
				RATE	BTAX, M\$	ATAX, M\$
BTAX RATE OF RETURN (PCT)	10.34	ATAX RATE OF RETURN (PCT)	7.85			
BTAX PAYOUT YEARS	11.96	ATAX PAYOUT YEARS	12.29			
BTAX PAYOUT YEARS (DISC)	18.92	ATAX PAYOUT YEARS (DISC)	31.00			
BTAX NET INCOME/INVEST	1.88	ATAX NET INCOME/INVEST	1.53	.0	1536778.673	937434.993
BTAX NET INCOME/INVEST (DISC)	1.02	ATAX NET INCOME/INVEST (DISC)	.89	2.0	1057710.865	598543.718
				5.0	530911.438	229668.114
				8.0	181637.991	-12136.352
PRODUCTION START DATE	1/ 1/ 0	PROJECT LIFE (YEARS)	31.00	10.0	20222.445	-122542.922
MONTHS IN FIRST LINE	12.00	DISCOUNT RATE (PCT)	10.00	12.0	52266.320	-203148.237
GROSS WELLS	1.00	PRIOR DEPL. BASIS (M\$)	.000	15.0	-220768.704	-283228.681
		PRIOR DEPR. BASIS (M\$)	.000	18.0	-294348.376	-329296.354
				20.0	-325111.327	-347066.091
MAX. OIL PI (B)	31.93	MAX. GAS PRICE (\$/M)	.00			
GROSS OIL	1.00	GROSS GAS	.00			

CUMULATIVE OI (BL) .000  
REMAINING OIL (MBBL) 400000.000  
ULTIMATE OIL (MBBL) 400000.000

CUMULATIVE GAS (MMCF)  
REMAINING GAS (MMCF)  
ULTIMATE GAS (MMCF)

.000  
.000  
.000

INITIAL W.I. FRACTION 1.00000000  
INITIAL NET OIL FRACTION .87500000  
INITIAL NET GAS FRACTION .00000000

FINAL W.I. FRACTION  
FINAL NET OIL FRACTION  
FINAL NET GAS FRACTION

1.00000000  
.87500000  
.00000000

30.0	-364991.240	-356022.485
35.0	-352729.850	-338576.562
40.0	-333737.681	-317122.309
45.0	-312534.725	-294890.952
50.0	-291381.027	-273463.093
60.0	-252918.684	-235426.734
70.0	-221186.583	-204516.130
80.0	-195770.946	-179930.323
90.0	-175553.633	-160450.900
100.0	-159432.548	-144963.012

OGRE(R) 1 BATAK  
 FILE NAME: KUVLUM ( 17)  
 CASE NAME: MIN ECON SIZE  
 CMD NAME: STDD1304( 300)

DATA . PORT

DATE: 02/24/94  
 TIME: 16:13:09

101 DETERMINE MINIMUM ECONOMIC SIZE  
 102 PROD 100 WELLS RESERVES = 600 MMHLS  
 103 SINGLE (LARGE) DRILLING & PRODUCTION PLATFORM

117 CASE \$COM  
 \* 107 KUVLUM DEVELOPMENT PROJECT  
 \* 120 01 94 12 1 1 94 10 1  
 \* 131 DRILL ACRS 7 DELAY 0 0 0  
 \* 132 PRODFAC ACRS 7 DELAY 0 0 0  
 \* 133 PIPELINE ACRS 7 DELAY 0 0 0  
 \* 134 DRILLSITE ACRS 7 DELAY 0 0 0  
 168!  
 169! TOTAL TAX IS 39 PERCENT  
 \* 170 39  
 \* 600 SET IDCAMORT = MAJOR

	W.I. FRACTION	OP. COST (\$/W/MO)	OP. COST (\$/MO.)	ADV. TAX (PCT)	MAJOR PH. NAME	PROD DATE (MO/DY/YR)	
210	1.00000000	.00	.00	.000	OIL	1/ 1/ 0	

	PHASE NAME	CUM PROD (MUNITS)	REV. INT FRACTION	PRICE (\$/UNIT)	SEV. TAX (PCT)	NO. OF WELLS	RATIO TO MAJOR PH
221	OIL	.000	.87500000	.000	.000	1.0	

300 CASE \$RESERVES200MM

300 SERIES LINES:

	MAN	OIL
* 305	FACT	3000.000
* 310		
* 311	12.	10000.000
* 312	12.	14000.000
* 313	12.	14000.000
* 314	12.	14000.000
* 315	12.	14000.000
* 316	12.	14000.000
* 317	12.	13600.000
* 318	12.	12600.000
* 319	12.	11600.000
* 320	12.	10600.000
* 321	12.	9200.000
* 322	12.	8200.000
* 323	12.	7600.000
* 324	12.	6800.000
* 325	12.	6200.000
* 326	12.	5400.000
* 327	12.	4800.000
* 328	12.	4400.000
* 329	12.	3800.000
* 330	12.	3400.000
* 331	12.	3000.000
* 332	12.	2600.000
* 333	12.	2200.000
* 334	12.	2000.000
* 335	12.	2000.000

600 SEPT

\* 600 DATA : 12.33 12.89 13.61 14.36  
 \* 605 15.16 16.00 16.89 17.15 17.41 17.67 17.94  
 \* 610 18.21 18.76 19.32 19.90 20.50 21.11  
 \* 615 21.74 22.40 23.07 23.76 24.47 25.21  
 \* 620 25.96 26.74 27.54 28.37 29.22 30.10  
 \* 621 31.00 31.93

611! OPERATING COST

615 DATA OPCOST 1000 : 0 0 0 0 0 0

616 8720 LIFE

617!

618!

619!

620 DATA OPCOST : ESC 3 4

630 DATA ESCINV : 0 3 TO FRAME 40

800! INVESTMENTS FOR THE COASTAL PIPELINE

801!

	INV NAME	INV. POINT	(G OR N)	TANG-M\$	INTANG-M\$	LSEHLD-M\$	RISK FRAC	OVHD FLAG
802	PIPELINE	-54.000 MOS	G	6500.000	.000	.000	1.000	
803	PIPELINE	-42.000 MOS	G	6500.000	.000	.000	1.000	
804	PIPELINE	-30.000 MOS	G	58500.000	.000	.000	1.000	
805	PIPELINE	-18.000 MOS	G	52000.000	.000	.000	1.000	
806	PIPELINE	-6.000 MOS	G	6500.000	.000	.000	1.000	
807!	INVESTMENTS FOR THE MAIN PIPELINE							
808	PIPELINE	-54.000 MOS	G	7350.000	.000	.000	1.000	
811	PIPELINE	-42.000 MOS	G	7350.000	.000	.000	1.000	
812	PIPELINE	-30.000 MOS	G	66150.000	.000	.000	1.000	
813	PIPELINE	-18.000 MOS	G	58800.000	.000	.000	1.000	
814	PIPELINE	-6.000 MOS	G	7350.000	.000	.000	1.000	
815!								
816!	INVESTMENTS FOR MAIN PRODUCTION PLATFORM							
817!	STRUCTURE							
818	PRODFAC	-42.000 MOS	G	105000.000	.000	.000	1.000	
819	PRODFAC	-30.000 MOS	G	157500.000	.000	.000	1.000	
820	PRODFAC	-18.000 MOS	G	157500.000	.000	.000	1.000	
821	PRODFAC	-6.000 MOS	G	105000.000	.000	.000	1.000	
822!	PRODUCTION FACILITIES							
823	PRODFAC	-30.000 MOS	G	21000.000	.000	.000	1.000	
824	PRODFAC	-18.000 MOS	G	147000.000	.000	.000	1.000	
825	PRODFAC	-6.000 MOS	G	252000.000	.000	.000	1.000	
826!								
827!	INVESTMENTS FOR PERMITTING							
828	PRODFAC	-66.000 MOS	G	5000.000	.000	.000	1.000	
829	PRODFAC	-54.000 MOS	G	5000.000	.000	.000	1.000	
830	PRODFAC	-42.000 MOS	G	5000.000	.000	.000	1.000	
831	PRODFAC	-30.000 MOS	G	5000.000	.000	.000	1.000	
832!	DELINEATION WELLS THEN PRODUCTION WELLS							
833!								
834	DRILL	-6.000 MOS	G	10500.000	61200.000	.000	1.000	
835	DRILL	-72.000 MOS	G	10530.000	59670.000	.000	1.000	
836	DRILL	6.000 MOS	G	10800.000	61200.000	.000	1.000	
837	DRILL	18.000 MOS	G	10800.000	61200.000	.000	1.000	
838	DRILL	30.000 MOS	G	12600.000	71400.000	.000	1.000	
839!								
840	ESC	USING	ESGINV					

850 NOLOSS OFF

DATE: 02/24/94  
TIME: 16:13:09  
FILE: KUVLUM  
GETA: 17

.....

AS OF JANUARY 1, 1994

S TOT	600000.000	.000	525000.000	.000	20.58	.00	1.010803492.000	.000	.000	10803492.000
REM.	.000	.000	.000	.000	.00	.00	.0	.000	.000	.000
TOTAL	600000.000	.000	525000.000	.000	20.58	.00	1.010803492.000	.000	.000	10803492.000

-END- MO-YR	-OPERATIONS, M\$-				-CAPITAL COSTS, M\$-				CASH FLOW BTAX, M\$	10.00 PCT CUM. DISC BTAX, M\$
	SEVERANCE TAXES	AD VAL TAXES	NET OPER EXPENSES	OPERATIONS CASH FLOW	TANGIBLE COSTS	INTANG. COSTS	LSHOLD COSTS	SALVAGE VALUE		
12-94	.000	.000	.000	.000	15530.000	59670.000	.000	.000	-75200.000	-74967.313
12-95	.000	.000	.000	.000	19415.500	.000	.000	.000	-19415.500	-91796.361
12-96	.000	.000	.000	.000	131392.465	.000	.000	.000	-131392.465	-195331.733
12-97	.000	.000	.000	.000	336723.825	.000	.000	.000	-336723.825	-436544.032
12-98	.000	.000	.000	.000	467423.809	.000	.000	.000	-467423.809	-740943.400
12-99	.000	.000	.000	.000	442436.950	70947.573	.000	.000	-513384.524	-1044880.002
12- 0	.000	.000	124945.632	318416.868	12895.765	73076.001	.000	.000	232445.103	-919712.066
12- 1	.000	.000	128094.001	501568.499	13282.638	75268.281	.000	.000	413017.581	-717539.138
12- 2	.00	.000	132554.821	507262.679	15961.303	9	.000	.000	400853.992	-539154.940
12- 3	.00	.000	136531.466	512841.034	.000	0	.000	.000	512841.034	-331703.417
12- 4	.000	.000	0.000	0.000	0.000	0.000	.000	.000	0.000	340.000

12-5	.000	.000	144846.232	524371.268	.000	.000	.000	524371.268	34333.740
12-6	.000	.000	149191.619	520540.381	.000	.000	.000	520540.381	192535.106
12-7	.000	.000	153667.368	485341.632	.000	.000	.000	485341.632	326629.513
12-8	.000	.000	158277.389	447677.611	.000	.000	.000	447677.611	439073.389
12-9	.000	.000	163025.710	407386.790	.000	.000	.000	407386.790	532095.179
12-10	.000	.000	167916.482	341890.018	.000	.000	.000	341890.018	603064.636
12-11	.000	.000	172953.976	294999.524	.000	.000	.000	294999.524	658733.671
12-12	.000	.000	178142.596	268737.404	.000	.000	.000	268737.404	704836.525
12-13	.000	.000	183486.873	228312.627	.000	.000	.000	228312.627	740443.652
12-14	.000	.000	188991.480	197702.520	.000	.000	.000	197702.520	768473.873
12-15	.000	.000	194661.224	152201.026	.000	.000	.000	152201.026	788091.172
12-16	.000	.000	200501.061	117144.939	.000	.000	.000	117144.939	801817.440
12-17	.000	.000	206516.093	93321.907	.000	.000	.000	93321.907	811758.206
12-18	.000	.000	212711.575	54019.925	.000	.000	.000	54019.925	816989.361
12-19	.000	.000	219092.923	26701.577	.000	.000	.000	26701.577	819340.010
12-20	.000	.000	225665.710	-2251.960	.000	.000	.000	-2251.960	819159.783
12-21	.000	.000	232435.682	-33009.182	.000	.000	.000	-33009.182	816758.185
12-22	.000	.000	239408.752	-65581.252	.000	.000	.000	-65581.252	812420.555
12-23	.000	.000	246591.015	-83841.015	.000	.000	.000	-83841.015	807379.323
12-24	.000	.000	253988.745	-86356.245	.000	.000	.000	-86356.245	802658.897
12-25	.000	.000	.000	.000	.000	.000	.000	.000	802658.897
S TOT	.000	.000	4555425.835	6248066.165	1455062.255	369409.238	.000	.000	4423594.672
REM.	.000	.000	.000	.000	.000	.000	.000	.000	802658.897
TOTAL	.000	.000	4555425.835	6248066.165	1455062.255	369409.238	.000	.000	4423594.672



DETERMINE MI M ECONOMIC SIZE  
 PROD 100 WELL RESERVES = 600 MMBBLS  
 SINGLE (LARGE) DRILLING & PRODUCTION PIA

DATE: 02/24/94  
 TIME: 16:13:09  
 FILE: KUVIUM  
 GET#: 17

# AFTER TAX ECONOMICS

## KUVIUM DEVELOPMENT PROJECT

AS OF JANUARY 1, 1994

-END- MO-YR	OPER CASH FLOW, M\$	DEPR. EXP., M\$	DEPL. EXP., M\$	INTANG. EXP., M\$	INTEREST EXP., M\$	TAXABLE INCOME M\$	TAX CREDIT M\$	TAXES PAYABLE M\$	CASH FLOW ATAK, M\$	10.00 PCT CUM. DISC ATAK, M\$
12-94	.000	.000	.000	45349.200	.000	-45349.200	.000	-17686.188	-57513.812	-58097.811
12-95	.000	.000	.000	3580.200	.000	-3580.200	.000	-1396.278	-18019.222	-73716.129
12-96	.000	.000	.000	3580.200	.000	-3580.200	.000	-1396.278	-129996.187	-176150.838
12-97	.000	.000	.000	3580.200	.000	-3580.200	.000	-1396.278	-335327.547	-416362.534
12-98	.000	.000	.000	3580.200	.000	-3580.200	.000	-1396.278	-466027.531	-719852.263
12-99	.000	.000	.000	51791.729	.000	-51791.729	.000	-20198.774	-493185.750	-1011826.154
12- 0	318416.868	203692.408	.000	57602.335	.000	57122.125	.000	22277.629	210167.474	-898652.683
12- 1	501568.499	351080.459	.000	63587.259	.000	86900.781	.000	33891.305	379126.276	-713068.271
12- 2	507262.679	254937.298	.000	79184.101	.000	173141.280	.000	67525.099	333328.893	-564730.426
12- 3	512841.034	184388.319	.000	18584.354	.000	309868.361	.000	120848.661	391992.373	-406163.913
12- 4	518667.590	131705.904	.000	16455.927	.000	370505.759	.000	144497.246	374170.344	-268566.415
12- 5	524371.268	130434.127	.000	12135.220	.000	381801.921	.000	148902.749	375468.519	-143043.788
12- 6	520540.381	129864.309	.000	7684.891	.000	382991.181	.000	149366.560	371173.821	-30237.543
12- 7	485341.632	66230.034	.000	2713.422	.000	416398.176	.000	162395.289	322946.343	58988.882
12- 8	447677.611	2017.217	.000	.000	.000	445660.394	.000	173807.554	273870.057	127777.247
12- 9	407386.790	712.194	.000	.000	.000	406674.596	.000	158603.092	248783.698	184583.961
12-10	341890.018	.000	.000	.000	.000	341890.018	.000	133337.107	208552.911	227875.330
12-11	294999.524	.000	.000	.000	.000	294999.524	.000	115049.814	179949.710	261833.441
12-12	268737.404	.000	.000	.000	.000	268737.404	.000	104807.588	163929.816	289956.182
12-13	228312.627	.000	.000	.000	.000	228312.627	.000	89041.925	139270.702	311676.530
12-14	197702.520	.000	.000	.000	.000	197702.520	.000	77103.983	120598.537	328774.965
12-15	152201.026	.000	.000	.000	.000	152201.026	.000	59358.400	92842.626	340741.518
12-16	117144.939	.000	.000	.000	.000	117144.939	.000	45686.526	71458.413	349114.542
12-17	93321.907	.000	.000	.000	.000	93321.907	.000	36395.544	56926.363	355178.410
12-18	54019.925	.000	.000	.000	.000	54019.925	.000	21067.771	32952.154	358369.414
12-19	26701.577	.000	.000	.000	.000	26701.577	.000	10413.615	16287.962	359803.310
12-20	-2251.960	.000	.000	.000	.000	-2251.960	.000	-878.264	-1373.696	359693.372
12-21	-33009.182	.000	.000	.000	.000	-33009.182	.000	-12873.581	-20135.601	358228.397
12-22	-65581.252	.000	.000	.000	.000	-65581.252	.000	-25576.688	-40004.564	355582.442
12-23	-83841.015	.000	.000	.000	.000	-83841.015	.000	-32697.996	-51143.019	352507.290
12-24	-86356.245	.000	.000	.000	.000	-86356.245	.000	-33678.936	-52677.309	349627.830
12-25	.000	-.013	.000	.000	.000	.013	.000	.005	-.005	349627.830
S TOT	6248066.165	1455062.256	.000	369409.238	.000	4423594.671	.000	1725201.923	2698392.749	349627.830
REM.	.000	.000	.000	.000	.000	.000	.000	.000	.000	349627.830
TOTAL	6248066.165	1455062.256	.000	369409.238	.000	4423594.671	.000	1725201.923	2698392.749	349627.830

BTAX RATE OF RETURN (PCT)	19.00	ATAK RATE OF RETURN (PCT)	14.83	----PRESENT WORTH PROFILE----
BTAX PAYOUT YEARS	9.97	ATAK PAYOUT YEARS	10.50	DISC PW OF NET PW OF NET
BTAX PAYOUT YEARS (DISC)	11.80	ATAK PAYOUT YEARS (DISC)	13.34	RATE BTAX, M\$ ATAX, M\$
BTAX NET INCOME/INVEST	3.42	ATAK NET INCOME/INVEST	2.48	----
BTAX NET INCOME/INVEST (DISC)	1.68	ATAK NET INCOME/INVEST (DISC)	1.30	2.0 4423594.672 2698392.749
				5.0 3214436.762 1912292.538
				8.0 1170181.170 586155.159
				12.0 526866.334 173410.373
				15.0 235455.847 -10387.909
				18.0 44399.593 -128049.098
				20.0 2.46 -1813.005
				25.0 -10252.812 -258612.632

PRODUCTION START DATE	1/ 1/ 0	PROJECT LIFE (YEARS)	31.00
MONTHS IN FIRST LINE	12.00	DISCOUNT RATE (PCT)	10.00
GROSS WELLS	1.00	PRIOR DEPR. BASIS (M\$)	.000
		PRIOR DEPR. BASIS (M\$)	.000

CUMULATIVE OIL (MBBL) .000  
REMAINING OIL (MBBL) 600000.000  
ULTIMATE OIL (MBBL) 600000.000

CUMULATIVE GAS (MMCF)  
REMAINING GAS (MMCF)  
ULTIMATE GAS (MMCF)

.000  
.000  
.000

INITIAL W.I. FRACTION 1.00000000  
INITIAL NET OIL FRACTION .87500000  
INITIAL NET GAS FRACTION .00000000

FINAL W.I. FRACTION  
FINAL NET OIL FRACTION  
FINAL NET GAS FRACTION

1.00000000  
.87500000  
.00000000

30.0	-246441.619	-288099.880
35.0	-272310.039	-293424.683
40.0	-278009.830	-286572.481
45.0	-273233.017	-273943.644
50.0	-263257.103	-258963.308
60.0	-238018.667	-228383.917
70.0	-213035.143	-201129.336
80.0	-191230.993	-178400.111
90.0	-173016.952	-159881.246
100.0	-158037.021	-144890.756

OGRE(R) 1 BATAK  
 FILE NAME: KUVLUM ( 17)  
 CASE NAME: MIN ECON SIZE  
 CMD NAME: STDE1758( 300)

DATA PORT

DATE: 02/24/94  
 TIME: 16:18:04

101 DETERMINE MINIMUM ECONOMIC SIZE  
 102 PROD 100 WELLS RESERVES = 800 MMBSLS  
 103 SINGLE (LARGE) DRILLING & PRODUCTION PLATFORM

117 CASE \$COM  
 \* 107 KUVLUM DEVELOPMENT PROJECT  
 \* 120 01 94 12 1 1 94 10 1  
 \* 131 DRILL ACRS 7 DELAY 0 0 0  
 \* 132 PRODFAC ACRS 7 DELAY 0 0 0  
 \* 133 PIPELINE ACRS 7 DELAY 0 0 0  
 \* 134 DRILLSITE ACRS 7 DELAY 0 0 0  
 168!  
 169! TOTAL TAX IS 39 PERCENT  
 \* 170 39  
 \* 600 SET IDCAMORT = MAJOR

	W.I. FRACTION	OP. COST (\$/W/MO)	OP. COST (\$/MO.)	ADV. TAX (PCT)	MAJOR PH. NAME	PROD DATE (MO/DY/YR)
210	1.00000000	.00	.00	.000	OIL	1/ 1/ 0

	PHASE NAME	CUM PROD (MUNITS)	REV. INT FRACTION	PRICE (\$/UNIT)	SEV. TAX (PCT)	NO. OF WELLS	RATIO TO MAJOR PH
221	OIL	.000	.87500000	.000	.000	1.0	

300 CASE \$RESERVES200MM

300 SERIES LINES:

	MAN	OIL
* 305	FACT	4000.000
* 310	12.	10000.000
* 311	12.	14000.000
* 312	12.	14000.000
* 313	12.	14000.000
* 314	12.	14000.000
* 315	12.	14000.000
* 316	12.	14000.000
* 317	12.	13600.000
* 318	12.	12600.000
* 319	12.	11600.000
* 320	12.	10600.000
* 321	12.	9200.000
* 322	12.	8200.000
* 323	12.	7600.000
* 324	12.	6800.000
* 325	12.	6200.000
* 326	12.	5400.000
* 327	12.	4800.000
* 328	12.	4400.000
* 329	12.	3800.000
* 330	12.	3400.000
* 331	12.	3000.000
* 332	12.	2600.000
* 333	12.	2200.000
* 334	12.	2000.000
* 335	12.	2000.000

600 SERI: ES:

\* 600 DATA OILP : 12.33 12.89 13.61 14.36  
 \* 605 15.16 16.00 16.89 17.15 17.41 17.67 17.94  
 \* 610 18.21 18.76 19.32 19.90 20.50 21.11  
 \* 615 21.74 22.40 23.07 23.76 24.47 25.21  
 \* 620 25.96 26.74 27.54 28.37 29.22 30.10  
 \* 621 31.00 31.93

611! OPERATING COST

615 DATA OPCOST 1000 : 0 0 0 0 0 0

616 9980 LIFE

617!

618!

619!

620 DATA OPCOST : ESC 3

630 DATA ESCINV : 0 3 TO FRAME 40

800! INVESTMENTS FOR THE COASTAL PIPELINE

801!

	INV NAME	INV. POINT	(G OR N)	TANG-M\$	INTANG-M\$	LSEHLD-M\$	RISK FRAC	OVHD FLAG
802	PIPELINE	-54.000 MOS	G	6500.000	.000	.000	1.000	
803	PIPELINE	-42.000 MOS	G	6500.000	.000	.000	1.000	
804	PIPELINE	-30.000 MOS	G	58500.000	.000	.000	1.000	
805	PIPELINE	-18.000 MOS	G	52000.000	.000	.000	1.000	
806	PIPELINE	-6.000 MOS	G	6500.000	.000	.000	1.000	
807!	INVESTMENTS FOR THE MAIN PIPELINE							
808	PIPELINE	-54.000 MOS	G	7350.000	.000	.000	1.000	
811	PIPELINE	-42.000 MOS	G	7350.000	.000	.000	1.000	
812	PIPELINE	-30.000 MOS	G	66150.000	.000	.000	1.000	
813	PIPELINE	-18.000 MOS	G	58800.000	.000	.000	1.000	
814	PIPELINE	-6.000 MOS	G	7350.000	.000	.000	1.000	
815!								
816!	INVESTMENTS FOR MAIN PRODUCTION PLATFORM							
817!	STRUCTURE							
818	PRODFAC	-42.000 MOS	G	105000.000	.000	.000	1.000	
819	PRODFAC	-30.000 MOS	G	157500.000	.000	.000	1.000	
820	PRODFAC	-18.000 MOS	G	157500.000	.000	.000	1.000	
821	PRODFAC	-6.000 MOS	G	105000.000	.000	.000	1.000	
822!	PRODUCTION FACILITIES							
823	PRODFAC	-30.000 MOS	G	25000.000	.000	.000	1.000	
824	PRODFAC	-18.000 MOS	G	161000.000	.000	.000	1.000	
825	PRODFAC	-6.000 MOS	G	276000.000	.000	.000	1.000	
826!								
827!	INVESTMENTS FOR PERMITTING							
828	PRODFAC	-66.000 MOS	G	5000.000	.000	.000	1.000	
829	PRODFAC	-54.000 MOS	G	5000.000	.000	.000	1.000	
830	PRODFAC	-42.000 MOS	G	5000.000	.000	.000	1.000	
831	PRODFAC	-30.000 MOS	G	5000.000	.000	.000	1.000	
832!	DELINEATION WELLS THEN PRODUCTION WELLS							
833!								
834	DRILL	-6.000 MOS	G	10600.000	61200.000	.000	1.000	
835	DRILL	-72.000 MOS	G	10530.000	59670.000	.000	1.000	
836	DRILL	6.000 MOS	G	10800.000	61200.000	.000	1.000	
837	DRILL	18.000 MOS	G	10800.000	61200.000	.000	1.000	
838	DRILL	30.000 MOS	G	12600.000	71400.000	.000	1.000	
839!								
840	ESC	USING	ESGINV					

850 NOLOSS OFF

DETERMINE MI. M ECONOMIC SIZE  
 PROD 100 WELLS RESERVES = 800 MMBBLS  
 SINGLE (LARGE) DRILLING & PRODUCTION PLA

DATE: 02/24/94  
 TIME: 16:18:04  
 FILE: KUVLUM  
 GETI: 17

# RESERVES AND ECONOMICS

## KUVLUM DEVELOPMENT PROJECT

AS OF JANUARY 1, 1994

END- MO-YR	GROSS PRODUCTION		NET PRODUCTION		PRICES		NO. OF WELLS	OPERATIONS, M\$			
	OIL, MMBL	GAS, MMCF	OIL, MMBL	GAS, MMCF	OIL \$/B	GAS \$/M		OIL REVENUE	GAS REVENUE	OTHER REVENUE	TOTAL REVENUE
12-94	.000	.000	.000	.000	12.33	.00	.0	.000	.000	.000	.000
12-95	.000	.000	.000	.000	12.89	.00	.0	.000	.000	.000	.000
12-96	.000	.000	.000	.000	13.61	.00	.0	.000	.000	.000	.000
12-97	.000	.000	.000	.000	14.36	.00	.0	.000	.000	.000	.000
12-98	.000	.000	.000	.000	15.16	.00	.0	.000	.000	.000	.000
12-99	.000	.000	.000	.000	16.00	.00	.0	.000	.000	.000	.000
12- 0	40000.000	.000	35000.000	.000	16.89	.00	1.0	591150.000	.000	.000	591150.000
12- 1	56000.000	.000	49000.000	.000	17.15	.00	1.0	840350.000	.000	.000	840350.000
12- 2	56000.000	.000	49000.000	.000	17.41	.00	1.0	853090.000	.000	.000	853090.000
12- 3	56000.000	.000	49000.000	.000	17.67	.00	1.0	865830.000	.000	.000	865830.000
12- 4	56000.000	.000	49000.000	.000	17.94	.00	1.0	879060.000	.000	.000	879060.000
12- 5	56000.000	.000	49000.000	.000	18.21	.00	1.0	892290.000	.000	.000	892290.000
12- 6	54400.000	.000	47600.000	.000	18.76	.00	1.0	892976.000	.000	.000	892976.000
12- 7	50400.000	.000	44100.000	.000	19.32	.00	1.0	852012.000	.000	.000	852012.000
12- 8	46400.000	.000	40600.000	.000	19.90	.00	1.0	807940.000	.000	.000	807940.000
12- 9	42400.000	.000	37100.000	.000	20.50	.00	1.0	760550.000	.000	.000	760550.000
12-10	36800.000	.000	32200.000	.000	21.11	.00	1.0	679742.000	.000	.000	679742.000
12-11	32800.000	.000	28700.000	.000	21.74	.00	1.0	623938.000	.000	.000	623938.000
12-12	30400.000	.000	26600.000	.000	22.40	.00	1.0	595840.000	.000	.000	595840.000
12-13	27200.000	.000	23800.000	.000	23.07	.00	1.0	549066.000	.000	.000	549066.000
12-14	24800.000	.000	21700.000	.000	23.76	.00	1.0	515592.000	.000	.000	515592.000
12-15	21600.000	.000	18900.000	.000	24.47	.00	1.0	462483.000	.000	.000	462483.000
12-16	19200.000	.000	16800.000	.000	25.21	.00	1.0	423528.000	.000	.000	423528.000
12-17	17600.000	.000	15400.000	.000	25.96	.00	1.0	399784.000	.000	.000	399784.000
12-18	15200.000	.000	13300.000	.000	26.74	.00	1.0	355642.000	.000	.000	355642.000
12-19	13600.000	.000	11900.000	.000	27.54	.00	1.0	327726.000	.000	.000	327726.000
12-20	12000.000	.000	10500.000	.000	28.37	.00	1.0	297885.000	.000	.000	297885.000
12-21	10400.000	.000	9100.000	.000	29.22	.00	1.0	265902.000	.000	.000	265902.000
12-22	8800.000	.000	7700.000	.000	30.10	.00	1.0	231770.000	.000	.000	231770.000
12-23	8000.000	.000	7000.000	.000	31.00	.00	1.0	217000.000	.000	.000	217000.000
12-24	8000.000	.000	7000.000	.000	31.93	.00	1.0	223510.000	.000	.000	223510.000
12-25	.000	.000	.000	.000	.00	.00	1.0	.000	.000	.000	.000
S TOT	800000.000	.000	700000.000	.000	20.58	.00	1.014404656	.000	.000	.000	14404656.000
REM.	.000	.000	.000	.000	.00	.00	.0	.000	.000	.000	.000
TOTAL	800000.000	.000	700000.000	.000	20.58	.00	.014404656	.000	.000	.000	14404656.000

END- MO-YR	OPERATIONS, M\$				CAPITAL COSTS, M\$				10.00 PCT	
	SEVERANCE TAXES	AD VAL TAXES	NET OPER EXPENSES	OPERATIONS CASH FLOW	TANGIBLE COSTS	INTANG. COSTS	LEASEHOLD COSTS	SALVAGE VALUE	CASH FLOW BTAX, M\$	CUM. DISC BTAX, M\$
12-94	.000	.000	.000	.000	15530.000	59670.000	.000	.000	-75200.000	-74967.313
12-95	.000	.000	.000	.000	19415.500	.000	.000	.000	-19415.500	-91796.361
12-96	.000	.000	.000	.000	131392.465	.000	.000	.000	-131392.465	-195331.733
12-97	.000	.000	.000	.000	338909.279	.000	.000	.000	-338909.279	-438109.583
12-98	.000	.000	.000	.000	483180.932	.000	.000	.000	-483180.932	-752770.428
12-99	.000	.000	.000	.000	470259.528	70947.573	.000	.000	-541207.102	-1073178.699
12- 0	.000	.000	142999.703	448150.297	12895.765	73076.001	.000	.000	362178.532	-878161.180
12- 1	.000	.000	147289.694	693060.306	13282.638	75268.281	.000	.000	604509.388	-582260.235
12- 2	.000	.000	151708.385	701381.615	15961.303	90447.384	.000	.000	594972.928	-317499.766
12- 3	.000	.000	156259.636	709570.364	.000	.000	.000	.000	709570.364	-30468.419
12- 4	.000	.000	160947.426	718112.574	.000	.000	.000	.000	718112.574	233610.483

12- 5		.000	161375.848	7265	.000		.000	726	152	490
1		.000	170749.124	722226.876	.000		.000	.000	722226.876	695988.373
12- 7	0	.000	175871.598	676140.402	.000		.000	.000	676140.402	882798.324
12- 8	.000	.000	181147.745	626792.255	.000	.000	.000	.000	626792.255	1040230.702
12- 9	.000	.000	186582.178	573967.822	.000	.000	.000	.000	573967.822	1171289.233
12-10	.000	.000	192179.643	487562.357	.000	.000	.000	.000	487562.357	1272497.324
12-11	.000	.000	197945.032	425992.968	.000	.000	.000	.000	425992.968	1352885.988
12-12	.000	.000	203883.383	391956.617	.000	.000	.000	.000	391956.617	1420127.535
12-13	.000	.000	209999.885	339066.115	.000	.000	.000	.000	339066.115	1473007.529
12-14	.000	.000	216299.881	299292.119	.000	.000	.000	.000	299292.119	1515441.102
12-15	.000	.000	222788.878	239694.122	.000	.000	.000	.000	239694.122	1546335.449
12-16	.000	.000	229472.544	194055.456	.000	.000	.000	.000	194055.456	1569073.582
12-17	.000	.000	236356.721	163427.279	.000	.000	.000	.000	163427.279	1586482.061
12-18	.000	.000	243447.422	112194.578	.000	.000	.000	.000	112194.578	1597346.704
12-19	.000	.000	250750.845	76975.155	.000	.000	.000	.000	76975.155	1604123.142
12-20	.000	.000	258273.370	39611.630	.000	.000	.000	.000	39611.630	1607293.300
12-21	.000	.000	266021.571	-119.571	.000	.000	.000	.000	-119.571	1607284.601
12-22	.000	.000	274002.218	-42232.218	.000	.000	.000	.000	-42232.218	1604491.306
12-23	.000	.000	282222.285	-65222.285	.000	.000	.000	.000	-65222.285	1600569.590
12-24	.000	.000	290688.954	-67178.954	.000	.000	.000	.000	-67178.954	1596897.437
12-25	.000	.000	.000	.000	.000	.000	.000	.000	.000	1596897.437
S TOT	.000	.000	5213663.969	9190992.031	1500827.410	369409.238	.000	.000	7320755.383	1596897.437
REM.	.000	.000	.000	.000	.000	.000	.000	.000	.000	1596897.437
TOTAL	.000	.000	5213663.969	9190992.031	1500827.410	369409.238	.000	.000	7320755.383	1596897.437

DETERMINE MII 4 ECONOMIC SIZE  
 PROD 100 WELLS RESERVES = 800 MMBBLS  
 SINGLE (LARGE) DRILLING & PRODUCTION PLA

DATE: 02/24/94  
 TIME: 16:18:04  
 FILE: KUVLUM  
 GET: 17

# AFTER TAX ECONOMICS

## KUVLUM DEVELOPMENT PROJECT

AS OF JANUARY 1, 1994

-END- MO-YR	OPER CASH FLOW, M\$	DEPR. EXP., M\$	DEPL. EXP., M\$	INTANG. EXP., M\$	INTEREST EXP., M\$	TAXABLE INCOME M\$	TAX CREDIT M\$	TAXES PAYABLE M\$	CASH FLOW ATA, M\$	10.00 PCT CUM. DISC ATA, M\$
12-94	.000	.000	.000	45349.200	.000	-45349.200	.000	-17686.188	-57513.812	-58097.811
12-95	.000	.000	.000	3580.200	.000	-3580.200	.000	-1396.278	-18019.222	-73716.129
12-96	.000	.000	.000	3580.200	.000	-3580.200	.000	-1396.278	-129996.187	-176150.838
12-97	.000	.000	.000	3580.200	.000	-3580.200	.000	-1396.278	-337513.001	-417928.085
12-98	.000	.000	.000	3580.200	.000	-3580.200	.000	-1396.278	-481784.654	-731679.291
12-99	.000	.000	.000	51791.729	.000	-51791.729	.000	-20198.774	-521008.328	-1040124.851
12- 0	448150.297	210230.418	.000	57602.335	.000	180317.544	.000	70323.842	291854.690	-882970.287
12- 1	693060.306	362288.346	.000	63587.259	.000	267184.701	.000	104202.033	500307.355	-638072.307
12- 2	701381.615	262942.539	.000	79184.101	.000	359254.975	.000	140109.440	454863.488	-435655.735
12- 3	709570.364	190106.675	.000	18584.354	.000	500879.335	.000	195342.941	514227.423	-227643.398
12- 4	718112.574	135790.444	.000	16455.927	.000	565866.203	.000	220687.819	497424.755	-44720.291
12- 5	726514.152	134518.668	.000	12135.220	.000	579860.264	.000	226145.503	500368.649	122557.614
12- 6	722226.076	133948.849	.000	7684.891	.000	580593.136	.000	226431.323	495795.553	273238.592
12- 7	676140.402	68272.074	.000	2713.422	.000	605154.906	.000	236010.414	440129.988	394841.533
12- 8	626792.255	2017.218	.000	.000	.000	624775.037	.000	243662.264	383129.991	491072.884
12- 9	573967.822	712.193	.000	.000	.000	573255.629	.000	223569.695	350398.127	571082.010
12-10	487562.357	.000	.000	.000	.000	487562.357	.000	190149.319	297413.038	632818.945
12-11	425992.968	.000	.000	.000	.000	425992.968	.000	166137.258	259855.710	681856.030
12-12	391956.617	.000	.000	.000	.000	391956.617	.000	152863.081	239093.536	722873.373
12-13	339066.115	.000	.000	.000	.000	339066.115	.000	132235.785	206830.330	755130.169
12-14	299292.119	.000	.000	.000	.000	299292.119	.000	116723.926	182568.193	781014.649
12-15	239694.122	.000	.000	.000	.000	239694.122	.000	93480.708	146213.414	799860.201
12-16	194055.456	.000	.000	.000	.000	194055.456	.000	75681.628	118373.828	813730.462
12-17	163427.279	.000	.000	.000	.000	163427.279	.000	63736.639	99690.640	824349.634
12-18	112194.578	.000	.000	.000	.000	112194.578	.000	43755.885	68438.693	830977.066
12-19	76975.155	.000	.000	.000	.000	76975.155	.000	30020.310	46954.845	835110.693
12-20	39611.630	.000	.000	.000	.000	39611.630	.000	15448.536	24163.094	837044.489
12-21	-119.571	.000	.000	.000	.000	-119.571	.000	-46.633	-72.938	837039.182
12-22	-42232.218	.000	.000	.000	.000	-42232.218	.000	-16470.565	-25761.653	835335.272
12-23	-65222.285	.000	.000	.000	.000	-65222.285	.000	-25436.691	-39785.594	832943.025
12-24	-67178.954	.000	.000	.000	.000	-67178.954	.000	-26199.792	-40979.162	830703.012
12-25	.000	-.014	.000	.000	.000	.014	.000	.005	-.005	830703.012
S TOT	9190992.031	1500827.410	.000	369409.238	.000	7320755.383	.000	2855094.599	4465660.784	830703.012
REM.	.000	.000	.000	.000	.000	.000	.000	.000	.000	830703.012
TOTAL	9190992.031	1500827.410	.000	369409.238	.000	7320755.383	.000	2855094.599	4465660.784	830703.012

BTAX RATE OF RETURN (PCT)				ATA, RATE OF RETURN (PCT)				-----PRESENT WORTH PROFILE-----			
BTAX PAYOUT YEARS				ATA, PAYOUT YEARS				DISC	PW OF NET	PW OF NET	
BTAX PAYOUT YEARS (DISC)				ATA, PAYOUT YEARS (DISC)				RATE	BTAX, M\$	ATA, M\$	
BTAX NET INCOME/INVEST				ATA, NET INCOME/INVEST							
BTAX NET INCOME/INVEST (DISC)				ATA, NET INCOME/INVEST (DISC)							
25.16				19.80							
9.04				9.58							
10.12				11.27							
4.91				3.39							
2.32				1.69							
PRODUCTION START DATE	1/ 1/ 0			PROJECT LIFE (YEARS)	31.00			8.0	2171113.914	1193577.586	
MONTHS IN FIRST LINE	12.00			DISCOUNT RATE (PCT)	10.00			10.0	1596897.437	830703.012	
GROSS WELLS	1.00			PRIOR DEPL. BASIS (M\$)	.000			12.0	1164060.524	558537.463	
				PRIOR DEPR. BASIS (M\$)	.000			15.0	701795.370	270417.334	
								18.0	392205.800	80520.016	
								20.0	243908.903	-8761.879	
								25.0	4124.105	-148072.231	

MAX. OIL F /B/ 31.93  
 GROSS OIL 1.00  
 MAX. GAS PRICE (\$/M) .00  
 GROSS GAS PRICE .00

CUMULATIVE OIL (BBL)	.000	CUMULATIVE GAS (MMCF)	.000	30.0	-122.44	150.0
REMAINING OIL (BBL)	800000.000	REMAINING GAS (MMCF)	.000	35.0	-187003.183	-243990.303
ULTIMATE OIL (MBBL)	800000.000	ULTIMATE GAS (MMCF)	.000	40.0	-218172.741	-252367.963
				45.0	-230457.851	-249868.622
				50.0	-232181.569	-241777.773
				60.0	-220954.409	-219338.852
				70.0	-203266.248	-196227.366
INITIAL W.I. FRACTION	1.00000000	FINAL W.I. FRACTION	1.00000000	80.0	-185461.115	-175706.593
INITIAL NET OIL FRACTION	.87500000	FINAL NET OIL FRACTION	.87500000	90.0	-169530.294	-158406.205
INITIAL NET GAS FRACTION	.00000000	FINAL NET GAS FRACTION	.00000000	100.0	-155897.309	-144104.881



OGRE(R) V: BATA  
 FILE NAME: KUVLUM ( 13)  
 CASE NAME: TOTAL DEVELOPMENT 40 WELLS  
 CMD NAME: STDA4342( 300)

DATA I PORT

DATE: 02/25/94  
 TIME: 08:43:48

101 KUVLUM DEVELOPMENT  
 102 COMBINED 40 WELL CASE

117 CASE \$COM  
 \* 107 KUVLUM DEVELOPMENT PROJECT  
 \* 120 01 94 12 1 1 94 10 1  
 \* 131 DRILL ACRS 7 DELAY 0 0 0  
 \* 132 PRODFAC ACRS 7 DELAY 0 0 0  
 \* 133 PIPELINE ACRS 7 DELAY 0 0 0  
 \* 134 DRILLSITE ACRS 7 DELAY 0 0 0  
 168!  
 169! TOTAL TAX IS 39 PERCENT  
 \* 170 39  
 \* 600 SET IDCAMORT = MAJOR

	W.I. FRACTION	OP. COST (\$/W/MO)	OP. COST (\$/MO.)	ADV. TAX (PCT)	MAJOR PH. NAME	PROD DATE (MO/DY/YR)	
210	1.00000000	.00	.00	.000	OIL	1/ 1/ 0	
	PHASE NAME	CUM PROD (MUNITS)	REV. INT FRACTION	PRICE (\$/UNIT)	REV. TAX (PCT)	NO. OF WELLS	RATIO TO MAJOR PH
221	OIL	.000	.87500000	.000	.000	1.0	

300 SERIES LINES:

	MAN	OIL
301	FACT	1000.000
302		
311	12.	31250.000
312	12.	43750.000
313	12.	43750.000
314	12.	43750.000
315	12.	43750.000
316	12.	43750.000
317	12.	42500.000
318	12.	39380.000
319	12.	36250.000
320	12.	33130.000
321	12.	28750.000
322	12.	25630.000
323	12.	23750.000
324	12.	21250.000
325	12.	19380.000
326	12.	16880.000
327	12.	15000.000
328	12.	13750.000
329	12.	11880.000
330	12.	10630.000
331	12.	9380.000
332	12.	8130.000
333	12.	6880.000
334	12.	6250.000
335	12.	6250.000

610 CASE \$OILLOW

600 SERIES LINES:

\* 600 D/ 12.33 12.89 13.61 14.36

10 18 32 20 11  
 \* 615 21.74 0 23.07 23.76 24.47 25.21  
 \* 620 25.96 74 27.54 28.37 29.22 30.10  
 \* 621 31.00 31.93

611! OPERATING COST

612!

615 DATA OPCOST 1000 : 0 0 0 0 0 0

616 8720 LIFE

617!

618!

619!

620 DATA OPCOST : ESC 3 &

630 DATA ESCINV : 0 3 TO FRAME 40

800! INVESTMENTS FOR THE COASTAL PIPELINE

801!

	INV NAME	INV. POINT	(G OR N)	TANG-M\$	INTANG-M\$	LSEHLD-M\$	RISK FRAC	OVHD FLAG
802	PIPELINE	-54.000 MOS	G	6500.000	.000	.000	1.000	
803	PIPELINE	-42.000 MOS	G	6500.000	.000	.000	1.000	
804	PIPELINE	-30.000 MOS	G	58500.000	.000	.000	1.000	
805	PIPELINE	-18.000 MOS	G	52000.000	.000	.000	1.000	
806	PIPELINE	-6.000 MOS	G	6500.000	.000	.000	1.000	
807!	INVESTMENTS FOR THE MAIN PIPELINE							
808	PIPELINE	-54.000 MOS	G	7400.000	.000	.000	1.000	
811	PIPELINE	-42.000 MOS	G	7400.000	.000	.000	1.000	
812	PIPELINE	-30.000 MOS	G	66600.000	.000	.000	1.000	
813	PIPELINE	-18.000 MOS	G	59200.000	.000	.000	1.000	
815	PIPELINE	-6.000 MOS	G	7400.000	.000	.000	1.000	
816!	INVESTMENTS FOR MAIN PRODUCTION PLATFORM							
817!	STRUCTURE							
818	PRODFAC	-42.000 MOS	G	105000.000	.000	.000	1.000	
819	PRODFAC	-30.000 MOS	G	157500.000	.000	.000	1.000	
820	PRODFAC	-18.000 MOS	G	157500.000	.000	.000	1.000	
821	PRODFAC	-6.000 MOS	G	105000.000	.000	.000	1.000	
822!	PRODUCTION FACILITIES							
823	PRODFAC	-30.000 MOS	G	20050.000	.000	.000	1.000	
824	PRODFAC	-18.000 MOS	G	140400.000	.000	.000	1.000	
825	PRODFAC	-6.000 MOS	G	240600.000	.000	.000	1.000	
826!								
827!	INVESTMENTS FOR PERMITTING							
828	PRODFAC	-66.000 MOS	G	5000.000	.000	.000	1.000	
829	PRODFAC	-54.000 MOS	G	5000.000	.000	.000	1.000	
830	PRODFAC	-42.000 MOS	G	5000.000	.000	.000	1.000	
831	PRODFAC	-30.000 MOS	G	5000.000	.000	.000	1.000	
832!								
833!	DELINEATION WELLS THEN PRODUCTION WELLS							
834!								
835	DRILL	-72.000 MOS	G	10530.000	59670.000	.000	1.000	
836	DRILL	-6.000 MOS	G	10800.000	61200.000	.000	1.000	
837!								
838	DRILL	6.000 MOS	G	7700.000	40800.000	.000	1.000	
839!								
840	ESC	USING ESCINV						

850 NOLOSS OFF

## KUVLUM DEVELOPMENT PROJECT

AS OF JANUARY 1, 1994

S TOT	625050.000	.000	546918.750	.000	20.58	.00	1.011254738.954	.000	.000	11254738.954
REM.	.000	.000	.000	.000	.00	.00	.0	.000	.000	.000
TOTAL	625050.000	.000	546918.750	.000	20.58	.00	1.011254738.954	.000	.000	11254738.954

-END- MO-YR	-OPERATIONS, M\$-				-CAPITAL COSTS, M\$-				CASH FLOW BTAX, M\$	10.00 PCT CUM. DISC BTAX, M\$
	SEVERANCE TAXES	AD VAL TAXES	NET OPER EXPENSES	OPERATIONS CASH FLOW	TANGIBLE COSTS	INTANG. COSTS	HOUSEHOLD COSTS	SALVAGE VALUE		
12-94	.000	.000	.000	.000	15530.000	59670.000	.000	.000	-75200.000	-74967.313
12-95	.000	.000	.000	.000	19467.000	.000	.000	.000	-19467.000	-91841.000
12-96	.000	.000	.000	.000	131445.510	.000	.000	.000	-131445.510	-195418.171
12-97	.000	.000	.000	.000	336177.462	.000	.000	.000	-336177.462	-436239.082
12-98	.000	.000	.000	.000	460445.654	.000	.000	.000	-460445.654	-736094.082
12-99	.000	.000	.000	.000	429279.190	70947.573	.000	.000	-500226.763	-1032240.958
12- 0	.000	.000	124945.632	336890.306	8597.177	48717.334	.000	.000	279375.756	-881705.293
12- 1	.000	.000	126694.001	527829.437	.000	.000	.000	.000	527829.437	-623350.692
12- 2	.000	.000	132554.821	533921.742	.000	.000	.000	.000	533921.742	-385773.825
12- 3	.000	.000	136531.466	539898.222	.000	.000	.000	.000	539898.222	-167377.283
12- 4	.000	.000	54627.215	54627.215	.000	.000	.000	.000	54627.215	-334.000

12- 5	.000	.000	149191.619	548445.881	.000	.000	.000	552255.331	218083.831
12- 6	.000	.000	153667.368	512051.532	.000	.000	.000	548445.881	384766.169
12- 7	.000	.000	158277.389	472925.736	.000	.000	.000	512051.532	526240.220
12- 8	.000	.000	163025.710	431243.665	.000	.000	.000	472925.736	645025.707
12- 9	.000	.000	167916.482	363131.956	.000	.000	.000	431243.665	743494.922
12-10	.000	.000	172953.976	314592.699	.000	.000	.000	363131.956	818873.776
12-11	.000	.000	178142.596	287357.404	.000	.000	.000	314592.699	878240.218
12-12	.000	.000	183486.873	245470.940	.000	.000	.000	287357.404	927537.399
12-13	.000	.000	188991.480	213918.720	.000	.000	.000	245470.940	965820.499
12-14	.000	.000	194661.224	166760.676	.000	.000	.000	213918.720	996149.850
12-15	.000	.000	200501.061	130380.189	.000	.000	.000	166760.676	1017643.753
12-16	.000	.000	206516.093	105815.157	.000	.000	.000	130380.189	1032920.840
12-17	.000	.000	212711.575	65250.725	.000	.000	.000	105815.157	1044192.403
12-18	.000	.000	219092.923	37063.502	.000	.000	.000	65250.725	1050511.120
12-19	.000	.000	225665.710	7181.065	.000	.000	.000	37063.502	1053773.972
12-20	.000	.000	232435.682	-24571.907	.000	.000	.000	7181.065	1054348.680
12-21	.000	.000	239408.752	-58206.752	.000	.000	.000	-24571.907	1052560.940
12-22	.000	.000	246591.015	-77059.765	.000	.000	.000	-58206.752	1048711.069
12-23	.000	.000	253988.745	-79371.557	.000	.000	.000	-77059.765	1044077.583
12-24	.000	.000	.000	.000	.000	.000	.000	-79371.557	1039738.955
12-25	.000	.000	.000	.000	.000	.000	.000	.000	1039738.955
S TOT	.000	.000	4555425.835	6699313.119	1400941.992	179334.907	.000	.000	5119036.220
REM.	.000	.000	.000	.000	.000	.000	.000	.000	1039738.955
TOTAL	.000	.000	4555425.835	6699313.119	1400941.992	179334.907	.000	.000	5119036.220

DATE: 02/25/94  
TIME: 08:43:48  
FILE: KVVLM  
GET: 13

**KUYLUM DEVELOPMENT PROJECT**

AS OF JANUARY 1, 1994

-END- MO-YR	OPER CASH FLOW, M\$	DEPR. EXP., M\$	DEPL. EXP., M\$	INTANG. EXP., M\$	INTEREST EXP., M\$	TAXABLE INCOME M\$	TAX CREDIT M\$	TAXES PAYABLE M\$	CASH FLOW ATAX, M\$	10.00 PCT CUM. DISC ATAX, M\$
12-94	.000	.000	.000	45349.200	.000	-45349.200	.000	-17686.188	-57513.812	-58097.811
12-95	.000	.000	.000	3580.200	.000	-3580.200	.000	-1396.278	-18070.722	-73760.768
12-96	.000	.000	.000	3580.200	.000	-3580.200	.000	-1396.278	-130049.232	-176237.276
12-97	.000	.000	.000	3580.200	.000	-3580.200	.000	-1396.278	-334781.184	-416057.584
12-98	.000	.000	.000	3580.200	.000	-3580.200	.000	-1396.278	-459049.376	-715002.945
12-99	.000	.000	.000	51791.729	.000	-51791.729	.000	-20198.774	-480027.989	-999187.110
12- 0	336890.306	200138.576	.000	39820.508	.000	96931.222	.000	37803.177	241772.619	-869002.998
12- 1	527829.437	343090.691	.000	7179.894	.000	177558.852	.000	69247.952	458581.485	-644544.658
12- 2	533921.742	245052.781	.000	7179.894	.000	281689.067	.000	109858.736	424063.006	-455851.161
12- 3	539898.222	175047.701	.000	7179.894	.000	357670.627	.000	139491.544	400406.678	-293880.941
12- 4	546138.215	125034.075	.000	5051.467	.000	416052.673	.000	162260.542	383877.673	-152713.667
12- 5	552255.331	125034.076	.000	1461.520	.000	425759.735	.000	166046.297	386209.034	-23600.386
12- 6	548445.881	125034.075	.000	.000	.000	423411.806	.000	165130.604	383315.277	92895.861
12- 7	512051.532	62510.030	.000	.000	.000	449541.502	.000	175321.186	336730.346	185930.650
12- 8	472925.736	.000	.000	.000	.000	472925.736	.000	184441.037	288484.699	258389.797
12- 9	431243.665	.000	.000	.000	.000	431243.665	.000	168185.029	263058.636	318456.018
12-10	363131.956	.000	.000	.000	.000	363131.956	.000	141621.463	221510.493	364437.119
12-11	314592.699	.000	.000	.000	.000	314592.699	.000	122691.153	191901.546	400650.648
12-12	287357.404	.000	.000	.000	.000	287357.404	.000	112069.388	175288.016	430721.928
12-13	245470.940	.000	.000	.000	.000	245470.940	.000	95733.667	149737.273	454074.619
12-14	213918.720	.000	.000	.000	.000	213918.720	.000	83428.301	130490.419	472575.523
12-15	166760.676	.000	.000	.000	.000	166760.676	.000	65036.664	101724.012	485686.804
12-16	130380.189	.000	.000	.000	.000	130380.189	.000	50848.274	79531.915	495005.827
12-17	105815.157	.000	.000	.000	.000	105815.157	.000	41267.911	64547.246	501881.481
12-18	65250.725	.000	.000	.000	.000	65250.725	.000	25447.783	39802.942	505735.899
12-19	37063.502	.000	.000	.000	.000	37063.502	.000	14454.766	22608.736	507726.239
12-20	7181.065	.000	.000	.000	.000	7181.065	.000	2800.615	4380.450	508076.811
12-21	-24571.907	.000	.000	.000	.000	-24571.907	.000	-9583.044	-14988.863	506986.290
12-22	-58206.752	.000	.000	.000	.000	-58206.752	.000	-22700.633	-35506.119	504637.869
12-23	-77059.765	.000	.000	.000	.000	-77059.765	.000	-30053.308	-47006.457	501811.443
12-24	-79371.557	.000	.000	.000	.000	-79371.557	.000	-30954.907	-48416.650	499164.880
12-25	.000	-.013	.000	.000	.000	.013	.000	.005	-.005	499164.880
S TOT	6699313.119	1400941.992	.000	179334.907	.000	5119036.220	.000	1996424.128	3122612.092	499164.880
REM.	.000	.000	.000	.000	.000	.000	.000	.000	.000	499164.880
TOTAL	6699313.119	1400941.992	.000	179334.907	.000	5119036.220	.000	1996424.128	3122612.092	499164.880

			-----PRESENT WORTH PROFILE-----		
			DISC	PW OF NET	PW OF NET
			RATE	BTAX, M\$	ATAX, M\$
BTAX RATE OF RETURN (PCT)	21.79	ATAX RATE OF RETURN (PCT)	16.93		
BTAX PAYOUT YEARS	9.34	ATAX PAYOUT YEARS	9.89		
BTAX PAYOUT YEARS (DISC)	10.83	ATAX PAYOUT YEARS (DISC)	12.20		
BTAX NET INCOME/INVEST	4.24	ATAX NET INCOME/INVEST	2.98	0	5119036.220
BTAX NET INCOME/INVEST (DISC)	1.98	ATAX NET INCOME/INVEST (DISC)	1.47	2.0	3757377.248
				5.0	2355253.566
PRODUCTION START DATE	1/ 1/ 0	PROJECT LIFE (YEARS)	31.00	8.0	1456203.240
MONTHS IN FIRST LINE	12.00	DISCOUNT RATE (PCT)	10.00	10.0	1039738.955
GROSS WELLS	1.00	PRIOR DEPR. BASIS (M\$)	0.00	12.0	765303.251
		PRIOR DEPR. BASIS (M\$)	0.00	15.0	499164.880
				18.0	259471.469
				20.0	88713.229
					-48928.409
					-112777.115
					0951.5

CUMULATIVE O. (BL) .000  
REMAINING OIL (MBBL) 625050.000  
ULTIMATE OIL (MBBL) 625050.000

CUMULATIVE GAS (MMCF) .000  
REMAINING GAS (MMCF) .000  
ULTIMATE GAS (MMCF) .000

INITIAL W.I. FRACTION 1.00000000  
INITIAL NET OIL FRACTION .87500000  
INITIAL NET GAS FRACTION .00000000

FINAL W.I. FRACTION 1.00000000  
FINAL NET OIL FRACTION .87500000  
FINAL NET GAS FRACTION .00000000

30.0	-192944.843	-252226.795
35.0	-232844.232	-266631.544
40.0	-248374.533	-266222.815
45.0	-250636.330	-258262.309
50.0	-245793.561	-246723.941
60.0	-227217.216	-220675.771
70.0	-206083.325	-196086.927
80.0	-186603.896	-174993.455
90.0	-169846.769	-157514.739
100.0	-155809.493	-143206.340

OGRE(R) V: BATAK  
 FILE NAME: KUVLUM ( 11)  
 CASE NAME: PROD7OWL  
 CMD NAME: STDD4913( 300)

DATA I P O R T

DATE: 02/25/94  
 TIME: 08:49:17

101 COMPLETE DEVELOPMENT 210MBOPD PROFILE  
 102 COMBINED 70 WELL CASE

117 CASE \$COM  
 \* 107 KUVLUM DEVELOPMENT PROJECT  
 \* 120 01 94 12 1 1 94 10 1  
 \* 131 DRILL ACRS 7 DELAY 0 0 0  
 \* 132 PRODFAC ACRS 7 DELAY 0 0 0  
 \* 133 PIPELINE ACRS 7 DELAY 0 0 0  
 \* 134 DRILLSITE ACRS 7 DELAY 0 0 0  
 168!  
 169! TOTAL TAX IS 39 PERCENT  
 \* 170 39  
 \* 600 SET IDCAMORT = MAJOR

	W.I. FRACTION	OP. COST (\$/W/MO)	OP. COST (\$/MO.)	ADV. TAX (PCT)	MAJOR PH. NAME	PROD DATE (MO/DY/YR)
210	1.00000000	.00	.00	.000	OIL	1/ 1/ 0

	PHASE NAME	CUM PROD (MUNITS)	REV. INT FRACTION	PRICE (\$/UNIT)	REV. TAX (PCT)	NO. OF WELLS	RATIO TO MAJOR PH
221	OIL	.000	.87500000	.000	.000	1.0	

300 SERIES LINES:

	MAN	OIL
305	FACT	1000.000
310		
311	12.	54750.000
312	12.	76650.000
313	12.	76650.000
314	12.	76650.000
315	12.	76650.000
316	12.	76650.000
317	12.	74460.000
318	12.	68990.000
319	12.	63510.000
320	12.	58040.000
321	12.	50370.000
322	12.	44900.000
323	12.	41610.000
324	12.	37230.000
325	12.	33950.000
326	12.	29570.000
327	12.	26280.000
328	12.	24090.000
329	12.	20810.000
330	12.	18620.000
331	12.	16430.000
332	12.	14240.000
333	12.	12050.000
334	12.	10950.000
335	12.	10950.000

610 CASE \$OILLOW

600 SERIES LINES:

600 D. P : 12.33 12.89 13.61 14.36

610 10.2 13.32 19.90 20.50 21.11  
 \* 615 21.7 40 23.07 23.76 24.47 25.21  
 \* 620 25.96 74 27.54 28.37 29.22 30.10  
 \* 621 31.00 31.93

611! OPERATING COST

615 DATA OPCOST 1000 : 0 0 0 0 0 0

616 11600 LIFE

617 DATA OPCOST : ESC 3 %

618!

619!

620!

630 DATA ESCINV : 0 3 TO FRAME 40

800! INVESTMENTS FOR THE COASTAL PIPELINE

801!

	INV NAME	INV. POINT	(G OR N)	TANG-M\$	INTANG-M\$	LSEHLD-M\$	RISK FRAC	OVHD FLAG
802	PIPELINE	-54.000 MOS	G	6500.000	.000	.000	1.000	
803	PIPELINE	-42.000 MOS	G	6500.000	.000	.000	1.000	
804	PIPELINE	-30.000 MOS	G	58500.000	.000	.000	1.000	
805	PIPELINE	-18.000 MOS	G	52000.000	.000	.000	1.000	
806	PIPELINE	-6.000 MOS	G	6500.000	.000	.000	1.000	
807!	INVESTMENTS FOR THE MAIN PIPELINE							
808	PIPELINE	-54.000 MOS	G	7400.000	.000	.000	1.000	
811	PIPELINE	-42.000 MOS	G	7400.000	.000	.000	1.000	
812	PIPELINE	-30.000 MOS	G	66600.000	.000	.000	1.000	
813	PIPELINE	-18.000 MOS	G	59200.000	.000	.000	1.000	
814	PIPELINE	-6.000 MOS	G	7400.000	.000	.000	1.000	
815!								
816!	INVESTMENTS FOR MAIN PRODUCTION PLATFORM							
817!	STRUCTURE							
818	PRODFAC	-42.000 MOS	G	105000.000	.000	.000	1.000	
819	PRODFAC	-30.000 MOS	G	157500.000	.000	.000	1.000	
820	PRODFAC	-18.000 MOS	G	157500.000	.000	.000	1.000	
821	PRODFAC	-6.000 MOS	G	105000.000	.000	.000	1.000	
822!	PRODUCTION FACILITIES							
823	PRODFAC	-30.000 MOS	G	20500.000	.000	.000	1.000	
824	PRODFAC	-18.000 MOS	G	185000.000	.000	.000	1.000	
825	PRODFAC	-6.000 MOS	G	317000.000	.000	.000	1.000	
826!								
827!	INVESTMENTS FOR PERMITTING							
828	PRODFAC	-66.000 MOS	G	5000.000	.000	.000	1.000	
829	PRODFAC	-54.000 MOS	G	5000.000	.000	.000	1.000	
830	PRODFAC	-42.000 MOS	G	5000.000	.000	.000	1.000	
831	PRODFAC	-30.000 MOS	G	5000.000	.000	.000	1.000	
832!								
833!	DELINEATION WELLS THEN PRODUCTION WELLS							
834!								
835	DRILL	-72.000 MOS	G	10530.000	59670.000	.000	1.000	
836	DRILL	-6.000 MOS	G	10800.000	61200.000	.000	1.000	
837	DRILL	6.000 MOS	G	10800.000	61200.000	.000	1.000	
838	DRILL	18.000 MOS	G	9900.000	56100.000	.000	1.000	
839!								
840	ESC	USING	ESGINV					

850 NOLOSS OFF



RESERVES AND ECONOMICS

KUVLUM DEVELOPMENT PROJECT

AS OF JANUARY 1, 1994

-END- MO-YR	---GROSS PRODUCTION---		---NET PRODUCTION---		---PRICES---		NO. OF WELLS	---OPERATIONS, M\$---		
	OIL, MBBL	GAS, MMCF	OIL, MBBL	GAS, MMCF	OIL \$/B	GAS \$/M		OIL REVENUE	GAS REVENUE	OTHER REVENUE
12-94	.000	.000	.000	.000	12.33	.00	.0	.000	.000	.000
12-95	.000	.000	.000	.000	12.89	.00	.0	.000	.000	.000
12-96	.000	.000	.000	.000	13.61	.00	.0	.000	.000	.000
12-97	.000	.000	.000	.000	14.36	.00	.0	.000	.000	.000
12-98	.000	.000	.000	.000	15.16	.00	.0	.000	.000	.000
12-99	.000	.000	.000	.000	16.00	.00	.0	.000	.000	.000
12- 0	54750.000	.000	47906.250	.000	16.89	.00	1.0	809136.563	.000	.000
12- 1	76650.000	.000	67068.750	.000	17.15	.00	1.0	1150229.063	.000	.000
12- 2	76650.000	.000	67068.750	.000	17.41	.00	1.0	1167666.938	.000	.000
12- 3	76650.000	.000	67068.750	.000	17.67	.00	1.0	1185104.813	.000	.000
12- 4	76650.000	.000	67068.750	.000	17.94	.00	1.0	1203213.375	.000	.000
12- 5	76650.000	.000	67068.750	.000	18.21	.00	1.0	1221321.938	.000	.000
12- 6	74460.000	.000	65152.500	.000	18.76	.00	1.0	1222260.900	.000	.000
12- 7	68990.000	.000	60366.250	.000	19.32	.00	1.0	1166275.950	.000	.000
12- 8	63510.000	.000	55571.250	.000	19.90	.00	1.0	1105867.875	.000	.000
12- 9	58040.000	.000	50785.000	.000	20.50	.00	1.0	1041092.500	.000	.000
12-10	50370.000	.000	44073.750	.000	21.11	.00	1.0	930396.863	.000	.000
12-11	44900.000	.000	39287.500	.000	21.74	.00	1.0	854110.250	.000	.000
12-12	41610.000	.000	36408.750	.000	22.40	.00	1.0	815556.000	.000	.000
12-13	37230.000	.000	32576.250	.000	23.07	.00	1.0	751534.088	.000	.000
12-14	33950.000	.000	29706.250	.000	23.76	.00	1.0	705820.500	.000	.000
12-15	29570.000	.000	25873.750	.000	24.47	.00	1.0	633130.663	.000	.000
12-16	26280.000	.000	22995.000	.000	25.21	.00	1.0	579703.950	.000	.000
12-17	24090.000	.000	21078.750	.000	25.96	.00	1.0	547204.350	.000	.000
12-18	20810.000	.000	18208.750	.000	26.74	.00	1.0	486901.975	.000	.000
12-19	18620.000	.000	16292.500	.000	27.54	.00	1.0	448695.450	.000	.000
12-20	16430.000	.000	14376.250	.000	28.37	.00	1.0	407854.213	.000	.000
12-21	14240.000	.000	12460.000	.000	29.22	.00	1.0	364081.200	.000	.000
12-22	12050.000	.000	10543.750	.000	30.10	.00	1.0	317366.875	.000	.000
12-23	10950.000	.000	9581.250	.000	31.00	.00	1.0	297018.750	.000	.000
12-24	10950.000	.000	9581.250	.000	31.93	.00	1.0	305929.313	.000	.000
12-25	.000	.000	.000	.000	.00	.00	1.0	.000	.000	.000
S TOT	1095050.000	.000	958168.750	.000	20.58	.00	1.0	19717474.355	.000	.000
REM.	.000	.000	.000	.000	.00	.00	.0	.000	.000	.000
TOTAL	1095050.000	.000	958168.750	.000	20.58	.00	1.0	19717474.355	.000	.000

-END- MO-YR	---OPERATIONS, M\$---				---CAPITAL COSTS, M\$---				10.00 PCT	
	SEVERANCE TAXES	AD VAL TAXES	NET OPER EXPENSES	OPERATIONS CASH FLOW	TANGIBLE COSTS	INTANG. COSTS	LSEHOLD COSTS	SALVAGE VALUE	CASH FLOW BTAX, M\$	CUM. DISC BTAX, M\$
12-94	.000	.000	.000	.000	15530.000	59670.000	.000	.000	-75200.000	-74967.313
12-95	.000	.000	.000	.000	19467.000	.000	.000	.000	-19467.000	-91841.000
12-96	.000	.000	.000	.000	131445.510	.000	.000	.000	-131445.510	-195418.171
12-97	.000	.000	.000	.000	343225.551	.000	.000	.000	-343225.551	-441287.985
12-98	.000	.000	.000	.000	510643.347	.000	.000	.000	-510643.347	-773833.117
12-99	.000	.000	.000	.000	517847.729	70947.573	.000	.000	-588795.302	-1122414.804
12- 0	.000	.000	166212.080	642924.483	12895.765	73076.001	.000	.000	556932.716	-822529.206
12- 1	.000	.000	171198.442	979030.621	12175.751	68995.924	.000	.000	897858.946	-383046.084
12- 2	.000	.000	176334.395	991332.543	.000	.000	.000	.000	991332.543	58062.905
12- 3	.000	.000	181624.427	1003480.386	.000	.000	.000	.000	1003480.386	463985.053
12- 4	.000	.000	707.000	10.000	.000	.000	.000	.000	40.000	837.000



AFTER TAX ECONOMICS

KUVLUM DEVELOPMENT PROJECT

AS OF JANUARY 1, 1994

-END- MO-YR	OPER CASH FLOW, M\$	DEPR. EXP., M\$	DEPL. EXP., M\$	INTANG. EXP., M\$	INTEREST EXP., M\$	TAXABLE INCOME M\$	TAX CREDIT M\$	TAXES PAYABLE M\$	CASH FLOW ATAX, M\$	10.00 PCT CUM. DISC ATAX, M\$
12-94	.000	.000	.000	45349.200	.000	-45349.200	.000	-17686.188	-57513.812	-58097.811
12-95	.000	.000	.000	3580.200	.000	-3580.200	.000	-1396.278	-18070.722	-73760.768
12-96	.000	.000	.000	3580.200	.000	-3580.200	.000	-1396.278	-130049.232	-176237.276
12-97	.000	.000	.000	3580.200	.000	-3580.200	.000	-1396.278	-341829.273	-421106.487
12-98	.000	.000	.000	3580.200	.000	-3580.200	.000	-1396.278	-509247.069	-752741.980
12-99	.000	.000	.000	51791.729	.000	-51791.729	.000	-20198.774	-568596.528	-1089360.956
12- 0	642924.483	221583.707	.000	57602.335	.000	363738.441	.000	141857.992	415094.726	-865852.908
12- 1	979030.621	381592.770	.000	59008.439	.000	538429.412	.000	209987.471	687871.475	-529150.732
12- 2	991332.543	274292.374	.000	12781.170	.000	704258.999	.000	274661.010	716671.533	-210256.474
12- 3	1003480.386	195934.090	.000	12781.170	.000	794765.126	.000	309958.399	693521.987	70283.075
12- 4	1016140.215	139953.013	.000	10652.743	.000	865534.459	.000	337558.439	678581.776	319824.911
12- 5	1028636.583	139518.339	.000	6332.035	.000	882786.209	.000	344286.621	684349.962	548609.484
12- 6	1023794.985	139518.339	.000	2069.878	.000	882206.768	.000	344060.640	679734.345	755192.693
12- 7	961856.057	70294.754	.000	.000	.000	891561.303	.000	347708.908	614147.149	924874.609
12- 8	895315.385	543.282	.000	.000	.000	894772.103	.000	348961.120	546354.265	1062103.253
12- 9	824223.436	.000	.000	.000	.000	824223.436	.000	321447.140	502776.296	1176906.070
12-10	707021.727	.000	.000	.000	.000	707021.727	.000	275738.474	431283.253	1266431.756
12-11	624033.860	.000	.000	.000	.000	624033.860	.000	243373.205	380660.655	1338265.809
12-12	578577.318	.000	.000	.000	.000	578577.318	.000	225645.154	352932.164	1398812.572
12-13	507446.045	.000	.000	.000	.000	507446.045	.000	197903.958	309542.087	1447088.065
12-14	454409.816	.000	.000	.000	.000	454409.816	.000	177219.828	277189.988	1486388.003
12-15	374177.659	.000	.000	.000	.000	374177.659	.000	145929.287	228248.372	1515807.099
12-16	312982.355	.000	.000	.000	.000	312982.355	.000	122063.118	190919.237	1538177.751
12-17	272481.108	.000	.000	.000	.000	272481.108	.000	106267.632	166213.476	1555883.019
12-18	203937.035	.000	.000	.000	.000	203937.035	.000	79535.444	124401.591	1567929.758
12-19	157241.562	.000	.000	.000	.000	157241.562	.000	61324.209	95917.353	1576373.755
12-20	107656.709	.000	.000	.000	.000	107656.709	.000	41986.117	65670.592	1581629.438
12-21	54877.770	.000	.000	.000	.000	54877.770	.000	21402.330	33475.440	1584064.959
12-22	-1112.657	.000	.000	.000	.000	-1112.657	.000	-433.936	-678.721	1584020.067
12-23	-31015.168	.000	.000	.000	.000	-31015.168	.000	-12095.916	-18919.252	1582882.481
12-24	-31945.623	.000	.000	.000	.000	-31945.623	.000	-12458.793	-19486.830	1581817.287
12-25	.000	-.014	.000	.000	.000	.014	.000	.005	-.005	1581817.287
S TOT	13657504.210	1563230.654	.000	272689.498	.000	11821584.058	.000	4610417.782	7211166.277	1581817.287
REM.	.000	.000	.000	.000	.000	.000	.000	.000	.000	1581817.287
TOTAL	13657504.210	1563230.654	.000	272689.498	.000	11821584.058	.000	4610417.782	7211166.277	1581817.287

-----PRESENT WORTH PROFILE-----			
BTAX RATE OF RETURN (PCT)	32.91	ATAX RATE OF RETURN (PCT)	26.03
BTAX PAYOUT YEARS	8.22	ATAX PAYOUT YEARS	8.73
BTAX PAYOUT YEARS (DISC)	8.87	ATAX PAYOUT YEARS (DISC)	9.75
BTAX NET INCOME/INVEST	7.44	ATAX NET INCOME/INVEST	4.93
BTAX NET INCOME/INVEST (DISC)	3.35	ATAX NET INCOME/INVEST (DISC)	2.31
			10.00
			11.00
			12.00
			13.00
			14.00
			15.00
			16.00
			17.00
			18.00
			19.00
			20.00
			21.00
			22.00
			23.00
			24.00
			25.00
			26.00
			27.00
			28.00
			29.00
			30.00
			31.00
			32.00
			33.00
			34.00
			35.00
			36.00
			37.00
			38.00
			39.00
			40.00
			41.00
			42.00
			43.00
			44.00
			45.00
			46.00
			47.00
			48.00
			49.00
			50.00
			51.00
			52.00
			53.00
			54.00
			55.00
			56.00
			57.00
			58.00
			59.00
			60.00
			61.00
			62.00
			63.00
			64.00
			65.00
			66.00
			67.00
			68.00
			69.00
			70.00
			71.00
			72.00
			73.00
			74.00
			75.00
			76.00
			77.00
			78.00
			79.00
			80.00
			81.00
			82.00
			83.00
			84.00
			85.00
			86.00
			87.00
			88.00
			89.00
			90.00
			91.00
			92.00
			93.00
			94.00
			95.00
			96.00
			97.00
			98.00
			99.00
			100.00

MAX. OIL S/B) 31.93 MAX. GAS PRICE (\$/M)

CUMULATIVE O (BL) .000  
REMAINING OIL (MBBL) 1095050.000  
ULTIMATE OIL (MBBL) 1095050.000

CUMULATIVE GAS (MMCF) .000  
REMAINING GAS (MMCF) .000  
ULTIMATE GAS (MMCF) .000

.000  
.000  
.000

30.0 -73.1223  
35.0 -52829.624 -166047.241  
40.0 -124116.427 -198506.024  
45.0 -163316.023 -212052.496  
50.0 -183511.375 -214886.061  
60.0 -194407.922 -205354.256  
70.0 -188219.676 -188793.850  
80.0 -176694.573 -171743.947  
90.0 -164328.721 -156339.984  
100.0 -152782.566 -143096.186

INITIAL W.I. FRACTION 1.00000000  
INITIAL NET OIL FRACTION .87500000  
INITIAL NET GAS FRACTION .00000000

FINAL W.I. FRACTION  
FINAL NET OIL FRACTION  
FINAL NET GAS FRACTION

1.00000000  
.87500000  
.00000000

OGRE(R) ' . BATAK  
 FILE NAME: ..UVLUM ( 12)  
 CASE NAME: PROD100W  
 CMD NAME: STDA4221( 300)

DATA PORT

DATE: 03/10/94  
 TIME: 10:42:26

101 TOTAL DEVELOPMENT 300MBOPD PROFILE  
 102 PROD 100 WELLS

117 CASE \$COM

\* 107 KUVLUM DEVELOPMENT PROJECT  
 \* 120 01 94 12 1 1 94 10 1  
 \* 131 DRILL ACRS 7 DELAY 0 0 0  
 \* 132 PRODFAC ACRS 7 DELAY 0 0 0  
 \* 133 PIPELINE ACRS 7 DELAY 0 0 0  
 \* 134 DRILSITE ACRS 7 DELAY 0 0 0

168!

169! TOTAL TAX IS 39 PERCENT

\* 170 39

\* 600 SET IDCAMORT = MAJOR

	W.I. FRACTION	OP. COST (\$/W/MO)	OP. COST (\$/MO.)	ADV. TAX (PCT)	MAJOR PH. NAME	PROD DATE (MO/DY/YR)	
210	1.00000000	.00	.00	.000	GIL	1/ 1/ 0	
	PHASE NAME	CUM PROD (MUNITS)	REV. INT FRACTION	PRICE (\$/UNIT)	REV. TAX (PCT)	NO. OF WELLS	RATIO TO MAJOR PH
221	OIL	.000	.87500000	.000	.000	1.0	

300 SERIES LINES:

	MAN	OIL
305	FACT	1000.000
310		
311	12.	78250.000
312	12.	109550.000
313	12.	109550.000
314	12.	109550.000
315	12.	109550.000
316	12.	109550.000
317	12.	106420.000
318	12.	98595.000
319	12.	90770.000
320	12.	82945.000
321	12.	71990.000
322	12.	64165.000
323	12.	59470.000
324	12.	53210.000
325	12.	48515.000
326	12.	42255.000
327	12.	37560.000
328	12.	34430.000
329	12.	29735.000
330	12.	26605.000
331	12.	23475.000
332	12.	20345.000
333	12.	17215.000
334	12.	15650.000
335	12.	15650.000

610 CASE \$OILLOW

600 SERIES LINES:

\* 600 DA ? : 12.33 12.89 13.61 14.36

610 16.21 19.32 19.90 20.30 21.11  
 \* 615 21.74 J 23.07 23.76 24.47 25.21  
 \* 620 25.96 26.74 27.54 28.37 29.22 30.10  
 \* 621 31.00 31.93  
 611! OPERATING COST  
 615 DATA OPCOST 1000 : 0 0 0 0 0 0  
 616 14580 LIFE  
 617!  
 618!  
 619!  
 620 DATA OPCOST : ESC 3 %  
 630 DATA ESCINV : 0 3 TO FRAME 40  
 800! INVESTMENTS FOR THE COASTAL PIPELINE  
 801!

	INV NAME	INV. POINT	(G OR H)	TANG-M\$	INTANG-M\$	LSEHLD-M\$	RISK FRAC	OVHD FLAG
802	PIPELINE	-54.000 MOS	G	6500.000	.000	.000	1.000	
803	PIPELINE	-42.000 MOS	G	6500.000	.000	.000	1.000	
804	PIPELINE	-30.000 MOS	G	58500.000	.000	.000	1.000	
805	PIPELINE	-18.000 MOS	G	52000.000	.000	.000	1.000	
806	PIPELINE	-6.000 MOS	G	6500.000	.000	.000	1.000	
807!	INVESTMENTS FOR THE MAIN PIPELINE							
808	PIPELINE	-54.000 MOS	G	7400.000	.000	.000	1.000	
811	PIPELINE	-42.000 MOS	G	7400.000	.000	.000	1.000	
812	PIPELINE	-30.000 MOS	G	65600.000	.000	.000	1.000	
813	PIPELINE	-18.000 MOS	G	59200.000	.000	.000	1.000	
814	PIPELINE	-6.000 MOS	G	7400.000	.000	.000	1.000	
815!								
816!	INVESTMENTS FOR MAIN PRODUCTION PLATFORM							
817!	STRUCTURE							
818	PRODFAC	-42.000 MOS	G	105000.000	.000	.000	1.000	
819	PRODFAC	-30.000 MOS	G	157500.000	.000	.000	1.000	
820	PRODFAC	-18.000 MOS	G	157500.000	.000	.000	1.000	
821	PRODFAC	-6.000 MOS	G	105000.000	.000	.000	1.000	
822!	PRODUCTION FACILITIES							
823	PRODFAC	-30.000 MOS	G	30650.000	.000	.000	1.000	
824	PRODFAC	-18.000 MOS	G	214600.000	.000	.000	1.000	
825	PRODFAC	-6.000 MOS	G	367800.000	.000	.000	1.000	
826!								
827!	INVESTMENTS FOR PERMITTING							
828	PRODFAC	-66.000 MOS	G	5000.000	.000	.000	1.000	
829	PRODFAC	-54.000 MOS	G	5000.000	.000	.000	1.000	
830	PRODFAC	-42.000 MOS	G	5000.000	.000	.000	1.000	
831	PRODFAC	-30.000 MOS	G	5000.000	.000	.000	1.000	
832!	DELINEATION WELLS THEN PRODUCTION WELLS							
833!								
834	DRILL	-6.000 MOS	G	10800.000	61200.000	.000	1.000	
835	DRILL	-72.000 MOS	G	10530.000	59670.000	.000	1.000	
836	DRILL	-6.000 MOS	G	10800.000	61200.000	.000	1.000	
837	DRILL	6.000 MOS	G	10800.000	61200.000	.000	1.000	
838	DRILL	18.000 MOS	G	10800.000	61200.000	.000	1.000	
839	DRILL	30.000 MOS	G	12600.000	71400.000	.000	1.000	
840	ESC	USING ESCINV						

850 NOLOSS OFF

DATE: 03/10/94  
TIME: 10:42:26  
FILE: KUVLUM  
GET#: 12

## AS OF JANUARY 1, 1994

---PRICES---

-END- MO-YR	-OPERATIONS, M\$-				-CAPITAL COSTS, M\$-				CASH FLOW BTAX, M\$	10.00 PCT CUM. DISC BTAX, M\$
	SEVERANCE TAXES	AD VAL TAXES	NET OPER EXPENSES	OPERATIONS CASH FLOW	TANGIBLE COSTS	INTANG. COSTS	LEASEHOLD COSTS	SALVAGE VALUE		
12-94	.000	.000	.000	.000	15530.000	59670.000	.000	.000	-75200.000	-74967.313
12-95	.000	.000	.000	.000	19467.000	.000	.000	.000	-19467.000	-91841.000
12-96	.000	.000	.000	.000	131445.510	.000	.000	.000	-131445.510	-195418.171
12-97	.000	.000	.000	.000	347760.368	.000	.000	.000	-347760.368	-444536.504
12-98	.000	.000	.000	.000	543958.408	.000	.000	.000	-543958.408	-798777.329
12-99	.000	.000	.000	.000	589259.012	141895.147	.000	.000	-731154.159	-1231639.054
12-00	.000	.000	200011.300	047526.700	12005.765	12076.001	.000	.000	061554.033	762753.516
12- 1	.000	.000	215178.731	1428755.956	13282.638	75268.281	.000	.000	1340205.038	-111757.300
12- 2	.00	.000	221634.093	1447223.220	15961.303	90.4	.000	.000	1340814.533	484877.108
12- 3	.0	.000	228283.116	1465496.822	.000	.0	.000	.000	1465496.822	1077601.503
12- 4	.000	.000	228133.116	1465496.822	.000	.0	.000	.000	1465496.822	1077601.503

12- 5	.000	.000	242185.558	1503356.755	.000	.000	.000	1503356.755	2126198.949
12- 6	.000	.000	249451.125	1497433.175	.000	.000	.000	1497433.175	2581295.197
12- 7	.000	.000	256934.659	1409813.816	.000	.000	.000	1409813.816	2970810.820
12- 8	.000	.000	264642.698	1315889.927	.000	.000	.000	1315889.927	3301324.924
12- 9	.000	.000	272581.979	1215243.959	.000	.000	.000	1215243.959	3578811.016
12-10	.000	.000	280759.439	1048985.849	.000	.000	.000	1048985.849	3796559.276
12-11	.000	.000	289182.222	931396.491	.000	.000	.000	931396.491	3972322.082
12-12	.000	.000	297857.688	867754.312	.000	.000	.000	867754.312	4121188.409
12-13	.000	.000	306793.419	767316.944	.000	.000	.000	767316.944	4240857.446
12-14	.000	.000	315997.222	692629.628	.000	.000	.000	692629.628	4339058.328
12-15	.000	.000	325477.138	579255.231	.000	.000	.000	579255.231	4413718.950
12-16	.000	.000	335241.452	493285.198	.000	.000	.000	493285.198	4471518.843
12-17	.000	.000	345298.696	436778.754	.000	.000	.000	436778.754	4518045.063
12-18	.000	.000	355657.657	340067.006	.000	.000	.000	340067.006	4550976.303
12-19	.000	.000	366327.387	274786.601	.000	.000	.000	274786.601	4575166.892
12-20	.000	.000	377317.208	205420.323	.000	.000	.000	205420.323	4591606.885
12-21	.000	.000	388636.724	131534.064	.000	.000	.000	131534.064	4601176.705
12-22	.000	.000	400295.826	53104.237	.000	.000	.000	53104.237	4604689.089
12-23	.000	.000	412304.701	12201.549	.000	.000	.000	12201.549	4605422.749
12-24	.000	.000	424673.842	12567.596	.000	.000	.000	12567.596	4606109.722
12-25	.000	.000	.000	.000	.000	.000	.000	.000	4606109.722
S TOT	.000	.000	7616755.580	20562352.726	1689560.003	440356.812	.000	.000	18432435.911
REM.	.000	.000	.000	.000	.000	.000	.000	.000	4606109.722
TOTAL	.000	.000	7616755.580	20562352.726	1689560.003	440356.812	.000	.000	18432435.911



TOTAL DEVELOPMENT 300MBOPD PROFILE  
PROD 100 WELLS

DATE: 03/10/94  
TIME: 10:42:26  
FILE: KUVLUM  
GET: 12

AFTER TAX ECONOMICS

KUVLUM DEVELOPMENT PROJECT

AS OF JANUARY 1, 1994

-END- MO-YR	OPER CASH FLOW, M\$	DEPR. EXP., M\$	DEPL. EXP., M\$	INTANG. EXP., M\$	INTEREST EXP., M\$	TAXABLE INCOME M\$	TAX CREDIT M\$	TAXES PAYABLE M\$	CASH FLOW ATAX, M\$	10.00 PCT CUM. DISC ATAX, M\$
12-94	.000	.000	.000	45349.200	.000	-45349.200	.000	-17686.188	-57513.812	-58097.811
12-95	.000	.000	.000	3580.200	.000	-3580.200	.000	-1396.278	-18070.722	-73760.768
12-96	.000	.000	.000	3580.200	.000	-3580.200	.000	-1396.278	-130049.232	-176237.276
12-97	.000	.000	.000	3580.200	.000	-3580.200	.000	-1396.278	-346364.090	-424355.006
12-98	.000	.000	.000	3580.200	.000	-3580.200	.000	-1396.278	-542562.130	-777686.192
12-99	.000	.000	.000	103583.457	.000	-103583.457	.000	-40397.548	-690756.611	-1186622.495
12- 0	947525.798	237192.757	.000	61859.189	.000	648473.852	.000	252904.802	608649.231	-858903.055
12- 1	1428755.956	408508.957	.000	67844.114	.000	952402.885	.000	371437.125	968767.913	-384711.302
12- 2	1447223.220	295955.645	.000	83440.956	.000	1067826.619	.000	416452.381	924362.152	26616.077
12- 3	1465496.822	213688.813	.000	22841.209	.000	1228966.800	.000	479297.052	986199.770	425547.969
12- 4	1484529.515	152634.828	.000	18584.354	.000	1313310.333	.000	512191.030	972338.485	783115.973
12- 5	1503356.755	151363.052	.000	12135.220	.000	1339858.483	.000	522544.808	980811.947	1111010.552
12- 6	1497433.175	150793.234	.000	7684.891	.000	1338955.050	.000	522192.469	975240.706	1407403.335
12- 7	1409813.816	76693.322	.000	2713.422	.000	1330407.072	.000	518858.758	890955.058	1653564.148
12- 8	1315889.927	2017.218	.000	.000	.000	1313872.709	.000	512410.357	803479.570	1855375.352
12- 9	1215243.959	712.193	.000	.000	.000	1214531.766	.000	473667.389	741576.570	2024705.290
12-10	1048985.849	.000	.000	.000	.000	1048985.849	.000	409104.481	639881.368	2157531.729
12-11	931396.491	.000	.000	.000	.000	931396.491	.000	363244.631	568151.860	2264747.040
12-12	867754.312	.000	.000	.000	.000	867754.312	.000	338424.182	529330.130	2355555.500
12-13	767316.944	.000	.000	.000	.000	767316.944	.000	299253.608	468063.336	2428553.613
12-14	692629.628	.000	.000	.000	.000	692629.628	.000	270125.555	422504.073	2488456.151
12-15	579255.231	.000	.000	.000	.000	579255.231	.000	225909.540	353345.691	2533999.130
12-16	493285.198	.000	.000	.000	.000	493285.198	.000	192381.227	300903.971	2569257.065
12-17	436778.754	.000	.000	.000	.000	436778.754	.000	170343.714	266435.040	2597638.059
12-18	340067.006	.000	.000	.000	.000	340067.006	.000	132626.132	207440.874	2617726.115
12-19	274786.601	.000	.000	.000	.000	274786.601	.000	107166.774	167619.827	2632482.375
12-20	205420.323	.000	.000	.000	.000	205420.323	.000	80113.926	125306.397	2642510.771
12-21	131534.064	.000	.000	.000	.000	131534.064	.000	51298.285	80235.779	2648348.361
12-22	53104.237	.000	.000	.000	.000	53104.237	.000	20710.652	32393.585	2650490.915
12-23	12201.549	.000	.000	.000	.000	12201.549	.000	4758.604	7442.945	2650938.448
12-24	12567.596	.000	.000	.000	.000	12567.596	.000	4901.362	7666.234	2651357.502
12-25	.000	-.016	.000	.000	.000	.016	.000	.006	-.006	2651357.502
S TOT	20562352.726	1689560.003	.000	440356.817	.000	18432435.911	.000	7188650.002	11243785.909	2651357.502
REM.	.000	.000	.000	.000	.000	.000	.000	.000	.000	2651357.502
TOTAL	20562352.726	1689560.003	.000	440356.817	.000	18432435.911	.000	7188650.002	11243785.909	2651357.502

BTAX RATE OF RETURN (PCT)	39.94	ATAX RATE OF RETURN (PCT)	32.21
BTAX PAYOUT YEARS	7.83	ATAX PAYOUT YEARS	8.30
BTAX PAYOUT YEARS (DISC)	8.25	ATAX PAYOUT YEARS (DISC)	8.94
BTAX NET INCOME/INVEST	9.65	ATAX NET INCOME/INVEST	6.28
BTAX NET INCOME/INVEST (DISC)	4.37	ATAX NET INCOME/INVEST (DISC)	2.94

-----PRESENT WORTH PROFILE-----

PRODUCTION START DATE	1/ 1/ 0	PROJECT LIFE (YEARS)	31.00	DISC	PW OF NET	PW OF NET
MONTHS IN FIRST LINE	12.00	DISCOUNT RATE (PCT)	10.00	RATE	BTAX, M\$	ATAX, M\$
GROSS WELLS	1.00	PRIOR DEPR. BASIS (M\$)	.000		2.0	13681406.647
		PRIOR DEPR. BASIS (M\$)	.000		5.0	8943228.528
					8.0	5972765.050
					10.0	4606109.722
					12.0	3572264.229
					15.0	2457363.834
					18.0	1696527.830
					20.0	1323717.400
						634496.110

MAX. OIL P (B) 31.93 MAX. GAS PRICE (\$/M) .00

CUMULATIVE OIL (MBBL)	.000	CUMULATIVE GAS (MMCF)	.000
REMAINING OIL (MBBL)	1565000.000	REMAINING GAS (MMCF)	.000
ULTIMATE OIL (MBBL)	1565000.000	ULTIMATE GAS (MMCF)	.000

INITIAL W.I. FRACTION	1.00000000	FINAL W.I. FRACTION	1.00000000
INITIAL NET OIL FRACTION	.87500000	FINAL NET OIL FRACTION	.87500000
INITIAL NET GAS FRACTION	.00000000	FINAL NET GAS FRACTION	.00000000

30.0	336349.415	51863.170
35.0	124793.922	-65167.506
40.0	-1396.755	-130155.595
45.0	-76968.499	-165035.286
50.0	-121822.067	-182165.592
60.0	-161759.000	-189151.662
70.0	-170316.050	-180704.310
80.0	-166654.957	-167802.102
90.0	-158643.858	-154573.026
100.0	-149578.942	-142482.304

# **KUVLUM PREDECISION STUDIES** **Arctic Consulting Listing**

<u>Company Name</u> <u>Contact Name(s)</u> <u>Titles</u>	<u>Phone/(Fax)</u> <u>Address</u>	<u>Areas of Expertise</u>
ABAM Engineers, Inc. Mike Lanier, VP Robert Mast, PE	206/952-6100 FAX: 206/952-4686 33301 9th Avenue South Federal Way, WA 98003	Arctic offshore structures and port facilities
AOE Consultants, Ltd. Dave Stenning, Principal	403/266-9700 FAX: 403/265-9722 1501, 300 Fifth Ave SW Calgary, Alberta Canada T2P 3C4	Ice engineering, project management
Arctic Geoscience Mike Schlagel, President	907/522-4300 FAX: 907/522-4301 10900 O'Malley Center Drive, #205 Anchorage, AK 99515	Geotechnical and geophysical investigations
C-Core Jack I. Clark, Ph.D. President & CEO	709/737-8350 FAX: 709/737-4706 Memorial University of Newfoundland St. John's, Newfoundland Canada A1B 3X5	Cold ocean research, Arctic design, pipeline research
Canarctic Shipping Company Limited Martin P. Luce, Exec. VP	613/234-8414/ FAX: 613/234-9747 150 Metcalfe Street, 19th Floor P. O. Box 39 Ottawa, Ontario Canada K2P 1P1	Ice-breaking tankers Marine transportation
CANATEC Consultants Ltd. Roger Pilkington, Ph.D. President	403/264-5575 FAX: 403/237-0660 Suite 1730 700 - Sixth Avenue SW Calgary, Alberta Canada T2P 0T8	Environmental, Ice, Geographical, Engineering
CANMAR John Fitzpatrick Sr. Structural Engineer	403/298-2818 FAX: 403/298-3532 PO Box 200, Station M Calgary, Alberta Canada T2P 2H8	Arctic structural design, tanker design
Center for Frontier Engineering Research W. D. Roggensack, Ph.D. Vice President Exploration and Prod. Tech	403/450-3300 FAX: 403/450-3700 200 Karl Clark Road Edmonton, Alberta Canada T6N 1E2	Arctic design and research

Coastal Frontiers Corporation Craig B. Leidersdorf, Principal	818/341-8133/ FAX: 818/341-4498 808/499-6675 924 Eton Avenue, Suite H Chatsworth, CA 91311	Coastal engineering Hindcast studies
Cold Oceans Design Associates Ltd. A. B. Gus Cammaert	709/737-3418 FAX: 709/737-4706 P. O. Box 9194, Station B St. John's, Newfoundland Canada A1A 2X9	Arctic marine facilities
Cold Regions Research and Engineering Laboratory (CRREL) O. A. Ayorinde	603/646 4289 72 Lyme Road Hanover, NH 03755-1290	Ice mechanics
K. R. Croasdale and Assoc. Ltd. Ken Croasdale	403/243-7787 FAX: 403/287-7889 334 - 40th Avenue SW Calgary, Alberta Canada T2S 0X4	Ice mechanics, Sea ice conditions
Fairweather Forecasting Chuck Samuels, President	907/258-9165 FAX: 907/258-9167 715 L St. Anchorage, AK 99510-0360	Weather reports, Arctic ice movements and data
Ben C. Gerwick, Inc. C. R. Firth, Vice President	415/398-8972 FAX: 415/433-8189 601 Montgomery Street San Francisco, CA 94111	Offshore Arctic structures and foundations, marine construction.
Global Marine Sherman B. Wetmore Dir., Engr. Development	713/496-8453 FAX: 713/531-1260 777 N. Eldridge Road Houston, TX 77210-4379	Arctic structure design and ice loads
IceCasting, Inc. Bob Prichard, President	206/363-3394 FAX: 206/363-3394 11042 Sand Point Way N.E. Seattle, WA 98125-5846	Arctic ice forecasting and movements
Institute for Marine Dynamics National Research Council Don Spencer	709/772-4294 FAX: 709/772-2462 Kerwin Place P. O. Box 12093 Postal Station A St. John's Newfoundland Canada A1B 3T5	Ice mechanics research
Interface Consulting, Intl. Robert C. Byrd Senior Consultant	713/496-6262 FAX: 713/496-6292 11767 Katy Freeway, Suite 1000 Houston, TX 77079	Project management, Arctic related studies

S. H. Iyer, Ph.D. President	403/288-5611 5651 Dalcastle Rise N.W. Calgary, Alberta Canada T3A 2A6	Offshore and Arctic engineering consultant
R. A. Kreig & Associates Ray Kreig, President	907/276-2025 FAX: 907/258-9614 201 Barrow Street, #1 Anchorage, AK 99501-2429	Terrain analysis Pipeline ROW assessment Facility siting
Kvaerner Mesa-Yards Inc. Mesa-Yards Arctic Research Centre Goran Wilkman, Manager	358-0-194-2540/ FAX: 358-0-194-2527 121246 masah sf (tlx) Kaanaantle 1 SF-00560 Helsinki, Finland	Ice-breaking tankers
Merlin Associates C. C. Yost Bob DeNapoli	713/586-0045/ FAX: 713/586-7965 P. O. Box 692188 Houston, TX	LNG facility cost information
M. C. Metz and Associates Michael C. Metz	303/278-2248 FAX: 303/278-3245 14379 W. Ellsworth Ave. (res) Golden, CO 80401	Geotechnical, pipeline civil, Facility siting
Pennine Engineering, Ltd. Gary Pidcock, President	403/253-9648 FAX: 403/255-5660 69 Medford Place S.W. Calgary, Alberta Canada T2V 2G1	Arctic drilling, and project management consultant
Sandwell, Inc. Sandwell Swan Wooster Div. D. M. (Dan) Masterson, Mgr., Engineering Services	403/237-8035 FAX: 403/237-9898 0382 1572 (tlx) 805, 940 - Sixth Avenue SW Calgary, Alberta Canada T2P 3T1	Port facilities, offshore structures Arctic structures
P.E. Sperry, PE	702/293-6858 FAX: 702/293-6058 636 Paloma Drive Boulder City, NV 89005	Tunnel construction consultant
Woodward-Clyde Consultants Joseph M. Colonell, Ph.D. Mgr. of Alaska Operations	907/561-1020 FAX: 907/563-3198 701 Sesame Street Anchorage, AK 99503	Geotechnical, tunneling, environmental engineering
B. Wright and Associates Brian Wright, President	403/266-7519 FAX: 403/297-9724 1630, 540 Fifth Ave. S.W. Calgary, Alberta Canada T2P 0M2	Arctic structure design, ice loading

**EVALUATION  
OF  
SAR SATELLITE IMAGERY  
AS A  
DATA SOURCE  
FOR  
DESIGN AND OPERATIONAL  
ICE CRITERIA  
AT ARCO'S KUVLUM FIELD**



**VAUDREY & ASSOCIATES, INC.**

**EVALUATION OF SAR SATELLITE IMAGERY  
AS A DATA SOURCE FOR  
DESIGN AND OPERATIONAL ICE CRITERIA  
AT ARCO'S KUVLUM FIELD**

by

Kennon D. Vaudrey

Prepared for:

ARCO Alaska, Inc.  
Anchorage, Alaska

Prepared by:

Vaudrey & Associates, Inc.  
San Luis Obispo, California

March 1994

## TABLE OF CONTENTS

<u>Section</u>	<u>Page Number</u>
1. Background and Objective.....	1
2. SAR Satellite Resource Centers.....	3
2.1 ERS-1 Satellite Description.....	3
2.2 Canadian Centre for Remote Sensing (CCRS).....	3
2.3 Ice Centre Environment Canada (ICEC) .....	4
2.4 RADARSAT International (RSI).....	6
2.5 Alaskan SAR Facility (ASF) .....	7
3. SAR Data Selection and Acquisition.....	10
4. Data Evaluation and Analysis.....	11
4.1 Multiyear Floes.....	11
4.2 Ice Islands.....	15
4.3 Shear Zone Rubble and First-Year Floebergs.....	19
4.4 Summer Ice Coverage .....	22
5. Summary and Recommendations.....	23
6. References.....	25
Appendix - Addendum to ARCO's Floeberg Study Based on Analysis of 1992 SAR Satellite Imagery .....	A-1



## LIST OF FIGURES

<u>Number</u>	<u>Description</u>	<u>Page Number</u>
Figure 1.	Lo-Res SAR Image ID 58368 - Multiyear Floes .....	12
Figure 2.	Full-Res SAR Image ID 58368 - Multiyear Floes .....	13
Figure 3.	Full-Res SAR Image ID 22454 - Ice Islands .....	17
Figure 4.	Full-Res SAR Image ID 23867 - Ellesmere Ice Shelf .....	18
Figure 5.	Full-Res SAR Image ID 24420 - 1992 Winter Shear Zone and Floeberg Source.....	20
Figure 6.	Lo-Res SAR Image ID 35134 - Floeberg Hazard to 1992 Summer Drilling at Kuvlum.....	21

**EVALUATION OF SAR SATELLITE IMAGERY  
AS A DATA SOURCE FOR  
DESIGN AND OPERATIONAL ICE CRITERIA  
AT ARCO'S KUVLUM FIELD**

**1. BACKGROUND AND OBJECTIVE**

Production platforms in the Camden Bay region of the eastern Beaufort Sea will be subjected to ice loading from different ice types and features. Ice encounter frequencies and ice loads computed for each encounter require the statistical representation (e.g., Vaudrey, 1992) of a number of extreme ice feature parameters (e.g., multiyear ice fraction, multiyear floe diameter, drift velocity, ice island population, ice island diameter, ice island concentration).

Multiyear ice fraction and floe diameter are required to determine encounter frequencies with platforms. In addition, floe diameter is required for momentum calculations during a summer multiyear floe impact with a structure. In the past, the most reliable method of acquiring multiyear ice fraction and floe size or diameter data has been Synthetic Aperture Radar (SAR) imagery acquired by aircraft (e.g., Intera, 1982-84; Vaudrey, 1990). However, SAR imagery acquired by satellites is a recent source of ice data and still has to be validated as a reliable data source. The European (ERS-1) satellite was launched in July 1991 and has a 30 meter resolution, only 2-3 times less than Intera's STAR-1 airborne SAR system with a resolution of 10-15 meters.

Ice velocity is another design parameter required to predict the ice flux (amount of ice to move past a platform during a given season) in order to compute the encounter frequency of a multiyear floe or ice island collision. Sequential SAR satellite images may be useful to determine pack ice drift, acquired when the ERS-1 satellite is functioning in a 3-day repeat cycle. Ice drift may be sufficient to provide the ice flux, but an "instantaneous" velocity (over a 1-2 hour period or less) is still needed (e.g., Vaudrey, 1987) for momentum calculations during a summer multiyear floe/ridge impact with an offshore structure.

It is anticipated that remote sensing (Vaudrey, 1988a), such as SAR satellite imagery, can be utilized to help develop a long-term prediction of an encounter between an offshore production platform and a drifting ice island, a significantly more hazardous ice feature than multiyear floes, but also extremely more rare. The prediction model (e.g., Vaudrey, 1988b) should include an estimation of the current ice island population, island concentration, and ice island size or diameter distribution, all of which can be determined from the archives of SAR satellite imagery. In addition, SAR satellite imagery may be used during operations as a predictive tool in near-real time to track ice islands as they move into Alaskan coastal waters and become a potential hazard to platforms.

The objective of this study is to evaluate SAR satellite imagery as a data source for developing design and operational ice criteria at the Kuvlum Field. The study is broken down into the following tasks: (1) SAR satellite resource center assessment, (2) SAR data selection and acquisition, and (3) SAR satellite imagery evaluation and analysis. The last task is subdivided further, according to the following extreme ice features: (1) multiyear floes, (2) ice islands, (3) shear zone rubble and first-year floebergs, and (4) summer ice coverage.

## **2. SAR SATELLITE RESOURCE CENTERS**

### **2.1 *ERS-1 Satellite Description***

In July 1991 the European Space Agency launched ERS-1, carrying an array of active microwave sensors to gather data primarily for the fields of oceanography, meteorology, glaciology, and climatology. For the first time data are being collected routinely from remote areas of the polar regions and southern oceans. The ERS-1 satellite has a sun-synchronous, near polar, quasi-circular orbit with a period of about 100 minutes. The satellite can be programmed for a repeat cycle of 3 days, 35 days, or 176 days.

The Active Microwave Instrument (AMI) aboard the ERS-1 satellite is comprised of two separate radars, one being a Synthetic Aperture Radar (SAR). The SAR provides all-weather (through cloud cover and darkness) imagery, 100 kilometers wide, to the right of the satellite track. The SAR operates at a frequency of 5.3 GHz (C-band) and has a linear vertical (VV) polarization and an incidence angle of 23°. In the image mode, the SAR has a spatial resolution of 26 m across track and 30 m along track. Imagery is acquired for a maximum duration of 10 minutes per orbit to conserve power. Since the data rate is too high for onboard storage, imagery is acquired only within the reception zone of a ground receiving station. The primary ground station for acquiring SAR data over the Alaskan Beaufort Sea is the Alaskan SAR Facility located in Fairbanks.

### **2.2 *Canadian Centre for Remote Sensing (CCRS)***

The Radar Data Development Program (RDDP) is a federal government program led by the Department of Energy, Mines and Resources at the Canadian Centre for Remote Sensing (CCRS). The main goal of the RDDP is to ensure that Canadians are able to use SAR effectively for resource management and environmental monitoring. One of the prime reasons for developing radar remote sensing capabilities in Canada has been the ability of SAR to provide reliable reconnaissance and surveillance data of sea ice conditions in Canadian waters, particularly during periods of unfavorable weather conditions and darkness.

Compared to other radar remote sensing applications investigated under the RDDP, the sea ice effort has been more successful in developing the operational use of SAR imagery. The work is focused on three main goals: 1) preparation of ice forecast charts by the Ice Centre Environment Canada (ICEC), 2) ice reconnaissance for ship navigation in ice-infested waters, and 3) delivery of SAR ice products to end users, such as offshore oil operators.

During a visit to Ottawa in June 1993, Mike Manore of the CCRS was interviewed. He indicated that they have performed a study to compare ERS-1 SAR imagery to airborne SAR imagery (STAR2) developed by Intera Consultants Ltd. (Calgary) for CCRS. The STAR2 imagery provides greater detail at floe boundaries. For example, a large multiyear conglomerate floe identified on ERS-1 SAR imagery shows up as several individual floes on STAR2 imagery. The primary difference in the two SAR systems is the steep angle of incidence of  $23^\circ$  for the ERS-1 SAR, while STAR2 has a range of incidence angles from  $60^\circ$  to  $85^\circ$ . A secondary difference between the two systems is the frequency bandwidth (C-band for ERS-1 SAR, X-band for STAR2).

The CCRS is currently developing an operational ice motion algorithm for automated tracking of ice between sequential SAR images, but Bruce Ramsey of the Canadian Ice Centre indicates that such a system is not currently being used on an operational basis at ICEC. In addition, the CCRS has made a digital mosaic of ERS-1 SAR imagery for the Arctic islands, from Banks I. to Baffin I. and north to Ellesmere I. They have used data over an 18-day period from both Canadian ground tracking stations at Prince Albert (Saskatchewan) and Gatineau (Quebec).

### *2.3 Ice Centre Environment Canada (ICEC)*

The Ice Centre is the Canadian governmental agency that provides daily and weekly ice charts for navigation and fishing along the east coast and between the Arctic islands. The ice charts contain ice edge location, ice concentration, ice type, and predicted ice thicknesses. Their primary

sources are: 1) airborne SAR imagery (Intera's STAR2), 2) Side-Looking Airborne Radar (SLAR) aboard a government owned DASH-7 aircraft, and 3) NOAA-AVHRR imagery. All of this imagery is available in near-real time, downlinked directly to the ICEC. There is no available user interface to obtain the raw imagery data, only the ice charts that are supplied by mail or fax from the ICEC. One exception is a direct downlink capability to some vessels, including the Canadian Coast Guard, navigating the St. Lawrence seaway.

Ice charts produced for the Canadian Beaufort Sea are based primarily on NOAA-AVHRR imagery with details during the summer shipping season supplied by SLAR and ice observers aboard weekly DASH-7 flights. There is no airborne SAR imagery (STAR2) available for the Beaufort Sea on a routine basis. The ICEC also has the software capability (same as or similar to Fairweather, Inc. in Anchorage) to enhance the NOAA-AVHRR imagery by removing hazy, thin cloud layers. Thus far, no satellite SAR imagery is used in an operational sense by the ICEC.

Currently, ERS-1 SAR imagery is retransmitted in a reduced resolution (approximately every fourth pixel or 2000 lines per image) format from processed imagery received from the Gatineau tracking station. None of this data is archived, only used and erased after 1-2 weeks. No information is received from Prince Albert at this time; however, the ICEC hopes to establish a link with Prince Albert (via Gatineau) before the Canadian RADARSAT satellite is launched in 1995.

Overall coverage of the Canadian east coast is provided by NOAA-AVHRR imagery, and details are provided primarily by airborne SAR imagery (STAR2). The ERS-1 SAR imagery is currently limited to supplement airborne SAR imagery along the east coast (Gatineau station mask does not reach the Beaufort Sea) of Canada to provide very specific details. The ERS-1 SAR imagery is very good for early detection of ice growth which damps the wave action in protected bays and lagoons and virtually eliminates the open water backscatter.

The operations people at the ICEC do not like ERS-1 SAR imagery, because there is significant open water backscatter due to wind-generated "choppiness" of the water surface. The backscatter virtually obliterates low ice concentrations (2 to 3 tenths ice coverage or less) in the open ocean away from bays and lagoons. In addition, ERS-1 SAR imagery makes the ice surface appear almost completely "white" at high temperatures (near freezing), even before surface ponding occurs. Other complaints of ERS-1 SAR imagery from ICEC ice analysts are: 1) areal coverage of each SAR image is too small, 2) imagery acquisition is not frequent enough for eastern Canada, and 3) the imagery has a "gray" scale that is too flat to differentiate multiyear ice, first-year ice, and young ice in the high Arctic. The overall conclusion is that the operations people at the ICEC are not impressed by ERS-1 SAR imagery and use it only as a "last resort".

Interviews with ICEC ice analysts yielded the following discussion of ice type identification using SAR imagery: "Multiyear ice is distinguished from first-year ice primarily by the brightness levels or tonal quality (gray scale). However, both of these parameters can be modified during processing and enhancement. Therefore, ICEC frequently relies on secondary parameters, such as floe shapes (multiyear is more circular), shape and size of melt ponds, and drainage and fracture patterns (texture)."

#### 2.4 *RADARSAT International (RSI)*

In addition to the two Canadian government agencies, there is RADARSAT International (RSI), a private Canadian consortium located in Ottawa and Richmond, BC, that is contracted by the CCRS to process and distribute SAR satellite imagery in an operational (near-real time) mode once the Canadian RADARSAT satellite is launched in 1995. RSI has also been designated as the North American distributor for ERS-1 SAR satellite imagery on a commercial basis. However, they too must acquire any SAR satellite data of the Alaskan Beaufort Sea, west of Barter Island, from the Alaskan SAR Facility (ASF) in Fairbanks, then turn around and sell it for about 30 times what ASF charges for a NASA-approved research project.

## 2.5 *Alaskan SAR Facility (ASF)*

The Alaskan SAR Facility (ASF) is a NASA-funded project, set up to house and coordinate reception of satellite SAR data, a processing system for the generation of SAR images, an archive to support science investigations, and an operations system. Receiving and data processing systems are implemented by the Jet Propulsion Laboratory (JPL) of Pasadena, California, and the operations and archives are the responsibility of the University of Alaska, Fairbanks (UAF).

The ASF currently is a ground station for the ERS-1 and the Japanese (JERS-1) SAR satellites, but ASF will also be a ground station for reception of RADARSAT SAR imagery when the Canadian satellite is launched in 1995. The process of recording data from the satellite (signal data) is called a data take. Data takes are a minimum of one minute to a maximum of ten minutes long. The signal data covers a long curved swath on the ground. Signal data is not directly usable and must be correlated into images. The images produced by ASF are 100 km by 100 km. There are approximately 5 images created per 1 minute of signal data.

The satellite will normally transmit SAR data to the ground station when it is more than 5 degrees above the horizon (relative to the ground station). There is an area on the ground that can be viewed directly by the satellite while it is transmitting data to the ground station. This ground area is known as the station mask. In the case of the ASF the station mask is a circle with a radius of approximately 3009 km centered on Fairbanks. Real time SAR data is constrained to fall within this station mask.

It should be noted that about 2-3 minutes per data take of any ERS-1 satellite pass over the Beaufort, Chukchi, or Bering Seas is dedicated for retransmission to the Navy-NOAA Joint Ice Center in Suitland, Maryland (U.S. counterpart to the Canadian ICEC). These SAR data are utilized, along with passive microwave (SSM/I) and NOAA-AVHRR imagery, to produce weekly ice charts, which give ice edge position, ice concentration, ice type, and predicted ice thickness.



**SAR Data Products.** After receiving and processing the signal data, they are stored in the ASF archives as catalogued data sets. Very little JERS-1 data are collected and archived, so the vast majority of the data products available to users come from ERS-1 SAR imagery. The ASF data sets, which can be directly ordered by approved users, include both SAR Data and Geophysical Processor System (GPS) Data.

The archived SAR and GPS Data are catalogued by data take ID and image ID numbers. SAR data products are categorized as either Full-Res or Low-Res Images. Both are available in several different types of media, including black and white prints or transparencies and digitally on computer-compatible tapes (CCT's) or 8 mm tape cartridges.

Full-Res images are 4-look SAR images with 30 m resolution and 12.5 m pixel spacing over a 100 km by 100 km area. These are 8192 x 8192 x 8 bit (64 MB) amplitude images suitable for making black and white photographs or displaying on a graphics workstation. The image location is given for the four corners and the center of each image. The net rms location error is about 200 meters. These images are standard products and created routinely when new data are collected.

Lo-Res images are produced by an 8 x 8 averaging process of the Full-Res images. Thus, Lo-Res images have a 240 m resolution and 100 m pixel spacing. The resulting image is 1024 x 1024 x 8 bits or only 1 megabyte. These images are the easiest for the ASF to handle, resulting in faster service and lower operating costs. ASF recommends that Lo-Res images be used as the primary data source. When absolutely required, the more costly Full-Res images can be ordered. Lo-Res images are also standard data products and are the basis of the browse file archived at the Geodata Center of the ASF.

The Geophysical Processor System (GPS) Data derives digital products from ASF SAR images. Since ERS-1 SAR imagery is a single frequency (C-band), single polarization (VV) radar, the geophysical algorithms are tuned for images with these characteristics. Three geophysical

algorithms have been implemented to generate: (1) Ice motion vectors, (2) Ice type classification, and (3) Wave spectra. All of the images used in ice motion analysis and ice classification are geocoded (transformed from a planimetric representation into a standard cartographic projection).

The GPS ice motion tracker compares two Lo-Res images taken nominally 3 days apart in order to determine the movement of ice floes identifiable in both images to estimate the velocity field for the area that overlaps both images. Typically, the registration accuracy is better than 300 m and is approximately 100 m in areas with relatively little ice deformation.

The GPS ice classifier differentiates ice types from pixel samples in Lo-Res images, based on their normalized backscatter coefficient. Typically, the principal ice types which can be identified in the ESR-1 SAR data are: multiyear, undeformed first-year, deformed first-year, and new ice/smooth open water. The number and accuracy of the identified ice types in a single image depends on the season and air temperature at the time of data acquisition. The results of the classifier are available as: 1) a classification map which gives the ice type of each pixel, and 2) a grid product which provides the fraction of each ice type over a 5 km x 5 km grid.

The ice type classifier is currently programmed to process only data acquired during freeze-up and winter and located away from the seasonal ice zone. Specifically, the classifier is restricted to process images acquired between Julian day 270-365 and 1-120, located north of 73° latitude. The user of ice type products should be aware of the shortcomings of the classifier algorithm, such as:

- Open water may be incorrectly labeled as first-year or multiyear ice due to its wind-dependent backscatter characteristics.
- Backscatter of highly deformed first-year ice is expected to be comparable to that of multiyear ice. For example, the deformed rubble in the shear zone along the coast have high backscatter.
- Surface melt tend to mask out multiyear ice signature.

### **3. SAR DATA SELECTION AND ACQUISITION**

As part of this study, a research proposal was submitted to NASA through the ASF to acquire and evaluate SAR data products from the ASF. The constraints of becoming an approved NASA user or principal investigator are: 1) the results of the proposed project should demonstrate a potential commercial application of the SAR data, and 2) a summary of the evaluation and findings must be submitted to the ASF, which has the right to publish them in the open literature. Approval by ASF and NASA was granted, and the remainder of this report discusses SAR data selection and acquisition from the ASF and SAR data evaluation and analysis, presented in Section 4.

As part of the NASA/ASF proposal, the Mission Planning group of ASF was requested to acquire future SAR imagery within an area containing the Kuvlum Prospect and bounded by a rectangle, ranging from 70° N to 72° N and from 135° W to 150° W. The request was considered almost redundant by Mission Planning since they are acquiring and processing every ERS-1 satellite pass that crosses this area as part of their standard operating procedure.

All of the SAR data was selected from several searches of the ASF online catalogue, which contains over 50,000 ERS-1 SAR images. To reduce the number of selected SAR images, specific seasonal and location criteria were employed for each search. The primary search was performed during a visit to the ASF in May 1993. The potential SAR data search list was pared down further by reviewing and assessing laser print copies of Lo-Res images in the browse file located in the Geodata Center of the ASF. Ultimately, a representative sample of 57 Lo-Res and 5 Full-Res ERS-1 SAR images was selected for evaluation and limited analysis. Photographic prints of each selected image were ordered and received from the ASF Geodata Center.

## 4. DATA EVALUATION AND ANALYSIS

### 4.1 *Multiyear Floes*

A search of midwinter SAR data acquired during 1991-92 and 1992-93 produced several images with a significant multiyear floe population in the region to the north and east of ARCO's Kuvlum Prospect. Multiyear floes were positively identified using ERS-1 SAR satellite imagery through a combination of tone (brightness), shape, and texture. Most of the floes visually designated as multiyear ice are brighter than the surrounding ice and have a generally circular or ellipsoidal shape with a mottled texture. Some of the larger multiyear floes appear to be "composite" floes, made up of several smaller multiyear floes, while other floes that are grouped together appear to be fragments of a larger single floe. Both Low-Res and Full-Res images from the ASF are processed at a scale of 1:500,000 (100 km by 100 km scene), which makes it very difficult, if not impossible, to detect individual floes smaller than 300 meters.

Using visual identification, multiyear ice fraction can be determined as a percentage of the area covered by each satellite image. The definition of ice fraction, as used here, indicates each ice type as a percentage of the total area. Thus, if open water were present in the image, the multiyear ice fraction, first-year ice fraction, and open water fraction would add up to 100%.

The multiyear ice fraction analysis can be performed at the same time as the multiyear floe size or diameter distribution. The analysis consists of identifying each individual floe, determining its size or diameter, and adding it to the population. The multiyear ice fraction is computed by multiplying the total number of floes identified for each image by the average floe area, then dividing that value by the total area covered by the SAR image. An example SAR image (Image ID 58368, center coordinates of 71.4°N, 144.3°W), acquired on May 2, 1993, was analyzed. For comparison between a Lo-Res laser print and a Full-Res contact photographic print, this SAR image is shown in Figure 1 (Lo-Res) and Figure 2 (Full-Res).

PLT  
ILLUM

0 20 KM

FIGURE 1

MISSION SENSOR PARAMETERS

PLATFORM ID: E-EP51  
SAR ID: SAR  
WAVELENGTH: E1 S 09392.01  
FREQUENCY: C-Band, LP-Pes  
WAVELENGTH: 5.3001E+09Hz  
POLARIZATION: VV  
TIME CENTER TIME:  
1993 122:21:15:59.964(02-MAY)

PROCESSING PARAMETERS

PRODUCT TYPE:  
Standard Low-Pes Positive Paper  
PRODUCT ID: 58368200  
RADIOMETRIC PRESENTATION:  
Amplitude  
CENTER INCIDENCE ANGLE:  
22.9842 deg  
Film Generation Time:  
1993 344:00:57:33.74 (10-DEC)

SCENE AND IMAGE PARAMETERS

SCENE ID: 58368200  
IMAGE GENERATION DATE:  
1993 135:03:54:38.000(15-MAY)  
IMAGE SIZE: 1024\* 1024  
PIXEL SPACING= 100.00m  
CENTER LAT= 71.41deg  
CENTER LON= -144.26deg  
HEADING= 206.05deg

Ground Plane Projection

SCALE ERROR= 0.18E-02  
LOCATION ERROR= 0.14E+03m  
SKEW DIST= 0.0005000  
ORIENTATION ERR= 0.0010000

ALASKA SAR FACILITY  
STANDARD FULL-RES FILM  
IMAGE ID: 58368100  
OS ORDER: U00000006423 004

FLY  
ILLUM  
0 10.00KM



FIGURE 2

MISSION SENSOR PARAMETERS

PLATFORM ID: SAR-ERR1  
SENSOR ID: SAR-ERR1  
DATE: 1993 09392.01  
FREQUENCY: 5.3001E+09HZ  
Polarization: VV  
Scene Center Time: 1993 122:31:13.39 9641 02-MAY

PROCESSING PARAMETERS

PRODUCT TYPE:  
PRODUCT ID: 58368100  
RADIOMETRIC PRESENTATION:  
AMPLITUDE  
CENTER INCIDENCE ANGLE:  
22.9842 DEG  
FILM GENERATION TIME:  
1993 347:15:31.50 55 (13-DEC)

SCENE AND IMAGE PARAMETERS

SCENE ID: 58368100  
IMAGE GENERATION DATE:  
1993 133:03:54.30 000 (15-MAY)  
IMAGE SIZE: 8192 8192  
PIXEL SPACING: 71 12.50M  
CENTER LAT: -144.418 DEC  
HEADING: 206.05 DEC

GROUND PLANE PROJECTION

SCALE ERROR= 0.18E-02  
LOCATION ERROR= 0.14E+03M  
SKEW DIST= 0.0005000  
ORIENTATION ERR= 0.0013000

IMAGE GENERATED BY NASA ASF. SAR DATA (C) ESA. 1993

PROCESSOR AND PHOTO LAYOUT DEVELOPED BY NASA JPL.

The multiyear ice fraction analysis was performed on the Full-Res SAR image, shown in Figure 2. A multiyear ice fraction of 22% was computed with about 1700 individual multiyear floes identified. The average floe size or diameter was 1100 meters with a standard deviation of 640 meters. The largest multiyear floe had a diameter of 6000 meters, and the minimum or "cutoff" floe size was 300 meters. It should be noted that there are actually many floes in the multiyear ice population that are smaller than 300 meters, but they cannot be identified and counted due to the limitation imposed by the scale at which the SAR satellite imagery is processed.

This problem of scale means that any multiyear floe size distribution developed from SAR satellite imagery processed at the ASF will be truncated, without including any of the multiyear floe population having diameters smaller than 300 meters. Such a distribution is biased toward larger diameter floes, and any statistical analysis using these distributions to develop multiyear floe encounters and the resulting ice loads for production structures will be overly conservative. However, other data (including aerial photography and airborne SAR imagery) exist which can provide a representation of multiyear floe sizes smaller than 300 meters. Additional analysis can be performed to merge these data sets and obtain a more complete and accurate overall floe size distribution.

The ice type classifier built into the geophysical processor system (GPS) could not be utilized during this study of the region around the Kuvlum Prospect since it is restricted to process image data acquired in the pack ice north of 73°N. The primary reason for this restriction is that the algorithm of the ice type classifier cannot distinguish between highly deformed first-year ice and multiyear floes due to a similarity in the backscatter of these two ice types. In addition, during the summer, surface melt ponds tend to mask out the multiyear ice signature, and open water between ice floes may be incorrectly labeled as multiyear ice due to wind dependent backscatter characteristics of the open water.

Ice velocity determined from the ice motion tracker built into the geophysical processor (GPS) was found to be very limited. The algorithm tracks the ice motion by locating common ice features in a pair of images viewed at different times. However, the time differential is restricted to a period of 3 days or more, which produces an ice velocity equivalent to the nominal pack ice drift. In addition, most of the SAR images chosen for ice motion analysis were located far offshore in the perennial pack ice. This type of ice motion product, as currently configured, is not very useful for developing a design ice movement criterion for offshore structures.

#### 4.2 *Ice Islands*

During a visit to the ASF in Fairbanks, Dr. Martin Jeffries (who has been studying ice islands) at the Geophysical Institute was interviewed. He said that ice islands can positively be identified using SAR satellite imagery. The surface "rolls" (gently undulating ridges and troughs) and brightness of an ice island produces a unique signature on SAR imagery.

Several ice islands, including Hobson's Choice, have been located on ERS-1 SAR imagery. Hobson's Choice can be seen in a Full-Res SAR image as the elongated white object embedded in a vast multiyear floe in the lower right-hand corner of Figure 3 (Image ID 22454), acquired on September 22, 1991. The dark, parallel lines within Hobson's Choice are the surface undulations. Two additional ice islands can be detected embedded in another multiyear floe in the lower left-hand corner of Figure 3. However, all of these ice islands and fragments have been found between the islands of the Canadian Archipelago, not in the Beaufort Gyre of the Arctic Ocean. No ice islands were detected during a brief scan of the acquired ERS-1 SAR imagery of the high-latitude Arctic Ocean; however, the search was not complete.

Another potential use of SAR satellite imagery is to check on the existing ice shelves of Ellesmere Island on a periodic basis (once a year or so) to determine if a "shelf breakout" has occurred since shelf disintegration is the primary source of ice islands in the Arctic Ocean. Currently, Dr. Jeffries



is performing such an assessment of the Ellesmere ice shelves as part of his ongoing research project.

An example of a Full-Res SAR image of some of the Ellesmere Island ice shelves is shown in Figure 4 (Image ID 23867), acquired on March 17, 1992. "North" is to the lower right where the multiyear pack ice of the Arctic Ocean can be seen as it slowly moves to the west past the island. The Milne Ice Shelf, showing two major cracks, is the most prominent ice shelf shown in this SAR image, located near the upper right-hand edge of Figure 4. Just east (below) of the Milne Ice Shelf is the smaller Ayles Ice Shelf, also displaying several cracks. The largest ice shelf on Ellesmere Island, the Ward Hunt Ice Shelf, is located outside of the image just below the lower edge of Figure 4. In fact, the western end of the Ward Hunt Ice Shelf (including the "milky" colored Cape Discovery Ice Rise) can be seen at the bottom of the image. The "white" fiord running across the bottom third of the image is the McClintock Inlet, which also had a large ice shelf at its mouth. However, the McClintock Ice Shelf virtually disintegrated between 1962 and 1966, producing a significant increase in the ice island population and accounted for many of the ice island sightings along the Alaskan Beaufort Sea coast in the late 1960's and throughout the 1970's.

ALASKA SAR FACILITY  
STANDARD FULL-RES FILM  
IMAGE ID: 22454100  
AOS ORDER: U0000003465 016

FLY  
ILLUM

00.0000

Two ice islands

Hobson's Choice

FIGURE 3

<b>MISSION SENSOR PARAMETERS</b>		<b>PROCESSING PARAMETERS</b>		<b>SCENE AND IMAGE PARAMETERS</b>		<b>GROUND PLANE PROJECTION</b>	
ATFORM ID: E-ERSI		PRODUCT TYPE:		SCENE ID: 22454100		SCALE ERROR= 0.18E-02	
TAKE: S1S00961.01		PRODUCT ID: 22454100		IMAGE GENERATION DATE:		LOCATION ERROR= 0.14E+03M	
DE: C BAND HR-RES		RADIOMETRIC PRESENTATION:		1992 178:15:25:43.000 (26-JUN)		SKEW DIST= 0.0005000	
FREQUENCY: 3001E+09HZ		AMPLITUDE		IMAGE SIZE: 8192x 8192		ORIENTATION ERR= 0.0010000	
POLARIZATION: VV		CENTER INCIDENCE ANGLE:		PIXEL SPACING= 77.12M			
CENTER TIME: 23 0353 DEC		23 0353 DEC		CENTER LAT= -99.350 DEC			
991 265:03:22:48.R42(22-SEP)		FILM GENERATION TIME:		HEADING= 322.78DEC			
AGE GENERATED BY NASA ASF. SAR DATA (C) ESA. 1991		1992 189:04:34:30.85 (07-JUL.)					
PROCESSOR AND PHOTO LAYOUT DEVELOPED BY NASA/JPL.							

ALASKA SAR FACILITY  
 STANDARD FULL-RES FILM  
 IMAGE ID: 23867100  
 ACQUISITION ORDER: U0000006114 002

FLT  
 ILLUM  
 0 20.00KM



FIGURE 4

MISSION SENSOR PARAMETERS

PLATFORM ID: E-ERSI  
 SENSOR ID: SAR  
 DATA TAKE: E1 S: 03496.01  
 FREQUENCY: C BAND, HR-RES  
 POLARIZATION: VV  
 CENTER TIME: 1993 00 11 03 705 (17-MAR)  
 DATE: 92 77 00 11 03 705 (17-MAR)

PROCESSING PARAMETERS

PRODUCT TYPE:  
 PRODUCT ID: 23867100  
 RADIOMETRIC PRESENTATION:  
 AMPLITUDE  
 CENTER INCIDENCE ANGLE:  
 2.0325 DEG  
 FILM GENERATION TIME:  
 1993 07 11 12 22 26.50 (28-SEP)

SCENE AND IMAGE PARAMETERS

SCENE ID: 23867100  
 IMAGE GENERATION DATE:  
 1993 04 16 4 000 (11-JUL)  
 IMAGE SIZE: 8192  
 PIXEL SPACING: 12.30M  
 CENTER LAT: 82.700 DEG  
 CENTER LON: 77.900 DEG  
 HEADING: 297.49 DEG

GROUND PLANE PROJECTION

SCALE ERROR= 0.18E-02  
 LOCATION ERROR= 0.14E+03M  
 SKEW DIST= 0.0005000  
 ORIENTATION ERR= 0.0010000

PROCESSOR AND PHOTO LAYOUT DEVELOPED BY NASA JPL

#### 4.3 *Shear Zone Rubble and First-Year Floebergs*

The shear zone can be located and the extent of grounded ice rubble can be determined from SAR satellite imagery acquired in the winter. First-year floebergs, generated in the shear zone during the winter, can become potential hazards to drilling operations during the summer (Beaudril 1992 Limited, 1993). As an example, a sequence of seven images acquired from March through May 1992 and during August 1992 was used to located floeberg sources and track a vast floeberg, which grounded north of the Kuvlum drill site during summer drilling.

The deep-water floeberg source is shown on the Full-Res SAR Image ID 35134, acquired on May 4, 1992 (Figure 5) as a narrow band of gray-to-white ice, indicating heavily deformed first-year ice. The vast floeberg AB is shown still embedded as part of the recently formed shear zone. Another Low-Res SAR Image ID 24420, acquired on August 31, 1992 (Figure 6), shows the location of the same Floeberg A'B', approximately 3 miles north of the Kuvlum drill site. The *Kulluk* can be seen as a tiny, white dot on the SAR imagery in Figure 6. Floeberg AB moved a total of 53 miles to the east-southeast from its place of origin north of Prudhoe Bay to the Kuvlum site.

A letter report was submitted to ARCO on July 1, 1993, containing a detailed discussion of: 1) the storms in April 1992 that created the deep-water floeberg source, 2) a historical perspective of the late winter of 1992, and 3) the identification and movement of Floeberg AB. This letter report is reproduced in the Appendix to provide a more complete understanding of the formation of floebergs and their potential hazard to summer drilling operations.

ALASKA SAR FACILITY  
STANDARD FULL-RES FILM  
IMAGE ID: 24420100  
S ORDER: S0000000771 001

N  
FLT  
ILLUM  
0 20.00KM

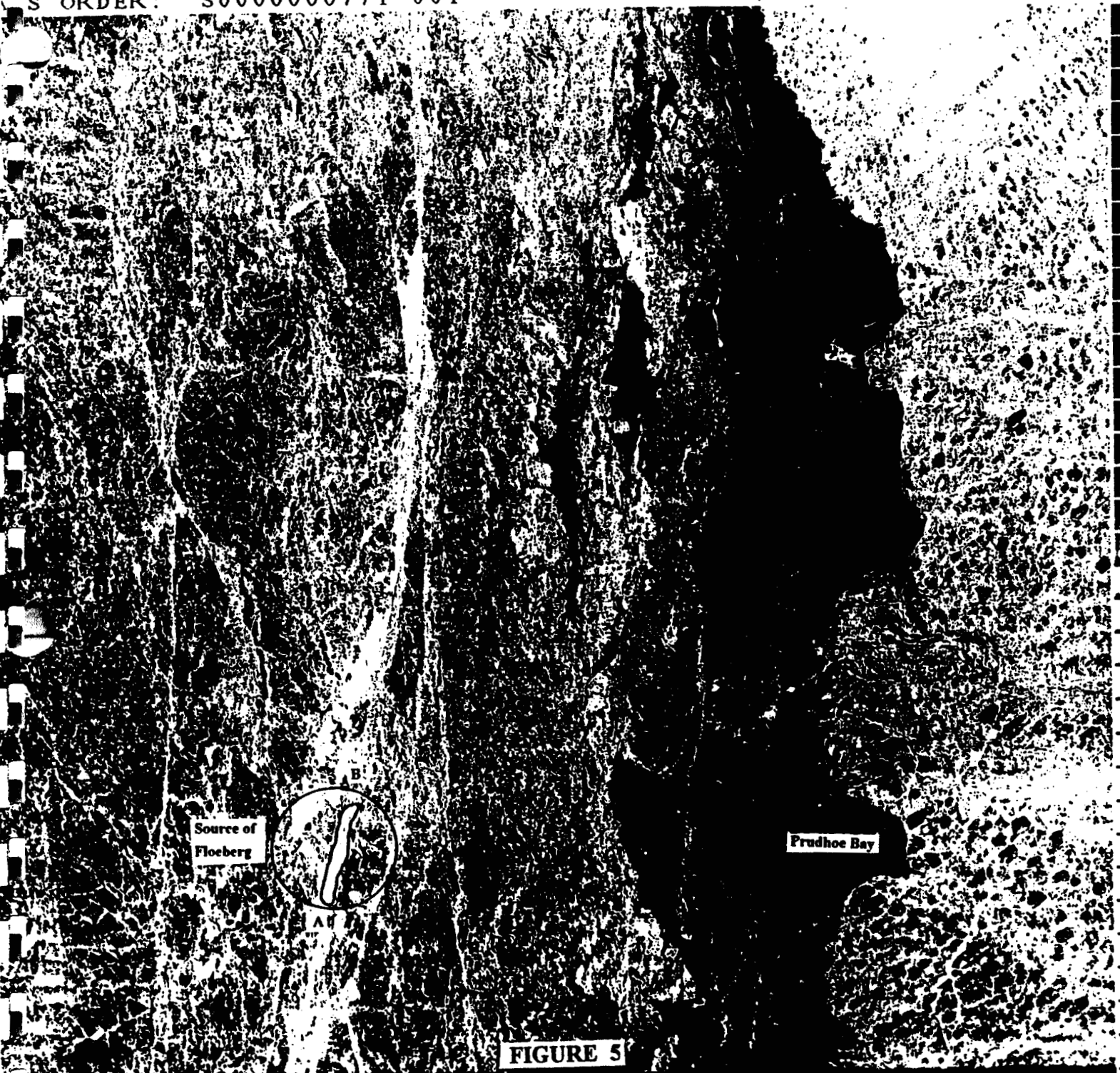


FIGURE 5

MISSION SENSOR PARAMETERS

PLATFORM ID: E-ERSI  
SCENE ID: SAR  
TAKE: S-04196-91  
BAND: HR-RES  
FREQUENCY: 5-3001E-09HZ  
Polarization: VV  
CENTER TIME: 25-21:24-55.302(04-MAY)  
1993

PROCESSING PARAMETERS

PRODUCT TYPE:  
PRODUCT ID: 24420100  
RADIOMETRIC PRESENTATION:  
AMPLITUDE  
CENTER INCIDENCE ANGLE:  
23.0403 DEG  
FILM GENERATION TIME:  
1993 347:10:40:33.62 (13-DEC)

SCENE AND IMAGE PARAMETERS

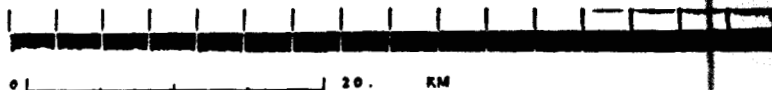
SCENE ID: 24420100  
IMAGE GENERATION DATE:  
1992 197:10:05:16.000(15-JUL)  
IMAGE SIZE: 8192  
PIXEL SPACING: 12.20M  
CENTER LAT: 70.490DEG  
CENTER LON: -147.400DEG  
HEADING: 204.950DEG

GROUND PLANE PROJECTION

SCALE ERROR= 0.18E-02  
LOCATION ERROR= 0.14E+03M  
SKEW DIST= 0.0005000  
ORIENTATION ERR= 0.0010000

PROCESSOR AND PHOTO LAYOUT DEVELOPED BY NASA JPL

GENERATED BY NASA ASF. SAR DATA (C) ESA, 1992



## 5. SUMMARY AND RECOMMENDATIONS

The objective of this study was to evaluate SAR satellite imagery as a data source for developing design and operational ice criteria at the Kuvlum Prospect. Results of the evaluation can be summarized in the following list of positive and negative comments:

### *Positives:*

1. SAR satellite imagery provides a valuable data source, as a supplement to the existing aircraft SAR data base collected in the early 1980's, for developing both multiyear ice fraction and multiyear floe diameter distributions as input parameters to design criteria for offshore structures.
2. SAR satellite imagery can be used to identify, locate, and track any ice islands currently rotating within the Beaufort Gyre and to determine if new ice islands have calved from the ice shelves of Ellesmere Island.
3. SAR satellite imagery acquired in the winter can be used to locate the shear zone and determine the extent of grounded ice rubble in order to assess the potential hazard to summer drilling operations from floebergs generated in the shear zone.

### *Negatives:*

1. ERS-1 SAR satellite imagery cannot be used in the summer to locate the ice edge, determine the ice concentration, or identify specific ice types (e.g., multiyear or first-year ice features) because open-water backscatter, due to surface roughness from wind-generated waves, frequently masks out the ice signature.
2. Multiyear floe size analysis using SAR satellite imagery processed at a scale of 1:500,000 results in a truncated distribution that does not contain any floes smaller than 300 meters. This shortcoming requires that the SAR satellite data be merged with other existing data bases before appropriate design criteria can be developed.

3. The ice motion tracker built into the Alaskan SAR Facility geophysical processor is very limited since movement is recorded over a period of 3 days or more, resulting in an ice velocity equivalent to the nominal pack ice drift, which is not very useful for developing design ice movement criteria for offshore structures.
4. The ice type classifier built into the Alaskan SAR Facility geophysical processor cannot be utilized for the region around the Kuvlum Prospect since it is restricted to process imagery acquired in the pack ice north of 73°N. The classifier cannot distinguish between multiyear floes and highly deformed first-year ice due to a similarity in the backscatter characteristics of these two ice types.

In addition to the evaluation summary, it is recommended that the following analyses be performed using SAR satellite imagery to develop design criteria for offshore production facilities at the Kuvlum Prospect:

1. A number of existing data bases (including several years of airborne SAR imagery and aerial photography) should be combined with SAR satellite imagery and analyzed to develop multiyear ice feature statistics as input to compute ice encounter frequencies and design ice loading for offshore production structures.
2. Ice island information should be developed from the archives at the Alaskan SAR Facility and combined with other available data to obtain a set of ice island statistics, including an estimate of the overall population, movement, and diameter. These resulting statistics should be inserted into a long-term forecasting model for predicting the encounter frequency of an offshore platform or a subsea pipeline in the Camden Bay region with an ice island.



## **6. REFERENCES**

1. Beaudril 1992 Limited (1993), ARCO Floeberg Study, Calgary, Alberta.
2. Intera Environmental Consultants Inc. (1982), Synthetic Aperture Radar (SAR) Study of the Beaufort and Chukchi Sea Ice - 1981, AOGA Project 144, Houston, Texas.
3. Intera Environmental Consultants Inc. (1983a), Synthetic Aperture Radar Program of the Bering, Chukchi, and Beaufort Sea Ice - 1982, AOGA Project 177, Houston, Texas.
4. Intera Environmental Consultants Inc. (1983b), Synthetic Aperture Radar Program of the Bering, Chukchi, and Beaufort Sea Ice - 1983, AOGA Project 218, Houston, Texas.
5. Intera Arctic Services Inc. (1984), Beaufort Sea: 1984 Alaska SAR Project, AOGA Project 257, Lakewood, Colorado.
6. Vaudrey & Associates, Inc. (1987), 1985-86 Ice Motion Measurements in Camden Bay, AOGA Project 328, San Luis Obispo, California.
7. Vaudrey & Associates, Inc. (1988a), Ice Island Identification and Tracking Using Remote Sensing, AOGA Project 363, San Luis Obispo, California.
8. Vaudrey & Associates, Inc. (1988b), Ice Island Parameter Statistics and Ice Island Encounter Frequency with Production Structures in Alaskan Beaufort Sea and Chukchi Sea, prepared for Unocal Oil & Gas Division (Anchorage, Alaska), San Luis Obispo, California.
9. Vaudrey & Associates, Inc. (1990), 1989 Multiyear Floe Concentration and Distribution in the Beaufort and Chukchi Seas Developed from SAR Imagery, AOGA Project 373, San Luis Obispo, California.
10. Vaudrey & Associates, Inc. (1992), Multiyear Ice Statistics for the Beaufort and Chukchi Seas, prepared for Chevron Oil Field Research Company (La Habra, California), San Luis Obispo, California.



**APPENDIX**

**ADDENDUM TO ARCO'S FLOEBERG STUDY  
BASED ON ANALYSIS OF 1992 SAR SATELLITE IMAGERY**

## APPENDIX

### **ADDENDUM TO ARCO'S FLOEBERG STUDY BASED ON ANALYSIS OF 1992 SAR SATELLITE IMAGERY**

**Introduction.** The scope of work for the SAR Satellite Imagery Project was expanded to include mid-to-late winter and summer 1992 coverage of the nearshore Beaufort Sea from Prudhoe Bay to Camden Bay. The objective of this expanded effort is to determine the possible source of floebergs that were a hazard to drilling at the Kuvlum site during the 1992 summer season. A sequence of seven SAR satellite images was obtained for March-May 1992 (March 12, April 15, April 23, and May 4) and August 1992 (August 1, August 14, and August 31). The ice conditions were compared from image to image to locate and track identifiable ice features, including floebergs. Since most floeberg sources are created during shearing ice motion produced by windy conditions, the late-winter 1992 storms most likely to have developed the hazardous floebergs are identified and used to determine if similar storm events occurred during the past two decades.

**Deep-Water Floeberg Source.** By March 12, 1992, the typical nearshore shear zone was not very apparent, but there was a distinct zone of shearing between 70°-50' and 71°N, at 148°W, and between 70°-30' and 70°-40'N, at 146°W (see Figure A-1). The lack of grounded ice in the 60-foot water depth made the ice relatively unstable and susceptible to movement, especially during a westerly storm. Between two consecutive SAR images acquired on March 12 and April 15, almost the entire ice cover offshore of the barrier islands between Cross I. and Flaxman I. moved about 7 nautical miles to the east-southeast. It is very likely that most of this movement occurred as a result of two relatively short duration, westerly storms on April 5-6 and April 11-12. The first storm was more intense with sustained winds of 25-30 knots, gusting to 35-40 knots. The second storm had sustained winds of only 15-20 knots.

Both of these westerly storms loosened the ice cover and produced an open-water lead just south of the existing zone of shearing. This lack of confinement created the conditions for extensive shear rubble formation during an easterly storm wind, if such a wind occurred within 1-2 weeks after the westerly storm. A sustained, intense east-northeasterly wind began at midday on April 15 and continued for the next 60 hours. The April 15-18 easterly storm generated sustained winds of 25-30 knots with gusts to 45 knots.

A SAR image acquired on May 4 (Figure 5 in the main body of the report) depicts a 1-2 mile wide zone of heavily deformed shear rubble (shown as a shaded area on Figure A-1), running in a WNW-ESE direction parallel to the barrier island chain between 146° and 149°W about 15-18 nautical miles offshore. In addition, a 2-3 mile wide shear zone east of Barter Island appears on a SAR image acquired on April 23. It is also shown on Figure A-1 as a shaded area.

The shear rubble that formed during the easterly storm on April 15-18 was partially grounded or floating in water depths of 90-100 feet west of Cross Island and 115-120 feet north and east of Cross Island. The offshore boundary of the shear zone east of Barter Island was located in water depths of 110-120 feet.

Using several ice features that were positively identified on each of the two consecutive SAR images acquired on April 15 and May 4, an ice movement of 43 NM was measured for the pack ice offshore of the newly-formed shear zone, but the ice remained relatively landfast for a distance of 8-10 nautical miles offshore of the barrier islands. The ice motion during the April 15-18 storm was undoubtedly greater than 43 NM since a moderate (15-20 knot) westerly wind blew steadily from April 29 through May 4. These westerly winds would have moved the ice back to the east some distance, even though the ice motion would have been minimized by the westward transport of the Beaufort Gyre.

The bottom line is that a deep-water source of potential floebergs formed to the west of the Kuvlum site during an unusual late-winter 1992 storm sequence (first a westerly to reduce confinement of the ice cover, followed by an easterly to create the shear rubble).

***Floeberg Identification and Movement.*** On August 31, 1992, a SAR satellite image (Figure 6 in the main body of the report) clearly shows the *Kulluk* on location at the Kuvlum site with two vast floebergs about 3 miles north of the site (shown on Figure A-1). One of the floebergs (marked B'-A' on Figure A-1) was approximately 6 miles long and 0.7 mile wide. This floeberg was also found on SAR images acquired on August 1 and August 14 and its position plotted on Figure A-1. The August 1 SAR image shows that the shear zone was breaking up east of 147°W, but the identified floeberg (marked A-B on Figure A-1) remained embedded in its original position within the shear zone, 15 NM north of Cross Island. Even though most of the ice cover had broken up by August 1, Floeberg A-B was in the same position as shown in the SAR image on May 4 (Figure 5).

Since Floeberg A-B remained landfast north of Cross Island for 3½ months (mid-April to early August), it may have been partially grounded or confined within a partially grounded shear zone, located in 115'-120' of water. After the ice surrounding the floeberg broke up in late July, westerly winds during early August 1992 drove Floeberg A-B to the southeast along the 120-foot isobath (see August 14 position of Floeberg A"-B" on Figure A-1). The floeberg continued its southeasterly trek toward the Kuvlum site during westerly winds in mid-August. Floeberg A-B moved a total of 53 nautical miles to the ESE (from its origin north of Cross Island to the Kuvlum site). Due to its deep-water origin in about 120 feet of water, either Floeberg A-B or a similar floeberg from the same zone of shearing could have run aground in the vicinity of the Kuvlum site (105-foot water depth) while creating a 10'-15' deep gouge (recorded by an ROV).

***Historical Perspective of 1992.*** The formation of floating shear rubble in deep water by a sequence of intense westerly and easterly storm winds during late winter is an unusual event. Meteorological observations acquired at Barrow for March and April from 1970 through 1991 were investigated to determine the return period for the storm events that occurred in April 1992. The criteria for storm sequence selection were: (1) westerly storm followed within 10 days by an easterly storm, (2) wind speeds  $\geq 22$  knots for  $\geq 24$  hours from the west and for  $\geq 48$  hours from the east, and (3) easterly wind direction in the range of 050°-070°.

No other westerly-easterly storm sequence that met the above criteria was found in the 22-year data base. This indicates that the return period was  $\geq 25$  years for the set of April 1992 storm events. Typical wind conditions during late winter are easterly winds up to 12-18 knots, interrupted occasionally by brief ( $< 24$  hours), intense (18-25 knots) westerly storms.

There were several individual storm events that met the criteria, but the wind reversal was missing. As examples, strong easterly winds blew on April 3-5, 1983, and on April 12-15, 1971, but there was no westerly storm that preceded either of the easterly events.

Numerous wind reversals from west to east occurred (e.g., April 1986), but the sustained wind speeds were lower and the duration was shorter than the criteria presented above. For example, a 20-knot westerly occurred on April 6-7, 1989, followed by a 15-20 knot easterly wind on April 16-18, but the westerly attained 20 knots for only 12 hours and the easterly exceeded 20 knots for only 18 hours.

**Summary and Conclusions.** A deep-water source of potential floebergs formed to the west of the Kuvlum drill site during an April 1992 storm sequence (first a westerly to reduce confinement of the ice cover, followed by an easterly to create the shear rubble). Based on 23 years (1970-1992) of meteorological records at Barrow, the set of April 1992 storm events had a return period of 25 years or more.

A sequence of seven SAR satellite images acquired from March through May 1992 and during August 1992 was used to locate floeberg sources and track a vast floeberg (approximately 6 miles long and 0.7 mile wide) which grounded north of the Kuvlum site during drilling. The identified floeberg was originally part of a deep-water shear zone that developed in 115-120 feet of water, 15 nautical miles north of Cross Island, during a ENE storm on April 15-18, 1992.

The floeberg remained landfast north of Cross Island for  $3\frac{1}{2}$  months. After break-up of the ice surrounding the floeberg, westerly winds during the first half of August 1992 drove the floeberg into the vicinity of the Kuvlum drill site. The floeberg moved a total of 53 nautical miles to the ESE (from its origin north of Cross Island to the Kuvlum site).

Due to its deep-water origin in about 120 feet of water, it is possible that such a floeberg ran aground in the vicinity of the Kuvlum site (105-foot water depth) and produced the 10'-15' deep gouge documented by an ROV.

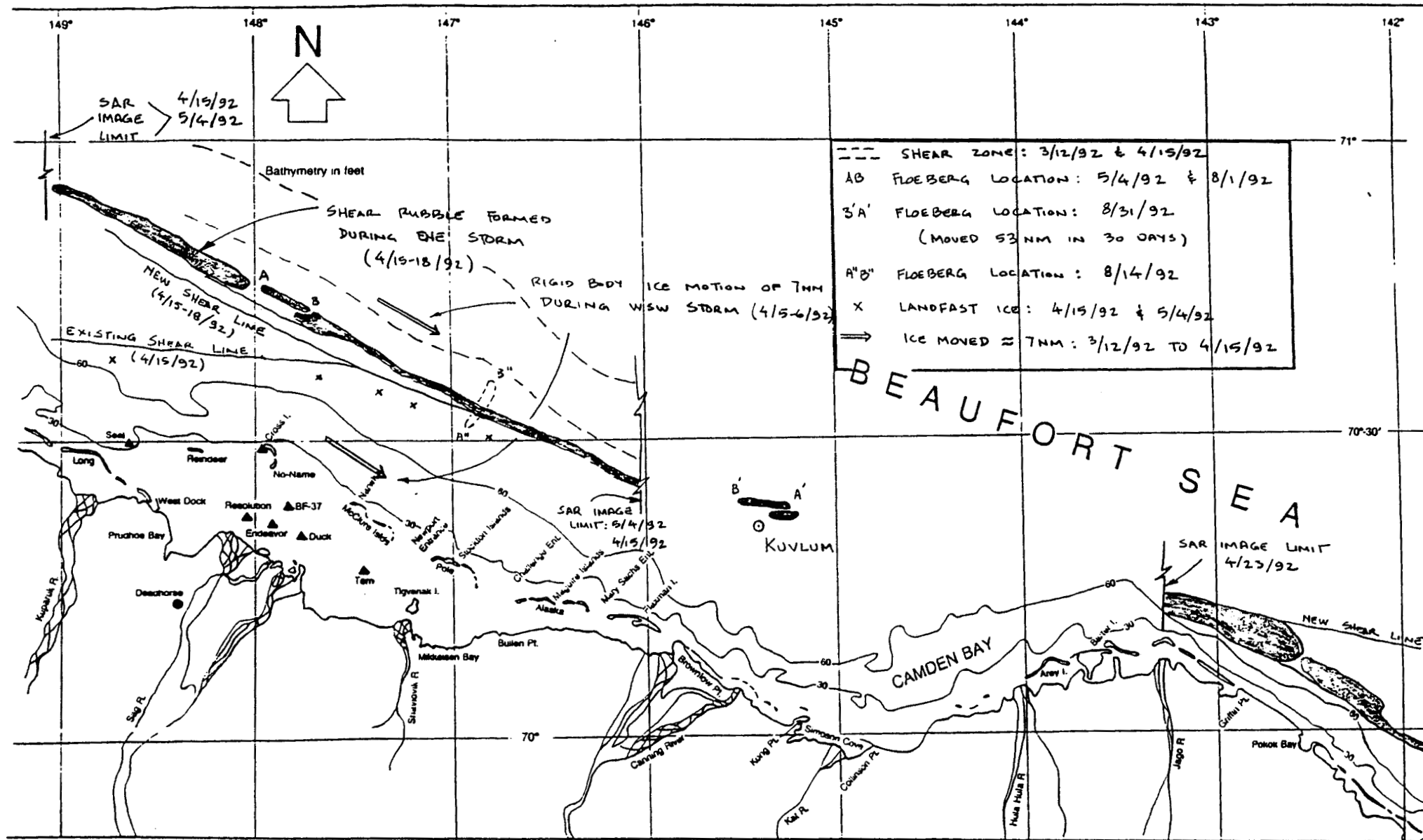


FIGURE A-1.

# **ARCO Alaska Floeberg Study**

## **May 1993**

### **Summary**

Beaudril, Ltd was contracted to coordinate a study of large ice features present in the Camden Bay area. Numerous experts were employed to provide their particular area of expertise. The cover and executive summary are provided in the following section. The full report was provided at the July 21, 1993 Kuvlum Predecision Studies Engineering meeting.

---

## **Arco Alaska Floeberg Study**

0311

05

04

04

05

*B. Wright & Associates Ltd.  
Canatec Consultants Ltd.  
K. Vaudrey & Associates Ltd.  
B. Dixit  
Beaudril (1992) Ltd.*

**May 1993**

---

## Table of Contents

Contents	i
List of Figures	iv
List of Tables	vii
Executive Summary	1-1
1.0 Purpose	2-1
2.0 Introduction	2-1
3.0 Background	3-1
4.0 Objectives	4-1
5.0 Methodology	5-1
6.0 Ice Conditions Overview	6-1
6.1 General	6-1
6.2 Ice Zonation	6-2
6.3 Winter Conditions	6-4
6.4 Summer Conditions	6-13
7.0 Floeberg Overview	7-1
7.1 General	7-1
7.2 Past Observations	7-5
8.0 Floeberg Assessment	8-1
8.1 Data Base	8-1



8.1.1	Information Identification	8-1
8.1.2	Data Types	8-2
8.2	Data Analysis	8-14
8.2.1	General	8-14
8.2.2	Winter Floeberg Sources	8-15
8.2.3	Summer Floeberg Occurrence	8-16
8.3	The Origin of Floebergs	8-21
8.3.1	Ice Morphology and the Origin of Floebergs	8-21
8.3.2	Parameters Affecting Floeberg Numbers	8-24
8.4	Interpretation and Processes	8-26
8.4.1	Can We Compare Floeberg Counts from Different Sources?	8-26
8.4.2	Comparison of Grounded Rubble Areas and Floebergs	8-32
8.4.3	Annual Behaviour of Ice and Floebergs	8-34
8.4.4	Effect of Winds	8-35
8.4.5	Is Kuvlum in a "Floeberg Alley"?	8-35
8.4.6	Was 1992 a "Bad" Year?	8-45
8.4.7	Floeberg Size Distribution	8-48
8.4.8	Are Floebergs Indicated in the AES Ice Maps?	8-50
8.4.9	Is there a Relationship Between Floebergs and Ice Concentration?	8-55
9.0	Floeberg Implications on Floating Drilling & Production	9-1
9.1	General	9-1
9.2	Implications on Floating Drilling Systems	9-3
9.3	Downtime Due to Floebergs	9-7

9.4	Combined Ice Downtime	9-15
9.4.1	Kulluk	9-15
9.4.2	Drillships	9-30
9.5	Implications on Production	9-37
10.0	Floeberg Prediction	10-1
10.1	Long Term Prediction	10-1
10.2	Practical Prediction	10-5
Appendix A	Environmental Alert Procedures	
Appendix B	Ice Management Overview	
Appendix C	Year by Year Floeberg Summaries	
Appendix D	Ice Chart Interpretations	
Appendix E	Floeberg Counting Circles	

## List of Figures

Figure 2.1	Floebergs at Kuvlum in 1992	2-3
Figure 2.2	Ice Management of Flobergs at Kuvlum	2-5
Figure 3.1	Artificial Islands in the Beaufort Sea	3-3
Figure 3.2	Beaufort Sea Caisson Islands	3-3
Figure 3.3	Drillship in the Beaufort Sea	3-4
Figure 3.4	Kulluk in the Beaufort Sea	3-4
Figure 3.5	Floebergs at Kuvlum	3-7
Figure 3.6	Large Floebergs at Kuvlum in 1992	3-8
Figure 3.7	Floeberg Clusters at Kuvlum	3-9
Figure 3.8	Floeberg Management at Kuvlum	3-9
Figure 5.1	Study Methodology	5-2
Figure 5.2	Large Floebergs at Kuvlum in 1992	5-3
Figure 5.3	Location Map	5-5
Figure 6.1	Winter Ice Zonation in the Beaufort Sea	6-3
Figure 6.2	Pressure Ridging at the Landfast Ice Edge	6-5
Figure 6.3	Pressure and Shear Ridging	6-6
Figure 6.4	Ridge and Rubble Fields at the Fast Ice Edge	6-8
Figure 6.5	Winter Seasonal Pack Ice	6-10
Figure 6.6	Polar Pack Ice Edge During Break-up	6-11
Figure 6.7	Multi-year Ice Floes and Ridges	6-12
Figure 6.8	Extreme First Year Pressure Ridge	6-14
Figure 6.9	Shear Ridge Fields at the Fast Ice Edge	6-15
Figure 6.10	July NOAA Image of Break-up Conditions	6-17
Figure 6.11	Summer Ice Intrusion	6-18
Figure 6.12	Extreme Floebergs at Kuvlum in 1992	6-20
Figure 7.1	Floebergs at Kuvlum in 1992	7-3
Figure 7.2	Multi-year Hummock Field in the Beaufort Sea	7-4
Figure 7.3	Grounded Shear Ridge Complex off Oliktok	7-6
Figure 7.4	1975 SLAR Image Showing Grounded Ridge Field	7-9
Figure 7.5	Cross Section of Grounded Shear Ridge Field	7-10
Figure 7.6	Floebergs at Pitsiulak in 1983	7-12

Figure 7.7	Cross Section of Floebergs from 1983	7-13
Figure 8.1	Example of SAR Imagery	8-4
Figure 8.2	Example of Landsat Imagery	8-8
Figure 8.3	Example of NOAA-AVHRR Imagery	8-10
Figure 8.4	Example of AES Ice Chart	8-12
Figure 8.5	Example of Floeberg Counting Procedure	8-19
Figure 8.6a	Floeberg Count Comparison - Belcher, 1988	8-28
Figure 8.6b	Floeberg Count Comparison - Belcher, 1989	8-29
Figure 8.6c	Floeberg Count Comparison - Kuvlum, 1992	8-30
Figure 8.6d	Floeberg Count Comparison - Kuvlum, 1992	8-31
Figure 8.7	Winter Ridge Areas versus Floeberg Counts	8-33
Figure 8.8	Location Map	8-36
Figure 8.9a	Floeberg Densities 1973-74	8-37
Figure 8.9b	Floeberg Densities 1975-76	8-38
Figure 8.9c	Floeberg Densities 1977-79	8-39
Figure 8.9d	Floeberg Densities 1980-81	8-40
Figure 8.9e	Floeberg Densities 1984-85	8-41
Figure 8.9f	Floeberg Densities 1986-88	8-42
Figure 8.9g	Floeberg Densities 1989	8-43
Figure 8.10a	Floeberg Counts by Year	8-46
Figure 8.10b	Floeberg Counts by Year	8-47
Figure 8.11	Floeberg Size Distribution	8-49
Figure 8.12a	SAR/AES Comparison	8-52
Figure 8.12b	SAR/AES Comparison	8-53
Figure 8.12c	SAR/AES Comparison	8-54
Figure 8.13	Ice Concentration versus Floeberg Density	8-56
Figure 9.1	Floeberg Density versus Downtime, 1992	9-8
Figure 9.2	Ice Concentration versus Downtime, 1992	9-8
Figure 9.3	Floeberg Encounter Return Period by Year	9-12
Figure 9.4	Operating Season Assessment Methodology	9-21
Figure 9.5	Kulluk Operating Season Profile	9-23
Figure 9.6	Kulluk Operating Season Probabilities	9-24
Figure 9.7	Kulluk Operating Day Probabilities	9-25
Figure 9.8	Drillship Operating Season Profile	9-33
Figure 9.9	Drillship Operating Season Probabilities	9-34

**Figure 9.10** Drillship Operating Day Probabilities

9-35

**Figure 10.1** Recommended Floeberg Prediction Approach

10-6

11-0  
12-0  
13-0  
14-0  
15-0  
16-0  
17-0  
18-0  
19-0  
20-0  
21-0  
22-0  
23-0  
24-0  
25-0  
26-0  
27-0  
28-0  
29-0  
30-0  
31-0  
32-0  
33-0  
34-0  
35-0  
36-0  
37-0  
38-0  
39-0  
40-0  
41-0  
42-0  
43-0  
44-0  
45-0  
46-0  
47-0  
48-0  
49-0  
50-0  
51-0  
52-0  
53-0  
54-0  
55-0  
56-0  
57-0  
58-0  
59-0  
60-0  
61-0  
62-0  
63-0  
64-0  
65-0  
66-0  
67-0  
68-0  
69-0  
70-0  
71-0  
72-0  
73-0  
74-0  
75-0  
76-0  
77-0  
78-0  
79-0  
80-0  
81-0  
82-0  
83-0  
84-0  
85-0  
86-0  
87-0  
88-0  
89-0  
90-0  
91-0  
92-0  
93-0  
94-0  
95-0  
96-0  
97-0  
98-0  
99-0  
100-0

---

## List of Tables

Table 8.1	Floeberg Ice Information Data Base	8-58
Table 8.2	Ice and Floeberg Data Summaries by Year	8-64
Table 8.3	Floeberg Data Summary	8-75
Table 9.1	Parametric Assessment of Floeberg Encounters	9-11
Table 9.2	Average Floeberg Encounter Return Period	9-11
Table 9.3	Characteristic Break-up Conditions	9-17
Table 9.4	Characteristic Summer Conditions	9-18
Table 9.5	Characteristic Freeze-up Conditions	9-19
Table 9.6	Expected Kulluk Operating Days	9-26
Table 9.7	Overall Kulluk Downtime for 100 Day Program	9-29
Table 9.8	Expected Drillship Operating Days	9-36
Table 9.9	Overall Drillship Downtime for 50 Day Program	9-36

---

## Executive Summary

### Introduction

In this report, the term floeberg has been used to describe large, rough ice features that are comprised of severe ridge and rubble field fragments, and have been observed drifting in the Kuvlum area. Because of their size and thickness, the presence of these floebergs represents a concern to the efficiency of floating drilling operations and, in the longer term, a design issue for bottom founded production structures and pipelines. Large floebergs cannot be practically managed by the icebreakers that support floating drilling vessels, and were the primary cause of drilling downtime during 1992 Kulluk operations at Kuvlum.

This study has been conducted to obtain a better understanding of floeberg occurrences at Kuvlum, in light of the problems experienced during the 1992 drilling season. The objectives of the work were:

- to identify and review ice information relevant to floeberg occurrences at Kuvlum
- to establish the source areas where floebergs originate and determine their expected summer occurrence frequencies at Kuvlum

- to assess the effect of expected floeberg populations on the efficiency of floating drilling operations at Kuvlum and highlight their implications on production structures and seafloor facilities
- to discuss possible approaches for predicting expected floeberg conditions at Kuvlum prior to the summer drilling season

#### Floeberg Data Base

In order to gain a better understanding of floeberg populations at Kuvlum and to quantify their occurrence frequencies, a large amount of historical ice information was reviewed. This information included various forms of satellite imagery, visual observations from winter and summer field reconnaissance flights, recent airborne radar imagery and historical ice charts. The information provided intermittent observations over the 1973 to 1992 period, which increased in terms of both quality and frequency of coverage with time. Although the information spanning the early 1970's to early 1980's period was useful for some aspects of the floeberg assessment work, airborne radar imagery that was available from drilling operations conducted over six of the past ten years provided the best information source. This radar data, supplemented by direct wellsite observations, was used almost exclusively for detailed analyses of floeberg sizes and occurrence frequencies.



## Floeberg Assessment

The key results of the floeberg assessment work are summarized as follows.

- most floebergs found in the vicinity of Kuvlum originate from grounded ridge formations located off Barter Island and the Barrier Islands in winter
- large floebergs ( $> 0.6\text{nm}$ ) in length are quite common in the Kuvlum area during the summer, with average seasonal densities over the floating drilling season varying between 0.8 and 3.4 large floebergs per  $100\text{nm}^2$
- Kuvlum is not in "floeberg alley" but can be affected by a significant number of floebergs in any given year
- the number of large and very large floebergs ( $> 0.6\text{nm}$ ) that are expected at Kuvlum and the surrounding area is substantially less than smaller floebergs and rough floes in the 0.15m to 0.6nm range
- average seasonal densities for these smaller, more manageable floebergs and rough floes range from 10 to 30 per  $100\text{nm}^2$  over the floating drilling season
- the number of floebergs observed around Kuvlum normally decreases over the course of the open water season, with the highest densities occurring two to three weeks after general ice break-up, and, during ice intrusions from the north or northwest
- there is a relationship between the number of floebergs expected during the summer season and the

areal extent of grounded ridge formations found in the area during winter, with higher summer floeberg densities associated with larger winter source areas

- most floebergs are formed from grounded ridge fields in water depths between 40 and 80 feet, and as a result, floeberg keels in excess of 100 feet that could ground in the Kuvlum area are considered uncommon
- there is no clear correlation between observed floeberg populations and regional summer ice conditions shown in the historical ice charts and as a result, the longer term ice chart data base cannot be used to "extend" the floeberg information that has been developed in this study

#### **Floeberg Effects on Floating Drilling Operations**

The effect of floebergs on the efficiency of floating drilling operations at Kuvlum was considered in terms of downtime potential. In a practical sense, the key points to note about the influence of floebergs on floating drilling operations are as follows.

- floebergs in the large (>0.6nm) and very large (>1.8nm) size categories are of primary concern in terms of drilling downtime, since they are considered largely unmanageable
- large floebergs are of equal consequence to the Kulluk and drillship systems, but the Kulluk, with icebreaker

support, is much less susceptible to downtime from smaller floebergs and other ice conditions

- floebergs less than 0.6nm in size can often be managed (given a reasonable level of icebreaker support) and normally, are of less concern

- however, smaller floebergs moving at high speeds, associated with high ice concentrations or occurring in poor visibility, can result in some downtime

- floebergs with keels in the order of 100 feet in depth are rare, with grounding occurrences like the one experienced at Kuvlum in 1992 (which resulted in the longest downtime episode) considered as very infrequent

- floeberg encounters leading to drilling disruptions will be episodic, in the sense of occurring quite sporadically in time

- encounters with large floebergs can be expected every one to two weeks in August of most years, and tend to decrease thereafter, except during ice intrusions

- 1992 was characterized by persistently high and uniform floeberg densities throughout the operating season, and in this regard was different in comparison to most other years

- in years with normal floeberg densities at Kuvlum, an average encounter return period of 25 days should be expected for large floebergs, and about 8 days of downtime assigned to either the Kulluk or a drillship

as the result of large floeberg encounters assuming a 100 day drilling season

- in years with high floeberg populations, encounter return periods of about 10 days should be expected for large floebergs, with as much as 20 days of potential downtime estimated for a 100 day floating drilling program.

#### Combined Ice Downtime

Floebergs will be an ongoing concern for floating drilling operations in the Kuvlum area in terms of potential downtime. However, floebergs are not the only source of downtime. High ice concentrations, large rough floes moving at high speeds and multi-year ice also represent potentially hazardous ice situations for drillship and Kulluk stationkeeping operations. In this study, a downtime analysis was also carried out to assess the expected interruption times associated with other adverse ice conditions and the results used to estimate combined ice downtimes for the Kulluk and drillship systems, as highlighted below.

#### *Kulluk*

- in a normal year, assuming a drilling season of 100 days, between 2 and 5 days of Kulluk downtime should be assigned for drilling interruptions caused by adverse ice conditions, other than large floebergs

in poor ice years and again, assuming 100 days of planned Kulluk drilling operations, about 15 days of downtime should be reasonably expected due to adverse ice conditions, excluding large floebergs

when the downtimes from floebergs and other adverse ice conditions are reasonably combined, about 10 and 25 days of Kulluk downtime can be expected in normal and poor years respectively, for a 100 day Kuvlum drilling program

### **Drillship**

in a normal year, assuming a drilling season of 50 days, between 10 and 15 days of drillship downtime should be assigned for drilling interruptions caused by adverse ice conditions, other than large floebergs

in poor ice years, drillship operations will be inefficient, with about 25 days of downtime reasonably expected due to adverse ice conditions, excluding large floebergs, and essentially no operating time in extremely bad years

- when downtime from floebergs and other adverse ice conditions are realistically combined, about 15 and 30 days of drillship downtime can be expected in normal and poor years respectively, for a 50 day Kuvlum drilling program

### Floeberg Implications on Production Systems

From the perspective of long term Kuvlum development, the occurrence of large floebergs represents an obvious design concern for production structures in terms of ice loads, and subsea facilities in terms of ice scour. Since several floeberg encounters can be expected over the course of a seasonal drilling operation at Kuvlum, there is no question that large floebergs will be experienced at and around this location many times during a 20 to 25 year production time frame. Because of their size, thickness and, with ongoing consolidation, their overall strength, the potential effects of floebergs will be one of the key ice design issues to address. However, the effects of other extreme features such as heavily ridged multi-year ice floes are also significant design concerns and will require equal attention. Some implications of floebergs on the design of production systems for Kuvlum are briefly highlighted as follows.

#### *Production Structures*

- production structures will have to be designed to sustain the ice loads resulting from summer and winter interactions with large floebergs, as well as those from multi-year floes and potentially, small ice island fragments
- the global ice loads associated with floebergs will probably be of the same order as those from other extreme ice features, because of their size, thickness and overall strength

- although floebergs originate as first year ice features, their persistence over time should be recognized in long term Kuvlum design work, with populations of second and multi-year "floebergs" also being important to define

- in terms of production structure concepts, designs that can "filter out" extremely thick and large ice features such as floebergs, by dissipating their kinetic energy over relatively long distances and enhancing the likelihood of large scale vertical fragmentation seem desirable (eg: structures with wide protective berms and/or grounded ice rubble)

- for large thick floeberg features, there appears to be little benefit to significantly sloped structures, since flexural failure forces will not be any less than ice crushing forces, for the ice thickness ranges anticipated

- a very preliminary "data base" on floebergs has been developed in this study but systematic, longer term work that is focussed on floebergs and other ice parameters of importance will be required to support future production structure design work for Kuvlum

#### ***Seafloor Facilities***

- the grounding of floebergs with deep keels and the related potential for seafloor scouring (or gouging) represents a concern for the design of any subsea facilities and pipelines associated with Kuvlum development

- the seafloor is known to be heavily scoured around and shoreward of Kuvlum but the relative scouring contributions from deep floebergs and other thick ice forms is not understood
- the implications of floebergs and other deep keel ice features will have to be addressed in the context of the overall scour problem since the scour issue is an extremely important design consideration for seafloor facilities

#### Floeberg Prediction

In order to better plan and schedule floating drilling operations in the Kuvlum area, a predictive capability for forecasting seasonal ice conditions, including floebergs, well in advance of drilling would be an obvious benefit. Some techniques for the long term prediction of summer ice conditions along the Alaskan Coast have been developed, but their results have shown little "skill" in forecast terms. In addition to being of questionable reliability, these long term outlooks are coarse in terms of their spatial and temporal resolution, and practically, of limited value for drilling season considerations. At present, long term predictions of generalized seasonal ice conditions represent an art rather than a science, and attempts to predict ice cover details such as floeberg occurrences are not even attempted.

In terms of general ice clearance, the best approach is to review the long term forecasts that are issued by the Joint Ice Centre and AES and "be aware" of the resultant season predictions. However, regardless of the forecast, the



drilling system should be capable of accomplishing the drilling program objectives within a reasonable range of expected ice conditions variability. In addition, the drilling operation should be sufficiently flexible to quickly react to changes in observed ice conditions in terms of mobilization.

Direct and ongoing monitoring of regional ice conditions around Kuvlum is very important to practically assess the manner in which the operating season is developing, including the likely presence of floebergs and other ice features considered hazardous to operations. From the standpoint of floeberg occurrences at Kuvlum, predictions are very difficult. Here, the best approach is to monitor winter floeberg source areas and the drifting floebergs that calve from them, and strategically respond to potential floeberg encounters, if and when they enter the Kuvlum operating area. A practical "prediction strategy" is recommended in this report that acknowledges the difficulties associated with floeberg prediction and provides a stepwise scheme to monitor probable levels of floeberg occurrence prior to and during Kuvlum drilling operations. This approach includes:

- the use of sequential satellite imagery to assess the extent of winter floeberg source areas, monitor the development of summer floeberg populations, and maintain a regional floeberg inventory over the course of the Kuvlum operating season
- the development and implementation of a strategic monitoring program for large floebergs or groups of floebergs, using ice movement buoys and visual reconnaissance, carried out on an incremental basis

within the scope of the Kuvlum environmental and whale monitoring programs

This regional observation and monitoring approach can be used as a basis for practical floeberg occurrence predictions at Kuvlum. In addition, specific floeberg observations obtained from this type of program would be very useful in confirming and extending the information developed in this study, and would also begin to improve the floeberg data base that will be required for various production considerations in the longer term.

FINAL REPORT

LONG TERM FORECAST OF BREAKUP IN THE VICINITY OF THE  
KUVLUM WELL

PREPARED BY IGOR APPEL

FAIRWEATHER FORECASTING  
715 L ST  
ANCHORAGE, AK 99501

PREPARED FOR

ARCO ALASKA, INC  
P.O. BOX 100360  
ANCHORAGE, AK 99510-0360

September 1, 1993

## EXECUTIVE SUMMARY

This report is a compilation of four intermediate reports on a study of long range forecasting of sea ice breakup for the well site "Kuvlum" which is located in Camden Bay on the Beaufort Sea. The site is west of Barter Island, Alaska.

For the purposes of this study "breakup" was defined as when the sea ice at the location of the well site "Kuvlum" reached five-tenths concentration or less. At this stage of ice deterioration it was felt that drilling operations could commence at the well site.

Forecasts for the initial date when ice concentration at the Kuvlum site would be 5/10ths or less were issued on the first day of April, May and June:

April 1st Forecast.-- After studying the dynamic influences of the atmosphere, the preliminary long-term forecast showed an opportunity to begin working in Camden Bay in the fourth week of July 1993. It was noted that it might be possible to carry out an activity plan in 1993 that is close to the upper limits.

May 1st Forecast.-- The second report continued the study of dynamic influences and also studied thermal influences on breakup. This report concluded that breakup would occur 3 to 4 days earlier than that indicated in the preliminary report.

June 1st Forecast.-- In the report issued the first of June, after allowing for conditions which had occurred in April and May, and the study of the effects of multi-year ice, the forecast for breakup was moved forward to 10-17 July.

Ice concentration around the Kuvlum site became less than 5/10ths in the middle of June. However, that decrease of concentration was not stable and during most of the first half of July the ice concentration in the vicinity of the site was more than 5/10ths and became less only on the 14th of July. The early opening in the vicinity of the Kuvlum site this year was caused by an open water zone intruding from the east.

The actual beginning of breakup, characterized by retreat of the compacted ice cover from the larger part of the Alaska coast, occurred between July 7th and 17th (see Figures 1 and 2).

The initial distribution of open water (or ice cover concentration) to the east from the region under study is an additional factor influencing breakup processes in the vicinity of site that will require further study.

## 1.0 INTRODUCTION

Long-range forecasting of ice cover presents one of the most difficult problems in studying polar sea ice. Current methods are based on different principles and quite obviously there is no general agreement on the best approach.

The factors determining ice cover evolution are as follows: dynamic influences, thermal influences, and ice distribution features. A procedure to forecast breakup was developed simultaneously with an investigation of features determining long-range interrelationships in the atmosphere-sea ice system. The large amount of data necessary for the forecast required significant effort to extract the necessary data from the database, to transform them into the proper grid format, and to correct the numerous mistakes contained in the gridded ice data.

A large number of hydrometeorological data for the last two decades were received, analyzed, converted to the necessary format and used in this research. That database includes daily pressure fields for a greater part of the northern hemisphere, air temperature, weekly values of total and partial ice concentration for a dense grid in the Arctic Ocean, and other hydrometeorological characteristics.

During work on the methodology to forecast breakup in the vicinity of Camden Bay, several different processes which affect the evolution of ice cover were studied and statistical relationships between them and breakup were revealed. The relationships were carefully investigated both quantitatively and qualitatively.

The adaptation of a numerical model to the regional conditions of the Beaufort Sea was carried out simultaneously while preparing the necessary hydrometeorological data and optimal approach for using weather observations and satellite imagery.

## 2.0 GENERAL APPROACH

### 2.1 SCALES OF STUDY

The task of predicting ice cover redistribution is made difficult by the many hydrometeorological factors influencing the ice cover condition. Quite different temporal and spatial scales are characteristic of these processes and not all of the processes can be predicted. Therefore we need to group the processes according to their scales and then to study their influence upon ice cover redistribution. Moreover statistical relationships should be explainable by the influence of corresponding physical processes. Therefore, statistical methods are used only if their results can be explained by physical processes and are then called *Physical Statistical Methods*.

The long-range character of the prediction clearly defines the corresponding temporal scale. It is the scale of seasonal changes. Using such scales leads to a peculiarity of long-range forecasting. Such forecasts can take into account only the long-term tendencies of ice cover

evolution. In this case short variations of ice condition are viewed only as an oscillation around the main seasonal changes.

A more difficult task is to choose spatial scales. Ice evolution features of different scales are described by different approaches. Small scale features are taken into account by the thermodynamic model, whereas coarse behavior of the ice cover is the task of statistical study.

## **2.2 REGION OF STUDY**

The main goal is a long term ice forecast for Camden Bay. The ice conditions in this region are determined by the influence of the southern periphery of the great anticyclonic circulation of the Arctic Ocean ice cover.

Thus the region of study is bounded on the south by the coast of the continent and on the north by the northernmost possible position of the desirable ice concentration isoline. In years with very light ice conditions, the position of the five tenths isoline reaches latitude  $75^{\circ}\text{N}$ , due north of Camden Bay. Therefore, this latitude was chosen as the northern boundary of the area under study. The east - west boundaries of the area under study are of secondary importance and it was decided to use a comparable dimension longitudinally. As a result the region was limited by longitudes  $140^{\circ}\text{W}$  to  $150^{\circ}\text{W}$ , with the site approximately between them. This region is called the *original study area*.

Later it was determined that the distribution of ice along the route from Summers Harbor to Camden Bay was also of interest. Therefore, the area of study was expanded to the east to the coast of Banks Island. The expanded area not only takes into account the travel route of the drill rig but also includes the distribution of ice cover upstream of the predominant ice motion.

Determining the air pressure field study area was much easier. All observations of air pressure in the region to the north of  $40^{\circ}$  latitude were taken into consideration.

## **2.3 DATA SOURCES**

The main ice concentration data were obtained for the period 1972-1990 in a gridded digital format from the National Snow and Ice Data Center (NSIDC) in Boulder, Colorado. Northern hemisphere digital satellite data, passive microwave SSMI and SMMR, for the period 1978-1989 were also used. The data from NSIDC contained errors and a great deal of effort was devoted to the analysis of ice distribution maps from that source. Ice maps for the period after 1990 were obtained from the Environment and Natural Resources Institute, UAA and NSIDC.

The distribution of total ice concentration was investigated for a period of almost 20 years. Investigation was carried out for a region limited by the Arctic coast of Alaska and Canada,  $150^{\circ}\text{W}$ ,  $75^{\circ}\text{N}$ , and  $122^{\circ}\text{W}$ . The ice data base consists of total concentration for a grid, all points of which are separated by .25 degrees of latitude and .5 degrees of longitude.

Historical data for atmospheric pressure were obtained from the National Center For Atmospheric Research (NCAR), Boulder, Colorado and from the Polar Science Center, University of Washington. This gridded data covers the entire period of record 1946-1992 for the northern hemisphere. Pressure data for recent months were obtained from the Climate Analysis Center, an arm of the National Meteorological Center.

## 2.4 PROCESSING AND ANALYSIS OF DATA

During the study probability maps of concentrations equal to or greater than five-tenths were produced. These probabilities were evaluated for every week of June, July, and August. For the same weeks the mean position of the five-tenths isoline and mean square root deviation for every half degree of longitude were evaluated.

The area covered by ice concentration with five-tenths or more was taken into consideration along with the position of this isoline. Summer changes in ice concentration in the vicinity of the site for the years of record were divided into three groups of heavy, mean and light ice condition. Then the differences in influencing factors for these groups of years were considered.

To reveal informative features of these influencing factors, causes of anomalous ice cover formation were studied. The relationship between long-range changes in influencing factors and the ice cover state is weak and therefore difficult to analyze. Thus it is very important to identify true interrelations and separate out variables with chance correlation.

## 3.0 DYNAMIC INFLUENCES

### 3.1 LARGE SCALE TRANSPORT

Mean monthly pressure fields were used to characterize large scale transport. Actual pressure data as well as normalized pressure were used for investigation. The procedure to get normalized data was as follows: calculate mean multi-year pressure fields for every month; compute mean square root deviation for every month for 20 years; and determine a pressure deviation normalized about the mean square root deviation value for the corresponding month.

The differences in pressure fields for typical groups of years were plotted on a map and were analyzed. It is important to note that these are not pressure field characteristics, but are pressure field anomalies.

The general conclusions which are characteristic of the evolution of air pressure fields from July to June during years preceding summers with light ice conditions in the vicinity of the site are as follows:

a. Cyclonic circulation over adjoining parts of the Arctic Ocean during the previous July-August, evidently anticyclonic during January-June, and a transitional period in September-December with small vorticity.

b. The outflow of ice cover in July-August, movement along the coast to the west in October-April, and again obvious outflow in May-June.

The next step of research was to investigate the relationship between the breakup of ice cover in the region under study and the monthly features of atmospheric circulation developed during the previous year. Two different spatial scales of atmospheric circulation characteristics were considered: local geostrophic wind at the site and the difference between pressure in the local center of air pressure anomalies. The influence of geostrophic wind in the vicinity of the site is negligible for all months. For studying seasonal changes in the ice cover redistribution it is better to take into account the general peculiarity of the circulation system determining processes in the study region.

The most prominent contribution to the future development of ice cover breakup is made by a larger feature of atmospheric circulation, the difference between pressure in the local centers of air pressure anomalies. The differences between anomalies was chosen as the main influencing factor.

Comparison of the interrelation between ice conditions during breakup and two types of pressure gradients shows that there is little difference between using normalized pressure and actual pressure in predicting ice conditions.

Monthly air pressure fields for each month of the year preceding breakup were further analyzed. Four alternating zones of positive and negative air pressure deflection are characteristic of the difference between monthly pressure for the two groups of years preceding light and heavy ice conditions in summer.

In general for all 12 months analyzed (from July until June) the boundaries of these zones could be most clearly defined for latitudes  $50^{\circ}\text{N}$  -  $75^{\circ}\text{N}$ . Also local extremes of air pressure anomalies are usually found in that latitude belt. The average location of the boundary between the pressure anomaly zone in the Pacific Ocean sector and the pressure anomaly zone over the North American continent lies across the Beaufort Sea. An evaluation of the role of pressure differences between the two local atmospheric anomaly centers, Pacific oceanic and North American continental, was made.

Prior to a typical light ice summer, the high pressure anomaly over the North American continent and the low pressure anomaly over the Pacific Ocean lead to a northward shift in the pack ice along a boundary separating these two pressure anomaly zones, this in turn explains light ice conditions in the Kuvlum vicinity.



### 3.2 VORTICITY OF AIR MOTION

The transfer of air masses described in the previous section deals with large scale motion in the atmosphere. The average distance between adjoining local centers of air pressure anomalies is approximately 4,000 - 5,000 km. This section is devoted to the research of air pressure field features at the smaller synoptic scale.

There is a quasi-circular motion associated with the synoptic air formation of cyclones and anticyclones. In the northern hemisphere air motion in an anticyclone is clockwise and in a cyclone is counter-clockwise. Correspondingly the vorticity in an anticyclone is negative and in a cyclone is positive. Vorticity is defined as the velocity of rotation.

The analysis shows vorticity to have a significant influence on summer breakup. This investigation of vorticity covers the entire Pacific Ocean-American part of the Arctic Ocean. The period of study was four months, from February through May, and daily data on vorticity were used. The most informative scale of vorticity is a quasi-circular motion with a typical radius of 1,000 km. This scale is characteristic not only of atmospheric cyclones and anticyclones but also is characteristic of the anticyclone gyre of ice motion in the Pacific Ocean-American region of the Arctic Ocean. The radius of the gyre is approximately equal to 1,000 km.

Since the main goal of our study was to investigate seasonal changes it was desirable to smooth the data by averaging. A weekly scale was chosen for averaging. A thorough analysis of vorticity changes has identified the best position for the center point from which to calculate vorticity. This center point is situated inside the anticyclonic gyre of ice motion in the Arctic Ocean.

Vorticity changes at this center point were calculated for three groups of years: 1) years preceding light ice conditions; 2) years preceding heavy ice conditions; and 3) all other years. There are large differences between the three groups considered. For each group of years there are periods with anticyclonic conditions lasting more than one month. However, the duration of the periods and their start time is quite different. Long stable periods of anticyclonic rotation of the ice cover leads to the outflow of ice from the area adjoining the Kuvlum site and creates light ice conditions during breakup.

The intensity of anticyclonic circulation also corresponds to the severity of the next summer's ice conditions. The mean value of Laplacian air pressure in April was finally chosen as the index which describes the influence of vorticity on subsequent ice conditions.

#### 4.0 THERMAL INFLUENCES

A primary thermal factor influencing sea ice cover evolution is air temperature. Air temperature data were collected from four stations, Barrow, Barter Island, Inuvik, and Sachs Harbour. These stations are separated by approximately equal distance and provide observations at different points along the coast in the study area.

A quantitative and qualitative analysis of the relationship between the portion of the original study area covered by 5/10ths or greater ice concentration in July and average monthly temperature at these stations was made for each of the 12 preceding months. The results show the relationship between ice conditions during breakup and prior air temperatures is usually weak, but some systematic features are revealed.

First, the sign of the correlation is negative in more than 80% of all cases. This means that increasing temperature during previous months results (statistically) in lighter ice conditions the next summer. The greater number of exceptions to this is at Sachs Harbour, far from Camden Bay. An unexpected positive correlation was obtained only for April and May at the three other meteorological stations.

It is important to note there are positive coefficients of correlation in April for all four stations studied. This testifies to the unique role of April processes in the subsequent sea ice cover evolution and particularly in breakup. A similar unique role for April was noted in analyzing the influence of vorticity.

The statistical correlation of ice conditions during breakup with previous average monthly temperatures is qualitatively similar for different months with the exception of the spring months, April and May.

From theoretical investigations it is known that the timing of air temperature changes in winter does not influence the final thickness of ice growth. Therefore temperature from several months can be averaged. So three-month averages of temperature were made from July until March. Conclusions for the averaged data are approximately the same as for monthly data. They are as follows:

A. The most prominent relationship exists between ice conditions in the vicinity of the Kuvlum site and air temperature at Barrow, even though Barrow is situated farther from the site than Barter Island. The greater the influence of the ocean on hydrometeorological conditions at a station the better correlation between air temperature at the station and ice coverage. In the synoptic spatial scale Barrow is surrounded mostly by sea. Therefore air temperature at Barrow is more informative for studying sea ice conditions than the other three stations.

B. The relationship between air temperature at Barrow and ice coverage the next summer is strongest for temperatures from the previous July-October. There are large areas of open water or new ice during this period. Air temperature determines the temperature of water as well as

the processes of melting and freezing. As a result the distribution of temperature and salinity depends mainly on air temperature and influences following thermal and dynamic processes of the ocean-ice cover system. In winter the influence of air temperature is less while the sea is covered by ice and the surface temperature is rather uniform.

## 5.0 REDISTRIBUTION AND INFLUENCE OF OLD ICE

The duration of floating drill rig operations in the arctic seas is mainly determined by ice conditions. Ice concentration is the main influencing factor as the effect of ice floes in a compacted ice cover is integrated.

Usually the ice cover is a mixture of ice of different ages. The thicker the ice the greater the danger for floating rig operations. Every year a large part of the ice cover in the Camden Bay vicinity consists of second year ice and multi-year ice. We use the term "old" ice for any type of ice that has survived at least one summer's melt.

The distribution of old ice is an index which characterizes the ice cover. As a rule, during winter and spring months, thick first year ice or old ice adjoins the coast. Polynyas and zones of young ice can be created along the coast and then disappear without influencing the subsequent ice distribution in the vicinity of Camden Bay. Retreat of the ice cover is not an unusual event. Often such atmospheric circulation causing ice pack retreat takes place in May. The mean duration of such processes is one week.

Old ice is of interest not only as an ice distribution characteristic but also as a parameter to track ice motion. Changes in the old ice boundary reflect a redistribution of ice cover due to motion.

Digitized data on ice distribution were used to study interannual and seasonal changes in old ice coverage. The dataset contains information not only about total concentration but also about partial concentration of ice in different stages of development.

An analysis of historical data of old ice distribution in the last week of March, April, May and June was carried out. The intention was to explore the influence of the previous ice cover condition upon the subsequent summer breakup.

The data on old ice concentration was extracted from the gridded sea ice database. A preliminary analysis of the data confirmed that they are not reliable. Sometimes the stage of ice development was undetermined or unknown. The latter cases were eliminated from consideration. Moreover often the presence of old ice was noted but its concentration was not determined. The large number of observations with unknown old ice concentrations precluded the use of old ice concentration data.

Only the presence or absence of old ice was identified. Rather often large unexplainable changes in old ice coverage were detected. These changes are fictitious, the result of erroneous data.

Therefore only averaged data were used. Two different kinds of averaging were done: a) averaging of the same month from different years; and b) averaging of different months from every year.

The result of monthly averaging of the presence of multi-year ice gives the probability of old ice of any concentration. The changes in ice concentration from month to month reflects mean seasonal redistribution of old ice and corresponds to the mean monthly pressure field.

The northerly retreat of all old ice isolines far from the Beaufort Sea coast is typical for April. It is explained by the west-northwest drift direction peculiar to the anticyclone over the adjoining part of the Arctic Ocean with isobars oriented parallel to the northern coast of Alaska. On the contrary in May the probability of old ice increases for all parts of the Beaufort Sea despite the seemingly constant baric conditions. Anticyclone circulation similar to April is observed in May over the Arctic Ocean, however the general system of winds is changing. There is a large inflow of ice into the Beaufort Sea across the east side of its northern boundary. That inflow of ice along the Canadian archipelago leads to an increase in the probability of old ice across most of the Beaufort Sea and an advance of the old ice boundary toward the coastline.

Finally in June the historical mean ice motion in accordance with air pressure fields becomes westward across the Beaufort Sea. It causes a northerly retreat of isolines and a decrease in old ice probability for all parts of the Beaufort Sea with an exception, the region near the coast from  $142^{\circ}\text{W}$  westward to Pt. Barrow. This region with an increasing probability of old ice is a narrow belt along the coast, approximately 60 miles wide. But that belt is situated in the vicinity of interest, Camden Bay and areas to the north.

These changes in the probability of old ice can be explained. During May southward motion of the ice cover usually forms a tongue of ice in the proximity of Mackenzie Bay. The location of old ice in that region is the most southern in the Beaufort Sea. Later in June that tongue moves to the west. And as a result, changes for the worse in ice conditions are typical in June for the study area.

The next step in investigating the influence of old ice is to evaluate the relationship between old ice distribution in the spring and the subsequent breakup. The accuracy of the old ice data is not sufficient to describe a qualitative relationship. Therefore the study is limited to only a quantitative description. The small number of years with reliable old ice concentration data was segregated into three groups characterized by large, mean, and small amounts of old ice during spring in the region under study. Then ice conditions during the summer breakup period were compared with the previous coverage by old ice. The results are as follows. Large concentrations of old ice in the spring can result in light, mean, and heavy ice conditions during the next summer. Small amounts of old ice in the spring leads to various summer ice conditions. Mean amounts of old ice also results in different breakup dates.

Such a conclusion is characteristic for seas where in spring zones of young and thin ice cover are small or absent. For those seas dynamic ice redistribution processes are predominant in the

formation of summer ice conditions whereas thermal processes and the initial state of ice cover in spring are secondary.

Thus one can make the conclusion that the location of old ice before breakup does not influence processes during breakup. Obvious confirmation of this thesis is as follows. In spring and summer of 1991 along the northern coast of Alaska there was a huge zone of first-year ice approximately 120 miles wide. In 1992 a zone of predominantly old ice adjoined the coast. But, the summer of 1991 was characterized by very heavy ice conditions whereas in the 1992 breakup began early and ice conditions were light.

## **6.0 STATISTICAL EVALUATION OF THE RELATIONSHIP BETWEEN SUMMER BREAKUP AND PRECEDING PROCESSES**

During the study three main factors determining processes of the subsequent breakup were identified: large scale air transport during the 12 previous months; vorticity of geostrophic wind in April; and temperature at Barrow averaged for every three months. The influence of each of these factors has been analyzed separately.

It is not correct to assume that those factors are fully independent. In this case some difficulties arise in the statistical analysis. There is no general approach to solve the problem and therefore different variations were considered and the best one was chosen.

To exclude undesirable calculation errors peculiar to correlations with a large number of determining factors, a generalized index characterizing the development of processes during preceding years was constructed. The index presents the sum of influential factors, relatively weighted, determining the contribution of each predictor to the intensity of the following breakup. This index serves to evaluate the severity of the subsequent ice conditions during breakup. Finally, these procedures have led to the opportunity to construct a quantitative relationship between total ice concentration distribution and the development of processes during previous year.

The task was as follows. There are 17 predictors: 12 informative pressure gradients, one for every month of the year; 4 seasonal values of air temperature at Barrow; and vorticity of the geostrophic wind over the Arctic Ocean in April. Each of them contributes to the development of hydrometeorological conditions in the vicinity of the Kuvlum site. The contribution is determined by the statistical relationship between every predictor and the area covered by total concentration of 5/10ths or more in the region under study. All years with the necessary datasets were taken into consideration.

First of all the hypothesis about the independence of the predictors was investigated. In this case the anomaly of ice coverage is simply the sum of anomalies contributed by every predictor. Calculations based on this approach yield resulting variability that is three times more than observed.

The conclusion is that the predictors considered are not independent and therefore their contributions should be weighted. The weight necessary for computations depends upon the mean square root deviation of every predictor, the coefficient of correlation, the coefficient of regression for each predictor, and accuracy of the coefficient of regression. The desired combination of influencing factors was determined.

## **7.0 LONG-TERM FORECASTS AND DEVELOPMENT OF ICE PROCESSES**

After developing the forecast method an estimate of confidence in the forecast was made. Usually the forecast methodology can be evaluated by comparing forecast data with observed data from previous years. It is necessary to emphasize that such a comparison should be done only for years that were not included in the development of the original forecast methodology.

Data from 1991 and 1992 were used to verify the quality of the forecast. The initial dates when ice concentration decreased enough to begin working were quite different in these two years. There were very heavy conditions in 1991 and an early breakup in 1992. Therefore these data are good cases to verify.

First of all it is important to note that the type of wind vorticity in April of these years coincides with the severity of ice conditions the following summer. Circulation in a counter-clockwise direction predominated in 1991 and an obvious clockwise motion occurred in 1992. That example, although it follows the expected trends, does not mean that atmospheric circulation in April alone determines the breakup conditions every year. The severity of ice conditions depends upon the combined effect of all processes investigated.

The forecast verification, using data through April of the year, leads to the following results. The forecast for 1991 derives an extreme index of severity leading to the conclusion that it would have been impossible to start operations before the end of August. The 1992 predicted initial date with ice concentration less than 5/10ths was 7 July 1992, the midpoint between the first and second week of July.

By comparison, actual observations taken from Navy/NOAA ice charts indicate that the initial date with ice concentration less than 5/10ths was mid-September 1991, and mid-July in 1992. These results can be interpreted as an approximate estimate of the forecast accuracy.

Once this methodology was established the current year values of the predictors were obtained. The first long-term forecast of breakup in Camden Bay was made on 1 April. Each subsequent month the forecast method was improved and the values of influencing factors for every new month were taken into account.

In accordance with the first forecast the appearance of conditions for working at the site was expected in the fourth week of July. It was anticipated that the upcoming breakup in the region under study would follow the processes characteristic for group of years with a high rate of ice

cover area decrease in the eastern part of the Beaufort Sea.

The first long-term forecast indicated that favorable ice conditions would exist in August and later and thus it might be possible to carry out drilling operations in 1993 that are close to the upper limits.

Mean monthly air circulation and vorticity of wind over the Arctic Ocean in April was favorable for light ice conditions. As a result after the April forecast the first predicted appearance of conditions for working at the site was expected in the third to fourth week of July. This date was 3 to 4 days earlier than the prediction in the April report.

In May new predictor weighting was made. It caused small changes in calculations made in previous reports. The most significant contribution to summer breakup processes is the month of April. After recalculating weights its contribution increased. April of the current year was very favorable for creating light summer ice conditions. Therefore after modifying predictor weights lighter ice conditions were projected.

Both the dynamic and thermal processes of May this year also had the same tendency, leading to the lightening of expected breakup conditions. Results of calculations in May showed that July ice coverage of 5/10ths or more concentration was less than the predicted value only in one-third of all cases.

The May breakup forecast states that the most probable time to start working in Camden Bay is during the period from the end of the second week in July to the beginning of the third week in July, or approximately 10-17 July. The 7 day change in the forecast is explained mainly by recalculation of predictor weights for months preceding May, and in part by favorable dynamical and thermal conditions during May.

It was emphasized that long-term ice forecasting takes into account only the long-term influences of ice cover evolution, i.e. seasonal changes. A similar statement is correct for all spatial scales as some small features of ice distribution can be hardly predictable. Therefore the statistical long-term forecast of breakup presents the prediction of the beginning of a stable retreat of the compacted ice cover from the coastline.

The appearance of a small concentration zone along all the north coast of Alaska means the beginning of a new kind of ice cover redistribution process that could be conventionally named the summer redistribution.

Results of the study had shown that usually the decrease in coverage of high ice concentrations is caused by the outflow of the ice cover from the coast. This hypothesis was used as a basis for the proposed method to forecast breakup. Retreat of the ice edge was forecasted to be approximately on 10-17 July.

During almost all the period from March through May the ice cover adjoined the coast of the Beaufort Sea. At the end of the third week of May very favorable southeast winds led to the development of a wide polynya along a large section of the Beaufort Sea coast. Later the area of open water began to decrease in size and was completely closed in the region between Pt. Barrow and 142° W on 1 June.

Thus at the beginning of June compacted ice cover adjoined almost all the northern coast of Alaska from Pt. Barrow to the U.S./Canadian border with few exceptions at the very eastern end of Alaska coast. But in the Canadian part of the Beaufort Sea a wide polynya persisted.

During all of June in accordance with our forecast a compacted ice cover adjoined a greater part of the northern Alaska coast. During 7-13 June a narrow zone of open water had opened constantly westward and had reached longitude 146.5° W. West of the opening the ice cover remained along the Alaskan coast.

Nevertheless the ice concentration around the Kuvlum site became less than 5/10ths in the middle of June, though that decrease of concentration was not stable. During most of the first half of July the ice concentration in the vicinity of the site was more than 5/10ths and became less on 14 July.

To the west from the *original area of study* the ice concentration along the coast was more than 5/10ths during June and beginning of July including 7 July (Figure 1). Later it became less than 5/10ths along some parts of the coast and on 17 July the ice concentration was less than 5/10ths along all the coast (Figure 2).

Thus summer processes began during the period 7-17 July in good correspondence with the ice cover retreat forecast of 10-17 July. It was noted above that a stable decrease of concentration less than 5/10ths in the vicinity of Kuvlum well was observed during the same period, on July 14th. The reason for this opening was not retreat of the ice edge from the coast but penetration westward of a lead from the east.

Such a probability was not taken into account during the study and was not forecast. Moreover the statistical study had shown that the most influential predictor was motion perpendicular to the coast. Ice distribution in the beginning of June and even in the middle of May 1993 was characterized by the existence of a significant zone of open water.

The existence of open water zones was not taken into account during the elaboration of the long-range ice forecast. Early appearance of the open water zones is an extremely rare event and therefore its influence was not revealed in statistical analysis.

Statistical analysis is a relevant method to study factors existing every year. But the influence of factors that seldom appear should be investigated another way. This is especially true when considering ice cover spatial distribution.



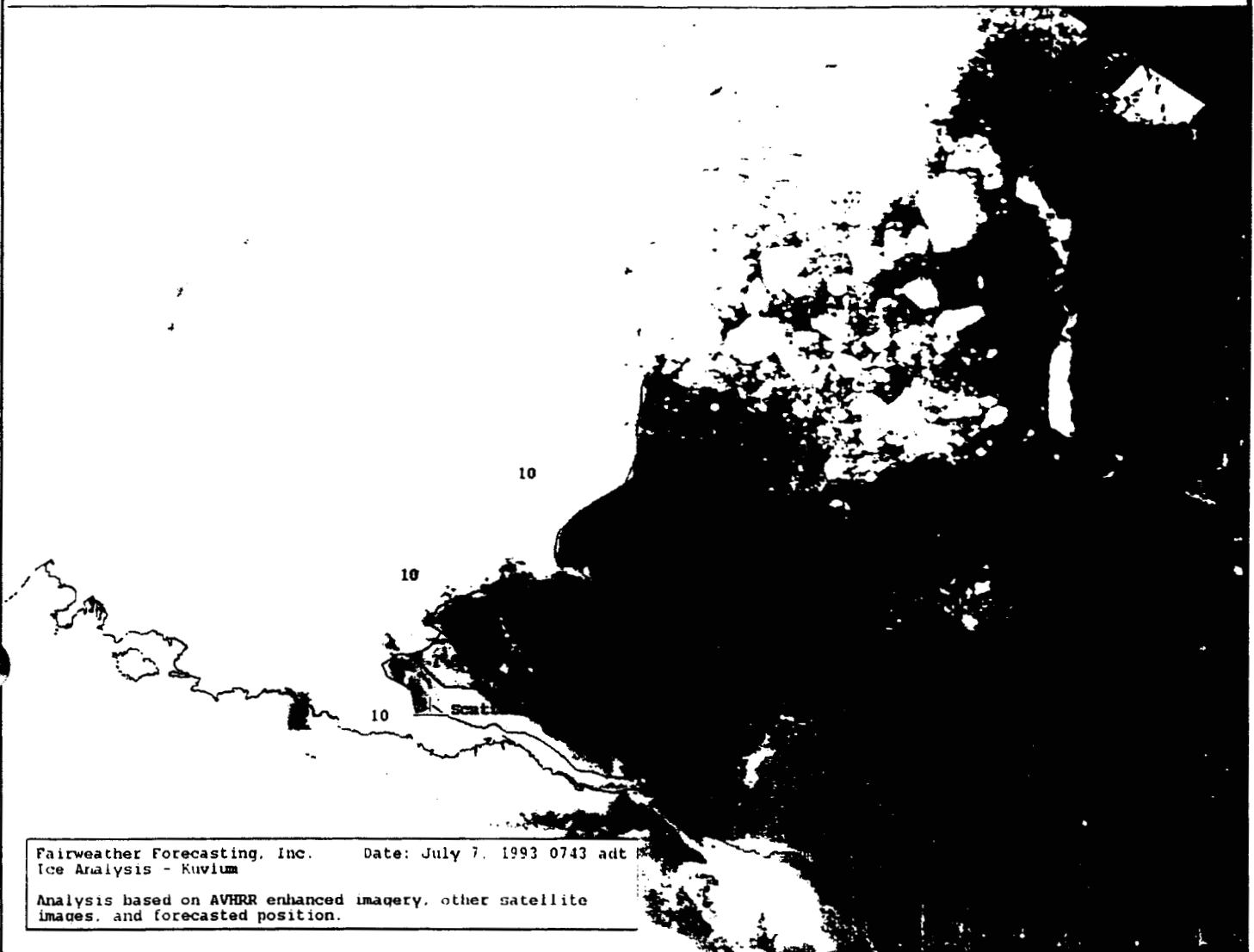


**Figure 1** Beaufort sea ice conditions on 7 July 1993.

Allowing for features of initial ice cover concentration distribution can be easily realized using a numerical method describing the evolution of the ice cover state under the influence of thermal and dynamical processes. Such a method was applied to calculate the motion of the open water zone.

Results show that in accordance with the numerical forecast the concentration in the vicinity of site at the end of June is less than 5/10ths.

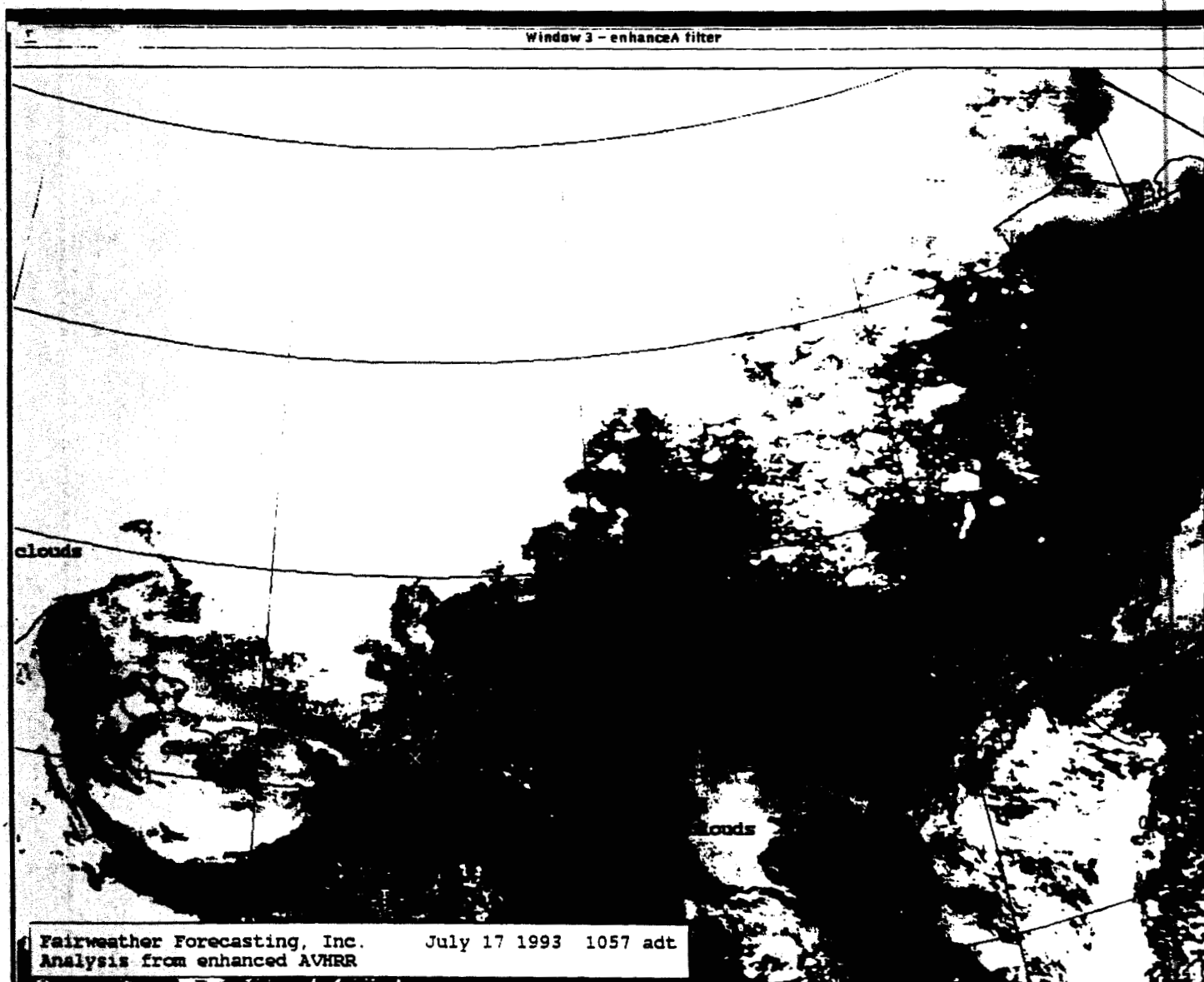


Figure 2 Beaufort Sea ice conditions on 17 July 1993.

Usually breakup in Camden Bay is a result of ice cover retreat from the coast. But in some years evidently breakup comes from east. This case should be analyzed, the reasons for the anomalous phenomena be revealed, and the opportunity to forecast be determined.

## 8.0 SUMMARY

Three parameters were used in developing the forecast method: 1) large scale atmospheric transport, 2) vorticity (velocity of rotation) of wind over the Arctic Ocean, and 3) air temperature at Barrow. These identified features of different influential processes seem to be explainable in physical terms. The overall picture of cause and effect relationships is systematic.

The forecast methodology was verified using data for ice conditions during the summer of 1991 and 1992. The results of the verification indicate a good degree of forecast accuracy.

Forecasts for the initial date when ice concentration at the Kuvlum site would be 5/10ths or less were issued on the first day of April, May, and June. The first preliminary long-term forecast indicated an opportunity to begin working in Camden Bay in the fourth week of July. It was noted that it might be possible to carry out an activity plan in 1993 that is close to the upper limits. Later by taking into consideration the effects of April and May 1993 the final forecast indicated that breakup would occur during the period 10-17 July.

The actual beginning of summer processes characterized by retreat of the compacted ice cover from the larger part of the Alaska coast to the east from Barrow occurred on July 7th - 17th. The earlier opening in the vicinity of the site this year was observed in the middle of June and is explained by an open water zone coming from the east.

There is no reason to doubt the reliability of the hypothesis used to create the long-range forecast method. The influencing factors are considered correctly but not all of them are taken into account by the method.

## 9.0 RECOMMENDATIONS

The term "breakup" has many connotations and is not easily quantifiable. In the present study, the first appearance of ice concentration of five-tenths or less was the target. Due to the instability of such an isoline, this is not a reliable indicator of when work should be started. A much more reliable indicator of future stability of ice coverage would be the beginning of "Summer Processes", characterized by retreat of the compacted ice cover from the larger part of the Alaska coast. Other recommendations for future study are as follows:

a. As was noted earlier, the open water intrusion into the area of the site from the East was not predicted and, since it is essentially a function of shorter term processes, may not be reliably predicted several months in advance. However, intermediate range forecasts of 4 - 6 weeks may be possible. Further study is required of these processes to determine the possibility of forecasting such events at intermediate ranges.

b. Determine features of seasonal atmospheric circulation and characteristic dates of seasonal transition using daily pressure observations rather than monthly averages as used in this study.

c. The large number of errors in the ice data base need to be corrected and calculations redone to eliminate this source of error. There is also a possibility that ice data for that region may be available from other sources.

**SPECTACLED EIDER AND  
TUNDRA SWAN SURVEYS: KUVLUM CORRIDOR,  
SAGAVANIRKTOK RIVER TO STAINES RIVER**

DRAFT REPORT

**CONFIDENTIAL  
NOT TO BE CIRCULATED  
OR DUPLICATED**

**DRAFT**

Prepared for

**ARCO Alaska, Inc.  
P. O. Box 100360  
Anchorage, AK 99510-0360**

Prepared by

**Laurence C. Byrne  
Robert J. Ritchie  
Debora A. Flint**

**Alaska Biological Research, Inc.  
P. O. Box 81934  
Fairbanks, AK 99708**

January 1994



Printed on 100% post-consumer recycled paper.

A10.18

**EXECUTIVE SUMMARY**

**DRAFT**

The primary objectives of the Kuvlum Corridor waterfowl surveys were to determine the density and distribution of Spectacled Eiders and the density and distribution of Tundra Swan individuals and nests during the breeding season. A secondary objective was to determine the efficacy of using a fixed-wing aircraft instead of a helicopter as a survey platform for Spectacled Eiders.

Waterfowl surveys were conducted in the Kuvlum Corridor, an area 8 km wide that parallels the coastline for approximately 83 km between the Sagavanirktok and Staines rivers. The study area was partitioned into two strata, based on geomorphologic and habitat differences. Stratum 1 extended from the Sagavanirktok River to approximately 8 km east of the Shaviovik River, Stratum 2 extended from the eastern boundary of Stratum 1 to the Staines River. Surveys for comparing platforms (i.e., aircraft) were flown in Stratum 1 of the Kuvlum Corridor, as well as in a portion of the Kuparuk Oilfield.

**EIDERS**

Eighty-three Spectacled Eiders and 168 King Eiders were observed during breeding surveys. Most Spectacled Eiders (90%) and King Eiders (74%) were observed in Stratum 1. Spectacled Eiders were most often (> 90%) observed in two habitat types: shallow open fresh water and freshwater lakes with emergent vegetation. Eighty-eight percent of all King Eiders were observed in three habitats: shallow open fresh water, freshwater lakes with emergent vegetation, and deep open lakes.

Three methods were used to estimate eider density: simple density; USFWS (1987) protocol with a visibility correction factor; and line transect methodology (Quang and Lanctot 1991).

The density of Spectacled Eiders in Stratum 1 was 3.4 - 4.0 times as great as their density in Stratum 2, depending on the method of density estimation. The density of King Eiders in Stratum 1 was only slightly higher than their density in Stratum 2, regardless of estimation technique. Density estimates for Spectacled Eiders in Stratum 1 ranged from 0.21 to 0.97 birds/km<sup>2</sup> depending on the method used; in Stratum 2 estimates ranged from 0.03 to 0.24 birds/km<sup>2</sup>. Density estimates for King Eiders in Stratum 1 ranged from 0.35 to 1.66 birds/km<sup>2</sup> depending on the method used; in Stratum 2 estimates ranged from 0.30 to 1.57 birds/km<sup>2</sup>.

**CONFIDENTIAL**  
**NOT TO BE CIRCULATED**  
**OR DUPLICATED**

Density estimates for Spectacled Eider pairs ranged from 0.07 to 0.49 pairs/km<sup>2</sup> in Stratum 1; Stratum 2 estimates ranged from 0.03 to 0.12. Density estimates for King Eider pairs in Stratum 1 ranged from 0.11 to 0.83 pairs/km<sup>2</sup>; Stratum 2 estimates ranged from 0.08 to 0.78 pairs/km<sup>2</sup>.

Comparisons of fixed-wing and helicopter survey platforms revealed that observers were able to see more Spectacled Eiders and King Eiders from the helicopter. In addition, fewer flying birds were observed during the helicopter survey than during the fixed-wing survey. However, line transect density estimates from the fixed-wing and helicopter data were within 8% of one another suggesting that using appropriate survey methodology from fixed-wing aircraft can produce density estimates that are comparable to those produced from helicopter surveys and at considerable cost savings.

## **TUNDRA SWANS**

Eighty-one Tundra Swans were seen at 50 locations in the Kuvlum Corridor. Stratum 1 contained 74 swans and 14 nests while Stratum 2 contained 7 swans and no nests. Only 14 nests were found in the entire area and most swans (74%) were not associated with nests and probably were failed or non-breeders.

Density of total swans was 0.17 birds/km<sup>2</sup> in Stratum 1 and 0.02 birds/km<sup>2</sup> in Stratum 2. Densities of nests in Stratum 1 was 0.02 nests/km<sup>2</sup>. The density of Tundra Swan nests

and adults during June in Stratum 1 were similar to densities calculated for other populations on the Arctic Coastal Plain.

Tundra Swans were almost absent from Stratum 2, apparently due to the lack of suitable lakes east of the Kavik River. Furthermore, the general distribution of Tundra Swans observed in the study area in 1993 conforms closely with earlier depictions of this area as a region with low use by breeding waterfowl pairs, relative to the region west of the Kavik River (Stratum 1).

**DRAFT**

**CONFIDENTIAL  
NOT TO BE CIRCULATED  
OR DUPLICATED**



DRAFT

CONFIDENTIAL  
NOT TO BE CIRCULATED  
OR DUPLICATED

## TABLE OF CONTENTS

EXECUTIVE SUMMARY .....	i
LIST OF TABLES .....	v
LIST OF FIGURES .....	v
ACKNOWLEDGMENTS .....	vi
INTRODUCTION .....	1
STUDY AREA .....	3
METHODS .....	6
EIDER SURVEYS .....	6
TUNDRA SWAN SURVEYS .....	9
DATA ANALYSIS .....	10
RESULTS AND DISCUSSION .....	12
EIDERS .....	12
ABUNDANCE .....	12
HABITAT USE .....	12
DISTRIBUTION .....	14
DENSITY .....	17
Spectacled Eiders .....	17
King Eiders .....	20
PLATFORM COMPARISON .....	21
TUNDRA SWANS .....	24
ABUNDANCE, DISTRIBUTION, AND DENSITY .....	24
LITERATURE CITED .....	27
APPENDIX 1 .....	30
APPENDIX 2 .....	31

# DRAFT

## LIST OF TABLES

CONFIDENTIAL  
NOT TO BE CIRCULATED  
OR DUPLICATED

Table 1. Habitat classes and description used in eider surveys of the Kuvlum Corridor study area, June 1993..	8
Table 2. Number and percentage of birds observed on the water by habitat.	13
Table 3. Density estimates (birds/km <sup>2</sup> or pairs/km <sup>2</sup> ) of Spectacled and King eiders, as calculated by three methods, in the Kuvlum Corridor study area, 16-17 June 1993.	18
Table 4. Density estimates for Spectacled Eiders (birds/km <sup>2</sup> or pairs/km <sup>2</sup> ) from aerial and ground surveys on the North Slope of Alaska.	19
Table 5. Density estimates for King Eiders (birds/km <sup>2</sup> or pairs/km <sup>2</sup> ) from aerial and ground surveys on the North Slope of Alaska.	22
Table 6. Density estimates (birds/km <sup>2</sup> or pairs/km <sup>2</sup> ) from comparative platform surveys for Spectacled Eiders in the Kuvlum Corridor and the Kuparuk Oilfield.	23
Table 7. Numbers and densities (birds/km <sup>2</sup> or pairs/km <sup>2</sup> ) of Tundra Swans and nests recorded during aerial surveys in the Kuvlum Corridor study area, Alaska, 25-26 June 1993.	25

## LIST OF FIGURES

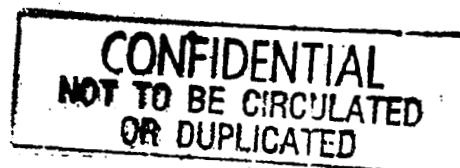
Figure 1. Kuvlum Corridor study area where aerial surveys for Spectacled Eiders and Tundra Swans were flown, 16-17 June 1993.	4
Figure 2. Survey lines for an aerial survey of Spectacled Eiders in the Kuvlum Corridor study area, 16-17 June, 1993.	7
Figure 3. Distribution of Spectacled Eiders observed during an aerial survey in the Kuvlum Corridor study area, 16-17 June, 1993.	15
Figure 4. Distribution of King Eiders observed during an aerial survey in the Kuvlum Corridor study area, 16-17 June 1993.	16

DRAFT

Kuvlum Spectacled Eiders & Tundra Swans

Figure 5. Distribution of Tundra Swans and nests observed during an aerial survey in the Kuvlum Corridor study area, 25-26 June, 1993.....26

DRAFT

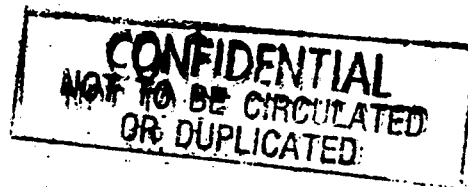


## ACKNOWLEDGMENTS

This study was funded by ARCO Alaska, Inc., and managed by Mike Joyce (ARCO). We appreciate the help of the many individuals involved in this project. Jim King acted as an observer for part of the Tundra Swan survey. Victoria Domke, Tamarack Air, developed the instrumentation and software for acquiring and recording GPS locations. Professor Pham Xuan Quang, University of Alaska - Fairbanks, offered advise on line transect methodology and analyzed portions of the data. Sandy Hamilton, Tamarack Air, was the pilot for all of the fixed-wing portions of the surveys. Steve Murphy, Rick Johnson and Betty Anderson reviewed draft versions of this report and made many helpful suggestions. Allison Zusi-Cobb prepared all maps, Mike Smith helped with various digitizing tasks, and Terrence Davis was instrumental in typing and formatting this report.

DRAFT

## INTRODUCTION



Recent oil exploration and discovery in the region between the Staines and Sagavanirktok rivers has created a need to undertake baseline surveys of wildlife resources in the region. In general, wildlife surveys associated with oilfield development have not extended east of the Sagavanirktok River. Exceptions to this include regional Brant (*Branta bernicula*) and Snow Goose (*Chen caerulescens*) surveys conducted between Prudhoe Bay and the Staines River (e.g., Johnson and Troy 1987, Ritchie et al. 1991, Burgess et al. 1992), caribou surveys near Bullen Point (WCC 1983, Lawhead and Cameron 1988), and extensive offshore surveys of barrier islands and coastal lagoons (e.g., Gavin 1974, Divoky 1978). In 1993, in response to developments at the Kuvlum site offshore of the Staines River, Alaska, Inc., contracted with Alaska Biological Research, Inc., (ABR) to conduct surveys of nesting waterfowl along an onshore area likely to contain the transportation and utility corridor that will be required if commercial deposits of oil are discovered.

Spectacled Eiders (*Somateria fischeri*) and Tundra Swans (*Cygnus columbianus*) were preeminent in our design of surveys because of their status and their influence in planning other developments in northern Alaska. Spectacled Eiders recently were listed as a threatened species under regulations of the Endangered Species Act. Their numbers have declined severely in western Alaska and research in Prudhoe Bay suggests similar declines (Warnock and Troy 1992). Any future developments will require intensive searches for Spectacled Eider nests, so mapping their distribution and identifying locations of abundance will be invaluable for long-term planning of oilfield developments. Tundra Swans have received considerable attention from both the regulatory agencies and the oil industry, and have been considered an indicator species for the productivity and well-being of all waterfowl in the area (King 1970, King and Hodges 1980).

The main objectives of the Spectacled Eider and Tundra Swan surveys in the Kuvlum Corridor in 1993 were:

- 1) to determine the density and distribution of Spectacled Eiders during a pre-nesting breeding-pair survey;
- 2) to determine the density and distribution of Tundra Swan nests and adults during the breeding season; and
- 3) to verify the efficacy of using fixed-wing aircraft instead of helicopters as survey platforms for Spectacled Eiders.

**DRAFT**

**CONFIDENTIAL  
NOT TO BE CIRCULATED  
OR DUPLICATED**

DRAFT

## STUDY AREA

CONFIDENTIAL  
NOT TO BE CIRCULATED  
OR DUPLICATED

The study area for the Kuvlum Corridor (Figure 1) is 8.0 km (5.0 mi) wide and parallels the coast of the Beaufort Sea for approximately 83.0 km (52.0 mi), from the west channel of the Sagavanirktok River eastward to the Staines River. The northern border of the study area ranges from 0.3 to 9.6 km (0.25 - 6.0 mi) inland, but is generally about 1.6 km (1.0 mi) from the coast. The total area within the Kuvlum Corridor study area is approximately 669.0 km<sup>2</sup> (261.3 mi<sup>2</sup>).

Based on differences in geomorphology and associated habitats, the study area was partitioned into two strata. Stratum 1 (376.4 km<sup>2</sup>) extends from the western channel of the Sagavanirktok River to approximately 5 miles east of the Shaviovik River. This area is underlain by an alluvial plain of fine-grained silt deposits, which are susceptible to thaw lake processes. Consequently, the area is a complex mosaic of deep open lakes, shallow ponds, marshes, and wet and moist meadows. In many drained-lake basins, numerous habitats occur in close proximity and are referred to as basin wetland complexes (Bergman et al. 1977). In addition to increasing habitat diversity, thaw lake processes also contribute to higher primary productivity because organic material and nutrients are released during shoreline erosion.

Stratum 2 (292.6 km<sup>2</sup>) extends from the eastern boundary of Stratum 1 to the Staines River. This region is underlain with glacial outwash sand and gravel, which forms a large deltaic fan at the mouth of the Canning River. Characteristic of this region is the lack of thaw lakes and drained-lake basins, presumably due to the coarse-textured sediments that are more thaw stable than fine-grained sediments. As a result, habitats are less diverse, waterbodies are more limited in number and size, and the area is dominated almost exclusively by nonpatterned moist tundra (Walker and Everett 1991).

Four of the eight transects used for the platform comparisons were flown in Stratum 1 of the Kuvlum Corridor study area. The other four transects were flown in the Kuparuk Oilfield, approximately 60 km to the west. These transects were located between a north-south line approximately 1 km (0.6 mi) east of the Milne Point road to a

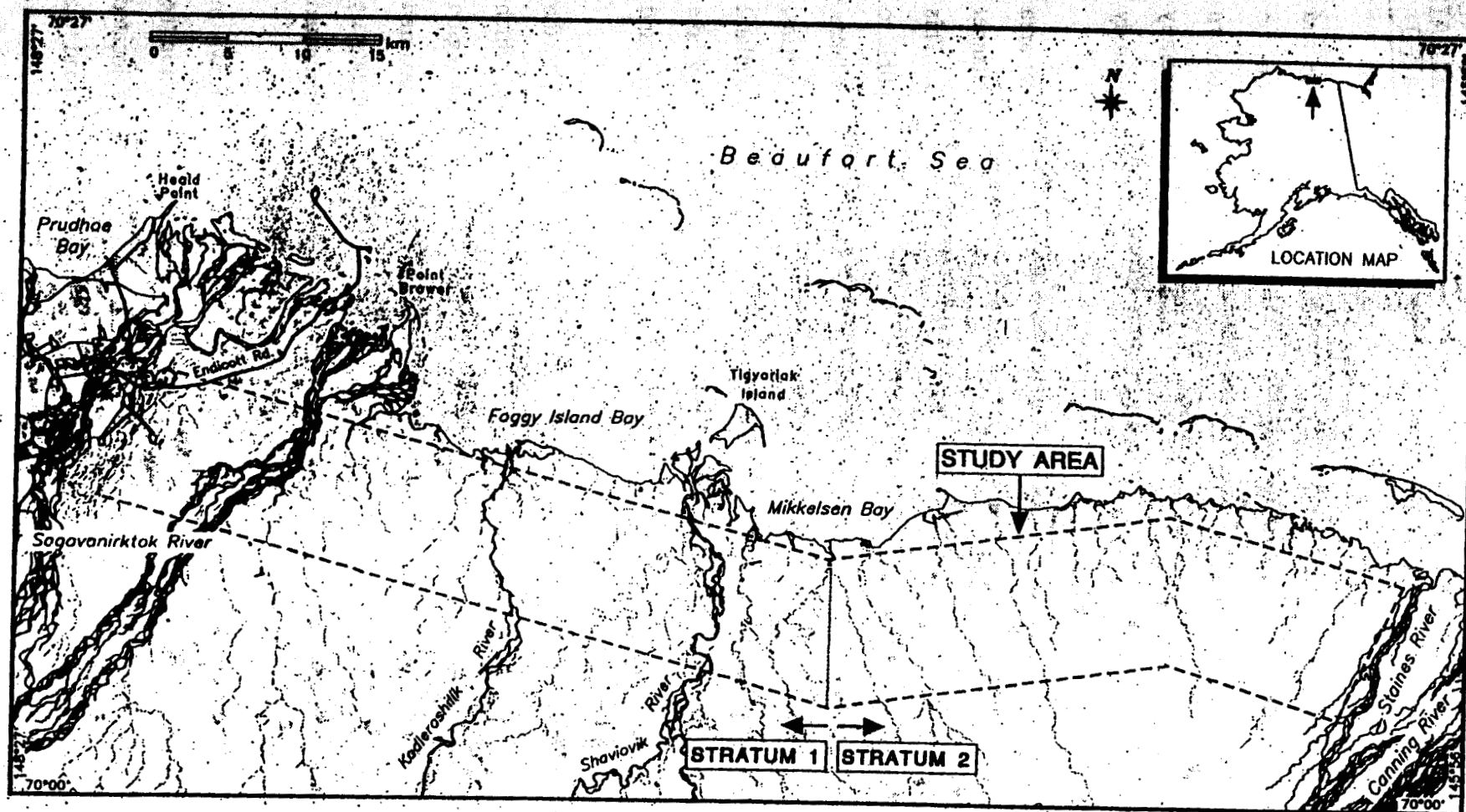


Figure 1. Kuvlum Corridor study area where aerial surveys for Spectacled Eiders and Tundra Swans were flown, June 1993. The study area was divided into two strata based on habitat and geomorphological differences.

DRAFT

STUDY AREA

CONFIDENTIAL  
NOT TO BE CIRCULATED  
OR DUPLICATED

north-south line approximately 4.2 km (2.5 mi) west of the mouth of Kalubik Creek (149° 24' W to 150° 13' W longitude). The area extended north-south from approximately 70° 21' N to 70° 27' N latitude.

**DRAFT**

**CONFIDENTIAL  
NOT TO BE CIRCULATED  
OR DUPLICATED**



# DRAFT

## METHODS

CONFIDENTIAL  
NOT TO BE CIRCULATED  
OR DUPLICATED

### EIDER SURVEYS

Aerial surveys for Spectacled Eiders were conducted in the Kuvlum Corridor study area on 16 and 17 June 1993. Surveys were flown in a Cessna 185 at an altitude of 38-46 m (125-150 ft) above ground level (agl) and at a speed of approximately 145 km/h (90 mi/h). Survey lines were oriented parallel to the northern and southern borders of the study area (Figure 2). A total of 500.1 km<sup>2</sup> were surveyed. Transects in Stratum 1 were located approximately 0.4 km apart for about 94% coverage of the area (353.8 km<sup>2</sup> surveyed). (An approximately 30-m wide blind strip beneath the plane was not surveyed.) Stratum 2 was flown at 50% coverage (transects 0.8 km apart; 146.3 km<sup>2</sup> surveyed). Transect lines were navigated by use of a Garmin 100 global positioning system (GPS) unit.

Two observers on opposite sides of the plane each surveyed a strip 200 m (656 ft) wide. Colored tape on the struts of the plane delimited the midpoint and outer boundary of the survey strip to facilitate estimation of distance from the aircraft to the eiders. On hand-held tape recorders, observers recorded date, time, transect number, species (including Spectacled Eider, King Eider [*Somateria spectabilis*], Common Eider [*Somateria mollissima*] and unidentified eiders), number of birds, sex, number of pairs, habitat, and perpendicular distance from the plane for all eiders observed. Seven general habitat types were used (Table 1). Locations of observations projected onto the transect line were stored in the GPS unit.

Platform-comparison surveys were flown on 16 and 17 June 1993. Eight transects, each approximately 78 km (49 miles) long, were surveyed for eiders in both a Cessna 185 fixed-wing aircraft and in a Bell 206B Jet Ranger helicopter. (Observations made on transects surveyed with the Cessna 185 were included as part of the Kuvlum Corridor eider survey.) Speed, altitude, and area surveyed were the same as described above for the entire Kuvlum Corridor survey. The same observers flew both the fixed-wing and helicopter portions of the surveys. Time between surveys using different

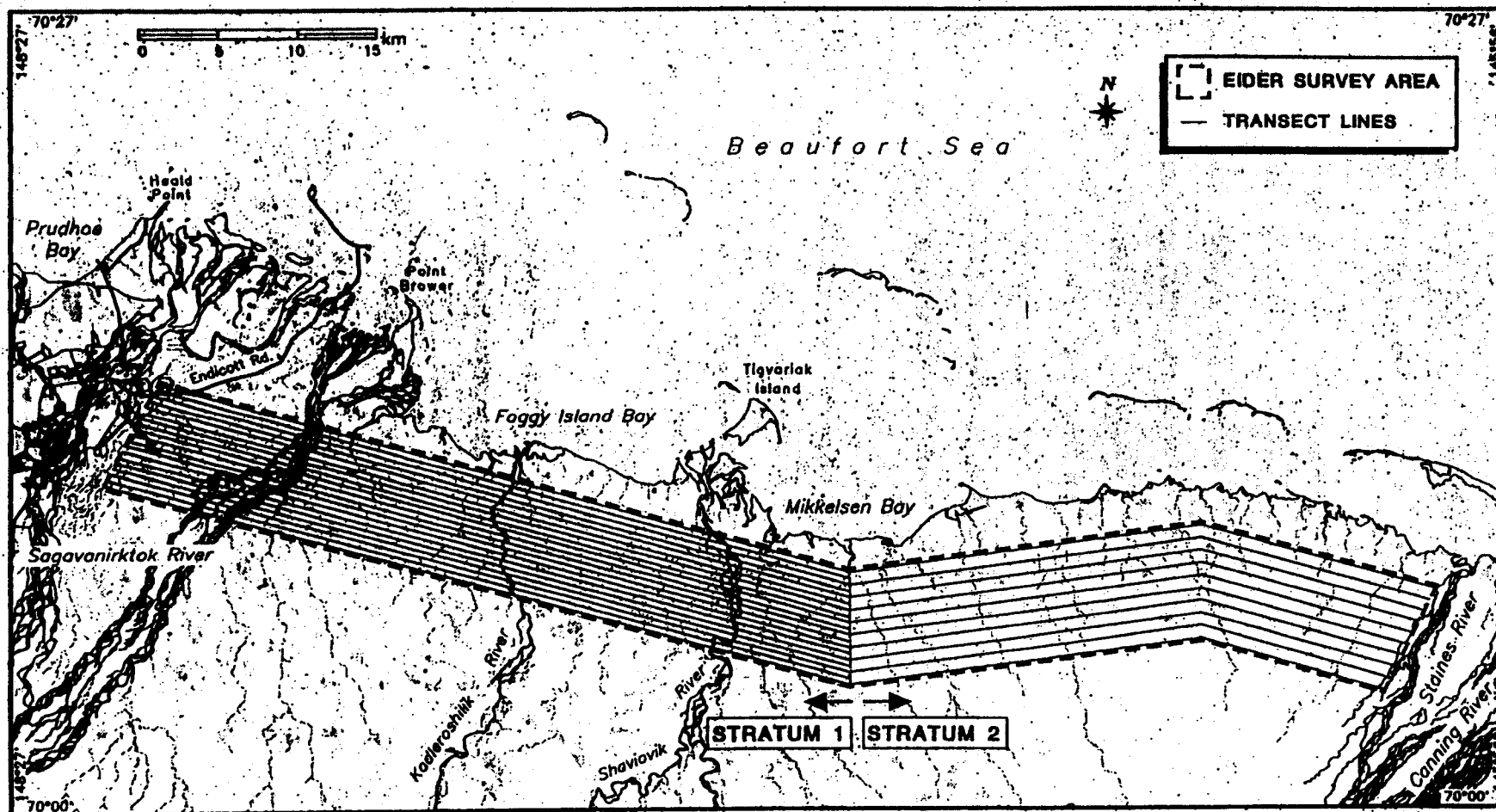


Figure 2. Survey lines used for an aerial survey of Spectacled Eiders in the Kuvlum Corridor study area, 16-17 June, 1993.

CONFIDENTIAL  
NOT TO BE CIRCULATED  
OR DUPLICATED

DRAFT

Table 1. Habitat classes and description used in eider surveys of the Kuvlum Corridor, June 1993. Descriptions follow Bergman et al. (1977) and Jorgenson et al. (1989).

Habitat Class	Description
Shallow open fresh water	Includes shallow (1 m deep) ponds and small lakes with little emergent vegetation (approximately 5% of the area).
Fresh water lake with emergents	Includes ponds and lakes (drained lakes) in which sedges and/or grasses cover at least 5% of the surface area. The sedge, <i>Carex aquatilis</i> , or the grass, <i>Arctophila fulva</i> , are the dominant emergents.
Deep open lake	Deep open lakes (> 1 m deep) are generally greater than 10 ha (24.7 acres) in extent. Emergents usually are present in less than 5% of the area.
Flooded / wet tundra	Includes both nonpatterned and low polygon tundra that are flooded in the spring by melt. <i>Carex aquatilis</i> , tolerant of flooding, is the dominant plant in the depression.
Beaded stream	Small streams linking pools that form at ice-wedge intersections. Flooding may occur during spring thaw but by mid-July water flow is greatly reduced. Pools may have stands of emergent <i>Arctophila</i> .
River with a gravel base	On the coastal plain these are major streams and rivers with broad flood plains and high discharge in the spring. By late summer, flow has significantly diminished exposing large gravel bars.
Open nearshore waters	Included in this category are shallow estuaries, lagoons, and embayments of the Beaufort Sea, located inshore of the barrier islands. The water is usually brackish and subject to seasonal change.

CONFIDENTIAL  
NOT TO BE CIRCULATED  
OR DUPLICATED

platforms varied from one to two hours. Data from the left and right sides of the helicopter were analyzed separately due to differences in view for the front and rear observer. That is, the observer in the left front seat was able to observe a strip from the survey line out 200 m, aided by a floor window in the helicopter. The observer in the right rear seat was unable to observe an approximately 10-m wide strip extending from the survey line.

An early objective of this study was to determine the feasibility of censusing a 400-m-wide transect for eiders, rather than the standard 200-m-wide transect set by USFWS protocol. It was obvious to observers early in the surveys, however, that 400 m was too great a distance to identify eiders to species. Therefore, efforts to more accurately quantify the usefulness of this transect were abandoned.

### TUNDRA SWAN SURVEYS

CONFIDENTIAL  
NOT TO BE CIRCULATED  
OR DUPLICATED

Aerial survey methods in 1993 followed the USFWS Tundra Swan Survey Protocol (USFWS 1991). A Cessna 185 aircraft was flown along 1.6 km-wide transects oriented parallel to the northern border of the study area. The aircraft was flown at 150 m agl and at 145 km/h. Survey dates (25 and 26 June 1993) were selected to be consistent with the timing of nesting (i.e., females incubating).

During sampling, each of two observers scanned a transect approximately 800-m wide on each side of the aircraft, while the pilot navigated and scanned ahead of the aircraft. A standardized set of codes for pairs of swans, single swans, flocks, and nests was employed (USFWS 1991). All observations were recorded on 1:63,360 USGS maps.

Location of all Tundra Swan sightings and nests were entered onto digital maps (developed from 1:63,360 USGS maps by AeroMap U.S., Inc.) that corresponded to the appropriate field map. Areas (km<sup>2</sup>) used for density calculations (Appendix 1) were measured from these base maps using ATLAS GIS software (Strategic Mapping, Inc. Santa Clara, CA). Summary statistics for nesting surveys followed the format established in 1988 and modified in 1990 for use in the Kuparuk and Prudhoe Bay oil fields (Ritchie et al. 1989, 1991).

**CONFIDENTIAL**  
**NOT TO BE CIRCULATED**  
**OR DUPLICATED**

## DATA ANALYSIS

Three methods were used to calculate density estimates for eiders. First, a simple density estimate (birds observed divided by area surveyed) was calculated. Second, a density using estimated pairs was calculated following the USFWS Standard Operating Procedures for Aerial Waterfowl Breeding Ground Population Surveys (1987). This method takes into account that the survey was conducted during the period when males and females should be paired and that male waterfowl in breeding plumage are more visible than female waterfowl during the breeding season. The following rules were used in estimating eider numbers by this procedure:

- 1) a male and a female observed in close proximity were counted as a pair;
- 2) a lone male was counted as a pair (lone females were not counted);
- 3) two to four males in a small flock were counted as an equivalent number of pairs;
- 4) flocks with more than 4 males were counted as that size group and not as pairs, unless males were determined to be associated with females, which were then counted as pairs; and
- 5) flying birds were counted if it was thought they were flushed from the transect being surveyed.

**DRAFT**

The total number of birds tallied by this method is divided by the area surveyed to arrive at an unadjusted density estimate. To account for unobserved birds this estimate is multiplied by a visibility correction factor (vcf). The USFWS uses a standard vcf of 3.58 for eiders (Lensink 1968 in USFWS 1987).

Third, densities of Spectacled Eiders, King Eiders and all eiders combined within the Kuvlum Corridor were estimated using line transect theory (Burnham et al. 1980, Quang 1991, Quang and Lanctot 1991). This method corrects for 'visibility bias' caused by differences in detectability of survey objects (in this case eider ducks) at varying distances from the survey line. Visibility bias can be caused by a number of factors, such as bad weather, velocity of the aircraft, observer fatigue, and vegetative cover type.

(Quang and Lanctot 1991). Burnham et al. (1980) assumed perfect detectability along the survey line, meaning that if an object were located along that line it would be detected with probability equal to 1. Probability of detection then decreases as distance from the line increases. Quang and Lanctot (1991) observed that in aerial surveys a 'blind strip' exists beneath the aircraft so that any object within that strip, including along the survey line, cannot be detected. They propose that detectability increases to a line of perfect detectability at some undetermined distance from the survey line and then decreases. The location of the line of perfect detectability varies for different observers, aircraft, vegetation types, etc. The method of Quang and Lanctot (1991) was used for the analysis of our survey data. Densities estimated with the line transect method apply to the surveyed area plus the blind strip.

The simple method of density estimation is a conservative approximation of eiders in the area. It is an estimate of density based solely on the birds observed; no attempt is made to account for unseen birds. The USFWS and line transect methods acknowledge that only a portion of the birds in an area are likely to be observed. Because no flocks of eiders containing more than four males were observed during the survey of the Kuvlum Corridor, the unadjusted USFWS density estimates are essentially based on double the number of males observed. A more accurate estimate is possible by including flying birds, but the number of birds that were unseen is still unknown. The vcf adjusts the estimates to account for this deficiency. In contrast, the line transect method attempts to model the detectability of the eiders being surveyed in a given area; densities estimated with this method are based on both the number of observed and unobserved (estimated) ducks, without using a constant vcf multiplier.

**DRAFT****CONFIDENTIAL  
NOT TO BE CIRCULATED  
OR DUPLICATED**

DRAFT

## RESULTS AND DISCUSSION

### EIDERS

CONFIDENTIAL  
NOT TO BE CIRCULATED  
OR DUPLICATED

#### ABUNDANCE

Eighty-three Spectacled Eiders, including both flying and non-flying birds, were observed at 49 locations during aerial surveys in the Kuvlum Corridor. Ninety percent (75 birds at 43 locations) of all Spectacled Eiders were observed on the water; the remaining eight eiders were observed flying (at 6 locations). Birds observed on the water comprised 47 males and 28 females. All females were paired with males for a total of 28 pairs. The unpaired males could represent non-breeders, breeding males that had not yet paired with females, or males paired with females that were not observed. Group size ranged from one to four, with only one observation of four birds (two pairs).

One hundred sixty-eight King Eiders were observed at 97 locations. Of these birds, 118 (at 68 locations) were observed on the water, while 50 birds (at 29 locations) were observed flying. Birds observed on the water comprised 83 males and 35 females. All females observed were paired with males for a total of 35 pairs. Group size ranged from 1 to 6 birds, with only one observation of 6 birds (3 pairs). Two Common Eiders (both males) were observed, one each at two locations.

#### HABITAT USE

Excluding flying birds, over 90% of all Spectacled Eiders were observed on either fresh water lakes with emergent vegetation (66.7%) or shallow open fresh water (24.0%) in the study area (Table 2). This pattern was similar for both Stratum 1 and Stratum 2. Other North Slope studies (Bergman et al. 1977; Derksen et al. 1981; Warnock and Troy 1992) reported similar habitat preferences of Spectacled Eider for freshwater bodies with emergent vegetation, especially *Arctophila*, during the breeding season. Spectacled Eiders also showed a preference for impoundments in the Prudhoe Bay area (Warnock and Troy 1992), but this artificial habitat type is not present in the Kuvlum Corridor.

DRAFT

Table 2. Number and percentage of birds observed on the water by habitat following Bergman et al. (1977) and Jorgenson et al. (1989).

Stratum/Habitat	Spectacled Eider		King Eider		All Eiders	
	Number	Percent	Number	Percent	Number	Percent
STRATUM 1						
Shallow open fresh water	14	20.6	21	22.3	35	21.5
Fresh water lake with emergents	47	69.1	39	41.5	86	52.7
Deep open lake	1	1.5	21	22.3	22	13.5
Flooded / wet tundra	1	1.5	1	1.1	2	1.2
Beaded stream	0	0.0	5	5.3	5	3.1
River with a gravel base	2	2.9	6	6.4	8	4.9
Not recorded	3	4.4	1	1.1	5	3.1
Total	68	100.0	94	100.0	163	100.0
STRATUM 2						
Shallow open fresh water	4	57.1	8	33.3	12	37.5
Fresh water lake with emergents	3	42.9	12	50.0	16	50.0
Deep open lake	0	0.0	3	12.5	3	9.4
Flooded / wet tundra	0	0.0	0	0.0	0	0.0
Beaded stream	0	0.0	0	0.0	0	0.0
River with a gravel base	0	0.0	1	4.2	1	3.1
Not recorded	0	0.0	0	0.0	0	0.0
Total	7	100.0	24	100.0	32	100.0
TOTAL AREA						
Shallow open fresh water	18	24.0	29	24.6	47	24.1
Fresh water lake with emergents	50	66.7	51	43.3	102	52.3
Deep open lake	1	1.3	24	20.3	25	12.8
Flooded / wet tundra	1	1.3	1	0.8	2	1.0
Beaded stream	0	0.0	6	5.1	6	3.1
River with a gravel base	2	2.7	6	5.1	8	4.1
Not recorded	3	4.0	1	0.8	5	2.6
Total	75	100.0	118	100.0	195	100.0

DRAFT

CONFIDENTIAL  
NOT TO BE CIRCULATED  
OR DUPLICATED

RESULTS AND DISCUSSION



Habitat use by King Eiders appeared to be less specific with over 88% of all observations located in three habitats: fresh water lakes with emergents (43.3%), shallow open fresh water (24.6%), and deep open lakes (20.3%). Habitat use was similar in both strata.

CONFIDENTIAL  
NOT TO BE CIRCULATED  
OR DUPLICATED

## DISTRIBUTION

In Stratum 1, 74 Spectacled Eiders were observed at 44 locations; nine were observed at five locations in Stratum 2 (Figure 3). (Fewer observations are displayed in Stratum 2 due to the less intensive sampling effort employed [near total coverage in Stratum 1 compared to 50% coverage in Stratum 2]). Observations were fairly evenly distributed throughout Stratum 1, although the area between the Kadleroshilik and Shaviovik rivers contained a dense clustering of eiders. All observations of more than one male and/or pair also occurred in this area. Only five observations of Spectacled Eiders were made in Stratum 2, all in the western half of that stratum. Warnock and Troy (1992) reported that the highest densities of Spectacled Eiders were found 20-25 km (12-15 mi) inland in their Prudhoe Bay study area. The Kuvlum Corridor does not extend as far inland as their study area, but the distribution of Spectacled Eiders in our study area appears to vary somewhat with distance from the coast. In Stratum 1, densities were lower within 4 km of the coast, and increased farther inland, approximately 4 - 8 km from the coast. In Stratum 2, all Spectacled Eiders were observed within approximately 7 km of the coast, perhaps due to the lack of lakes in the southern portion of the stratum.

More King Eiders (124) were observed in Stratum 1 than in Stratum 2 (44 eiders) (Figure 4). Numbers of King Eiders were highest in Stratum 1 between the eastern channel of the Sagavanirktok River and the Kadleroshilik River and then declined gradually to the east. Unlike Spectacled Eiders, King Eiders were observed at several locations in the eastern portion of Stratum 2.

Two Common Eiders were observed: one near the northeastern corner of Stratum 1 and one near the northwestern corner of Stratum 2.

DRAFT

CONFIDENTIAL  
NOT TO BE CIRCULATED  
OR DUPLICATED

RESULTS AND DISCUSSION

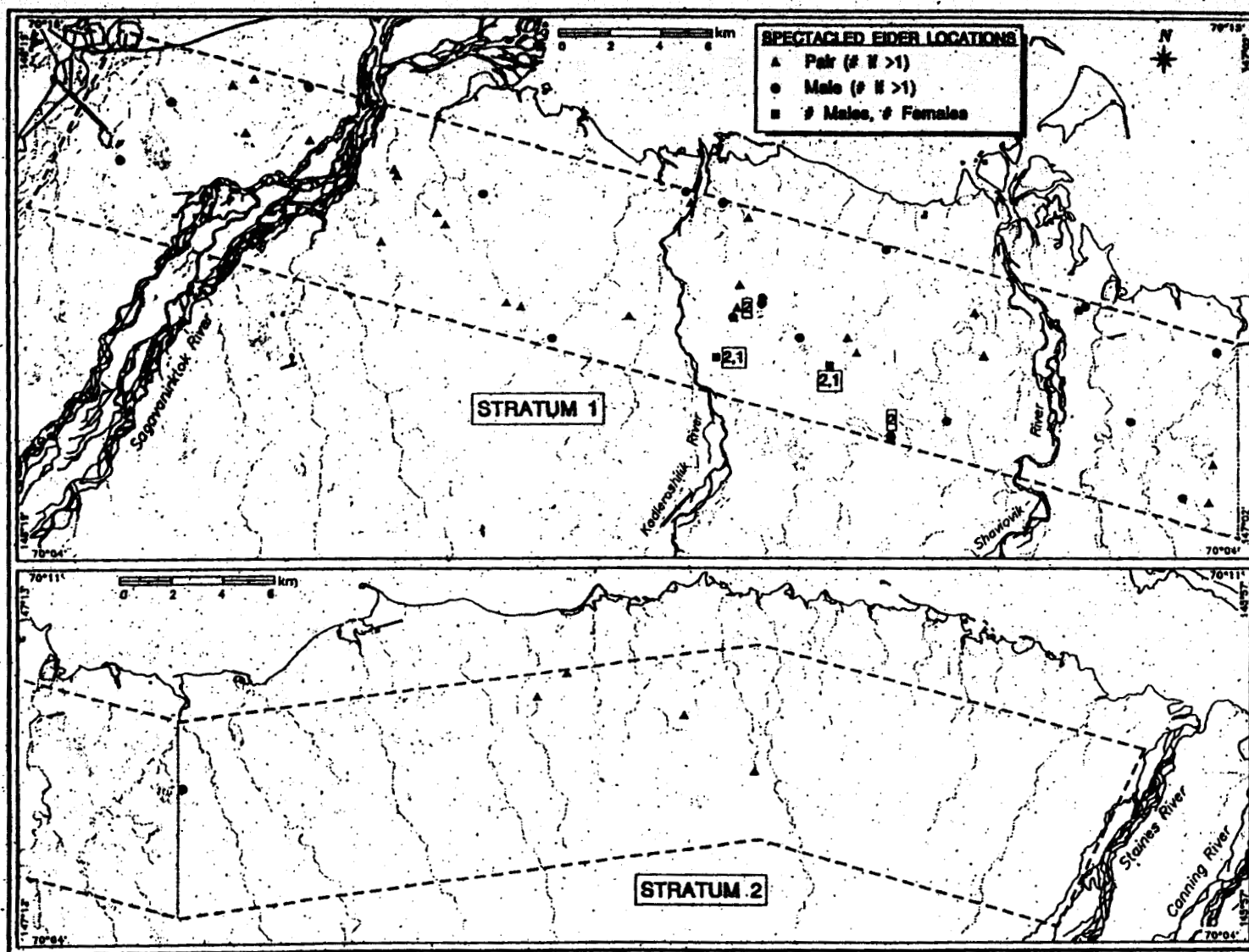


Figure 3. Distribution of Spectacled Eiders observed during an aerial survey in the Kuvlum Corridor study area, 16-17 June, 1993.

DRAFT

CONFIDENTIAL  
NOT TO BE CIRCULATED  
OR DUPLICATED

RESULTS AND DISCUSSION

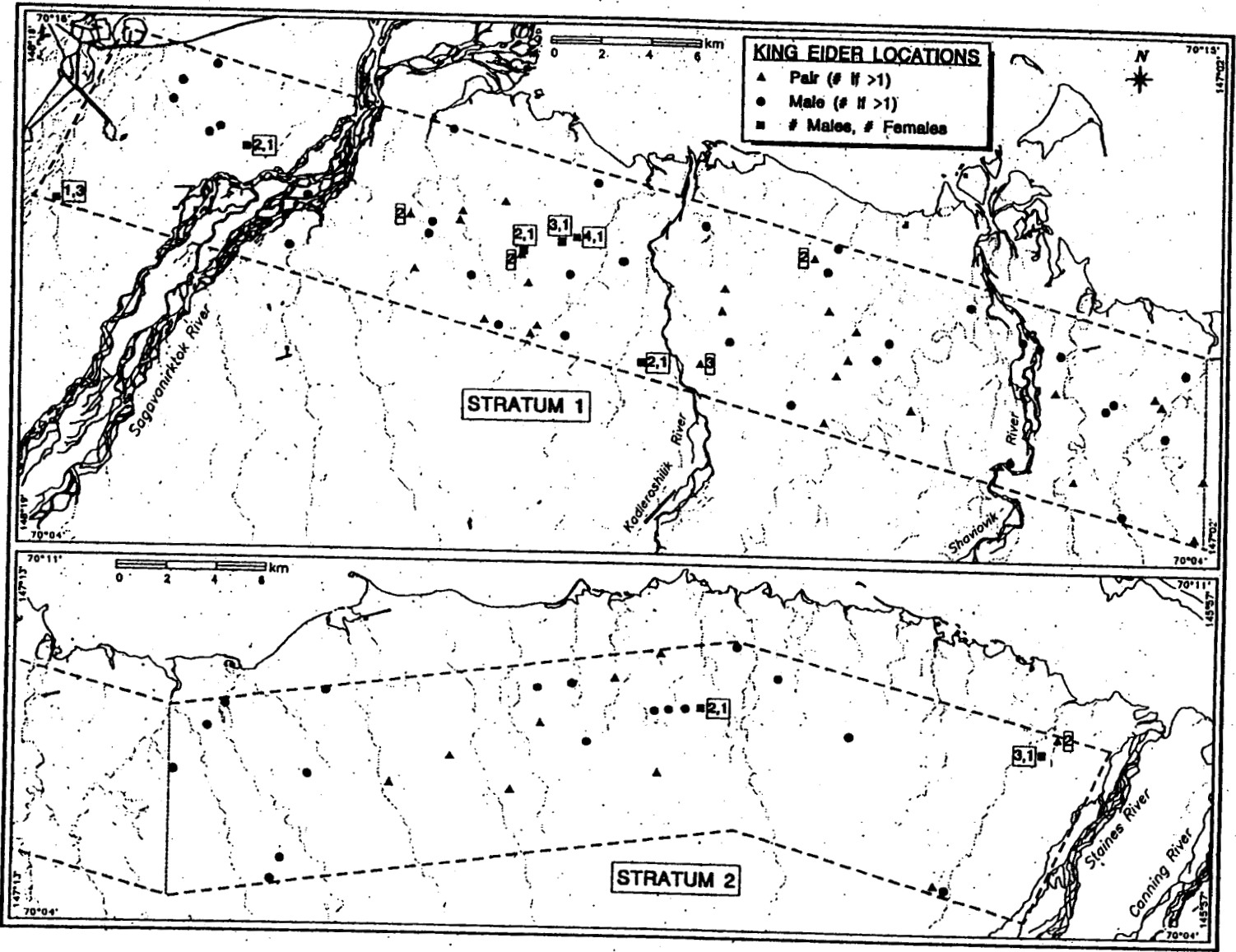


Figure 4 Distribution of King Eiders observed during an aerial survey in the Kuvlum Corridor study area, 16-17 June 1993

CONFIDENTIAL  
NOT TO BE CIRCULATED  
OR DUPLICATED

RESULTS AND DISCUSSION

DRAFT

## DENSITY

For both Spectacled and King eiders in the Kuvlum Corridor, the general relationship of density estimates for total birds was

simple estimates < line transect estimates < USFWS (vcf = 3.58) estimates

(Table 3). We believe that the simple estimate is biased low because it is based solely on observed birds, and we acknowledge that not all birds in the survey area were detected. The biased estimate is at least 358% low if the USFWS standard correction factor is accurate (Lensink 1968 in USFWS 1987; Conant et al. 1991). At the other extreme is the density estimate based on USFWS methodology and a vcf of 3.58. This technique generated a density estimate (0.97 birds/km<sup>2</sup>) that was much higher than any reported from aerial surveys on the Arctic Coastal Plain (Table 4). However, because this correction factor was formulated from results of surveys on the Yukon Kuskokwim Delta in habitats much different than those found on the North Slope, its use in determining densities in the Kuvlum Corridor may not be appropriate. The USFWS is currently investigating the question of visibility correction factors for waterfowl surveys on the North Slope (J. Hodges, USFWS, pers. comm.). The line transect density estimates fall between estimates generated by the two other techniques and we hypothesize that the true density is in this range as well. However, the size and direction of the bias associated with these estimates is unknown. Line transect methodology is sensitive to accurate distance estimation, sample size, and inter-observer variability. Although we think that the line transect densities are the best estimates presented here, further work would be required (e.g., ground verification) to determine how well they estimate the true density.

## Spectacled Eiders

Densities of Spectacled Eiders in Stratum 1 were calculated by all three methods (Table 3), but the density of Spectacled Eiders in Stratum 2 could not be estimated with

DRAFT

Table 4. Density estimates for Spectacled Eiders (birds/km<sup>2</sup> or pairs/km<sup>2</sup>) from aerial and ground surveys on the North Slope of Alaska.

Criterion / Study	Study Area	Method	
		Aerial Survey	Ground Survey
<div>CONFIDENTIAL NOT TO BE CIRCULATED OR DUPLICATED</div>			
TOTAL BIRDS			
Larned et al. (1992)	Arctic Coastal Plain	0.16	—
Smith et al. (1993)	Colville River Delta	0.04	—
Smith et al. (1994) <sup>a</sup>	Colville River Delta	0.09 - 0.10	—
Smith et al. (1994) <sup>a</sup>	East of Colville River Delta	0.04	—
Anderson et al. (1994) <sup>a</sup> (two surveys)	Kuparuk Oilfield	0.08 - 0.20	—
Warnock and Troy (1992) (four surveys)	Prudhoe Bay Oilfield	—	0.12 - 0.99
Anderson (ABR, unpubl. data) (five years data)	Lisburne Development Area	—	0.60 - 1.20
Troy and Wickliffe (1990)	Pt. McIntyre	—	0.00 - 0.05
Johnson et al. (1990)	Pt. McIntyre	—	0.00 - 0.06
PAIRS			
Warnock and Troy (1992)	Prudhoe Bay Oilfield	0.13	—
Smith et al. (1994) <sup>a</sup>	Colville River Delta	0.01 - 0.05	—
Smith et al. (1994) <sup>a</sup>	East of Colville River Delta	0.06 - 0.14	—
Anderson et al. (1994) <sup>a</sup> (two surveys)	Kuparuk Oilfield	0.02 - 0.12	—

<sup>a</sup> Two methods of estimation were used.

observations in Stratum 2. Although the requirement of a large sample may appear to be a limitation of using the line transect technique to sample a rare bird such as the Spectacled Eider, this was not a problem in Stratum 1, an area only slightly larger than

# DRAFT

**CONFIDENTIAL**  
**NOT TO BE CIRCULATED**  
**OR DUPLICATED**

## RESULTS AND DISCUSSION

Table 3. Density estimates (birds/km<sup>2</sup> or pairs/km<sup>2</sup>) of Spectacled and King eiders, as calculated by three methods, in the Kuvlum Corridor Study Area, June 1993.

Method / Criteria	Species / Area			
	Spectacled Eider		King Eider	
	Stratum 1	Stratum 2	Stratum 1	Stratum 2
<b>SIMPLE METHOD</b>				
Total birds	0.21	0.06	0.35	0.30
Total pairs	0.07	0.03	0.11	0.08
<b>USFWS METHOD</b>				
Total birds (unadjusted)	0.27	0.07	0.46	0.44
Total birds (vcf=3.58) <sup>a</sup>	0.97	0.24	1.66	1.57
Total pairs (unadjusted)	0.14	0.03	0.23	0.22
Total pairs (vcf=3.58) <sup>a</sup>	0.49	0.12	0.83	0.78
<b>LINE TRANSECT METHOD<sup>b</sup></b>				
Total birds	0.35	—	0.61	—
Total pairs	—	—	0.18	—

<sup>a</sup> vcf = visibility correction factor: 3.58 from Lensink (1968).

<sup>b</sup> The line transect method of density estimation requires a sample size > 25. Dashes indicate data sets with inadequate sample size. Line transect densities are based on non-flying birds only.

the line transect method because of small sample size, although the density could be approximated. For Stratum 1, the ratio of

$$\text{simple density of non-flying birds} / \text{line transect density} = 1.88$$

Applying this ratio to the simple density of non-flying birds in Stratum 2 yields a density estimate of 0.09 birds/km<sup>2</sup>.

Densities of Spectacled Eiders, regardless of the estimation method employed, differed greatly between the two strata (Table 3). Stratum 1 supported a density of Spectacled Eiders 3.4 - 4.0 times greater than in Stratum 2. A comparison of line transect density estimates for the two strata was not possible because of the small number of

# DRAFT

CONFIDENTIAL  
NOT TO BE CIRCULATED  
OR DUPLICATED

## RESULTS AND DISCUSSION

Stratum 2 and that had a much higher density of Spectacled Eiders. In regions with low densities, the area surveyed would have to be increased until an adequate sample size was attained. Even if Stratum 2 were sampled with the same effort used in Stratum 1, it is doubtful that an adequate sample size ( $> 25$  birds) would have been attained.

Our density estimates for Spectacled Eiders ranged from 0.21 to 0.97 birds/km<sup>2</sup> for Stratum 1, and from 0.06 to 0.24 birds/km<sup>2</sup> depending on the method of estimation (Table 3). Other studies on the North Slope have estimated the density of Spectacled Eiders from aerial breeding surveys, and densities ranged from 0.04 to 0.18 birds/km<sup>2</sup> (Table 4). All density estimates for Stratum 1 were higher than any of the estimates from the other studies; the range of density estimates from other studies largely overlapped the range of values for Stratum 2 estimates.

No densities from ground surveys for Spectacled Eiders have been reported in the Kuvlum Corridor, but various studies have reported Spectacled Eider densities based on other North Slope areas. Estimates from ground surveys are not comparable to estimates from aerial surveys and are included here only to give a sense of the geographical and temporal variability of Spectacled Eider densities on the North Slope. Density estimates among ground studies are highly variable, depending on such factors as timing of the survey, habitat quality, size of the study area, road accessibility, amount of survey coverage, and time taken to complete the survey. Density estimates from other studies ranged from 0.00 to 1.20 birds/km<sup>2</sup> (Table 4).

Our pair density estimates ranged from 0.07 to 0.49 pairs/km<sup>2</sup> for Stratum 1 and from 0.03 to 0.12 pairs/km<sup>2</sup> for Stratum 2. Pair density estimates from other aerial surveys on the North Slope ranged from 0.02 to 0.13 pairs/km<sup>2</sup> (Table 4).

### King Eiders

The density of King Eiders in Stratum 2 could not be estimated with the line transect method because of small sample size. For Stratum 1, the ratio of

$$\text{simple density of non-flying birds} / \text{line transect density} = 2.47$$

**DRAFT****CONFIDENTIAL  
NOT TO BE CIRCULATED  
OR DUPLICATED****RESULTS AND DISCUSSION****Table 6.** Density estimates (birds/km<sup>2</sup> or pairs/km<sup>2</sup>) from comparative platform surveys for Spectacled Eiders in the Kuylum Corridor and the Kuparuk Oilfield.

	Fixed-wing <sup>a</sup>	Platform	
		Helicopter <sup>b</sup> (front seat)	(back seat)
Number of non-flying birds observed	29	26	25
Number of flying birds observed	11	1	3
Total number of birds observed	40	27	28
Total number of pairs observed	14	10	9
<b>SIMPLE METHOD</b>			
Total birds	0.159	0.214	0.222
Total pairs	0.055	0.079	0.071
<b>USFWS METHOD</b>			
Number of birds tallied <sup>c</sup>	52	34	34
Total birds (unadjusted)	0.206	0.269	0.269
Total birds (vcf=3.58)	0.738	0.963	0.963
Number pairs tallied	26	17	17
Total pairs (unadjusted)	0.103	0.135	0.135
Total pairs (vcf=3.58)	0.369	0.483	0.483
<b>LINE TRANSECT METHOD</b>			
Total birds	0.286	0.298	0.311

<sup>a</sup> Two observers (one front, one rear); 252.3 km<sup>2</sup> surveyed.<sup>b</sup> One observer in front with greater visibility, one observer in back; 126.2 km<sup>2</sup> surveyed/observer.<sup>c</sup> Birds tallied following USFWS (1987).

wing survey (Table 6). In addition, nearly 50% of the King Eiders observed from the fixed-wing were flying as compared to 10% from the helicopter. This difference is not what we expected because other studies have depicted helicopters as more disruptive to waterfowl than fixed-wing aircraft (Ward and Stehn 1989).

**DRAFT**



DRAFT

CONFIDENTIAL  
NOT TO BE CIRCULATED  
OR DUPLICATED

## RESULTS AND DISCUSSION

Although helicopters proved to be a better platform than the fixed-wing aircraft for locating Spectacled Eiders, line transect density estimates generated from the two platforms were within 8% of one another (Table 6). Even though different numbers of birds were sighted from the two platforms, the density estimates were similar because the line transect technique effectively accounted for birds not detected during the survey.

We can conclude from these comparisons that the helicopter is more suitable when the specific locations of as many birds as possible are required for subsequent ground surveys or other site-specific objectives. Fixed-winged aircraft, however, appear to be more suitable for surveying eiders over large remote areas where acquiring density estimates is a main objective. Until empirically defined visibility correction factors are established, generating accurate densities may best be accomplished using line transect techniques.

A question unresolved by this study is whether fixed-wing aircraft actually do cause eiders to take flight more readily than during overflights by helicopters. This question is of particular relevance to surveys employing line transect techniques because only non-flying birds are used to calculate densities. Additional comparisons and evaluations of the reactions of birds to both platforms would be required to resolve this question.

## TUNDRA SWANS

### ABUNDANCE, DISTRIBUTION, AND DENSITY

During nesting surveys in June 1993, 81 Tundra Swans were seen at 50 locations (Table 7; Figure 5). More swans (74) and nests (14) were observed in Stratum 1 as compared to Stratum 2 (7 swans and no nests). Only 14 nests were found in the entire area and most swans (74%) were not associated with nests and probably were failed or non-breeders (Appendix 2).

Table 7. Numbers and densities (birds/km<sup>2</sup> or pairs/ km<sup>2</sup>) of Tundra Swans and nests recorded during aerial surveys in the Kuvlum Corridor study area, Alaska, 25-26 June, 1993.

Location	Nests	Adults with Nests	Adults without Nests	Total Swans
Stratum 1	14 (0.031)	21 (0.046)	49 (0.110)	70 (0.154)
Stratum 2	0 (0)	0 (0)	5 (0.014)	5 (0.014)
Total	14 (0.017)	21 (0.026)	54 (0.070)	75 (0.093)

Density of total swans was 0.17 birds/km<sup>2</sup> in Stratum 1 and 0.02 birds/km<sup>2</sup> in Stratum 2. Density of nests in Stratum 1 was 0.02 nests/km<sup>2</sup>. The density of Tundra Swan nests and adults during June in Stratum 1 were similar to densities calculated for other Alaska coastal plain populations. Nest densities between 0.02 and 0.04 for nests/km<sup>2</sup> and 0.15 - 0.17 birds/km<sup>2</sup> have been reported for the OGL 54 and Kuparuk areas (Ritchie et al. 1991) and Prudhoe Bay (Stickney et al. 1992). Similar densities of nests and adults were recorded in a portion of Stratum 1 surveyed for Tundra Swans in 1992 (Stickney et al. 1993). No other standard USFWS surveys have been conducted in this region (see Groves et al. 1989).

Tundra Swans were almost absent from Stratum 2, apparently due to the lack of large lakes east of the Kavik River. King and Hodges (1980) concluded that the density of nesting swans could be estimated using the numbers of lakes present in an area. The general distribution of Tundra Swans observed in the study area in 1993 conforms closely with Gavin's (1970) depiction of this area between the Kavik and Staines rivers as a region with low use by breeding waterfowl pairs, relative to the region west of the Kavik River. Only two Tundra Swan nests and a few adults were located in the area between Bullen Point and the Staines River immediately north of Stratum 2 in 1983 (WCC 1983a).

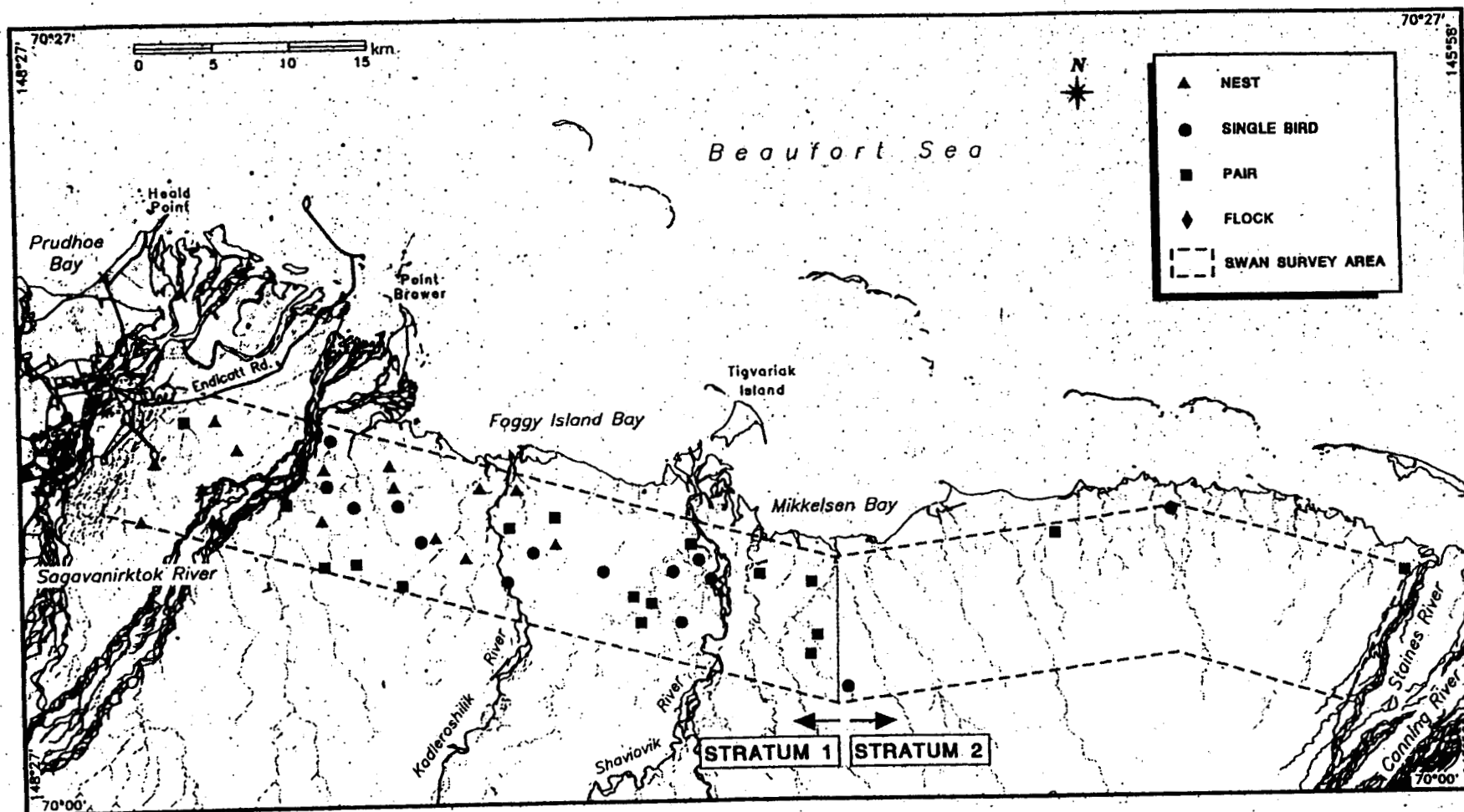


Figure 5. Distribution of Tundra Swans and nests observed during an aerial survey in the Kuvlum Corridor study area, 25-26 June, 1993.

CONFIDENTIAL  
NOT TO BE CIRCULATED  
OR DUPLICATED

DRAFT

RESULTS AND DISCUSSION

## LITERATURE CITED

- Anderson, B. A., Cooper, B. A., R. J. Ritchie. in prep. Spectacled Eider surveys in the Kuparuk Oilfield. Unpubl. draft. rep. prep. for ARCO, Alaska, Inc. Anchorage, AK. by Alaska Biological Research, Inc. Fairbanks.
- Bergman, R. D., R. L. Howard, K. F. Abraham, and M. W. Weller. 1977. Water birds and their wetland resources in relation to oil development at Storkersen Point, Alaska. U.S. Fish Wildl. Serv., Resour. Publ. 129: 1-38.
- Johnson, C. B., S. M. Murphy, C. C. Cranor, M. T. Jorgenson, and B. A. Kugler. 1990. Point McIntyre waterbird and noise monitoring program. Unpubl. rep. prep. for ARCO Alaska, Inc., Anchorage, AK. by Alaska Biological Research, Inc., Fairbanks, and Acentech, Inc., Los Angeles. 132 pp.
- Johnson, S. R. and D. M. Troy. 1987. The status of Lesser Snow Geese in the Sagavanirktok River Delta area, Alaska: a 7- year summary. Unpubl. rep. prep. for SOHIO, Alaska, Petroleum Co., Anchorage, AK. by LGL, Alaska Research Associates, Anchorage.
- Jorgenson, M. T., S. M. Murphy, and B. A. Anderson. 1989. A hierarchical classification of avian habitats on the North slope of Alaska. Paper presented at the Third Alaska Bird Conf. and Workshop, 20-22 March 1989, Univ. Alaska, Fairbanks. [abstract].
- King, J. G. 1970. The swans and geese of Alaska's Arctic Slope. Wildfowl 21: 11-17.
- King, J. G. and J. I. Hodges. 1980. A correlation between *Cygnus columbianus columbianus* territories and waterbodies in western Alaska. In: G.V. T. Matthews and M. Smart, eds. Proc. Second Int. Swan Symp., Sapporo, Japan. IWRB, Slimbridge, Glos., UK.
- Lawhead, B. E. and R. D. Cameron. 1988. Caribou distribution on the calving grounds of the Central Arctic herd, 1987. Unpubl. rep. prep. for ARCO Alaska, Inc. and Kuparuk River Unit, Anchorage, AK. by Alaska Biological Research, Inc., and Alaska Dep. Fish and Game, Fairbanks, AK. 59 pp + appendices
- Larned, W. W., G. R. Balogh, R. A. Stehn, and W. I. Butler. 1992. The status of eider breeding populations in Alaska, 1992. Unpubl. rep. U.S. Fish and Wildl. Serv. Anchorage, AK. 55 pp.
- Lensink, C. J. 1968. Refuge narrative report, Clarence Rhode National Wildlife Range. U.S. Fish and Wildl. Serv. Library, Anchorage, AK.

## LITERATURE CITED

- U.S. Fish and Wildlife Service. 1991. Trumpeter and Tundra Swan survey protocol - 1991. Unpubl. memo. prepared by USFWS, Off. Migr. Bird Manage., Juneau, AK. 9 pp.
- Walker, D. A., and K. R. Everett. 1991. Loess ecosystems of northern Alaska: regional gradient and topo sequence at Prudhoe Bay. Ecological Monograph 6(14): 437-464.
- Warnock, N. D. and D. M. Troy. 1992. Distribution and abundance of Spectacled Eiders at Prudhoe Bay, Alaska: 1991. Unpubl. rep. prep. for BP Exploration (Alaska) Inc., Anchorage, Alaska by Troy Ecological Research Associates, Anchorage, AK. 20 pp.
- Woodward-Clyde Consultants and Alaska Biological Research. 1983a. Terrestrial Environmental Study for Point Thompson Development Project. Unpubl. final rep. prep. for EXXON Company, USA, Thousand Oaks, CA.
- Woodward-Clyde Consultants and Alaska Biological Research. 1983b. Lisburne Development Area: 1983 environmental studies. Unpubl. rep prep. for Alaska, Inc., Anchorage.

# DRAFT

CONFIDENTIAL  
NOT TO BE CIRCULATED  
OR DUPLICATED

Appendix 1. Area (km<sup>2</sup>) covered by aerial surveys for Tundra Swans in two strata, Kuvlum Corridor, Alaska, 25-26 June, 1993.

		Transect Lengths (km) <sup>a</sup>		Areal Coverage (km <sup>2</sup> ) <sup>a</sup>	
		Stratum 1	Stratum 2	Stratum 1	Stratum 2
USGS Quadrangle					
Beechey Point	A-3	15.30	0	24.48	0
	A-2	140.34	0	224.54	0
	A-1	128.39	12.75	205.42	20.40
Flaxman Island	A-4	0	69.12	0	110.59
	A-5	0	138.07	0	220.91
Total		284.03	219.94	454.44	351.90

<sup>a</sup> Calculated from digitized maps of each USGS Quadrangle.

Appendix 2. Number of Tundra Swans and nests recorded (by quadrangle) during aerial surveys in the Kuvlum Corridor study area, Alaska, 25-26 June, 1993.

Location	USGS Quadrangle	Adults with Nests			Total Nests	Adults without Nests				Total Swans
		Pair	Single Adult	Total		Pair	Single Adult	Flocks	Flocked Swans	
Beechey Point	A-3	1	1	3	2	0	0	0	0	3
	A-2	6	5	17	11	7	6	2	6	43
	A-1	0	1					0	0	28
Flaxman Island	A-4	0	0					0	0	2
	A-5	0	0					0	0	5
Total		7	7	21	14	20	14	2	6	81

CONFIDENTIAL  
NOT TO BE CIRCULATED  
OR DUPLICATED

DRAFT